ISSN 1948-5204 (online)

World Journal of *Gastrointestinal Oncology*

Monthly Volume 17 Number 1 January 15, 2025

Published by Baishideng Publishing Group Inc

World Journal of Gastrointestinal Oncology

Contents

Monthly Volume 17 Number 1 January 15, 2025

EDITORIAL

ORIGINAL ARTICLE

Case Control Study

Retrospective Cohort Study

Retrospective Study

LETTER TO THE EDITOR

ABOUT COVER

Editorial Board Member of *World Journal of Gastrointestinal Oncology*, Wey-Ran Lin, AGAF, MD, PhD, Professor, Department of Gastroenterology and Hepatology, Linkou Chang Gung Memorial Hospital, Taoyuan 333, Taiwan. t12360@cgmh.org.tw

AIMS AND SCOPE

The primary aim of *World Journal of Gastrointestinal Oncology* (*WJGO*, *World J Gastrointest Oncol*) is to provide scholars and readers from various fields of gastrointestinal oncology with a platform to publish high-quality basic and clinical research articles and communicate their research findings online.

WJGO mainly publishes articles reporting research results and findings obtained in the field of gastrointestinal oncology and covering a wide range of topics including liver cell adenoma, gastric neoplasms, appendiceal neoplasms, biliary tract neoplasms, hepatocellular carcinoma, pancreatic carcinoma, cecal neoplasms, colonic neoplasms, colorectal neoplasms, duodenal neoplasms, esophageal neoplasms, gallbladder neoplasms, *etc*.

INDEXING/ABSTRACTING

The *WJGO* is now abstracted and indexed in PubMed, PubMed Central, Science Citation Index Expanded (SCIE, also known as SciSearch®), Journal Citation Reports/Science Edition, Scopus, Reference Citation Analysis, China Science and Technology Journal Database, and Superstar Journals Database. The 2024 edition of Journal Citation Reports® cites the 2023 journal impact factor (JIF) for *WJGO* as 2.5; JIF without journal self cites: 2.5; 5-year JIF: 2.8; JIF Rank: 72/143 in gastroenterology and hepatology; JIF Quartile: Q3; and 5-year JIF Quartile: Q2. The *WJGO*'s CiteScore for 2023 is 4.2 and Scopus CiteScore rank 2023: Gastroenterology is 80/167; Oncology is 196/404.

RESPONSIBLE EDITORS FOR THIS ISSUE

Production Editor: *Si Zhao*; **Production Department Director:** *Xiang Li*; **Cover Editor:** *Jia-Ru Fan*.

NAME OF JOURNAL
World Journal of Gastrointestinal Oncology

ISSN
ISSN 1948-5204 (online)

LAUNCH DATE
February 15, 2009

FREQUENCY
Monthly

EDITORS-IN-CHIEF
Monjur Ahmed, Florin Burada

EDITORIAL BOARD MEMBERS
https://www.wjgnet.com/1948-5204/editorialboard.htm

PUBLICATION DATE
January 15, 2025

INSTRUCTIONS TO AUTHORS
https://www.wjgnet.com/bpg/gerinfo/204

GUIDELINES FOR ETHICS DOCUMENTS
https://www.wjgnet.com/bpg/GerInfo/287

GUIDELINES FOR NON-NATIVE SPEAKERS OF ENGLISH
https://www.wjgnet.com/bpg/gerinfo/240

PUBLICATION ETHICS
https://www.wjgnet.com/bpg/GerInfo/288

PUBLICATION MISCONDUCT
https://www.wjgnet.com/bpg/gerinfo/208

ARTICLE PROCESSING CHARGE
https://www.wjgnet.com/bpg/gerinfo/242

STEPS FOR SUBMITTING MANUSCRIPTS
https://www.wjgnet.com/bpg/GerInfo/239

ONLINE SUBMISSION
https://www.f6publishing.com

World Journal of Gastrointestinal Oncology

Submit a Manuscript: https://www.f6publishing.com

World J Gastrointest Oncol 2025 January 15; 17(1): 93983

DOI: 10.4251/wjgo.v17.i1.93983

ISSN 1948-5204 (online)

EDITORIAL

Antiviral therapy for hepatitis B virus infection is beneficial for the prognosis hepatocellular carcinoma

Hui Wan, Yu-Xin Zhang, Guan-Yue Shan, Jun-Ya Cheng, Duan-Rui Qiao, Yi-Ying Liu, Wen-Na Shi, Hai-Jun Li

Specialty type: Gastroenterology and hepatology

Provenance and peer review: Invited article; Externally peer reviewed.

Peer-review model: Single blind

Peer-review report's classification
Scientific Quality: Grade C
Novelty: Grade B
Creativity or Innovation: Grade C
Scientific Significance: Grade B

P-Reviewer: Keppeke GD

Received: March 9, 2024
Revised: September 20, 2024
Accepted: September 29, 2024
Published online: January 15, 2025
Processing time: 277 Days and 22.1 Hours

Hui Wan, Yu-Xin Zhang, Guan-Yue Shan, Jun-Ya Cheng, Duan-Rui Qiao, Yi-Ying Liu, Wen-Na Shi, Institute of Translational Medicine, The First Hospital of Jilin University, Changchun 130061, Jilin Province, China

Jun-Ya Cheng, Duan-Rui Qiao, Yi-Ying Liu, Wen-Na Shi, Department of Bioengineering, Pharmacy School of Jilin University, Changchun 130061, Jilin Province, China

Hai-Jun Li, Institute of Liver Diseases, Institute of Translational Medicine, The First Hospital of Jilin University, Changchun 130061, Jilin Province, China

Corresponding author: Hai-Jun Li, MD, PhD, Associate Professor, Institute of Liver Diseases, Institute of Translational Medicine, The First Hospital of Jilin University, No. 71 Xinmin Street, Changchun 130061, Jilin Province, China. hjli2012@jlu.edu.cn

Abstract

In this editorial, we comment on the article by Mu *et al*, published in the recent issue of the *World Journal of Gastrointestinal Oncology*. We pay special attention to the immune tolerance mechanism caused by hepatitis B virus (HBV) infection, the pathogenesis of hepatocellular carcinoma (HCC), and the role of antiviral therapy in treating HCC related to HBV infection. HBV infection leads to systemic innate immune tolerance by directly inhibiting pattern recognition receptor recognition and antiviral signaling pathways, as well as by inhibiting the immune functions of macrophages, natural killer cells and dendritic cells. In addition, HBV leads to an immunosuppressive cascade by expressing inhibitory molecules to induce exhaustion of HBV-specific cluster of differentiation 8 + T cells, ultimately leading to long-term viral infection. The loss of immune cell function caused by HBV infection ultimately leads to HCC. Long-term antiviral therapy can improve the prognosis of patients with HCC and prevent tumor recurrence and metastasis.

Key Words: Hepatitis B virus; Hepatocellular carcinoma; Hepatitis B virus-DNA; Immune tolerance; Antiviral therapy

Core Tip: Hepatocellular carcinoma (HCC) is the seventh most common cancer in the world and is usually associated with hepatitis B virus (HBV) infection. Radical resection and antiviral therapy are considered key clinical treatments for patients with HBV-related HCC. However, many patients have their HCC and HBV infection detected at the same time, so they receive remedial antiviral treatment beginning in the perioperative period, missing the opportunity for long-term preoperative antiviral therapy. Therefore, evaluating the clinical efficacy and relevant factors of perioperative remedial antiviral therapy will be valuable.

Citation: Wan H, Zhang YX, Shan GY, Cheng JY, Qiao DR, Liu YY, Shi WN, Li HJ. Antiviral therapy for hepatitis B virus infection is beneficial for the prognosis hepatocellular carcinoma. *World J Gastrointest Oncol* 2025; 17(1): 93983
URL: https://www.wjgnet.com/1948-5204/full/v17/i1/93983.htm
DOI: https://dx.doi.org/10.4251/wjgo.v17.i1.93983

INTRODUCTION

Hepatocellular carcinoma (HCC) is currently one of the most common malignant tumors in the world, with its incidence rate ranking seventh in the world and its mortality ranking third in the world[1]. HCC is a complex and multifactorial disease, and its occurrence and development are influenced by both genetic and environmental factors. Multiple studies have shown that factors affecting HCC include hepatitis B virus (HBV) infection, hepatitis C virus (HCV) infection, alcohol consumption, and nonalcoholic fatty liver disease[2].

The immune tolerance caused by HBV can be divided into hepatic innate immune tolerance and adaptive immune tolerance. Hepatic intrinsic immunity is the frontline defense mechanism against HBV attacks, and pattern recognition receptors (PRRs) play important roles in immune responses. Numerous studies have shown that HBV infection interferes with PRR-mediated antiviral signaling[3-5]. HBV infection is one of the risk factors for HCC, accounting for 50%-80% of HCC cases worldwide. The tumor immune microenvironment of HCC is characterized by immunosuppression through a variety of mechanisms, including the recruitment of immunosuppressive cells, a reduction in antitumor effector cells, changes in cytokine levels, and increased expression of immune checkpoint proteins[6]. HBV infection leads to systemic innate immune tolerance by directly inhibiting PRR recognition and antiviral signaling pathways, as well as by inhibiting the immune functions of macrophages, natural killer (NK) cells and dendritic cells (DCs). In addition, HBV leads to an immunosuppressive cascade by expressing inhibitory molecules such as programmed death (PD)-1, programmed cell death 1 ligand 1 (PD-L1), cytotoxic T lymphocyte-associated protein 4 (CTLA-4), interleukin (IL)-10, T-cell immunoglobulin and mucin domain-containing protein 3 (Tim-3) to induce exhaustion of HBV-specific cluster of differentiation (CD) 8 + T cells, ultimately leading to long-term viral infection. The loss of immune cell function caused by HBV infection ultimately leads to HCC. In this editorial, we comment on the article by Mu *et al*[7]. We elucidate the mechanisms of HBV infection and the pathogenesis of liver cancer and suggest that long-term antiviral therapy can improve the prognosis of patients with HCC and prevent tumor recurrence and metastasis.

THE IMMUNE TOLERANCE MECHANISM OF HBV INFECTION

HBV has four open reading frames, namely, the S region, C region, P region, and X region, which encode hepatitis B surface antigen (HBsAg), hepatitis B core antigen (HBcAg), HBV polymerase, and hepatitis B X protein (HBx), respectively[8]. Because HBV does not cause the breakdown of infected cells through extensive proliferation, the immune system relies mainly on CD8 + T cells or NK cells to kill infected cells, release the virus, and then eliminate the virus with antibodies. Moreover, cytokines such as interferon (IFN)-α or tumor necrosis factor (TNF)-α can directly inhibit HBV replication or induce its degradation by activating apolipoprotein B mRNA editing enzyme catalytic subunit nucleic acid editing enzymes[9]. However, when the function of immune cells is disrupted or the release of cytokines is inhibited, immune tolerance can occur.

The immune tolerance caused by HBV can be divided into hepatic innate immune tolerance and adaptive immune tolerance. Hepatic intrinsic immunity is the first line of defense against HBV attacks, and PRRs play important roles in immune responses. Numerous studies have shown that HBV infection interferes with PRR-mediated antiviral signaling pathways[3-5]. HBeAg, HBsAg, and other viral particles inhibited the antiviral function induced by toll-like receptors (TLRs) in HBV-infected individuals[10]. The reduction in TLR3, TLR4, and TLR9 expression in hepatocytes is significantly reduced during the immune tolerance stage of HBV infection, and the TLR signaling pathway is disrupted. In addition, HBV polymerase inhibits TLR3-mediated IFN-α/β induction by blocking the activation of interferon regulatory factor 3 (IRF3). Research has indicated that HBV polymerase inhibits the phosphorylation, dimerization, and nuclear translocation of IRF3[11]. In addition, Lang *et al*[12] reported that HBeAg can inhibit the function of TLRs by inhibiting the activation of NF-κB[12]. HBsAg inhibits TLR2 on monocytes/macrophages by blocking the c-Jun N-terminal kinase-mitogen-activated protein kinase pathway and provides innate immune suppression[13]. HBV targets TLRs and downstream signaling pathways, leading to endogenous immune tolerance in the liver. Retinoic acid-inducible gene-I (RIG-I) is a cytoplasmic antiviral nucleic acid sensor that generates type 1 IFN, thereby inhibiting HBV replication[14]. HBx and HBV polymerase interfere with the RIG-I signaling pathway in human liver cells by disrupting the interaction

between interferon beta promoter stimulator 1 and RIG-I and inhibiting the production of type I IFN[15].

Kupffer cells (KCs) and monocyte derived macrophages are two main types of macrophages in the liver. As an immunosuppressive organ, the liver exhibits an anti-inflammatory phenotype through the secretion of immune regulatory cytokines such as IL-10 under physiological conditions. However, during virus infection, the liver recruits Ly6c + monocytes to secrete pro-inflammatory factors IL-6 and IL-1β and TNF-α, controlling infection through inflammatory response[16]. Up-regulation of IL-10 during HBV infection can impair lymphocyte function and decelerate HBV clearance [17]. HBV infection promotes the production of IL-18 in KCs and affects the activity of NK cells. Research has shown that not only does the level of pro-inflammatory factors secreted by liver resident KCs decrease, but the level of pro-inflammatory factors secreted by M1 macrophages from periphery also decreases after HBV infected. In addition, HBV can enhance liver immune tolerance by stimulating monocyte differentiation into M2 macrophage, which is beneficial for infection maintenance[18]. Moreover, M2 macrophage may also be involved in the occurrence and development of HCC by releasing inhibitory regulatory factors.

NK cell number, IFN-γ production and cell lysis ability weakened in chronic hepatitis B (CHB) patients[19]. There are inhibitory receptors such as NK group 2A (NKG2A), Tim-3, and killer cell lectin like receptor G1 (KLRG1), and activate receptors such as NK group 2C, NK group 2D (NKG2D) and CD16 on NK cell surface[20,21]. HBeAg increase the expression of NKG2A and Tim-3 on the surface of peripheral blood NK cells of CHB patients[22,23]. The inhibitory KLRG1 + NK cells increased in the blood and liver of HBsAg positive CHB patients. In addition, peripheral blood mononuclear cells and NKG2D + NK cells in the liver of CHB patients decreased[24]. The phenotypic changes of NK cells are the basis of functional defects and the result of immune dysfunction. IFN-γ and TNF-α production decreased in conventional NK cells of CHB patients may related to the CD122 low expression on cell surface[25]. IL-15 mediated activation of the protein kinase B mammalian target of rapamycin pathway is impaired in NK cells of CHB patients[26]. The high level of inhibitory cytokine IL-10 in the liver of CHB patients has a significant inhibitory effect on the production of IFN-γ by NK cells[27].

DCs are specialized antigen-presenting cells, as well as participating in the production of cytokines which affect T cell polarization. The DC subpopulations mainly include myeloid DCs (mDCs) and plasma like DCs. The mDCs frequency reduced in CHB patients but it would be recovered after antiviral therapy[28]. The intrahepatic mDC was positively correlated with serum alanine aminotransferase level, and significantly negatively correlated with plasma HBV load[29]. The mDCs from HBV patients showed functional defects resulting in a reduction of IL-2, IFN-γ and TNF-α production by T cells due of IL-12 reduction[30]. NK cell and DC interactions caused by HBV may significantly impair the efficacy of antiviral immune response in CHB patients[31]. In conclusion, the persistence of HBV not only directly inhibits PRRs recognition and antiviral signal pathway, leading to endogenous immune tolerance of cells, but also inhibits the function of innate immune cells (including macrophages, NK cells and DCs), leading to hepatic innate immune tolerance.

The persistent existence of HBV will lead to CD8 + T cell frequency reduction and functional defects. In CHB infection, CD8 + T cells lose their proliferation capacity and antiviral function, which is characterized by excessive inhibitory signals, reduced production of cytokines, and T cells exhaustion[32]. PD-1 is a co-inhibitory receptor that has been shown to increase expression on antigen specific T cells during chronic viral infection and weaken T cell activation through co-inhibitory signaling. Blocking the PD-1/PD-L1 pathway can restore the function of exhausted T cells[33]. During the persistence of HBV, PD-1 was up-regulated on both peripheral blood monocytes and intrahepatic lymphocytes, especially on HBV specific CD8 + T cells. PD-1 interacted with PD-L1 on antigen presenting cells, leading to the functional inhibition and apoptosis of CD8 + T cells[34]. In CHB infection, the proportion of liver infiltrating T-reg cells increased. Multiple molecules are involved in T-reg-mediated immunosuppression, including CTLA-4, IL-10 and Tim-3. CTLA-4 and Tim-3 are up-regulated on HBV specific CD8 + T cells, which is closely related to the viral load, and plays an important role in T cell depletion in persistent HBV infection[35]. In addition, the immunosuppressive environment in the liver during HBV infection contributes to T cell tolerance. The level of IL-10 and transforming growth factor (TGF)-β is closely related to virus replication. The cell-intrinsic production of TGF-β mediates apoptosis of CD8 + T cells, thus blocking TGF-β may contribute to T cell reconstitution[36]. In summary, HBV forms an immunosuppressive cascade by inhibitory molecules such as PD-1, PD-L1, CTLA-4, IL-10, Tim-3 and immune cells CD8 + T cells, ultimately leading to long-term viral infection (shown in Figure 1).

THE PATHOGENESIS OF HCC

HCC is currently one of the most common malignant tumors worldwide[1]. The occurrence and development of HCC are influenced by both genetic and environmental factors. Multiple studies have shown that factors affect HCC, including HBV infection, HCV infection, alcohol consumption, and nonalcoholic fatty liver disease[2]. At present, the occurrence and development of HCC is a multigene, multistep and multistage process. With the development of molecular biology, research on the pathogenesis of HCC is gradually becoming systematic, which may provide new approaches for the treatment of HCC.

The occurrence of HCC is related to the unbalance activation of oncogenes and antioncogenes. Under normal circumstances, oncogenes maintain low expression levels and play important physiological functions. But under certain conditions, such as viral infection, chemical carcinogens or radiation effects, oncogenes can be abnormally activated and induce cancerous transformation. Common oncogenes include the *RAS* family, *MYC* family, *SRC* family, *SIS* family and *MYB* family[37]. Antioncogenes play a crucial negative regulatory role in controlling cell growth, proliferation, and differentiation. They interact with oncogenes to maintain a normal physiological activity of cells. *P53* is an important antioncogene that can induce apoptosis of cancer cells. However, when *P53* mutates, it loses control of cell proliferation

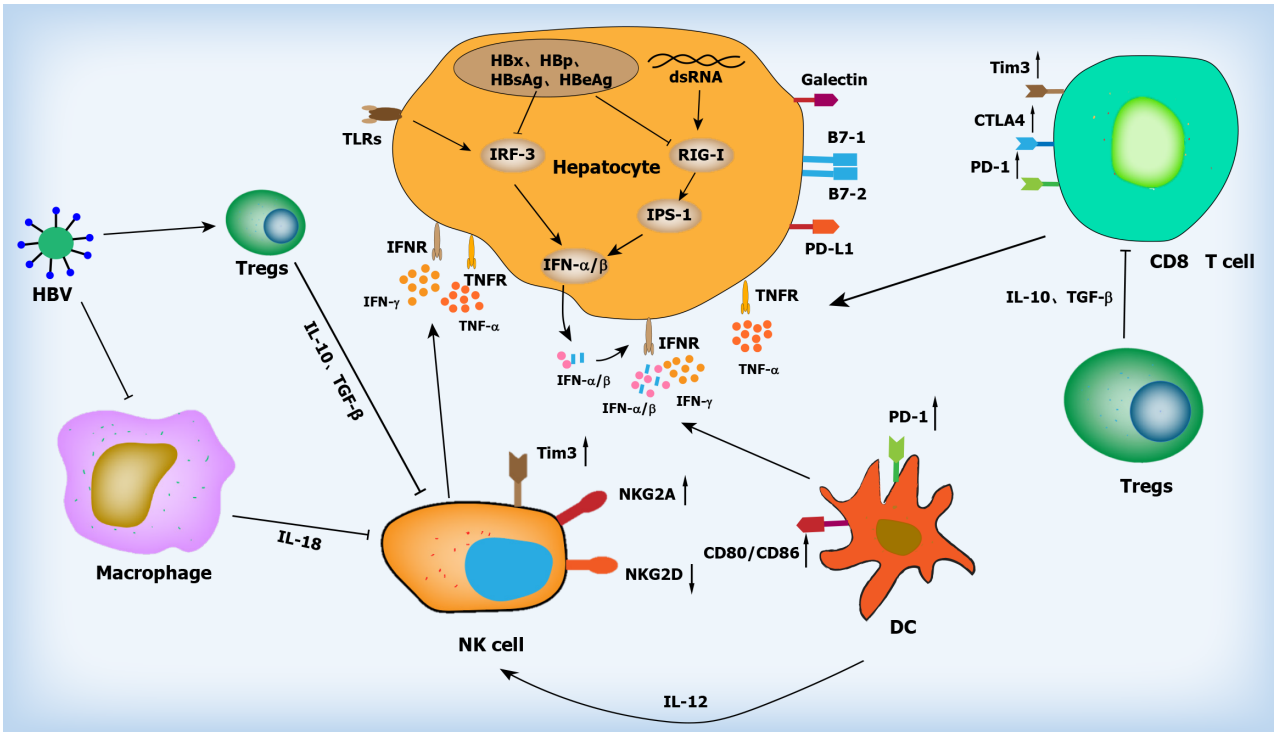

Figure 1 Hepatitis B virus immune tolerance mechanism. In hepatocyte, hepatitis B virus (HBV) inhibits toll-like receptors mediated interferon (IFN)-α/β production by blocking the activation of interferon regulatory factor 3 HBV interferes with the retinoic acid-inducible gene-I (RIG-I) signaling pathway in hepatocyte and inhibits the production of IFN-α/β by disrupting the interaction between mitochondrial antiviral-signaling protein and RIG-I. HBV affects the activation of natural killer (NK) cells by inhibiting the production of interleukin (IL)-18 by macrophages. HBV promotes the generation of Tregs, which release IL-10 and transforming growth factor β to increase the expression of surface inhibitory receptors on NK cells and CD8 + T cells, thereby reducing IFN and tumor necrosis factor-α release. The expression of immune checkpoints on the surface of CD8 + T cells increases, leading to T cell exhaustion, resulting in immune tolerance of HBV. IL: Interleukin; HBV: Hepatitis B virus; NK: Natural killer; IFN: Interferon; NKG2A: Natural killer group 2A; NKG2D: Natural killer group 2D; Tim-3: T-cell immunoglobulin and mucin domain-containing protein 3; DC: Dendritic cell; CD: Cluster of differentiation; PD-1: Programmed death-1; CTLA4: Cytotoxic T lymphocyte-associated protein 4; TGF: Transforming growth factor; PD-L1: Programmed cell death 1 ligand 1; TNF: Tumor necrosis factor; TLR: Toll-like receptors; IRF-3: Interferon regulatory factor 3; IPS-1: Interferon-β promoter stimulator 1; RIG-I: Retinoic acid-inducible gene-I.

and leads cell canceration[38]. *P53* can inhibit tumor progression by controlling the composition of microRNAs carried by exosomes and secreting cytokines. On the contrary, *P53* mutants can promote tumor progression by regulating the content of exosomes, leading M2 macrophages polarization and form immunosuppressive microenvironment[39]. *P21* gene is closely linking tumor inhibition with cell cycle control processes[40]. *P16* is a fundamental gene in the cell cycle, whose expression products are directly involved in the negative regulation of cell proliferation[41]. The bnormal methylation of *P53*, *P21* and *P16* in serum DNA play an important role in early detection of HCC[42]. These findings indicate that the inactivation of *P16* is a major event in the development of liver cancer. In addition, there are a large number of antioncogenes, such as *PTEN*, *Rb*, which are closely related to the occurrence of HCC.

The occurrence of HCC is also related to abnormal activation of signaling pathways. The key proteins in Wingless (Wnt)/β-catenin signaling pathway undergo mutations will lead to abnormal cell proliferation and promote HCC occurrence. Frizzled family, casein kinase 1, desheveled, glycogen synthase kinase 3, *APC*, *AXIN*, β-catenin and transcription factor T-cell factor (TCF)/lymphoid enhancer factor family compose the main Wnt signaling pathway[43, 44]. When there is no Wnt signal, β-catenin is effectively phosphorylated and polyubiquitinated in the *AXIN* complex. *AXIN* gene mutations can prevent β-catenin degradation, which accumulates in the cytoplasm and enters the nucleus to bind to TCF family proteins, enhances the transcription of downstream genes such as *c-MYC*, survivin and *Cyclin-D1*, promotes cell proliferation, and inhibits cell apoptosis. Abnormal activation of the Wnt pathway can cause unlimited proliferation of tumor cells and invasion and metastasis of tumors[45]. The expression of β-catenin and its downstream target genes such as *c-MYC* and *Cyclin-D1* is reduced when *Wnt-10B* gene knockout. Therefore, the abnormal expression of Wnt is involved in HCC occurrence[46]. *PARP6* can affect wnt/β-catenin by inhibiting the expression of *XRCC6* to inhibit HCC progression[47]. Curcumin inhibit the proliferation of liver cancer cells, induce cell cycle arrest and apoptosis by reducing the expression of β-catenin and inducing inactivation of wnt/β-catenin signaling pathway[48]. Based on these themes, future experiments will focus on developing new therapies for wnt/β-catenin in HCC treatment[49].

The Hedgehog (Hh) signaling pathway controls cell growth and proliferation, and the occurrence of tumors is a result of uncontrolled cell growth and proliferation[50]. In the presence of Hh ligands, when Hh ligands bind to patched (Ptch)-1, Ptch-1 is internalized, which relieves the inhibition of smoothened (Smo). Smo dissociates *SUFU* from *GLI* and then forms *GLI* activators, which promotes the expression of target genes. In the absence of Hh ligands, Ptch-1 inhibits the expression of Smo, and Gli binds to *SUFU* to form *GLIR*, inhibiting the expression of target genes. Zhou *et al*[51] discovered that the molecular mechanism of chemotherapy resistance in HCC has been revealed by targeting the Hh

signaling pathway, providing new insights for alleviating resistance in refractory HCC. He *et al*[52] demonstrated that circznf609 activates the Hh pathway by regulating the expression of *GLI2*, thereby enhancing the proliferation and metastasis of liver cancer cells. In summary, numerous studies have shown that abnormal expression of the Hh pathway promotes the occurrence of HCC.

The *NOTCH* signaling pathway is also closely related to the occurrence of HCC. *NOTCH* signaling affects multiple processes of normal cellular morphogenesis, including apoptosis, proliferation, and formation of cell boundaries[53,54]. In the pathogenesis of HCC, the *NOTCH* signaling pathway can play a pathogenic role by regulating other HCC related signaling pathways. *NOTCH* signaling can promote the progression of HCC by upregulating the Wnt signaling pathway [55]. *NOTCH1* and Akt may play a crucial role in the resistance of HCC cells to sorafenib. Valproic acid may overcome resistance and enhance the sensitivity of HCC cells to sorafenib by inhibiting the *NOTCH*/Akt signaling pathway[54]. Xie *et al*[56] described a significant correlation between high expression of *TSPAN5* and some clinical pathological features, including invasion length, vascular invasion, clinical staging and low overall survival rate in HCC patients. In clinical HCC samples, the expression of *TSPAN5* is closely related to many key molecules involved in *NOTCH* signaling, highlighting its role in regulating *NOTCH* signaling and demonstrating the important role of the *NOTCH* signaling pathway in the pathogenesis of HCC. In addition, the abnormal activation of epidermal growth factor (EGF)/EGF receptor signaling pathway, MAPK signaling pathway, vascular endothelial growth factor (VEGF)/VEGF receptor signaling pathway also promotes tumor cell proliferation. There are complex intersections and cascades between various signaling pathways, and these reaction processes are crucial for the treatment of HCC (shown in Figure 2).

RELATION BETWEEN HBV AND HCC

Most HCCs arise from underlying chronic inflammation, including HBV and HCV infections, alcoholic steatohepatitis, nonalcoholic steatohepatitis, and exposure to toxic substances such as aflatoxins. HBV infection is one of the risk factors for HCC, accounting for 50%-80% of HCC cases worldwide. The tumor immune microenvironment of HCC is characterized by immunosuppression through a variety of mechanisms, including the recruitment of immunosuppressive cells, a reduction in antitumor effector cells, changes in cytokine levels and increased expression of immune checkpoint proteins[8]. The tumor microenvironment can induce macrophage differentiation. Macrophages can differentiate into M1-type and M2-type macrophages in different microenvironments. Many activated macrophages infiltrate tumor tissue; these activated macrophages are named tumor-associated macrophages (TAMs), which have multiple M2 phenotypes and can promote tumor growth, invasion, and metastasis by secreting a variety of active substances. TAMs are among the most infiltrative inflammatory cells in the tumor microenvironment and can inhibit the antitumor immune effect of HCC. Some studies have shown that immunosuppressive cytokines, such as IL-4, IL-13, C-C motif chemokine ligand 2, chemokine (C-X-C Motif) ligand 12, and colony stimulating factor-1, can promote the differentiation of TAMs, leading to innate or adaptive immunity defects[57]. TAMs can block antitumor immune responses and accelerate tumor progression by increasing the expression of *PDGF*, *EGF* and *IGF*[58].

NK cells, as an important part of immune system, play an important role at different stages of HCC development. Their function is primarily regulated by interactions with other immune cells, which are mediated by different types of cytokines, ligands, and their receptors. Tregs can impair the function of NK cells by releasing a variety of cytokines (IL-8, IL-10, and TGF-β1). Recent studies have shown that in HBV transgenic mice, NK cell-derived IFN-γ induces HCC through the epithelial cell adhesion molecule-epithelial mesenchymal transition axis and promotes HBsAg-positive hepatocyte injury through activated NK cells, thereby stimulating HCC development[59]. Studies have shown reduced cytotoxicity and production of IFN-γ and TNF-α in NK cells in HBV-induced HCC patients compared to healthy individuals[60].

TAMs can inhibit anti-tumor responses by damaging effector T cells, reducing cytotoxicity in NK cells, reducing tumor-infiltrating lymphocytes, and amplifying immune checkpoint signaling in HCCs[61]. Immune checkpoints mainly include PD-1/PD-L1, CTLA-4 and Tim-3, which play a key role in the process of tumor immune evasion. PD-1 is expressed on activated B cells, T cells, DCs, and NK cells and inhibits the activation of these immune cells by binding to PD-L1 to generate inhibitory signals, protecting tumor cells from attack[62]. Interestingly, in HCC patients, immune checkpoint-related molecules are often overexpressed due to long-term chronic inflammation, leading to apoptosis of CD8 + T cells, which are less active against tumors[63].

CONCLUSION

Elevated levels of HBV-DNA during the perioperative period are associated with postoperative recurrence of liver cancer. Therefore, antiviral therapy is necessary to suppress serum HBV DNA levels. Currently, antiviral drugs include nucleotide analogs (NAs), viral DNA polymerase inhibitors, and polyethylene glycol IFN (PEG-IFN-α). The NAs used for antiviral therapy include tenofovir disoproxil fumarate, tenofovir alafenamide fumarate, entecavir, *etc.*, which can effectively inhibit HBV replication and reduce the viral load to undetectable levels after 48 weeks of treatment[64]. A recent meta-analysis revealed that antiviral therapy with NA can reduce HCC-related mortality and postoperative recurrence of HCC and improve the overall survival rate of patients with HBV-related HCC[65]. However, NA therapy rarely reduces HBsAg levels, and virus replication typically rebounds after the termination of NA therapy[66]. Therefore, to maintain beneficial therapeutic effects, lifelong NA treatment is necessary. IFN-α has dual antiviral and anti-proliferative properties. Some meta-analyses have indicated that IFN-α effectively clears HBeAg and continuously decreases

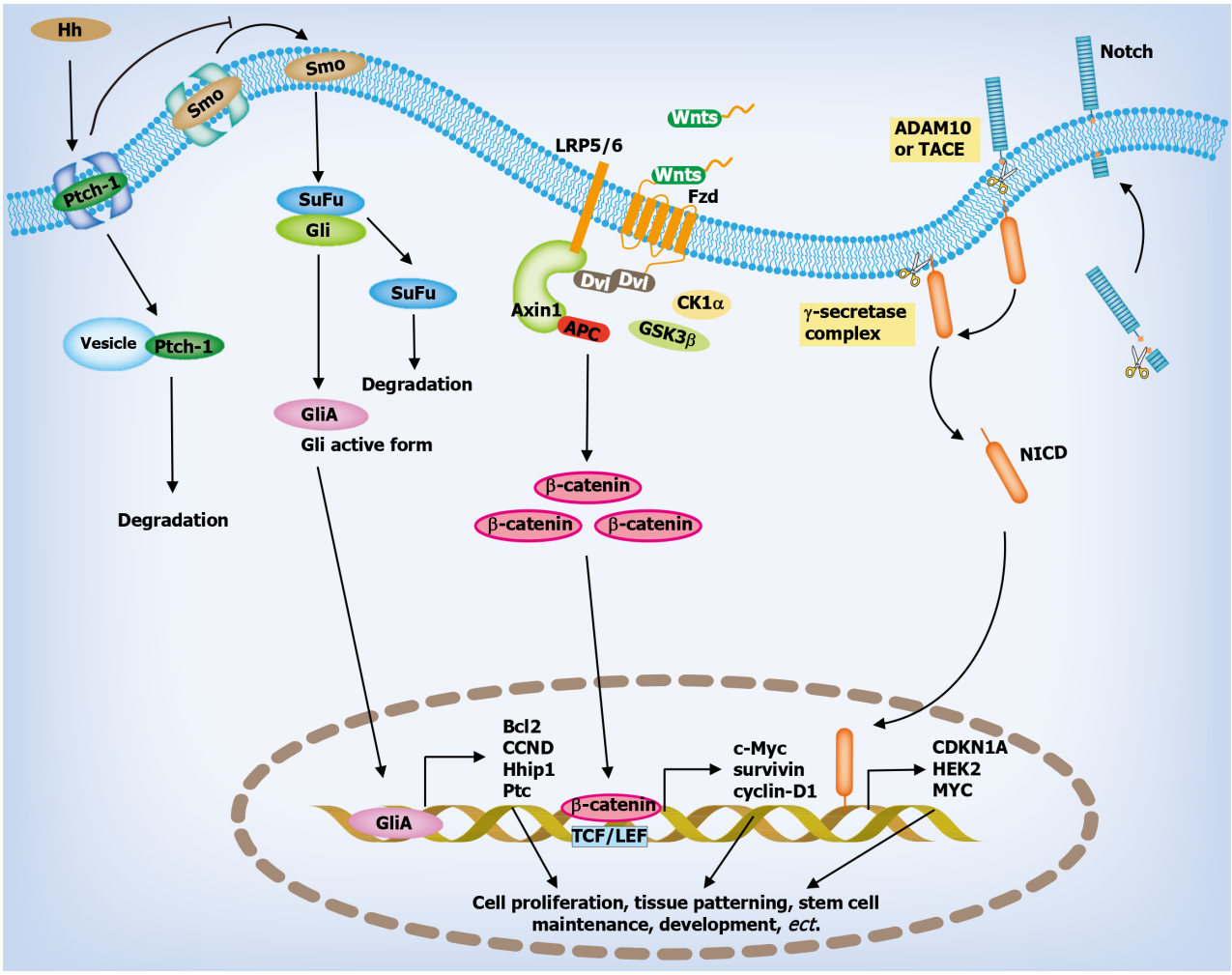

Figure 2 The pathogenesis of liver cancer. The occurrence of hepatocellular carcinoma is related to the abnormal activation of multiple signaling pathways. When there is a wnt signal, abnormalities in the *AXIN* gene can inhibit β-catenin degradation, accumulating in the cytoplasm and entering the nucleus to bind with T-cell factor family proteins, enhancing downstream gene transcription. In the presence of hedgehog (Hh) ligands, the binding of Hh ligand to patched (Ptch)-1 can lead to the endocytosis of Ptch-1, thereby relieving the inhibition of smoothened (Smo). The accumulation and activation of Smo lead to the dissociation of suppressor of fused and *GLI*, forming *GLI* activators that promote the expression of target genes. Notch protein is cleaved by furin like proteins and expressed on the cell surface in the form of heterodimers. After binding with ligands, it is cleaved by proteases, and then cleaved by γ-secretase complex in the transmembrane region. At this time, the activated molecule notch intracellular domain enters the nucleus to regulate the transcription of target genes. Hh: Hedgehog; Smo: Smoothened; TCF/LEF: Transcription factor T-cell factor/lymphoid enhancer factor.

serum HBV-DNA levels[67]. A recent study using urokinase-type plasminogen activator/severe combined immunodeficiency liver-humanized mice revealed that PEG-IFN-α treatment resulted in a decrease in HBx, restoration of structure maintenance of chromosome (SMC) 5/6, and decreased cccDNA transcriptional activity. However, the antiviral effect did not persist after treatment, and SMC5/6 degraded again[68]. A recent report involving RNA sequencing of liver biopsies from patients with CHB after PEG-IFN-α treatment revealed that hepatic tumor protein p53 binding protein 2 levels were significantly higher in the HBsAg loss group than in the HBsAg persistence group, indicating an increased probability of serum HBsAg loss in PEG-IFN-α-treated CHB patients[69]. In short, the rational and long-term use of antiviral drugs that target different HBV components and activate antiviral immune responses can improve patient prognosis and reduce the recurrence and metastasis of HCC.

FOOTNOTES

Author contributions: Zhang YX, Shan GY, Qian DR, and Shi WN collected the information; Cheng JY and Liu YY drew and modified the illustrations; Wan H wrote the paper; Li HJ revised the paper.

Supported by the Natural Science Foundation of China, No. 81970529; the Natural Science Foundation of Jilin Province, No. 20230508074RC and No. YDZJ202401218ZYTS.

Conflict-of-interest statement: The authors declare that they have no conflict of interest.

Country of origin: China

ORCID number: Guan-Yue Shan 0000-0002-3380-9418; Duan-Rui Qiao 0000-0001-6875-2143; Hai-Jun Li 0000-0002-2515-3076.

S-Editor: Fan M
L-Editor: A
P-Editor: Zhang L

REFERENCES

1 **Sung H**, Ferlay J, Siegel RL, Laversanne M, Soerjomataram I, Jemal A, Bray F. Global Cancer Statistics 2020: GLOBOCAN Estimates of Incidence and Mortality Worldwide for 36 Cancers in 185 Countries. *CA Cancer J Clin* 2021; **71**: 209-249 [PMID: 33538338 DOI: 10.3322/caac.21660]
2 **Llovet JM**, Kelley RK, Villanueva A, Singal AG, Pikarsky E, Roayaie S, Lencioni R, Koike K, Zucman-Rossi J, Finn RS. Hepatocellular carcinoma. *Nat Rev Dis Primers* 2021; **7**: 6 [PMID: 33479224 DOI: 10.1038/s41572-020-00240-3]
3 **Wu J**, Lu M, Meng Z, Trippler M, Broering R, Szczeponek A, Krux F, Dittmer U, Roggendorf M, Gerken G, Schlaak JF. Toll-like receptor-mediated control of HBV replication by nonparenchymal liver cells in mice. *Hepatology* 2007; **46**: 1769-1778 [PMID: 17929296 DOI: 10.1002/hep.21897]
4 **Xu C**, Fan J, Liu D, Tuerdi A, Chen J, Wei Y, Pan Y, Dang H, Wei X, Yousif AS, Yogaratnam J, Zhou Q, Lichenstein H, Xu T. Alpha-kinase 1 (ALPK1) agonist DF-006 demonstrates potent efficacy in mouse and primary human hepatocyte (PHH) models of hepatitis B. *Hepatology* 2023; **77**: 275-289 [PMID: 35699669 DOI: 10.1002/hep.32614]
5 **Wu J**, Meng Z, Jiang M, Pei R, Trippler M, Broering R, Bucchi A, Sowa JP, Dittmer U, Yang D, Roggendorf M, Gerken G, Lu M, Schlaak JF. Hepatitis B virus suppresses toll-like receptor-mediated innate immune responses in murine parenchymal and nonparenchymal liver cells. *Hepatology* 2009; **49**: 1132-1140 [PMID: 19140219 DOI: 10.1002/hep.22751]
6 **Zhou J**, Wang W, Li Q. Potential therapeutic targets in the tumor microenvironment of hepatocellular carcinoma: reversing the protumor effect of tumor-associated macrophages. *J Exp Clin Cancer Res* 2021; **40**: 73 [PMID: 33596985 DOI: 10.1186/s13046-021-01873-2]
7 **Mu F**, Hu LS, Xu K, Zhao Z, Yang BC, Wang YM, Guo K, Shi JH, Lv Y, Wang B. Perioperative remedial antiviral therapy in hepatitis B virus-related hepatocellular carcinoma resection: How to achieve a better outcome. *World J Gastrointest Oncol* 2024; **16**: 1833-1848 [PMID: 38764825 DOI: 10.4251/wjgo.v16.i5.1833]
8 **Faure-Dupuy S**, Delphin M, Aillot L, Dimier L, Lebossé F, Fresquet J, Parent R, Matter MS, Rivoire M, Bendriss-Vermare N, Salvetti A, Heide D, Flores L, Klumpp K, Lam A, Zoulim F, Heikenwälder M, Durantel D, Lucifora J. Hepatitis B virus-induced modulation of liver macrophage function promotes hepatocyte infection. *J Hepatol* 2019; **71**: 1086-1098 [PMID: 31349000 DOI: 10.1016/j.jhep.2019.06.032]
9 **Matsumoto T**, Marusawa H, Endo Y, Ueda Y, Matsumoto Y, Chiba T. Expression of APOBEC2 is transcriptionally regulated by NF-kappaB in human hepatocytes. *FEBS Lett* 2006; **580**: 731-735 [PMID: 16427049 DOI: 10.1016/j.febslet.2005.12.081]
10 **Vincent IE**, Zannetti C, Lucifora J, Norder H, Protzer U, Hainaut P, Zoulim F, Tommasino M, Trépo C, Hasan U, Chemin I. Hepatitis B virus impairs TLR9 expression and function in plasmacytoid dendritic cells. *PLoS One* 2011; **6**: e26315 [PMID: 22046272 DOI: 10.1371/journal.pone.0026315]
11 **Yu S**, Chen J, Wu M, Chen H, Kato N, Yuan Z. Hepatitis B virus polymerase inhibits RIG-I- and Toll-like receptor 3-mediated beta interferon induction in human hepatocytes through interference with interferon regulatory factor 3 activation and dampening of the interaction between TBK1/IKKepsilon and DDX3. *J Gen Virol* 2010; **91**: 2080-2090 [PMID: 20375222 DOI: 10.1099/vir.0.020552-0]
12 **Lang T**, Lo C, Skinner N, Locarnini S, Visvanathan K, Mansell A. The hepatitis B e antigen (HBeAg) targets and suppresses activation of the toll-like receptor signaling pathway. *J Hepatol* 2011; **55**: 762-769 [PMID: 21334391 DOI: 10.1016/j.jhep.2010.12.042]
13 **Wang S**, Chen Z, Hu C, Qian F, Cheng Y, Wu M, Shi B, Chen J, Hu Y, Yuan Z. Hepatitis B virus surface antigen selectively inhibits TLR2 ligand-induced IL-12 production in monocytes/macrophages by interfering with JNK activation. *J Immunol* 2013; **190**: 5142-5151 [PMID: 23585678 DOI: 10.4049/jimmunol.1201625]
14 **Zhou L**, He R, Fang P, Li M, Yu H, Wang Q, Yu Y, Wang F, Zhang Y, Chen A, Peng N, Lin Y, Zhang R, Trilling M, Broering R, Lu M, Zhu Y, Liu S. Hepatitis B virus rigs the cellular metabolome to avoid innate immune recognition. *Nat Commun* 2021; **12**: 98 [PMID: 33397935 DOI: 10.1038/s41467-020-20316-8]
15 **Kumar M**, Jung SY, Hodgson AJ, Madden CR, Qin J, Slagle BL. Hepatitis B virus regulatory HBx protein binds to adaptor protein IPS-1 and inhibits the activation of beta interferon. *J Virol* 2011; **85**: 987-995 [PMID: 21068253 DOI: 10.1128/JVI.01825-10]
16 **Li H**, Zheng HW, Chen H, Xing ZZ, You H, Cong M, Jia JD. Hepatitis B virus particles preferably induce Kupffer cells to produce TGF-β1 over pro-inflammatory cytokines. *Dig Liver Dis* 2012; **44**: 328-333 [PMID: 22177317 DOI: 10.1016/j.dld.2011.11.005]
17 **Li M**, Sun R, Xu L, Yin W, Chen Y, Zheng X, Lian Z, Wei H, Tian Z. Kupffer Cells Support Hepatitis B Virus-Mediated CD8+ T Cell Exhaustion *via* Hepatitis B Core Antigen-TLR2 Interactions in Mice. *J Immunol* 2015; **195**: 3100-3109 [PMID: 26304988 DOI: 10.4049/jimmunol.1500839]
18 **Scott CL**, Zheng F, De Baetselier P, Martens L, Saeys Y, De Prijck S, Lippens S, Abels C, Schoonooghe S, Raes G, Devoogdt N, Lambrecht BN, Beschin A, Guilliams M. Bone marrow-derived monocytes give rise to self-renewing and fully differentiated Kupffer cells. *Nat Commun* 2016; **7**: 10321 [PMID: 26813785 DOI: 10.1038/ncomms10321]
19 **Stelma F**, de Niet A, Tempelmans Plat-Sinnige MJ, Jansen L, Takkenberg RB, Reesink HW, Kootstra NA, van Leeuwen EM. Natural Killer Cell Characteristics in Patients With Chronic Hepatitis B Virus (HBV) Infection Are Associated With HBV Surface Antigen Clearance After Combination Treatment With Pegylated Interferon Alfa-2a and Adefovir. *J Infect Dis* 2015; **212**: 1042-1051 [PMID: 25791117 DOI:

10.1093/infdis/jiv180]
20 **Oliviero B**, Varchetta S, Paudice E, Michelone G, Zaramella M, Mavilio D, De Filippi F, Bruno S, Mondelli MU. Natural killer cell functional dichotomy in chronic hepatitis B and chronic hepatitis C virus infections. *Gastroenterology* 2009; **137**: 1151-1160, 1160.e1 [PMID: 19470388 DOI: 10.1053/j.gastro.2009.05.047]
21 **Sun C**, Fu B, Gao Y, Liao X, Sun R, Tian Z, Wei H. TGF-β1 down-regulation of NKG2D/DAP10 and 2B4/SAP expression on human NK cells contributes to HBV persistence. *PLoS Pathog* 2012; **8**: e1002594 [PMID: 22438812 DOI: 10.1371/journal.ppat.1002594]
22 **Li F**, Wei H, Wei H, Gao Y, Xu L, Yin W, Sun R, Tian Z. Blocking the natural killer cell inhibitory receptor NKG2A increases activity of human natural killer cells and clears hepatitis B virus infection in mice. *Gastroenterology* 2013; **144**: 392-401 [PMID: 23103614 DOI: 10.1053/j.gastro.2012.10.039]
23 **Ju Y**, Hou N, Meng J, Wang X, Zhang X, Zhao D, Liu Y, Zhu F, Zhang L, Sun W, Liang X, Gao L, Ma C. T cell immunoglobulin- and mucin-domain-containing molecule-3 (Tim-3) mediates natural killer cell suppression in chronic hepatitis B. *J Hepatol* 2010; **52**: 322-329 [PMID: 20133006 DOI: 10.1016/j.jhep.2009.12.005]
24 **Nandi M**, Pal S, Ghosh S, Chakraborty BC, Dey D, Baidya A, Shil A, Chattopadhyaya S, Banerjee S, Santra A, Chowdhury A, Datta S. CD8(+)CD28(-) T cells: key cytotoxic players impacting disease pathogenesis in chronic HBV infection. *Clin Sci (Lond)* 2019; **133**: 1917-1934 [PMID: 31477625 DOI: 10.1042/CS20190369]
25 **Han W**, Ni Q, Liu K, Yao Y, Zhao D, Liu X, Chen Y. Decreased CD122 on CD56(dim) NK associated with its impairment in asymptomatic chronic HBV carriers with high levels of HBV DNA, HBsAg and HBeAg. *Life Sci* 2018; **195**: 53-60 [PMID: 29307521 DOI: 10.1016/j.lfs.2018.01.001]
26 **Marotel M**, Villard M, Drouillard A, Tout I, Besson L, Allatif O, Pujol M, Rocca Y, Ainouze M, Roblot G, Viel S, Gomez M, Loustaud V, Alain S, Durantel D, Walzer T, Hasan U, Marçais A. Peripheral natural killer cells in chronic hepatitis B patients display multiple molecular features of T cell exhaustion. *Elife* 2021; **10** [PMID: 33507150 DOI: 10.7554/eLife.60095]
27 **Micco L**, Peppa D, Loggi E, Schurich A, Jefferson L, Cursaro C, Panno AM, Bernardi M, Brander C, Bihl F, Andreone P, Maini MK. Differential boosting of innate and adaptive antiviral responses during pegylated-interferon-alpha therapy of chronic hepatitis B. *J Hepatol* 2013; **58**: 225-233 [PMID: 23046671 DOI: 10.1016/j.jhep.2012.09.029]
28 **van der Molen RG**, Sprengers D, Biesta PJ, Kusters JG, Janssen HL. Favorable effect of adefovir on the number and functionality of myeloid dendritic cells of patients with chronic HBV. *Hepatology* 2006; **44**: 907-914 [PMID: 17006907 DOI: 10.1002/hep.21340]
29 **Zhang Z**, Chen D, Yao J, Zhang H, Jin L, Shi M, Zhang H, Wang FS. Increased infiltration of intrahepatic DC subsets closely correlate with viral control and liver injury in immune active pediatric patients with chronic hepatitis B. *Clin Immunol* 2007; **122**: 173-180 [PMID: 17052956 DOI: 10.1016/j.clim.2006.09.006]
30 **Beckebaum S**, Cicinnati VR, Zhang X, Ferencik S, Frilling A, Grosse-Wilde H, Broelsch CE, Gerken G. Hepatitis B virus-induced defect of monocyte-derived dendritic cells leads to impaired T helper type 1 response in vitro: mechanisms for viral immune escape. *Immunology* 2003; **109**: 487-495 [PMID: 12871214 DOI: 10.1046/j.1365-2567.2003.01699.x]
31 **De Pasquale C**, Campana S, Barberi C, Sidoti Migliore G, Oliveri D, Lanza M, Musolino C, Raimondo G, Ferrone S, Pollicino T, Ferlazzo G. Human Hepatitis B Virus Negatively Impacts the Protective Immune Crosstalk Between Natural Killer and Dendritic Cells. *Hepatology* 2021; **74**: 550-565 [PMID: 33482027 DOI: 10.1002/hep.31725]
32 **van der Burg SH**, Arens R, Melief CJ. Immunotherapy for persistent viral infections and associated disease. *Trends Immunol* 2011; **32**: 97-103 [PMID: 21227751 DOI: 10.1016/j.it.2010.12.006]
33 **Maier H**, Isogawa M, Freeman GJ, Chisari FV. PD-1:PD-L1 interactions contribute to the functional suppression of virus-specific CD8+ T lymphocytes in the liver. *J Immunol* 2007; **178**: 2714-2720 [PMID: 17312113 DOI: 10.4049/jimmunol.178.5.2714]
34 **Xu B**, Zhang Z, Shi Y, Chen XY, Wang FS. [PD-1 up-regulation influenced apoptosis of HBV-specific CD8 T cells in patients with acute resolved hepatitis B]. *Zhonghua Yi Xue Za Zhi* 2009; **89**: 1158-1161 [PMID: 19595077 DOI: 10.3760/cma.j.issn.0376-2491.2009.17.003]
35 **Kondo Y**, Kobayashi K, Ueno Y, Shiina M, Niitsuma H, Kanno N, Kobayashi T, Shimosegawa T. Mechanism of T cell hyporesponsiveness to HBcAg is associated with regulatory T cells in chronic hepatitis B. *World J Gastroenterol* 2006; **12**: 4310-4317 [PMID: 16865771 DOI: 10.3748/wjg.v12.i27.4310]
36 **Tinoco R**, Alcalde V, Yang Y, Sauer K, Zuniga EI. Cell-intrinsic transforming growth factor-beta signaling mediates virus-specific CD8+ T cell deletion and viral persistence in vivo. *Immunity* 2009; **31**: 145-157 [PMID: 19604493 DOI: 10.1016/j.immuni.2009.06.015]
37 **Anderson MW**, Reynolds SH, You M, Maronpot RM. Role of proto-oncogene activation in carcinogenesis. *Environ Health Perspect* 1992; **98**: 13-24 [PMID: 1486840 DOI: 10.1289/ehp.929813]
38 **Levine AJ**. p53: 800 million years of evolution and 40 years of discovery. *Nat Rev Cancer* 2020; **20**: 471-480 [PMID: 32404993 DOI: 10.1038/s41568-020-0262-1]
39 **Hassin O**, Oren M. Drugging p53 in cancer: one protein, many targets. *Nat Rev Drug Discov* 2023; **22**: 127-144 [PMID: 36216888 DOI: 10.1038/s41573-022-00571-8]
40 **Suzuki H**, Ito R, Ikeda K, Tamura TA. TATA-binding protein (TBP)-like protein is required for p53-dependent transcriptional activation of upstream promoter of p21Waf1/Cip1 gene. *J Biol Chem* 2012; **287**: 19792-19803 [PMID: 22511763 DOI: 10.1074/jbc.M112.369629]
41 **Kaneto H**, Sasaki S, Yamamoto H, Itoh F, Toyota M, Suzuki H, Ozeki I, Iwata N, Ohmura T, Satoh T, Karino Y, Satoh T, Toyota J, Satoh M, Endo T, Omata M, Imai K. Detection of hypermethylation of the p16(INK4A) gene promoter in chronic hepatitis and cirrhosis associated with hepatitis B or C virus. *Gut* 2001; **48**: 372-377 [PMID: 11171828 DOI: 10.1136/gut.48.3.372]
42 **Zhang YJ**, Ahsan H, Chen Y, Lunn RM, Wang LY, Chen SY, Lee PH, Chen CJ, Santella RM. High frequency of promoter hypermethylation of RASSF1A and p16 and its relationship to aflatoxin B1-DNA adduct levels in human hepatocellular carcinoma. *Mol Carcinog* 2002; **35**: 85-92 [PMID: 12325038 DOI: 10.1002/mc.10076]
43 **Nusse R**. An ancient cluster of Wnt paralogues. *Trends Genet* 2001; **17**: 443 [PMID: 11491115 DOI: 10.1016/s0168-9525(01)02349-6]
44 **Dierick H**, Bejsovec A. Cellular mechanisms of wingless/Wnt signal transduction. *Curr Top Dev Biol* 1999; **43**: 153-190 [PMID: 9891886 DOI: 10.1016/s0070-2153(08)60381-6]
45 **Luis TC**, Ichii M, Brugman MH, Kincade P, Staal FJ. Wnt signaling strength regulates normal hematopoiesis and its deregulation is involved in leukemia development. *Leukemia* 2012; **26**: 414-421 [PMID: 22173215 DOI: 10.1038/leu.2011.387]
46 **Bengochea A**, de Souza MM, Lefrançois L, Le Roux E, Galy O, Chemin I, Kim M, Wands JR, Trepo C, Hainaut P, Scoazec JY, Vitvitski L, Merle P. Common dysregulation of Wnt/Frizzled receptor elements in human hepatocellular carcinoma. *Br J Cancer* 2008; **99**: 143-150 [PMID: 18577996 DOI: 10.1038/sj.bjc.6604422]
47 **Tang B**, Zhang Y, Wang W, Qi G, Shimamoto F. PARP6 suppresses the proliferation and metastasis of hepatocellular carcinoma by degrading

XRCC6 to regulate the Wnt/β-catenin pathway. *Am J Cancer Res* 2020; **10**: 2100-2113 [PMID: 32775003]

48 **Shao J**, Shi CJ, Li Y, Zhang FW, Pan FF, Fu WM, Zhang JF. LincROR Mediates the Suppressive Effects of Curcumin on Hepatocellular Carcinoma Through Inactivating Wnt/β-Catenin Signaling. *Front Pharmacol* 2020; **11**: 847 [PMID: 32714183 DOI: 10.3389/fphar.2020.00847]

49 **Deldar Abad Paskeh M**, Mirzaei S, Ashrafizadeh M, Zarrabi A, Sethi G. Wnt/β-Catenin Signaling as a Driver of Hepatocellular Carcinoma Progression: An Emphasis on Molecular Pathways. *J Hepatocell Carcinoma* 2021; **8**: 1415-1444 [PMID: 34858888 DOI: 10.2147/JHC.S336858]

50 **Cheng WT**, Xu K, Tian DY, Zhang ZG, Liu LJ, Chen Y. Role of Hedgehog signaling pathway in proliferation and invasiveness of hepatocellular carcinoma cells. *Int J Oncol* 2009; **34**: 829-836 [PMID: 19212688 DOI: 10.3892/ijo_00000209]

51 **Zhou XT**, Ding J, Li HY, Zuo JL, Ge SY, Jia HL, Wu J. Hedgehog signalling mediates drug resistance through targeting TAP1 in hepatocellular carcinoma. *J Cell Mol Med* 2020; **24**: 4298-4311 [PMID: 32108992 DOI: 10.1111/jcmm.15090]

52 **He Y**, Huang H, Jin L, Zhang F, Zeng M, Wei L, Tang S, Chen D, Wang W. CircZNF609 enhances hepatocellular carcinoma cell proliferation, metastasis, and stemness by activating the Hedgehog pathway through the regulation of miR-15a-5p/15b-5p and GLI2 expressions. *Cell Death Dis* 2020; **11**: 358 [PMID: 32398664 DOI: 10.1038/s41419-020-2441-0]

53 **Geissler K**, Zach O. Pathways involved in Drosophila and human cancer development: the Notch, Hedgehog, Wingless, Runt, and Trithorax pathway. *Ann Hematol* 2012; **91**: 645-669 [PMID: 22418742 DOI: 10.1007/s00277-012-1435-0]

54 **Yang X**, Liu J, Liang Q, Sun G. Valproic acid reverses sorafenib resistance through inhibiting activated Notch/Akt signaling pathway in hepatocellular carcinoma. *Fundam Clin Pharmacol* 2021; **35**: 690-699 [PMID: 33015852 DOI: 10.1111/fcp.12608]

55 **Ye YC**, Zhao JL, Lu YT, Gao CC, Yang Y, Liang SQ, Lu YY, Wang L, Yue SQ, Dou KF, Qin HY, Han H. NOTCH Signaling *via* WNT Regulates the Proliferation of Alternative, CCR2-Independent Tumor-Associated Macrophages in Hepatocellular Carcinoma. *Cancer Res* 2019; **79**: 4160-4172 [PMID: 31266773 DOI: 10.1158/0008-5472.CAN-18-1691]

56 **Xie Q**, Guo H, He P, Deng H, Gao Y, Dong N, Niu W, Liu T, Li M, Wang S, Wu Y, Li JL. Tspan5 promotes epithelial-mesenchymal transition and tumour metastasis of hepatocellular carcinoma by activating Notch signalling. *Mol Oncol* 2021; **15**: 3184-3202 [PMID: 33955149 DOI: 10.1002/1878-0261.12980]

57 **Cai H**, Zhu XD, Ao JY, Ye BG, Zhang YY, Chai ZT, Wang CH, Shi WK, Cao MQ, Li XL, Sun HC. Colony-stimulating factor-1-induced AIF1 expression in tumor-associated macrophages enhances the progression of hepatocellular carcinoma. *Oncoimmunology* 2017; **6**: e1333213 [PMID: 28932635 DOI: 10.1080/2162402X.2017.1333213]

58 **Cheng K**, Cai N, Zhu J, Yang X, Liang H, Zhang W. Tumor-associated macrophages in liver cancer: From mechanisms to therapy. *Cancer Commun (Lond)* 2022; **42**: 1112-1140 [PMID: 36069342 DOI: 10.1002/cac2.12345]

59 **Chen Y**, Hao X, Sun R, Wei H, Tian Z. Natural Killer Cell-Derived Interferon-Gamma Promotes Hepatocellular Carcinoma Through the Epithelial Cell Adhesion Molecule-Epithelial-to-Mesenchymal Transition Axis in Hepatitis B Virus Transgenic Mice. *Hepatology* 2019; **69**: 1735-1750 [PMID: 30329167 DOI: 10.1002/hep.30317]

60 **Xu D**, Han Q, Hou Z, Zhang C, Zhang J. miR-146a negatively regulates NK cell functions *via* STAT1 signaling. *Cell Mol Immunol* 2017; **14**: 712-720 [PMID: 26996068 DOI: 10.1038/cmi.2015.113]

61 **Zhang J**, Hu C, Xie X, Qi L, Li C, Li S. Immune Checkpoint Inhibitors in HBV-Caused Hepatocellular Carcinoma Therapy. *Vaccines (Basel)* 2023; **11** [PMID: 36992198 DOI: 10.3390/vaccines11030614]

62 **Butte MJ**, Keir ME, Phamduy TB, Sharpe AH, Freeman GJ. Programmed death-1 ligand 1 interacts specifically with the B7-1 costimulatory molecule to inhibit T cell responses. *Immunity* 2007; **27**: 111-122 [PMID: 17629517 DOI: 10.1016/j.immuni.2007.05.016]

63 **Dai X**, Xue J, Hu J, Yang SL, Chen GG, Lai PBS, Yu C, Zeng C, Fang X, Pan X, Zhang T. Positive Expression of Programmed Death Ligand 1 in Peritumoral Liver Tissue is Associated with Poor Survival after Curative Resection of Hepatocellular Carcinoma. *Transl Oncol* 2017; **10**: 511-517 [PMID: 28558264 DOI: 10.1016/j.tranon.2017.03.009]

64 **Rinker F**, Zimmer CL, Höner Zu Siederdissen C, Manns MP, Kraft ARM, Wedemeyer H, Björkström NK, Cornberg M. Hepatitis B virus-specific T cell responses after stopping nucleos(t)ide analogue therapy in HBeAg-negative chronic hepatitis B. *J Hepatol* 2018; **69**: 584-593 [PMID: 29758333 DOI: 10.1016/j.jhep.2018.05.004]

65 **Liu H**, Han CL, Tian BW, Ding ZN, Yang YF, Ma YL, Yang CC, Meng GX, Xue JS, Wang DX, Dong ZR, Chen ZQ, Hong JG, Li T. Tenofovir versus entecavir on the prognosis of hepatitis B virus-related hepatocellular carcinoma: a systematic review and meta-analysis. *Expert Rev Gastroenterol Hepatol* 2023; **17**: 623-633 [PMID: 37148261 DOI: 10.1080/17474124.2023.2212161]

66 **Kim GA**, Lim YS, An J, Lee D, Shim JH, Kim KM, Lee HC, Chung YH, Lee YS, Suh DJ. HBsAg seroclearance after nucleoside analogue therapy in patients with chronic hepatitis B: clinical outcomes and durability. *Gut* 2014; **63**: 1325-1332 [PMID: 24162593 DOI: 10.1136/gutjnl-2013-305517]

67 **Tinè F**, Liberati A, Craxì A, Almasio P, Pagliaro L. Interferon treatment in patients with chronic hepatitis B: a meta-analysis of the published literature. *J Hepatol* 1993; **18**: 154-162 [PMID: 7691924 DOI: 10.1016/s0168-8278(05)80241-7]

68 **Allweiss L**, Giersch K, Pirosu A, Volz T, Muench RC, Beran RK, Urban S, Javanbakht H, Fletcher SP, Lütgehetmann M, Dandri M. Therapeutic shutdown of HBV transcripts promotes reappearance of the SMC5/6 complex and silencing of the viral genome in vivo. *Gut* 2022; **71**: 372-381 [PMID: 33509930 DOI: 10.1136/gutjnl-2020-322571]

69 **Guan G**, Zhang T, Ning J, Tao C, Gao N, Zeng Z, Guo H, Chen CC, Yang J, Zhang J, Gu W, Yang E, Liu R, Guo X, Ren S, Wang L, Wei G, Zheng S, Gao Z, Chen X, Lu F, Chen X. Higher TP53BP2 expression is associated with HBsAg loss in peginterferon-α-treated patients with chronic hepatitis B. *J Hepatol* 2024; **80**: 41-52 [PMID: 37858684 DOI: 10.1016/j.jhep.2023.09.039]

World Journal of Gastrointestinal Oncology

Submit a Manuscript: https://www.f6publishing.com

World J Gastrointest Oncol 2025 January 15; 17(1): 98572

DOI: 10.4251/wjgo.v17.i1.98572

ISSN 1948-5204 (online)

EDITORIAL

TRIPLET combined with microwave ablation: A novel treatment for advanced hepatocellular carcinoma

Fei-Yu Zhao, Guo-Wei Si, Nian-Song Qian

Specialty type: Oncology

Provenance and peer review: Invited article; Externally peer reviewed.

Peer-review model: Single blind

Peer-review report's classification

Scientific Quality: Grade C, Grade D

Novelty: Grade C, Grade C

Creativity or Innovation: Grade B, Grade C

Scientific Significance: Grade B, Grade B

P-Reviewer: Majeed NF

Received: June 29, 2024

Revised: August 21, 2024

Accepted: September 9, 2024

Published online: January 15, 2025

Processing time: 165 Days and 17 Hours

Fei-Yu Zhao, Department of Thoracic Oncology, Respiratory and Critical Care Medicine, The Eighth Medical Center of People's Liberation Army General Hospital, Beijing 100853, China

Guo-Wei Si, Department of Gastroenterology, Fourth Medical Centre, General Hospital of the People's Liberation Army, Beijing 100142, China

Nian-Song Qian, Senior Department of Thoracic Oncology, Respiratory and Critical Care Medicine, The Eighth Medical Center of People's Liberation Army General Hospital, Beijing 100091, China

Corresponding author: Nian-Song Qian, MD, Chief Physician, Senior Department of Thoracic Oncology, Respiratory and Critical Care Medicine, The Eighth Medical Center of People's Liberation Army General Hospital, No. 28 Fuxing Road, Beijing 100091, China. qianniansong1@163.com

Abstract

This editorial comments on a study by Zuo *et al*. The focus is on the efficacy of hepatic arterial infusion chemotherapy combined with camrelizumab and apatinib (the TRIPLET regimen), alongside microwave ablation therapy, in treating advanced hepatocellular carcinoma (HCC). The potential application of this combination therapy for patients with advanced HCC is evaluated.

Key Words: Microwave ablation; Hepatic arterial infusion chemotherapy; Apatinib; Camrelizumab; Hepatocellular carcinoma

Core Tip: This article examines the efficacy of combining microwave ablation with the TRIPLET regimen in patients with advanced hepatocellular carcinoma. While both treatments show promise individually, their combined efficacy and safety require further clinical investigation.

Citation: Zhao FY, Si GW, Qian NS. TRIPLET combined with microwave ablation: A novel treatment for advanced hepatocellular carcinoma. *World J Gastrointest Oncol* 2025; 17(1): 98572
URL: https://www.wjgnet.com/1948-5204/full/v17/i1/98572.htm
DOI: https://dx.doi.org/10.4251/wjgo.v17.i1.98572

INTRODUCTION

Globally, primary liver cancer ranks as the sixth most common cancer diagnosis and the third leading cause of cancer-induced mortality, with hepatocellular carcinoma (HCC) accounting for 75%-80% of these cases[1]. Hepatic arterial infusion chemotherapy (HAIC) employing a combination of oxaliplatin, fluorouracil, and folinic acid (FOLFOX) effectively reduces intrahepatic tumor load by delivering chemotherapeutic agents directly to the arteries supplying the tumor[2]. Camrelizumab, a programmed death receptor 1 inhibitor, has been approved for the treatment of liver cancer [3]. Apatinib, the first highly selective tyrosine kinase inhibitor targeting vascular endothelial growth factor 2 in China, has shown efficacy in patients with advanced HCC[4].

The combination of HAIC with camrelizumab and apatinib, known as the TRIPLET regimen, has demonstrated efficacy in several studies for the treatment of advanced HCC[5]. Additionally, microwave ablation (MWA) is widely used as an effective local treatment for HCC and may potentially eliminate residual lesions after the TRIPLET regimen. However, the therapeutic efficacy of combining the TRIPLET regimen with MWA has yet to be thoroughly investigated.

In this editorial, we review and analyze the study by Zuo *et al*[6], published in the *World Journal of Gastrointestinal Oncology*, which explores this combination treatment.

EFFICACY

In their study, Zuo *et al*[6] divided patients into two groups to assess changes and treatment efficacy through detailed clinical follow-up and imaging data. The patients were categorized into the TRIPLET (T-A) group with 122 cases and the TRIPLET combined with MWA (T-M) group with 95 cases. Two statistical methods were used to make the study more rigorous, but the results were consistent. After a propensity score matchin, the study compared the outcomes of the T-A group with those of the T-M group, yielding the following results.

The objective response rate (ORR) of the T-M group (85.4%) was significantly higher than that of the T-A group (65.9%; $P < 0.001$). The 1-year, 2-year, and 3-year cumulative overall survival (OS) rates of the T-M group were 98.7%, 93.4%, and 82.0% respectively, while those of the T-A group were 85.1%, 63.1%, and 55.0% respectively (HR = 0.22; 95%CI: 0.10-0.49; $P < 0.001$). Safety is also an issue to be focused on. The incidence of major complications in the T-A group was 4.9% (6/122), and that in the T-M group was 5.3% (5/95), with $P = 1.000$, suggesting that there was no significant difference in safety between the T-M and T-A groups. These outcomes indicate that the T-M approach provides better ORR and OS benefits than the T-A regimen.

The therapeutic rationale for the T-M therapy likely stems from the advantages offered by MWA, such as the ability to target larger treatment areas and shorter treatment times[7], which effectively eliminate residual lesions after the TRIPLET regimen in advanced HCC. However, the precise mechanisms behind these benefits are not yet fully understood, necessitating further clinical studies in the future.

SHORTCOMINGS

As the authors themselves acknowledge, the study has a few limitations. First, this was a retrospective study with a small number of patients and a relatively short retrospective follow-up period. This calls for prospective randomized controlled trials to validate the findings. Secondly, the primary cause of HCC in China is hepatitis B virus infection, whereas in Western countries, it is often alcohol consumption. This raises questions about the applicability of the T-M protocol in different geographic and etiologic contexts. It is worth noting that this study addresses MWA and the results may not be generalisable to thermal ablation in general.

Additionally, the study notes that most patients undergoing MWA were under 70 years old. Since many elderly patients may not tolerate MWA well, further research is needed to determine the efficacy of this treatment for older patients with HCC.

Financial considerations also play a crucial role. The TRIPLET regimen combined with MWA is likely to be more costly than the TRIPLET regimen alone. Therefore, it is important to investigate this combined approach while considering financial factors and the varying healthcare policies of different countries.

CONCLUSION

The combination of MWA therapy with the TRIPLET regimen (HAIC with camrelizumab and apatinib) significantly

improves OS. This approach could represent a promising new treatment option for these patients.

FOOTNOTES

Author contributions: Zhao FY wrote this paper; Si GW revised it; Qian NS provided ideas for writing it.

Conflict-of-interest statement: There are no conflicts of interest in this article.

Country of origin: China

ORCID number: Nian-Song Qian 0000-0002-3297-4294.

S-Editor: Lin C
L-Editor: A
P-Editor: Zhao S

REFERENCES

1 **Samant H**, Amiri HS, Zibari GB. Addressing the worldwide hepatocellular carcinoma: epidemiology, prevention and management. *J Gastrointest Oncol* 2021; **12**: S361-S373 [PMID: 34422400 DOI: 10.21037/jgo.2020.02.08]
2 **Ge N**, Wang H, He C, Wang X, Huang J, Yang Y. Optimal interventional treatment for liver cancer: HAIC, TACE or iTACE? *J Interv Med* 2023; **6**: 59-63 [PMID: 37409063 DOI: 10.1016/j.jimed.2023.03.001]
3 **Markham A**, Keam SJ. Camrelizumab: First Global Approval. *Drugs* 2019; **79**: 1355-1361 [PMID: 31313098 DOI: 10.1007/s40265-019-01167-0]
4 **Sun T**, Ren Y, Kan X, Chen L, Zhang W, Yang F, Zheng C. Advanced Hepatocellular Carcinoma With Hepatic Arterioportal Shunts: Combination Treatment of Transarterial Chemoembolization With Apatinib. *Front Mol Biosci* 2020; **7**: 607520 [PMID: 33344507 DOI: 10.3389/fmolb.2020.607520]
5 **Zhang TQ**, Geng ZJ, Zuo MX, Li JB, Huang JH, Huang ZL, Wu PH, Gu YK. Camrelizumab (a PD-1 inhibitor) plus apatinib (an VEGFR-2 inhibitor) and hepatic artery infusion chemotherapy for hepatocellular carcinoma in Barcelona Clinic Liver Cancer stage C (TRIPLET): a phase II study. *Signal Transduct Target Ther* 2023; **8**: 413 [PMID: 37884523 DOI: 10.1038/s41392-023-01663-6]
6 **Zuo MX**, An C, Cao YZ, Pan JY, Xie LP, Yang XJ, Li W, Wu PH. Camrelizumab, apatinib and hepatic artery infusion chemotherapy combined with microwave ablation for advanced hepatocellular carcinoma. *World J Gastrointest Oncol* 2024; **16**: 3481-3495 [PMID: 39171171 DOI: 10.4251/wjgo.v16.i8.3481]
7 **Izzo F**, Granata V, Grassi R, Fusco R, Palaia R, Delrio P, Carrafiello G, Azoulay D, Petrillo A, Curley SA. Radiofrequency Ablation and Microwave Ablation in Liver Tumors: An Update. *Oncologist* 2019; **24**: e990-e1005 [PMID: 31217342 DOI: 10.1634/theoncologist.2018-0337]

World Journal of Gastrointestinal Oncology

Submit a Manuscript: https://www.f6publishing.com

World J Gastrointest Oncol 2025 January 15; 17(1): 98872

DOI: 10.4251/wjgo.v17.i1.98872

ISSN 1948-5204 (online)

EDITORIAL

Characteristics of gut microbiota dysbiosis in patients with colorectal polyps

Xian-Rong Wu, Xiao-Hong He, Yong-Fang Xie

Specialty type: Oncology

Provenance and peer review: Invited article; Externally peer reviewed.

Peer-review model: Single blind

Peer-review report's classification

Scientific Quality: Grade B, Grade C

Novelty: Grade B, Grade B

Creativity or Innovation: Grade B, Grade B

Scientific Significance: Grade B, Grade B

P-Reviewer: Wang XX; Zhao K

Received: July 9, 2024

Revised: September 5, 2024

Accepted: September 19, 2024

Published online: January 15, 2025

Processing time: 156 Days and 5.7 Hours

Xian-Rong Wu, Xiao-Hong He, Yong-Fang Xie, School of Life Health Information Science and Engineering, Chongqing Post and Communications University, Chongqing 400065, China

Co-first authors: Xian-Rong Wu and Xiao-Hong He.

Corresponding author: Yong-Fang Xie, MD, Doctor, School of Life Health Information Science and Engineering, Chongqing Post and Communications University, No. 2 Chongwen Road, Nanan District, Chongqing 400065, China. xyf1688@126.com

Abstract

This editorial, inspired by a recent study published in the *World Journal of Gastrointestinal Oncology*, covers the research findings on microbiota changes in various diseases. In recurrent colorectal polyps, the abundances of *Klebsiella*, *Parvimonas*, and *Clostridium* increase, while those of *Bifidobacterium* and *Lactobacillus* decrease. This dysbiosis may promote the formation and recurrence of polyps. Similar microbial changes have also been observed in colorectal cancer, inflammatory bowel disease, autism spectrum disorder, and metabolic syndrome, indicating the role of increased pathogens and decreased probiotics in these conditions. Regulating the gut microbiota, particularly by increasing probiotic levels, may help prevent polyp recurrence and promote gut health. This microbial intervention strategy holds promise as an adjunctive treatment for patients with colorectal polyps.

Key Words: Recurrent colorectal polyps; Gut microbiota dysbiosis; Klebsiella; Probiotics; Intestinal inflammation; Microbial intervention strategy

Core Tip: This review addresses gut microbiota dysbiosis in patients with recurrent colorectal polyps, noting increased levels of *Klebsiella, Parvimonas,* and *Clostridium* and decreased levels of *Bifidobacterium* and *Lactobacillus*. This dysbiosis may promote polyp formation and recurrence by creating an inflammatory gut environment. A reduction in probiotics weakens intestinal barrier function, while an increase in pathogens further degrades the gut through their metabolic products and toxins. These changes are also observed in colorectal cancer, inflammatory bowel disease, autism spectrum disorder, and metabolic syndrome. Regulating the gut microbiota, particularly by increasing the use of probiotics, may restore gut health and prevent polyp recurrence. Future research should explore specific mechanisms and evaluate long-term effects.

Citation: Wu XR, He XH, Xie YF. Characteristics of gut microbiota dysbiosis in patients with colorectal polyps. *World J Gastrointest Oncol* 2025; 17(1): 98872
URL: https://www.wjgnet.com/1948-5204/full/v17/i1/98872.htm
DOI: https://dx.doi.org/10.4251/wjgo.v17.i1.98872

INTRODUCTION

Recurrent colorectal polyps are a key precursor to the development of colorectal cancer, the second leading cause of cancer-related deaths worldwide[1]. Adenomatous polyps (APs) are the most common precancerous lesions of colorectal cancer, with a recurrence rate of 20%–50%[2]. Studies have shown that gut microbiota dysbiosis plays an important role in the formation and recurrence of polyps[3]. Dysbiosis is characterized by a decrease in beneficial bacteria such as *Bifidobacterium* and *Lactobacillus* and an increase in pathogenic bacteria such as *Klebsiella*, *Sutterella*, and *Cronobacter*[4]. This increase in pathogenic bacteria may promote the formation and recurrence of polyps by fostering an inflammatory environment in the gut[5]. Additionally, changes in the gut microbiota are associated not only with polyp recurrence but also with colorectal cancer, inflammatory bowel disease (IBD), autism spectrum disorder (ASD), and metabolic syndrome [6]. Regulating the gut microbiota, particularly by increasing the levels of probiotics and reducing the abundance of pathogenic bacteria, may help prevent polyp recurrence and promote gut health[7]. This microbial intervention strategy holds promise as an adjunctive treatment for patients with colorectal polyps, and further research will help determine its efficacy and underlying mechanisms[8].

MICROBIOTA CHANGES IN DIFFERENT DISEASES

The formation of recurrent colorectal polyps is closely related to intestinal dysbiosis, which involves not only changes in the composition of the gut microbiota but also alterations in metabolic products and the significance of the gut under physiological and pathological conditions. The gut plays a critical role in maintaining overall health, with its barrier function, immune regulation, metabolic activities, and connections to neurological and psychological health exerting significant influence under both normal and pathological states[9]. The physical barrier formed by intestinal epithelial cells and the mucosal immune system represents the first line of defense against pathogenic invasion and maintains systemic homeostasis. When intestinal barrier function is compromised, as observed in IBD, increased intestinal permeability may trigger systemic inflammation, exacerbating disease progression[10]. Moreover, the gut microbiota plays a key role in host metabolism and immune regulation, with the production of short-chain fatty acids (SCFAs) providing energy to the intestinal epithelium, exerting anti-inflammatory effects, and protecting the barrier[11]. Certain probiotics, such as *Bifidobacterium* and *Lactobacillus*, can inhibit inflammatory responses and maintain immune homeostasis in the gut by modulating the T-cell balance[12]. Furthermore, the bidirectional communication between the gut and brain, known as the gut-brain axis, highlights the impact of the gut microbiota on neurological and psychological health. For example, dysbiosis observed in patients with ASD may affect behavior and cognitive function through the gut-brain axis[13]. Patients with metabolic syndrome exhibit significant changes in the gut microbiota, such as a decrease in beneficial bacteria and an increase in pathogenic bacteria, which are closely associated with insulin resistance and lipid metabolism abnormalities[14]. Similar dysbiosis plays a crucial role in diseases such as obesity and colorectal cancer, affecting energy metabolism and the inflammatory status[15]. Research suggests that certain pathogenic bacteria, such as *Escherichia coli* and *Klebsiella*, can produce genotoxic substances that promote the development of colorectal cancer[16]. Modulating the gut microbiota, particularly by increasing the use of probiotics and prebiotics, may have potential in the prevention and treatment of colorectal cancer and other related diseases[17]. The impact of gut dysbiosis extends beyond individual gut health and may influence overall systemic health through complex biochemical pathways, which is particularly evident in the pathological process of colorectal polyps and their recurrence[18]. Therefore, further exploration of changes in the gut microbiota in various diseases not only aids in understanding the pathogenesis of these conditions but also provides new directions for clinical interventions. Studies have shown that the following bacterial groups are significantly associated with recurrent colorectal polyps: *Klebsiella*, *Sutterella*, *Cronobacter*, *Bifidobacterium*, and *Lactobacillus*. *Klebsiella* is a gram-negative bacterium that is commonly associated with intestinal infections and antibiotic resistance. In patients with non APs or APs, the abundance of this bacterium is significantly increased, which may be one of the key factors in gut microbiota dysbiosis. These findings suggest that Klebsiella plays a potential role in the formation and recurrence of polyps[19]. *Sutterella* is also a gram-negative bacterium associated with intestinal inflammation and

diseases. Studies have shown that the abundance of this bacterium is significantly greater in polyp patients than in healthy individuals, especially in patients with recurrent polyps. These findings indicate that *Sutterella* may play a role in polyp recurrence by promoting the formation of an inflammatory environment in the gut, further supporting this conclusion[20]. *Cronobacter* is another gram-negative bacterium that is known to be associated with foodborne diseases and infections. In polyp patients, particularly those with Aps, the abundance of *Cronobacter* is significantly increased. The increase in this bacterium may be related to the formation and development of polyps, suggesting its role in gut microbiota dysbiosis[21]. *Bifidobacterium* and *Lactobacillus* are two common probiotics that are generally beneficial for gut health. However, in all types of polyp patients, the levels of these two probiotics are reduced. The decrease in *Bifidobacterium* levels may be associated with the formation and recurrence of polyps, while the reduction in *Lactobacillus* further supports the role of gut microbiota dysbiosis in polyp formation[22]. A decrease in probiotic levels may weaken intestinal barrier function and increase gut inflammation, thereby promoting the formation and recurrence of polyps. These bacterial groups are closely related to gut microbiota dysbiosis and recurrent colorectal polyps. Increasing the levels of probiotics and targeting specific pathogenic bacteria may help prevent polyp recurrence and promote gut health. In addition, these bacterial groups are closely related to other diseases in the body. Table 1 below details the changes in the microbiota in different diseases[23-27].

Colorectal cancer

Colorectal cancer is a common malignant tumor, with symptoms including abdominal pain, bloody stools, weight loss, and bowel dysfunction. Changes in the microbiota are characterized by a decrease in the abundance of probiotics such as *Bifidobacterium* and *Lactobacillus* and an increase in the abundance of pathogenic bacteria such as *Klebsiella*, *Sutterella*, and *Cronobacter*[28]. This dysbiosis may promote intestinal inflammation and the development and progression of cancer.

IBD

IBD includes Crohn's disease and ulcerative colitis, characterized by chronic intestinal inflammation. Symptoms include abdominal pain, diarrhea, weight loss, and fatigue. Studies have shown that the levels of *Bifidobacterium* and *Lactobacillus* decrease in IBD patients, while the levels of *Klebsiella*, *Sutterella*, and *Cronobacter* increase. These changes in the microbiota may lead to weakened intestinal barrier function and persistent inflammation[29].

ASD

ASD is a neurodevelopmental disorder characterized by impaired social communication, repetitive behaviors, and restricted interests. The gut microbiota of individuals with autism shows a decrease in *Bifidobacterium* and *Lactobacillus* and an increase in *Klebsiella*, *Sutterella*, and *Cronobacter*. These changes may be associated with intestinal dysfunction and systemic inflammation[30].

Metabolic syndrome

Metabolic syndrome includes hypertension, high blood sugar, excess abdominal fat, and abnormal cholesterol or triglyceride levels, increasing the risk of heart disease, stroke, and diabetes. In patients with metabolic syndrome, the levels of *Bifidobacterium* and *Lactobacillus* decrease, while the levels of *Klebsiella*, *Sutterella*, and *Cronobacter* increase. This dysbiosis may lead to increased intestinal permeability and systemic inflammation[31].

MICROBIOTA CHANGES IN DIFFERENT TYPES OF POLYPS

Studies have shown that changes in the gut microbiota in different diseases significantly impact health. In patients with colorectal cancer, the abundances of *Klebsiella*, *Sutterella*, and *Cronobacter* significantly increase, while those of *Bifidobacterium* and *Lactobacillus* significantly decrease[32]. This dysbiosis pattern is also observed in patients with IBD and ASD [33]. These changes suggest that the increase in pathogenic bacteria and the decrease in probiotics may promote intestinal inflammation and disease progression. Specifically, in colorectal polyps, there are significant differences in the gut microbiota composition between polyp patients and healthy individuals. The levels of *Bifidobacterium* and *Lactobacillus* are relatively higher and the levels of *Klebsiella, Sutterella*, and *Cronobacter* are relatively lower in the gut of healthy individuals, helping to maintain intestinal balance and health[34]. In contrast, the levels of *Bifidobacterium* and *Lactobacillus* are significantly lower, while the levels of *Klebsiella, Sutterella,* and *Cronobacter* are significantly higher in the gut of healthy individuals. This dysbiosis may deteriorate the intestinal environment, promoting the formation and development of polyps[35]. Even in patients who have previously had adenomas but currently have no adenomas, their gut microbiota has not fully returned to normal, showing changes similar to those in non adenomatous and APs patients. These findings suggest that targeted regulation of the gut microbiota, particularly by increasing probiotic levels and reducing the abundance of pathogenic bacteria, may help prevent polyp recurrence and promote gut health. Further studies also indicate that dysbiosis is reflected not only in the composition of the microbiota but also in the levels of metabolites. Changes in metabolites in patients with colorectal polyps include a decrease in SCFAs, such as butyrate and propionate, and an increase in amine metabolites and bile acids, which may further promote inflammation and the development of polyps. Table 2 provides a detailed description of the microbiota changes in patients with different types of colorectal polyps and healthy individuals. In healthy individuals, the gut contains high levels of probiotics (such as *Bifidobacterium* and *Lactobacillus*) and low levels of pathogenic bacteria. This balance helps maintain gut health and immune function. However, in non APs patients, probiotic levels significantly decrease, while pathogenic bacteria, especially *Klebsiella, Sutterella,* and *Cronobacter*, increase. The increase in these pathogenic bacteria may be associated with

Table 1 Relationship between gut microbiota and colorectal polyps

Disease/microbiota	*Bifidobacterium*	*Lactobacillus*	*Klebsiella*	*Sutterella*	*Cronobacter*	Ref.
Colorectal cancer	Decrease	Decrease	Increase	Increase	Increase	[23,24]
Inflammatory bowel disease	Decrease	Decrease	Increase	Increase	Increase	[25]
Autism spectrum disorder	Decrease	Decrease	Increase	Increase	Increase	[26]
Metabolic syndrome	Decrease	Decrease	Increase	Increase	Increase	[27]

Table 2 Changes in microbiota in patients with different types of colorectal polyps and healthy individuals

Microbiota/disease state	Healthy individuals	Non-adenomatous polyp patients	Adenomatous polyp patients	Previous adenoma patients (currently no adenoma)	Ref.
Bifidobacterium	High	Decreased	Decreased	Decreased	[36]
Lactobacillus	High	Decreased	Decreased	Decreased	[37]
Klebsiella	Low	Increased	Increased	Increased	[38]
Sutterella	Low	Increased	Increased	Increased	[39]
Cronobacter	Low	Increased	Increased	Increased	[40]

intestinal inflammation and polyp formation[36-41]. The situation in APs patients is similar to that in non APs patients, with a significant reduction in probiotic levels and an increase in pathogenic bacteria. This dysbiosis is considered an important factor in the formation and development of adenomas[42]. Studies have shown that the gut microbiota also shows similar characteristics in patients who have previously had adenomas, with decreased probiotics and increased pathogenic bacteria[43]. These changes indicate that gut microbiota dysbiosis is a significant risk factor for colorectal polyps, especially recurrent APs. Restoring probiotic levels and targeting specific pathogenic bacteria may become important strategies for preventing polyp recurrence[42,43]. By regulating the gut microbiota, particularly by increasing the abundance of probiotics such as *Bifidobacterium* and *Lactobacillus*, it is possible to help restore normal gut function, reduce inflammation, and thus lower the recurrence rate of polyps[44]. This microbial intervention strategy holds promise as an adjunctive treatment for patients with colorectal polyps, and further research will help determine its efficacy and underlying mechanisms[41]. Studies have shown that different plant extracts have significant effects on regulating the gut microbiota. The extract of Salvia miltiorrhiza improves gut microbiota dysbiosis in hypertensive rats induced by a high-salt diet by regulating the Th17/Treg cell balance, significantly increasing the proportion of beneficial bacteria such as Prevotellaceae[45]. Huanglian-derived polysaccharides increase the growth of beneficial bacteria and the concentration of SCFAs, especially butyric acid, in a high-fat diet/streptozotocin-induced type 2 diabetes mouse model [46]. Phyllostachys nigra polysaccharides significantly improve the gut microbiota structure and reduce insulin resistance by regulating glucose and lipid metabolism in diabetic mice[47]. Phyllanthus emblica extract significantly alters the gut microbiota structure in high-fat diet-induced hyperlipidemic mice, increasing the proportion of specific probiotics, such as *Akkermansia* and *Bacteroides*, while reducing harmful bacteria and lowering SCFA levels[48]. These findings suggest that by balancing the gut microbiota, the symptoms of related diseases can be effectively improved, indicating potential therapeutic effects on gut microbiota dysbiosis in patients with colorectal polyps.

METABOLITE CHANGES

Studies have shown that gut microbiota dysbiosis manifests not only in microbial composition but also in significant differences in metabolite levels. Changes in metabolites in colorectal polyp patients are particularly prominent and involve key metabolites such as SCFAs, vitamin synthesis metabolites, bile acids, and amine metabolites. Specifically, in the gut of healthy individuals, the levels of SCFAs such as butyrate and propionate are high, and these metabolites play important roles in maintaining gut health and reducing inflammation. However, in non APs and APs patients, the levels of butyrate and propionate significantly decrease, indicating weakened anti-inflammatory and barrier functions of the gut [49-51]. Additionally, the levels of bile acids such as deoxycholic acid significantly increase in polyp patients, further promoting the formation of an inflammatory environment in the gut. This change is particularly evident in APs patients. In contrast, patients who previously had adenomas but currently have no adenomas have partially restored normal metabolite levels, but their bile acid and amine metabolite levels are still higher than those of healthy individuals, suggesting long-term effects of dysbiosis[49-51]. Amine metabolites such as cadaverine and histamine also increase in polyp patients, further exacerbating the pathological state of the gut[52]. In summary, these changes in metabolites not only deepen our understanding of the role of gut microbiota dysbiosis in polyp formation but also provide new directions for future prevention and treatment strategies. The following table details the changes in metabolites in patients with different types of colorectal polyps and in healthy individuals. These changes indicate that dysbiosis is reflected not only

in the composition of the microbiota but also in significant differences in metabolite levels. Changes in metabolites in colorectal polyp patients include decreases in SCFAs such as butyrate and propionate and increases in amine metabolites and bile acids. These changes may further promote inflammation and the development of polyps. Specifically, butyrate and propionate levels are increased in healthy individuals. Table 3 provides a detailed description of the metabolite changes in patients with different types of colorectal polyps and healthy individuals. These changes indicate that dysbiosis is reflected not only in the composition of the microbiota but also in significant differences in metabolite levels. Changes in metabolites in colorectal polyp patients include decreases in SCFAs such as butyrate and propionate and increases in amine metabolites and bile acids. These changes may further promote inflammation and the development of polyps. Specifically, butyrate and propionate levels are increased in healthy individuals, and these metabolites help maintain gut health and reduce inflammation[53-56]. However, in non APs and APs patients, butyrate and propionate levels are significantly decreased, indicating a weakened intestinal barrier function and anti-inflammatory capacity[57, 58]. Additionally, the levels of deoxycholic acid and amine metabolites in these patients increase, further exacerbating intestinal inflammation and the development of polyps[59]. Even in patients who previously had adenomas but currently have no adenomas, their metabolite levels have not fully returned to normal, showing changes similar to those in non adenomatous and APs patients. These findings suggest that the impact of dysbiosis may be long-term and that restoring normal microbiota and metabolite levels may require more time[60]. Overall, these findings emphasize the importance of targeted regulation of the gut microbiota and metabolites. Increasing the levels of probiotics such as *Bifidobacterium* and *Lactobacillus*, reducing the abundance of pathogenic bacteria such as *Klebsiella, Sutterella,* and *Cronobacter*, and restoring the levels of SCFAs while reducing harmful metabolites may help prevent the recurrence of colorectal polyps and promote overall gut health.

This study investigated the characteristics of gut microbiota dysbiosis in patients with recurrent colorectal polyps and further analyzed the broad impact of this dysbiosis on other systemic diseases. The results demonstrate that the gut microbiota plays a crucial role in host health and the development of various diseases. Specifically, gut dysbiosis is not only significant in digestive system diseases but also has far-reaching effects on multiple conditions, including ASD, metabolic syndrome, and neurodegenerative diseases. These findings provide new perspectives on the relationship between the gut microbiota and various diseases and offer important references for future clinical treatment strategies. In patients with recurrent colorectal polyps, gut dysbiosis is characterized by a significant increase in pathogenic bacteria abundance and a marked decrease in probiotic levels. This dysbiosis may promote the formation and recurrence of polyps through multiple mechanisms. The overgrowth of pathogenic bacteria, such as *Klebsiella* and *Clostridium* species, can disrupt intestinal barrier function, leading to local inflammatory responses. This inflammatory response not only directly damages intestinal epithelial cells but also promotes polyp growth and increases the risk of carcinogenesis by inducing a chronic inflammatory environment[61,62]. Additionally, the metabolic products of the gut microbiota play crucial roles in regulating the tumor microenvironment. For example, SCFAs produced by certain pathogenic bacteria can regulate host immune responses and directly participate in polyp formation and progression by influencing gene expression in intestinal epithelial cells[63]. However, the impact of gut dysbiosis extends far beyond colorectal polyps or other digestive system diseases. In recent years, increasing research has revealed the central role of the gut microbiota in various systemic diseases. Particularly in ASD, patients often exhibit significant gut microbiota dysbiosis, which is closely related to their neurobehavioral abnormalities. Patients with ASD exhibit a significantly reduced gut microbiota diversity, a general decrease in probiotic levels, and an increased abundance of potential pathogens such as *Clostridium* and *Bacteroides species*. This dysbiosis is not only associated with digestive system symptoms but may also affect central nervous system function through the "gut-brain axis", contributing to the core symptoms of ASD, such as social deficits and behavioral abnormalities[64,65]. Specifically, studies suggest that a reduction in SCFA levels in ASD patients may exacerbate neuroinflammation, which is a significant factor leading to cognitive impairment in these patients[66]. In metabolic syndrome, the impact of gut dysbiosis is profound. Metabolic syndrome involves obesity, diabetes, and cardiovascular diseases, and it has a complex pathogenesis. Research shows that the ratio of *Firmicutes* to *Bacteroidetes* is significantly imbalanced in the gut of obese patients, leading to increased energy intake efficiency and fat storage[67]. This dysbiosis may also trigger systemic inflammatory responses by increasing intestinal permeability, further exacerbating the symptoms of metabolic syndrome[68]. Even with lifestyle interventions such as dietary control or exercise, these gut microbiota characteristics may persist long-term in patients, indicating the long-term role of the gut microbiota in metabolic syndrome[69]. The role of gut dysbiosis in neurodegenerative diseases has also garnered significant attention in recent years. Patients with Alzheimer's disease and Parkinson's disease exhibit significantly reduced gut microbiota diversity, along with the proliferation of pathogenic bacteria and a decrease in probiotics. Gut dysbiosis may affect central nervous system health through multiple pathways. It may disrupt the blood-brain barrier, increasing the likelihood of harmful metabolites such as lipopolysaccharides entering the brain, thereby triggering neuroinflammation[70,71]. Chronic inflammation in the gut caused by dysbiosis may further affect brain neuron function through systemic circulation, ultimately exacerbating the progression of neurodegenerative diseases[72]. These findings underscore the central role of the gut microbiota in host health. Gut dysbiosis not only affects the digestive system but also influences overall health through complex biochemical signaling pathways. The chronic inflammation and metabolic disorders triggered by gut dysbiosis not only exacerbate disease progression but also may play a critical role in the early stages of disease onset. Therefore, targeted interventions that modulate the gut microbiota, such as probiotic supplementation, prebiotic application, or fecal microbiota transplantation, may offer new strategies for preventing and treating various diseases. However, the long-term effects and safety of these interventions need to be validated through larger-scale clinical studies.

Table 3 Metabolite changes in patients with different types of colorectal polyps and healthy individuals

Metabolites/disease state	Healthy individuals	Non-adenomatous polyp patients	Adenomatous polyp patients	Previous adenoma patients (currently no adenoma)	Ref.
SCFAs					
Butyrate	High	Significantly decreased	Significantly decreased	Restored to near normal levels, but lower than healthy individuals	[53]
Propionate	High	decreased	Decreased	Partially restored, but still lower than healthy individuals	[53]
Vitamin synthesis metabolites					
Vitamin B complex	High	No significant change	No significant change	No significant change	[54]
Bile acids					
Deoxycholic acid	Normal levels	Increased	Significantly Increased	Partially restored, but still higher than healthy individuals	[55]
Amine metabolites					
Cadaverine, histamine	Normal levels	No significant change	Increased	Decreased, but still higher than healthy individuals	[56]

SCFAs: Short-chain fatty acids.

CONCLUSION

Studies have shown that gut microbiota dysbiosis is a significant characteristic in patients with recurrent colorectal polyps. Specifically, the abundances of *Klebsiella, Sutterella*, and *Cronobacter* increase, while those of *Bifidobacterium* and *Lactobacillus* significantly decrease. This dysbiosis may promote the formation and recurrence of polyps by fostering an inflammatory environment in the gut. In the gut of colorectal polyp patients, a reduction in probiotics such as *Bifidobacterium* and *Lactobacillus* weakens intestinal barrier function, leading to increased inflammatory responses in the gut. Conversely, the increase in pathogenic bacteria such as *Klebsiella, Sutterella*, and *Cronobacter* may further deteriorate the gut environment through their metabolic products and toxic factors, promoting the growth and recurrence of polyps. Similar changes in the microbiota have also been observed in patients with colorectal cancer, IBD, ASD, and metabolic syndrome. The increase in pathogenic bacteria and decrease in probiotics in these diseases further support the important role of dysbiosis in disease progression. Specifically, *Klebsiella* is associated with intestinal infections and antibiotic resistance, *Sutterella* is closely linked to intestinal inflammation and diseases, and *Cronobacter* is known to be associated with foodborne diseases and infections. Future research should further explore the specific mechanisms of the gut microbiota and metabolites, develop personalized microbial intervention plans, and evaluate the long-term effects of gut microbiota regulation on the prevention of polyp recurrence. These studies will provide more effective prevention and treatment strategies for clinical practice and will further advance the treatment of colorectal polyps and related diseases. Regulating the gut microbiota, particularly by increasing the levels of probiotics such as *Bifidobacterium* and *Lactobacillus*, may help restore gut health and prevent the recurrence of polyps. This microbial intervention strategy holds potential not only for patients with colorectal polyps but also for the treatment of other related diseases. In summary, regulating the gut microbiota and restoring a healthy balance are key strategies for the prevention and treatment of colorectal polyps and related diseases.

FOOTNOTES

Author contributions: Wu XR, He XH compiled and drafted the literature review, and proposed the overall framework of the article; contributed to assisted in the literature review, provided critical academic insights and analysis, and made significant revisions to the article; Xie YF oversaw the overall direction of the article, reviewed and revised various sections, ensuring the accuracy and completeness of the academic content.

Conflict-of-interest statement: The authors declare no potential conflict of interests.

Country of origin: China

ORCID number: Yong-Fang Xie 0000-0002-8210-5732.

S-Editor: Liu H
L-Editor: A
P-Editor: Zhang XD

REFERENCES

1 **Yin LL**, Qi PQ, Hu YF, Fu XJ, He RS, Wang MM, Deng YJ, Xiong SY, Yu QW, Hu JP, Zhou L, Zhou ZB, Xiong Y, Deng H. Dysbiosis promotes recurrence of adenomatous polyps in the distal colorectum. *World J Gastrointest Oncol* 2024; **16**: 3600-3623 [PMID: 39171160 DOI: 10.4251/wjgo.v16.i8.3600]
2 **Lynch JP**, Chimungu JG, Brown KM. Root anatomical phenes associated with water acquisition from drying soil: targets for crop improvement. *J Exp Bot* 2014; **65**: 6155-6166 [PMID: 24759880 DOI: 10.1093/jxb/eru162]
3 **Bruno RM**, Taddei S. Renal denervation: a blunt weapon against isolated systolic hypertension? *Eur Heart J* 2017; **38**: 101-103 [PMID: 27694190 DOI: 10.1093/eurheartj/ehw460]
4 **Ahn J**, Sinha R, Pei Z, Dominianni C, Wu J, Shi J, Goedert JJ, Hayes RB, Yang L. Human gut microbiome and risk for colorectal cancer. *J Natl Cancer Inst* 2013; **105**: 1907-1911 [PMID: 24316595 DOI: 10.1093/jnci/djt300]
5 **Gruszczyk J**, Kanjee U, Chan LJ, Menant S, Malleret B, Lim NTY, Schmidt CQ, Mok YF, Lin KM, Pearson RD, Rangel G, Smith BJ, Call MJ, Weekes MP, Griffin MDW, Murphy JM, Abraham J, Sriprawat K, Menezes MJ, Ferreira MU, Russell B, Renia L, Duraisingh MT, Tham WH. Transferrin receptor 1 is a reticulocyte-specific receptor for Plasmodium vivax. *Science* 2018; **359**: 48-55 [PMID: 29302006 DOI: 10.1126/science.aan1078]
6 **Zhang JJ**, Su H, Zhang L, Liao BS, Xiao SM, Dong LL, Hu ZG, Wang P, Li XW, Huang ZH, Gao ZM, Zhang LJ, Shen L, Cheng RY, Xu J, Chen SL. Comprehensive Characterization for Ginsenosides Biosynthesis in Ginseng Root by Integration Analysis of Chemical and Transcriptome. *Molecules* 2017; **22** [PMID: 28561788 DOI: 10.3390/molecules22060889]
7 **See RM**, Teo YN, Teo YH, Syn NL, Yip ASY, Leong S, Wee CF, Cheong AJY, Lee CH, Chan MY, Yeo TC, Wong RCC, Chang P, Hong CC, Chai P, Sia CH. Effects of Sodium-Glucose Cotransporter 2 on Amputation Events: A Systematic Review and Meta-Analysis of Randomized-Controlled Trials. *Pharmacology* 2022; **107**: 123-130 [PMID: 34942623 DOI: 10.1159/000520903]
8 **Arthur JC**, Perez-Chanona E, Mühlbauer M, Tomkovich S, Uronis JM, Fan TJ, Campbell BJ, Abujamel T, Dogan B, Rogers AB, Rhodes JM, Stintzi A, Simpson KW, Hansen JJ, Keku TO, Fodor AA, Jobin C. Intestinal inflammation targets cancer-inducing activity of the microbiota. *Science* 2012; **338**: 120-123 [PMID: 22903521 DOI: 10.1126/science.1224820]
9 **Kraemer WJ**, Ratamess NA, Nindl BC. Recovery responses of testosterone, growth hormone, and IGF-1 after resistance exercise. *J Appl Physiol (1985)* 2017; **122**: 549-558 [PMID: 27856715 DOI: 10.1152/japplphysiol.00599.2016]
10 **Brandwein-Gensler M**, Siegal GP. Striking pathology gold: a singular experience with daily reverberations: sinonasal hemangiopericytoma (glomangiopericytoma) and oncogenic osteomalacia. *Head Neck Pathol* 2012; **6**: 64-74 [PMID: 22430770 DOI: 10.1007/s12105-012-0337-8]
11 **Flint HJ**, Scott KP, Duncan SH, Louis P, Forano E. Microbial degradation of complex carbohydrates in the gut. *Gut Microbes* 2012; **3**: 289-306 [PMID: 22572875 DOI: 10.4161/gmic.19897]
12 **Rooks MG**, Garrett WS. Gut microbiota, metabolites and host immunity. *Nat Rev Immunol* 2016; **16**: 341-352 [PMID: 27231050 DOI: 10.1038/nri.2016.42]
13 **Cryan JF**, Dinan TG. Mind-altering microorganisms: the impact of the gut microbiota on brain and behaviour. *Nat Rev Neurosci* 2012; **13**: 701-712 [PMID: 22968153 DOI: 10.1038/nrn3346]
14 **Le Chatelier E**, Nielsen T, Qin J, Prifti E, Hildebrand F, Falony G, Almeida M, Arumugam M, Batto JM, Kennedy S, Leonard P, Li J, Burgdorf K, Grarup N, Jørgensen T, Brandslund I, Nielsen HB, Juncker AS, Bertalan M, Levenez F, Pons N, Rasmussen S, Sunagawa S, Tap J, Tims S, Zoetendal EG, Brunak S, Clément K, Doré J, Kleerebezem M, Kristiansen K, Renault P, Sicheritz-Ponten T, de Vos WM, Zucker JD, Raes J, Hansen T; MetaHIT consortium, Bork P, Wang J, Ehrlich SD, Pedersen O. Richness of human gut microbiome correlates with metabolic markers. *Nature* 2013; **500**: 541-546 [PMID: 23985870 DOI: 10.1038/nature12506]
15 **Huo RX**, Wang YJ, Hou SB, Wang W, Zhang CZ, Wan XH. Gut mucosal microbiota profiles linked to colorectal cancer recurrence. *World J Gastroenterol* 2022; **28**: 1946-1964 [PMID: 35664963 DOI: 10.3748/wjg.v28.i18.1946]
16 **Schwabe RF**, Jobin C. The microbiome and cancer. *Nat Rev Cancer* 2013; **13**: 800-812 [PMID: 24132111 DOI: 10.1038/nrc3610]
17 **Mutukula N**, Elkabetz Y. "Neural Killer" Cells: Autologous Cytotoxic Neural Stem Cells for Fighting Glioma. *Cell Stem Cell* 2017; **20**: 426-428 [PMID: 28388425 DOI: 10.1016/j.stem.2017.03.019]
18 **Garcia-Martin I**, Penketh RJA, Garay SM, Jones RE, Grimstead JW, Baird DM, John RM. Symptoms of Prenatal Depression Associated with Shorter Telomeres in Female Placenta. *Int J Mol Sci* 2021; **22** [PMID: 34299077 DOI: 10.3390/ijms22147458]
19 **Jaba Deva Krupa A**, Dhanalakshmi S, R K. An improved parallel sub-filter adaptive noise canceler for the extraction of fetal ECG. *Biomed Tech (Berl)* 2021; **66**: 503-514 [PMID: 33946135 DOI: 10.1515/bmt-2020-0313]
20 **Sibanda A**, Carnes D, Visentin D, Cleary M. A systematic review of the use of music interventions to improve outcomes for patients undergoing hip or knee surgery. *J Adv Nurs* 2019; **75**: 502-516 [PMID: 30230564 DOI: 10.1111/jan.13860]
21 **Anwar S**, Nasrullah M, Hosen MJ. COVID-19 and Bangladesh: Challenges and How to Address Them. *Front Public Health* 2020; **8**: 154 [PMID: 32426318 DOI: 10.3389/fpubh.2020.00154]
22 **Musolino AM**, Supino MC. The Role of Lung Ultrasound in Diagnosis and Follow-Up of Children With Coronavirus Disease 2019. *Pediatr Crit Care Med* 2020; **21**: 783 [PMID: 32427688 DOI: 10.1097/PCC.0000000000002436]
23 **Wang T**, Cai G, Qiu Y, Fei N, Zhang M, Pang X, Jia W, Cai S, Zhao L. Structural segregation of gut microbiota between colorectal cancer patients and healthy volunteers. *ISME J* 2012; **6**: 320-329 [PMID: 21850056 DOI: 10.1038/ismej.2011.109]
24 **Louis P**, Flint HJ. Diversity, metabolism and microbial ecology of butyrate-producing bacteria from the human large intestine. *FEMS Microbiol Lett* 2009; **294**: 1-8 [PMID: 19222573 DOI: 10.1111/j.1574-6968.2009.01514.x]
25 **Ott SJ**, Musfeldt M, Wenderoth DF, Hampe J, Brant O, Fölsch UR, Timmis KN, Schreiber S. Reduction in diversity of the colonic mucosa associated bacterial microflora in patients with active inflammatory bowel disease. *Gut* 2004; **53**: 685-693 [PMID: 15082587 DOI: 10.1136/gut.2003.025403]

26 **Carroll C**, Booth A, Cooper K. A worked example of "best fit" framework synthesis: a systematic review of views concerning the taking of some potential chemopreventive agents. *BMC Med Res Methodol* 2011; **11**: 29 [PMID: 21410933 DOI: 10.1186/1471-2288-11-29]

27 **Karlsson FH**, Fåk F, Nookaew I, Tremaroli V, Fagerberg B, Petranovic D, Bäckhed F, Nielsen J. Symptomatic atherosclerosis is associated with an altered gut metagenome. *Nat Commun* 2012; **3**: 1245 [PMID: 23212374 DOI: 10.1038/ncomms2266]

28 **Allen-Vercoe E**, Strauss J, Chadee K. The role of the intestinal microbiota in colorectal cancer and colitis-associated cancer: From mice to humans. *Curr Issues Mol Biol* 2011; **14**: 15-32

29 **Sartor RB**, Wu GD. Roles for Intestinal Bacteria, Viruses, and Fungi in Pathogenesis of Inflammatory Bowel Diseases and Therapeutic Approaches. *Gastroenterology* 2017; **152**: 327-339.e4 [PMID: 27769810 DOI: 10.1053/j.gastro.2016.10.012]

30 **Wang CF**, Yang SH, Lin SH, Chen PC, Lo YC, Pan HC, Lai HY, Liao LD, Lin HC, Chen HY, Huang WC, Huang WJ, Chen YY. A proof-of-principle simulation for closed-loop control based on preexisting experimental thalamic DBS-enhanced instrumental learning. *Brain Stimul* 2017; **10**: 672-683 [PMID: 28298263 DOI: 10.1016/j.brs.2017.02.004]

31 **Gulsrud AC**, Hellemann GS, Freeman SF, Kasari C. Two to ten years: developmental trajectories of joint attention in children with ASD who received targeted social communication interventions. *Autism Res* 2014; **7**: 207-215 [PMID: 24550145 DOI: 10.1002/aur.1360]

32 **Giordano A**, Rossi G, Probo M, Moretti P, Paltrinieri S. Colorimetric and electrophoretic evaluation of lipoprotein fractions in healthy neonatal calves: Comparison with results from adult cows and from calves with inflammatory conditions. *Res Vet Sci* 2017; **111**: 108-112 [PMID: 28226299 DOI: 10.1016/j.rvsc.2017.02.007]

33 **Frank DN**, St Amand AL, Feldman RA, Boedeker EC, Harpaz N, Pace NR. Molecular-phylogenetic characterization of microbial community imbalances in human inflammatory bowel diseases. *Proc Natl Acad Sci U S A* 2007; **104**: 13780-13785 [PMID: 17699621 DOI: 10.1073/pnas.0706625104]

34 **Sears CL**, Garrett WS. Microbes, microbiota, and colon cancer. *Cell Host Microbe* 2014; **15**: 317-328 [PMID: 24629338 DOI: 10.1016/j.chom.2014.02.007]

35 **Sobhani I**, Tap J, Roudot-Thoraval F, Roperch JP, Letulle S, Langella P, Corthier G, Tran Van Nhieu J, Furet JP. Microbial dysbiosis in colorectal cancer (CRC) patients. *PLoS One* 2011; **6**: e16393 [PMID: 21297998 DOI: 10.1371/journal.pone.0016393]

36 **Albert U**, De Cori D, Aguglia A, Barbaro F, Lanfranco F, Bogetto F, Maina G. Effects of maintenance lithium treatment on serum parathyroid hormone and calcium levels: a retrospective longitudinal naturalistic study. *Neuropsychiatr Dis Treat* 2015; **11**: 1785-1791 [PMID: 26229473 DOI: 10.2147/NDT.S86103]

37 **Agosta F**, Galantucci S, Valsasina P, Canu E, Meani A, Marcone A, Magnani G, Falini A, Comi G, Filippi M. Disrupted brain connectome in semantic variant of primary progressive aphasia. *Neurobiol Aging* 2014; **35**: 2646-2655 [PMID: 24970567 DOI: 10.1016/j.neurobiolaging.2014.05.017]

38 **Moazen M**, Calder P, Koroma P, Wright J, Taylor S, Blunn G. An experimental evaluation of fracture movement in two alternative tibial fracture fixation models using a vibrating platform. *Proc Inst Mech Eng H* 2019; **233**: 595-599 [PMID: 30894097 DOI: 10.1177/0954411919837304]

39 **Shakhpazyan NK**, Mikhaleva LM, Bedzhanyan AL, Gioeva ZV, Mikhalev AI, Midiber KY, Pechnikova VV, Biryukov AE. Exploring the Role of the Gut Microbiota in Modulating Colorectal Cancer Immunity. *Cells* 2024; **13**: 1437 [DOI: 10.3390/cells13171437]

40 **De Vriese AS**, Wetzels JF, Glassock RJ, Sethi S, Fervenza FC. Therapeutic trials in adult FSGS: lessons learned and the road forward. *Nat Rev Nephrol* 2021; **17**: 619-630 [PMID: 34017116 DOI: 10.1038/s41581-021-00427-1]

41 **Human Microbiome Project Consortium**. Structure, function and diversity of the healthy human microbiome. *Nature* 2012; **486**: 207-214 [PMID: 22699609 DOI: 10.1038/nature11234]

42 **Nakatsu G**, Li X, Zhou H, Sheng J, Wong SH, Wu WK, Ng SC, Tsoi H, Dong Y, Zhang N, He Y, Kang Q, Cao L, Wang K, Zhang J, Liang Q, Yu J, Sung JJ. Gut mucosal microbiome across stages of colorectal carcinogenesis. *Nat Commun* 2015; **6**: 8727 [PMID: 26515465 DOI: 10.1038/ncomms9727]

43 **Zeller G**, Tap J, Voigt AY, Sunagawa S, Kultima JR, Costea PI, Amiot A, Böhm J, Brunetti F, Habermann N, Hercog R, Koch M, Luciani A, Mende DR, Schneider MA, Schrotz-King P, Tournigand C, Tran Van Nhieu J, Yamada T, Zimmermann J, Benes V, Kloor M, Ulrich CM, von Knebel Doeberitz M, Sobhani I, Bork P. Potential of fecal microbiota for early-stage detection of colorectal cancer. *Mol Syst Biol* 2014; **10**: 766 [PMID: 25432777 DOI: 10.15252/msb.20145645]

44 **Bartling B**, Schwarzmann L, Pliquett RU, Simm A, Hofmann B. Simultaneous influence of sex and age on blood pressure difference between supine and sitting body positions. *Z Gerontol Geriatr* 2021; **54**: 597-604 [PMID: 32647989 DOI: 10.1007/s00391-020-01756-9]

45 **Çaylan N**, Yalçın SS, Tezel B, Aydın Ş, Özen Ö, Şengelen M, Çakır B. Evaluation of injury-related under-five mortality in Turkey between 2014-2017. *Turk J Pediatr* 2021; **63**: 37-47 [PMID: 33686825 DOI: 10.24953/turkjped.2021.01.005]

46 **Zhao Y**, Jia M, Zhang C, Feng X, Chen J, Li Q, Zhang Y, Xu W, Dong Y, Jiang Y, Liu Y, Huang P. Reproducibility of ultrasound-guided attenuation parameter (UGAP) to the noninvasive evaluation of hepatic steatosis. *Sci Rep* 2022; **12**: 2876 [PMID: 35190618 DOI: 10.1038/s41598-022-06879-0]

47 **Lattanzi R**, Severini C, Maftei D, Saso L, Badiani A. The Role of Prokineticin 2 in Oxidative Stress and in Neuropathological Processes. *Front Pharmacol* 2021; **12**: 640441 [PMID: 33732160 DOI: 10.3389/fphar.2021.640441]

48 **Xu YF**, Yao Y, Ma M, Yang SH, Jiang P, Wang J, Tsuneyama K, Wang C, Liu X, Li L, Lian ZX. The Proinflammatory Cytokines IL-18, IL-21, and IFN-γ Differentially Regulate Liver Inflammation and Anti-Mitochondrial Antibody Level in a Murine Model of Primary Biliary Cholangitis. *J Immunol Res* 2022; **2022**: 7111445 [PMID: 35300072 DOI: 10.1155/2022/7111445]

49 **Kose KC**, Inanmaz ME, Isik C, Basar H, Caliskan I, Bal E. Short segment pedicle screw instrumentation with an index level screw and cantilevered hyperlordotic reduction in the treatment of type-A fractures of the thoracolumbar spine. *Bone Joint J* 2014; **96-B**: 541-547 [PMID: 24692625 DOI: 10.1302/0301-620X.96B4.33249]

50 **Ben Said S**, Or D. Synthetic Microbial Ecology: Engineering Habitats for Modular Consortia. *Front Microbiol* 2017; **8**: 1125 [PMID: 28670307 DOI: 10.3389/fmicb.2017.01125]

51 **Koh A**, De Vadder F, Kovatcheva-Datchary P, Bäckhed F. From Dietary Fiber to Host Physiology: Short-Chain Fatty Acids as Key Bacterial Metabolites. *Cell* 2016; **165**: 1332-1345 [PMID: 27259147 DOI: 10.1016/j.cell.2016.05.041]

52 **Ridlon JM**, Harris SC, Bhowmik S, Kang DJ, Hylemon PB. Consequences of bile salt biotransformations by intestinal bacteria. *Gut Microbes* 2016; **7**: 22-39 [PMID: 26939849 DOI: 10.1080/19490976.2015.1127483]

53 **Donohoe DR**, Garge N, Zhang X, Sun W, O'Connell TM, Bunger MK, Bultman SJ. The microbiome and butyrate regulate energy metabolism and autophagy in the mammalian colon. *Cell Metab* 2011; **13**: 517-526 [PMID: 21531334 DOI: 10.1016/j.cmet.2011.02.018]

54 **Mannarino CF**, Moreira JC, Ferreira JA, Arias AR. [Assessment of impacts of combined treatment of solid urban waste landfill leachate and

sewage on aquatic biota]. *Cien Saude Colet* 2013; **18**: 3235-3243 [PMID: 24196889 DOI: 10.1590/s1413-81232013001100014]

55 **Wilcox JA**, Boire AA. Palliation for all people: alleviating racial disparities in supportive care for brain metastases. *Neuro Oncol* 2020; **22**: 1239-1240 [PMID: 32692819 DOI: 10.1093/neuonc/noaa174]

56 **Hamer HM**, Jonkers D, Venema K, Vanhoutvin S, Troost FJ, Brummer RJ. Review article: the role of butyrate on colonic function. *Aliment Pharmacol Ther* 2008; **27**: 104-119 [PMID: 17973645 DOI: 10.1111/j.1365-2036.2007.03562.x]

57 **Nunes-Alves C**. Parasite physiology: linking virulence and transmission in malaria. *Nat Rev Microbiol* 2014; **12**: 655 [PMID: 25198141 DOI: 10.1038/nrmicro3354]

58 **Gunduz-Cinar O**, Brockway E, Lederle L, Wilcox T, Halladay LR, Ding Y, Oh H, Busch EF, Kaugars K, Flynn S, Limoges A, Bukalo O, MacPherson KP, Masneuf S, Pinard C, Sibille E, Chesler EJ, Holmes A. Identification of a novel gene regulating amygdala-mediated fear extinction. *Mol Psychiatry* 2019; **24**: 601-612 [PMID: 29311651 DOI: 10.1038/s41380-017-0003-3]

59 **Gagnière J**, Raisch J, Veziant J, Barnich N, Bonnet R, Buc E, Bringer MA, Pezet D, Bonnet M. Gut microbiota imbalance and colorectal cancer. *World J Gastroenterol* 2016; **22**: 501-518 [PMID: 26811603 DOI: 10.3748/wjg.v22.i2.501]

60 **Famularo G**, Minisola G, Bravi MC, Colucci P, Gasbarrone L. Tetany, hypomagnesemia, and proton-pump inhibitors. *Am J Med* 2012; **125**: e7-e8 [PMID: 22800870 DOI: 10.1016/j.amjmed.2012.04.027]

61 **Kostic AD**, Chun E, Robertson L, Glickman JN, Gallini CA, Michaud M, Clancy TE, Chung DC, Lochhead P, Hold GL, El-Omar EM, Brenner D, Fuchs CS, Meyerson M, Garrett WS. Fusobacterium nucleatum potentiates intestinal tumorigenesis and modulates the tumor-immune microenvironment. *Cell Host Microbe* 2013; **14**: 207-215 [PMID: 23954159 DOI: 10.1016/j.chom.2013.07.007]

62 **Dülger AC**, Aslan M, Olmez S, Esen R, Taşdemir M, Aytemiz E, Ebinc S, Kalkan NÖ. Co-occurrence of hepatocellular cancer and non-Hodgkin lymphoma. *Pol Arch Med Wewn* 2013; **123**: 127-128 [PMID: 23535859 DOI: 10.1007/s13277-013-0684-4]

63 **Al-Qadami GH**, Secombe KR, Subramaniam CB, Wardill HR, Bowen JM. Gut Microbiota-Derived Short-Chain Fatty Acids: Impact on Cancer Treatment Response and Toxicities. *Microorganisms* 2022; **10** [PMID: 36296324 DOI: 10.3390/microorganisms10102048]

64 **Holland-Bill L**, Christiansen CF, Ulrichsen SP, Ring T, Lunde Jørgensen JO, Sørensen HT. Preadmission Diuretic Use and Mortality in Patients Hospitalized With Hyponatremia: A Propensity Score-Matched Cohort Study. *Am J Ther* 2019; **26**: e79-e91 [PMID: 28005557 DOI: 10.1097/MJT.0000000000000544]

65 **Pavlou S**, Augustine J, Cunning R, Harkin K, Stitt AW, Xu H, Chen M. Attenuating Diabetic Vascular and Neuronal Defects by Targeting P2rx7. *Int J Mol Sci* 2019; **20** [PMID: 31035433 DOI: 10.3390/ijms20092101]

66 **Davies MN**, Pere H, Bosschem I, Haesebrouck F, Flahou B, Tartour E, Flower DR, Tough DF, Bayry J. In Silico Adjuvant Design and Validation. *Methods Mol Biol* 2017; **1494**: 107-125 [PMID: 27718189 DOI: 10.1007/978-1-4939-6445-1_8]

67 **Maruyama H**, Shiba M, Ishikawa-Kakiya Y, Kato K, Ominami M, Fukunaga S, Otani K, Hosomi S, Tanaka F, Kamata N, Taira K, Nagami Y, Yamagami H, Tanigawa T, Watanabe T, Yamamoto A, Kabata D, Shintani A, Fujiwara Y. Positive correlation between pancreatic volume and post-endoscopic retrograde cholangiopancreatography pancreatitis. *J Gastroenterol Hepatol* 2020; **35**: 769-776 [PMID: 31618801 DOI: 10.1111/jgh.14878]

68 **Ley RE**, Turnbaugh PJ, Klein S, Gordon JI. Microbial ecology: human gut microbes associated with obesity. *Nature* 2006; **444**: 1022-1023 [PMID: 17183309 DOI: 10.1038/4441022a]

69 **Saulnier DM**, Kolida S, Gibson GR. Microbiology of the human intestinal tract and approaches for its dietary modulation. *Curr Pharm Des* 2009; **15**: 1403-1414 [PMID: 19442165 DOI: 10.2174/138161209788168128]

70 **Sampson TR**, Mazmanian SK. Control of brain development, function, and behavior by the microbiome. *Cell Host Microbe* 2015; **17**: 565-576 [PMID: 25974299 DOI: 10.1016/j.chom.2015.04.011]

71 **Hill-Burns EM**, Debelius JW, Morton JT, Wissemann WT, Lewis MR, Wallen ZD, Peddada SD, Factor SA, Molho E, Zabetian CP, Knight R, Payami H. Parkinson's disease and Parkinson's disease medications have distinct signatures of the gut microbiome. *Mov Disord* 2017; **32**: 739-749 [PMID: 28195358 DOI: 10.1002/mds.26942]

72 **Wang L**, Ye J, Wang H, Xie H, Qiu Y. The novel link between planar möbius aromatic and third order nonlinear optical properties of metal-bridged polycyclic complexes. *Sci Rep* 2017; **7**: 10182 [PMID: 28860567 DOI: 10.1038/s41598-017-10739-7]

World Journal of Gastrointestinal Oncology

Submit a Manuscript: https://www.f6publishing.com

World J Gastrointest Oncol 2025 January 15; 17(1): 99834

DOI: 10.4251/wjgo.v17.i1.99834

ISSN 1948-5204 (online)

EDITORIAL

Advanced hepatocellular carcinoma treatment strategies: Are transarterial approaches leading the way?

Stefan Patauner, Giovanni Scotton, Francesca Notte, Antonio Frena

Specialty type: Oncology

Provenance and peer review: Invited article; Externally peer reviewed.

Peer-review model: Single blind

Peer-review report's classification

Scientific Quality: Grade B, Grade C

Novelty: Grade B, Grade B

Creativity or Innovation: Grade B, Grade B

Scientific Significance: Grade B, Grade B

P-Reviewer: Gupta T; Zhao P

Received: July 31, 2024

Revised: September 20, 2024

Accepted: September 25, 2024

Published online: January 15, 2025

Processing time: 133 Days and 21.1 Hours

Stefan Patauner, Giovanni Scotton, Francesca Notte, Antonio Frena, Department of General and Pediatric Surgery, Bolzano Central Hospital - SABES, Bolzano 39100, Trentino-Alto Adige, Italy

Co-first authors: Stefan Patauner and Giovanni Scotton.

Corresponding author: Antonio Frena, MD, PhD, Surgeon, Department of General and Pediatric Surgery, Bolzano Central Hospital - SABES, Via Boehler 5, Bolzano 39100, Trentino-Alto Adige, Italy. antonio.frena@sabes.it

Abstract

Hepatocellular carcinoma (HCC) is a leading cause of cancer-related mortality worldwide, with advanced stages posing significant treatment challenges. Although hepatic arterial infusion chemotherapy (HAIC) has emerged as a promising modality for treating advanced HCC, particularly in Asian clinical practice, its adoption in Western medicine remains limited due to a lack of large-scale randomized controlled trials. This editorial reviews and comments on the meta-analysis conducted by Zhou *et al*, which evaluates the efficacy and safety of HAIC and its combination strategies for advanced HCC. The authors performed a comprehensive meta-analysis of various clinical trials and cohort studies comparing HAIC and its combinations to other first-line treatments, such as sorafenib and transarterial chemoembolization (TACE). In this work, HAIC showed significantly better results regarding overall survival and progression-free survival compared to sorafenib or TACE alone and their combination. HAIC in combination with lenvatinib, ablation, programmed cell death 1 inhibitors, and radiotherapy further enhanced patient outcomes, indicating a synergistic effect. This editorial focuses on the critical role of multimodal treatment strategies in managing advanced HCC. It advocates for a paradigm shift towards integrated treatment approaches to enhance survival rates and improve the quality of life in patients with advanced HCC.

Key Words: Hepatocellular carcinoma; Hepatic arterial infusion chemotherapy; Transarterial chemoembolization; Sorafenib; Combined therapy

Core Tip: The treatment landscape for hepatocellular carcinoma (HCC) is various, including surgical resection, ablation, transplantation, transarterial, and systemic therapies. Each modality is selected based on tumor characteristics, liver function, and patient performance status. This editorial explores the role of hepatic arterial infusion chemotherapy and its combination strategies for advanced HCC, highlighting its potential advantages and advocating for its broader acceptance based on recent meta-analysis findings.

Citation: Patauner S, Scotton G, Notte F, Frena A. Advanced hepatocellular carcinoma treatment strategies: Are transarterial approaches leading the way? *World J Gastrointest Oncol* 2025; 17(1): 99834
URL: https://www.wjgnet.com/1948-5204/full/v17/i1/99834.htm
DOI: https://dx.doi.org/10.4251/wjgo.v17.i1.99834

INTRODUCTION

Hepatocellular carcinoma (HCC) is the most common type of primary liver cancer in adults and the fourth leading cause of mortality in cancer patients worldwide[1]. Five-year survival of HCC is approximately 18%[2]. Only 20%-30% of HCC patients are eligible for curative treatment. For the remaining majority, the prognosis remains poor, particularly when HCC is diagnosed at an advanced stage, where curative options such as surgical resection, liver transplantation, or ablation are no longer feasible. Advanced HCC typically consists of extensive liver involvement, vascular invasion, and distant metastases, making treatment especially challenging[1].

Different treatment options have been described for patients affected by HCC depending on tumor stage with/without vascular invasion, number and size of the lesions, underlying liver function (Child-Pugh, model for end-stage liver disease score), and patient performance status (ECOG PS 0-4).

According to the Barcelona Clinic Liver Cancer (BCLC) organization, patients with very early stage (0) and early stage (A) HCC can be treated with surgical resection, ablation, or liver transplantation[3,4].

According to the European Association for the Study of the Liver (EASL) guidelines, surgical resection is the preferred treatment for patients with single tumors larger than 2 cm, preserved liver function (Child-Pugh A or B), good performance status (PS 1-2), and an adequate volume of remaining liver. Depending on the tumor size (< 5 cm) and liver function (Child-Pugh A), the 5- and 10-year survival rates after resection are favorable at 70% and 35%, respectively. However, the 5-year recurrence rate remains high at 70%[5,6].

The advancement of minimally invasive surgery, which is associated with fewer postoperative complications and a potentially minimal impact on liver function[7-10], supports the consideration of resection for patients who would initially have been chosen for ablation. This is particularly relevant for patients with peripheral tumors where ablation might be contraindicated due to risks like tract seeding or damage to neighboring organs[7].

For patients classified as BCLC 0-A who do not qualify for surgical resection or liver transplantation, ablation can be a viable alternative.

Ablation techniques include radiofrequency ablation (RFA), microwave ablation, and the injection of chemical agents (such as ethanol, boiling saline, and acetic acid), as well as laser therapy and cryotherapy. Microwave ablation has shown promise with favorable response rates for tumors ranging from 3 to 5 cm in size and those near blood vessels or the gallbladder[11]. It generally requires fewer sessions and provides survival rates comparable to those achieved with RFA. For very early HCCs (≤ 2 cm), ablation can offer similar survival outcomes to resection but with better cost-effectiveness [11-13]. However, for single, larger early-stage HCCs, surgical resection remains the preferred approach due to its superior survival rates[13,14].

Liver transplantation is the best treatment for patients who meet the Milan criteria (single nodule ≤ 5 cm in diameter or up to three nodules, each ≤ 3 cm, without macrovascular invasion or extrahepatic spread) or extended liver transplant criteria. By eliminating both the tumor(s) and the underlying cirrhosis, this approach offers 5-year and 10-year survival rates of approximately 60%-80% and 50%, respectively. Additionally, the recurrence rate of HCC post-transplantation is under 15%, which is better than the recurrence rate following surgical resection[15].

Transarterial treatments are an option for patients with BCLC stage 0-A who have failed first-line therapies and are considered standard care for those with BCLC intermediate stage (B) disease. This includes patients with multinodular HCC that have no vascular invasion or extrahepatic spread, preserved portal flow, good liver function (Child A-B), and a favorable performance status (PS 0). The main transarterial treatments are transarterial chemoembolization (TACE), hepatic arterial infusion chemotherapy (HAIC), and selective internal radiation therapy (SIRT). These approaches take advantage of the fact that while normal liver tissue receives over 75% of its blood supply from the portal vein, liver tumors receive approximately 80% of their blood from the hepatic artery.

TACE, introduced in the 1970s for unresectable HCC, remains the standard treatment for intermediate-stage HCC with relatively preserved liver function. The TACE procedure involves intra-arterial injection of a cytotoxic agent followed by embolization of the tumor-feeding artery, combining the effects of targeted tumor ischemia and chemotherapy. After undergoing TACE, overall survival rates of 70.3%, 40.4%, and 32.4% were reported at 1, 3, and 5 years, respectively[16]. Combining TACE with sorafenib has shown improved progression-free survival (PFS) compared to TACE alone. While the role of TACE as a bridge to liver transplantation is not yet well-defined, it can be effective in downstaging patients with advanced HCC[17].

SIRT (also known as TARE) involves the intra-arterial infusion of yttrium-90 microspheres and is considered for patients with BCLC intermediate stage (B). It has demonstrated comparable results to TACE and can be considered for patients with single nodules ≤ 8 cm[18]. When used as a bridge to transplantation, SIRT shows similar outcomes to RFA and TACE[17].

Systemic therapy encompasses the adoption of multikinase inhibitors like sorafenib and lenvatinib and immunotherapy. Sorafenib, approved in 2007, targets pathways involved in cell proliferation and angiogenesis. It benefits HCC patients with Child-Pugh A or B7 liver function. Lenvatinib, approved in 2018, demonstrated non-inferiority to sorafenib. Lenvatinib is used globally, but sorafenib is less favored in Asia due to its lower efficacy in hepatitis B virus (HBV)-HCC patients[19]. Immune checkpoint inhibitors (ICIs) have enriched the panel of advanced HCC treatments. For example, pembrolizumab, targeting programmed cell death 1, was approved in the United States as a second-line treatment after sorafenib failure[20].

THE ROLE OF HAIC

HAIC is a locoregional treatment that utilizes a catheter technique to directly and continuously deliver high doses of anticancer drugs to liver tumors. This approach increases the local concentration of drugs within the tumor while minimizing systemic side effects. HAIC typically involves the implantation of a catheter and port system, enabling repeated administration of chemotherapeutic agents.

HAIC treatment is currently not included in the guidelines of the American Association for the Study of Liver Diseases, the EASL, or the Asian Pacific Association for the Study of the Liver, due to insufficient clinical evidence to make strong recommendations. Despite this, HAIC has been utilized in Asia, especially in Japan and South Korea, to enhance the prognosis of advanced HCC and has been incorporated into treatment guidelines[21]. The potential of HAIC may be underestimated due to the small sample sizes in previous studies and the lack of larger randomized trials.

Recently, the Japanese Society of Implantable Port Assisted Treatment has proposed clinical practice guidelines for HAIC with a port system, which could facilitate broader adoption of this treatment[22,23].

The primary advantage of HAIC compared to other systemic treatments is its substantial increase in local drug concentration due to the higher first-pass effect in the liver. This results in enhanced antitumor efficacy while minimizing systemic toxicity. In this regard, most studies on HAIC have reported a zero rate of treatment discontinuation due to infusion-related complications. Another significant advantage of HAIC lies in its application for patients with portal vein tumor thrombus. Most guidelines consider unresectable HCC with significant portal vein tumor thrombosis unsuitable for TACE, with sorafenib being the standard recommended treatment. However, before sorafenib approval for advanced HCC, HAIC was already routinely used in the Asian region, particularly in Japan and Korea, demonstrating promising results and likely surpassing the outcomes achieved with sorafenib alone. These findings prompted the design of trials comparing various HAIC regimens (such as cisplatin and 5-FU based) with sorafenib alone and their combinations[24]. While cisplatin and 5-FU based HAIC are the most commonly used regimens in Japan, they do not appear to outperform TACE in combination therapy. On the other hand, more aggressive HAIC regimens, such as 5-FU, leucovorin, and oxaliplatin (FOLFOX)-HAIC, have shown a distinct advantage over TACE in terms of both efficacy and safety[25].

The heterogeneity of the published studies and the different chemotherapy regimens used represent a jungle that is very difficult to navigate. A review of 1026 publications on HAIC for HCC reveals a significant increase in research output since 1990, with the most significant rise occurring in the past decade[26]. Notably, 83 studies were published in 2021, the highest number in the reviewed period. Regarding institutional and national contributions, Japan leads with 456 publications, followed by China (197), South Korea (96), and the United States (83). Overall, HAIC has gained prominence in HCC treatment, exploring its efficacy in combination with targeted and immunotherapy treatments.

The flip side of the coin is that several challenges hinder a clear evaluation of its efficacy. One of the key issues is the presence of too many variables across studies, making them difficult to compare. These variables include the size of the HCC, whether portal vein infiltration is present, and the degree of cirrhosis or hepatic arterialization. Additionally, the statistical analysis methods used in different studies vary, further complicating the comparison of results. Patient populations differ significantly, leading to heterogeneity in the outcomes. Furthermore, most of the studies come from Asia and this geographical dominance limits the global applicability of HAIC. To improve comparability, it would be crucial to establish global databases that classify patients into macro-categories based on factors such as HCC type, tumor size, liver function, and treatment line (first or second). This would enable the creation of a unified treatment strategy, allowing for more accurate comparisons. While HAIC shows generally favorable results, other studies suggest combining it with other treatments, indicating that HAIC alone might not be sufficient in most cases.

The meta-analysis conducted by Zhou *et al*[27] contributes to this context by seeking to organize and clarify the substantial heterogeneity present in the published studies[27].

The article is titled "Efficacy of HAIC and its combination strategies for advanced HCC: A network meta-analysis" and evaluates the effectiveness of HAIC both as a standalone treatment and in combination with other therapies for patients with advanced HCC. This meta-analysis offers a thorough comparison of HAIC with other first-line treatments, such as sorafenib and TACE, providing valuable insights into its potential advantages. The findings suggest that HAIC yields slightly better outcomes than both TACE and sorafenib in advanced HCC cases. Additionally, combined therapies (*e.g.*, HAIC + TACE) showed modestly enhanced results in overall survival, PFS, complete response, partial response, overall response rate, and disease control rate compared to HAIC alone.

The analysis by Zhou *et al*[27] emphasizes the underutilization of HAIC in Western medical practice, primarily due to the lack of randomized controlled trials supporting its use. This meta-analysis, by integrating data from various

randomized controlled trials and cohort studies, bridges this gap and advocates for broader acceptance of HAIC based on its demonstrated efficacy and safety. While challenges remain in its clinical integration, the compelling evidence presented in this study paves the way for renewed interest and further research in HAIC, promising improved outcomes for patients with advanced HCC.

THE EAST-WEST DIFFERENCE

The choice of treatment is governed by factors such as underlying comorbidities, the stage of the disease, liver function, and overall performance status. The management of HCC varies significantly between Eastern and Western countries due to differences in epidemiological and etiological factors. In Eastern countries, HCC is predominantly associated with HBV, hepatitis C virus, and aflatoxin exposure. Conversely, in Western countries, HCC is more commonly linked to metabolic syndrome and alcohol abuse. The prevalence of obesity, diabetes, and non-alcoholic fatty liver disease contributes significantly to HCC cases in these regions[28,29].

Guidelines for HCC differ between Western and Eastern countries. The Western guidelines (American Association for the Study of Liver Diseases, EASL-European Organization of Research and Treatment of Cancer) incorporate the BCLC staging classification in the therapeutic algorithm, leading to narrower resection indications (resection for non-cirrhotic livers, resection for a single tumor of any size or 2-3 nodules within 3 cm, no resection for vascular invasion). In contrast, eastern countries (China, Hong Kong, Japan, and Korea) do not have unified guidelines and do not use the BCLC in the therapeutic algorithm. For example, China and Japan consider resection for tumors of any size, including advanced stages with portal vein thrombi, if embolectomy through the portal vein can be attempted[30,31].

Western guidelines recommend TACE for BCLC stage B HCC, while Eastern guidelines may favor surgical resection if sufficient liver reserve is possible, even with portal vein involvement. In Western countries, macrovascular invasion is often managed with systemic therapies, while in Asia, TACE remains an option, and where expertise is available, HAIC serves as an alternative to TACE or initial systemic chemotherapy. The Japanese guideline recommended HAIC for HCC patients with more than four tumors, portal or macrovascular invasion, or those who have failed TACE[32].

The integration of local and systemic therapies in a multimodal approach ensures comprehensive tumor control. Local treatments such as HAIC and TACE deliver high concentrations of chemotherapeutic agents directly to the tumor site, achieving greater tumor shrinkage. When combined with systemic therapies, which address micrometastasis and circulating tumor cells, this approach maximizes tumor control and delays progression. One of the major challenges in advanced HCC treatment is the development of resistance to single-agent therapies. Multimodal approaches can mitigate this issue by targeting different pathways involved in tumor growth and survival. For example, combining HAIC with ICIs not only attacks the tumor directly but also modulates the immune environment, making it more hostile to cancer cells. This multifaceted attack can prevent the emergence of resistant tumor clones.

CONCLUSION

HAIC represents a promising locoregional treatment for advanced HCC, offering targeted drug delivery directly to liver tumors and minimizing systemic side effects. Despite not being widely endorsed by major liver disease guidelines due to limited evidence, HAIC has demonstrated notable efficacy in Asian countries. Although HAIC impact is sometimes overshadowed by other treatments like sorafenib or TACE, emerging evidence, including Zhou *et al*'s meta-analysis[27], suggests HAIC efficacy, particularly when used in combination therapies. Addressing the existing variability and geographical biases through comprehensive global databases and further randomized trials could enhance HAIC global adoption and optimize treatment outcomes for advanced HCC.

FOOTNOTES

Author contributions: Frena A designed the overall concept of the manuscript and revised the manuscript; Patauner S and Scotton G equally contributed to the design, review of the literature and writing of the manuscript; Notte F contributed to the review of the literature and editing of the manuscript; All authors contributed to this paper.

Conflict-of-interest statement: All the authors report no relevant conflicts of interest for this article.

Country of origin: Italy

ORCID number: Stefan Patauner 0000-0001-7592-0934; Giovanni Scotton 0000-0003-2222-3822; Francesca Notte 0000-0002-3559-1782; Antonio Frena 0000-0001-9461-5345.

S-Editor: Li L
L-Editor: Webster JR
P-Editor: Cai YX

REFERENCES

1 **Bray F**, Ferlay J, Soerjomataram I, Siegel RL, Torre LA, Jemal A. Global cancer statistics 2018: GLOBOCAN estimates of incidence and mortality worldwide for 36 cancers in 185 countries. *CA Cancer J Clin* 2018; **68**: 394-424 [PMID: 30207593 DOI: 10.3322/caac.21492]
2 **Jemal A**, Ward EM, Johnson CJ, Cronin KA, Ma J, Ryerson B, Mariotto A, Lake AJ, Wilson R, Sherman RL, Anderson RN, Henley SJ, Kohler BA, Penberthy L, Feuer EJ, Weir HK. Annual Report to the Nation on the Status of Cancer, 1975-2014, Featuring Survival. *J Natl Cancer Inst* 2017; **109** [PMID: 28376154 DOI: 10.1093/jnci/djx030]
3 **Reig M**, Forner A, Rimola J, Ferrer-Fàbrega J, Burrel M, Garcia-Criado Á, Kelley RK, Galle PR, Mazzaferro V, Salem R, Sangro B, Singal AG, Vogel A, Fuster J, Ayuso C, Bruix J. BCLC strategy for prognosis prediction and treatment recommendation: The 2022 update. *J Hepatol* 2022; **76**: 681-693 [PMID: 34801630 DOI: 10.1016/j.jhep.2021.11.018]
4 **Bruix J**, Reig M, Sherman M. Evidence-Based Diagnosis, Staging, and Treatment of Patients With Hepatocellular Carcinoma. *Gastroenterology* 2016; **150**: 835-853 [PMID: 26795574 DOI: 10.1053/j.gastro.2015.12.041]
5 **European Association for the Study of the Liver**. EASL Clinical Practice Guidelines: Management of hepatocellular carcinoma. *J Hepatol* 2018; **69**: 182-236 [PMID: 29628281 DOI: 10.1016/j.jhep.2018.03.019]
6 **Berzigotti A**, Reig M, Abraldes JG, Bosch J, Bruix J. Portal hypertension and the outcome of surgery for hepatocellular carcinoma in compensated cirrhosis: a systematic review and meta-analysis. *Hepatology* 2015; **61**: 526-536 [PMID: 25212123 DOI: 10.1002/hep.27431]
7 **Molina V**, Sampson-Dávila J, Ferrer J, Fondevila C, Díaz Del Gobbo R, Calatayud D, Bruix J, García-Valdecasas JC, Fuster J. Benefits of laparoscopic liver resection in patients with hepatocellular carcinoma and portal hypertension: a case-matched study. *Surg Endosc* 2018; **32**: 2345-2354 [PMID: 29218665 DOI: 10.1007/s00464-017-5930-1]
8 **Witowski J**, Rubinkiewicz M, Mizera M, Wysocki M, Gajewska N, Sitkowski M, Małczak P, Major P, Budzyński A, Pędziwiatr M. Meta-analysis of short- and long-term outcomes after pure laparoscopic versus open liver surgery in hepatocellular carcinoma patients. *Surg Endosc* 2019; **33**: 1491-1507 [PMID: 30203210 DOI: 10.1007/s00464-018-6431-6]
9 **Morise Z**, Ciria R, Cherqui D, Chen KH, Belli G, Wakabayashi G. Can we expand the indications for laparoscopic liver resection? A systematic review and meta-analysis of laparoscopic liver resection for patients with hepatocellular carcinoma and chronic liver disease. *J Hepatobiliary Pancreat Sci* 2015; **22**: 342-352 [PMID: 25663288 DOI: 10.1002/jhbp.215]
10 **Troisi RI**, Berardi G, Morise Z, Cipriani F, Ariizumi S, Sposito C, Panetta V, Simonelli I, Kim S, Goh BKP, Kubo S, Tanaka S, Takeda Y, Ettorre GM, Russolillo N, Wilson GC, Cimino M, Montalti R, Giglio MC, Igarashi K, Chan CY, Torzilli G, Cheung TT, Mazzaferro V, Kaneko H, Ferrero A, Geller DA, Han HS, Kanazawa A, Wakabayashi G, Aldrighetti L, Yamamoto M. Laparoscopic and open liver resection for hepatocellular carcinoma with Child-Pugh B cirrhosis: multicentre propensity score-matched study. *Br J Surg* 2021; **108**: 196-204 [PMID: 33711132 DOI: 10.1093/bjs/znaa041]
11 **Yu J**, Yu XL, Han ZY, Cheng ZG, Liu FY, Zhai HY, Mu MJ, Liu YM, Liang P. Percutaneous cooled-probe microwave versus radiofrequency ablation in early-stage hepatocellular carcinoma: a phase III randomised controlled trial. *Gut* 2017; **66**: 1172-1173 [PMID: 27884919 DOI: 10.1136/gutjnl-2016-312629]
12 **Cho YK**, Kim JK, Kim WT, Chung JW. Hepatic resection versus radiofrequency ablation for very early stage hepatocellular carcinoma: a Markov model analysis. *Hepatology* 2010; **51**: 1284-1290 [PMID: 20099299 DOI: 10.1002/hep.23466]
13 **Cucchetti A**, Piscaglia F, Cescon M, Colecchia A, Ercolani G, Bolondi L, Pinna AD. Cost-effectiveness of hepatic resection versus percutaneous radiofrequency ablation for early hepatocellular carcinoma. *J Hepatol* 2013; **59**: 300-307 [PMID: 23603669 DOI: 10.1016/j.jhep.2013.04.009]
14 **Shouval D**. Focus. *J Hepatol* 2012; **57**: 713-714 [PMID: 22824817 DOI: 10.1016/j.jhep.2012.07.022]
15 **Mazzaferro V**, Llovet JM, Miceli R, Bhoori S, Schiavo M, Mariani L, Camerini T, Roayaie S, Schwartz ME, Grazi GL, Adam R, Neuhaus P, Salizzoni M, Bruix J, Forner A, De Carlis L, Cillo U, Burroughs AK, Troisi R, Rossi M, Gerunda GE, Lerut J, Belghiti J, Boin I, Gugenheim J, Rochling F, Van Hoek B, Majno P; Metroticket Investigator Study Group. Predicting survival after liver transplantation in patients with hepatocellular carcinoma beyond the Milan criteria: a retrospective, exploratory analysis. *Lancet Oncol* 2009; **10**: 35-43 [PMID: 19058754 DOI: 10.1016/S1470-2045(08)70284-5]
16 **Lencioni R**, de Baere T, Soulen MC, Rilling WS, Geschwind JF. Lipiodol transarterial chemoembolization for hepatocellular carcinoma: A systematic review of efficacy and safety data. *Hepatology* 2016; **64**: 106-116 [PMID: 26765068 DOI: 10.1002/hep.28453]
17 **Sapisochin G**, Barry A, Doherty M, Fischer S, Goldaracena N, Rosales R, Russo M, Beecroft R, Ghanekar A, Bhat M, Brierley J, Greig PD, Knox JJ, Dawson LA, Grant DR. Stereotactic body radiotherapy vs. TACE or RFA as a bridge to transplant in patients with hepatocellular carcinoma. An intention-to-treat analysis. *J Hepatol* 2017; **67**: 92-99 [PMID: 28257902 DOI: 10.1016/j.jhep.2017.02.022]
18 **Salem R**, Johnson GE, Kim E, Riaz A, Bishay V, Boucher E, Fowers K, Lewandowski R, Padia SA. Yttrium-90 Radioembolization for the Treatment of Solitary, Unresectable HCC: The LEGACY Study. *Hepatology* 2021; **74**: 2342-2352 [PMID: 33739462 DOI: 10.1002/hep.31819]
19 **Kudo M**, Finn RS, Qin S, Han KH, Ikeda K, Piscaglia F, Baron A, Park JW, Han G, Jassem J, Blanc JF, Vogel A, Komov D, Evans TRJ, Lopez C, Dutcus C, Guo M, Saito K, Kraljevic S, Tamai T, Ren M, Cheng AL. Lenvatinib versus sorafenib in first-line treatment of patients with unresectable hepatocellular carcinoma: a randomised phase 3 non-inferiority trial. *Lancet* 2018; **391**: 1163-1173 [PMID: 29433850 DOI: 10.1016/S0140-6736(18)30207-1]
20 **Zhu AX**, Finn RS, Edeline J, Cattan S, Ogasawara S, Palmer D, Verslype C, Zagonel V, Fartoux L, Vogel A, Sarker D, Verset G, Chan SL, Knox J, Daniele B, Webber AL, Ebbinghaus SW, Ma J, Siegel AB, Cheng AL, Kudo M; KEYNOTE-224 investigators. Pembrolizumab in patients with advanced hepatocellular carcinoma previously treated with sorafenib (KEYNOTE-224): a non-randomised, open-label phase 2 trial. *Lancet Oncol* 2018; **19**: 940-952 [PMID: 29875066 DOI: 10.1016/S1470-2045(18)30351-6]
21 **Kokudo N**, Takemura N, Hasegawa K, Takayama T, Kubo S, Shimada M, Nagano H, Hatano E, Izumi N, Kaneko S, Kudo M, Iijima H, Genda T, Tateishi R, Torimura T, Igaki H, Kobayashi S, Sakurai H, Murakami T, Watadani T, Matsuyama Y. Clinical practice guidelines for

hepatocellular carcinoma: The Japan Society of Hepatology 2017 (4th JSH-HCC guidelines) 2019 update. *Hepatol Res* 2019; **49**: 1109-1113 [PMID: 31336394 DOI: 10.1111/hepr.13411]

22 **Ueshima K**, Komemushi A, Aramaki T, Iwamoto H, Obi S, Sato Y, Tanaka T, Matsueda K, Moriguchi M, Saito H, Sone M, Yamagami T, Inaba Y, Kudo M, Arai Y. Clinical Practice Guidelines for Hepatic Arterial Infusion Chemotherapy with a Port System Proposed by the Japanese Society of Interventional Radiology and Japanese Society of Implantable Port Assisted Treatment. *Liver Cancer* 2022; **11**: 407-425 [PMID: 36158592 DOI: 10.1159/000524893]

23 **Iwamoto H**, Shimose S, Shirono T, Niizeki T, Kawaguchi T. Hepatic arterial infusion chemotherapy for advanced hepatocellular carcinoma in the era of chemo-diversity. *Clin Mol Hepatol* 2023; **29**: 593-604 [PMID: 36775834 DOI: 10.3350/cmh.2022.0391]

24 **Zhao M**, Guo Z, Zou YH, Li X, Yan ZP, Chen MS, Fan WJ, Li HL, Yang JJ, Chen XM, Xu LF, Zhang YW, Zhu KS, Sun JH, Li JP, Jin Y, Yu HP, Duan F, Xiong B, Yin GW, Lin HL, Ma YL, Wang HM, Gu SZ, Si TG, Wang XD, Zhao C, Yu WC, Guo JH, Zhai J, Huang YH, Wang WY, Lin HF, Gu YK, Chen JZ, Wang JP, Zhang YM, Yi JZ, Lyu N. Arterial chemotherapy for hepatocellular carcinoma in China: consensus recommendations. *Hepatol Int* 2024; **18**: 4-31 [PMID: 37864725 DOI: 10.1007/s12072-023-10599-6]

25 **Li QJ**, He MK, Chen HW, Fang WQ, Zhou YM, Xu L, Wei W, Zhang YJ, Guo Y, Guo RP, Chen MS, Shi M. Hepatic Arterial Infusion of Oxaliplatin, Fluorouracil, and Leucovorin Versus Transarterial Chemoembolization for Large Hepatocellular Carcinoma: A Randomized Phase III Trial. *J Clin Oncol* 2022; **40**: 150-160 [PMID: 34648352 DOI: 10.1200/JCO.21.00608]

26 **Li M**, Zhang K, He J, Zhang W, Lv T, Wang L, Xing W, Yu H. Hepatic arterial infusion chemotherapy in hepatocellular carcinoma: A bibliometric and knowledge-map analysis. *Front Oncol* 2022; **12**: 1071860 [PMID: 36686799 DOI: 10.3389/fonc.2022.1071860]

27 **Zhou SA**, Zhou QM, Wu L, Chen ZH, Wu F, Chen ZR, Xu LQ, Gan BL, Jin HS, Shi N. Efficacy of hepatic arterial infusion chemotherapy and its combination strategies for advanced hepatocellular carcinoma: A network meta-analysis. *World J Gastrointest Oncol* 2024; **16**: 3672-3686 [PMID: 39171172 DOI: 10.4251/wjgo.v16.i8.3672]

28 **Feng MY**, Chan SL. Management of Hepatocellular Carcinoma: The East-West Difference. *Curr Chin Sci* 2023; **3**: 467-476 [DOI: 10.2174/2210298103666230912143208]

29 **Lee VHF**, Seong J, Yoon SM, Wong TCL, Wang B, Zhang JL, Chiang CL, Ho PPY, Dawson LA. Contrasting Some Differences in Managing Advanced Unresectable Hepatocellular Carcinoma Between the East and the West. *Clin Oncol (R Coll Radiol)* 2019; **31**: 560-569 [PMID: 31279433 DOI: 10.1016/j.clon.2019.06.002]

30 **Zhou J**, Sun H, Wang Z, Cong W, Wang J, Zeng M, Zhou W, Bie P, Liu L, Wen T, Han G, Wang M, Liu R, Lu L, Ren Z, Chen M, Zeng Z, Liang P, Liang C, Chen M, Yan F, Wang W, Ji Y, Yun J, Cai D, Chen Y, Cheng W, Cheng S, Dai C, Guo W, Hua B, Huang X, Jia W, Li Y, Li Y, Liang J, Liu T, Lv G, Mao Y, Peng T, Ren W, Shi H, Shi G, Tao K, Wang W, Wang X, Wang Z, Xiang B, Xing B, Xu J, Yang J, Yang J, Yang Y, Yang Y, Ye S, Yin Z, Zhang B, Zhang B, Zhang L, Zhang S, Zhang T, Zhao Y, Zheng H, Zhu J, Zhu K, Liu R, Shi Y, Xiao Y, Dai Z, Teng G, Cai J, Wang W, Cai X, Li Q, Shen F, Qin S, Dong J, Fan J. Guidelines for the Diagnosis and Treatment of Hepatocellular Carcinoma (2019 Edition). *Liver Cancer* 2020; **9**: 682-720 [PMID: 33442540 DOI: 10.1159/000509424]

31 **Kokudo N**, Hasegawa K, Akahane M, Igaki H, Izumi N, Ichida T, Uemoto S, Kaneko S, Kawasaki S, Ku Y, Kudo M, Kubo S, Takayama T, Tateishi R, Fukuda T, Matsui O, Matsuyama Y, Murakami T, Arii S, Okazaki M, Makuuchi M. Evidence-based Clinical Practice Guidelines for Hepatocellular Carcinoma: The Japan Society of Hepatology 2013 update (3rd JSH-HCC Guidelines). *Hepatol Res* 2015; **45** [PMID: 25625806 DOI: 10.1111/hepr.12464]

32 **Kudo M**, Matsui O, Izumi N, Iijima H, Kadoya M, Imai Y, Okusaka T, Miyayama S, Tsuchiya K, Ueshima K, Hiraoka A, Ikeda M, Ogasawara S, Yamashita T, Minami T, Yamakado K; Liver Cancer Study Group of Japan. JSH Consensus-Based Clinical Practice Guidelines for the Management of Hepatocellular Carcinoma: 2014 Update by the Liver Cancer Study Group of Japan. *Liver Cancer* 2014; **3**: 458-468 [PMID: 26280007 DOI: 10.1159/000343875]

World Journal of Gastrointestinal Oncology

Submit a Manuscript: https://www.f6publishing.com

World J Gastrointest Oncol 2025 January 15; 17(1): 100713

DOI: 10.4251/wjgo.v17.i1.100713

ISSN 1948-5204 (online)

EDITORIAL

Exosomes as promising frontier approaches in future cancer therapy

Fatt-Yang Chew, Chin-Hung Tsai, Kuang-Hsi Chang, Yu-Kang Chang, Ruey-Hwang Chou, Yi-Jui Liu

Specialty type: Gastroenterology and hepatology

Provenance and peer review: Invited article; Externally peer reviewed.

Peer-review model: Single blind

Peer-review report's classification

Scientific Quality: Grade B
Novelty: Grade A
Creativity or Innovation: Grade A
Scientific Significance: Grade A

P-Reviewer: Gugulothu D

Received: August 24, 2024
Revised: October 9, 2024
Accepted: October 29, 2024
Published online: January 15, 2025
Processing time: 110 Days and 2.1 Hours

Fatt-Yang Chew, Department of Medical Imaging, China Medical University Hospital, Taichung 404, Taiwan

Fatt-Yang Chew, Department of Radiology, School of Medicine, China Medical University, Taichung 404, Taiwan

Chin-Hung Tsai, Department of Cancer Center, Tungs' Taichung MetroHarbor Hospital, Taichung 435, Taiwan

Chin-Hung Tsai, Department of Chest Medicine, Tungs' Taichung MetroHarbor Hospital, Taichung 435, Taiwan

Chin-Hung Tsai, Yu-Kang Chang, Department of Post-Baccalaureate Medicine, College of Medicine, National Chung Hsing University, Taichung 402, Taiwan

Kuang-Hsi Chang, Yu-Kang Chang, Department of Medical Research, Tungs' Taichung MetroHarbor Hospital, Taichung 435, Taiwan

Kuang-Hsi Chang, Center for General Education, China Medical University, Taichung 404, Taiwan

Kuang-Hsi Chang, General Education Center, Jen-Teh Junior College of Medicine, Nursing and Management, Miaoli 356, Taiwan

Yu-Kang Chang, Department of Nursing, Jen-Teh Junior College of Medicine, Nursing and Management, Miaoli 356, Taiwan

Ruey-Hwang Chou, Graduate Institute of Biomedical Sciences, China Medical University, Taichung 404, Taiwan

Ruey-Hwang Chou, Center for Molecular Medicine, China Medical University Hospital, Taichung 404, Taiwan

Ruey-Hwang Chou, Department of Medical Laboratory and Biotechnology, Asia University, Taichung 413, Taiwan

Yi-Jui Liu, Department of Automatic Control Engineering, Feng Chia University, Taichung 407, Taiwan

Co-first authors: Fatt-Yang Chew and Chin-Hung Tsai.

Co-corresponding authors: Ruey-Hwang Chou and Yi-Jui Liu.

Corresponding author: Yi-Jui Liu, PhD, Professor, Department of Automatic Control Engi-

neering, Feng Chia University, No. 100 Wenhwa Road, Seatwen, Taichung 407, Taiwan. erliu@fcu.edu.tw

Abstract

In this editorial, we will discuss the article by Tang *et al* published in the recent issue of the *World Journal of Gastrointestinal Oncology*. They explored an innovative approach to enhancing gemcitabine (GEM) delivery and efficacy using human bone marrow mesenchymal stem cells (HU-BMSCs)-derived exosomes. The manufacture of GEM-loaded HU-BMSCs-derived exosomes (Exo-GEM) has been optimized. The Tang *et al*'s study demonstrated that Exo-GEM exhibits enhanced cytotoxicity and apoptosis-inducing effects compared to free GEM, highlighting the potential of exosome-based drug delivery systems as a more effective and targeted approach to chemotherapy in pancreatic cancer. Additional *in vivo* studies are required to confirm the safety and effectiveness of Exo-GEM before it can be considered for clinical use.

Key Words: Mesenchymal stem cells; Exosomes; Gemcitabine; Pancreatic cancer; Apoptosis

Core Tip: The method of loading gemcitabine into exosomes is crucial for the effectiveness of the delivery system. The study ascertained that electroporation and sonication were more efficient than incubation in delivering gemcitabine into the human bone marrow mesenchymal stem cells-derived exosomes. Exosomes gemcitabine (Exo-GEM) demonstrated potent cytotoxicity against pancreatic cancer cells by enhancing GEM-induced apoptosis. Exo-GEM offers a promising strategy for targeted therapy in pancreatic cancer by harnessing the natural advantages of exosomes, such as high biocompatibility and the ability to navigate tumor microenvironments. Exo-GEM could deliver chemotherapy more precisely to cancer cells, reducing side effects in healthy cells.

Citation: Chew FY, Tsai CH, Chang KH, Chang YK, Chou RH, Liu YJ. Exosomes as promising frontier approaches in future cancer therapy. *World J Gastrointest Oncol* 2025; 17(1): 100713
URL: https://www.wjgnet.com/1948-5204/full/v17/i1/100713.htm
DOI: https://dx.doi.org/10.4251/wjgo.v17.i1.100713

INTRODUCTION

Pancreatic cancer is a malignant and aggressive disease characterized by invasion, rapid progression of the disease, and resistance to treatment. The most common type of pancreatic cancer is pancreatic ductal adenocarcinoma (PDAC), which accounts for about 90% of cases[1]. Typical symptoms in pancreatic cancer patients include abdominal pain, back pain, unexplained weight loss, jaundice, lightening of stool, darkening of urine, no hunger, *etc.*, but there are usually no obvious symptoms in its early stage[2]. Due to the lack of an accurate early diagnostic test and specific symptoms, pancreatic cancer is usually diagnosed late or after it has metastasized to other organs[3].

At present, the main treatments for pancreatic cancer are surgery, radiation therapy, and chemotherapy. However, only around 20% of patients with pancreatic cancer are resectable, and the remaining 80% are not amenable to surgery. Gemcitabine (GEM) is sold under the brand name Gemzar and is the standard first-line treatment for metastatic pancreatic cancer patients[4]. However, its efficacy is often limited due to rapid metabolism, poor delivery efficiency, and the development of drug resistance.

Treatment efficacy is limited by strong biological barriers to drug/material transport into deep tissues, including macrophage uptake, fluid dynamics in blood vessels, and high intratumoral pressure[5]. Exosomes are natural biological nanoparticles secreted by cells (usually 30 nm-150 nm in diameter) and contain many biomolecules, including nucleic acids, proteins, and lipids. Exosomes act as novel mediators in intercellular communication, serving as messengers to mediate physiological and pathological processes[6]. Exosomes have been tested as drug delivery vehicles for cancer treatment due to their unique properties, such as size, innate stability, low immunogenicity, excellent tissue/cell penetration ability and ability to mimic synthetic liposomes in carrying various anticancer drugs/materials[7]. These nanoscale vesicles, *i.e.* exosomes, have garnered considerable interest in the fields of biology and medical sciences.

For example, Kamerkar *et al*[8] used inhibitory exosomes (iExosomes) derived from normal fibroblast-like mesenchymal cells containing RNA interference (RNAi) sequences designed to target $KRAS^{G12D}$. These iExosomes express cluster of differentiation 47 (CD47), which protects them from phagocytosis, ultimately enabling their enhanced efficacy to suppress cancer and increase survival in multiple mouse models of pancreatic cancer[8]. In addition to delivering RNAi to block the expression of *KRAS* in pancreatic cancer cells, exosomes can also carry clustered regularly interspaced short palindromic repeats/CRISPR-associated protein 9 (CRISPR/Cas9) plasmid DNA for targeted gene deletion to replace the viral delivery system. McAndrews *et al*[9] used typical transfection protocols to effect the encapsulation of CRISPR/Cas9 plasmid DNA by non-autologous exosomes. The CRISPR/Cas9 DNA was designed to provoke targeted $KRAS^{G12D}$ gene

deletion in PDAC cells, proving that exosomes loaded with CRISPR/Cas9 can target mutated *KRAS*^{G12D} oncogenic alleles to suppress tumor growth in syngeneic subcutaneous and orthotopic models of pancreatic cancer[9].

Numerous studies have demonstrated that exosomes are potential carriers of therapeutic anti-cancer small molecules, including curcumin, paclitaxel, doxorubicin, and GEM[10-13]. Previous studies have revealed that exosomes gemcitabine (Exo-GEM) derived from tumors, M1 macrophages, and mesenchymal stem cells (MSCs) demonstrate a remarkable capacity to overcome drug resistance in pancreatic cancer[13-16]. However, the efficiency of Exo-GEM to specifically target pancreatic cancer cells has yet to be fully established. The study by Tang *et al*[17] in the recent issue of *World Journal of Gastrointestinal Oncology* has explored an innovative approach to improve GEM delivery and efficacy through the use of human bone marrow MSCs (HU-BMSCs)-derived exosomes[17].

CARGO LOADING AND EFFICACY OF EXOSOMES

Cargo, such as drugs and materials, can be loaded into or onto exosomes *via* three main approaches: (1) Biological methods, such as viral transduction[18] and incubation[19]; (2) Chemical methods, including saponin-assisted permeation [20], transfection by calcium phosphate[21], transfection using diethylaminoethyl-dextran[22], creating lipopolyplexes with polyethylenimine[23], merging liposomes with exosomes[24] *etc.*; and (3) Physical methods, *e.g.*, sonication[25], extrusion[26], freeze-thaw cycles[27], electroporation[28], and dialysis[29] (Figure 1). It is important to note that while various methods can efficiently load different types of cargo into exosomes, these processes can potentially damage both exosomes and their cargo due to the destructive impact of the techniques. To ensure optimal loading, the ideal combination of key parameters, such as the intensity of physical interactions, operation time, cell type, and the concentration of reagents and exosomes should be carefully determined[7,30].

The recent study by Tang *et al*[17] compared three methods for loading GEM into the HU-BMSCs-derived exosomes: Electroporation, sonication, and incubation. Both electroporation and sonication showed significantly higher loading and encapsulation efficacy by approximately sixfold compared to incubation. Exo-GEM exhibited significantly higher cytotoxicity and induced more apoptosis against the human PDAC cell lines-Panc-1 and MiaPaca-2-than free GEM. The findings suggest that Exo-GEM may help overcome the challenges associated with conventional GEM chemotherapy, such as drug resistance and inadequate solubility[17]. Further modifications of the exosomes' surface, such as conjugation with tumor-specific antibodies or ligands, might be considered for the next generation of Exo-GEM. Effectively delivering GEM by exosomes to the target cells could potentially improve the therapeutic outcomes of PDAC patients.

SAFETY AND ADMINISTRATION ROUTES OF EXOSOMES

Conventional administration of GEM by intravenous (IV) injection is associated with well-known toxicities, including hematological, gastrointestinal, and liver-related side effects[31]. Exosomes have the potential to enhance drug targeting, reduce systemic toxicity, and provide controlled release, thereby mitigating many of the adverse effects typically associated with conventional GEM treatment[32]. The IV administration of exosomes is the most common route and a convenient method for drug delivery, providing low immunogenicity and rapid therapeutic effects[33-35]. Intraperitoneal administration of exosomes could target organs affected by cancer within the peritoneal cavity, such as the ovaries[36]. Subcutaneous administration allows for a slower and more sustained release of exosomes[37,38].

Exo-GEM treatment significantly inhibited tumor growth and extended survival in tumor-bearing mice but caused minimal damage to normal tissues, suggesting exosomes are safe and effective carriers for the targeted delivery of GEM against pancreatic cancer[13]. Research on exosomes as therapeutic agents and drug delivery carriers has been predominantly carried out in animal models. Several clinical studies revealed no major toxicity or serious adverse events after administering dendritic cell-derived exosomes loaded with major histocompatibility complex class I or II peptides to enhance the immune response for the treatment of cancer patients[38-40]. Further clinical trials are essential to fully assess the long-term safety and efficacy of exosome-based therapies.

POTENTIAL CLINICAL APPLICATIONS

The study by Tang *et al*[17] opens new avenues for the clinical application of exosome-based drug delivery systems in the treatment of pancreatic cancer[17]. Exo-GEM could significantly impact the delivery of chemotherapy for pancreatic cancer patients. By enhancing the delivery and effectiveness of GEM, this approach may allow for lower dosages, leading to fewer side effects and an improved quality of life for pancreatic cancer patients. Additional *in vivo* studies are needed to validate the safety and effectiveness of Exo-GEM before it can be considered for clinical application. Several pilot clinical trials of exosome-based therapies have been launched, such as the curcumin-loaded plant exosomes for colon cancer, MSC-derived exosomes with *KRAS*^{G12D} siRNA (iExosomes) for metastatic pancreatic cancer, exosomes with antisense oligonucleotide-signal transducer and activator of transcription 6 (exoASO-STAT6)/(CDK-004) to target cancer-specific signaling pathways for patients with advanced hepatocellular carcinoma and patients with liver metastases, and vaccination with tumor antigen-loaded dendritic cell-derived exosomes (DEX2) for non-small cell lung cancer (Table 1).

Table 1 The clinical trials of cargoes for cancer therapy

Study title	Conditions	Interventions	NCT number	Study status	Sponsor
Study investigating the ability of plant exosomes to deliver curcumin to normal and colon cancer tissue	Colon cancer	Dietary supplement: Curcumin conjugated with plant exosomes	NCT01294072	Recruiting	University of Louisville
Inhibitory exosomes in treating participants with metastatic pancreas cancer with *KRAS*^{G12D} mutation	*KRAS* NP004976.2: p.G12D; Metastatic Pancreatic Adenocarcinoma; Pancreatic ductal adenocarcinoma; Stage IV pancreatic cancer	Drug: Mesenchymal stromal cells-derived exosomes with *KRAS* ^{G12D} siRNA	NCT03608631	Active; Not Recruiting	M.D. Anderson Cancer Center
A study of exoASO-STAT6 (CDK-004) in patients with advanced hepatocellular carcinoma and patients with liver metastases from either primary gastric cancer or colorectal cancer	Advanced hepatocellular carcinoma; Gastric cancer metastatic to liver; Colorectal cancer metastatic to liver	Drug: CDK-004	NCT05375604	Terminated	Codiak BioSciences
Trial of a vaccination with tumor antigen-loaded dendritic cell-derived exosomes	Non small cell lung cancer	Biological: DEX2	NCT01159288	Completed	Gustave Roussy, Cancer Campus, Grand Paris

Data collected from ClinicalTrials.gov accessed on August 20, 2024. exoASO-STAT6: Exosomes with antisense oligonucleotide-signal transducer and activator of transcription 6; CDK-004: Codiak BioSciences product-004; DEX: Dendritic cell-derived exosomes; NCT: National clinical trial.

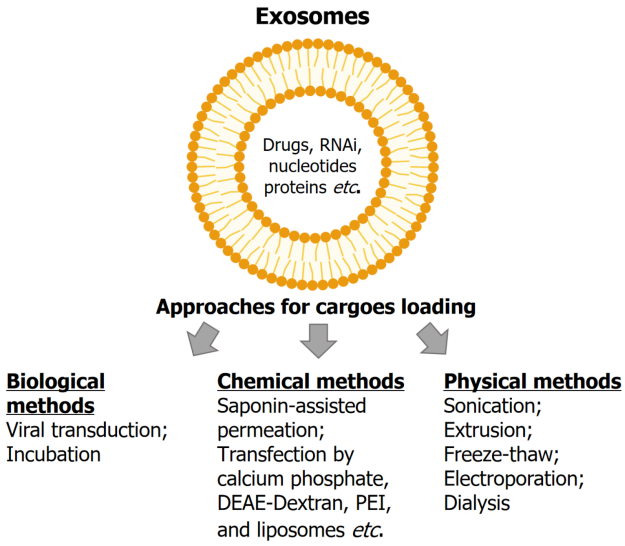

Figure 1 Schematic diagram of approaches for cargoes loading to exosomes. The scheme illustrates the approaches including biological, chemical, and physical methods, which are used to load cargoes, such as drugs, RNA interference, nucleotides, and proteins, into or onto the exosomes. RNAi: RNA interference; DEAE: Diethylaminoethyl; PEI: Polyethylenimine.

CONCLUSION

The study by Tang *et al*[17] marks a significant advancement in cancer therapy, particularly in the treatment of pancreatic cancer. The fabrication of Exo-GEM has been optimized. By demonstrating the enhanced cytotoxicity and apoptosis-inducing effects of Exo-GEM compared to free GEM, the research highlights the potential of exosome-based drug delivery systems as a more effective and targeted approach to chemotherapy[17]. Although further research is necessary to validate these findings *in vivo* and explore their clinical applications, this study establishes a strong foundation for a promising new direction in cancer treatment. The use of HU-BMSCs-derived exosomes for drug delivery could potentially address some of the major challenges in current cancer therapies, offering renewed hope for patients facing this devastating disease.

FOOTNOTES

Author contributions: Chew FY and Tsai CH contributed to writing, editing the manuscript, and review of literature; Chang KH, and Chang YK contributed to the discussion and review of the manuscript; Liu YJ and Chou RH contributed to the review, discussion, and

design the overall concept of the manuscript.

Supported by the grants of China Medical University Hospital, No. DMR-112-173 and No. DMR-113-089; and the grant from Tungs' Taichung Metro Harbor Hospital, No. TTMHH-R1120013.

Conflict-of-interest statement: The authors declare that they have no conflict of interest.

Country of origin: Taiwan

ORCID number: Fatt-Yang Chew 0000-0002-8965-6131; Ruey-Hwang Chou 0000-0002-2297-2180; Yi-Jui Liu 0000-0001-5865-6836.

S-Editor: Fan M
L-Editor: A
P-Editor: Zhao YQ

REFERENCES

1 **Pishvaian MJ**, Brody JR. Therapeutic Implications of Molecular Subtyping for Pancreatic Cancer. *Oncology (Williston Park)* 2017; **31**: 159-166, 168 [PMID: 28299752]
2 **Bardeesy N**, DePinho RA. Pancreatic cancer biology and genetics. *Nat Rev Cancer* 2002; **2**: 897-909 [PMID: 12459728 DOI: 10.1038/nrc949]
3 **Bond-Smith G**, Banga N, Hammond TM, Imber CJ. Pancreatic adenocarcinoma. *BMJ* 2012; **344**: e2476 [PMID: 22592847 DOI: 10.1136/bmj.e2476]
4 **Teague A**, Lim KH, Wang-Gillam A. Advanced pancreatic adenocarcinoma: a review of current treatment strategies and developing therapies. *Ther Adv Med Oncol* 2015; **7**: 68-84 [PMID: 25755680 DOI: 10.1177/1758834014564775]
5 **Blanco E**, Shen H, Ferrari M. Principles of nanoparticle design for overcoming biological barriers to drug delivery. *Nat Biotechnol* 2015; **33**: 941-951 [PMID: 26348965 DOI: 10.1038/nbt.3330]
6 **Di Bella MA**. Overview and Update on Extracellular Vesicles: Considerations on Exosomes and Their Application in Modern Medicine. *Biology (Basel)* 2022; **11** [PMID: 35741325 DOI: 10.3390/biology11060804]
7 **Chen H**, Wang L, Zeng X, Schwarz H, Nanda HS, Peng X, Zhou Y. Exosomes, a New Star for Targeted Delivery. *Front Cell Dev Biol* 2021; **9**: 751079 [PMID: 34692704 DOI: 10.3389/fcell.2021.751079]
8 **Kamerkar S**, LeBleu VS, Sugimoto H, Yang S, Ruivo CF, Melo SA, Lee JJ, Kalluri R. Exosomes facilitate therapeutic targeting of oncogenic KRAS in pancreatic cancer. *Nature* 2017; **546**: 498-503 [PMID: 28607485 DOI: 10.1038/nature22341]
9 **McAndrews KM**, Xiao F, Chronopoulos A, LeBleu VS, Kugeratski FG, Kalluri R. Exosome-mediated delivery of CRISPR/Cas9 for targeting of oncogenic Kras(G12D) in pancreatic cancer. *Life Sci Alliance* 2021; **4** [PMID: 34282051 DOI: 10.26508/lsa.202000875]
10 **Song H**, Liu B, Dong B, Xu J, Zhou H, Na S, Liu Y, Pan Y, Chen F, Li L, Wang J. Exosome-Based Delivery of Natural Products in Cancer Therapy. *Front Cell Dev Biol* 2021; **9**: 650426 [PMID: 33738290 DOI: 10.3389/fcell.2021.650426]
11 **Saari H**, Lázaro-Ibáñez E, Viitala T, Vuorimaa-Laukkanen E, Siljander P, Yliperttula M. Microvesicle- and exosome-mediated drug delivery enhances the cytotoxicity of Paclitaxel in autologous prostate cancer cells. *J Control Release* 2015; **220**: 727-737 [PMID: 26390807 DOI: 10.1016/j.jconrel.2015.09.031]
12 **Gomari H**, Forouzandeh Moghadam M, Soleimani M, Ghavami M, Khodashenas S. Targeted delivery of doxorubicin to HER2 positive tumor models. *Int J Nanomedicine* 2019; **14**: 5679-5690 [PMID: 31413568 DOI: 10.2147/IJN.S210731]
13 **Li YJ**, Wu JY, Wang JM, Hu XB, Cai JX, Xiang DX. Gemcitabine loaded autologous exosomes for effective and safe chemotherapy of pancreatic cancer. *Acta Biomater* 2020; **101**: 519-530 [PMID: 31629893 DOI: 10.1016/j.actbio.2019.10.022]
14 **Zhao Y**, Zheng Y, Zhu Y, Zhang Y, Zhu H, Liu T. M1 Macrophage-Derived Exosomes Loaded with Gemcitabine and Deferasirox against Chemoresistant Pancreatic Cancer. *Pharmaceutics* 2021; **13** [PMID: 34575569 DOI: 10.3390/pharmaceutics13091493]
15 **Klimova D**, Jakubechova J, Altanerova U, Nicodemou A, Styk J, Szemes T, Repiska V, Altaner C. Extracellular vesicles derived from dental mesenchymal stem/stromal cells with gemcitabine as a cargo have an inhibitory effect on the growth of pancreatic carcinoma cell lines in vitro. *Mol Cell Probes* 2023; **67**: 101894 [PMID: 36706931 DOI: 10.1016/j.mcp.2023.101894]
16 **Zhou Y**, Zhou W, Chen X, Wang Q, Li C, Chen Q, Zhang Y, Lu Y, Ding X, Jiang C. Bone marrow mesenchymal stem cells-derived exosomes for penetrating and targeted chemotherapy of pancreatic cancer. *Acta Pharm Sin B* 2020; **10**: 1563-1575 [PMID: 32963950 DOI: 10.1016/j.apsb.2019.11.013]
17 **Tang ZG**, Chen TM, Lu Y, Wang Z, Wang XC, Kong Y. Human bone marrow mesenchymal stem cell-derived exosomes loaded with gemcitabine inhibit pancreatic cancer cell proliferation by enhancing apoptosis. *World J Gastrointest Oncol* 2024; **16**: 4006-4013 [PMID: 39350998 DOI: 10.4251/wjgo.v16.i9.4006]
18 **Shi J**, Jiang X, Gao S, Zhu Y, Liu J, Gu T, Shi E. Gene-modified Exosomes Protect the Brain Against Prolonged Deep Hypothermic Circulatory Arrest. *Ann Thorac Surg* 2021; **111**: 576-585 [PMID: 32652066 DOI: 10.1016/j.athoracsur.2020.05.075]
19 **Brossa A**, Tapparo M, Fonsato V, Papadimitriou E, Delena M, Camussi G, Bussolati B. Coincubation as miR-Loading Strategy to Improve the Anti-Tumor Effect of Stem Cell-Derived EVs. *Pharmaceutics* 2021; **13** [PMID: 33429869 DOI: 10.3390/pharmaceutics13010076]
20 **Thakur A**, Sidu RK, Zou H, Alam MK, Yang M, Lee Y. Inhibition of Glioma Cells' Proliferation by Doxorubicin-Loaded Exosomes *via* Microfluidics. *Int J Nanomedicine* 2020; **15**: 8331-8343 [PMID: 33149579 DOI: 10.2147/IJN.S263956]
21 **Zhang D**, Lee H, Zhu Z, Minhas JK, Jin Y. Enrichment of selective miRNAs in exosomes and delivery of exosomal miRNAs in vitro and in

vivo. *Am J Physiol Lung Cell Mol Physiol* 2017; **312**: L110-L121 [PMID: 27881406 DOI: 10.1152/ajplung.00423.2016]

22 **Lokossou AG**, Toudic C, Nguyen PT, Elisseeff X, Vargas A, Rassart É, Lafond J, Leduc L, Bourgault S, Gilbert C, Scorza T, Tolosa J, Barbeau B. Endogenous retrovirus-encoded Syncytin-2 contributes to exosome-mediated immunosuppression of T cells†. *Biol Reprod* 2020; **102**: 185-198 [PMID: 31318021 DOI: 10.1093/biolre/ioz124]

23 **Zhupanyn P**, Ewe A, Büch T, Malek A, Rademacher P, Müller C, Reinert A, Jaimes Y, Aigner A. Extracellular vesicle (ECV)-modified polyethylenimine (PEI) complexes for enhanced siRNA delivery in vitro and in vivo. *J Control Release* 2020; **319**: 63-76 [PMID: 31866504 DOI: 10.1016/j.jconrel.2019.12.032]

24 **Wang H**, Chen FS, Zhang ZL, Zhou HX, Ma H, Li XQ. MiR-126-3p-Enriched Extracellular Vesicles from Hypoxia-Preconditioned VSC 4.1 Neurons Attenuate Ischaemia-Reperfusion-Induced Pain Hypersensitivity by Regulating the PIK3R2-Mediated Pathway. *Mol Neurobiol* 2021; **58**: 821-834 [PMID: 33029740 DOI: 10.1007/s12035-020-02159-y]

25 **Lamichhane TN**, Jeyaram A, Patel DB, Parajuli B, Livingston NK, Arumugasaamy N, Schardt JS, Jay SM. Oncogene Knockdown *via* Active Loading of Small RNAs into Extracellular Vesicles by Sonication. *Cell Mol Bioeng* 2016; **9**: 315-324 [PMID: 27800035 DOI: 10.1007/s12195-016-0457-4]

26 **Fuhrmann G**, Serio A, Mazo M, Nair R, Stevens MM. Active loading into extracellular vesicles significantly improves the cellular uptake and photodynamic effect of porphyrins. *J Control Release* 2015; **205**: 35-44 [PMID: 25483424 DOI: 10.1016/j.jconrel.2014.11.029]

27 **Hajipour H**, Farzadi L, Roshangar L, Latifi Z, Kahroba H, Shahnazi V, Hamdi K, Ghasemzadeh A, Fattahi A, Nouri M. A human chorionic gonadotropin (hCG) delivery platform using engineered uterine exosomes to improve endometrial receptivity. *Life Sci* 2021; **275**: 119351 [PMID: 33737084 DOI: 10.1016/j.lfs.2021.119351]

28 **Johnsen KB**, Gudbergsson JM, Skov MN, Christiansen G, Gurevich L, Moos T, Duroux M. Evaluation of electroporation-induced adverse effects on adipose-derived stem cell exosomes. *Cytotechnology* 2016; **68**: 2125-2138 [PMID: 26856590 DOI: 10.1007/s10616-016-9952-7]

29 **Jeyaram A**, Lamichhane TN, Wang S, Zou L, Dahal E, Kronstadt SM, Levy D, Parajuli B, Knudsen DR, Chao W, Jay SM. Enhanced Loading of Functional miRNA Cargo *via* pH Gradient Modification of Extracellular Vesicles. *Mol Ther* 2020; **28**: 975-985 [PMID: 31911034 DOI: 10.1016/j.ymthe.2019.12.007]

30 **de Liyis BG**, Nolan J, Maharjana MA. Fibroblast growth factor receptor 1-bound extracellular vesicle as novel therapy for osteoarthritis. *Biomedicine (Taipei)* 2022; **12**: 1-9 [PMID: 35836973 DOI: 10.37796/2211-8039.1308]

31 **Keshishyan S**, Sehdev V, Reeves D, Ray SD. Cytostatic Agents. *Side Effects of Drugs Annual* 2015 [DOI: 10.1016/bs.seda.2015.08.009]

32 **Stefańska K**, Józkowiak M, Angelova Volponi A, Shibli JA, Golkar-Narenji A, Antosik P, Bukowska D, Piotrowska-Kempisty H, Mozdziak P, Dzięgiel P, Podhorska-Okołów M, Zabel M, Dyszkiewicz-Konwińska M, Kempisty B. The Role of Exosomes in Human Carcinogenesis and Cancer Therapy-Recent Findings from Molecular and Clinical Research. *Cells* 2023; **12** [PMID: 36766698 DOI: 10.3390/cells12030356]

33 **Takahashi Y**, Nishikawa M, Shinotsuka H, Matsui Y, Ohara S, Imai T, Takakura Y. Visualization and in vivo tracking of the exosomes of murine melanoma B16-BL6 cells in mice after intravenous injection. *J Biotechnol* 2013; **165**: 77-84 [PMID: 23562828 DOI: 10.1016/j.jbiotec.2013.03.013]

34 **Riau AK**, Ong HS, Yam GHF, Mehta JS. Sustained Delivery System for Stem Cell-Derived Exosomes. *Front Pharmacol* 2019; **10**: 1368 [PMID: 31798457 DOI: 10.3389/fphar.2019.01368]

35 **Smyth T**, Kullberg M, Malik N, Smith-Jones P, Graner MW, Anchordoquy TJ. Biodistribution and delivery efficiency of unmodified tumor-derived exosomes. *J Control Release* 2015; **199**: 145-155 [PMID: 25523519 DOI: 10.1016/j.jconrel.2014.12.013]

36 **Shimizu A**, Sawada K, Kobayashi M, Oi Y, Oride T, Kinose Y, Kodama M, Hashimoto K, Kimura T. Patient-Derived Exosomes as siRNA Carriers in Ovarian Cancer Treatment. *Cancers (Basel)* 2024; **16** [PMID: 38672564 DOI: 10.3390/cancers16081482]

37 **Wiklander OP**, Nordin JZ, O'Loughlin A, Gustafsson Y, Corso G, Mäger I, Vader P, Lee Y, Sork H, Seow Y, Heldring N, Alvarez-Erviti L, Smith CI, Le Blanc K, Macchiarini P, Jungebluth P, Wood MJ, Andaloussi SE. Extracellular vesicle in vivo biodistribution is determined by cell source, route of administration and targeting. *J Extracell Vesicles* 2015; **4**: 26316 [PMID: 25899407 DOI: 10.3402/jev.v4.26316]

38 **Escudier B**, Dorval T, Chaput N, André F, Caby MP, Novault S, Flament C, Leboulaire C, Borg C, Amigorena S, Boccaccio C, Bonnerot C, Dhellin O, Movassagh M, Piperno S, Robert C, Serra V, Valente N, Le Pecq JB, Spatz A, Lantz O, Tursz T, Angevin E, Zitvogel L. Vaccination of metastatic melanoma patients with autologous dendritic cell (DC) derived-exosomes: results of thefirst phase I clinical trial. *J Transl Med* 2005; **3**: 10 [PMID: 15740633 DOI: 10.1186/1479-5876-3-10]

39 **Morse MA**, Garst J, Osada T, Khan S, Hobeika A, Clay TM, Valente N, Shreeniwas R, Sutton MA, Delcayre A, Hsu DH, Le Pecq JB, Lyerly HK. A phase I study of dexosome immunotherapy in patients with advanced non-small cell lung cancer. *J Transl Med* 2005; **3**: 9 [PMID: 15723705 DOI: 10.1186/1479-5876-3-9]

40 **Besse B**, Charrier M, Lapierre V, Dansin E, Lantz O, Planchard D, Le Chevalier T, Livartoski A, Barlesi F, Laplanche A, Ploix S, Vimond N, Peguillet I, Théry C, Lacroix L, Zoernig I, Dhodapkar K, Dhodapkar M, Viaud S, Soria JC, Reiners KS, Pogge von Strandmann E, Vély F, Rusakiewicz S, Eggermont A, Pitt JM, Zitvogel L, Chaput N. Dendritic cell-derived exosomes as maintenance immunotherapy after first line chemotherapy in NSCLC. *Oncoimmunology* 2016; **5**: e1071008 [PMID: 27141373 DOI: 10.1080/2162402X.2015.1071008]

World Journal of Gastrointestinal Oncology

Submit a Manuscript: https://www.f6publishing.com

World J Gastrointest Oncol 2025 January 15; 17(1): 101477

DOI: 10.4251/wjgo.v17.i1.101477

ISSN 1948-5204 (online)

EDITORIAL

Unraveling the landscape of pediatric pancreatic tumors: Insights from Japan

Savvas Lampridis

Specialty type: Oncology

Provenance and peer review: Invited article; Externally peer reviewed.

Peer-review model: Single blind

Peer-review report's classification

Scientific Quality: Grade A, Grade B

Novelty: Grade A, Grade B

Creativity or Innovation: Grade A, Grade B

Scientific Significance: Grade A, Grade B

P-Reviewer: Haworth IS; Wen J

Received: September 15, 2024

Revised: October 3, 2024

Accepted: October 18, 2024

Published online: January 15, 2025

Processing time: 87 Days and 16.4 Hours

Savvas Lampridis, Faculty of Medicine, Imperial College London, London SW7 2AZ, United Kingdom

Savvas Lampridis, Department of Surgical Oncology, 424 General Military Training Hospital, Thessaloniki 56429, Greece

Corresponding author: Savvas Lampridis, MD, MSc, Editor-in-Chief, Researcher, Surgical Oncologist, Faculty of Medicine, Imperial College London, South Kensington Campus, London SW7 2AZ, United Kingdom. savvas.lampridis@doctors.org.uk

Abstract

Pediatric pancreatic tumors, though rare, pose significant diagnostic and management challenges. The recent, 22-year nationwide survey on pediatric pancreatic tumors in Japan by Makita *et al* offers valuable insights into this uncommon entity, revealing striking geographical variations and questioning current treatment paradigms. This editorial commentary analyzes the study's key findings, including the predominance of solid pseudopapillary neoplasms and their younger age of onset, which contrast sharply with Western data. It explores the implications for clinical practice and research, emphasizing the need for population-specific approaches to diagnosis and treatment. The revealed limited institutional experience and surgical management patterns prompt a reevaluation of optimal care delivery for these complex cases, suggesting benefits of centralizing healthcare services. Furthermore, the commentary advocates for international collaborative studies to elucidate the genetic, environmental, and lifestyle factors influencing the development and progression of pediatric pancreatic tumors across diverse populations. It also outlines future directions, calling for advancements in precision medicine and innovative care delivery models to improve global patient outcomes. Unraveling Makita *et al*'s findings within the broader landscape of pediatric oncology can stimulate further research and clinical advancements in managing pancreatic and other rare tumors in children.

Key Words: Child; Epidemiology; Japan; Pancreatic endocrine tumors; Pancreatic neoplasms; Pancreatoblastoma; Pediatric oncology; Solid pseudopapillary neoplasm; Surgical management; Survey

Core Tip: This editorial analyzes a 22-year nationwide survey on pediatric pancreatic tumors in Japan. The predominance of solid pseudopapillary neoplasms and their younger age of onset contrast sharply with Western data, highlighting the need for population-specific approaches. Centralizing healthcare services could address the limited experience with these rare tumors observed at many institutions. The commentary also advocates for precision medicine, innovative care delivery models, and international collaborative studies on genetic and environmental factors across diverse populations. These insights could significantly improve the diagnosis, treatment, and management of pediatric pancreatic and other rare neoplasms globally, stimulating further research and clinical advancements.

Citation: Lampridis S. Unraveling the landscape of pediatric pancreatic tumors: Insights from Japan. *World J Gastrointest Oncol* 2025; 17(1): 101477
URL: https://www.wjgnet.com/1948-5204/full/v17/i1/101477.htm
DOI: https://dx.doi.org/10.4251/wjgo.v17.i1.101477

INTRODUCTION

Pediatric pancreatic tumors represent rare but formidable adversaries in childhood oncology. These neoplasms, accounting for less than 0.1% of all pediatric cancers, include a diverse spectrum of histological types, each with its own prognostic implications[1-4]. Despite their rarity, most pancreatic tumors present significant diagnostic and therapeutic challenges, frequently resulting in suboptimal outcomes[5,6]. The complex nature of these tumors, coupled with the vital physiological functions of the pancreas, demands a nuanced approach to treatment: One that carefully balances aggressive intervention with organ preservation, particularly in growing children.

In this issue of the *World Journal of Gastrointestinal Oncology*, Makita *et al*[7] present a nationwide survey on pediatric pancreatic tumors in Japan, offering a fresh perspective on this uncommon entity. By meticulously documenting 213 cases over a 22-year period, the authors have provided a comprehensive view of the epidemiological landscape, management strategies, and patient outcomes in a large Asian pediatric cohort. The results include a wide range of tumor types, from solid pseudopapillary neoplasms to endocrine tumors and pancreatoblastomas, providing valuable insights into their relative frequencies, clinical presentations, and treatment approaches. The authors also shed light on the surgical experiences across different institutions, highlighting the challenges in managing these rare tumors. This extensive survey not only contributes significantly to our understanding of pediatric pancreatic tumors in Japan but also provides an important point of comparison with data from other countries, revealing important geographical and ethnic variations in disease patterns.

INSIGHTS AND IMPLICATIONS

The striking predominance of solid pseudopapillary neoplasms in the Japanese pediatric population, accounting for 77% of all cases[7], stands as one of the most significant study findings. This figure sharply contrasts with Western data, where solid pseudopapillary neoplasms typically represent only 30%-32% of pediatric pancreatic tumors[1,2]. Such a marked disparity challenges our current understanding of the relevant epidemiology and raises critical questions about underlying causative factors. Genetic predisposition emerges as a potential explanation for this phenomenon. The *CTNNB1* gene mutation, affecting β-catenin and considered a hallmark of solid pseudopapillary neoplasms of the pancreas[8,9], may have a higher prevalence or penetrance in the Japanese population. This hypothesis opens new avenues for research into population-specific genetic markers for pancreatic tumor risk. It underscores the need for large-scale genomic studies across diverse populations to illuminate the complex interplay between genetics and tumor development. Environmental factors also warrant investigation. Could distinctive aspects of the Japanese lifestyle, such as dietary habits rich in soy products[10], influence the risk profile for specific pancreatic tumor types? The potential impact of other environmental exposures unique to Japan remains an area ripe for exploration.

To provide insights into the relative frequency of different tumor types, the findings from Japan can be contextualized by comparing them with data from other regions. In the United States, the Surveillance, Epidemiology, and End Results database[1] reveals a more balanced distribution of tumor types, with neuroendocrine tumors (33.8%) and solid pseudopapillary neoplasms (32.3%) occurring at almost equal rates. Additionally, a National Cancer Database study[2] in the United States reported a higher frequency of pancreatoblastoma (15.6%) compared to Japan (7.5%). European data also demonstrate variations. For instance, the Italian Tumori Rari in Età Pediatrica project documented an intermediate prevalence of solid pseudopapillary tumors (12 of 21 cases) over a 10-year period, while pancreatoblastomas were relatively more common (4 of 21 cases) than in Japan[11]. Interestingly, a single-institution study from China, conducted over 15 years, found that 5 out of 11 adolescents with pancreatic tumors treated with resection were diagnosed with solid pseudopapillary neoplasms, a finding that aligns more closely with the Japanese data[12]. In this study, the same number of patients were found to have neuroendocrine tumors, while one patient was diagnosed with pancreatic ductal adenocarcinoma. These comparisons highlight the geographical variations in pediatric pancreatic tumor distribution and show the importance of region-specific epidemiological understanding.

The high relative frequency of solid pseudopapillary neoplasms in Japanese children carries significant implications also for clinical practice. It suggests that clinicians in Japan should maintain a high level of suspicion for this histological type when evaluating pediatric pancreatic tumors. Conversely, clinicians in Western countries, such as the United States and United Kingdom, should remain vigilant for other tumor types that are equally or more prevalent in their populations, including endocrine tumors and pancreatoblastoma[1,2]. This geographical variation in tumor type distribution highlights the need for region-specific clinical approaches to diagnosis and management. From a research standpoint, this difference underscores the importance of international studies to elucidate the global landscape of pediatric pancreatic tumors. Such collaborative efforts could pave the way for the development of population-specific risk assessment tools, potentially improving early detection and patient outcomes across different ethnic groups.

Another key finding in the study by Makita *et al*[7] is the relatively young age at onset for solid pseudopapillary neoplasms in the Japanese cohort. The median presentation age of approximately 12 years is significantly lower than that reported in Western and Taiwanese data[1,2,13,14], revealing variations even within Asian populations. This earlier presentation has important implications for early detection strategies and challenges current screening practices for high-risk groups. Moreover, this gap in age of onset suggests that a uniform strategy for managing pediatric pancreatic tumors may be insufficient. This finding also prompts questions about potential modifiable risk factors contributing to earlier onset in certain populations. Tailored, population-based approaches should be employed to enhance prevention, early detection, and overall outcomes.

The surgical management patterns revealed in the study by Makita *et al*[7] highlight a significant challenge in pediatric oncology. Nearly 52% of the surveyed institutions across Japan had no experience with pancreatic tumor surgery in children over the study period. This striking statistic mirrors trends in the United States, where even the largest children's hospitals report an average of only 1-2 patients with pancreatic neoplasms per year[15,16]. This paucity of cases presents a serious obstacle to developing and maintaining surgical expertise, supporting the argument for centralization of care for these rare and complex cases. Centralization could concentrate expertise, thereby improving outcomes through higher case volumes and standardized care protocols[17,18]. Nevertheless, this approach raises questions about maintaining a distributed knowledge base within the broader pediatric surgical community, crucial for initial recognition and appropriate referral of these rare cases. Consequently, it may lead to delayed diagnosis and treatment, especially in geographically diverse countries like Japan[18,19]. Balancing the concentration of expertise with accessibility of care represents a key challenge in optimizing the management of rare pediatric cancers, such as pancreatic tumors.

Building on the challenges of surgical management, the study by Makita *et al*[7] further reveals that adult gastrointestinal surgeons were involved in roughly 40% of pediatric pancreatic tumor cases. This pattern highlights the need for cross-specialty expertise and prompts a reevaluation of training requirements for these complex procedures. While the current collaborative model between pediatric and adult specialists has yielded favorable outcomes, as evidenced by the reported survival rates, there remains scope for improvement. Developing specialized training programs for pediatric pancreatic surgery could strengthen the expertise of pediatric surgeons in this rare but critical field. However, the rarity of these tumors poses challenges in maintaining proficiency. A more pragmatic approach may involve establishing centers of excellence where pediatric surgeons can gain focused experience in pancreatic procedures while leveraging the expertise of adult gastrointestinal surgeons. This hybrid model could synergize pediatric-specific knowledge of child physiology and care with the technical proficiency of high-volume pancreatic surgeons. This integrated approach aligns with the concept of centralization discussed earlier, offering a potential solution to balance the concentration of expertise with the need for comprehensive pediatric care. By fostering collaboration between pediatric and adult specialists, such centers could address both the surgical complexity of these rare tumors and the unique needs of pediatric patients.

While the study by Makita *et al*[7] offers valuable insights, it is important to acknowledge and analyze its limitations. The retrospective, questionnaire-based design introduces several potential biases. Recall bias may affect the accuracy of data, particularly for cases from the earlier years of the 22-year study period. Additionally, there is a risk of selection bias favoring high-volume centers, potentially skewing the data towards more complex cases. The extended study period also raises concerns about the consistency of diagnostic criteria across different centers and over time, which may impact the comparability of cases.

Another limitation of the study is the exclusion of non-surgically treated cases. This approach may underestimate the true incidence of pancreatic tumors, particularly advanced or unresectable cases, leading to an incomplete picture of the full spectrum of pediatric pancreatic tumors in Japan. The study's focus on surgical cases omits valuable information about tumors managed non-operatively, potentially biasing the overall understanding of disease presentation and management.

The limited institutional experience highlighted in the study is also noteworthy. With 75 of 145 responding facilities reporting no experience with pediatric pancreatic tumor surgery over the 22-year period, and only 4 facilities managing more than 10 cases, the rarity of these tumors and the challenge in building expertise become apparent. This disparity in experience may influence the generalizability of the findings and highlights the need for centralized expertise in managing these rare cases.

Another limitation is the potential underrepresentation of certain patient groups. The survey was administered only to pediatric surgical units, potentially missing cases treated solely by adult gastrointestinal surgeons. This may particularly affect the representation of solid pseudopapillary neoplasms in older teenagers, whose care might be managed by adult surgeons due to their physical maturity. Consequently, the study might not capture the full spectrum of pediatric pancreatic tumors, especially in the adolescent population.

The lack of standardized data collection across institutions poses another challenge. This may result in inconsistencies in reporting and limit the ability to perform more granular analyses of factors such as specific surgical techniques or detailed pathological findings. The variability in data reporting could impact the reliability and comparability of the results across different centers.

To address these limitations and improve future studies, several strategies can be implemented. Establishing a prospective, multi-institutional registry with standardized data collection protocols would ensure consistency across centers and reduce recall bias. Such a registry should include all cases of pediatric pancreatic tumors, regardless of treatment approach, and incorporate regular quality checks and data audits to maintain accuracy.

Expanding data collection to include detailed pathological and molecular profiling of tumors, long-term follow-up data, and quality of life measures would provide a more comprehensive understanding of disease progression and treatment outcomes. Collaboration with adult gastrointestinal surgery departments is necessary to ensure comprehensive coverage of all pediatric cases, including those treated by adult surgeons.

Utilization of national databases, such as the National Clinical Database in Japan, would allow for more comprehensive case capture and validation of questionnaire-based data. This integration would provide a more accurate representation of the incidence and management of pediatric pancreatic tumors across all healthcare settings. Furthermore, establishing an international collaborative network would facilitate standardized data collection across different countries, enabling more robust international comparisons. Such collaboration could also pool resources for centralized pathology review and molecular analysis, ensuring consistency in diagnosis and classification across diverse populations.

FUTURE DIRECTIONS

The study by Makita *et al*[7] catalyzes broader discussions regarding rare pediatric neoplasms, such as pancreatic tumors. Their findings highlight the importance of understanding genetic, environmental, and lifestyle factors influencing these rare tumors across diverse populations. By pooling global data and resources, we can construct a more comprehensive picture of pediatric pancreatic tumors, aligning with the growing emphasis on precision medicine in oncology. Advanced genomic and proteomic profiling could reveal early detection biomarkers and novel therapeutic targets, paving the way for personalized treatment strategies that can improve outcomes while minimizing toxicity in young patients. The marked differences in tumor type distribution between Japanese and Western populations underscore the significance of geographic and ethnic variations in disease patterns, echoing recent calls for more diverse representation in cancer genomics studies[20]. As precision medicine advances, understanding these population-specific differences becomes crucial for developing targeted therapies and personalized treatment approaches, potentially revolutionizing pediatric oncology.

The insights from Makita *et al*[7] extend beyond scientific understanding. The study's revelation of limited institutional experience with rare pediatric pancreatic tumors highlights the importance of democratizing access to expertise. Virtual tumor boards and telemedicine networks could ensure that every child, regardless of location, benefits from the collective knowledge of the pediatric oncology community[21,22]. Coupled with standardized treatment protocols and quality metrics specific to pediatric pancreatic tumors, this approach could bridge the gap between high-volume centers and community hospitals, enhancing care quality and consistency across diverse healthcare settings.

As we look to the future, the work of Makita *et al*[7] serves as both a valuable resource and a call to action. It challenges us to think globally while acting locally. By embracing a holistic approach that combines collaborative research, precision medicine, and innovative care delivery, we can work towards a future where every child with a pancreatic tumor has access to optimal, evidence-based care. While the path forward may be challenging, the potential to transform outcomes for these young patients makes it a journey worth undertaking. As we advance, it is essential to maintain focus on the individual child at the center of our efforts, ensuring that our scientific and clinical progress translates into tangible benefits for patients and their families.

CONCLUSION

The nationwide survey by Makita *et al*[7] provides crucial insights into pediatric pancreatic tumors in Japan, highlighting important trends and challenges in their management. The predominance of solid pseudopapillary neoplasms in the Japanese cohort and the varying surgical experiences across institutions emphasize the need for further research and international collaboration. This study should serve as a steppingstone for more comprehensive, prospective investigations to validate and expand upon these findings. By integrating the lessons learned from this survey with ongoing advances in molecular diagnostics and precision medicine, we can work towards improving outcomes for children with rare tumors worldwide. The pediatric oncology community must continue to foster global collaboration and knowledge sharing to address the unique challenges posed by rare but impactful neoplasms.

FOOTNOTES

Author contributions: Lampridis S wrote the manuscript.

Conflict-of-interest statement: The author has no conflicts of interest to declare.

Country of origin: United Kingdom

ORCID number: Savvas Lampridis 0000-0003-2827-5826.

S-Editor: Qu XL
L-Editor: A
P-Editor: Wang WB

REFERENCES

1 **Qi X**, Zhou B, Liang F, Wang X. Prognostic factors of pancreatic tumors in children and adolescents: a population study based on the surveillance, epidemiology, and end results database. *BMC Gastroenterol* 2024; **24**: 108 [PMID: 38486208 DOI: 10.1186/s12876-024-03194-y]
2 **Picado O**, Ferrantella A, Zabalo C, Rao K, Thorson CM, Sola JE, Perez EA. Treatment patterns and outcomes for pancreatic tumors in children: an analysis of the National Cancer Database. *Pediatr Surg Int* 2020; **36**: 357-363 [PMID: 31989243 DOI: 10.1007/s00383-020-04617-z]
3 **Mostafa ME**, Erbarut-Seven I, Pehlivanoglu B, Adsay V. Pathologic classification of "pancreatic cancers": current concepts and challenges. *Chin Clin Oncol* 2017; **6**: 59 [PMID: 29307199 DOI: 10.21037/cco.2017.12.01]
4 **Chung EM**, Travis MD, Conran RM. Pancreatic tumors in children: radiologic-pathologic correlation. *Radiographics* 2006; **26**: 1211-1238 [PMID: 16844942 DOI: 10.1148/rg.264065012]
5 **Patterson KN**, Trout AT, Shenoy A, Abu-El-Haija M, Nathan JD. Solid pancreatic masses in children: A review of current evidence and clinical challenges. *Front Pediatr* 2022; **10**: 966943 [PMID: 36507125 DOI: 10.3389/fped.2022.966943]
6 **Grosfeld JL**, Vane DW, Rescorla FJ, McGuire W, West KW. Pancreatic tumors in childhood: analysis of 13 cases. *J Pediatr Surg* 1990; **25**: 1057-1062 [PMID: 2262858 DOI: 10.1016/0022-3468(90)90218-x]
7 **Makita S**, Uchida H, Kano M, Kawakubo N, Miyake H, Yoneda A, Tajiri T, Fukumoto K. Nationwide questionnaire survey on pediatric pancreatic tumors in Japan. *World J Gastrointest Oncol* 2024; **16**: 4166-4176 [DOI: 10.4251/wjgo.v16.i10.4166]
8 **Selenica P**, Raj N, Kumar R, Brown DN, Arqués O, Reidy D, Klimstra D, Snuderl M, Serrano J, Palmer HG, Weigelt B, Reis-Filho JS, Scaltriti M. Solid pseudopapillary neoplasms of the pancreas are dependent on the Wnt pathway. *Mol Oncol* 2019; **13**: 1684-1692 [PMID: 30972907 DOI: 10.1002/1878-0261.12490]
9 **Guo M**, Luo G, Jin K, Long J, Cheng H, Lu Y, Wang Z, Yang C, Xu J, Ni Q, Yu X, Liu C. Somatic Genetic Variation in Solid Pseudopapillary Tumor of the Pancreas by Whole Exome Sequencing. *Int J Mol Sci* 2017; **18** [PMID: 28054945 DOI: 10.3390/ijms18010081]
10 **Yamagiwa Y**, Sawada N, Shimazu T, Yamaji T, Goto A, Takachi R, Ishihara J, Iwasaki M, Inoue M, Tsugane S; JPHC Study Group. Soy Food Intake and Pancreatic Cancer Risk: The Japan Public Health Center-based Prospective Study. *Cancer Epidemiol Biomarkers Prev* 2020; **29**: 1214-1221 [PMID: 32169996 DOI: 10.1158/1055-9965.EPI-19-1254]
11 **Dall'igna P**, Cecchetto G, Bisogno G, Conte M, Chiesa PL, D'Angelo P, De Leonardis F, De Salvo G, Favini F, Ferrari A; TREP Group. Pancreatic tumors in children and adolescents: the Italian TREP project experience. *Pediatr Blood Cancer* 2010; **54**: 675-680 [PMID: 19998473 DOI: 10.1002/pbc.22385]
12 **Yao L**, Xie ZB, Jin C, Jiang YJ, Li J, Yang F, Lin QJ, Fu DL. Radical resection and enucleation in Chinese adolescents with pancreatic tumors: A 15-year case series. *Medicine (Baltimore)* 2017; **96**: e6438 [PMID: 28328854 DOI: 10.1097/MD.0000000000006438]
13 **Lin YJ**, Burkhart R, Lu TP, Wolfgang C, Wright M, Zheng L, Wu HY, Chen CH, Lee SY, Wu CH, He J, Tien YW. Solid Pseudopapillary Neoplasms of the Pancreas Across Races Demonstrate Disparities with Comparably Good Prognosis. *World J Surg* 2022; **46**: 3072-3080 [PMID: 36066663 DOI: 10.1007/s00268-022-06717-4]
14 **Leraas HJ**, Kim J, Sun Z, Ezekian B, Gulack BC, Reed CR, Tracy ET. Solid Pseudopapillary Neoplasm of the Pancreas in Children and Adults: A National Study of 369 Patients. *J Pediatr Hematol Oncol* 2018; **40**: e233-e236 [PMID: 29240036 DOI: 10.1097/MPH.0000000000001049]
15 **Rojas Y**, Warneke CL, Dhamne CA, Tsao K, Nuchtern JG, Lally KP, Vasudevan SA, Hayes-Jordan AA, Cass DL, Herzog CE, Hicks MJ, Kim ES, Austin MT. Primary malignant pancreatic neoplasms in children and adolescents: a 20 year experience. *J Pediatr Surg* 2012; **47**: 2199-2204 [PMID: 23217876 DOI: 10.1016/j.jpedsurg.2012.09.005]
16 **Yu DC**, Kozakewich HP, Perez-Atayde AR, Shamberger RC, Weldon CB. Childhood pancreatic tumors: a single institution experience. *J Pediatr Surg* 2009; **44**: 2267-2272 [PMID: 20006007 DOI: 10.1016/j.jpedsurg.2009.07.078]
17 **Grosman-Rimon L**, Li DHY, Collins BE, Wegier P. Can we improve healthcare with centralized management systems, supported by information technology, predictive analytics, and real-time data?: A review. *Medicine (Baltimore)* 2023; **102**: e35769 [PMID: 37960822 DOI: 10.1097/MD.0000000000035769]
18 **Sinsky CA**, Bavafa H, Roberts RG, Beasley JW. Standardization vs Customization: Finding the Right Balance. *Ann Fam Med* 2021; **19**: 171-177 [PMID: 33685879 DOI: 10.1370/afm.2654]
19 **Shinjo D**, Aramaki T. Geographic distribution of healthcare resources, healthcare service provision, and patient flow in Japan: a cross sectional study. *Soc Sci Med* 2012; **75**: 1954-1963 [PMID: 22920275 DOI: 10.1016/j.socscimed.2012.07.032]
20 **Spratt DE**, Chan T, Waldron L, Speers C, Feng FY, Ogunwobi OO, Osborne JR. Racial/Ethnic Disparities in Genomic Sequencing. *JAMA Oncol* 2016; **2**: 1070-1074 [PMID: 27366979 DOI: 10.1001/jamaoncol.2016.1854]
21 **AkbariRad M**, Keshvardoost S, Shariatmadari H, Firoozi A, Moodi Ghalibaf A. Virtual tumor boards: An approach to equity in cancer care. *Health Promot Perspect* 2023; **13**: 166-167 [PMID: 37808940 DOI: 10.34172/hpp.2023.23]
22 **Marshall CL**, Petersen NJ, Naik AD, Vander Velde N, Artinyan A, Albo D, Berger DH, Anaya DA. Implementation of a regional virtual tumor board: a prospective study evaluating feasibility and provider acceptance. *Telemed J E Health* 2014; **20**: 705-711 [PMID: 24845366 DOI: 10.1089/tmj.2013.0320]

World Journal of Gastrointestinal Oncology

Submit a Manuscript: https://www.f6publishing.com

World J Gastrointest Oncol 2025 January 15; 17(1): 96702

DOI: 10.4251/wjgo.v17.i1.96702

ISSN 1948-5204 (online)

ORIGINAL ARTICLE

Case Control Study

Activin A receptor type 1C single nucleotide polymorphisms associated with esophageal squamous cell carcinoma risk in Chinese population

Si-Yun Lin, Hou Huang, Jin-Jie Yu, Feng Su, Tian Jiang, Shao-Yuan Zhang, Lu Lv, Tao Long, Hui-Wen Pan, Jun-Qing Qi, Qiang Zhou, Wei-Feng Tang, Guo-Wen Ding, Li-Ming Wang, Li-Jie Tan, Jun Yin

Specialty type: Oncology

Provenance and peer review: Unsolicited article; Externally peer reviewed.

Peer-review model: Single blind

Peer-review report's classification

Scientific Quality: Grade C, Grade C

Novelty: Grade B, Grade C

Creativity or Innovation: Grade B, Grade C

Scientific Significance: Grade B, Grade C

P-Reviewer: Luo X; Zhan X

Received: May 13, 2024

Revised: September 1, 2024

Accepted: October 14, 2024

Published online: January 15, 2025

Processing time: 212 Days and 18.8 Hours

Si-Yun Lin, Jin-Jie Yu, Feng Su, Tian Jiang, Shao-Yuan Zhang, Li-Jie Tan, Jun Yin, Department of Thoracic Surgery, Zhongshan Hospital Affiliated to Fudan University, Shanghai 200032, China

Si-Yun Lin, Hou Huang, Shanghai Key Laboratory of Clinical Geriatric Medicine, Huadong Hospital Affiliated to Fudan University, Shanghai 200040, China

Lu Lv, Tao Long, Hui-Wen Pan, Jun-Qing Qi, Guo-Wen Ding, Department of Cardiothoracic Surgery, The Affiliated People's Hospital of Jiangsu University, Zhenjiang 212002, Jiangsu Province, China

Qiang Zhou, Department of Thoracic Surgery, Sichuan Cancer Hospital & Institute, Chengdu 610042, Sichuan Province, China

Wei-Feng Tang, Department of Cardiothoracic Surgery, Nanjing Drum Tower Hospital, The Affiliated Hospital of Nanjing University Medical School, Nanjing 210000, Jiangsu Province, China

Li-Ming Wang, Department of Respiratory and Critical Care Medicine, Shanghai Xuhui Central Hospital, Shanghai 200032, China

Co-first authors: Si-Yun Lin and Hou Huang.

Co-corresponding authors: Li-Jie Tan and Jun Yin.

Corresponding author: Jun Yin, MD, PhD, Professor, Department of Thoracic Surgery, Zhongshan Hospital Affiliated to Fudan University, No. 180 Fenglin Road, Xuhui District, Shanghai 200032, China. jun_yin@fudan.edu.cn

Abstract

BACKGROUND

Transforming growth factor-β (TGF-β) superfamily plays an important role in tumor progression and metastasis. Activin A receptor type 1C (ACVR1C) is a TGF-β type I receptor that is involved in tumorigenesis through binding to different ligands.

AIM
To evaluate the correlation between single nucleotide polymorphisms (SNPs) of ACVR1C and susceptibility to esophageal squamous cell carcinoma (ESCC) in Chinese Han population.

METHODS
In this hospital-based cohort study, 1043 ESCC patients and 1143 healthy controls were enrolled. Five SNPs (rs4664229, rs4556933, rs77886248, rs77263459, rs6734630) of ACVR1C were assessed by the ligation detection reaction method. Hardy-Weinberg equilibrium test, genetic model analysis, stratified analysis, linkage disequilibrium test, and haplotype analysis were conducted.

RESULTS
Participants carrying ACVR1C rs4556933 GA mutant had significantly decreased risk of ESCC, and those with rs77886248 TA mutant were related with higher risk, especially in older male smokers. In the haplotype analysis, ACVR1C $T_{rs4664229}A_{rs4556933}T_{rs77886248}C_{rs77263459}A_{rs6734630}$ increased risk of ESCC, while $T_{rs4664229}G_{rs4556933}T_{rs77886248}C_{rs77263459}A_{rs6734630}$ was associated with lower susceptibility to ESCC.

CONCLUSION
ACVR1C rs4556933 and rs77886248 SNPs were associated with the susceptibility to ESCC, which could provide a potential target for early diagnosis and treatment of ESCC in Chinese Han population.

Key Words: Activin A receptor type 1C; Single nucleotide polymorphisms; Esophageal squamous cell carcinoma; Genetic susceptibility; Hospital-based cohort study

Core Tip: In this study, a case-control approach was used to investigate the association between specific single nucleotide polymorphisms (SNPs) of the *ACVR1C* gene and the risk of esophageal squamous cell carcinoma (ESCC) in a Chinese Han population. The study included 2186 participants, comprising 1043 ESCC patients and 1143 healthy controls. Notably, the rs4556933 G>A SNP was significantly associated with ESCC risk across several genetic models. Stratified analysis indicated an increased risk in older males and smokers. These findings suggest that *ACVR1C* SNPs play a critical role in ESCC susceptibility, meriting further investigation into their involvement in cancer development.

Citation: Lin SY, Huang H, Yu JJ, Su F, Jiang T, Zhang SY, Lv L, Long T, Pan HW, Qi JQ, Zhou Q, Tang WF, Ding GW, Wang LM, Tan LJ, Yin J. Activin A receptor type 1C single nucleotide polymorphisms associated with esophageal squamous cell carcinoma risk in Chinese population. *World J Gastrointest Oncol* 2025; 17(1): 96702
URL: https://www.wjgnet.com/1948-5204/full/v17/i1/96702.htm
DOI: https://dx.doi.org/10.4251/wjgo.v17.i1.96702

INTRODUCTION

Esophageal cancer (EC) is a common malignancy of the upper digestive tract. The International Agency for Research on Cancer reported approximately 604000 new cases of EC, ranking seventh, and 540000 deaths, ranking sixth, worldwide in 2020[1]. The incidence of EC varies regionally, with China presenting a high-incidence area, with new cases accounting for over half of the global total count[2]. Moreover, in contrast to patients of Western origin, the pathological type detected in most Chinese patients is esophageal squamous cell carcinoma (ESCC).

The onset of ESCC is frequently inconsistent. Genetic, epigenetic, and environmental factors significantly contribute to ESCC pathogenesis; smoking and alcohol consumption are crucial exogenous risk factors[3]. Additionally, unhealthy dietary habits, such as hot eating, uneven intake, and excessive intake of pickled products, can increase the risk of tumorigenesis. Gene and chromosomal abnormalities are closely related to the occurrence and development of heterogeneity, a major characteristic of tumors. Therefore, further genetic studies are necessary to explore the pathogenic processes of ESCC and its association with genetic abnormalities, including single nucleotide polymorphisms (SNP), the most common type of genetic variation.

Activin A receptor type 1C (ACVR1C) is a transforming growth factor-β (TGF-β) type I receptor, with a single-span transmembrane domain, which is also known as activin receptor-like kinase 7 (ALK7). The receptors for TGF-β superfamily ligands comprise quadruplex complexes with two homodimers of type I and type II subunits[4]. More than thirty-five TGF-β superfamily receptors have been found in mammals[5,6]. The TGF-β superfamily includes TGF-β1-3, activins A and B, inhibins, growth differentiation factors, bone morphogenetic proteins, nodal proteins, and other ligand components; they are involved in cell proliferation, differentiation, adhesion, wound healing, and immune responses through binding in various ways[7]. Numerous studies have demonstrated the magnitude of TGF-β superfamily cytokines during tumor progression; the differential activities of TGF-βs and their core receptors in metastatic phenotypes

present the most crucial part of its involvement in tumorigenesis[8]. Therefore, the regular expression and functions of the TGF-β superfamily play a critical role in maintaining the stability of the organism.

ACVR1C is the seventh and most recently identified member of the type-I receptor subfamily. ACVR1C is highly expressed in tissues and cell types with endocrine or neuroendocrine functions compared with other TGF-β receptors, thus exhibiting its correlation with obesity, type II diabetes, and metabolic syndrome[9]. Early studies elucidated the large amount of mRNA expression encoding ALK7 in the adipose tissue, gastrointestinal tract, ovary, prostate, pancreas, and a few brain nuclei, especially in the cerebellum[10-12]. Moreover, it is involved in cancer-related apoptosis and cell proliferation *in vitro*. ACVR1C and its ligand Nodal have pro-apoptotic effects in various cancer cells, including breast cancer [13,14]. However, contrasting reports are also available[15,16]. Additionally, ACVR1C signaling acts as a homeostatic tissue barrier against tumorigenesis and metastasis[17]. Consequently, further research can clarify the pro-and anti-tumorigenic effects of ACVR1C.

Hence, in this study, we hypothesized that some SNPs of ACVR1C might be correlated with the susceptibility to ESCC and aimed to determine their correlation with esophageal tumorigenesis using an association analysis of candidate SNPs. We aimed to verify this hypothesis through a hospital-based cohort study in a Chinese Han population.

MATERIALS AND METHODS

Study design

This single-center, case-control study was conducted from October 1, 2008 to January 31, 2017. The Ethics Committee of Jiangsu University (Zhenjiang, China) and the Institutional Review Board (approval No. K20160036-W) approved this study. The research protocol was formulated and executed following the Ethical Principles for Medical Research Involving Human Subjects by the World Medical Association Declaration of Helsinki. All the participants provided informed consent.

A total of 2186 participants from the People's Hospital affiliated with Jiangsu University were retrospectively enrolled. The case group included 1043 patients with ESCC. All diagnoses were confirmed *via* pathological biopsies. Patients, who underwent neoadjuvant therapy, had other EC histological types, or had a history of other cancers, were excluded from the study. The control group included non-tumor patients with healthy physical examination and trauma during the same period. Propensity matching was conducted considering the distribution characteristics of the case groups such as sex, age, and residential area.

Demographic characteristics, including sex, age, and ESCC-related risk factors (smoking status and alcohol consumption), were recorded based on a questionnaire. Smoking was defined as the active smoking of ≥ 1 cigarette per day for one year. Alcohol consumption was defined as drinking at least three times per week for more of over six months. After obtaining the informed consent, 2 mL of fasting venous blood was drawn from each participant for subsequent tests.

DNA extraction and genotyping

The genomic DNA was extracted from peripheral blood using the QIAamp DNA Blood Mini Kit (Qiagen, Berlin, Germany). The ligation detection reaction (LDR) method was used for further SNP genotyping analysis with technical support from Genesky Biotechnology Inc. (Shanghai, China). Meanwhile, the consistency of all data was confirmed using 10% of the samples that were randomly selected. Double-track data entries were used to ensure the authenticity. To select the correlated SNPs loci and tagSNPs for further analyses, a pilot linkage disequilibrium (LD) analysis was performed using data sourced from the 1000Genomes project (1000G: PRJEB6930) of the National Center for Biotechnology Information SNP database.

Statistical analysis

SPSS 24.0 (Chicago, IL, United States), Haploview4.1, SHEsis software (online version)[18] were used to analyze the data. Hardy-Weinberg equilibrium (HWE) test was conducted to analyze the genotype distribution frequency of the control group by χ^2 test. SNPs in the control group with a P value greater than 0.05 were considered to be consistent with HWE, and could be further analyzed. χ^2 test was also applied to compare the differences in demographic characteristics between the ESCC case and control group.

Diverse genetic models and subgroup-stratified analyses were performed using logistic regression. Assuming alleles A and B are located in a single SNP: (1) Co-dominant model (risk associated with AB individuals lies between that of AA and BB individuals); (2) Dominant model (risk increased by allele B); (3) Recessive model (risk increased by two copies of allele B); and (4) Additive model (risk increased by r-fold for AB and 2r for BB) were considered[19]. Odds ratios (OR) and 95%CI were calculated to assess the strength of the association between SNPs and the risk of disease. Subsequently, adjusted OR and corresponding CI were calculated based on hierarchical variables, including age, sex, smoking, and alcohol consumption status. Finally, haplotype and LD analyses were performed using the SHEsis software. The coefficient of LD was evaluated using the D' and r^2 values. Bilateral test data were considered statistically significant at $P < 0.05$.

RESULTS

Characteristics of ESCC patients and healthy controls

The demographic characteristics and ESCC-related risk factors of the enrolled participants are listed in Table 1. We analyzed 1043 patients with ESCC (63.07 ± 7.27 years, mean age ± SD; 758 males and 285 females) and 1143 healthy controls (62.64 ± 9.90 years, mean age ± SD; 828 males and 315 females). Age and sex did not significantly differ between groups. However, smoking and alcohol consumption status significantly differed between the groups ($P < 0.001$), with higher rates for both parameters in the case group than in the control group.

The basic information on the five selected genotyped SNPs is presented in Table 2. All SNPs were located on chromosome 2. The minor allele frequency (MAF) of SNPs in the control group corresponded to that in the East Asian population, which was reflected in the 1000 Genomes database. The genotyping value was > 95%, indicating the reliability of the experimental results. The HWE test was conducted for the control group, which validated that the study population was in line with the Hardy-Weinberg balance ($P > 0.05$), and that the study population was representative.

Risk of ACVR1C SNPs with ESCC analyzed by genetic model

The associations between ESCC and each SNP are summarized in Table 3 and Figure 1. Based on four genetic models, the correlation between ESCC and various genotypes was analyzed. rs4556933 G>A was significantly associated with ESCC in the dominant, recessive, and additive models ($P < 0.001$, = 0.036, and 0.015, respectively). In addition, in the co-dominant model, the GA genotype of rs4556933 was associated with a lower risk of ESCC. The significant association between rs77886248 T>A and ESCC was reflected in only the dominant model ($P = 0.038$), which suggests that the TA and AA genotypes significantly increased the risk of ESCC between the case and healthy control groups. Nevertheless, genetic models showed no association of ESCC with rs4664229, rs77263459, and rs6734630 were not associated with ESCC, which is attributable to the marginal statistical significance observed in the genotype frequencies. The genotype distributions of the two significant SNPs are shown in Figure 2.

Stratified analysis of SNPs and the risk of ESCC in different subgroups

The stratified analyses based on sex, age, smoking status, and alcohol consumption better reflected the correlation between ACVR1C SNPs and susceptibility to ESCC (Table 4 and Table 5; Figure 3). In male participants older than 63 years, rs4556933 G>A was statistically significant in the dominant, recessive, and co-dominant models when comparing GG with GA ($P < 0.05$). Similar results were found in the dominant and co-dominant (TA *vs* TT) models of rs77886248 T>A ($P = 0.027/0.025$, with adjusted OR = 1.619/1.623, respectively), indicating that male sex is a risk factor for ESCC. For rs77886248, smoking was also associated with a higher risk of ESCC in the dominant and co-dominant (TA *vs* TT) models ($P = 0.035/0.024$, adjusted OR = 1.954/2.401).

Haplotype analysis of SNPs and susceptibility to ESCC

As listed in Table 6 and Table 7, the haplotype analysis of the five SNPs showed that $T_{rs4664229}G_{rs4556933}T_{rs77886248}T_{rs77263459}A_{rs6734630}$ was the most common genotype in all participants, included in the case and control groups (58.7% and 57.4%, respectively). $T_{rs4664229}A_{rs4556933}T_{rs77886248}C_{rs77263459}A_{rs6734630}$ was considered to increase the risk of ESCC ($P = 0.012$, OR = 1.211), whereas, $T_{rs4664229}G_{rs4556933}T_{rs77886248}C_{rs77263459}A_{rs6734630}$ was associated with lower susceptibility to ESCC ($P < 0.01$, OR = 0.126).

DISCUSSION

In this study, we demonstrate the relationship between functional ACVR1C polymorphisms and ESCC in a Chinese Han population through an association analysis of candidate SNPs. After collecting blood samples from 2186 participants and conducting LDR analysis, we identified five target SNP loci of AVCR1C. The LD analysis revealed a significant correlation among the five loci, especially between rs4556933 G>A and rs77263459 T>C. These loci are not in the same functional region; rs4556933 is a synonymous variant of the coding sequence and rs77263459 is an intron-associated variant. However, a strong LD is detected ($D = 0.849$, $r^2 = 0.588$), which indicates a similar influence on gene coding. In this study, the MAF of ACVR1C rs77886248, rs77263459, and rs6734630 in the control group were A = 0.0325, C = 0.2482, and G = 0.1050, respectively, which followed the East Asian population frequency distribution in the 1000Genomes database (A = 0.0387, C = 0.2361, G = 0.0913). The frequency of the first two alleles was significantly higher than that of the global data (A = 0.0078, C = 0.1042), whereas, the third allele showed lower frequency than the global data (G = 0.1865). This demonstrated differences in the frequency distribution of the gene polymorphism loci across species, which may have led to regional diversity in the incidence rate and pathological types of ESCC.

As a receptor binds to the TGF-β superfamily (ligands including Nodal, Activin A/B, and GDF3), ACVR1C is involved in the regulation of tumor progression and metastasis. Asnaghi *et al*[15] reported that ACVR1C/SMAD2 signaling promotes the invasion and growth of retinoblastoma[15]. However, Lonardo *et al*[20] suggested that downregulated ACVR1C is a marker of poor prognosis[20]. A significant association of ACVR1C rs4556933 G>A and rs77886248 T>A with ESCC was observed in certain genotypes and genetic models. In the co-dominant test, the GA genotype of rs4556933 reduced the risk of ESCC compared to the wild-type GG genotype ($P < 0.001$, OR = 0.598, 95%CI: 0.498-0.719); however, the TA genotype of rs77886248 served an independent risk factor for ESCC ($P < 0.001$, OR = 1.432, 95%CI: 1.034-1.983). However, compared to the wild-type genotype in the co-dominant model, the homozygous mutations of the selected SNPs exhibited no significant association with the risk of ESCC, which is potentially attributed to the hereditary modes

Table 1 distribution of selected demographic variables and risk factors in esophageal squamous cell carcinoma case and control groups, *n* (%)

Variable	Case group (*n* = 1043)	Control group (*n* = 1143)	*P* value
Age (years), mean ± SD	63.07 ± 7.27	62.64 ± 9.90	0.252
Age (years)			0.041
≥ 63	572 (54.84)	577 (50.48)	
< 63	471 (45.16)	566 (49.52)	
Sex			0.903
Male	758 (72.67)	828 (72.44)	
Female	285 (27.33)	315 (27.56)	
Smoking status			< 0.001
Never	589 (56.47)	810 (70.87)	
Ever	454 (43.53)	333 (29.13)	
Alcohol consumption			< 0.001
Never	714 (68.46)	1061 (92.82)	
Ever	329 (31.54)	82 (7.18)	

Table 2 Primary information of five selected genotyped single nucleotide polymorphisms of Activin A receptor type 1C: rs4664229 T>C, rs4556933 G>A, rs77886248 T>A, rs77263459 T>C, rs6734630 A>G

Genotyped SNPs	rs4664229	rs4556933	rs77886248	rs77263459	rs6734630
Alleles	T>C	G>A	T>A	T>C	A>G
Chromosome	2	2	2	2	2
Gene	ACVR1C				
Function	3 Prime UTR variant	Synonymous variant	Intron variant	Intron variant	3 Prime UTR Variant
Chromosome position	157530426	157587377	157565301	157621261	157528286
Regulome DB score[1]	4	4	7	5	7
TFBS	-	-	-	-	-
MAF in database (1000 Genomes)					
Global	C = 0.1414	A = 0.4403	A = 0.0078	C = 0.1042	G = 0.1865
East Asian	C = 0.0903	A = 0.3185	A = 0.0387	C = 0.2361	G = 0.0913
MAF in control	C = 0.1050	A = 0.3027	A = 0.0325	C = 0.2482	G = 0.1050
P value for HWE test in the controls	0.2551	0.6442	0.4526	0.5386	0.2630
Genotyping method	Ligation detection reaction				
Genotyping value, %	98.9	98.5	98.9	98.9	98.9

[1]http://www.regulomedb.org/.

TFBS: Transcription factor binding site (http://snpinfo.niehs.nih.gov/snpinfo/snpfuc.htm); HWE: Hardy-weinberg equilibrium; SNPs: Single nucleotide polymorphisms; ACVR1C: Activin A receptor type 1C; MAF: Minor allele frequency.

and complex mechanisms of SNP in tumor development and progression. Moreover, rs4556933 G>A significantly increased the risk of ESCC in the recessive test, suggesting that the effect of the homozygous mutant AA differs from that of the GA genotype. The hazardous effects of homozygous mutations are associated with tumor immune escape[21]. SNP polymorphism usually involves the transition or inversion-induced variation at a single base. Hence, haplotype analysis further validated the relationship between the five loci and ESCC risk.

Stratified analyses of the SNP rs4556933 revealed a significantly reduced risk of ESCC in subjects with a GA mutation, regardless of their subgroup. For males (age > 63 years) with AA mutants, the risk of ESCC increased, which is consistent

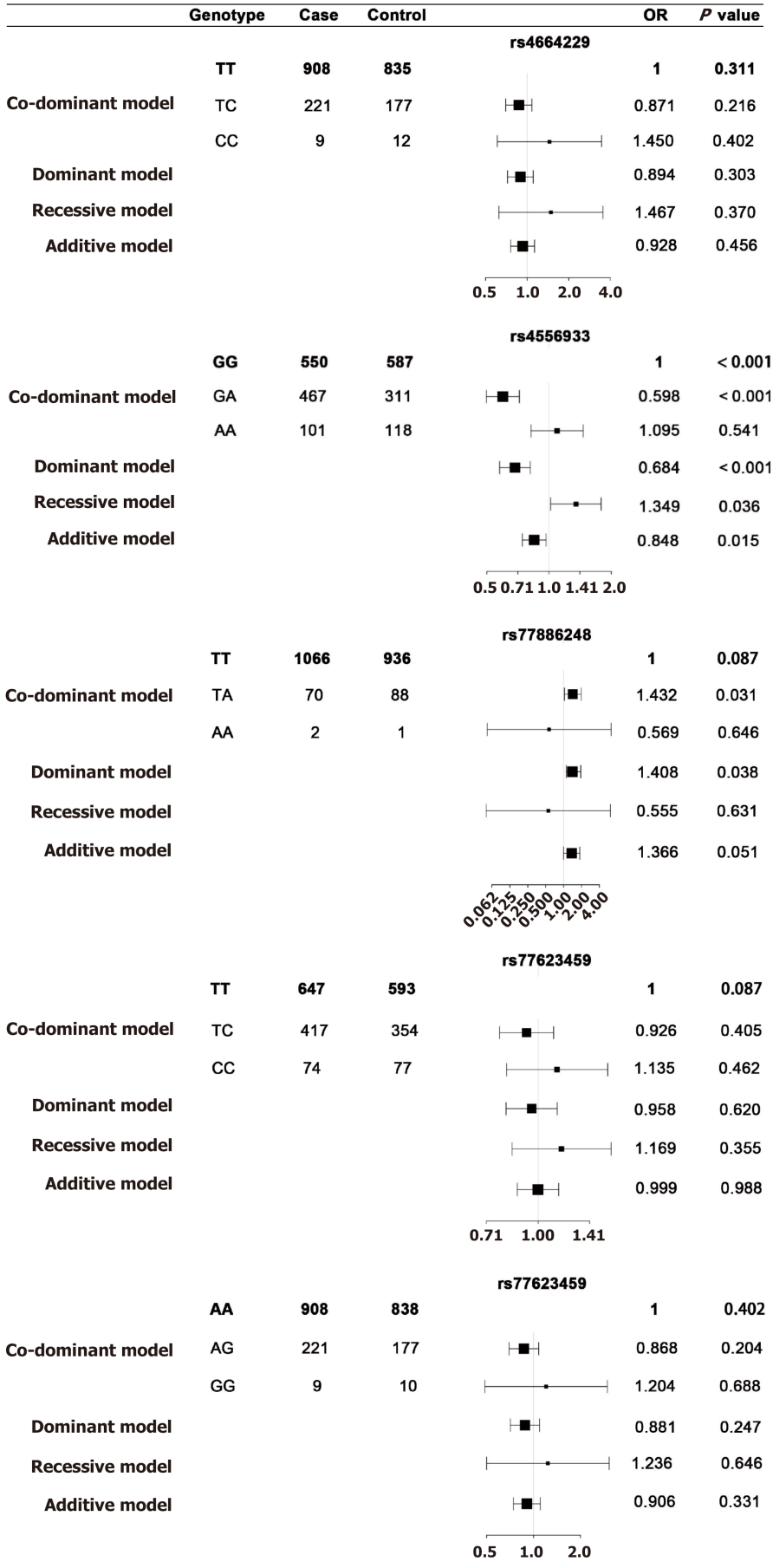

Figure 1 Forest plots of genetic modeling to analyze the risk of activin A receptor type 1C single nucleotide polymorphisms with esophageal squamous cell carcinoma. OR: Odds ratio.

Table 3 Analyses of associations between selected genotyped single nucleotide polymorphisms of activin A receptor type 1C on risk of esophageal squamous cell carcinoma

Locus	Genotype	Control	Case	Co-dominant model		Dominant model	Recessive model	Addictive model
				OR (95%CI)	*P* value	OR (95%CI)/*P* value	OR (95%CI)/*P* value	OR (95%CI)/*P* value
rs4664229	TT	908	835	1	0.311	0.894 (0.721-1.107)	1.487 (0.624-3.545)	0.928 (0.76-1.131)
	TC	221	177	0.871 (0.7-1.084)	0.216	0.303	0.37	0.456
	CC	9	12	1.45 (0.608-3.459)	0.402			
rs4556933	GG	550	587	1	< 0.001	0.684 (0.577-0.811)	1.349 (1.019-1.786)	0.848 (0.743-0.969)
	GA	487	311	0.598 (0.498-0.719)	< 0.001	< 0.001	0.036	0.015
	AA	101	118	1.095 (0.819-1.463)	0.541			
rs77886248	TT	1066	936	1	0.087	1.408 (1.019-1.944)	0.555 (0.05-6.126)	1.366 (0.999-1.870)
	TA	70	88	1.432 (1.034-1.983)	0.031	0.038	0.631	0.051
	AA	2	1	0.569 (0.052-6.29)	0.646			
rs77263459	TT	647	593	1	0.087	0.958 (0.807-1.136)	1.169 (0.84-1.628)	0.999 (0.870-1.147)
	TC	417	354	0.926 (0.773-1.109)	0.405	0.62	0.355	0.988
	CC	74	77	1.135 (0.810-1.592)	0.462			
rs6734630	AA	908	838	1	0.402	0.881 (0.711-1.092)	1.236 (0.5-3.054)	0.906 (0.743-1.105)
	GA	221	177	0.868 (0.697-1.08)	0.204	0.247	0.646	0.331
	GG	9	10	1.204 (0.487-2.977)	0.688			

OR: Odds ratio.

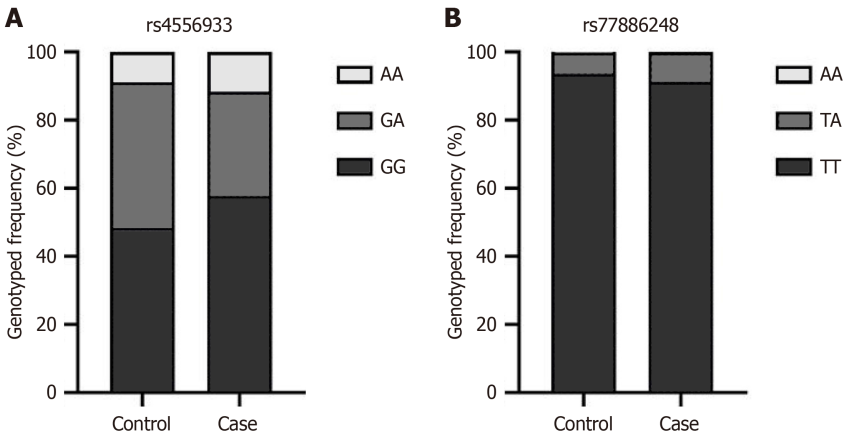

Figure 2 Genotype distributions of two significant single nucleotide polymorphisms. A: Rs4556933; B: Rs77886248.

with an epidemiological report in China[22]. Only a few studies have reflected the clinical significance of rs4556933 G>A; its correlation with preeclampsia pathogenesis was first reported in a Norwegian population[23]. The genetic function of rs4556933 reflects that it is a synonymous variant; it is considered a silent mutation owing to no alterations in protein sequences. As synonymous mutations are well accepted to be neutral or nearly neutral, they are often neglected in research on pathogenic or protective mutations. However, synonymous mutations in the oncogene *KRAS* were reported to have a relevant impact on gene expression and mRNA secondary structure[24]. Furthermore, synonymous variants can affect gene regulation *via* transcription, splicing, mRNA stability, and translation, inducing loss of function and poor prognosis in renal cell carcinoma[25,26]. Therefore, the correlation between this mutation and tumorigenesis may have

Table 4 Stratified analyses between rs4556933 polymorphism and esophageal squamous cell carcinoma risk by sex, age, smoking status and alcohol consumption

Variables	Control/case numbers				Adjusted OR/*P* value (95%CI of OR)				
	GG	GA	AA	GA + AA	GG	GA	AA	GA + AA	AA *vs* (GG + GA)
Sex									
Male	399/424	351/225	74/91	425/316	1	0.587/< 0.01 (0.464-0.742)	1.18/0.369 (0.823-1.691)	0.689/0.001 (0.555-0.855)	1.463/0.032 (1.033-2.071)
Female	151/163	136/86	27/27	163/113	1	0.57/0.02 (0.401-0.811)	0.898/0.718 (0.502-1.607)	0.624/0.005 (0.449-0.868)	1.156/0.614 (0.658-2.032)
Age									
≥ 63	290/324	241/163	45/66	286/229	1	0.588/< 0.01 (0.449-0.769)	1.283/0.257 (0.833-1.976)	0.697/0.004 (0.543-0.893)	1.582/0.032 (1.041-2.403)
< 63	260/263	246/148	56/52	302/200	1	0.568/< 0.01 (0.427-0.755)	0.932/0.754 (0.601-1.447)	0.634/0.001 (0.487-0.826)	1.198/0.406 (0.783-1.832)
Smoking status									
Ever	151/262	152/135	29/52	181/187	1	0.485/< 0.01 (0.344-0.683)	1.009/0.974 (0.583-1.749)	0.568/0.001 (0.412-0.782)	1.39/0.223 (0.818-2.362)
Never	399/325	335/176	72/66	407/242	1	0.645/< 0.01 (0.509-0.817)	1.156/0.442 (0.799-1.674)	0.734/0.006 (0.59-0.914)	1.38/0.078 (0.964-1.973)
Alcohol consumption									
Ever	31/190	45/92	6/38	51/130	1	0.326/< 0.01 (0.192-0.552)	1.019/0.969 (0.395-2.63)	0.407/< 0.01 (0.246-0.674)	1.745/0.23 (0.703-4.332)
Never	519/397	442/219	95/80	537/299	1	0.646/< 0.01 (0.524-0.797)	1.117/0.507 (0.806-1.548)	0.729/0.001 (0.601-0.885)	1.343/0.068 (0.978-1.842)

OR: Odds ratio.

Table 5 Stratified analyses between rs77886248 polymorphism and esophageal squamous cell carcinoma risk by sex, age, smoking status and alcohol consumption

Variables	Control/case numbers				Adjusted OR/*P* value (95%CI of OR)				
	TT	TA	AA	TA + AA	TT	TA	AA	TA + AA	AA *vs* (TA + AA)
Sex									
Male	779/680	44/64	1/1	45/65	1	1.619/0.027 (1.057-2.482)	1.772/0.686 (0.11-28.458)	1.623/0.025 (1.063-2.476)	1.714/0.704 (0.107-27.524)
Female	287/256	26/24	1/0	27/24	1	1.024/0.937 (0.57-1.839)	-/- (-)	0.979/0.942 (0.548-1.749)	-/- (-)
Age									
≥ 63	544/509	31/49	1/1	32/50	1	1.643/0.046 (1.009-2.675)	1.255/0.874 (0.76-20.757)	1.631/0.046 (1.009-2.639)	1.21/0.894 (0.073-20.012)
< 63	522/427	39/39	1/0	40/39	1	1.158/0.559 (0.707-1.898)	-/- (-)	1.134/0.616 (0.694-1.853)	-/- (-)
Smoking status									
Ever	314/405	18/45	0/1	18/46	1	1.954/0.035	-/- (-)	2.401/0.024	-/- (-)

						(1.049-3.642)		(1.099-3.791)	
Never	752/531	52/43	2/0	54/0	1	1.164/0.483	-/- (-)	1.118/0.604	-/- (-)
						(0.762-1.778)		(0.734-1.702)	
Alcohol consumption									
Ever	76/294	6/28	0/0	6/28	1	1.111/0.824	-/- (-)	1.111/0.824	-/- (-)
						(0.44-2.807)		(0.44-2.807)	
Never	990/642	64/60	2/1	66/61	1	1.41/0.068	0.722/0.793	1.389/0.078	0.704/0.777
						(0.975-2.038)	(0.64-8.61)	(0.964-1.999)	(0.062-7.959)

OR: Odds ratio.

Table 6 Haplotype frequencies in the case and control group, and risk of esophageal squamous cell carcinoma

Haplotypes	Case (%)	Control (%)	OR (95%CI)	*P* value
$T_{rs4664229}G_{rs4556933}T_{rs77886248}T_{rs77263459}A_{rs6734630}$	58.7	57.4	1.053 (0.929-1.192)	0.42
$T_{rs4664229}A_{rs4556933}T_{rs77886248}C_{rs77263459}A_{rs6734630}$	22.0	18.9	1.211 (1.043-1.407)	0.012
$C_{rs4664229}G_{rs4556933}T_{rs77886248}T_{rs77263459}G_{rs6734630}$	7.1	6.2	1.143 (0.898-1.454)	0.278
$T_{rs4664229}A_{rs4556933}T_{rs77886248}T_{rs77263459}A_{rs6734630}$	5.4	5.9	0.901 (0.695-1.167)	0.429
$T_{rs4664229}G_{rs4556933}A_{rs77886248}T_{rs77263459}A_{rs6734630}$	2.8	3.2	0.861 (0.605-1.226)	0.406
$T_{rs4664229}G_{rs4556933}T_{rs77886248}C_{rs77263459}A_{rs6734630}$	0.6	4.7	0.126 (0.072-0.221)	< 0.01
$C_{rs4664229}A_{rs4556933}T_{rs77886248}C_{rs77263459}G_{rs6734630}$	2.1	0.8	-	-
$C_{rs4664229}A_{rs4556933}T_{rs77886248}T_{rs77263459}G_{rs6734630}$	0.8	1.2	-	-
$C_{rs4664229}G_{rs4556933}A_{rs77886248}T_{rs77263459}G_{rs6734630}$	0.5	1.2	-	-
$C_{rs4664229}G_{rs4556933}T_{rs77886248}C_{rs77263459}G_{rs6734630}$	0.1	0.1	-	-

Table 7 Linkage disequilibrium analysis using parameter *D* and r^2

D'/ r^2	rs4556933	rs77886248	rs77263459	rs6734630
rs4664229	0.156/0.001	0.123/0.005	0.333/0.004	0.997/0.985
rs4556933	-	0.993/0.016	0.849/0.588	0.154/0.001
rs77886248	-	-	0.988/0.013	0.125/0.005
rs77263459	-	-	-	0.334/0.004

$D' > 0$, $r^2 > 0$ indicated linkage disequilibrium between different gene loci.

been underestimated. Additionally, an approximately two-fold increase in the risk of ESCC was detected in older smokers with the mutant genotype (TA and AA) of rs77886248 than in those with wild-type TT, which was consistent with a previous report[27].

Currently, neoadjuvant chemoradiotherapy or chemotherapy combined with surgical resection is considered the standard treatment for patients with locally advanced EC[28]. With the progress in immunotherapy, immune checkpoint inhibitors have been applied in the adjuvant and preoperative treatment stages, ranging from second-line treatment to advanced stages, all of which enhanced the pathologic complete response rate and prolonged disease-free survival[29, 30]. Therefore, identifying targets for efficacy assessments may help screen the potential benefit populations and provide tailored therapeutic strategies for patients. Minari *et al*[31] extracted and analyzed the correlation of SNPs in the programmed death ligand-1 (*PD-L1*) gene with immunotherapy efficacy in a cohort of 166 non-small cell lung cancer cases, and demonstrated an association of the *PD-L1* rs4143815 SNP with a long clinical benefit cohort ($P = 0.02$)[31]. Additionally, SNPs and treatment safety have a potential functional correlation, with 12 mutations or SNPs associated with an increased risk of melanoma immune-related adverse events[32].

Despite advances in novel therapies, the prognosis of EC remains poor. The early symptoms of EC are insidious; most cases exhibit are locally advanced stage when diagnosed, with lymph node metastasis, resulting in a high recurrence rate

A

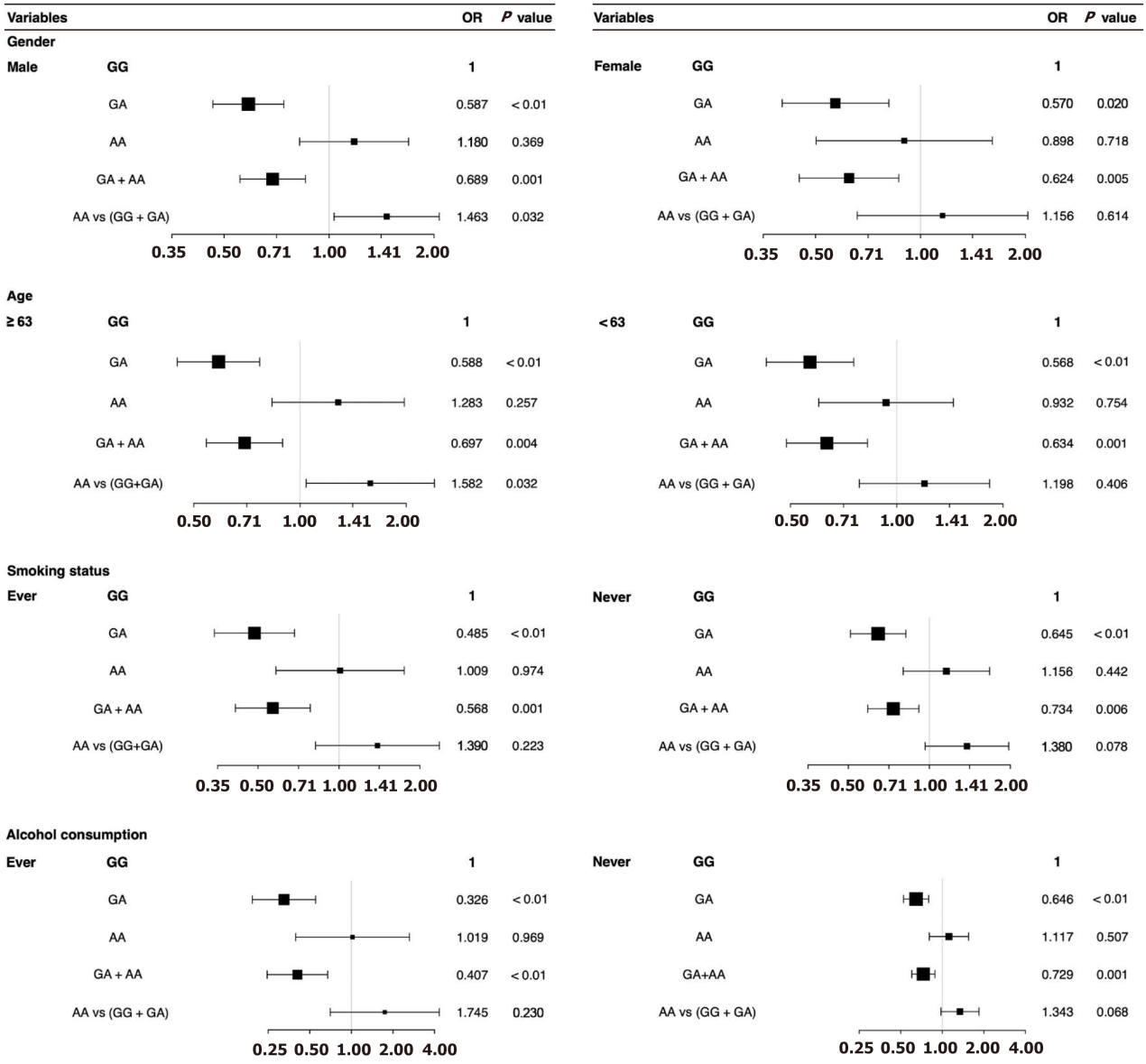
Variables
OR
P value
Gender
Male
GG
1
GA
0.587
< 0.01
AA
1.180
0.369
GA + AA
0.689
0.001
AA vs (GG + GA)
1.463
0.032
0.35 0.50 0.71 1.00 1.41 2.00
Variables
OR
P value
Female
GG
1
GA
0.570
0.020
AA
0.898
0.718
GA + AA
0.624
0.005
AA vs (GG + GA)
1.156
0.614
0.35 0.50 0.71 1.00 1.41 2.00
Age
≥ 63
GG
1
GA
0.588
< 0.01
AA
1.283
0.257
GA + AA
0.697
0.004
AA vs (GG+GA)
1.582
0.032
0.50 0.71 1.00 1.41 2.00
< 63
GG
1
GA
0.568
< 0.01
AA
0.932
0.754
GA + AA
0.634
0.001
AA vs (GG + GA)
1.198
0.406
0.50 0.71 1.00 1.41 2.00
Smoking status
Ever
GG
1
GA
0.485
< 0.01
AA
1.009
0.974
GA + AA
0.568
0.001
AA vs (GG+GA)
1.390
0.223
0.35 0.50 0.71 1.00 1.41 2.00
Never
GG
1
GA
0.645
< 0.01
AA
1.156
0.442
GA + AA
0.734
0.006
AA vs (GG + GA)
1.380
0.078
0.35 0.50 0.71 1.00 1.41 2.00
Alcohol consumption
Ever
GG
1
GA
0.326
< 0.01
AA
1.019
0.969
GA + AA
0.407
< 0.01
AA vs (GG + GA)
1.745
0.230
0.25 0.50 1.00 2.00 4.00
Never
GG
1
GA
0.646
< 0.01
AA
1.117
0.507
GA+AA
0.729
0.001
AA vs (GG + GA)
1.343
0.068
0.25 0.50 1.00 2.00 4.00

B

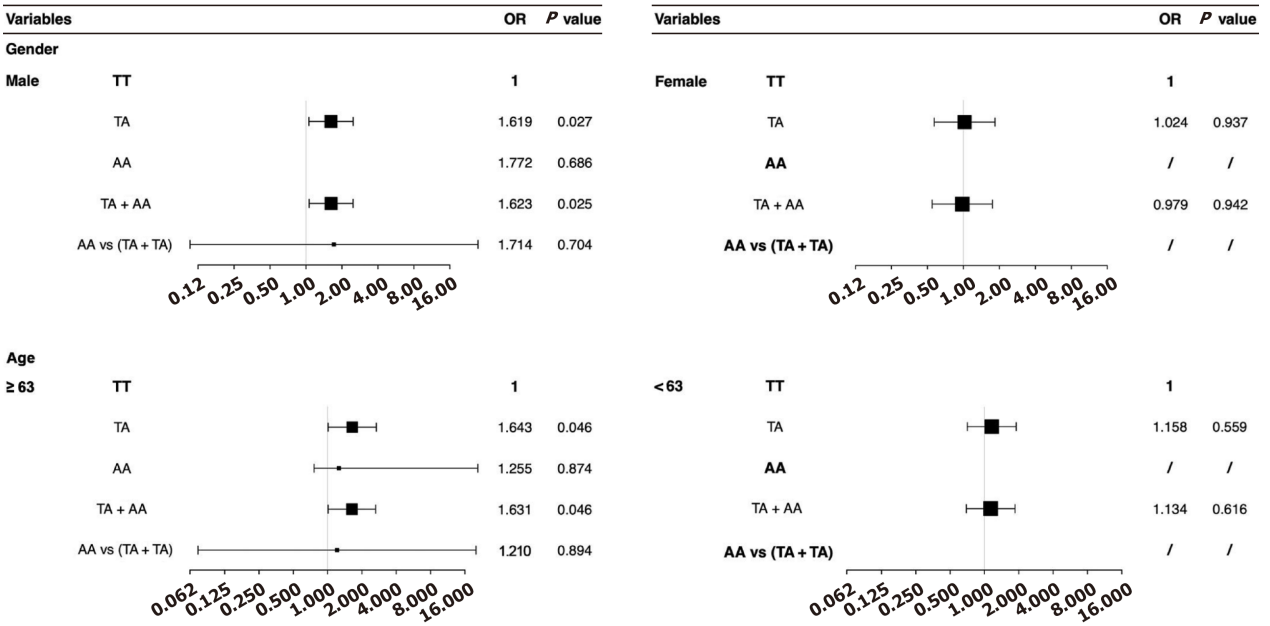
Variables
OR
P value
Gender
Male
TT
1
TA
1.619
0.027
AA
1.772
0.686
TA + AA
1.623
0.025
AA vs (TA + TA)
1.714
0.704
0.12 0.25 0.50 1.00 2.00 4.00 8.00 16.00
Variables
OR
P value
Female
TT
1
TA
1.024
0.937
AA
/
/
TA + AA
0.979
0.942
AA vs (TA + TA)
/
/
0.12 0.25 0.50 1.00 2.00 4.00 8.00 16.00
Age
≥ 63
TT
1
TA
1.643
0.046
AA
1.255
0.874
TA + AA
1.631
0.046
AA vs (TA + TA)
1.210
0.894
0.062 0.125 0.250 0.500 1.000 2.000 4.000 8.000 16.000
< 63
TT
1
TA
1.158
0.559
AA
/
/
TA + AA
1.134
0.616
AA vs (TA + TA)
/
/
0.062 0.125 0.250 0.500 1.000 2.000 4.000 8.000 16.000

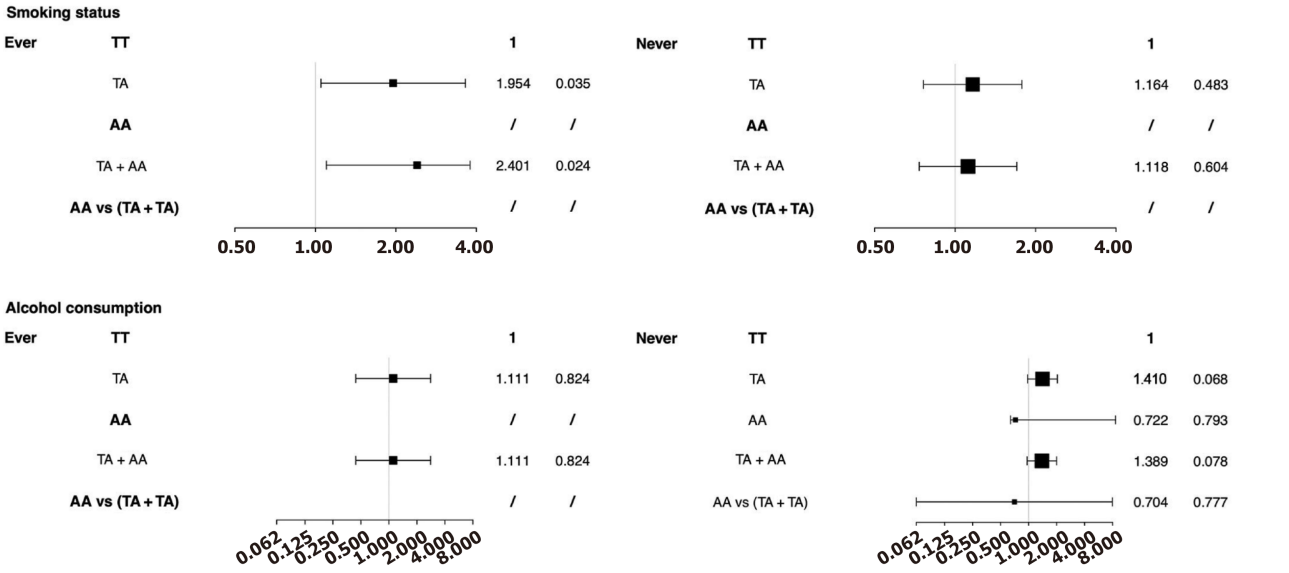

Figure 3 Forest plots. A: Forest plots of stratified analysis to rs4556933 genotype and esophageal squamous cell carcinoma (ESCC) risk; B: Forest plots of stratified analysis to rs77886248 genotype and ESCC risk. OR: Odds ratio.

and poor 5-year survival[33]. Therefore, the timely diagnosis and identification of new therapeutic targets are required. Among all subgroups analyzed in this study, subjects carrying the ACVR1C rs4556933 GA genotype exhibited a significantly reduced risk of ESCC, which can be considered a candidate locus involved in tumorigenesis and provide potential targets for diagnosis and treatment.

Our study has several limitations. First, this was a hospital-based cohort study and the control group might not accurately represent the general population. Second, owing to technical constraints, we could not verify gene expression through functional experiments in cells or animals. Moreover, beyond alcohol and smoking, other risk factors of ESCC, which include diet and nutrition, infection and microbiome, gastric atrophy, and family income, should be considered when defining subgroups. In a large-scale case-control study, the association of SNPs with disease progression will be further explored depending on the availability of complementary treatment modalities, efficacy evaluations, and long-term follow-up data.

CONCLUSION

In summary, the mutant of GA genotype in ACVR1C rs4556933 G>A showed a suggestive association with a lower risk of ESCC, while rs77886248 T>A increased the susceptibility to ESCC, especially in older male smokers of Chinese Han population.

FOOTNOTES

Author contributions: Yin J and Tan LJ conceptualized and designed the research; Yin J, Lv L, Long T, Pan HW, Qi JQ, Zhou Q and Tang WF screened patients and acquired clinical data; Yin J, Lv L and Long T collected blood specimen and performed laboratory analysis; Huang H and Lin SY performed Data analysis and wrote the first draft of the manuscript; Lin SY was responsible for data re-analysis and re-interpretation, figure plotting, comprehensive literature search, preparation and submission of the current version of the manuscript; Yu JJ, Su F and Zhang SY provided suggestions on the methodology and writing guidance; Jiang T and Wang LM helped revise the manuscript; Ding GW, Tan LJ and Yin J were responsible for study administration; All the authors have read and approved the final manuscript. Both Lin SY and Huang H have made crucial and indispensable contributions towards the completion of the project and thus qualified as the co-first authors of the paper. Both Tan LJ and Yin J have played important and indispensable roles in the experimental design, data interpretation and manuscript preparation as the co-corresponding authors. Yin J and Wang LM applied for and obtained the funds for this research project.

Supported by The National Natural Science Foundation of China, No. 82350127 and No. 82241013; the Shanghai Natural Science Foundation, No. 20ZR1411600; the Shanghai Shenkang Hospital Development Center, No. SHDC2020CR4039; the Bethune Ethicon Excellent Surgery Foundation, No. CESS2021TC04; and Xuhui District Medical Research Project of Shanghai, No. SHXH201805.

Institutional review board statement: The study was reviewed and approved by the Ethics Committee of Jiangsu University (Zhenjiang, China) and the Review Board of the institution (Approval No. K20160036-W).

Informed consent statement: All recruited participants were provided with informed consent.

Conflict-of-interest statement: All the authors report no relevant conflicts of interest for this article.

Data sharing statement: The dataset generated and analyzed during the current study are available in 1000Genomes project [1000G: PRJEB6930] from the NCBI SNP database. The genotype data of the selected SNPs used to support the findings of this study are available from the corresponding author on reasonable request at jun_yin@fudan.edu.cn.

STROBE statement: The authors have read the STROBE Statement—checklist of items, and the manuscript was prepared and revised according to the STROBE Statement—checklist of items.

Country of origin: China

ORCID number: Si-Yun Lin 0000-0003-0218-2533; Guo-Wen Ding 0000-0001-9788-5551; Li-Ming Wang 0000-0003-3831-8113; Jun Yin 0009-0008-5428-9969.

S-Editor: Li L
L-Editor: A
P-Editor: Zhao YQ

REFERENCES

1 **Sung H**, Ferlay J, Siegel RL, Laversanne M, Soerjomataram I, Jemal A, Bray F. Global Cancer Statistics 2020: GLOBOCAN Estimates of Incidence and Mortality Worldwide for 36 Cancers in 185 Countries. *CA Cancer J Clin* 2021; **71**: 209-249 [PMID: 33538338 DOI: 10.3322/caac.21660]
2 **Xia C**, Dong X, Li H, Cao M, Sun D, He S, Yang F, Yan X, Zhang S, Li N, Chen W. Cancer statistics in China and United States, 2022: profiles, trends, and determinants. *Chin Med J (Engl)* 2022; **135**: 584-590 [PMID: 35143424 DOI: 10.1097/CM9.0000000000002108]
3 **Abnet CC**, Arnold M, Wei WQ. Epidemiology of Esophageal Squamous Cell Carcinoma. *Gastroenterology* 2018; **154**: 360-373 [PMID: 28823862 DOI: 10.1053/j.gastro.2017.08.023]
4 **Massagué J**. TGFβ signalling in context. *Nat Rev Mol Cell Biol* 2012; **13**: 616-630 [PMID: 22992590 DOI: 10.1038/nrm3434]
5 **Tzavlaki K**, Moustakas A. TGF-β Signaling. *Biomolecules* 2020; **10** [PMID: 32210029 DOI: 10.3390/biom10030487]
6 **Heldin CH**, Miyazono K, ten Dijke P. TGF-beta signalling from cell membrane to nucleus through SMAD proteins. *Nature* 1997; **390**: 465-471 [PMID: 9393997 DOI: 10.1038/37284]
7 **Shi Y**, Massagué J. Mechanisms of TGF-beta signaling from cell membrane to the nucleus. *Cell* 2003; **113**: 685-700 [PMID: 12809600 DOI: 10.1016/s0092-8674(03)00432-x]
8 **David CJ**, Massagué J. Contextual determinants of TGFβ action in development, immunity and cancer. *Nat Rev Mol Cell Biol* 2018; **19**: 419-435 [PMID: 29643418 DOI: 10.1038/s41580-018-0007-0]
9 **Ibáñez CF**. Regulation of metabolic homeostasis by the TGF-β superfamily receptor ALK7. *FEBS J* 2022; **289**: 5776-5797 [PMID: 34173336 DOI: 10.1111/febs.16090]
10 **Rydén M**, Imamura T, Jörnvall H, Belluardo N, Neveu I, Trupp M, Okadome T, ten Dijke P, Ibáñez CF. A novel type I receptor serine-threonine kinase predominantly expressed in the adult central nervous system. *J Biol Chem* 1996; **271**: 30603-30609 [PMID: 8940033 DOI: 10.1074/jbc.271.48.30603]
11 **Lorentzon M**, Hoffer B, Ebendal T, Olson L, Tomac A. Habrec1, a novel serine/threonine kinase TGF-beta type I-like receptor, has a specific cellular expression suggesting function in the developing organism and adult brain. *Exp Neurol* 1996; **142**: 351-360 [PMID: 8934566 DOI: 10.1006/exnr.1996.0204]
12 **Kang Y**, Reddi AH. Identification and cloning of a novel type I serine/threonine kinase receptor of the TGF-beta/BMP superfamily in rat prostate. *Biochem Mol Biol Int* 1996; **40**: 993-1001 [PMID: 8955889 DOI: 10.1080/15216549600201623]
13 **Michael IP**, Saghafinia S, Hanahan D. A set of microRNAs coordinately controls tumorigenesis, invasion, and metastasis. *Proc Natl Acad Sci U S A* 2019; **116**: 24184-24195 [PMID: 31704767 DOI: 10.1073/pnas.1913307116]
14 **Hu T**, Su F, Jiang W, Dart DA. Overexpression of Activin Receptor-like Kinase 7 in Breast Cancer Cells Is Associated with Decreased Cell Growth and Adhesion. *Anticancer Res* 2017; **37**: 3441-3451 [PMID: 28668833 DOI: 10.21873/anticanres.11712]
15 **Asnaghi L**, White DT, Key N, Choi J, Mahale A, Alkatan H, Edward DP, Elkhamary SM, Al-Mesfer S, Maktabi A, Hurtado CG, Lee GY, Carcaboso AM, Mumm JS, Safieh LA, Eberhart CG. ACVR1C/SMAD2 signaling promotes invasion and growth in retinoblastoma. *Oncogene* 2019; **38**: 2056-2075 [PMID: 30401983 DOI: 10.1038/s41388-018-0543-2]
16 **Principe M**, Chanal M, Karam V, Wierinckx A, Mikaélian I, Gadet R, Auger C, Raverot V, Jouanneau E, Vasiljevic A, Hennino A, Raverot G, Bertolino P. ALK7 expression in prolactinoma is associated with reduced prolactin and increased proliferation. *Endocr Relat Cancer* 2018; **25**: 795-806 [PMID: 30012586 DOI: 10.1530/ERC-18-0082]
17 **Michael IP**, Saghafinia S, Tichet M, Zangger N, Marinoni I, Perren A, Hanahan D. ALK7 Signaling Manifests a Homeostatic Tissue Barrier That Is Abrogated during Tumorigenesis and Metastasis. *Dev Cell* 2019; **49**: 409-424.e6 [PMID: 31063757 DOI: 10.1016/j.devcel.2019.04.015]
18 **Shi YY**, He L. SHEsis, a powerful software platform for analyses of linkage disequilibrium, haplotype construction, and genetic association at polymorphism loci. *Cell Res* 2005; **15**: 97-98 [PMID: 15740637 DOI: 10.1038/sj.cr.7290272]

19 **Lewis CM**. Genetic association studies: design, analysis and interpretation. *Brief Bioinform* 2002; **3**: 146-153 [PMID: 12139434 DOI: 10.1093/bib/3.2.146]

20 **Lonardo E**, Hermann PC, Mueller MT, Huber S, Balic A, Miranda-Lorenzo I, Zagorac S, Alcala S, Rodriguez-Arabaolaza I, Ramirez JC, Torres-Ruíz R, Garcia E, Hidalgo M, Cebrián DÁ, Heuchel R, Löhr M, Berger F, Bartenstein P, Aicher A, Heeschen C. Nodal/Activin signaling drives self-renewal and tumorigenicity of pancreatic cancer stem cells and provides a target for combined drug therapy. *Cell Stem Cell* 2011; **9**: 433-446 [PMID: 22056140 DOI: 10.1016/j.stem.2011.10.001]

21 **Da Già MC**, Dietrich O, Truger M, Arampatzi P, Duell J, Heidemeier A, Zhou X, Danhof S, Kraus S, Chatterjee M, Meggendorfer M, Twardziok S, Goebeler ME, Topp MS, Hudecek M, Prommersberger S, Hege K, Kaiser S, Fuhr V, Weinhold N, Rosenwald A, Erhard F, Haferlach C, Einsele H, Kortüm KM, Saliba AE, Rasche L. Homozygous BCMA gene deletion in response to anti-BCMA CAR T cells in a patient with multiple myeloma. *Nat Med* 2021; **27**: 616-619 [PMID: 33619368 DOI: 10.1038/s41591-021-01245-5]

22 **Li J**, Xu J, Zheng Y, Gao Y, He S, Li H, Zou K, Li N, Tian J, Chen W, He J. Esophageal cancer: Epidemiology, risk factors and screening. *Chin J Cancer Res* 2021; **33**: 535-547 [PMID: 34815628 DOI: 10.21147/j.issn.1000-9604.2021.05.01]

23 **Roten LT**, Johnson MP, Forsmo S, Fitzpatrick E, Dyer TD, Brennecke SP, Blangero J, Moses EK, Austgulen R. Association between the candidate susceptibility gene ACVR2A on chromosome 2q22 and pre-eclampsia in a large Norwegian population-based study (the HUNT study). *Eur J Hum Genet* 2009; **17**: 250-257 [PMID: 18781190 DOI: 10.1038/ejhg.2008.158]

24 **Sharma Y**, Miladi M, Dukare S, Boulay K, Caudron-Herger M, Groß M, Backofen R, Diederichs S. A pan-cancer analysis of synonymous mutations. *Nat Commun* 2019; **10**: 2569 [PMID: 31189880 DOI: 10.1038/s41467-019-10489-2]

25 **Niersch J**, Vega-Rubín-de-Celis S, Bazarna A, Mergener S, Jendrossek V, Siveke JT, Peña-Llopis S. A BAP1 synonymous mutation results in exon skipping, loss of function and worse patient prognosis. *iScience* 2021; **24**: 102173 [PMID: 33681728 DOI: 10.1016/j.isci.2021.102173]

26 **Diederichs S**, Bartsch L, Berkmann JC, Fröse K, Heitmann J, Hoppe C, Iggena D, Jazmati D, Karschnia P, Linsenmeier M, Maulhardt T, Möhrmann L, Morstein J, Paffenholz SV, Röpenack P, Rückert T, Sandig L, Schell M, Steinmann A, Voss G, Wasmuth J, Weinberger ME, Wullenkord R. The dark matter of the cancer genome: aberrations in regulatory elements, untranslated regions, splice sites, non-coding RNA and synonymous mutations. *EMBO Mol Med* 2016; **8**: 442-457 [PMID: 26992833 DOI: 10.15252/emmm.201506055]

27 **Wang QL**, Ness-Jensen E, Santoni G, Xie SH, Lagergren J. Development and Validation of a Risk Prediction Model for Esophageal Squamous Cell Carcinoma Using Cohort Studies. *Am J Gastroenterol* 2021; **116**: 683-691 [PMID: 33982937 DOI: 10.14309/ajg.0000000000001094]

28 **Fick CN**, Dunne EG, Sihag S, Molena D, Cytryn SL, Janjigian YY, Wu AJ, Worrell SG, Hofstetter WL, Jones DR, Gray KD. Immunotherapy for Resectable Locally Advanced Esophageal Carcinoma. *Ann Thorac Surg* 2024; **118**: 130-140 [PMID: 38408631 DOI: 10.1016/j.athoracsur.2024.02.021]

29 **Qin J**, Xue L, Hao A, Guo X, Jiang T, Ni Y, Liu S, Chen Y, Jiang H, Zhang C, Kang M, Lin J, Li H, Li C, Tian H, Li L, Fu J, Zhang Y, Ma J, Wang X, Fu M, Yang H, Yang Z, Han Y, Chen L, Tan L, Dai T, Liao Y, Zhang W, Li B, Chen Q, Guo S, Qi Y, Wei L, Li Z, Tian Z, Kang X, Zhang R, Li Y, Wang Z, Chen X, Hou Z, Zheng R, Zhu W, He J, Li Y. Neoadjuvant chemotherapy with or without camrelizumab in resectable esophageal squamous cell carcinoma: the randomized phase 3 ESCORT-NEO/NCCES01 trial. *Nat Med* 2024; **30**: 2549-2557 [PMID: 38956195 DOI: 10.1038/s41591-024-03064-w]

30 **Kelly RJ**, Ajani JA, Kuzdzal J, Zander T, Van Cutsem E, Piessen G, Mendez G, Feliciano J, Motoyama S, Lièvre A, Uronis H, Elimova E, Grootscholten C, Geboes K, Zafar S, Snow S, Ko AH, Feeney K, Schenker M, Kocon P, Zhang J, Zhu L, Lei M, Singh P, Kondo K, Cleary JM, Moehler M; CheckMate 577 Investigators. Adjuvant Nivolumab in Resected Esophageal or Gastroesophageal Junction Cancer. *N Engl J Med* 2021; **384**: 1191-1203 [PMID: 33789008 DOI: 10.1056/NEJMoa2032125]

31 **Minari R**, Bonatti F, Mazzaschi G, Dodi A, Facchinetti F, Gelsomino F, Cinquegrani G, Squadrilli A, Bordi P, Buti S, Bersanelli M, Leonetti A, Cosenza A, Ferri L, Rapacchi E, Quaini F, Ardizzoni A, Tiseo M. PD-L1 SNPs as biomarkers to define benefit in patients with advanced NSCLC treated with immune checkpoint inhibitors. *Tumori* 2022; **108**: 47-55 [PMID: 34002648 DOI: 10.1177/03008916211014954]

32 **Abdel-Wahab N**, Diab A, Yu RK, Futreal A, Criswell LA, Tayar JH, Dadu R, Shannon V, Shete SS, Suarez-Almazor ME. Genetic determinants of immune-related adverse events in patients with melanoma receiving immune checkpoint inhibitors. *Cancer Immunol Immunother* 2021; **70**: 1939-1949 [PMID: 33409738 DOI: 10.1007/s00262-020-02797-0]

33 **van Hagen P**, Hulshof MC, van Lanschot JJ, Steyerberg EW, van Berge Henegouwen MI, Wijnhoven BP, Richel DJ, Nieuwenhuijzen GA, Hospers GA, Bonenkamp JJ, Cuesta MA, Blaisse RJ, Busch OR, ten Kate FJ, Creemers GJ, Punt CJ, Plukker JT, Verheul HM, Spillenaar Bilgen EJ, van Dekken H, van der Sangen MJ, Rozema T, Biermann K, Beukema JC, Piet AH, van Rij CM, Reinders JG, Tilanus HW, van der Gaast A; CROSS Group. Preoperative chemoradiotherapy for esophageal or junctional cancer. *N Engl J Med* 2012; **366**: 2074-2084 [PMID: 22646630 DOI: 10.1056/NEJMoa1112088]

World Journal of Gastrointestinal Oncology

Submit a Manuscript: https://www.f6publishing.com

World J Gastrointest Oncol 2025 January 15; 17(1): 96267

DOI: 10.4251/wjgo.v17.i1.96267

ISSN 1948-5204 (online)

ORIGINAL ARTICLE

Retrospective Cohort Study

Transarterial chemoembolization combined with lenvatinib and sintilimab *vs* lenvatinib alone in intermediate-advanced hepatocellular carcinoma

Fei-Da Wu, Hai-Feng Zhou, Wei Yang, Di Zhu, Bi-Fei Wu, Hai-Bin Shi, Sheng Liu, Wei-Zhong Zhou

Specialty type: Oncology

Provenance and peer review: Unsolicited article; Externally peer reviewed.

Peer-review model: Single blind

Peer-review report's classification

Scientific Quality: Grade A
Novelty: Grade A
Creativity or Innovation: Grade B
Scientific Significance: Grade A

P-Reviewer: Jiao Y

Received: May 1, 2024
Revised: October 16, 2024
Accepted: November 5, 2024
Published online: January 15, 2025
Processing time: 225 Days and 2.6 Hours

Fei-Da Wu, Hai-Feng Zhou, Wei Yang, Di Zhu, Bi-Fei Wu, Hai-Bin Shi, Sheng Liu, Wei-Zhong Zhou, Department of Interventional Radiology, The First Affiliated Hospital of Nanjing Medical University, Nanjing 210029, Jiangsu Province, China

Co-first authors: Fei-Da Wu and Hai-Feng Zhou.

Co-corresponding authors: Sheng Liu and Wei-Zhong Zhou.

Corresponding author: Wei-Zhong Zhou, MD, PhD, Department of Interventional Radiology, The First Affiliated Hospital of Nanjing Medical University, No. 300 Guangzhou Road, Gulou District, Nanjing 210029, Jiangsu Province, China. xmjbq007@163.com

Abstract

BACKGROUND

Hepatocellular carcinoma (HCC) is the most common form of liver cancer that has limited treatment options and a poor prognosis. Transarterial chemoembolization (TACE) is the first-line treatment for intermediate-stage HCC but can induce tumour hypoxia, thereby promoting angiogenesis. Recent studies suggested that combining TACE with anti-angiogenic therapies and immunotherapy might improve efficacy. Lenvatinib, a tyrosine kinase inhibitor, has demonstrated superior outcomes compared to sorafenib, while immune checkpoint inhibitors such as sintilimab show potential when combined with TACE. However, the efficacy and safety of TACE combined with lenvatinib and sintilimab (TACE + SL) compared to TACE with lenvatinib alone (TACE + L) in patients with intermediate-advanced HCC has not yet been investigated.

AIM

To evaluate the efficacy and safety of TACE + SL therapy in comparison to TACE + L therapy in patients with intermediate-advanced HCC.

METHODS

A retrospective analysis was performed on patients with intermediate-advanced HCC who received TACE plus lenvatinib with or without sintilimab between September 2019 and September 2022. Baseline characteristics were compared, and propensity score matching was applied. Overall survival (OS), progression-free survival (PFS), and objective response rate (ORR) were evaluated between the two

groups, and adverse events were analyzed.

RESULTS

The study included 57 patients, with 30 in the TACE + SL group and 27 in the TACE + L group. The TACE + SL group demonstrated significantly improved median PFS and OS compared to the TACE + L group (PFS: 14.1 months *vs* 9.6 months, $P = 0.016$; OS: 22.4 months *vs* 14.1 months, $P = 0.039$), along with a higher ORR (70.0% *vs* 55.6%). After propensity score matching, 30 patients were included, with the TACE + SL group again showing longer median PFS and a trend toward improved OS (PFS: 14.6 months *vs* 9.2 months, $P = 0.012$; OS: 23.9 months *vs* 16.3 months, $P = 0.063$), and a higher ORR (73.3% *vs* 53.3%). No severe adverse events were reported.

CONCLUSION

TACE + SL demonstrated superior outcomes in terms of OS and PFS, compared to TACE + L. These findings suggest that the addition of sintilimab might enhance the therapeutic response in patients with intermediate-advanced HCC.

Key Words: Hepatocellular carcinoma; Transarterial chemoembolization; Sintilimab; Lenvatinib; Immunotherapy; Programmed cell death 1; Prognosis

Core Tip: This study evaluates the efficacy and safety of combining transarterial chemoembolization (TACE) with lenvatinib and sintilimab compared to TACE with lenvatinib alone in patients with intermediate-advanced hepatocellular carcinoma. The results indicate that TACE with lenvatinib and sintilimab significantly improves overall survival (22.4 months *vs* 14.1 months) and progression-free survival (14.1 months *vs* 9.6 months), with a higher objective response rate (70% *vs* 55.6%). Notably, no severe adverse events were reported, suggesting that the combination therapy is effective and safe. These findings support the inclusion of sintilimab in hepatocellular carcinoma treatment regimens.

Citation: Wu FD, Zhou HF, Yang W, Zhu D, Wu BF, Shi HB, Liu S, Zhou WZ. Transarterial chemoembolization combined with lenvatinib and sintilimab *vs* lenvatinib alone in intermediate-advanced hepatocellular carcinoma. *World J Gastrointest Oncol* 2025; 17(1): 96267

URL: https://www.wjgnet.com/1948-5204/full/v17/i1/96267.htm

DOI: https://dx.doi.org/10.4251/wjgo.v17.i1.96267

INTRODUCTION

Hepatocellular carcinoma (HCC), the most prevalent form of liver cancer, is a leading cause of cancer-related mortality worldwide[1,2]. Due to its usually asymptomatic in its early stages, HCC is frequently diagnosed at advanced stages, resulting in limited therapeutic options and a poor prognosis. Transarterial chemoembolization (TACE) is the recommended first-line treatment for intermediate-stage HCC[3]; however, it can induce tumour hypoxia, promoting angiogenesis and tumour progression[4]. Recent studies indicate that combining TACE with anti-angiogenic therapy and immunotherapy can improve treatment efficacy for advanced HCC[5]. Lenvatinib, a tyrosine kinase inhibitor, is approved as a first-line treatment for HCC and has demonstrated superior outcomes compared to sorafenib[6,7]. Additionally, the combination of immune checkpoint inhibitors, including programmed cell death 1 (PD-1) inhibitors such as sintilimab, with TACE has demonstrated promising results across various solid tumours, including liver cancer[8-13]. Sintilimab, with a favourable safety profile compared to other treatments, has shown efficacy in clinical trials, improving overall survival (OS) and objective response rates (ORRs) in patients with advanced HCC, making it a compelling choice for combination therapy in this population[14]. The effectiveness of combining TACE, lenvatinib, and immunotherapy (*e.g.*, sintilimab) in patients with intermediate-advanced HCC remains uncertain. This retrospective study aims to evaluate the potential benefits and prognostic impact of this combination therapy in improving patient outcomes. Specifically, the efficacy and safety of combining TACE with lenvatinib and sintilimab (TACE + SL) and TACE combined with lenvatinib alone (TACE + L) were compared.

MATERIALS AND METHODS

Patients

This retrospective analysis included all patients with intermediate-advanced HCC treated at the First Affiliated Hospital of Nanjing Medical University who received TACE plus lenvatinib, with or without sintilimab, between September 2019 and September 2022. The study was approved by the Institutional Ethics Review Boards and conducted in accordance

with the World Medical Association Declaration of Helsinki. Inclusion criteria were Barcelona Clinic Liver Cancer (BCLC) stage B or C, Child-Pugh class A5, A6, or B7, Eastern Cooperative Oncology Group performance status ≤ 1, at least one assessable lesion, and ≥ 1 cycle of TACE plus lenvatinib with/without sintilimab. Exclusion criteria included < 1 month of lenvatinib or sintilimab treatment, secondary primary malignancies, follow-up < 6 months, incomplete clinical data, or loss to follow-up. Informed consent was waived due to the retrospective nature of the study.

TACE procedure

TACE was initiated before the administration of lenvatinib and sintilimab. A percutaneous femoral or radial artery approach was used for intubation, followed by angiography to identify the tumour-feeding artery. Chemoembolization was performed using super-selective emulsions of epirubicin and iodised oil *via* microcatheters, followed by the injection of gelatine sponge fragments to embolise the blood vessels supplying the tumour. Post-TACE syndrome was recorded, and liver function indicators were assessed within 1 week of each TACE treatment.

Lenvatinib and sintilimab administration

Lenvatinib was administered orally at a daily dose of 12 mg for patients weighing ≥ 60 kg or 8 mg for those weighing < 60 kg. Sintilimab was administered intravenously at a dose of 200 mg within 1 week of the initial TACE procedure, followed by subsequent doses every 3 weeks. In the event of severe adverse events (AEs), sintilimab and lenvatinib doses were adjusted through dose reduction, suspension, or discontinuation to ensure patient safety and manage treatment-related toxicities.

Follow-up and assessment

Patients were followed up every 6-8 weeks until the end of the study (June 30, 2023) or death. Follow-up assessments included routine physical examinations, laboratory blood tests, and contrast-enhanced computed tomography/magnetic resonance imaging scans to monitor treatment-related AEs. Tumour progression was assessed using the modified Response Evaluation Criteria in Solid Tumours. OS was defined as the time from treatment initiation to death from any cause or the most recent follow-up. Progression-free survival (PFS) was measured from treatment initiation to the date of disease progression. The ORR was calculated as the sum of complete responses and partial responses, while the disease control rate (DCR) included complete responses, partial responses, and stable disease.

Statistical analyses

All statistical analyses were performed using IBM SPSS Statistics 26 software and R 4.1.2 software. Propensity score matching (PSM) was applied to minimize selection bias and reduce the influence of potential confounding factors. Due to the small sample size, continuous variables were dichotomised to ensure comparability between the groups. Baseline variables were compared using the χ^2 test or Fisher's exact test for categorical variables, and the Student's *t*-test or Mann-Whitney *U* test for quantitative data, as appropriate. Survival analysis was conducted using the Kaplan-Meier method, with the log-rank test used to compare survival curves between groups. Univariate Cox regression analysis was performed, and factors with a *P*-value of < 0.2 were included in the multivariate regression using a backward stepwise selection approach ($P < 0.05$ for significance). A *P*-value of < 0.05 was considered statistically significant.

RESULTS

Patients' characteristics

This study enrolled 57 patients with HCC who met the inclusion criteria between September 2019 and September 2022 (Figure 1). The patients were divided into two groups: The TACE + SL group ($n = 30$) and the TACE + L group ($n = 27$), with ages ranging from 37 years to 80 years. The median follow-up duration was 19.2 months for the TACE + SL group and 17.5 months for the TACE + L group. Table 1 presents the clinical characteristics of the patients. PSM at a 1:1 ratio yielded 15 matched pairs. After matching, no statistically significant differences were observed in baseline characteristics between the two groups.

Efficacy outcomes

Before PSM, the median OS was 22.4 months for the TACE + SL group and 14.1 months for the TACE + L group ($P = 0.039$). The median PFS for the TACE + SL group was 14.1 months, compared to 9.6 months for the TACE + L group ($P = 0.016$) (Figure 2A and B). After PSM, the median OS for the TACE + SL group increased to 23.9 months, while it was 16.3 months for the TACE + L group ($P = 0.063$). The median PFS remained consistent, with 14.6 months in the TACE + SL group and 9.2 months in the TACE + L group ($P = 0.012$) (Figure 2C and D). The 1-year and 2-year survival rates for the TACE + SL group were 93.3% and 40.0%, respectively, compared to 80.0% and 13.3% in the TACE + L group (Table 2).

Tumour responses

Table 3 presents the tumour responses based on modified Response Evaluation Criteria in Solid Tumours. Before PSM, three patients (10.0%) in the TACE + SL group experienced disease progression, resulting in an ORR of 70.0% and a DCR of 90.0%. In contrast, 10 patients (37.0%) in the TACE + L group experienced disease progression, yielding an ORR of 55.6% and a DCR of 63.0%. After PSM, one patient (6.7%) in the TACE + SL group experienced disease progression, with an ORR of 73.3% and a DCR of 93.3%. Conversely, six patients (40.0%) in the TACE + L group experienced disease

Table 1 Patient characteristics before and after propensity score matching

Characteristic		Before PSM			After PSM		
		TACE + L	TACE + SL	*P* value	TACE + L	TACE + SL	*P* value
Gender				1.00			1.00
	Female	3	3		2	1	
	Male	24	27		13	14	
Age (year)				0.66			1.00
	≥ 60	16	15		8	8	
	< 60	11	15		7	7	
ECOG				1.00			0.43
	0	7	8		3	6	
	1	20	22		12	9	
Etiology				0.49			0.65
	HBV	22	21		13	11	
	Other	5	9		2	4	
Cirrhosis				1.00			1.00
	No	4	4		2	2	
	Yes	23	26		13	13	
Tumor number				0.35			0.71
	≥ 3	11	17		6	8	
	< 3	16	13		9	7	
Tumor size (cm)				0.43			1.00
	≥ 7	8	13		4	5	
	< 7	19	17		11	10	
PVTT				0.05			1.00
	No	22	16		11	11	
	Yes	5	14		4	4	
Metastases				1.00			0.33
	No	23	26		11	14	
	Yes	4	4		4	1	
BCLC				0.03			1.00
	B	22	15		11	11	
	C	5	15		4	4	
Child-Pugh class				1.00			1.00
	A	25	27		14	15	
	B	2	3		1	0	
AFP (ng/mL)				0.00			1.00
	≥ 100	2	17		2	2	
	< 100	25	13		13	13	

PSM: Propensity score matching; TACE + L: Transarterial chemoembolization with lenvatinib alone; TACE + SL: Transarterial chemoembolization combined with lenvatinib and sintilimab; ECOG: Eastern Cooperative Oncology Group; PVTT: Portal vein tumour thrombosis; BCLC: Barcelona Clinic Liver Cancer; AFP: Alpha-fetoprotein; HBV: Hepatitis B virus.

Table 2 Tumor response at 1 year based on modified response evaluation criteria in solid tumors, *n* (%)

	Unmatched group		Matched group	
	TACE + L (*n* = 27)	TACE + SL (*n* = 30)	TACE + L (*n* = 15)	TACE + SL (*n* = 15)
CR	4 (14.8)	6 (20.0)	1 (6.7)	2 (13.3)
PR	11 (40.7)	15 (50.0)	7 (46.7)	9 (60.0)
SD	2 (7.4)	6 (20.0)	1 (6.7)	3 (20.0)
PD	10 (37.0)	3 (10.0)	6 (40.0)	1 (6.7)
ORR	15 (55.6)	21 (70.0)	8 (53.3)	11 (73.3)
DCR	17 (63.0)	27 (90.0)	9 (60.0)	14 (93.3)
1-year OS	19 (70.4)	26 (86.7)	12 (80)	14 (93.3)

TACE + L: Transarterial chemoembolization with lenvatinib alone; TACE + SL: Transarterial chemoembolization combined with lenvatinib and sintilimab; CR: Complete response; PR: Partial response; SD: Stable response; PD: Progressive disease; ORR: Objective response rate; DCR: Disease control rate; OS: Overall survival.

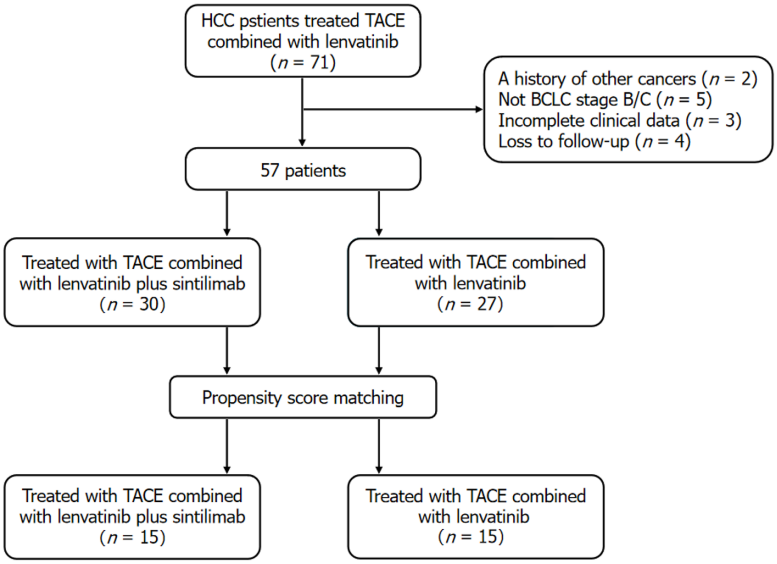

Figure 1 Flow diagram of patient enrollment. HCC: Hepatocellular carcinoma; TACE: Transarterial chemoembolization; BCLC: Barcelona Clinic Liver Cancer.

progression, leading to an ORR of 53.3% and a DCR of 60.0%. The ORR and DCR in the TACE + SL group were consistently higher than those in the TACE + L group before and after PSM.

Subgroup analysis

The subgroup analyses of factors associated with OS and PFS are presented in Supplementary Figure 1. The TACE + SL regimen demonstrated significantly longer PFS and OS among subgroups of patients with hepatitis B virus infection, absence of distant metastases, BCLC stage B, Child-Pugh class A, and alpha-fetoprotein (AFP) levels of ≤ 100 ng/mL.

Safety outcomes

AEs occurring during treatment were evaluated and classified according to the Common Terminology Criteria for AEs version 5.0, considering their frequency and severity (Table 2). No treatment-related deaths were reported, and all observed toxicities were manageable. In the TACE + SL group, the most commonly reported AEs during TACE included nausea (76.7%), abdominal pain (73.3%), and fever (76.7%). During the administration of lenvatinib and sintilimab, the most common AEs were hand-foot syndrome (33.3%) and hypertension (40.0%). These AEs were generally categorized as mild to moderate.

Table 3 Treatment-related adverse events, *n* (%)

Adverse events	TACE + SL (*n* = 30)			TACE + L (*n* = 27)		
Toxicity grade	/	1/2	3/4	/	1/2	3/4
Diarrhea	6 (20.0)	4	2	5 (18.5)	3	2
Transaminitis	14 (46.7)	12	2	13 (48.1)	8	5
Hand-foot skin reactions	10 (33.3)	7	3	7 (25.9)	6	1
Nausea with/without vomiting	23 (76.7)	20	3	17 (63.0)	15	2
Abdominal pain	22 (73.3)	18	4	22 (81.5)	19	3
Fatigue	9 (30.0)	6	3	7 (25.9)	5	2
Fever	23 (76.7)	20	3	17 (63.0)	15	2
Decreased WBC/PLT count	7 (23.3)	5	2	9 (33.3)	7	2
Thrombopenia	8 (26.7)	7	1	3 (11.1)	2	1
Decreased appetite	5 (16.7)	5	0	8 (30.0)	8	0
Hypertension	12 (40.0)	9	3	7 (26.0)	4	3
Hypothyroidism	7 (23.3)	6	1	/	/	/
Proteinuria	0 (0.0)	0	0	1 (3.7)	0	1

TACE + L: Transarterial chemoembolization with lenvatinib alone; TACE + SL: Transarterial chemoembolization combined with lenvatinib and sintilimab; WBC: White blood cell; PLT: Platelet.

DISCUSSION

This study evaluated the efficacy and safety of the TACE + SL regimen with the TACE + L regimen in treating patients with intermediate-advanced HCC. Our findings indicate that the TACE + SL regimen was associated with improved OS and PFS compared to the TACE + L regimen. These results suggest that the addition of lenvatinib and sintilimab to TACE might offer enhanced therapeutic benefits for patients with intermediate-advanced HCC. The improved outcomes observed in the TACE + SL group could be attributed to several factors. Firstly, lenvatinib, a multi-kinase inhibitor, has demonstrated efficacy as a first-line therapy for unresectable HCC[7,15,16]. Lenvatinib targets multiple angiogenic and oncogenic pathways, resulting in tumour regression and prolonged survival. By combining lenvatinib with TACE, the anti-tumour effect of TACE might be augmented, potentially inhibiting tumour progression[17-19]. Secondly, sintilimab, an anti-PD-1 monoclonal antibody, has shown promising efficacy across various cancers, including HCC[11,20]. By blocking the PD-1/programmed death ligand-1 interaction, sintilimab enhances the immune response, thereby restoring the anti-tumour immune response. When used in combination with TACE, sintilimab might further enhance immune-mediated tumour cell elimination, thereby improving overall treatment response.

Before PSM, baseline differences between the two groups, including portal vein tumour thrombosis (PVTT), BCLC stage, and AFP levels, could have influenced treatment outcomes. It is well established that PVTT, BCLC stage C, and elevated AFP levels are associated with poor prognosis in patients with HCC. Despite having a higher proportion of patients with PVTT, more advanced BCLC stages, and elevated AFP levels, the TACE + SL group exhibited longer OS and PFS compared to the TACE + L group. Subgroup analyses further suggested that the TACE + SL regimen might offer better prognostic outcomes, particularly among patients with hepatitis B virus infection, absence of distant metastases, BCLC stage B, Child-Pugh class A, and AFP ≤ 100 ng/mL. However, given the small sample size, the robustness of these subgroup results might be limited. After PSM, which balanced baseline characteristics between the two groups, no statistically significant difference in median OS was observed between the TACE + SL and TACE + L groups (P = 0.063). This lack of significance may be attributable to the small sample size and the fact that more patients in the TACE + SL group had not yet reached the endpoint due to a shorter follow-up period. However, the TACE + SL group demonstrated superior median PFS compared to the TACE + L group, suggesting the potential for longer OS in further studies. Patients with PVTT, BCLC stage C, and higher AFP levels might benefit more from the TACE + SL regimen compared to the TACE + L regimen. Therefore, large-scale clinical trials and mechanistic studies are required shortly.

The safety profile of the TACE + SL regimen was manageable, with no treatment-related deaths reported. The most common AEs reported during treatment included nausea, abdominal pain, fever, hand-foot syndrome, and hypertension. These AEs were generally mild to moderate in severity and did not significantly affect the patient's overall well-being. These findings align with those of previous studies on combination therapies for intermediate-advanced HCC[21,22]. Appropriate management and monitoring of these AEs were implemented throughout the study to ensure patient safety and optimize treatment outcomes. This study has certain limitations. First, the retrospective design and relatively small sample size might affect the generalizations and robustness of the findings. To enhance the reliability of these results, future investigations should include larger, multicentre cohorts with extensive follow-up periods, providing more

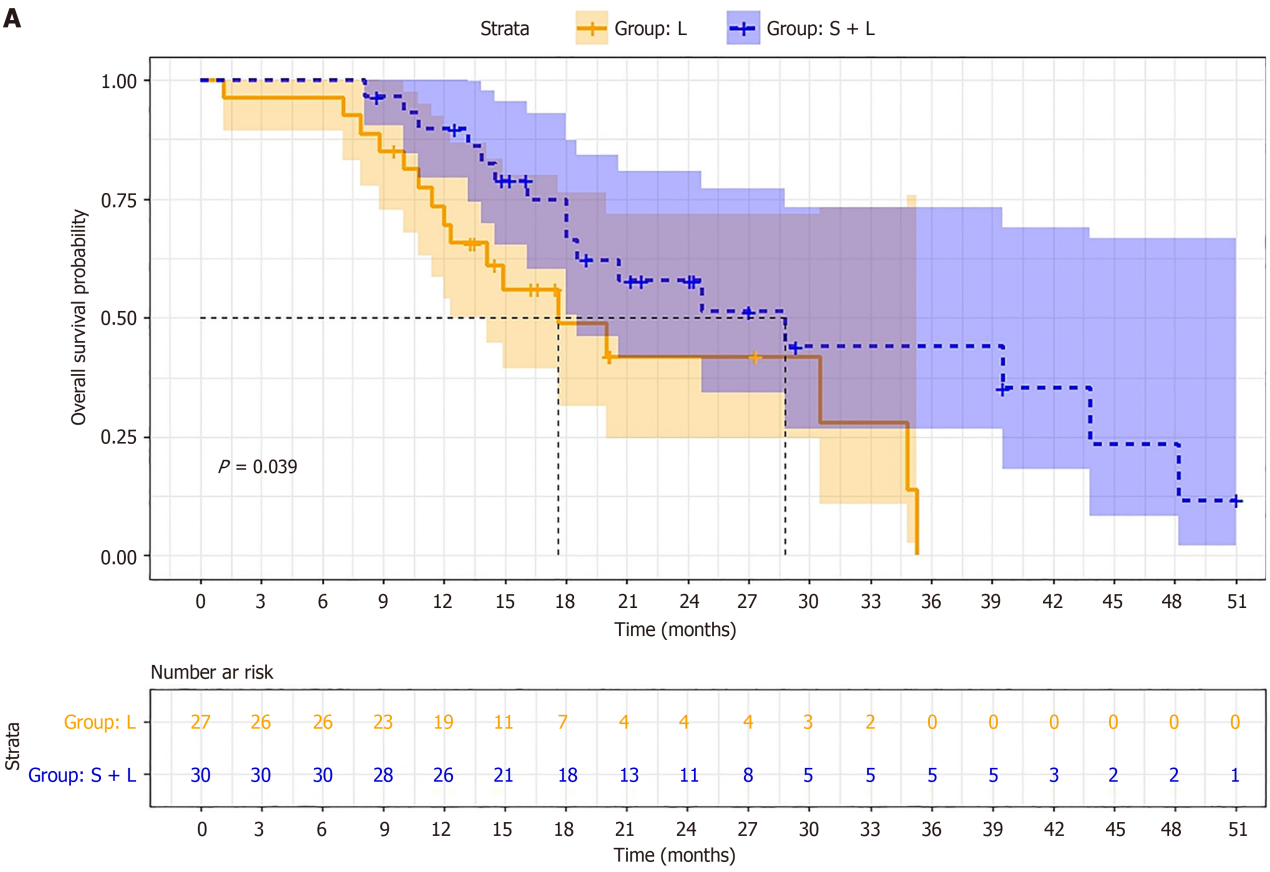
A
Strata
Group: L
Group: S + L
Overall survival probability
1.00
0.75
0.50
0.25
0.00
P = 0.039
0 3 6 9 12 15 18 21 24 27 30 33 36 39 42 45 48 51
Time (months)
Number ar risk
Strata
Group: L 27 26 26 23 19 11 7 4 4 4 3 2 0 0 0 0 0 0
Group: S + L 30 30 30 28 26 21 18 13 11 8 5 5 5 5 3 2 2 1
0 3 6 9 12 15 18 21 24 27 30 33 36 39 42 45 48 51
Time (months)

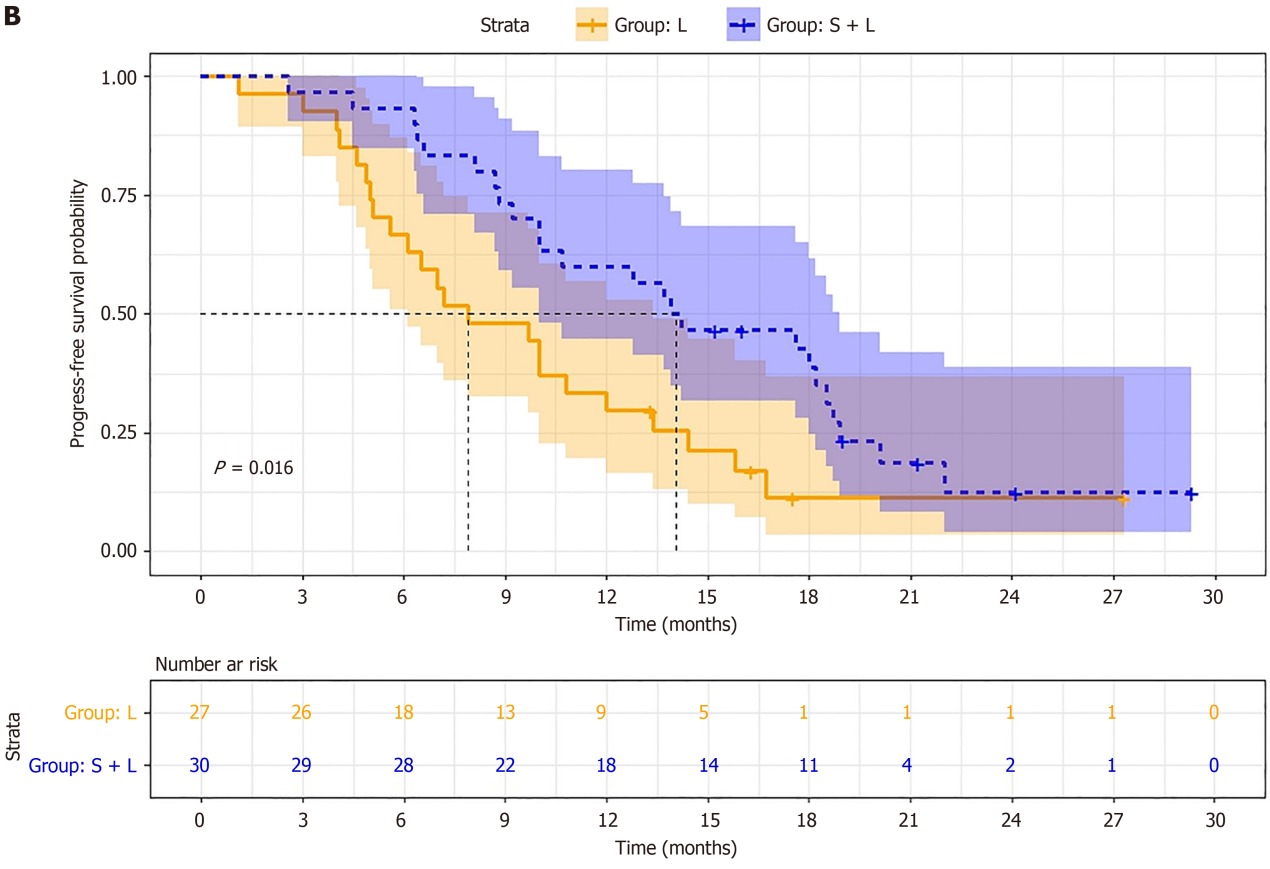
B
Strata
Group: L
Group: S + L
Progress-free survival probability
1.00
0.75
0.50
0.25
0.00
P = 0.016
0 3 6 9 12 15 18 21 24 27 30
Time (months)
Number ar risk
Strata
Group: L 27 26 18 13 9 5 1 1 1 1 0
Group: S + L 30 29 28 22 18 14 11 4 2 1 0
0 3 6 9 12 15 18 21 24 27 30
Time (months)

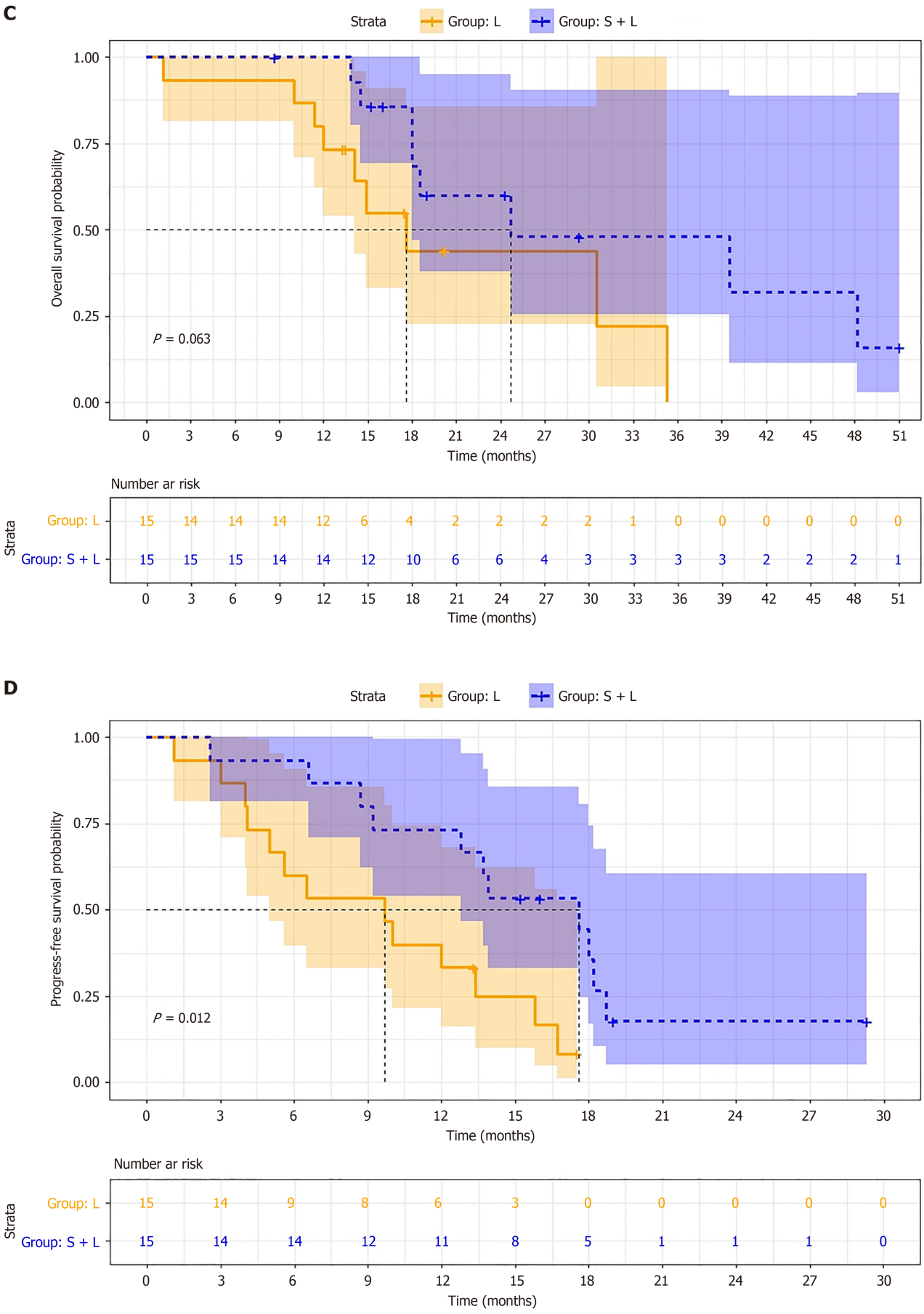

Figure 2 Kaplan-Meier survival for overall survival. A and B: Kaplan-Meier survival for overall survival and progression-free survival before propensity score matching; C and D: Kaplan-Meier survival for overall survival and progression-free survival after propensity score matching. Yellow and blue areas: Confidence

intervals. S + L: Sintilimab and lenvatinib; L: Lenvatinib.

comprehensive data on the long-term efficacy and safety of the combined TACE + SL regimen and strengthening the evidence base for this therapeutic approach. Second, the focus on patients with intermediate-advanced HCC raises concerns about the applicability of the findings to individuals with early-stage disease. Future research should investigate the efficacy and safety of the TACE + SL regimen across different stages of HCC, including early-stage patients. This could involve stratifying populations by disease stage and using randomized controlled trials to draw more definitive conclusions. Addressing these limitations will contribute to a more nuanced understanding of treatment modalities for HCC in subsequent studies.

CONCLUSION

In conclusion, our study demonstrated that the TACE + SL regimen is a promising treatment option for patients with intermediate-advanced HCC. The addition of lenvatinib and sintilimab to TACE improved OS and PFS compared to TACE combined with lenvatinib alone.

ACKNOWLEDGEMENTS

The authors thank the support of Yan Shen for patient recruitment and Zhong-Ling Pei for patient data aggregation. The authors also consulted Hai-Feng Zhou on analytical methodology. The authors thank patients with intermediate-advanced hepatocellular carcinoma at the First Affiliated Hospital of Nanjing Medical University for their immense contribution to this study.

FOOTNOTES

Author contributions: Wu FD and Zhou HF contributed equally to this article, they are the co-first authors of this manuscript. Wu FD analyzed the data and wrote the manuscript; Wu FD, Zhou HF, and Zhou WZ designed the research study; Wu FD, Zhu D, Yang W, and Wu BF performed the research; Shi HB, Liu S, and Zhou WZ provided financial support; Liu S and Zhou WZ made equally important contributions to the design, implementation and writing of this study, they are the co-corresponding authors of this manuscript; and all authors have read and approve the final manuscript.

Institutional review board statement: The study was reviewed and approved by the First Affiliated Hospital of Nanjing Medical University Institutional Review Board, approval No. 2023-SR-902.

Informed consent statement: The study was a retrospective study and therefore no informed consent was obtained from the participants.

Conflict-of-interest statement: All the authors report no relevant conflicts of interest for this article.

Data sharing statement: Technical appendix, statistical code, and dataset available from the corresponding author at xmjbq007@163.com.

STROBE statement: The authors have read the STROBE Statement-checklist of items, and the manuscript was prepared and revised according to the STROBE Statement-checklist of items.

Country of origin: China

ORCID number: Fei-Da Wu 0000-0002-4353-3398; Hai-Feng Zhou 0000-0002-9380-7879; Wei Yang 0000-0002-9625-8270; Sheng Liu 0000-0003-0090-8118; Wei-Zhong Zhou 0000-0001-8013-5607.

S-Editor: Bai Y
L-Editor: A
P-Editor: Zhao YQ

REFERENCES

1 **Sung H**, Ferlay J, Siegel RL, Laversanne M, Soerjomataram I, Jemal A, Bray F. Global Cancer Statistics 2020: GLOBOCAN Estimates of Incidence and Mortality Worldwide for 36 Cancers in 185 Countries. *CA Cancer J Clin* 2021; **71**: 209-249 [PMID: 33538338 DOI: 10.3322/caac.21660]

2 **Chen W**, Zheng R, Baade PD, Zhang S, Zeng H, Bray F, Jemal A, Yu XQ, He J. Cancer statistics in China, 2015. *CA Cancer J Clin* 2016; **66**: 115-132 [PMID: 26808342 DOI: 10.3322/caac.21338]

3 **Reig M**, Forner A, Rimola J, Ferrer-Fàbrega J, Burrel M, Garcia-Criado Á, Kelley RK, Galle PR, Mazzaferro V, Salem R, Sangro B, Singal AG, Vogel A, Fuster J, Ayuso C, Bruix J. BCLC strategy for prognosis prediction and treatment recommendation: The 2022 update. *J Hepatol* 2022; **76**: 681-693 [PMID: 34801630 DOI: 10.1016/j.jhep.2021.11.018]

4 **Zheng L**, Fang S, Wu F, Chen W, Chen M, Weng Q, Wu X, Song J, Zhao Z, Ji J. Efficacy and Safety of TACE Combined With Sorafenib Plus Immune Checkpoint Inhibitors for the Treatment of Intermediate and Advanced TACE-Refractory Hepatocellular Carcinoma: A Retrospective Study. *Front Mol Biosci* 2020; **7**: 609322 [PMID: 33521054 DOI: 10.3389/fmolb.2020.609322]

5 **Qin J**, Huang Y, Zhou H, Yi S. Efficacy of Sorafenib Combined With Immunotherapy Following Transarterial Chemoembolization for Advanced Hepatocellular Carcinoma: A Propensity Score Analysis. *Front Oncol* 2022; **12**: 807102 [PMID: 35463356 DOI: 10.3389/fonc.2022.807102]

6 **Villanueva A**. Hepatocellular Carcinoma. *N Engl J Med* 2019; **380**: 1450-1462 [PMID: 30970190 DOI: 10.1056/NEJMra1713263]

7 **Kudo M**, Finn RS, Qin S, Han KH, Ikeda K, Piscaglia F, Baron A, Park JW, Han G, Jassem J, Blanc JF, Vogel A, Komov D, Evans TRJ, Lopez C, Dutcus C, Guo M, Saito K, Kraljevic S, Tamai T, Ren M, Cheng AL. Lenvatinib versus sorafenib in first-line treatment of patients with unresectable hepatocellular carcinoma: a randomised phase 3 non-inferiority trial. *Lancet* 2018; **391**: 1163-1173 [PMID: 29433850 DOI: 10.1016/S0140-6736(18)30207-1]

8 **Guo J**, Wang S, Han Y, Jia Z, Wang R. Effects of transarterial chemoembolization on the immunological function of patients with hepatocellular carcinoma. *Oncol Lett* 2021; **22**: 554 [PMID: 34084221 DOI: 10.3892/ol.2021.12815]

9 **Zhang S**, Zhao Y, He L, Bo C, An Y, Li N, Ma W, Guo Y, Guo Y, Zhang C. Effect of camrelizumab plus transarterial chemoembolization on massive hepatocellular carcinoma. *Clin Res Hepatol Gastroenterol* 2022; **46**: 101851 [PMID: 34923180 DOI: 10.1016/j.clinre.2021.101851]

10 **Schmidt EV**. Developing combination strategies using PD-1 checkpoint inhibitors to treat cancer. *Semin Immunopathol* 2019; **41**: 21-30 [PMID: 30374524 DOI: 10.1007/s00281-018-0714-9]

11 **Ren Z**, Xu J, Bai Y, Xu A, Cang S, Du C, Li Q, Lu Y, Chen Y, Guo Y, Chen Z, Liu B, Jia W, Wu J, Wang J, Shao G, Zhang B, Shan Y, Meng Z, Wu J, Gu S, Yang W, Liu C, Shi X, Gao Z, Yin T, Cui J, Huang M, Xing B, Mao Y, Teng G, Qin Y, Wang J, Xia F, Yin G, Yang Y, Chen M, Wang Y, Zhou H, Fan J; ORIENT-32 study group. Sintilimab plus a bevacizumab biosimilar (IBI305) versus sorafenib in unresectable hepatocellular carcinoma (ORIENT-32): a randomised, open-label, phase 2-3 study. *Lancet Oncol* 2021; **22**: 977-990 [PMID: 34143971 DOI: 10.1016/S1470-2045(21)00252-7]

12 **Jin ZC**, Zhong BY, Chen JJ, Zhu HD, Sun JH, Yin GW, Ge NJ, Luo B, Ding WB, Li WH, Chen L, Wang YQ, Zhu XL, Yang WZ, Li HL, Teng GJ; CHANCE Investigators. Real-world efficacy and safety of TACE plus camrelizumab and apatinib in patients with HCC (CHANCE2211): a propensity score matching study. *Eur Radiol* 2023; **33**: 8669-8681 [PMID: 37368105 DOI: 10.1007/s00330-023-09754-2]

13 **Zhu HD**, Li HL, Huang MS, Yang WZ, Yin GW, Zhong BY, Sun JH, Jin ZC, Chen JJ, Ge NJ, Ding WB, Li WH, Huang JH, Mu W, Gu SZ, Li JP, Zhao H, Wen SW, Lei YM, Song YS, Yuan CW, Wang WD, Huang M, Zhao W, Wu JB, Wang S, Zhu X, Han JJ, Ren WX, Lu ZM, Xing WG, Fan Y, Lin HL, Zhang ZS, Xu GH, Hu WH, Tu Q, Su HY, Zheng CS, Chen Y, Zhao XY, Fang ZT, Wang Q, Zhao JW, Xu AB, Xu J, Wu QH, Niu HZ, Wang J, Dai F, Feng DP, Li QD, Shi RS, Li JR, Yang G, Shi HB, Ji JS, Liu YE, Cai Z, Yang P, Zhao Y, Zhu XL, Lu LG, Teng GJ; CHANCE001 Investigators. Transarterial chemoembolization with PD-(L)1 inhibitors plus molecular targeted therapies for hepatocellular carcinoma (CHANCE001). *Signal Transduct Target Ther* 2023; **8**: 58 [PMID: 36750721 DOI: 10.1038/s41392-022-01235-0]

14 **Fong KY**, Zhao JJ, Sultana R, Lee JJX, Lee SY, Chan SL, Yau T, Tai DWM, Sundar R, Too CW. First-Line Systemic Therapies for Advanced Hepatocellular Carcinoma: A Systematic Review and Patient-Level Network Meta-Analysis. *Liver Cancer* 2023; **12**: 7-18 [PMID: 36872922 DOI: 10.1159/000526639]

15 **Matsuki M**, Hoshi T, Yamamoto Y, Ikemori-Kawada M, Minoshima Y, Funahashi Y, Matsui J. Lenvatinib inhibits angiogenesis and tumor fibroblast growth factor signaling pathways in human hepatocellular carcinoma models. *Cancer Med* 2018; **7**: 2641-2653 [PMID: 29733511 DOI: 10.1002/cam4.1517]

16 **Yamamoto Y**, Matsui J, Matsushima T, Obaishi H, Miyazaki K, Nakamura K, Tohyama O, Semba T, Yamaguchi A, Hoshi SS, Mimura F, Haneda T, Fukuda Y, Kamata JI, Takahashi K, Matsukura M, Wakabayashi T, Asada M, Nomoto KI, Watanabe T, Dezso Z, Yoshimatsu K, Funahashi Y, Tsuruoka A. Lenvatinib, an angiogenesis inhibitor targeting VEGFR/FGFR, shows broad antitumor activity in human tumor xenograft models associated with microvessel density and pericyte coverage. *Vasc Cell* 2014; **6**: 18 [PMID: 25197551 DOI: 10.1186/2045-824X-6-18]

17 **Voron T**, Colussi O, Marcheteau E, Pernot S, Nizard M, Pointet AL, Latreche S, Bergaya S, Benhamouda N, Tanchot C, Stockmann C, Combe P, Berger A, Zinzindohoue F, Yagita H, Tartour E, Taieb J, Terme M. VEGF-A modulates expression of inhibitory checkpoints on CD8+ T cells in tumors. *J Exp Med* 2015; **212**: 139-148 [PMID: 25601652 DOI: 10.1084/jem.20140559]

18 **Khan KA**, Kerbel RS. Improving immunotherapy outcomes with anti-angiogenic treatments and vice versa. *Nat Rev Clin Oncol* 2018; **15**: 310-324 [PMID: 29434333 DOI: 10.1038/nrclinonc.2018.9]

19 **Rahma OE**, Hodi FS. The Intersection between Tumor Angiogenesis and Immune Suppression. *Clin Cancer Res* 2019; **25**: 5449-5457 [PMID: 30944124 DOI: 10.1158/1078-0432.CCR-18-1543]

20 **Hoy SM**. Sintilimab: First Global Approval. *Drugs* 2019; **79**: 341-346 [PMID: 30742278 DOI: 10.1007/s40265-019-1066-z]

21 **Zheng Y**, Xiang Y, Shi H, Lin Z, Cheng S, Zhu J. Transarterial Chemoembolization Combined with Atezolizumab Plus Bevacizumab versus Transarterial Chemoembolization Alone in Intermediate-stage Hepatocellular Carcinoma: A Multicenter Retrospective Study. *J Hepatocell Carcinoma* 2024; **11**: 1079-1093 [PMID: 38882440 DOI: 10.2147/JHC.S461630]

22 **Xiang YJ**, Wang K, Yu HM, Li XW, Cheng YQ, Wang WJ, Feng JK, Bo MH, Qin YY, Zheng YT, Shan YF, Zhou LP, Zhai J, Cheng SQ. Transarterial chemoembolization plus a PD-1 inhibitor with or without lenvatinib for intermediate-stage hepatocellular carcinoma. *Hepatol Res* 2022; **52**: 721-729 [PMID: 35536197 DOI: 10.1111/hepr.13773]

World Journal of Gastrointestinal Oncology

Submit a Manuscript: https://www.f6publishing.com

World J Gastrointest Oncol 2025 January 15; 17(1): 96598

DOI: 10.4251/wjgo.v17.i1.96598

ISSN 1948-5204 (online)

ORIGINAL ARTICLE

Retrospective Cohort Study

Multiparameter magnetic resonance imaging-based radiomics model for the prediction of rectal cancer metachronous liver metastasis

Zhi-Da Long, Xiao Yu, Zhi-Xiang Xing, Rui Wang

Specialty type: Gastroenterology and hepatology

Provenance and peer review: Unsolicited article; Externally peer reviewed.

Peer-review model: Single blind

Peer-review report's classification

Scientific Quality: Grade C, Grade C

Novelty: Grade B, Grade C

Creativity or Innovation: Grade B, Grade C

Scientific Significance: Grade B, Grade C

P-Reviewer: Asik M; Liu G

Received: May 10, 2024

Revised: September 6, 2024

Accepted: September 27, 2024

Published online: January 15, 2025

Processing time: 215 Days and 19.2 Hours

Zhi-Da Long, Xiao Yu, Zhi-Xiang Xing, Rui Wang, Department of Hepatobiliary and Pancreaticosplenic Surgery, Jingzhou Hospital Affiliated to Yangtze University, Jingzhou 434100, Hubei Province, China

Corresponding author: Rui Wang, MD, Doctor, Department of Hepatobiliary and Pancreaticosplenic Surgery, Jingzhou Hospital Affiliated to Yangtze University, No. 26 Chuyuan Road, Jingzhou District, Jingzhou 434100, Hubei Province, China. hyhq0216@163.com

Abstract

BACKGROUND

The liver, as the main target organ for hematogenous metastasis of colorectal cancer, early and accurate prediction of liver metastasis is crucial for the diagnosis and treatment of patients. Herein, this study aims to investigate the application value of a combined machine learning (ML) based model based on the multiparameter magnetic resonance imaging for prediction of rectal metachronous liver metastasis (MLM).

AIM

To investigate the efficacy of radiomics based on multiparametric magnetic resonance imaging images of preoperative first diagnosed rectal cancer in predicting MLM from rectal cancer.

METHODS

We retrospectively analyzed 301 patients with rectal cancer confirmed by surgical pathology at Jingzhou Central Hospital from January 2017 to December 2023. All participants were randomly assigned to the training or validation queue in a 7:3 ratio. We first apply generalized linear regression model (GLRM) and random forest model (RFM) algorithm to construct an MLM prediction model in the training queue, and evaluate the discriminative power of the MLM prediction model using area under curve (AUC) and decision curve analysis (DCA). Then, the robustness and generalizability of the MLM prediction model were evaluated based on the internal validation set between the validation queue groups.

RESULTS

Among the 301 patients included in the study, 16.28% were ultimately diagnosed with MLM through pathological examination. Multivariate analysis showed that carcinoembryonic antigen, and magnetic resonance imaging radiomics were independent predictors of MLM. Then, the GLRM prediction model was deve-

loped with a comprehensive nomogram to achieve satisfactory differentiation. The prediction performance of GLRM in the training and validation queue was 0.765 [95% confidence interval (CI): 0.710-0.820] and 0.767 (95%CI: 0.712-0.822), respectively. Compared with GLRM, RFM achieved superior performance with AUC of 0.919 (95%CI: 0.868-0.970) and 0.901 (95%CI: 0.850-0.952) in the training and validation queue, respectively. The DCA indicated that the predictive ability and net profit of clinical RFM were improved.

CONCLUSION

By combining multiparameter magnetic resonance imaging with the effectiveness and robustness of ML-based predictive models, the proposed clinical RFM can serve as an insight tool for preoperative assessment of MLM risk stratification and provide important information for individual diagnosis and treatment of rectal cancer patients.

Key Words: Rectal cancer; Metachronous liver metastases; Magnetic resonance imaging; Radiomics; Machine learning

Core Tip: In recent years, with the rapid development of data and information technology, imaging omics has been gradually applied in the clinical diagnosis and treatment of tumors, as it can non-invasive extract high-throughput heterogeneity information within tumors and integrate patient clinical information to improve the accuracy of models. Up to now, imaging omics models based on computed tomography or magnetic resonance imaging (MRI) images have shown potential application value in preoperative T and N staging and efficacy evaluation of rectal cancer. However, there is currently very little imaging omics research based on MRI of primary rectal cancer tumors. In fact, MRI is the most accurate imaging method for diagnosing rectal cancer, which can better display the invasion of adjacent lymph nodes, blood vessels, or surrounding organs by primary rectal cancer tumors. In view of this, this study attempts to establish a non-invasive preoperative prediction model for metachronous liver metastasis in rectal cancer based on the imaging omics features of the initial diagnosis MRI images of rectal cancer, combined with machine learning algorithms, and verify its effectiveness. This will provide clinical assistance for clinicians to make personalized monitoring and treatment decision.

Citation: Long ZD, Yu X, Xing ZX, Wang R. Multiparameter magnetic resonance imaging-based radiomics model for the prediction of rectal cancer metachronous liver metastasis. *World J Gastrointest Oncol* 2025; 17(1): 96598
URL: https://www.wjgnet.com/1948-5204/full/v17/i1/96598.htm
DOI: https://dx.doi.org/10.4251/wjgo.v17.i1.96598

INTRODUCTION

Throughout the world, colorectal cancer is a common malignant tumor of the digestive system, with its incidence rate and mortality ranking top[1]. According to the statistics of global cancer statistics, the global incidence rate and mortality of colorectal cancer in 2020 will be 10% and 9.4% respectively[2-4]. The liver, as the most common target organ for hematogenous metastasis of gastrointestinal malignant tumors, is also the most susceptible site for rectal cancer metastasis[5]. Previous studies have shown that approximately 35% to 55% of rectal cancer patients experience liver metastasis, and ultimately about 40% to 50% of rectal cancer patients die from liver metastasis[6-8]. At present, surgical resection of liver metastases is the only possible method for rectal cancer patients with liver metastases to achieve cure or prolong survival, and patients who can accept radical resection of liver metastases have a significantly higher 5-year survival rate than those who cannot be completely removed[9,10]. In addition, the more 15% to 25% of rectal cancer patients are diagnosed or undergo rectal cancer radical surgery without liver metastasis, the more likely they may eventually develop rectal metachronous liver metastasis (MLM) as the condition progresses[11,12]. Therefore, early detection and prediction of liver metastasis in rectal cancer and effective clinical intervention are crucial for the survival and prognosis of rectal cancer patients.

Up to now, there is no effective research method that can accurately predict the MLM of rectal cancer. There are studies based on computed tomography (CT) images of liver parenchyma to predict MLM by obtaining intensity features (such as grayscale values, entropy values, *etc.*), but the clinical promotion value is limited[13-15]. Previous researchers have attempted to analyze the association between clinical baseline features (such as tumor markers, lymph node metastasis status, *etc.*) and liver metastasis in rectal cancer, but there is currently no consensus or clear understanding of the relationship between MLM and clinical pathological parameters[16,17]. In addition, some scholars have studied the impact of gene mutations such as *KRAS*/*NRAS* on MLM, but genomics is an invasive examination that is expensive and difficult to widely promote in rectal cancer patients[18]. In view of this, it is urgent to seek convenient and high-precision prediction models that can be used to predict MLM to assist clinical decision-making.

In recent years, with the rapid development of data and information technology, imaging omics has been gradually applied in the clinical diagnosis and treatment of tumors, as it can non-invasive extract high-throughput heterogeneity information within tumors and integrate patient clinical information to improve the accuracy of models. Up to now, imaging omics models based on CT or magnetic resonance imaging (MRI) images have shown potential application value

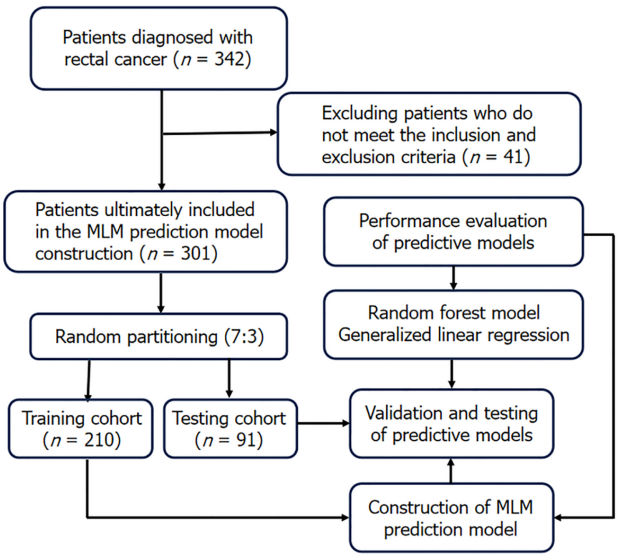

Figure 1 Patient inclusion and prediction model construction process. MLM: Metachronous liver metastasis.

in preoperative T and N staging and efficacy evaluation of rectal cancer[19,20]. However, there is currently very little imaging omics research based on MRI of primary rectal cancer tumors. In fact, MRI is the most accurate imaging method for diagnosing rectal cancer, which can better display the invasion of adjacent lymph nodes, blood vessels, or surrounding organs by primary rectal cancer tumors. In view of this, this study attempts to establish a non-invasive preoperative prediction model for MLM in rectal cancer based on the imaging omics features of the initial diagnosis MRI images of rectal cancer, combined with machine learning (ML) algorithms, and verify its effectiveness. This will provide clinical assistance for clinicians to make personalized monitoring and treatment decision.

MATERIALS AND METHODS

Patients

We retrospectively analyzed 301 patients with rectal cancer confirmed by surgical pathology at Jingzhou Central Hospital from January 2017 to December 2023. The inclusion criteria are as follows: (1) Patients confirmed by postoperative histopathology to have rectal adenocarcinoma; (2) Patients with regular follow-up before and after treatment, and complete follow-up imaging and clinical data; (3) Patients who were diagnosed with rectal cancer for the first time but did not find distant metastasis on enhanced CT or MRI; and (4) Patients who have no history of other primary malignant tumors and have not received anti-tumor treatment before their initial diagnosis. Exclusion criteria: (1) Patients confirmed by histopathology to have rectal mucinous adenocarcinoma (*i.e.*, due to the high malignancy of rectal mucinous adenocarcinoma and potential risk of metastasis); and (2) Patients with poor MR image quality or severe artifacts that cannot meet the analysis requirements. This study has been approved by the Ethics Committee of Jingzhou Central Hospital and complies with the Helsinki Declaration. All included patients were exempt from informed consent (No. 2024-154-01). The process and predictive model construction for patients included in the study were summarized in Figure 1.

Acquisition of rectal MRI images

Region of interest (ROI) drawing and radiomics feature extraction: A radiologist with more than 5 years of experience in abdominal and pelvic MRI diagnosis refers to all sequence images to determine the specific location and boundary of the primary tumor of rectal cancer on high-definition T2 weighted imaging (HD T2WI), diffusion weighted imaging (DWI) (b = 1000) The region of interest was drawn layer by layer on the image and reviewed by a senior radiologist with more than 10 years of experience in abdominal and pelvic MRI diagnosis. The ROIs of all layers of the entire tumor are fused to form a three-dimensional morphology of the tumor. Finally, the minimum absolute shrinkage and selection operator algorithm is used to extract and screen radiomic features related to MLM (including first-order features, morphological features, and second-order texture features, high-order texture features).

MRI imaging data collection and analysis

As shown in Supplementary Figure 1, the DWI (b = 1000) and oblique axial HD T2WI images in MRI of patients with rectal cancer were imported into ITK-SNAP software. We used the Z-Score standard to resample and normalize the original data to achieve image resampling and normalization. The gray value of the image is adjusted to the standard normal distribution. At the same time, consistency analysis is performed before screening radiomics features to eliminate radiomics features with poor consistency.

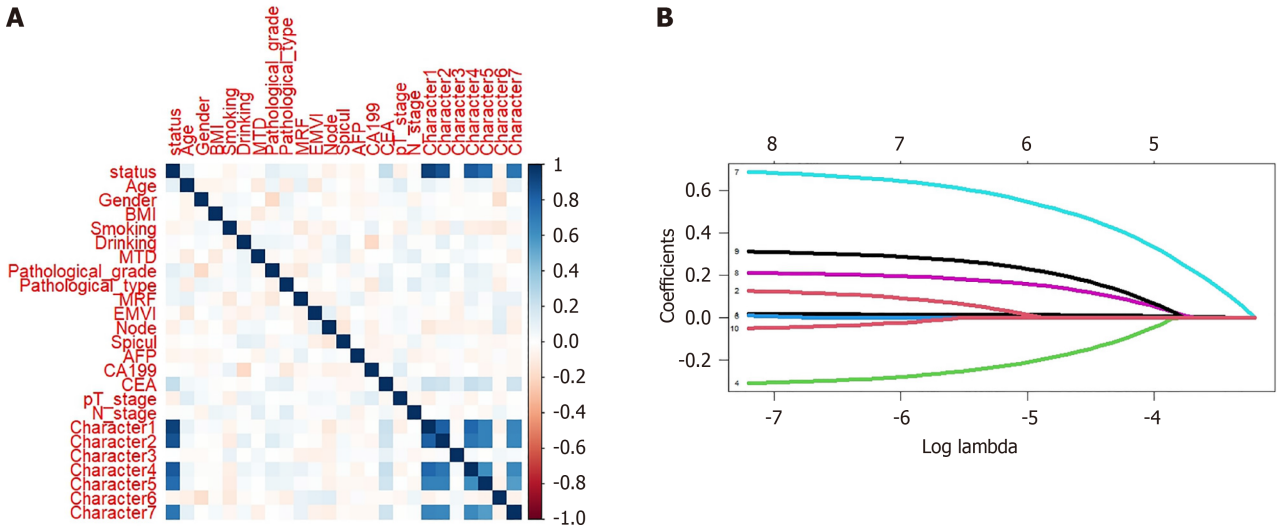

Figure 2 Selection of metachronous liver metastasis candidate predictive variables based on least absolute shrinkage and selection operator regression. A: Spearman correlation analysis; B: Least absolute shrinkage and selection operator regression analysis. BMI: Body mass index; MTD: Maximum tumor diameter; MRF: Mesenteric fascia; AFP: Alpha fetoprotein; CA: Carbohydrate antigen; CEA: Carcinoembryonic antigen.

Construction and validation of imaging-based radiomics MLM model

We adopted two commonly used ML algorithm prediction models in this MLM prediction, namely: Generalized linear regression model (GLRM) and random forest model (RFM). In addition, we also used the least absolute shrinkage and selection operator (LASSO) algorithm to reduce the dimensionality of the radiomics features extracted from the training set, and then used logistic regression analysis on the reduced feature set to construct radiomics labels and obtain each patient label score to reflect the risk of MLM. Screen radiomic features related to MLM. The prediction performance of the prediction model in the training set and validation set was evaluated using the receiver operating characteristic curve [*i.e.*, accuracy, sensitivity, specificity, and area under the curve (AUC)] and decision curve analysis. The DeLong test was used to compare AUCs between prediction models to select the radiomics prediction model with the best prediction performance.

Statistical analysis

In this study, statistical analysis and visualization of clinical baseline characteristics of patients between the MLM group and the non-MLM group were implemented using R software (version 4.2.3). All comparisons involving categorical variables (*i.e.*, percentile counts) were performed using the χ^2 test. If the continuous variables (*i.e.*, mean ± SD) conformed to the normal distribution, the *t* test was used. If they did not conform to the normal distribution, the Mann-Whitney *U* test was used. *P* less than 0.05 was considered as statistically significant difference between groups.

RESULTS

Patients' characteristics and radiomics features

Our study included 301 rectal cancer patients who underwent MR examination before treatment. Among them, 49 patients developed liver metastasis within 24 months after diagnosis of rectal cancer, including 22 males and 27 females. The average time for liver metastasis was 8.61 ± 6.50 months. In addition, the median follow-up time for all patients was 23.5 months. We also extracted 40 radiomics features from each patient's HD T2WI and DWI images, and ultimately found that there were five radiomics features compared between the MLM and nMLM groups [*i.e.* T2_wavelet.LHL_firstorder_RobustMeanAbsoluteDeviation (Character 1), T1_log.sigma.1.0.mm.3D_firstorder_Kurtosis (Character 2), ADC_wavelet.LHL_gldm_LargeDepenceHighGrayLevelEmphasis (Character 4), ADC_wavelet.HLL_glrlm_LongRunHighGrayLeveEmphasis (Character 5), T1_wavelet.HHL_glszm_GrayLevelNonUniformity (Character 7)]. The clinical baseline characteristics of all patients are summarized in Table 1 and Supplementary Table 1.

Candidate predictive factors selection related to MLM

We applied LASSO analysis to obtain the optimal feature subset from candidate MRI imaging parameters, and finally screen five imaging parameter candidate variables based on the parameter weights in the subset, namely feature 1, feature 2, feature 4, feature 5, and feature 7 (Figure 2). Additionally, multivariate logistic regression analysis was conducted to determine independent risk factors for MLM. The results showed that feature 1 [odds ratio (OR) = 1.19; 95% confidence interval (CI): 0.87-2.16], feature 2 (OR = 2.58; 95%CI: 1.14-3.99), feature 4 (OR = 1.13; 95%CI: 0.61-1.94), feature 5 (OR = 0.91; 95%CI: 0.19-2.06), and feature 7 (OR = 2.09; 95%CI: 1.05-3.55) were significantly associated with the occurrence of MLM (Table 2).

Table 1 Patient baseline characteristics and magnetic resonance imaging radiomics parameters, *n* (%)

Variables	Overall (*n* = 301)	MLM (*n* = 49)	Non-MLM (*n* = 252)	*P* value
Age [median (IQR)]	46.00 (31.00, 58.00)	51.00 (32.00, 60.00)	44.50 (30.00, 57.00)	0.074
Gender				
Male	136 (45.2)	22 (44.9)	114 (45.2)	1.000
Female	165 (54.8)	27 (55.1)	138 (54.8)	
BMI, kg/m^2 [median (IQR)]	23.50 (20.80, 26.10)	22.90 (20.70, 26.60)	23.55 (20.80, 26.02)	0.870
Smoking				
Yes	140 (46.5)	26 (53.1)	114 (45.2)	0.396
No	161 (53.5)	23 (46.9)	138 (54.8)	
Drinking				
Yes	142 (47.2)	22 (44.9)	120 (47.6)	0.847
No	159 (52.8)	27 (55.1)	132 (52.4)	
MTD, cm				
≤ 4	147 (48.8)	25 (51.0)	122 (48.4)	0.859
> 4	154 (51.2)	24 (49.0)	130 (51.6)	
Pathological grade				
I-II	142 (47.2)	17 (34.7)	125 (49.6)	0.079
III	159 (52.8)	32 (65.3)	127 (50.4)	
Pathological type				
Infiltrating	38 (12.6)	4 (8.2)	34 (13.5)	0.700
Ulcerative	111 (36.9)	18 (36.7)	93 (36.9)	
Cauliflower	74 (24.6)	12 (24.5)	62 (24.6)	
Uplift	78 (25.9)	15 (30.6)	63 (25.0)	
MRF				
Yes	162 (53.8)	23 (46.9)	139 (55.2)	0.368
No	139 (46.2)	26 (53.1)	113 (44.8)	
EMVI				
Yes	154 (51.2)	26 (53.1)	128 (50.8)	0.893
No	147 (48.8)	23 (46.9)	124 (49.2)	
Node				
Yes	133 (44.2)	26 (53.1)	107 (42.5)	0.226
No	168 (55.8)	23 (46.9)	145 (57.5)	
Spicule				
Yes	164 (54.5)	28 (57.1)	136 (54.0)	0.801
No	137 (45.5)	21 (42.9)	116 (46.0)	
AFP, ng/mL [median (IQR)]	2.81 (2.25, 3.41)	2.69 (2.16, 3.32)	2.82 (2.27, 3.42)	0.334
CA199, U/mL [median (IQR)]	9.61 (6.60, 12.66)	9.83 (6.64, 11.47)	9.59 (6.54, 12.73)	0.856
CEA, ng/mL [median (IQR)]				
0-5	167 (55.5)	14 (28.6)	153 (60.7)	< 0.001
≥ 5	134 (44.5)	35 (71.4)	99 (39.3)	
pT stage				
T2	158 (52.5)	30 (61.2)	128 (50.8)	0.237

T3	143 (47.5)	19 (38.8)	124 (49.2)	
N stage				
N0	94 (31.2)	16 (32.7)	78 (31.0)	0.936
N1	102 (33.9)	17 (34.7)	85 (33.7)	
N2	105 (34.9)	16 (32.7)	89 (35.3)	
Character 1 [median (IQR)]	0.46 (0.31, 0.63)	1.65 (1.44, 1.98)	0.41 (0.28, 0.55)	< 0.001
Character 2 [median (IQR)]	8.70 (7.70, 9.60)	13.00 (11.80, 14.80)	8.30 (7.57, 9.10)	< 0.001
Character 3 [median (IQR)]	169.30 (140.90, 198.10)	167.80 (145.20, 194.70)	172.25 (139.95, 198.25)	0.976
Character 4 [median (IQR)]	1.70 (1.20, 2.40)	4.50 (3.60, 5.10)	1.60 (1.10, 2.10)	< 0.001
Character 5 [median (IQR)]	3.60 (2.90, 4.20)	6.70 (4.80, 8.80)	3.40 (2.70, 4.00)	< 0.001
Character 6 [median (IQR)]	32.30 (22.30, 42.50)	29.80 (23.00, 39.30)	32.75 (22.08, 43.00)	0.364
Character 7 [median (IQR)]	4.20 (2.80, 5.30)	7.20 (5.90, 8.10)	3.75 (2.60, 4.80)	< 0.001

MLM: Metachronous liver metastasis; IQR: Interquartile range; BMI: Body mass index; MTD: Maximum tumor diameter; MRF: Mesenteric fascia; EMVI: Extramural venous invasion; AFP: Alpha fetoprotein; CA199: Carbohydrate antigen 199; CEA: Carcinoembryonic antigen; Character 1: T2_wavelet.LHL_firstorder_RobustMeanAbsoluteDeviation; Character 2: T1_log.sigma10.mm.3D_firstorder_Kurtosis; Character 3: T1_-lbp.3D.m1_firstorder_Skewness; Character 4: ADC_wavelet.LHL_gldm_LargeDepenceHighGrayLevelEmphasis; Character 5: ADC_-wavelet.HLL_glrlm_LongRunHighGrayLeveEmphasis; Character 6: T1_log.sigma30.mm.3D_glrlm_GrayLevelNonUniformity; Character 7: T1_wavelet.HHL_glszm_GrayLevelNonUniformity.

Table 2 Selection of metachronous liver metastasis predictive variables based on logistic regression

Variables	Univariate			Multivariate		
	OR	95%CI	*P* value	OR	95%CI	*P* value
Age [median (IQR)]	1.02	0.55-1.72	> 0.05			
Gender						
Male	1.00					
Female	0.86	0.23-1.02	> 0.05			
BMI, kg/m^2 [median (IQR)]	1.21	0.78-1.87	> 0.05			
Smoking						
Yes	1.00					
No	0.79	0.18-1.16	> 0.05			
Drinking						
Yes	1.00					
No	0.81	0.23-2.57	> 0.05			
MTD, cm						
≤ 4	1.00					
> 4	1.16	0.77-3.98	> 0.05			
Pathological grade						
I-II	1.00					
III	1.23	0.91-2.26	> 0.05			
Pathological type						
Infiltrating	1.00					
Ulcerative	0.63	0.12-1.16	> 0.05			
Cauliflower	0.78	0.23-1.65	> 0.05			

Uplift	1.12	0.88-2.37	> 0.05			
MRF						
Yes	1.00					
No	0.63	0.22-1.19	> 0.05			
EMVI						
Yes	1.00					
No	0.67	0.11-1.59	> 0.05			
Node						
Yes	1.00					
No	0.82	0.41-2.16	> 0.05			
Spicule						
Yes	1.00					
No	0.58	0.21-2.26	> 0.05			
AFP, ng/mL [median (IQR)]	1.23	0.88-1.77	> 0.05			
CA199, U/mL [median (IQR)]	1.15	0.91-1.65	> 0.05			
CEA, ng/mL [median (IQR)]	2.13	1.03-4.57	< 0.05	2.11	1.01-4.12	< 0.05
pT stage						
T2	1.00					
T3	1.13	0.75-2.16	> 0.05			
N stage						
N0	1.00					
N1	1.13	0.86-1.87	> 0.05			
N2	1.21	0.99-2.14	> 0.05			
Character 1 [median (IQR)]	1.23	0.77-1.96	< 0.05	1.19	0.87-2.16	< 0.05
Character 2 [median (IQR)]	2.67	1.12-4.13	< 0.05	2.58	1.14-3.99	< 0.05
Character 3 [median (IQR)]	1.58	0.88-2.03	> 0.05			
Character 4 [median (IQR)]	1.06	0.56-1.87	< 0.05	1.13	0.61-1.94	< 0.05
Character 5 [median (IQR)]	0.98	0.23-1.56	< 0.05	0.91	0.19-2.06	< 0.05
Character 6 [median (IQR)]	1.87	1.02-2.76	> 0.05			
Character 7 [median (IQR)]	2.23	1.11-3.87	< 0.05	2.09	1.05-3.55	< 0.05

OR: Odds ratio; CI: Confidence interval; IQR: Interquartile range; BMI: Body mass index; MTD: Maximum tumor diameter; MRF: Mesenteric fascia; EMVI: Extramural venous invasion; AFP: Alpha fetoprotein; CA199: Carbohydrate antigen 199; CEA: Carcinoembryonic antigen; Character 1: T2_wavelet.LHL_firstorder_RobustMeanAbsoluteDeviation; Character 2: T1_log.sigma10.mm.3D_firstorder_Kurtosis; Character 3: T1_-lbp.3D.m1_firstorder_Skewness; Character 4: ADC_wavelet.LHL_gldm_LargeDepenceHighGrayLevelEmphasis; Character 5: ADC_-wavelet.HLL_glrlm_LongRunHighGrayLeveEmphasis; Character 6: T1_log.sigma30.mm.3D_glrlm_GrayLevelNonUniformity; Character 7: T1_wavelet.HHL_glszm_GrayLevelNonUniformity.

Construction and evaluation of nomogram predictive model for MLM

Based on the independent risk factors for MLM mentioned above, a nomogram prediction model was established (Figure 3). In the training queue, the AUC was 0.765 (95%CI: 0.710-0.820), with a sensitivity of 0.75 and a specificity of 0.98. In the validation queue, the AUC was 0.767 (95%CI: 0.712-0.822), with a sensitivity of 0.64 and a specificity of 0.94 (Table 3). The calibration curve showed good consistency between the predicted probability and the actual probability, indicating that the nomogram has good predictive performance.

Construction and evaluation of random forest predictive model based on ML algorithm

In the RFM, according to the importance ranking of predictive variable characteristics, feature 1, feature 2, feature 4, and

Table 3 Evaluation of predictive performance of metachronous liver metastasis prediction model based on receiver operating characteristic

Prediction model	Training set				International set			
	AUC	95%CI	PPV	NPV	AUC	95%CI	PPV	NPV
RFM	0.919	0.868-0.970	0.94	0.99	0.901	0.850-0.952	0.94	0.99
GLRM	0.765	0.710-0.820	0.75	0.98	0.767	0.712-0.822	0.64	0.94

AUC: Area under the curve; CI: Confidence interval; PPV: Positive predictive value; NPV: Negative predictive value; RFM: Random forest model; GLRM: Generalized linear regression.

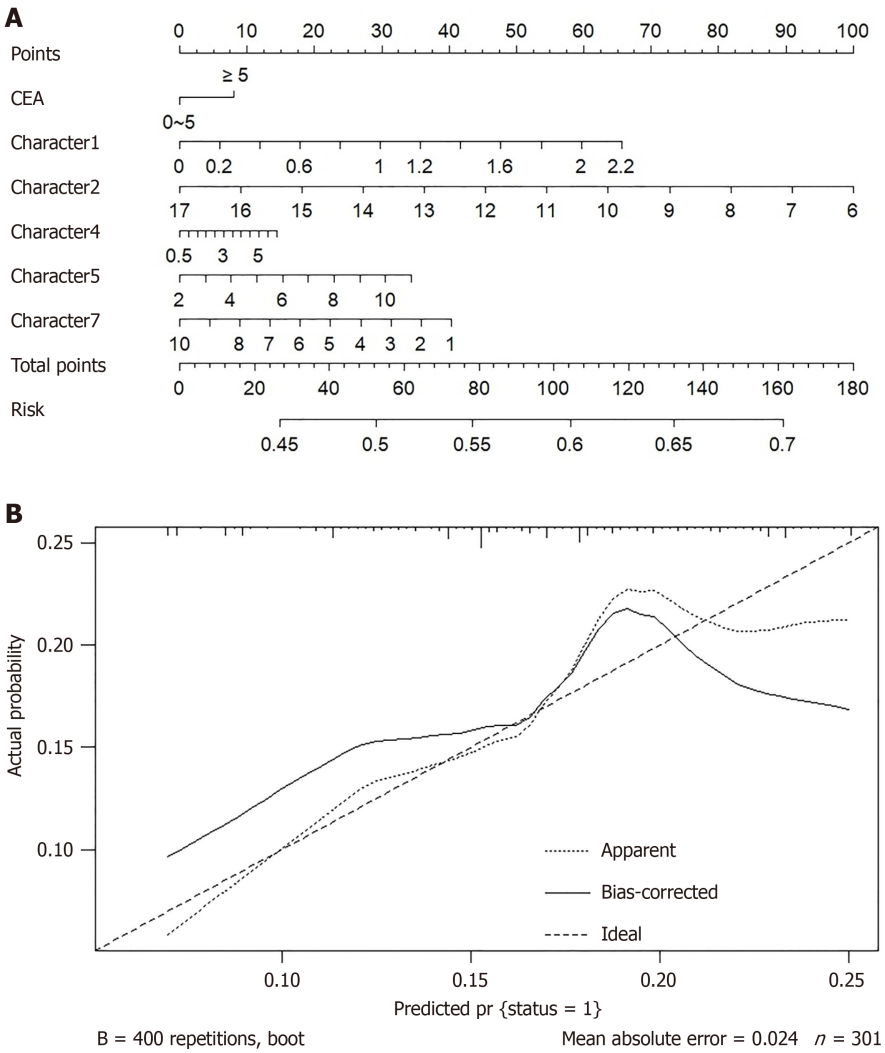

Figure 3 Nomogram visual prediction model for predicting metachronous liver metastasis. A: Nomogram; B: Calibration curve. CEA: Carcinoembryonic antigen.

feature 7 were identified as the four major important variables, while other clinical indices followed closely behind. Besides, the AUC of the training queue reached 0.919 (95%CI: 0.868-0.970), with a sensitivity of 0.94 and a specificity of 0.99 (Figure 4), significantly better than the AUC of traditional GLRM ($P < 0.05$). In the validation queue, the AUC of the RFM reached 0.901 (95%CI: 0.850-0.952), with a sensitivity of 0.94 and a specificity of 0.99. As shown in Figure 5, in terms of evaluating the predictive robustness of the model, RFM also demonstrates superior predictive performance compared to GLRM.

Meanwhile, we used SHapley additive explanations to evaluate the RFM, as shown in Supplementary Figure 2. It was also observed that feature 1, feature 2, feature 4, and feature 7 play the most crucial roles in predicting and interpreting RFM. Specifically, elasticity score, maximum diameter and Adler blood flow grading were associated with an increased risk of MLM.

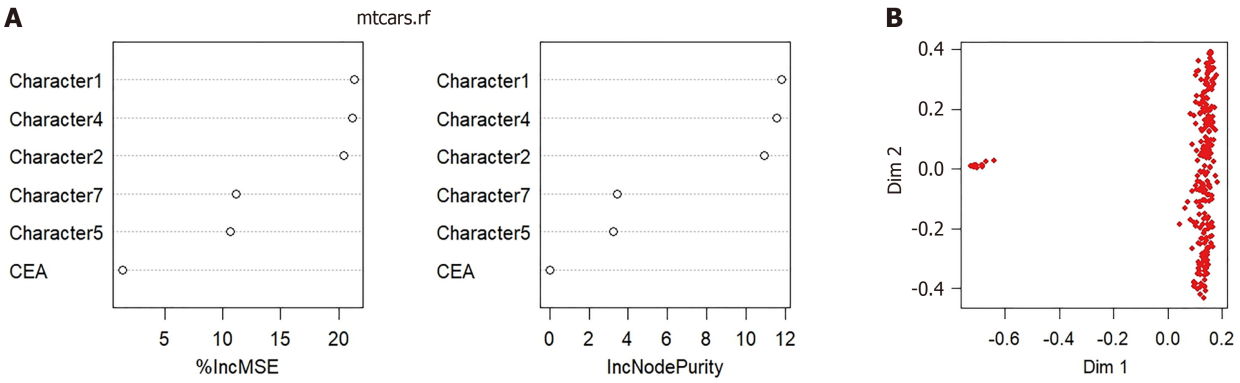

Figure 4 Random forest prediction model for predicting metachronous liver metastasis. A: The random forest prediction model based on machine learning algorithms; B: Predictive performance detection of models. The red dots represent patients with metachronous liver metastasis, and the blue dots represent patients without metachronous liver metastasis.

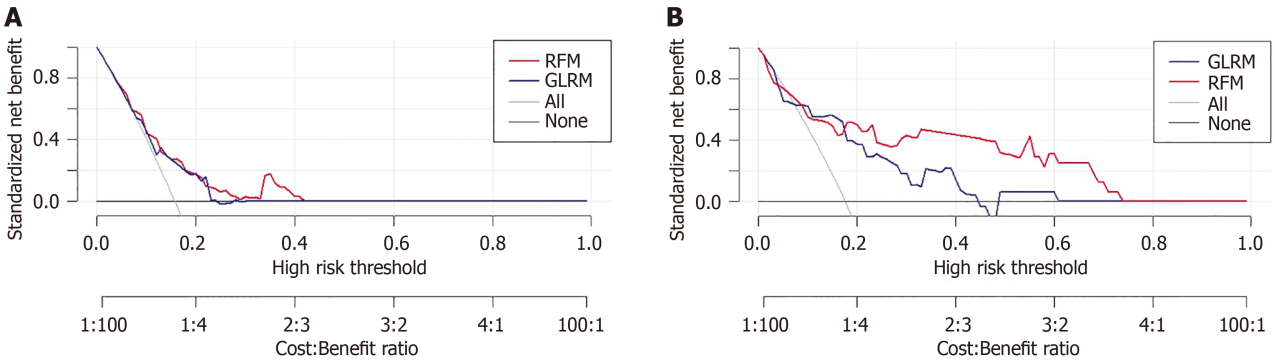

Figure 5 Performance evaluation of predictive models based on decision curve analysis. A: Training cohort; B: Testing cohort. RFM: Random forest model; GLRM: Generalized linear regression model.

DISCUSSION

Surgery is currently one of the main treatments for colorectal liver metastases[21,22]. However, most patients with colorectal liver metastases have missed the optimal treatment time when diagnosed, resulting in poor survival and poor prognosis[9,23]. Our study attempts to construct and validate a fusion radiomics MLM prediction model from the MRI images of the first diagnosed primary tumors of patients with rectal cancer (*i.e.*, high b-value DWI, HD T2WI), combined with the patient's clinical baseline characteristics and non-radiomics MRI features. The results suggest that compared with a single clinical predictor, the fused radiomics model has better predictive performance, suggesting that this prediction model has the potential to help clinicians adjust treatment plans based on the probability of liver metastasis, thereby improving the prognosis and long-term survival rate of rectal cancer patients.

Early detection of liver metastasis in rectal cancer has always been a major challenge in clinical diagnosis and treatment, especially in accurately predicting MLM, which is crucial for adjusting treatment plans reasonably[24-26]. However, there is currently no effective method in clinical practice. This study found that MRI has unparalleled advantages in multi parameter and multi plane imaging compared to other imaging examinations, and has become the preferred imaging method for tumor staging and re staging of rectal cancer patients after treatment. However, there are still few reports on predicting MLM based on MRI radiomics[27,28]. Previous studies reported using convolutional networks to analyze preoperative liver CT images of patients with rectal cancer, extract and analyze liver imaging features, and construct MLM predictions based on patient clinical characteristics[29-31]. Consistent with previous research, the GLRM model finally achieved AUCs of 0.765 and 0.767 in the validation set and training set respectively.

The results of this study also showed that the AUC of the RFM model built based on the radiomics and clinical baseline characteristics of HD T2WI and DWI of the primary tumor in the training set and validation set were 0.919 and 0.901 respectively, suggesting that MRI-based radiomics is effective for MLM. Unparalleled predictive advantage. We speculate that the high-definition T2WI sequence in the MRI sequence has the characteristics of small field of view, large matrix, high spatial resolution, and multiple signal acquisition times. Therefore, it can clearly display the invasion of adjacent structures by the tumor and help distinguish subtle differences, especially high b-value DWI sequences can show the degree of diffusion restriction of free water molecules in the tumor cell microenvironment and can reflect more heterogeneous information within the tumor.

Our study still inevitably has the following limitations. Firstly, this study is based on MRI images and clinical data of rectal cancer patients obtained from a single center institution. Subsequent studies still need to expand the sample size or

further evaluate the MLM prediction performance of the fusion prediction model in conjunction with multi center institutions, as well as obtain external queue validation; Secondly, due to limitations in case imaging data, this study only obtained plain MRI images of the rectum at the initial diagnosis of rectal cancer patients, and there is still a lack of comparison between enhanced MRI images of the rectum. Therefore, subsequent studies need to add imaging omics features in dynamic enhanced sequences; Thirdly, this study is a retrospective study. Due to incomplete follow-up data of some rectal cancer patients, the results may be compromised. Therefore, future studies still need to focus on prospective cohort studies to reduce data bias errors.

CONCLUSION

In general, a radiomics prediction model based on preoperative primary tumor MRI images of rectal cancer patients combined with relevant clinical baseline features has high accuracy in predicting MLM of rectal cancer. In particular, RFM is expected to provide auxiliary guidance for clinical and imaging physicians to monitor MLM of rectal cancer, and help provide effective information for patients to develop personalized treatment plans, thereby helping to improve the long-term survival and prognosis of rectal cancer patients.

FOOTNOTES

Author contributions: Wang R designed the research study; Long ZD has completed the preliminary data collection and visualization analysis; Yu X and Xing ZX have completed the initial draft and proofreading of their paper; All authors have made final corrections to the manuscript.

Institutional review board statement: This study has been approved by the Ethics Committee of Jingzhou Central Hospital and complies with the Helsinki Declaration. All included patients were exempt from informed consent, No. 2024-154-01.

Informed consent statement: As the study only involved retrospective chart reviews, informed written consents were not required in accordance with institutional IRB policy.

Conflict-of-interest statement: The authors declare that they have no conflict of interest.

Data sharing statement: Not applicable.

STROBE statement: The authors have read the STROBE Statement—a checklist of items, and the manuscript was prepared and revised according to the STROBE Statement-a checklist of items.

Country of origin: China

ORCID number: Rui Wang 0009-0004-5263-6745.

S-Editor: Fan M
L-Editor: A
P-Editor: Zhao YQ

REFERENCES

1 **Sung H**, Ferlay J, Siegel RL, Laversanne M, Soerjomataram I, Jemal A, Bray F. Global Cancer Statistics 2020: GLOBOCAN Estimates of Incidence and Mortality Worldwide for 36 Cancers in 185 Countries. *CA Cancer J Clin* 2021; **71**: 209-249 [PMID: 33538338 DOI: 10.3322/caac.21660]

2 **Keum N**, Giovannucci E. Global burden of colorectal cancer: emerging trends, risk factors and prevention strategies. *Nat Rev Gastroenterol Hepatol* 2019; **16**: 713-732 [PMID: 31455888 DOI: 10.1038/s41575-019-0189-8]

3 **Connell LC**, Mota JM, Braghiroli MI, Hoff PM. The Rising Incidence of Younger Patients With Colorectal Cancer: Questions About Screening, Biology, and Treatment. *Curr Treat Options Oncol* 2017; **18**: 23 [PMID: 28391421 DOI: 10.1007/s11864-017-0463-3]

4 **Cao W**, Chen HD, Yu YW, Li N, Chen WQ. Changing profiles of cancer burden worldwide and in China: a secondary analysis of the global cancer statistics 2020. *Chin Med J (Engl)* 2021; **134**: 783-791 [PMID: 33734139 DOI: 10.1097/CM9.0000000000001474]

5 **Engstrand J**, Nilsson H, Strömberg C, Jonas E, Freedman J. Colorectal cancer liver metastases - a population-based study on incidence, management and survival. *BMC Cancer* 2018; **18**: 78 [PMID: 29334918 DOI: 10.1186/s12885-017-3925-x]

6 **Suthananthan AE**, Bhandari M, Platell C. Influence of primary site on metastatic distribution and survival in stage IV colorectal cancer. *ANZ J Surg* 2018; **88**: 445-449 [PMID: 28512795 DOI: 10.1111/ans.13969]

7 **Tan EK**, Ooi LLPJ. Colorectal Cancer Liver Metastases – Understanding the Differences in the Management of Synchronous and Metachronous Disease. *Ann Acad Med Singap* 2010; **39**: 719-733 [DOI: 10.47102/annals-acadmedsg.v39n9p719]

8 **Slesser AA**, Georgiou P, Brown G, Mudan S, Goldin R, Tekkis P. The tumour biology of synchronous and metachronous colorectal liver metastases: a systematic review. *Clin Exp Metastasis* 2013; **30**: 457-470 [PMID: 23180209 DOI: 10.1007/s10585-012-9551-8]

9 **Akgül Ö**, Çetinkaya E, Ersöz Ş, Tez M. Role of surgery in colorectal cancer liver metastases. *World J Gastroenterol* 2014; **20**: 6113-6122 [PMID: 24876733 DOI: 10.3748/wjg.v20.i20.6113]

10 **Zhou JM**, Wang L, Mao AR. Value and prognostic factors of repeat hepatectomy for recurrent colorectal liver metastasis. *Hepatobiliary Pancreat Dis Int* 2023; **22**: 570-576 [PMID: 36858891 DOI: 10.1016/j.hbpd.2023.02.005]

11 **Barbon C**, Margonis GA, Andreatos N, Rezaee N, Sasaki K, Buettner S, Damaskos C, Pawlik TM, He J, Wolfgang CL, Weiss MJ. Colorectal Liver Metastases: Does the Future of Precision Medicine Lie in Genetic Testing? *J Gastrointest Surg* 2018; **22**: 1286-1296 [PMID: 29644557 DOI: 10.1007/s11605-018-3766-1]

12 **Hołówko W**, Grąt M, Hinderer B, Orlińska I, Krawczyk M. Prediction of survival in patients with unresectable colorectal liver metastases. *Pol Przegl Chir* 2014; **86**: 319-324 [PMID: 25222579 DOI: 10.2478/pjs-2014-0056]

13 **Li ZF**, Kang LQ, Liu FH, Zhao M, Guo SY, Lu S, Quan S. Radiomics based on preoperative rectal cancer MRI to predict the metachronous liver metastasis. *Abdom Radiol (NY)* 2023; **48**: 833-843 [PMID: 36529807 DOI: 10.1007/s00261-022-03773-1]

14 **Colloca GA**, Venturino A, Guarneri D. Different variables predict the outcome of patients with synchronous versus metachronous metastases of colorectal cancer. *Clin Transl Oncol* 2020; **22**: 1399-1406 [PMID: 31916018 DOI: 10.1007/s12094-019-02277-7]

15 **Liang M**, Cai Z, Zhang H, Huang C, Meng Y, Zhao L, Li D, Ma X, Zhao X. Machine Learning-based Analysis of Rectal Cancer MRI Radiomics for Prediction of Metachronous Liver Metastasis. *Acad Radiol* 2019; **26**: 1495-1504 [PMID: 30711405 DOI: 10.1016/j.acra.2018.12.019]

16 **Lu Z**, Sun J, Wang M, Jiang H, Chen G, Zhang W. A nomogram prediction model based on clinicopathological combined radiological features for metachronous liver metastasis of colorectal cancer. *J Cancer* 2024; **15**: 916-925 [PMID: 38230226 DOI: 10.7150/jca.88778]

17 **Liu Y**, Wang Y, Zhang H, Zheng M, Wang C, Hu Z, Wang Y, Xiong H, Hu H, Tang Q, Wang G. Nomogram for predicting occurrence of synchronous liver metastasis in colorectal cancer: a single-center retrospective study based on pathological factors. *World J Surg Oncol* 2022; **20**: 39 [PMID: 35183207 DOI: 10.1186/s12957-022-02516-2]

18 **Díez-Alonso M**, Mendoza-Moreno F, Jiménez-Álvarez L, Nuñez O, Blazquez-Martín A, Sanchez-Gollarte A, Matías-García B, Molina R, San-Juan A, Gutierrez-Calvo A. Prognostic factors of survival in stage IV colorectal cancer with synchronous liver metastasis: Negative effect of the KRAS mutation. *Mol Clin Oncol* 2021; **14**: 93 [PMID: 33767862 DOI: 10.3892/mco.2021.2255]

19 **Inchingolo R**, Maino C, Cannella R, Vernuccio F, Cortese F, Dezio M, Pisani AR, Giandola T, Gatti M, Giannini V, Ippolito D, Faletti R. Radiomics in colorectal cancer patients. *World J Gastroenterol* 2023; **29**: 2888-2904 [PMID: 37274803 DOI: 10.3748/wjg.v29.i19.2888]

20 **Staal FCR**, van der Reijd DJ, Taghavi M, Lambregts DMJ, Beets-Tan RGH, Maas M. Radiomics for the Prediction of Treatment Outcome and Survival in Patients With Colorectal Cancer: A Systematic Review. *Clin Colorectal Cancer* 2021; **20**: 52-71 [PMID: 33349519 DOI: 10.1016/j.clcc.2020.11.001]

21 **Kambakamba P**, Hoti E, Cremen S, Braun F, Becker T, Linecker M. The evolution of surgery for colorectal liver metastases: A persistent challenge to improve survival. *Surgery* 2021; **170**: 1732-1740 [PMID: 34304889 DOI: 10.1016/j.surg.2021.06.033]

22 **Rocca A**, Scacchi A, Cappuccio M, Avella P, Bugiantella W, De Rosa M, Costa G, Polistena A, Codacci-Pisanelli M, Amato B, Carbone F, Ceccarelli G. Robotic surgery for colorectal liver metastases resection: A systematic review. *Int J Med Robot* 2021; **17**: e2330 [PMID: 34498805 DOI: 10.1002/rcs.2330]

23 **Puijk RS**, Ruarus AH, Vroomen LGPH, van Tilborg AAJM, Scheffer HJ, Nielsen K, de Jong MC, de Vries JJJ, Zonderhuis BM, Eker HH, Kazemier G, Verheul H, van der Meijs BB, van Dam L, Sorgedrager N, Coupé VMH, van den Tol PMP, Meijerink MR; COLLISION Trial Group. Colorectal liver metastases: surgery versus thermal ablation (COLLISION) - a phase III single-blind prospective randomized controlled trial. *BMC Cancer* 2018; **18**: 821 [PMID: 30111304 DOI: 10.1186/s12885-018-4716-8]

24 **Adam R**, de Gramont A, Figueras J, Kokudo N, Kunstlinger F, Loyer E, Poston G, Rougier P, Rubbia-Brandt L, Sobrero A, Teh C, Tejpar S, Van Cutsem E, Vauthey JN, Påhlman L; of the EGOSLIM (Expert Group on OncoSurgery management of LIver Metastases) group. Managing synchronous liver metastases from colorectal cancer: a multidisciplinary international consensus. *Cancer Treat Rev* 2015; **41**: 729-741 [PMID: 26417845 DOI: 10.1016/j.ctrv.2015.06.006]

25 **Patel I**, Bartlett D, Dasari BV, Chatzizacharias N, Isaac J, Marudanayagam R, Mirza DF, Roberts JK, Sutcliffe RP. Detection of Colorectal Liver Metastases Using Near-Infrared Fluorescence Imaging During Hepatectomy: Prospective Single Centre UK Study. *J Gastrointest Cancer* 2023; **54**: 574-579 [PMID: 35616823 DOI: 10.1007/s12029-022-00836-w]

26 **Martin J**, Petrillo A, Smyth EC, Shaida N, Khwaja S, Cheow HK, Duckworth A, Heister P, Praseedom R, Jah A, Balakrishnan A, Harper S, Liau S, Kosmoliaptsis V, Huguet E. Colorectal liver metastases: Current management and future perspectives. *World J Clin Oncol* 2020; **11**: 761-808 [PMID: 33200074 DOI: 10.5306/wjco.v11.i10.761]

27 **Granata V**, Fusco R, Setola SV, Galdiero R, Maggialetti N, Patrone R, Ottaiano A, Nasti G, Silvestro L, Cassata A, Grassi F, Avallone A, Izzo F, Petrillo A. Colorectal liver metastases patients prognostic assessment: prospects and limits of radiomics and radiogenomics. *Infect Agent Cancer* 2023; **18**: 18 [PMID: 36927442 DOI: 10.1186/s13027-023-00495-x]

28 **Alshohoumi F**, Al-Hamdani A, Hedjam R, AlAbdulsalam A, Al Zaabi A. A Review of Radiomics in Predicting Therapeutic Response in Colorectal Liver Metastases: From Traditional to Artificial Intelligence Techniques. *Healthcare (Basel)* 2022; **10** [PMID: 36292522 DOI: 10.3390/healthcare10102075]

29 **Han Z**, Tong Y, Zhu X, Sun D, Jia N, Feng Y, Yan K, Wei Y, He J, Ju H. Development and external validation of MRI-based RAS mutation status prediction model for liver metastases of colorectal cancer. *J Surg Oncol* 2024; **129**: 556-567 [PMID: 37974474 DOI: 10.1002/jso.27508]

30 **Kijima S**, Sasaki T, Nagata K, Utano K, Lefor AT, Sugimoto H. Preoperative evaluation of colorectal cancer using CT colonography, MRI, and PET/CT. *World J Gastroenterol* 2014; **20**: 16964-16975 [PMID: 25493009 DOI: 10.3748/wjg.v20.i45.16964]

31 **Granata V**, Fusco R, Brunese MC, Ferrara G, Tatangelo F, Ottaiano A, Avallone A, Miele V, Normanno N, Izzo F, Petrillo A. Machine Learning and Radiomics Analysis for Tumor Budding Prediction in Colorectal Liver Metastases Magnetic Resonance Imaging Assessment. *Diagnostics (Basel)* 2024; **14** [PMID: 38248029 DOI: 10.3390/diagnostics14020152]

World Journal of Gastrointestinal Oncology

Submit a Manuscript: https://www.f6publishing.com

World J Gastrointest Oncol 2025 January 15; 17(1): 92908

DOI: 10.4251/wjgo.v17.i1.92908

ISSN 1948-5204 (online)

ORIGINAL ARTICLE

Retrospective Study

Association between autoimmune gastritis and gastric polyps: Clinical characteristics and risk factors

Jing-Zheng Jin, Xiao Liang, Shu-Peng Liu, Rui-Lan Wang, Qing-Wei Zhang, Yu-Feng Shen, Xiao-Bo Li

Specialty type: Gastroenterology and hepatology

Provenance and peer review: Unsolicited article; Externally peer reviewed.

Peer-review model: Single blind

Peer-review report's classification

Scientific Quality: Grade C
Novelty: Grade B
Creativity or Innovation: Grade B
Scientific Significance: Grade B

P-Reviewer: Soldera J

Received: February 10, 2024
Revised: August 23, 2024
Accepted: September 11, 2024
Published online: January 15, 2025
Processing time: 306 Days and 0.8 Hours

Jing-Zheng Jin, Division of Gastroenterology and Hepatology, Renji Hospital, Shanghai Jiao Tong University School of Medicine, Shanghai 200127, China

Jing-Zheng Jin, Xiao Liang, Shu-Peng Liu, Qing-Wei Zhang, Yu-Feng Shen, Division of Gastroenterology and Hepatology, Shanghai Institute of Digestive Diseases, Shanghai 200001, China

Xiao Liang, Shu-Peng Liu, Qing-Wei Zhang, Division of Gastroenterology and Hepatology, Renji Hospital Affiliated to Shanghai Jiao Tong University School of Medicine, Shanghai 200127, China

Rui-Lan Wang, Division of Gastroenterology and Hepatology, Sichuan Armed Police Corps Hospital, Leshan 610041, Sichuan Province, China

Yu-Feng Shen, Division of Gastroenterology and Hepatology, NHC Key Laboratory of Digestive Diseases, Renji Hospital, Shanghai Jiao Tong University School of Medicine, Shanghai 200127, China

Xiao-Bo Li, Department of Gastroenterology, Renji Hospital Affiliated to Shanghai Jiao Tong University School of Medicine Shanghai Institute of Digestive Diseases, Shanghai 200127, China

Co-first authors: Jing-Zheng Jin and Xiao Liang.

Co-corresponding authors: Yu-Feng Shen and Xiao-Bo Li.

Corresponding author: Xiao-Bo Li, MD, PhD, Doctor, Professor, Department of Gastroenterology, Renji Hospital Affiliated to Shanghai Jiao Tong University School of Medicine Shanghai Institute of Digestive Diseases, No. 160 Pujian Road, Pudong New Area, Shanghai 200127, China. lxb196911@163.com

Abstract

BACKGROUND

The relationship between autoimmune gastritis (AIG) and gastric polyps (GPs) is not well understood.

AIM

To explore the clinical characteristics and risk factors of AIG with GPs in patients.

METHODS
This double center retrospective study included 530 patients diagnosed with AIG from July 2019 to July 2023. We collected clinical, biochemical, serological, and demographic data were of each patient. Logistic regression analyses, both multivariate and univariate, were conducted to pinpoint independent risk factors for GPs in patients with AIG patients. Receiver operating characteristic curves were utilized to establish the optimal cutoff values, sensitivity, and specificity of these risk factors for predicting GPs in patients with AIG.

RESULTS
Patients with GPs had a higher median age than those without GPs [61 (52.25-69) years *vs* 58 (47-66) years, P = 0.006]. The gastrin-17 levels were significantly elevated in patients with GPs compared with those without GPs [91.9 (34.2-138.9) pmol/mL *vs* 60.9 (12.6-98.4) pmol/mL, $P < 0.001$]. Additionally, the positive rate of parietal cell antibody (PCA) antibody was higher in these patients than in those without GPs (88.6% *vs* 73.6%, $P < 0.001$). Multivariate and univariate analyses revealed that PCA positivity [odds ratio (OR) = 2.003, P = 0.017], pepsinogen II (OR = 1.053, P = 0.015), and enterochromaffin like cells hyperplasia (OR = 3.116, $P < 0.001$) were significant risk factors for GPs, while pepsinogen I was identified as a protective factor.

CONCLUSION
PCA positivity and enterochromaffin like cells hyperplasia are significant risk factor for the development of GPs in patients with AIG. Elevated gastrin-17 levels may also play a role in this process. These findings suggest potential targets for further research and therapeutic intervention in managing GPs in patients with AIG.

Key Words: Autoimmune gastritis; Gastric polyps; Neuroendocrine tumor; Risk factors; Nomogram

Core Tip: In this double-center retrospective study, we explore the clinical characteristics and risk factors associated with autoimmune gastritis (AIG) and gastric polyps in 530 patients diagnosed with AIG from July 2019 to July 2023. The study found that higher age, elevated gastrin-17 levels, and higher positivity rates of parietal cell antibody antibodies were significantly associated with the presence of gastric polyps in AIG patients. Through univariate and multivariate analyses, parietal cell antibody positivity, elevated pepsinogen II levels, and enterochromaffin like cells hyperplasia were identified as significant risk factors.

Citation: Jin JZ, Liang X, Liu SP, Wang RL, Zhang QW, Shen YF, Li XB. Association between autoimmune gastritis and gastric polyps: Clinical characteristics and risk factors. *World J Gastrointest Oncol* 2025; 17(1): 92908
URL: https://www.wjgnet.com/1948-5204/full/v17/i1/92908.htm
DOI: https://dx.doi.org/10.4251/wjgo.v17.i1.92908

INTRODUCTION

Gastric polyps (GPs) are protrusions that form within the stomach's mucosal or submucosal layers. They are typically asymptomatic and are often detected incidentally during routine endoscopic examinations. While most GPs are benign, there is a potential for some to harbor dysplasia, which can progress to invasive cancer. The prevalence of GPs varies among sources, with several high-powered studies, reporting rates between 2% to 6% in patients undergoing endoscopy [1,2]. The most commonly observed types of GPs include gastric hyperplastic polyps (GHPs), characterized by significant foveolar hyperplasia; fundic gland polyps (FGPs), which are marked by dilated and irregularly budding fundic glands primarily composed of parietal cells, with a smaller proportion of chief cells. Additionally, adenomatous polyps, which are associated with low-grade glandular dysplasia[3-6], and gastric neuroendocrine neoplasms (gNENs), which are well-differentiated epithelial tumors arising from neuroendocrine cells within the gastric mucosa, can also present as submucosal lesions with specific patterns[7]. All these types can produce a mucosal or submucosal protrusion that appears as a GP[8].

GPs almost never occur in normal gastric mucosa. The majority of GPs are found incidentally during endoscopic investigations, and not fully the exact mechanism behind the formation of GHPs remains unclear[9]. However, their development is thought to be associated with chronic inflammation, commonly linked to atrophic gastritis and *Helicobacter pylori* (*H. pylori*) infection[10,11]. Prolonged use of proton pump inhibitors (PPIs) may lead to hypergastrinemia, which is associated with the development of both FGPs and GHPs[12,13]. The primary risk factors for adenoma development include age and chronic irritation or inflammation of the tissue, which can lead to intestinal metaplasia. This metaplasia increase the risk of malignant transformation, often linked to acquired mutations in genes such as p53 and Ki-67[14,15].

Autoimmune gastritis (AIG) is a chronic organ-specific atrophic gastritis, that is not self-limiting. Endoscopic examination reveals atrophy is typically confined to the body and fundus mucosa of the stomach, sparing the gastric antrum[16]. The disease is characterized by self-reactive T cells, and activated B cells that produce antibodies (PCA) and anti-intrinsic factor antibodies (IFAs). This immune response leads to the destruction of parietal cells, which impairs intrinsic factor secretion, resulting in disorders of iron and vitamin B12 absorption[17]. The destruction of parietal and chief cells results in the replacement of gastric glands with either connective tissue or a different type of epithelial tissue [18]. This process results in lowered hydrochloric acid production, decreased blood levels of pepsinogen I (PG-I), and elevated gastrin levels[19]. Intestinal metaplasia of the gastric mucosa is a precursor to gastric adenoma and adenocarcinoma, according to the Correa cascade, and patients with AIG have an elevated risk of developing gastric adenocarcinoma compared to the general population[20]. Moreover, hypergastrinemia resulting from reduced stomach acid can lead to enterochromaffin-like (ECL) cell hyperplasia and an increased incidence of gNENs[21-23]. Although, hypergastrinemia is frequently observed in patients with AIG and those using long-term PPIs, definitive data linking AIG to GPs, are limited, with most studies focusing on adenocarcinoma and gNENs[24]. The main objective of this study was to evaluate the frequency of GPs in patients with AIG and to investigate the biochemical, clinical, and histological factors that may predict GP occurrence in this group.

MATERIALS AND METHODS

This double center retrospective study retrospectively enrolled patients diagnosed with AIG at the Renji Hospital Affiliated with Shanghai Jiao Tong University School of Medicine, Department of Gastroenterology, and the Sichuan Armed Police Corps Hospital, Department of Gastroenterology, from June 2019 to June 2023. The exclusion criteria comprised the absence of histologic data, inadequate biopsy samples, discordant laboratory or pathological findings, presence of active tumors, or severe organ failure. This study received approval from the Institutional Ethics Committee of Renji Hospital, Shanghai Jiao Tong University, School of Medicine, with a waiver for informed consent.

Clinical data were obtained from medical records and outpatient consultation systems. To ensure confidentiality, all patient data were anonymized following collection, recording, assessment, and analysis. AIG diagnosis was based on pathological features observed in endoscopic biopsy tissue, such as parietal cell destruction, chronic lymphocytic infiltration, and the presence or absence of pseudopyloric gland metaplasia and neuroendocrine cell hyperplasia. Endoscopic findings of characteristic atrophy, positive PCA or IFA, and elevated circulating gastrin-17 levels were used to support the diagnosis of AIG[18,25,26]. Baseline evaluations for all enrolled patients, included demographic data (sex, and age at AIG diagnosis), clinical data (comorbidities and previous treatments), serologic examination, and upper gastrointestinal endoscopic biopsy with histopathology.

Upper gastrointestinal endoscopy

All diagnostic and surveillance esophagogastroduodenoscopy (EGD) procedures were performed using standard gastroscopy techniques. Patients who had previously undergone PPI therapy were examined at least 2 weeks after discontinuation. According to the updated Sydney classification[27], each patients with AIG undergoing monitored EGD, patients with five gastric biopsies: Four from the antrum, corpus and fundus, one from the incisura angularis. The biopsy specimens were directly sent to the pathology laboratory for examination. All patients with suspected *H. pylori* infection underwent a rapid urease test.

For macroscopic polypoid mucosal lesions, the following data were recorded: Histologic features (*e.g.*, hyperplastic, fundic glandular, adenomatous, neuroendocrine, adenocarcinoma, or other neoplasm), and year of occurrence, location (antrum, body, or fundus), size, treatment modality. Lesions were biopsied, with the largest lesions removed if multiple polyps were present. Lesions less than or equal to 5 mm in diameter were removed using forceps as a "cold biopsy", while larger lesions required endoscopic mucosal resection. For lesions greater than 1 cm, narrow band imaging or endoscopic ultrasonography was performed to assess the extent of the lesion and invasion depth. Endoscopic mucosal dissection was planned if necessary.

For patients with uncomplicated AIG, endoscopic monitoring was scheduled every 1-3 years, based on the degree of atrophy and the presence of intestinal metaplasia. Patients with gNENs underwent annual endoscopic follow-up[18,28]. For those diagnosed with gastric adenocarcinoma, individualized evaluations were carried out to establish the most suitable intervention and follow-up plan.

Histopathological examination

The diagnosis of AIG was made based on histopathological findings, including the destruction of parietal cells, chronic lymphocytic infiltration, with or without pseudopyloric gland metaplasia and neuroendocrine cell hyperplasia[18]. Biopsies sample were collected during EGD according to the updated Sydney classification[27]. Each patient was evaluated for *H. pylori* infection. The severity of mucosal atrophy and the associated gastric cancer risk were staged using the Operative Link on Gastritis Assessment (OLGA) score (stages I-IV), while intestinal metaplasia was assessed using the Operative Link on Gastric Intestinal Metaplasia (OLGIM) score (stages I-IV)[29,31].

Additionally, pseudopyloric metaplasia was assessed. ECL cell proliferation was detected using chromogranin A staining following Solcia *et al*'s criteria[32,33], categorized as simple, linear, micronodular, or macronodular and defined as hyperplasia with a diameter greater than 150 μm. The specimens were preserved in formalin and processed through standard laboratory protocols. Gastric mucosa sections, with a thickness of 5 μm, were stained with hematoxylin and assessed for intestinal metaplasia using Alcian blue-PAS staining. Immunohistochemical analyses were conducted on

gNEN sections for chromogranin A, synaptophysin, and the Ki-67 proliferation index, utilizing the MIB-I antibody. All gastric neuroendocrine tumors (gNETs) were classified according to the 2019 World Health Organization classification system[34] and staged in accordance with the tumor node metastasis staging system as per ENETS guidelines[35].

Laboratory serological testing

Fasting blood samples for biochemical testing were obtained at 8 am. Serum samples were collected using standard blood collection tubes, while plasma samples were collected using ethylenediaminetetraacetic acid (1 mg/mL) or heparin tubes. Anemia was defined as a hemoglobin level of less than 12 g/dL in women and less than 13 g/dL in men. Macrocytic anemia was identified when the mean corpuscular volume exceeded 100 fL, while microcytic anemia was defined when the mean corpuscular volume was less than 80 fL. The reference ranges for white blood cells were (4-11) × 10^9/L, for platelets were (100-300) × 10^9/L, for thyroid-stimulating hormone were 0.4-4.91 mIU/mL, for vitamin B12 were 180-914 pg/mL, and for iron were 7.8-32.2 μmol/L. PCA and IFA antibodies were detected using dilution and direct enzyme-linked immunosorbent assay, with positivity defined as a value ≥ 1:20. The PG-I, PG-II and gastrin-17 level in peripheral blood were measured by enzyme-linked immunosorbent assay, with normal ranges being 70-165 μg/L, 3-15 μg/L and less than 7 pmol/mL, respectively. For patients on PPI therapy, blood tests should were to repeated at least 15 days after discontinuation of the medication.

Construction and validation of a clinical nomogram

A multivariate logistic regression analysis was conducted using several clinical parameters: Age, sex, PCA, IFA, previous *H. pylori* infection, OLGA score, OLGIM score, presence or absence of anemia, ECL hyperplasia, PG ratio, and levels of PG-I, PG-II, and gastrin-17. Backward stepwise regression, optimal subset selection, and likelihood ratio tests were applied, with the Akaike Information Criterion (AIC) as the stopping criterion. The AIC was used to evaluate the model's goodness of fit. To assist clinicians in predicting the likelihood of developing GPs in AIG patients, a clinical nomogram was developed based on multivariate logistic analysis of the main cohort. The model's discrimination was evaluated using receiver operating characteristic (ROC) curve analysis, with performance measured by the area under the curve. Odds ratios with 95% confidence intervals (CIs) for the final predictors were calculated. Calibration curves were used to compare predicted and observed probabilities, thereby assessing the model's accuracy.

Statistical analysis

The Kolmogorov-Smirnov test was employed to assess the normality of continuous variables. For variables with a normal distribution, data were presented as mean ± SD. For non-normally distributed variables, the median and interquartile range (IQR) were reported. Categorical variables were described using counts and percentages. To compare groups, the Mann-Whitney *U* test and Kruskal-Wallis test were utilized for non-parametric data, while proportions were compared using the χ^2 test or Fisher's exact test. Correlations between variables, such as sex, age, PPI usage, *H. pylori* infection status, PCA and/or IFA positivity, OLGA and OLGIM stages, PG ratio, types of GPs, and serum levels of gastrin-17, PG-I, PG-II, and vitamin B12, were analyzed using Pearson's or Spearman's correlation coefficients. Binary logistic regression was conducted to identify potential risk factors for GP development in AIG patients and to create a predictive model. A P value of less than 0.05 (two-tailed) was deemed statistically significant. All analyses were performed using R software (version 4.2.1; R Foundation for Statistical Computing, Vienna, Austria).

RESULTS

Clinical characteristics

The study flow chart is depicted in Figure 1. A total of 530 patients with AIG were initially enrolled; of these, 114 patients were excluded, from the analysis, leaving 166 patients with GPs and 364 patients without GPs. Continuous data was tested for normality. Table 1 summarizes the demographic, characteristics, clinical, biochemical, and histological baseline characteristics of the enrolled patient. The median age of the study population was 59 (IQR: 48-67) years, with a predominance of females (68.3%). Among the subjects, 17.2% had a history of *H. pylori* infection. The positive rates for PCA and IFA antibodies were 78.3% and 24.7%, respectively. Anemia was present in 40.0% of the patients, with iron deficiency anemia accounting for 30.8% and pernicious anemia for 12.5%. The median gastrin-17 level was 70.44 (IQR: 18.30-112.97). ECL hyperplasia was observed in 27.0% of the patients with AIG.

Characteristics and differences between patients with AIG with and without GPs

Patients with AIG were categorized two groups: Those with GPs (GP group) and those without GPs (NGP group). We compared the characteristics and differences between these two groups. Continuous data of non-normal distribution, were analyzed using the Wilcoxon rank-sum test, and differences in categorical data were assessed using the χ^2 test, with pairwise comparisons adjusted by the Bonferroni correction method. The results are summarized in Table 2. The median age of patients with GPs was significantly higher than that of patients without GPs [61 (IQR: 52.25-69) years *vs* 58 (IQR: 47-66) years, $P = 0.006$]. The gastrin-17 levels were also elevated in the GP group compared with the NGP group [91.9 (IQR: 34.2-138.9) pmol/mL *vs* 60.9 (IQR: 12.6-98.4) pmol/mL, $P < 0.001$]. The positive rate of PCA antibodies was also significantly higher in the GP group (88.6% *vs* 73.6%, $P < 0.001$).

Furthermore, there were significant differences in OLGA ($P < 0.001$), OLGIM ($P = 0.018$) staging, and ECL hyperplasia ($P < 0.001$) between the GP and NGP groups (Figure 2). Specifically, the proportion of OLGA stage II was lower in the GP

Table 1 Baseline data showing the demographic data, clinical, biochemical, and histological characteristics of autoimmune gastritis patients

Characteristics	
Patients (*N*)	530
Age (year), median (IQR)	59 (48-67)
Sex (female), *n* (%)	362 (68.30)
PCA positivity, *n* (%)	415 (78.3)
IFA positivity, *n* (%)	131 (24.7)
HP infection positivity, *n* (%)	91 (17.2)
Anemia, *n* (%)	212 (40.0)
Iron deficiency anemia, *n* (%), mild/moderate/severe	163 (30.8), 135/22/6
Pernicious anemia, *n* (%), mild/moderate/severe	66 (12.5), 48/11/7
Gastrin-17 (pmol/L), median (IQR)	70.44 (18.30-112.97)
PG-I (μg/L), median (IQR)	30.67 (20.08-48.61)
PG-II (μg/L), median (IQR)	8.07 (6.40-11.00)
PG-I/PG-II, median (IQR)	3.74 (2.05-6.20)
Vitamin B12 (pg/mL), median (IQR)	239.00 (136.20-355.50)
Norm, *n* (%)	331 (62.5)
Low level, *n* (%)	199 (37.6)
OLGA, *n* (%)	
0	44 (8.3)
I	120 (22.6)
II	179 (33.8)
III	146 (27.6)
IV	41 (7.7)
OLGIM, *n* (%)	
0	134 (25.3)
I	240 (45.3)
II	98 (18.5)
III	45 (8.5)
IV	13 (2.5)
ECL hyperplasia, *n* (%)	143 (27.0)
Absent	387 (73.0)
Linear	62 (11.7)
Micronodular	46 (8.7)
Macronodular	18 (3.4)
gNET	17 (3.2)

IQR: Interquartile range; PCA: Parietal cell antibodies; IFAs: Intrinsic factor antibodies; HP: *Helicobacter pylori*; PG: Pepsinogen; OLGA: Operative Link for Gastritis Assessment; OLGIM: Operative Link on Intestinal Metaplasia Assessment; ECL: Enterochromaffin-like; gNET: Gastric neuroendocrine tumor.

group than in the NGP group, while the proportions of OLGA stages III and IV were higher. There was no significant difference in the proportion of OLGA stages 0/I between the two groups. For OLGIM staging the GP group had a lower proportion of stages 0, I, and II and a higher proportion of stages III and IV than the NGP group. The degree of ECL hyperplasia, including linear, micronodular, and macronodular types, was more pronounced in the GP group than in the NGP group.

Table 2 Differences between patients with and without polyps

Group, *n* (%)	Gastric polyp, 166 (31.3)	Non-gastric polyp, 364 (68.7)	*P* value
Age (year), median (IQR)	61 (52.25-69)	58 (47-66)	0.006
Sex, *n* (%)	112 (67.5)	250 (68.7)	0.859
PCA positivity, *n* (%)	147 (88.6)	268 (73.6)	< 0.001
IFA positivity, *n* (%)	42 (25.3)	89 (24.5)	0.833
HP infection positivity, *n* (%)	24 (14.5)	67 (18.4)	0.264
Anemia, *n* (%)	70 (42.17)	159 (43.68)	0.302
Iron deficiency anemia, *n* (%), mild/moderate/severe	52 (31.33), 44/8/0	111 (30.49), 91/14/6	0.406
Pernicious anemia, *n* (%), mild/moderate/severe	18 (10.84), 14/3/1	48 (13.19), 34/8/6	0.851
Gastrin-17 (pmol/L), median (IQR)	91.9 (34.2-138.9)	60.9 (12.6-98.4)	< 0.001
PG-I (μg/L), median (IQR)	34.83 (22.8-45.7)	30.0 (18.1-58.2)	0.51
PG-II (μg/L), median (IQR)	8.8 (7.2-10.9)	7.8 (6.2-11)	0.019
PG-I/PG-II, median (IQR)	3.7 (2.4-5.0)	3.7 (1.9-6.7)	0.464
Vitamin B12 (pg/mL), median (IQR)	256.0 (130.0-357.2)	238.0 (137.0-354.5)	0.994
Norm/low level, *n* (%)	107 (64.46)/59 (35.54)	224 (61.54)/140 (38.46)	0.584
OLGA (0/I /II/III/IV)	11/34/39/61/21	33/86/140/85/20	< 0.001
OLGIM (0/I/II/III/IV)	38/63/39/21/5	96/177/59/24/8	0.018
ECL hyperplasia (absent/linear/micronodular/macronodular)	86/29/25/9	301/33/21/9	< 0.001

IQR: Interquartile range; PCA: Parietal cell antibodies; IFA: Intrinsic factor antibody; HP: *Helicobacter pylori*; PG: Pepsinogen; OLGA: Operative Link for Gastritis Assessment; OLGIM: Operative Link on Intestinal Metaplasia Assessment; ECL: Enterochromaffin-like.

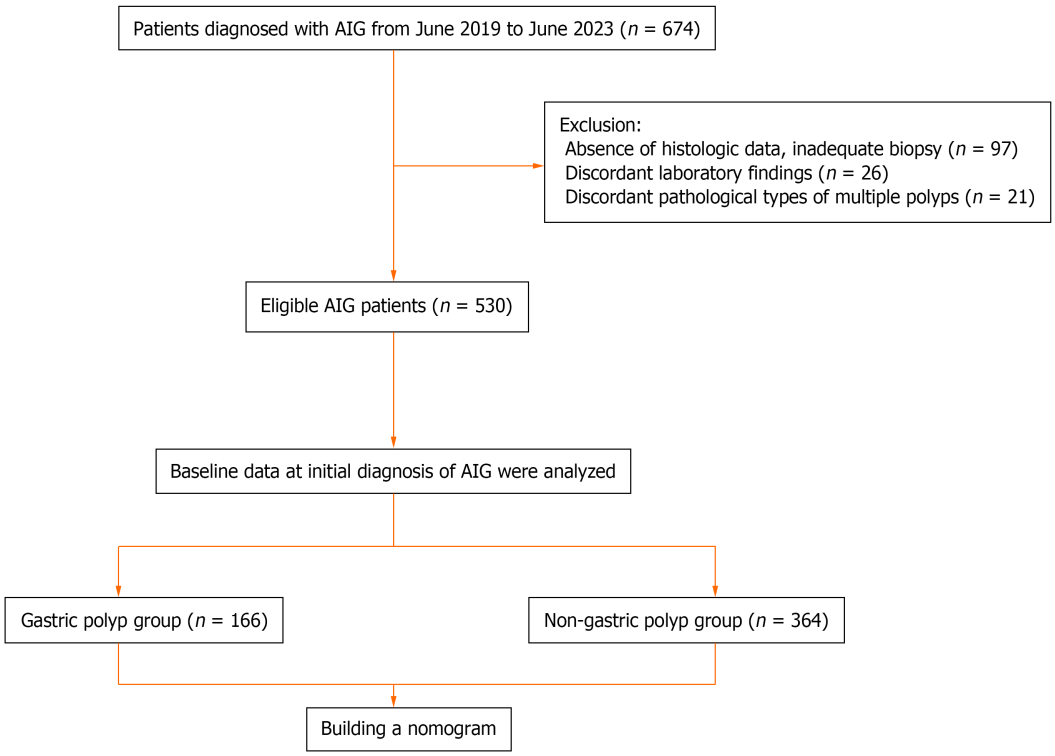

Figure 1 Flow chart depicting the study population and study design. AIG: Autoimmune gastritis.

Table 3 Pathological characteristics and distribution of gastric polyps

Pathology	HPs	Fundic polyps	gNET	Adenomas/LGD	Adenocarcinoma
Patients (*n*)	109	18	17	6	16
Polyps (*n*)	295	54	50	11	23
Diameter (mm), median (IQR)	5 (2-30)	2.5 (2-20)	5 (2-15)	12.5 (4-25)	20 (7-50)
Median number (IQR)	2 (1-3)	1.5 (1-3)	3 (1-4)	1 (1-3)	1 (1-1.25)
Single	49	9	6	5	12
Multiple	60	9	11	1	4
Distribution					
Fundus	34	49	1	1	0
Corpus	223	5	48	4	13
Caria	10	0	0	1	1
Antrum	28	0	1	0	9
OLGA (0/I/II/III/IV)	6/18/28/43/14	4/7/2/4/1	0/2/2/10/3	0/3/1/1/1	1/4/6/3/2
OLGIM (0/I/II/III/IV)	26/39/29/13/3	7/6/3/2/0	3/6/3/5/0	1/4/0/0/4	1/9/4/1/1
ECL hyperplasia					
Absent	61	12	0	4	9
Linear	22	1	0	2	4
Micronodular	19	3	0	0	3
Macronodular	7	2	0	0	0
gNET	0	0	17	0	0

HP: *Helicobacter pylori*; gNET: Gastric neuroendocrine tumor; LGD: Low-grade glandular dysplasia; IQR: Interquartile range; OLGA: Operative Link for Gastritis Assessment; OLGIM: Operative Link on Intestinal Metaplasia Assessment; ECL: Enterochromaffin-like.

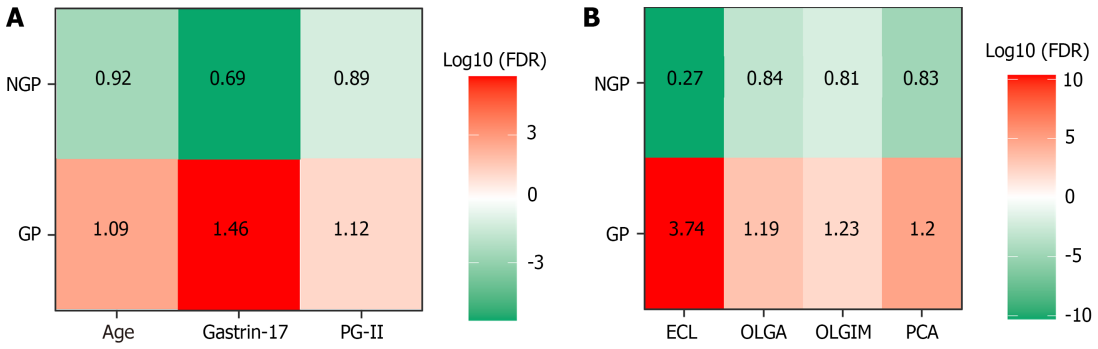

Figure 2 Group differences between the gastric polyp and without gastric polyp groups. A: Heat map of age and blood biochemical difference between gastric polyp group and without gastric polyp group; B: Heat map of histopathological differences between gastric polyp group and without gastric polyp group. GP: Gastric polyp; NGP: Without gastric polyp; FDR: False discovery rate; PG: Pepsinogen; ECL: Enterochromaffin-like; OLGA: Operative Link on Gastritis Assessment; OLGIM: Operative Link on Gastric Intestinal Metaplasia; PCA: Parietal cell antibody.

Characteristics of the GP group differences

Table 3 presents the pathological types and distribution of GPs, as well as the associated degrees of atrophy intestinal metaplasia, and ECL hyperplasia. Among the 166 patients with AIG with GPs, a total of 433 polyps were identified. Hyperplastic polyps were the most prevalent, accounting for 295 (68.1%) of the polyps in 109 (65.7%) patients (Figure 3). Other types included FGPs (12.5%), gNETs (11.6%), gastric adenocarcinoma (5.3%), and gastric adenoma (2.5%). The characteristics of patients across different polyp categories are detailed in Table 4, which presents the pathological features and distribution of GPs. Significant differences were observed in terms of age, sex, *H. pylori* infection, PG-I levels, and gastrin-17 levels. Patients with gNET exhibited the highest mean gastrin-17 levels, while those with gastric adenocarcinomas were the oldest on average (Figure 4A and B). Additionally, the highest mean OLGA stage was noted in patients

Table 4 Pathological characteristics and distribution of gastric polyps

Pathology	Gastric polyp groups (n = 166, N = 433[1])					P value
	HPs	Fundic polyps	gNET	Adenomas/LGD	Adenocarcinoma	
Age (year), median (IQR)	59 (51-67)	56.5 (44.5-71.2)	63 (56-72)	67 (62.8-71.2)	67.5 (61.2-71)	0.012
Sex (female), *n* (%)	75 (68.8)	12 (66.7)	15 (88.2)	4 (66.7)	6 (37.5)	0.041
PCA positivity, *n* (%)	94 (86.2)	15 (83.3)	15 (88.2)	5 (83.3)	15 (93.8)	0.904
IFA positivity, *n* (%)	26 (23.9)	6 (33.3)	3 (17.6)	2 (33.3)	8 (50)	0.185
HP infection positivity, *n* (%)	10 (9.2)	4 (22.2)	1 (5.9)	0 (0)	9 (56.2)	< 0.001
PG-I (μg/L), median (IQR)	33.3 (25-42.8)	38.2 (24.5-48.3)	37.8 (24.1-57.2)	11.5 (11-19.8)	37 (25.8-43.9)	0.033
PG-II (μg/L), median (IQR)	8.8 (7.2-11)	9.3 (7.1-10.4)	9.3 (7.5-10.6)	7.8 (7.1-8.7)	8.1 (7-10.4)	0.919
PGI/II, median (IQR)	3.7 (2.5-4.9)	3.8 (2.1-5.1)	4.4 (2.7-5.2)	1.4 (1.2-1.9)	4.5 (3.3-6.2)	0.06
Gastrin-17 (pmol/L), median (IQR)	91 (69.2-136.4)	81.9 (35.2-117.7)	137.7 (113-176.9)	95 (75.7-109.2)	96.7 (59.1-137.1)	0.013
Vitamin B12 (pg/mL), median (IQR)	264 (154-352)	257.5 (140-361.8)	210 (82-320)	144 (102-301.5)	256.5 (98.5-360.8)	0.71
Anemia, *n* (%)	38 (34.9)	9 (50)	5 (29.4)	4 (66.7)	5 (31.2)	0.35

[1]The total number of polyps.

HP: *Helicobacter pylori*; gNET: Gastric neuroendocrine tumor; LGD: Low-grade glandular dysplasia; IQR: Interquartile range; PCA: Parietal cell antibodies; IFA: Intrinsic factor antibody; PG: Pepsinogen.

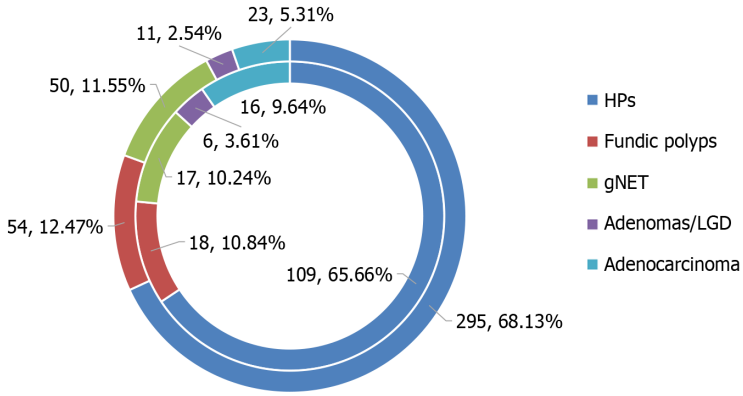

Figure 3 The proportion of gastric polyps and autoimmune gastritis patients. HP: *Helicobacter pylori*; gNET: Gastric neuroendocrine tumor; LGD: Low-grade glandular dysplasia.

with GHPs and gNET (Figure 4C and D).

Risk factors of GPs in patients with AIG

Univariate and multivariate binary logistic regression analyses were conducted to identify risk factors for the development of GPs in patients with AIG (Table 5). The univariate analysis indicated that age, PCA positivity, gastrin-17 level, PG-II level, and advanced OLGA and OLGIM stages (III and IV) were associated with an increased risk factors of GPs. Conversely, PG-I level, PG ratio, and ECL hyperplasia were identified as protective factors. Multivariate analysis showed that PCA positivity, PG-II, and ECL hyperplasia were independent risk factors, while PG-I served as a protective factor (Figure 5).

Construction and validation of the nomogram

To develop a predictive model, the optimal subset method was employed for variable selection, with AIC was used as the stopping criterion (Table 6). The final nomogram included age, OLGA stage, PCA positivity, PG ratio, and ECL hyperplasia (Figure 6A). An example of the nomogram score for a patient is illustrated in Figure 6B. ROC analysis revealed an area under the curve of 0.729 (95%CI: 0.683-0.775), indicating good diagnostic performance. The calibration curve demonstrated a good fit of the model with minimal error was small (Figure 6C and D).

Table 5 Univariate and multivariate analysis of the characteristics most associated with the development of gastric polyps in patients with autoimmune gastritis

Variable	Univariate analysis (95%CI)	*P* value	Multivariate analysis (95%CI)	*P* value
Age	1.023 (1.007-1.038)	0.003	1.015 (0.998-1.033)	0.084
Sex				
Male	1.057 (0.714-1.566)	0.781	1.019 (0.656-1.582)	0.933
Female				
PCA				
Positive	2.771 (1.629-4.716)	< 0.001	2.003 (1.130-3.549)	0.017
Negative				
IFA				
Positive	1.047 (0.685-1.599)	0.833	0.866 (0.538-1.394)	0.553
Negative				
HP infection				
Positive	0.749 (0.451-1.244)	0.265	0.897 (0.512-1.571)	0.704
Negative				
Anemia				
Yes	0.819 (0.561-1.196)	0.302	0.811 (0.533-1.233)	0.326
No				
Gastrin-17	1.007 (1.004-1.010)	< 0.001	1.002 (0.998-1.005)	0.306
PG-I	0.992 (0.985-0.998)	0.008	0.992 (0.985-0.999)	0.031
PG-II	1.037 (1.001-1.074)	0.044	1.053 (1.010-1.097)	0.015
PG-I/PG-II	0.927 (0.884-0.971)	0.002		
OLGA				
0-II				
III-IV	2.408 (1.648-3.519)	< 0.001	1.541 (0.963-2.464)	0.071
OLGIM				
0-II				
III-IV	1.927 (1.107-3.353)	0.020	0.954 (0.487-1.869)	0.891
ECL hyperplasia				
Absent				
Exist	0.225 (0.150-0.338)	< 0.001	3.116 (1.868-5.197)	< 0.001

PCA: Parietal cell antibodies; IFA: Intrinsic factor antibody; HP: *Helicobacter pylori*; PG: Pepsinogen; OLGA: Operative Link for Gastritis Assessment; OLGIM: Operative Link on Intestinal Metaplasia Assessment; ECL: Enterochromaffin-like; CI: Confidence interval.

DISCUSSION

AIG is a chronic atrophic gastritis with an immune-mediated etiology. Its onset is often insidious, and early stages may present without specific symptoms. As the disease progresses, patients may develop a range of symptoms including digestive, hematological, and neurological manifestations. In some cases, anemia becomes the predominant symptom, leading to a significant delays in diagnosis[36]. Progressive destruction of gastric parietal cells, mediated by PCA or IFA, results in gastric atrophy and/or intestinal or pseudopyloric metaplasia, creating an abnormal mucosal environment conducive to the formation of GPs. Furthermore, AIG is closely linked to gNETs[17]. Atrophy of the gastric body mucosa and decreased gastric acid secretion lead to the stimulation of gastric antral G cells, resulting in increased gastrin secretion. This, in turn, stimulates the proliferation of ECL cells, potentially culminating in gNET formation[37].

In our multicenter retrospective study, we aimed to investigate the pathological types of GPs and clinical and associated biochemical factors in patients with AIG. Among the 530 patients with AIG studied, 166 (31.3%) were found to have a total of 433 polypoid lesions. The study cohort was representative of the broader AIG patient population, with

Table 6 Multivariate logistics regression analysis of the optimal subset method model

Variable	Coefficient	OR (95%CI)	*P* value
Age	0.015	1.015 (0.999-1.032)	0.071
PCA			
Positive	0.778	2.178 (1.243-3.818)	0.007
Negative			
PG-I/PG-II	-0.069	0.927 (0.884-0.971)	0.008
OLGA			
0-II			
III-IV	0.375	1.455 (0.945-2.239)	0.088
ECL hyperplasia			
Absent			
Exist	1.247	3.479 (2.242-5.399)	< 0.001
Intercept	-1.711	-	-

OR: Odds ratio; CI: Confidence interval; PCA: Parietal cell antibodies; PG: Pepsinogen; OLGA: Operative Link for Gastritis Assessment; ECL: Enterochromaffin-like.

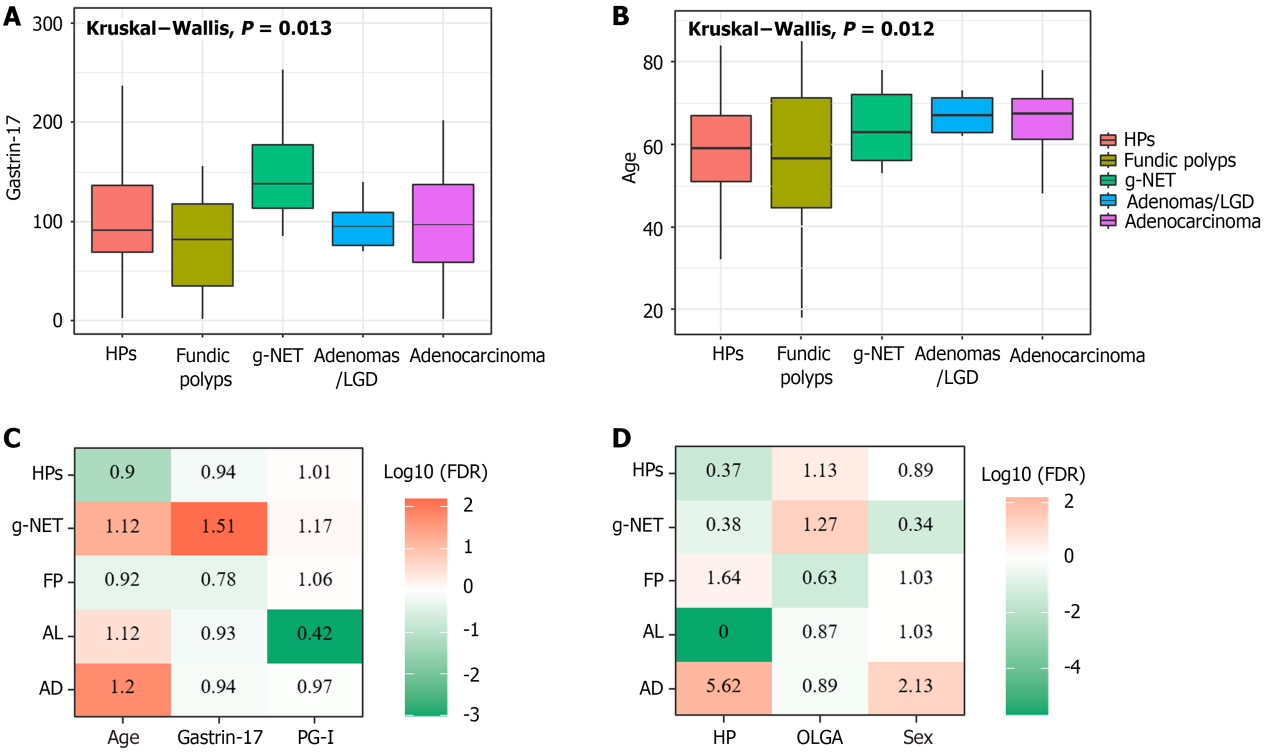

Figure 4 Differences among the gastric polyp groups. A: Gastrin-17 differences between groups; B: Age differences between groups; C: Heat map of age and blood biochemical differences between groups; D: Heat map of histopathological differences between groups. HP: *Helicobacter pylori*; gNET: Gastric neuroendocrine tumor; LGD: Llow-grade glandular dysplasia; FP: Fundic polyps; AL: Adenomas/low-grade glandular dysplasia; AD: Adenocarcinoma; PG: Pepsinogen; OLGA: Operative Link on Gastritis Assessment; FDR: False discovery rate.

68.3% being female and a median age of 59 years at diagnosis. Our findings align with previous studies, showing a significant incidence of gNETs in patients with AIG compared with the general population. Additionally, 16 patients with AIG (3.02%) were diagnosed with gastric adenocarcinoma. Of these, nine had a history of *H. pylori* infection, suggesting a potential link between past *H. pylori* infection and the development of gastric adenocarcinoma in patients with AIG.

Our study revealed no significant differences in sex between patients with AIG with GPs and those without. Additionally, previous *H. pylori* infection rates were similar across both groups, suggesting that *H. pylori* infection may not significantly impact abnormal epithelial cell proliferation in the context of AIG. The occurrence of GPs in patients

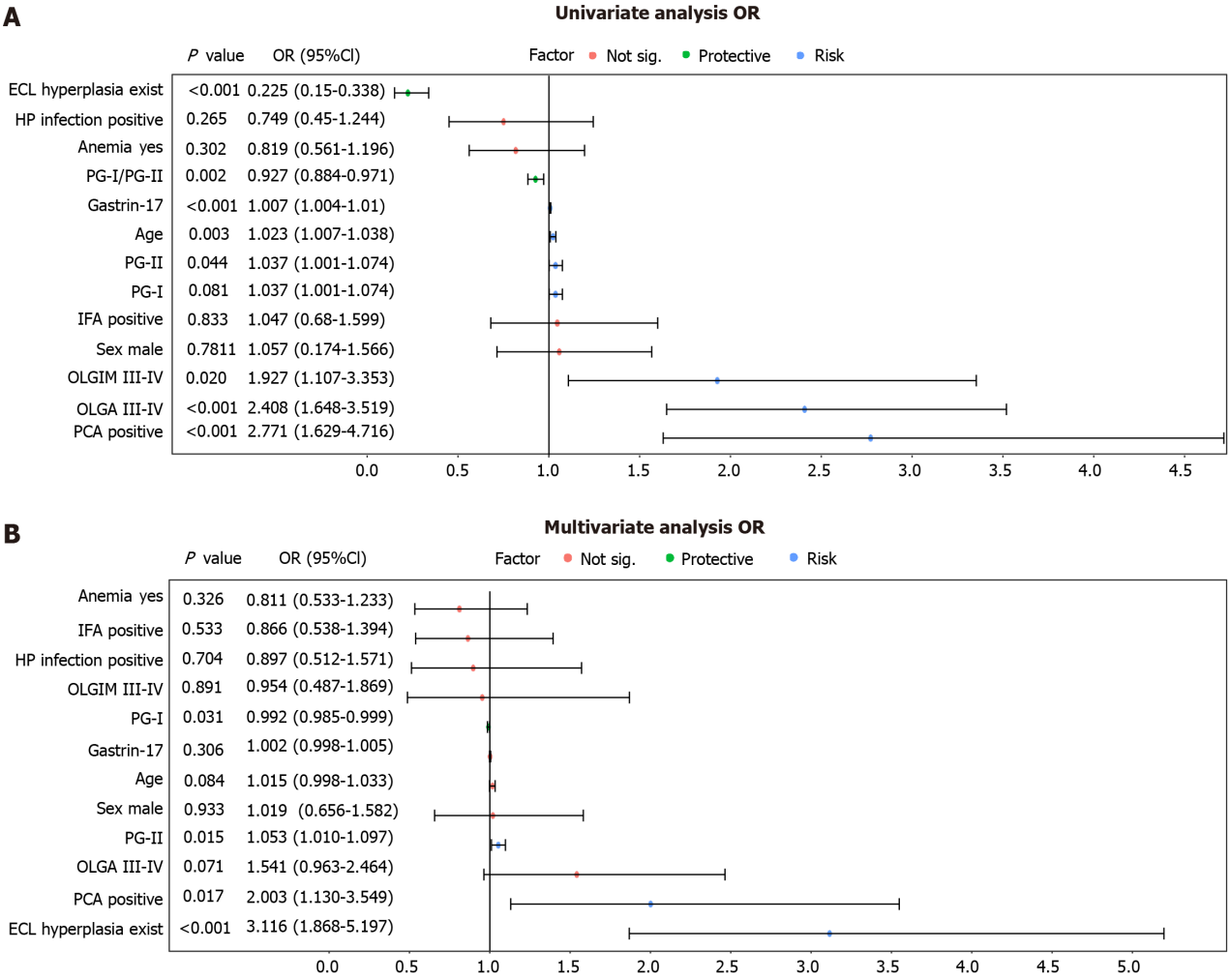

Figure 5 Forestplot depicting the results of univariate and multivariate analyses. A: Forest plots for univariate analysis; B: Forest plots for multivariate analysis. OR: Odds ratio; CI: Confidence interval; ECL: Enterochromaffin-like; HP: *Helicobacter pylori*; PG: Pepsinogen; IFA: Intrinsic factor antibody; OLGA: Operative Link on Gastritis Assessment; OLGIM: Operative Link on Gastric Intestinal Metaplasia; PCA: Parietal cell antibody.

with AIG was associated with PCA positivity and ECL hyperplasia, though the specific pathophysiological and molecular mechanisms remain unclear and warrant further investigation through basic research.

We observed that GPs were positively correlated with age, gastrin levels, and OLGA and OLGIM stages. However, OLGA and OLGIM staging scores may not be entirely reliable in predicting polyp formation in patients with AIG, as the histological lesions in AIG predominantly affect the fundus and body of the stomach rather than the antrum. Consequently, active endoscopic surveillance should be performed for all patients with AIG, irrespective of OLGA stage. Our study findings indicate that gastrin-17 levels were significantly higher in the GP group; this supports its role in ECL cell proliferation and the development of neuroendocrine lesions, while also maintaining its trophic effects on other epithelial components of the gastric mucosa. We speculate that elevated gastrin-17 levels contribute to abnormal mucosal proliferation, thereby facilitating to the growth of polyps in patients with AIG. Notably, PG-II levels were significantly was lower in the GP group, suggesting that atrophy of the antral mucosa might influence the occurrence of GPs. Histologically, a higher proportion of patients in the GP group, exhibited OLGA stages III-IV and more pronounced ECL hyperplasia than those in the NGP group. However, no significant differences were found in OLGA and ECL hyperplasia between benign and malignant polyps, potentially due to the low number of malignant polyps in our study sample. Additionally, anemia and vitamin B12 levels were not significantly associated with the presence of GPs.

This study represents the largest analysis to date of AIG and its relationship with GPs, featuring a substantial sample size of 530 patients. By using univariate and multivariate logistic regression analyses, we identified PCA positivity and ECL hyperplasia as significant risk factors for GPs in patients with AIG, while PG-I was found to be a protective factor. Although age and gastrin-17 did not achieve statistical significance in the regression models, they remain relevant variables in the context of AIG. The prediction model we developed, based on these logistic regression results, demonstrated good performance with an area under the ROC curve was of 0.729 (95%CI: 0.683-0.775). The use of fold cross-validation ensured robust consistency and extensibility, of the model, offering valuable insights for clinical practice. However, the model requires validation across diverse cohorts to enhance its clinical applicability and reliability.

Our study sheds light on the previously underexplored relationship between AIG GPs, leveraging a large and demographically diverse sample (68.3% women, median age: 59 years). Identified key risk factors, such as PCA positivity

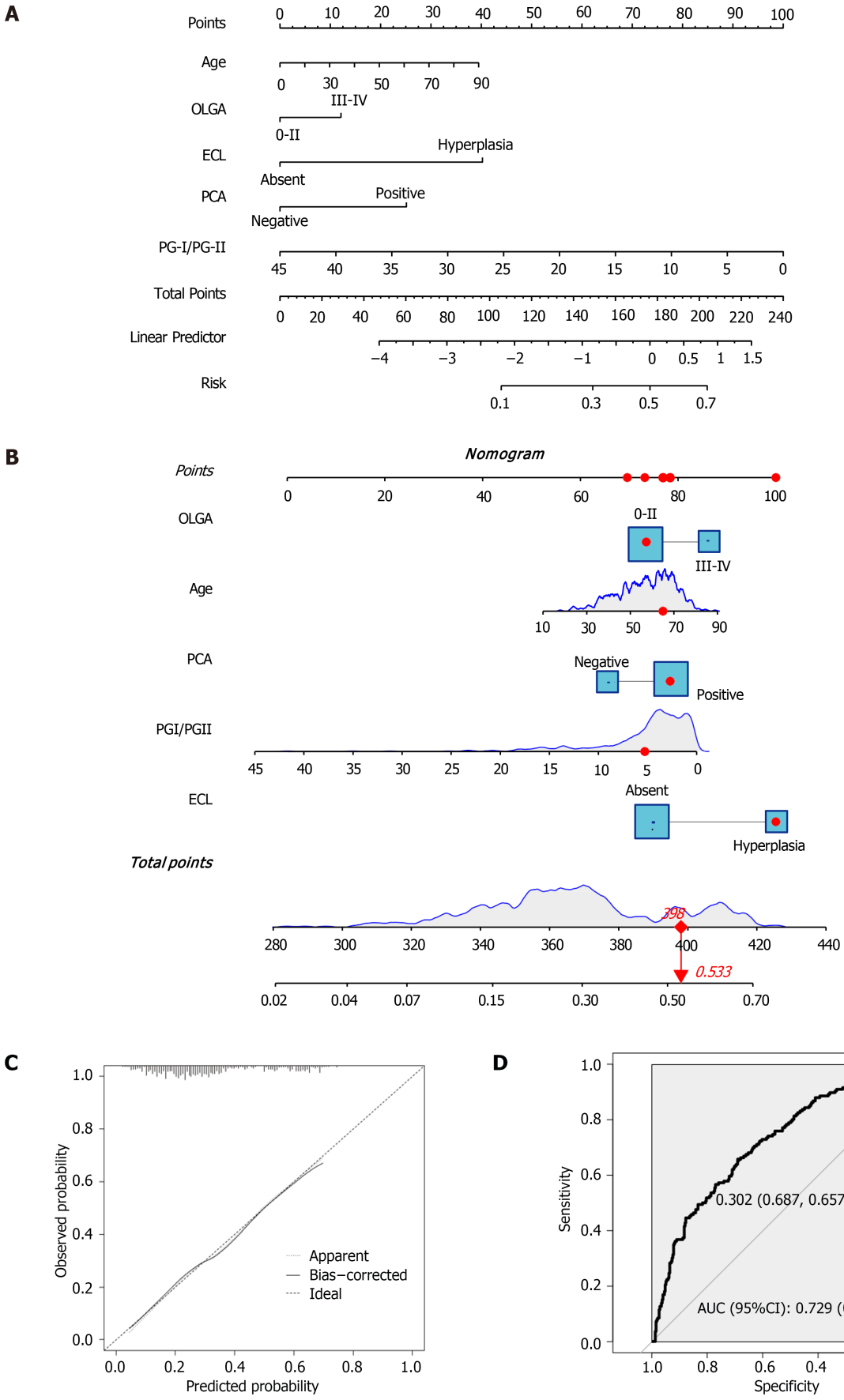

Figure 6 Nomogram, receiver operating characteristic curve, and forest plot depictions. A: Nomogram; B: An example of the nomogram; C: Calibration curve; D: Receiver operating characteristic curve. OLGA: Operative Link on Gastritis Assessment; ECL: Enterochromaffin-like; PCA: Parietal cell antibody; PG: Pepsinogen; AUC: Area under the receiver operating characteristic curve.

and ECL hyperplasia, provide useful tools for clinicians assessing the risk of GPs in patients with AIG. Despite the promising results, the study's cross-sectional design limits causal inference, and highlights the need for further research into the molecular mechanisms driving polyp development.

CONCLUSION

In conclusion, our study not only confirms the relationship between AIG and the occurrence of GPs, but also highlights the predominance of benign, particularly hyperplastic polyps. Nonetheless, the potential risk of malignant transformation should not be overlooked. Comprehensive endoscopic surveillance and follow-up, as recommended by the Sydney protocol are essential for patients undergoing polyp resection. While our findings elucidate the roles of PCA and ECL hyperplasia in predicting GPs, they do not fully explain the roles of PCA, ECL hyperplasia, and gastrin-17 in the development and malignant potential of these polyps. Future research, particularly longitudinal studies, is crucial to further elucidate these relationships and improve noninvasive monitoring strategies for gastric mucosa and epithelial hyperplasia in patients with AIG.

ACKNOWLEDGEMENTS

We are grateful to all the individuals who participated in the study.

FOOTNOTES

Author contributions: Jin JZ, Liang X, and Liu SP contributed equally to this research, Jin JZ and Liang X are the co-first authors of this manuscript. Jin JZ and Liang X conceptualized the study and authored the manuscript; Liu SP played a key role in designing the analysis plans; Wang RL were responsible for data collection and provided technical support throughout the research; Zhang QW, Shen YF, and Li XB also made equal contributions to the study; Zhang QW, Shen YF, and Li XB meticulously reviewed, proofread the manuscript, and suggested valuable improvements, they are the co-corresponding authors of this manuscript. All authors reviewed and approved the final version of the manuscript.

Supported by the Health Technology Project of Pudong New District Health Commission, No. PW2020D-12.

Institutional review board statement: This study received approval from the Institutional Ethics Committee of Renji Hospital, Shanghai Jiao Tong University, School of Medicine, Approval No. LY2024-141-B.

Informed consent statement: The informed consent was waived by the Institutional Ethics Committee of Renji Hospital, Shanghai Jiao Tong University, School of Medicine.

Conflict-of-interest statement: All the authors report no relevant conflicts of interest for this article.

Data sharing statement: No additional data are available.

Country of origin: China

ORCID number: Xiao-Bo Li 0009-0003-0583-8101.

S-Editor: Wang JJ
L-Editor: A
P-Editor: Cai YX

REFERENCES

1 **Carmack SW**, Genta RM, Schuler CM, Saboorian MH. The current spectrum of gastric polyps: a 1-year national study of over 120,000 patients. *Am J Gastroenterol* 2009; **104**: 1524-1532 [PMID: 19491866 DOI: 10.1038/ajg.2009.139]

2 **Park DY**, Lauwers GY. Gastric polyps: classification and management. *Arch Pathol Lab Med* 2008; **132**: 633-640 [PMID: 18384215 DOI: 10.5858/2008-132-633-GPCAM]

3 **Castro R**, Pimentel-Nunes P, Dinis-Ribeiro M. Evaluation and management of gastric epithelial polyps. *Best Pract Res Clin Gastroenterol* 2017; **31**: 381-387 [PMID: 28842047 DOI: 10.1016/j.bpg.2017.06.001]

4 **Carmack SW**, Genta RM, Graham DY, Lauwers GY. Management of gastric polyps: a pathology-based guide for gastroenterologists. *Nat Rev Gastroenterol Hepatol* 2009; **6**: 331-341 [PMID: 19421245 DOI: 10.1038/nrgastro.2009.70]

5 **Burt RW**. Gastric fundic gland polyps. *Gastroenterology* 2003; **125**: 1462-1469 [PMID: 14598262 DOI: 10.1016/j.gastro.2003.07.017]

6 **Cao H**, Wang B, Zhang Z, Zhang H, Qu R. Distribution trends of gastric polyps: an endoscopy database analysis of 24 121 northern Chinese patients. *J Gastroenterol Hepatol* 2012; **27**: 1175-1180 [PMID: 22414211 DOI: 10.1111/j.1440-1746.2012.07116.x]

7 **Ahmed M**. Gastrointestinal neuroendocrine tumors in 2020. *World J Gastrointest Oncol* 2020; **12**: 791-807 [PMID: 32879660 DOI: 10.4251/wjgo.v12.i8.791]

8 **Oberhuber G**, Stolte M. Gastric polyps: an update of their pathology and biological significance. *Virchows Arch* 2000; **437**: 581-590 [PMID: 11193468 DOI: 10.1007/s004280000330]

9 **Markowski AR**, Markowska A, Guzinska-Ustymowicz K. Pathophysiological and clinical aspects of gastric hyperplastic polyps. *World J Gastroenterol* 2016; **22**: 8883-8891 [PMID: 27833379 DOI: 10.3748/wjg.v22.i40.8883]

10 **Abraham SC**, Singh VK, Yardley JH, Wu TT. Hyperplastic polyps of the stomach: associations with histologic patterns of gastritis and gastric atrophy. *Am J Surg Pathol* 2001; **25**: 500-507 [PMID: 11257625 DOI: 10.1097/00000478-200104000-00010]

11 **Horvath B**, Pai RK. Prevalence of Helicobacter pylori in Gastric Hyperplastic Polyps. *Int J Surg Pathol* 2016; **24**: 704-708 [PMID: 27160432 DOI: 10.1177/1066896916648380]

12 **Cavalcoli F**, Zilli A, Conte D, Ciafardini C, Massironi S. Gastric neuroendocrine neoplasms and proton pump inhibitors: fact or coincidence? *Scand J Gastroenterol* 2015; **50**: 1397-1403 [PMID: 26059834 DOI: 10.3109/00365521.2015.1054426]

13 **Miyamoto S**, Kato M, Matsuda K, Abiko S, Tsuda M, Mizushima T, Yamamoto K, Ono S, Kudo T, Shimizu Y, Hatanaka KC, Tsunematsu I, Sakamoto N. Gastric Hyperplastic Polyps Associated with Proton Pump Inhibitor Use in a Case without a History of Helicobacter pylori Infection. *Intern Med* 2017; **56**: 1825-1829 [PMID: 28717077 DOI: 10.2169/internalmedicine.56.8040]

14 **Markowski AR**, Guzinska-Ustymowicz K. Gastric hyperplastic polyp with focal cancer. *Gastroenterol Rep (Oxf)* 2016; **4**: 158-161 [PMID: 25361760 DOI: 10.1093/gastro/gou077]

15 **Waldum H**, Fossmark R. Gastritis, Gastric Polyps and Gastric Cancer. *Int J Mol Sci* 2021; **22** [PMID: 34207192 DOI: 10.3390/ijms22126548]

16 **Terao S**, Suzuki S, Yaita H, Kurahara K, Shunto J, Furuta T, Maruyama Y, Ito M, Kamada T, Aoki R, Inoue K, Manabe N, Haruma K. Multicenter study of autoimmune gastritis in Japan: Clinical and endoscopic characteristics. *Dig Endosc* 2020; **32**: 364-372 [PMID: 31368581 DOI: 10.1111/den.13500]

17 **D'Elios MM**, Bergman MP, Azzurri A, Amedei A, Benagiano M, De Pont JJ, Cianchi F, Vandenbroucke-Grauls CM, Romagnani S, Appelmelk BJ, Del Prete G. H(+),K(+)-atpase (proton pump) is the target autoantigen of Th1-type cytotoxic T cells in autoimmune gastritis. *Gastroenterology* 2001; **120**: 377-386 [PMID: 11159878 DOI: 10.1053/gast.2001.21187]

18 **Shah SC**, Piazuelo MB, Kuipers EJ, Li D. AGA Clinical Practice Update on the Diagnosis and Management of Atrophic Gastritis: Expert Review. *Gastroenterology* 2021; **161**: 1325-1332.e7 [PMID: 34454714 DOI: 10.1053/j.gastro.2021.06.078]

19 **Magris R**, De Re V, Maiero S, Fornasarig M, Guarnieri G, Caggiari L, Mazzon C, Zanette G, Steffan A, Canzonieri V, Cannizzaro R. Low Pepsinogen I/II Ratio and High Gastrin-17 Levels Typify Chronic Atrophic Autoimmune Gastritis Patients With Gastric Neuroendocrine Tumors. *Clin Transl Gastroenterol* 2020; **11**: e00238 [PMID: 33094954 DOI: 10.14309/ctg.0000000000000238]

20 **Song M**, Camargo MC, Katki HA, Weinstein SJ, Männistö S, Albanes D, Surcel HM, Rabkin CS. Association of Antiparietal Cell and Anti-Intrinsic Factor Antibodies With Risk of Gastric Cancer. *JAMA Oncol* 2022; **8**: 268-274 [PMID: 34913949 DOI: 10.1001/jamaoncol.2021.5395]

21 **Butt J**, Lehtinen M, Öhman H, Waterboer T, Epplein M. Association of Helicobacter pylori and Autoimmune Gastritis With Stomach Cancer in a Cohort of Young Finnish Women. *Gastroenterology* 2022; **163**: 305-307.e4 [PMID: 35301012 DOI: 10.1053/j.gastro.2022.03.012]

22 **Weise F**, Vieth M, Reinhold D, Haybaeck J, Goni E, Lippert H, Ridwelski K, Lingohr P, Schildberg C, Vassos N, Kruschewski M, Krasniuk I, Grimminger PP, Waidmann O, Peitz U, Veits L, Kreuser N, Lang H, Bruns C, Moehler M, Lordick F, Gockel I, Schumacher J, Malfertheiner P, Venerito M. Gastric cancer in autoimmune gastritis: A case-control study from the German centers of the staR project on gastric cancer research. *United European Gastroenterol J* 2020; **8**: 175-184 [PMID: 32213076 DOI: 10.1177/2050640619891580]

23 **Lahner E**, Esposito G, Pilozzi E, Galli G, Corleto VD, Di Giulio E, Annibale B. Gastric cancer in patients with type I gastric carcinoids. *Gastric Cancer* 2015; **18**: 564-570 [PMID: 24890255 DOI: 10.1007/s10120-014-0393-8]

24 **Dilaghi E**, Bellisario M, Esposito G, Carabotti M, Annibale B, Lahner E. The Impact of Proton Pump Inhibitors on the Development of Gastric Neoplastic Lesions in Patients With Autoimmune Atrophic Gastritis. *Front Immunol* 2022; **13**: 910077 [PMID: 35935934 DOI: 10.3389/fimmu.2022.910077]

25 **Kishikawa H**, Nakamura K, Ojiro K, Katayama T, Arahata K, Takarabe S, Sasaki A, Miura S, Hayashi Y, Hoshi H, Kanai T, Nishida J. Relevance of pepsinogen, gastrin, and endoscopic atrophy in the diagnosis of autoimmune gastritis. *Sci Rep* 2022; **12**: 4202 [PMID: 35273265 DOI: 10.1038/s41598-022-07947-1]

26 **Hall SN**, Appelman HD. Autoimmune Gastritis. *Arch Pathol Lab Med* 2019; **143**: 1327-1331 [PMID: 31661309 DOI: 10.5858/arpa.2019-0345-RA]

27 **Misiewicz JJ**. The Sydney System: a new classification of gastritis. Introduction. *J Gastroenterol Hepatol* 1991; **6**: 207-208 [PMID: 1912430 DOI: 10.1111/j.1440-1746.1991.tb01467.x]

28 **Delle Fave G**, O'Toole D, Sundin A, Taal B, Ferolla P, Ramage JK, Ferone D, Ito T, Weber W, Zheng-Pei Z, De Herder WW, Pascher A, Ruszniewski P; Vienna Consensus Conference participants. ENETS Consensus Guidelines Update for Gastroduodenal Neuroendocrine Neoplasms. *Neuroendocrinology* 2016; **103**: 119-124 [PMID: 26784901 DOI: 10.1159/000443168]

29 **Rugge M**, Meggio A, Pennelli G, Piscioli F, Giacomelli L, De Pretis G, Graham DY. Gastritis staging in clinical practice: the OLGA staging system. *Gut* 2007; **56**: 631-636 [PMID: 17142647 DOI: 10.1136/gut.2006.106666]

30 **Yue H**, Shan L, Bin L. The significance of OLGA and OLGIM staging systems in the risk assessment of gastric cancer: a systematic review and meta-analysis. *Gastric Cancer* 2018; **21**: 579-587 [PMID: 29460004 DOI: 10.1007/s10120-018-0812-3]

31 **Capelle LG**, de Vries AC, Haringsma J, Ter Borg F, de Vries RA, Bruno MJ, van Dekken H, Meijer J, van Grieken NC, Kuipers EJ. The staging of gastritis with the OLGA system by using intestinal metaplasia as an accurate alternative for atrophic gastritis. *Gastrointest Endosc* 2010; **71**: 1150-1158 [PMID: 20381801 DOI: 10.1016/j.gie.2009.12.029]

32 **Solcia E**, Rindi G, Paolotti D, Luinetti O, Klersy C, Zangrandi A, La Rosa S, Capella C. Natural history, clinicopathologic classification and prognosis of gastric ECL cell tumors. *Yale J Biol Med* 1998; **71**: 285-290 [PMID: 10461359]

33 **Cockburn AN**, Morgan CJ, Genta RM. Neuroendocrine proliferations of the stomach: a pragmatic approach for the perplexed pathologist. *Adv*

Anat Pathol 2013; **20**: 148-157 [PMID: 23574771 DOI: 10.1097/PAP.0b013e31828d185d]

34 **Nagtegaal ID**, Odze RD, Klimstra D, Paradis V, Rugge M, Schirmacher P, Washington KM, Carneiro F, Cree IA; WHO Classification of Tumours Editorial Board. The 2019 WHO classification of tumours of the digestive system. *Histopathology* 2020; **76**: 182-188 [PMID: 31433515 DOI: 10.1111/his.13975]

35 **Capurso G**, Gaujoux S, Pescatori LC, Panzuto F, Panis Y, Pilozzi E, Terris B, de Mestier L, Prat F, Rinzivillo M, Coriat R, Coulevard A, Delle Fave G, Ruszniewski P. The ENETS TNM staging and grading system accurately predict prognosis in patients with rectal NENs. *Dig Liver Dis* 2019; **51**: 1725-1730 [PMID: 31405587 DOI: 10.1016/j.dld.2019.07.011]

36 **Lenti MV**, Miceli E, Cococcia S, Klersy C, Staiani M, Guglielmi F, Giuffrida P, Vanoli A, Luinetti O, De Grazia F, Di Stefano M, Corazza GR, Di Sabatino A. Determinants of diagnostic delay in autoimmune atrophic gastritis. *Aliment Pharmacol Ther* 2019; **50**: 167-175 [PMID: 31115910 DOI: 10.1111/apt.15317]

37 **Neumann WL**, Coss E, Rugge M, Genta RM. Autoimmune atrophic gastritis--pathogenesis, pathology and management. *Nat Rev Gastroenterol Hepatol* 2013; **10**: 529-541 [PMID: 23774773 DOI: 10.1038/nrgastro.2013.101]

World Journal of Gastrointestinal Oncology

Submit a Manuscript: https://www.f6publishing.com

World J Gastrointest Oncol 2025 January 15; 17(1): 96439

DOI: 10.4251/wjgo.v17.i1.96439

ISSN 1948-5204 (online)

ORIGINAL ARTICLE

Retrospective Study

Predictive value of a constructed artificial neural network model for microvascular invasion in hepatocellular carcinoma: A retrospective study

Hai-Yang Nong, Yong-Yi Cen, Shan-Jin Lu, Rui-Sui Huang, Qiong Chen, Li-Feng Huang, Jian-Ning Huang, Xue Wei, Man-Rong Liu, Lin Li, Ke Ding

Specialty type: Oncology

Provenance and peer review: Unsolicited article; Externally peer reviewed.

Peer-review model: Single blind

Peer-review report's classification

Scientific Quality: Grade C

Novelty: Grade B

Creativity or Innovation: Grade B

Scientific Significance: Grade B

P-Reviewer: Li XJ

Received: May 8, 2024

Revised: September 6, 2024

Accepted: November 7, 2024

Published online: January 15, 2025

Processing time: 218 Days and 7.5 Hours

Hai-Yang Nong, Shan-Jin Lu, Rui-Sui Huang, Qiong Chen, Li-Feng Huang, Jian-Ning Huang, Xue Wei, Ke Ding, Department of Radiology, The Third Affiliated Hospital of Guangxi Medical University, Nanning 530031, Guangxi Zhuang Autonomous Region, China

Hai-Yang Nong, Yong-Yi Cen, Department of Radiology, Affiliated Hospital of Youjiang Medical University for Nationalities, Baise 533000, Guangxi Zhuang Autonomous Region, China

Hai-Yang Nong, Yong-Yi Cen, Guangxi Clinical Medical Research Center for Hepatobiliary Diseases, Affiliated Hospital of Youiiang Medical University for Nationalities, Baise 533000, Guangxi Zhuang Autonomous Region, China

Man-Rong Liu, Department of Ultrasound, The Third Affiliated Hospital of Guangxi Medical University, Nanning 530031, Guangxi Zhuang Autonomous Region, China

Lin Li, Department of Hepatobiliary Surgery, The Third Affiliated Hospital of Guangxi Medical University, Nanning 530031, Guangxi Zhuang Autonomous Region, China

Co-first authors: Hai-Yang Nong and Yong-Yi Cen.

Co-corresponding authors: Man-Rong Liu and Ke Ding.

Corresponding author: Ke Ding, MD, Doctor, Department of Radiology, The Third Affiliated Hospital of Guangxi Medical University, No. 13 Dancun Road, Nanning 530031, Guangxi Zhuang Autonomous Region, China. 272480365@qq.com

Abstract

BACKGROUND

Microvascular invasion (MVI) is a significant risk factor for recurrence and metastasis following hepatocellular carcinoma (HCC) surgery. Currently, there is a paucity of preoperative evaluation approaches for MVI.

AIM

To investigate the predictive value of texture features and radiological signs based on multiparametric magnetic resonance imaging in the non-invasive preoperative prediction of MVI in HCC.

METHODS
Clinical data from 97 HCC patients were retrospectively collected from January 2019 to July 2022 at our hospital. Patients were classified into two groups: MVI-positive (n = 57) and MVI-negative (n = 40), based on postoperative pathological results. The correlation between relevant radiological signs and MVI status was analyzed. MaZda4.6 software and the mutual information method were employed to identify the top 10 dominant texture features, which were combined with radiological signs to construct artificial neural network (ANN) models for MVI prediction. The predictive performance of the ANN models was evaluated using area under the curve, sensitivity, and specificity. ANN models with relatively high predictive performance were screened using the DeLong test, and the regression model of multilayer feedforward ANN with backpropagation and error backpropagation learning method was used to evaluate the models' stability.

RESULTS
The absence of a pseudocapsule, an incomplete pseudocapsule, and the presence of tumor blood vessels were identified as independent predictors of HCC MVI. The ANN model constructed using the dominant features of the combined group (pseudocapsule status + tumor blood vessels + arterial phase + venous phase) demonstrated the best predictive performance for MVI status and was found to be automated, highly operable, and very stable.

CONCLUSION
The ANN model constructed using the dominant features of the combined group can be recommended as a non-invasive method for preoperative prediction of HCC MVI status.

Key Words: Hepatocellular carcinoma; Texture analysis; Magnetic resonance imaging; Microvascular invasion; Pseudocapsule; Tumor blood vessels

Core Tip: Whether artificial neural network (ANN) models mimicking human brain provide a high predictive value for hepatocellular carcinoma (HCC) microvascular invasion (MVI). The preoperative prediction ANN model constructed on multiparametric magnetic resonance imaging is acute and stable. ANN models have clinical values and benefits in non-invasively predicting MVI in HCC patients.

Citation: Nong HY, Cen YY, Lu SJ, Huang RS, Chen Q, Huang LF, Huang JN, Wei X, Liu MR, Li L, Ding K. Predictive value of a constructed artificial neural network model for microvascular invasion in hepatocellular carcinoma: A retrospective study. *World J Gastrointest Oncol* 2025; 17(1): 96439
URL: https://www.wjgnet.com/1948-5204/full/v17/i1/96439.htm
DOI: https://dx.doi.org/10.4251/wjgo.v17.i1.96439

INTRODUCTION

Primary liver cancer is one of the most common malignant tumors worldwide, with hepatocellular carcinoma (HCC) comprising approximately 85%-90% of all primary liver cancer cases[1]. Although surgical resection remains a primary treatment modality for HCC, the postoperative recurrence rate continues to be notably high[2]. Microvascular invasion (MVI) is recognized as a significant risk factor for tumor recurrence and metastasis following HCC surgery[3-5]. Currently, the evaluation criteria for MVI predominantly rely on postoperative pathological biopsy, and there is a notable lack of preoperative evaluation methods. Imaging texture analysis has been applied to various medical imaging settings to assist in disease diagnosis and treatment[6-9], as it can provide objective and quantitative image description features that reflect the physiological heterogeneity within the region of interest (ROI). Previous studies have often utilized computerized tomography (CT) images[10-13] and two-dimensional ROIs, which provide less information compared to three-dimensional (3D) ROIs[14-16]. Multiparametric liver magnetic resonance imaging (MRI) offers advantages in assessing tumor heterogeneity and has been employed for clinical diagnosis, staging classification, and efficacy evaluation of liver cancer[17,18]. However, previous investigations into the predictive performance of MRI imaging features for MVI have yielded inconsistent results and are highly dependent on the diagnosing physicians. Artificial neural networks (ANNs) are mathematical models that emulate the functions of the human brain. Consisting of a large number of interconnected neurons, ANNs exhibit high fault tolerance, parallel-distributed processing ability, adaptability, self-organization, and self-learning abilities, which enabling them to analyze relatively complex nonlinear systems[19]. This study aims to address the question: Will an ANN model that incorporates texture features from multiparametric MRI images, in conjunction with radiological signs, demonstrate a higher predictive value for HCC MVI? We hypothesize that the integration of artificial intelligence and traditional imaging features could represent a significant advancement in predicting MVI, thereby enhancing clinical applications.

MATERIALS AND METHODS

Study subjects

In accordance with the ethical principles of the Declaration of Helsinki, we conducted a retrospective analysis involving 97 patients with HCC, all of whom were confirmed by surgical pathology at our hospital between January 2019 and July 2022. This study received approval from our institutional review board, and informed consent was obtained from all patients (No. 2015-02-28-1).

Research methods

MVI assessment and grouping: MVI refers to the presence of cancer cell clusters within vascular lumens lined by endothelial cells, as detected under the microscope. Liver cancer is most commonly found to invade the branches of the portal vein (including intra-capsular blood vessels)[20]. Based on postoperative pathological observations, patients were classified into MVI-positive and MVI-negative groups.

MRI examination method: (1) MRI examination equipment: UMR790 3.0T MRI and SIEMENS Verio 3.0T MRI imaging devices; (2) Contrast agents: Gadobutrol Injection (0.1 mmol/kg, injection rate 1.5 mL/second) or gadopentetate dimeglumine (0.2 mmol/kg, injection rate 2.0 mL/second); and (3) Scanning range and parameter settings: The scanning range was from the top of the diaphragm to the lower edge of the liver.

Scanning parameter settings were as follows: (1) UMR790 3.0T MRI: Axial t1 gre-quick3d-tra [time of repetition (TR)/time of echo (TE) 2.65/1.03 ms], slice thickness 3 mm; Axial t2-arms-tra-fs-navi (TR/TE 4352/92.4 ms), slice thickness 6 mm. The contrast agent was administered *via* the cubital vein using a dual-barrel high-pressure injector. Following the contrast agent injection, 20 mL of 0.9% sterile saline was immediately injected at the same rate to flush the tube. An automatic monitoring scanning method was then employed to capture six arterial phases (AP) at 15 to 28 seconds post-contrast agent injection, with selection of the optimal late AP image. Portal venous phase (VP) images were subsequently obtained at 55 to 65 seconds, and delayed phase (DP) images were captured at 180 seconds; and (2) SIEMENS Verio 3.0T MRI: Axial-t1-vibe-fs-tra (TR/TE 3.92/1.39 ms), slice thickness 4 mm; Axial t2-blade-tra-fs-navi (TR/TE 4185.31/89.00 ms), slice thickness 6 mm. The contrast agent was similarly injected *via* the cubital vein using a dual-barrel high-pressure injector, followed by the immediate injection of 20 mL of 0.9% sterile saline at the same rate to flush the tube. Late AP, portal VP, and DP images were obtained at 25 to 30 seconds, 55 to 65 seconds, and 180 seconds after contrast agent injection, respectively.

HCC MRI radiological sign evaluation

Two radiologists independently evaluated the radiological signs without knowledge of the pathological diagnosis of patients. In cases of inconsistent evaluation results, a consensus was achieved through discussion or by consulting another senior diagnostic physician. The imaging criteria included in this study are based on the standardized diagnosis and treatment quality control indicators for Chinese primary HCC (2022 Edition)[21]. Examples of several MRI radiological signs are illustrated in Figure 1.

Grouping was based on several criteria, including maximum tumor diameter, pseudocapsule status, tumor blood vessels, cystic degeneration or necrosis, and cirrhosis: (1) Maximum tumor diameter: Lesions were measured using the medical imaging department's picture archiving and communication system (PACS) and categorized into two groups: < 3.0 cm and ≥ 3.0 cm, according to the maximum diameter of the tumor; (2) Pseudocapsule status: Based on the T1-weighted imaging (T1WI) sequence showing a low signal ring of 0.5 mm-3 mm at the edge of lesion, or a high signal shadow with ring-shaped delayed enhancement during the portal VP or DP. The pseudocapsule status was classified as either complete or incomplete/absent; (3) Tumor blood vessels: Based on whether thickened and tortuous enhancing blood vessels within the tumor showed during the AP of the MR-enhanced scan, and categorized as either with or without tumor blood vessels; (4) Cystic degeneration or necrosis: The observation of patchy low signal intensity on T1WI and high signal intensity on T2-weighted imaging (T2WI) within the lesion, combined with the absence of enhancement on the contrast-enhanced scan, suggests the presence of necrosis or cystic degeneration. Conversely, in the absence of these findings, it was classified as no detected necrosis or cystic degeneration; and (5) Cirrhosis: The identification of an irregular liver edge, blunt liver margin, widened liver fissures, disproportionate liver lobes, and diffuse reticular low signal changes in the liver parenchyma on T2WI sequence indicated cirrhosis. In contrast, the absence of these features was interpreted as indicative of no cirrhosis.

Texture analysis method based on multiparametric MRI

HCC lesion ROI delineation and texture feature extraction: T2WI, AP, VP, and DP images were exported from the PACS in BMP format. Initially, the MaZda 4.6 software (available from: http://www.eletel.p.lodz.pl/mazda/) was employed to manually delineate the ROI layer by layer on the enhanced scanning phase images with the clearest tumor boundaries. These delineated layers were subsequently fused to create a 3D volume of interest (VOI). The VOI was then copied to other enhanced images, and in instances of misalignment, adjustments were made based on the neighboring tissue structure to minimize placement errors across different scanning phase images. Given that the layer thickness of T2WI images differed from that of the enhanced images, ROIs needed to be manually delineated separately, layer by layer, before being fused into a single VOI. Finally, a senior radiologist meticulously reviewed the placement of all VOIs layers, examining them layer by layer. In cases of disagreement regarding the ROI delineation or VOI adjustments, the lesion was re-delineated or adjusted until consensus was achieved. To minimize the impact of partial volume effects, ROIs were manually delineated on all slices with locating 1 mm-2 mm inside the tumor lesion boundary. Before

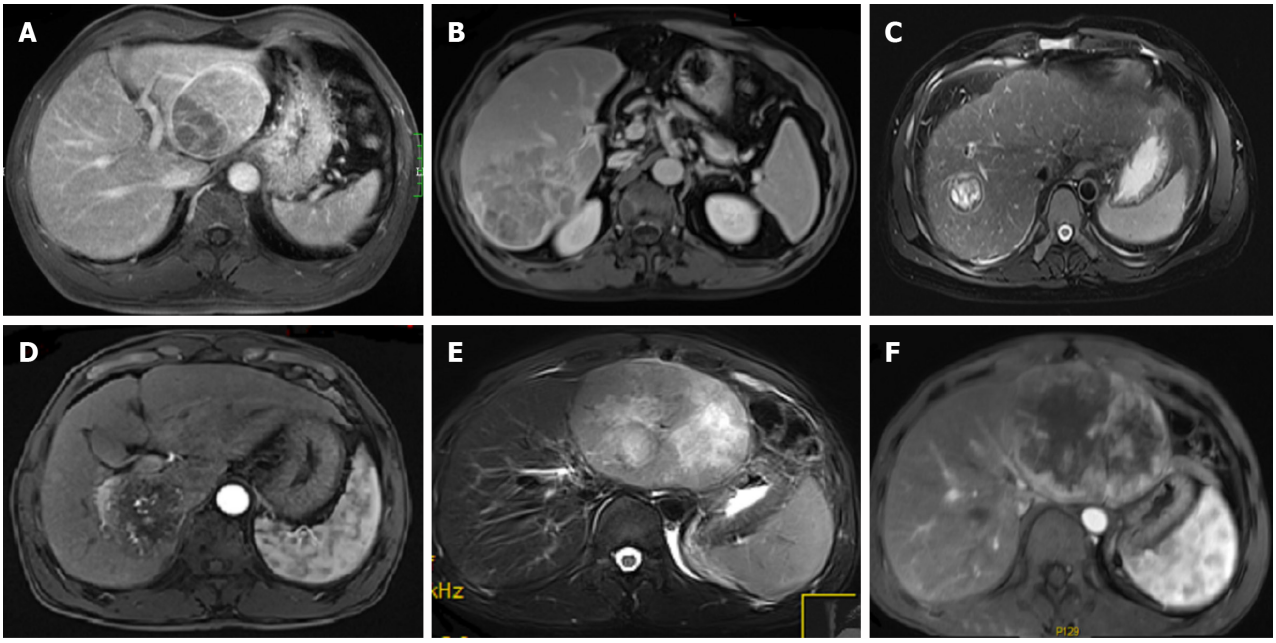

Figure 1 Representative examples of hepatocellular carcinoma magnetic resonance imaging radiological signs. A: Axial portal venous phase image: A high-signal ring surrounding the tumor lesion edge in the left lobe of the liver, demonstrating good continuity, indicative of a complete pseudocapsule; B: Axial delayed phase image: A high-signal ring around the tumor lesion edge in the right lobe of the liver with interrupted continuity, suggesting an incomplete pseudocapsule; C: Axial T2-weighted imaging image: Irregular liver margin and diffuse reticular slightly low-signal change of the liver parenchyma, characteristic of cirrhosis; D: Axial arterial phase image: Thickened and tortuous enhanced blood vessels within the tumor lesion in the right lobe of the liver, representing tumor vessels; E: Axial T2-weighted imaging image: Irregular patchy high-signal region within a large tumor, suggesting areas of cystic degeneration or necrosis; F: Axial delayed phase image: Corresponding to E, showing no enhancement in the areas of suspected cystic degeneration or necrosis.

extracting texture features, all enrolled MRI images were gray-level standardized to reduce the impact of imaging non-standardization on the stability of texture features[13,16]. A total of 94 texture feature parameters were extracted for each sequence separately.

Dimensionality reduction of HCC MRI texture features: The mutual information (MI) method included in the MaZda 4.6 software was used to select the top 10 dominant texture features from single sequence MRI (T2WI/AP/VP/DP) texture features. Python programmed MI was implemented for dimensionality reduction and selection of the top 10 dominant texture features from multiparametric MRI (T2WI + AP + VP + DP) texture features, totaling 94× 4 features.

Construction and evaluation of ANN models: Using the B11 program included in the MaZda 4.6 software, the dominant texture features obtained from dimensionality reduction of single sequence MRI and multiparametric MRI were used to construct ANN models separately. The ten dominant texture features from the multiparametric MRI were combined with radiological signs, which are independent predictors of HCC MVI, to develop the ANN model. The results were represented as misclassification rates (MCR). The predictive performance of the model for MVI was evaluated using the area under the receiver operating characteristic (ROC) curve (AUC), as well as sensitivity and specificity metrics. The DeLong test was employed to assess the statistical differences in AUC among the ANN models based on different features, leading to the selection of models that demonstrated relatively high performance. The flowchart illustrating the construction of the ANN models based on MRI texture features is presented in Figure 2.

Training and testing of ANN models with high prediction performance: A regression model based on multilayer feedforward backpropagation ANN and error backpropagation learning method was used for training and testing ANN models with high prediction performance. The ANN was implemented using the Python programming language, using features of ANN models demonstrating high prediction performance as input variables and postoperative pathological results of MVI-positive and MVI-negative groups as output variables. The dataset was divided into an 8:2 ratio using a random selection method, followed by input variable data standardization. The dense connection layer of the ANN model was configured with 256 neurons and utilized a sigmoid activation function, with input dimensions corresponding to the number of features. The hidden layer was composed of 128 neurons, also employing a sigmoid activation function. The optimizer used was root mean square propagation, and the loss function chosen was categorical cross entropy. The number of neurons in the hidden layer was determined based on the quantity of inputs in the input layer. During model training, the number of iterative calculations was set to 200, batch size was set to 64, and 30% of the data was used as a test set. The output layer consisted of two elements, with the first element representing patients in the MVI-positive group and the second element representing patients in the MVI-negative group. Finally, the accuracy rate and loss function values of the test set data pertaining to HCC MVI prediction were monitored, and the calculations were repeated 30 times. The average value obtained from these repetitions was considered the final result.

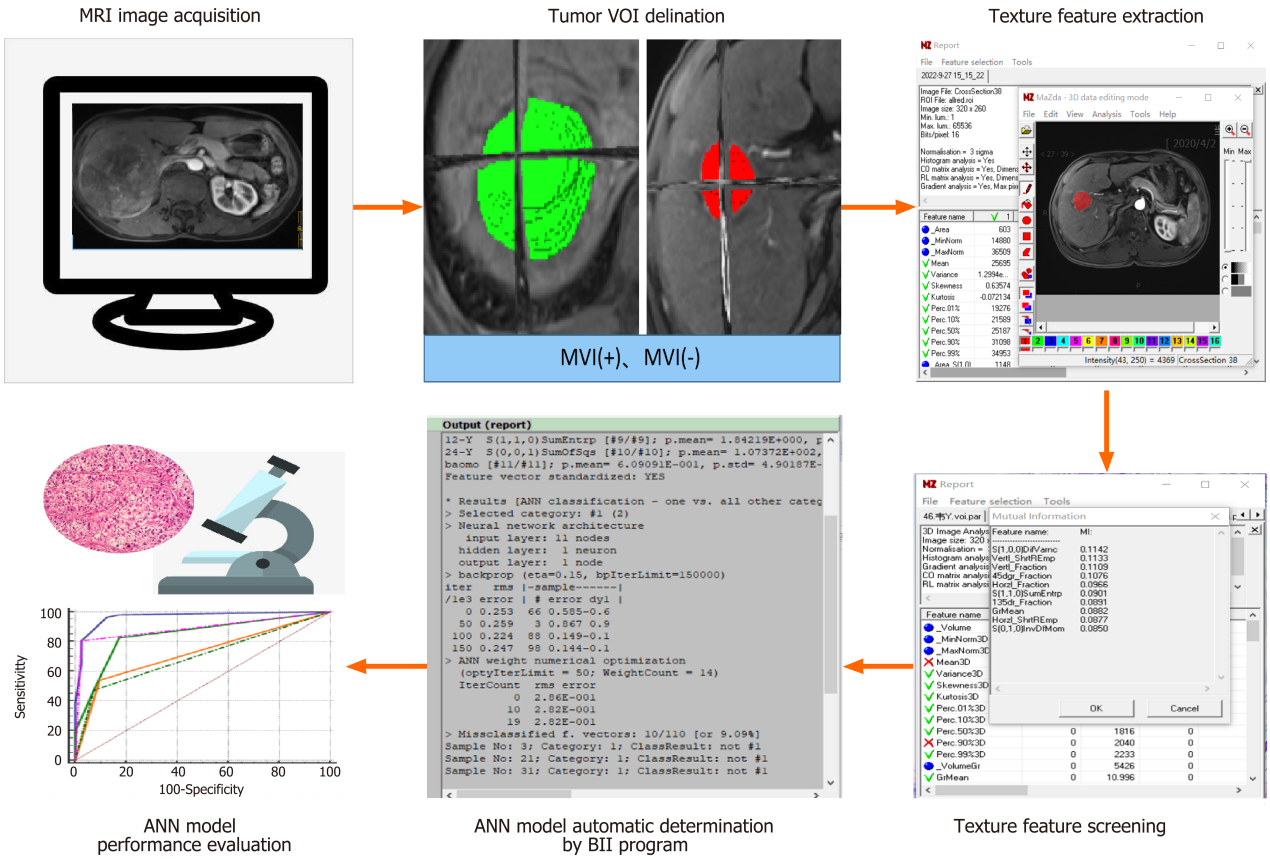

Figure 2 Flowchart of artificial neural network model construction based on magnetic resonance imaging texture features. MRI: Magnetic resonance imaging; ANN: Artificial neural network; VOI: Volume of interest; MVI: Microvascular invasion.

Statistical analysis

Statistical product and service solutions 26.0 software analysis package was used for this study, and two independent samples *t*-test was used for measures that conformed to normal distribution, and nonparametric Mann-Whitney *U* test was used for measures that did not conform to normal distribution; χ^2 test was used to analyze the relationship between MRI imaging signs and MVI expression; and for clinical or imaging features with $P < 0.05$, binary logistic regression was used to further screen for independent independent risk factors. Python 3.7 programming language with MI method was used to perform feature dimensionality reduction for multiparameter texture features and select the top 10 dominant features. The ANN model of the built-in B11 program of MaZda 4.6 software was used for prediction and classification. The performance of ANN models in predicting MVI status was represented by the MCR. The AUC, sensitivity, and specificity were metrics used to evaluate the predictive performance. To assess the statistical differences between the AUCs of different models, the DeLong test was applied, with a *P* value of less than 0.05 considered statistically significant.

RESULTS

Prediction of HCC MVI based on MRI radiological signs

Based on the postoperative pathological results, patients were divided into the MVI-positive group (57 cases in total, including 50 males and 7 females, aged 29-80 years, with an average age of 51.28 ± 12.54 years) and the MVI-negative group (40 cases in total, including 34 males and 6 females, aged 35-79 years, with an average age of 55.23 ± 11.33 years). The flowchart for the enrollment process of the study population is shown in Figure 3. The relationship between MRI imaging signs and HCC MVI positive and negative groups was analyzed using the χ^2 test, which are both categorical variables. Among the clinical and radiological signs including gender, age, tumor maximum diameter (≥ 3 cm or < 3 cm), pseudocapsule status (presence and complete or Absence/incomplete), tumor blood vessels (presence or absense), cystic degeneration or necrosis (presence or absense) and cirrhosis (presence or absense), it was found that tumor maximum diameter, pseudocapsule status, presence of tumor blood vessels, and presence of necrosis or cystic degeneration were significantly correlated with MVI status (all $P < 0.05$) (Table 1), while the presence of cirrhosis was not correlated with MVI ($P = 0.298$). For clinical or imaging features with significant correlation ($P < 0.05$), binary logistic regression was used to further screen independent risk factors. The results showed that the absence of pseudocapsule or incomplete pseudocapsule and tumor blood vessels were independent risk factors for MVI (Table 1).

Table 1 Binary logistic regression analysis for microvascular invasion prediction

Variables	β	SE	Wald	df	*P* value	OR (95%CI)
Tumor maximum diameter	-0.074	0.588	0.016	1	0.900	0.929 (0.293-2.942)
Pseudocapsule	2.093	0.639	10.733	1	0.001	8.111 (2.318-28.373)
Tumor blood vessels	2.051	0.788	6.775	1	0.009	7.775 (1.660-36.421)
Cystic degeneration or necrosis	0.098	0.677	0.021	1	0.885	1.103 (0.293-4.4155)

OR: Odds ratio; CI: Confidence interval.

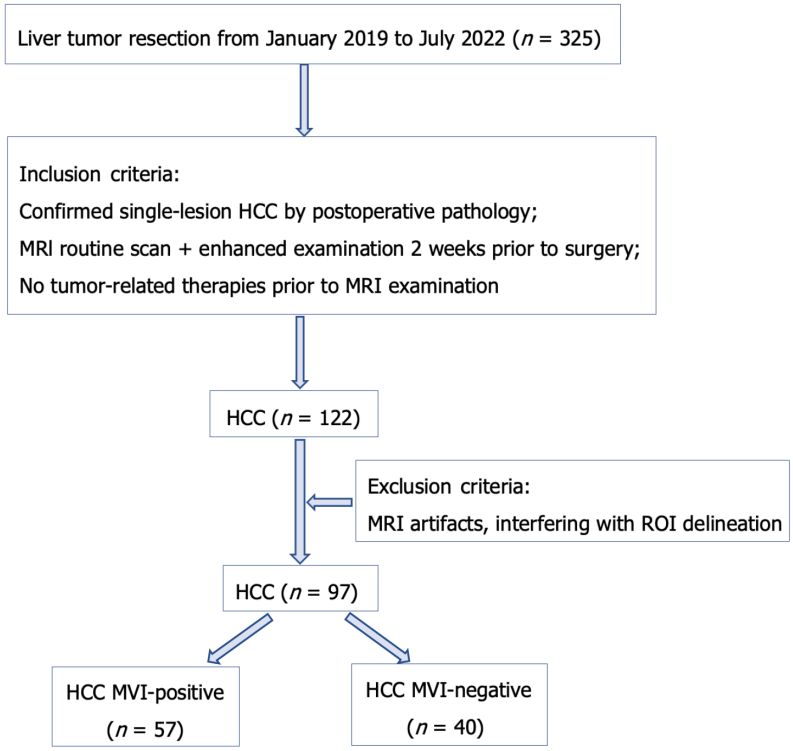

Figure 3 Flowchart of subject enrollment in this study. MRI: Magnetic resonance imaging; MVI: Microvascular invasion; HCC: Hepatocellular carcinoma; ROI: Region of interest.

Application and evaluation results of ANN models for MVI status prediction

The dominant texture features obtained from single sequence and multiparametric MRI after MI dimensionality reduction are shown in Table 2. The texture features of multiparametric MRI were derived from the gray-level gradients and long run length matrix features of AP and VP images. The performance of ANN models constructed on different features for MVI performance prediction is shown in Table 3, and the ROC curves are shown in Figure 4. Notably, the ANN model incorporating the combined group (pseudocapsule situation, tumor blood vessels, AP, and VP) exhibited the highest performance for predicting MVI, with metrics including MCR, sensitivity, specificity, and AUC recorded at 13.40%, 80.70%, 97.50%, and 0.891, respectively. Subsequently, a difference analysis of AUCs using ANN models constructed on dominant texture features from different MRI sequence and radiological signs were performed, and the results showed that the difference between the combined group and the single sequence or AP + VP ANN models was statistically significant ($P < 0.05$ for both comparisons). The ANN models constructed on T2WI, AP, VP, and AP + VP dominant texture features demonstrated comparable performance for predicting MVI, with no statistically significant difference between pairwise comparisons ($P > 0.05$ for all). These findings suggest that the ANN model utilizing features from the combined group demonstrates superior predictive performance, which warrants further testing and validation (the schematic diagram of the combined group ANN model structure is shown in Figure 5).

Training and testing results for the ANN model of high prediction performance

In this study, the ANN model for the combined group was trained and tested, with the accuracy rate and loss function values for the test set being monitored. After 30 iterations, the mean value was obtained as the final result. The results show that the test set data had an accuracy rate of 0.774 ± 0.335 for predicting HCC MVI, and the loss function value was 0.647 ± 0.061. These results suggest that the model demonstrates good stability.

Table 2 The dominant texture features selected after microvascular invasion dimensionality reduction

T2WI	AP	VP	DP	Multiparametric
GrSkewness	Z_ShrtREmp	Z_LngREmph	Perc.01% 3D	AP-S (0, 1, 0) SumAverg
135dr_GLevNonU	Z_Fraction	Z_Fraction	S (0, 0, 1) InvDfMom	AP-Horzl_Fraction
45dgr_GLevNonU	Z_LngREmph	S (1, 0, 0) SumAverg	GrMean	AP-Horzl_ShrtREmp
Horzl_GLevNonU	45dgr_ShrtREmp	S (0, 0, 1) SumAverg	Z_LngREmph	AP-Horzl_LngREmph
Z_RLNonUni	S (0, 0, 1) InvDfMom	S (1, 1, 0) SumAverg	Z_ShrtREmp	AP-S (0, 0, 1) InvDfMom
135dr_ShrtREmp	S (0, 0, 1) SumAverg	Vertl_RLNonUni	S (1, -1, 0) SumAverg	VP- 45dgr_RLNonUni
Horzl_Fraction	Skewness 3D	135dr_RLNonUni	S (1, -1, 0) SumVarnc	VP-Vertl_RLNonUni
135dr_RLNonUni	GrSkewness	Z_ShrtREmp	Z_Fraction	VP-S (0, 0, 1) SumAverg
Z_GLevNonU	45dgr_Fraction	Perc.10% 3D	S (0, 1, 0) SumVarnc	VP-Z_ShrtREmp
Vertl_GLevNonU	Kurtosis 3D	S (0, 1, 0) SumAverg	Perc.10% 3D	VP-Z_LngREmph

T2WI: T2-weighted imaging; 3D: Three-dimensional; AP: Arterial phases; VP: Venous phase; DP: Delayed phase.

Table 3 Hepatocellular carcinoma microvascular invasion prediction results from artificial neural network models constructed on different features, *n* (%)

Sequence	MCR (*n* = 97)	Sensitivity (%)	Specificity (%)	AUC (95%CI)
T2WI	25 (25.77)	80.70	65.00	0.729
AP	19 (19.59)	100.00	52.50	0.762
VP	24 (24.74)	70.17	82.50	0.763
DP	23 (23.71)	70.17	85.00	0.776
AP + VP	17 (17.53)	94.73	65.00	0.799
[1]Combined	13 (13.40)	80.70	97.50	0.891

[1]Combined = Pseudocapsule + tumor blood vessels + arterial phases + venous phase.
T2WI: T2-weighted imaging; MCR: Misclassification rate; AUC: Area under curve; AP: Arterial phases; VP: Venous phase; DP: Delayed phase; CI: Confidence interval.

DISCUSSION

MRI radiological signs in predicting MVI

When the tumor diameter exceeds 3.0 cm, significant alterations occur in the genetic material and biological invasiveness of HCC[22]. Based on this theoretical foundation, this study used 3.0 cm as the threshold for classifying HCC size. Previous studies have found that HCC tumor size, multiple nodular tumor morphology, irregular tumor margins, incomplete pseudocapsule, and abnormal intratumoral arteries are radiological signs related to MVI, while their clinical values and applicability vary. Huang *et al*[23] found that tumor size and incomplete pseudocapsule are independent risk factors for predicting MVI. In contrast, this study found that while tumor size is correlated with MVI status, it was not identified as an independent risk factor for predicting MVI, aligning with the findings of Kim *et al*[24] and Chou *et al*[25], and different from Huang *et al*[23]. This discrepancy may be attributed to selection bias regarding HCC lesion size. Furthermore, this study identifies the absence or incompleteness of a pseudocapsule as an independent risk factor for predicting MVI, aligning with the findings of Huang *et al*[23]. This observation supports the hypothesis that the pseudocapsule of HCC serves to inhibit cancer cell invasion into adjacent liver parenchyma. Additionally, cancer cell cords at the incomplete pseudocapsule can interact with normal liver cells, with tumor blood vessels directly linking tonormal liver sinusoids, thereby increasing the likelihood of MVI by cancer cells[26]. In addition to these above findings, we further proved that tumor blood vessels are also an independent risk factor for predicting MVI, consistent with the finding of Renzulli *et al*[27]. Unlike Renzulli *et al*[27] who combined intratumoral arteries and low density halo sign into a specific radiological sign/imaging feature called two-trait predictor of venous invasion for preoperative prediction of MVI, this study did not include low signal halo analysis due to the difficulty in distinguishing low signal halo and enhanced pseudocapsule on MRI images. In the study of preoperative MVI risk assessment for HCC by Yang *et al*[28], least absolute shrinkage and selection operator (LASSO) regression analysis was performed on a cohort of 405 patients who underwent HCC resection. In this study, HCC tumor necrosis or cystic degeneration shows statistical significance in detecting

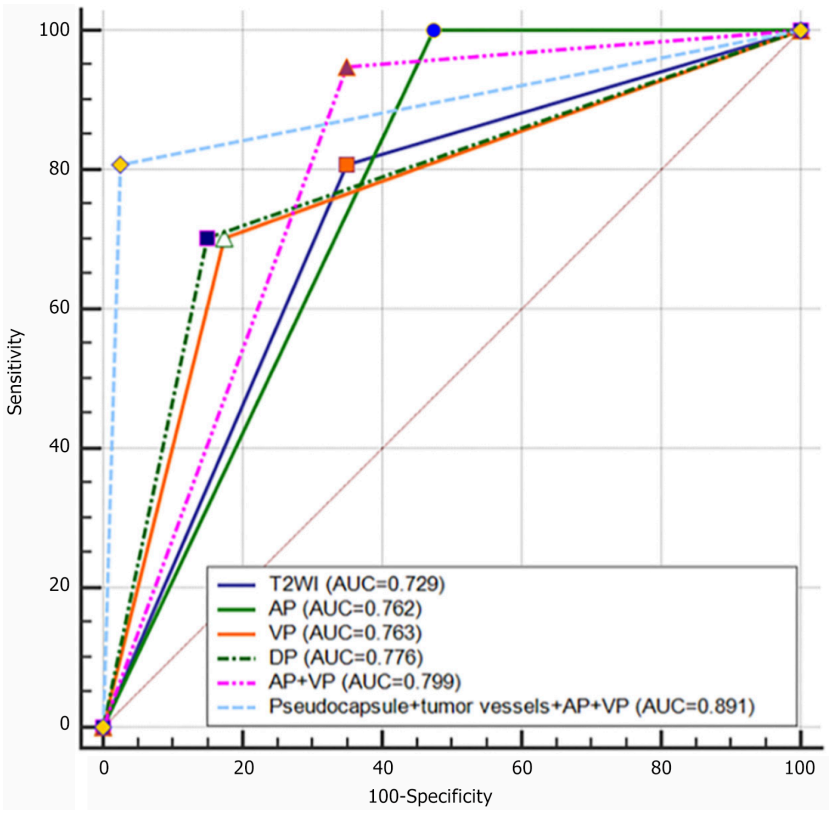

Figure 4 Receiver operating characteristic curves for predicting hepatocellular carcinoma microvascular invasion using artificial neural network models constructed on different sequence features. T2WI: T2-weighted imaging; AUC: Area under curve; AP: Arterial phases; VP: Venous phase; DP: Delayed phase.

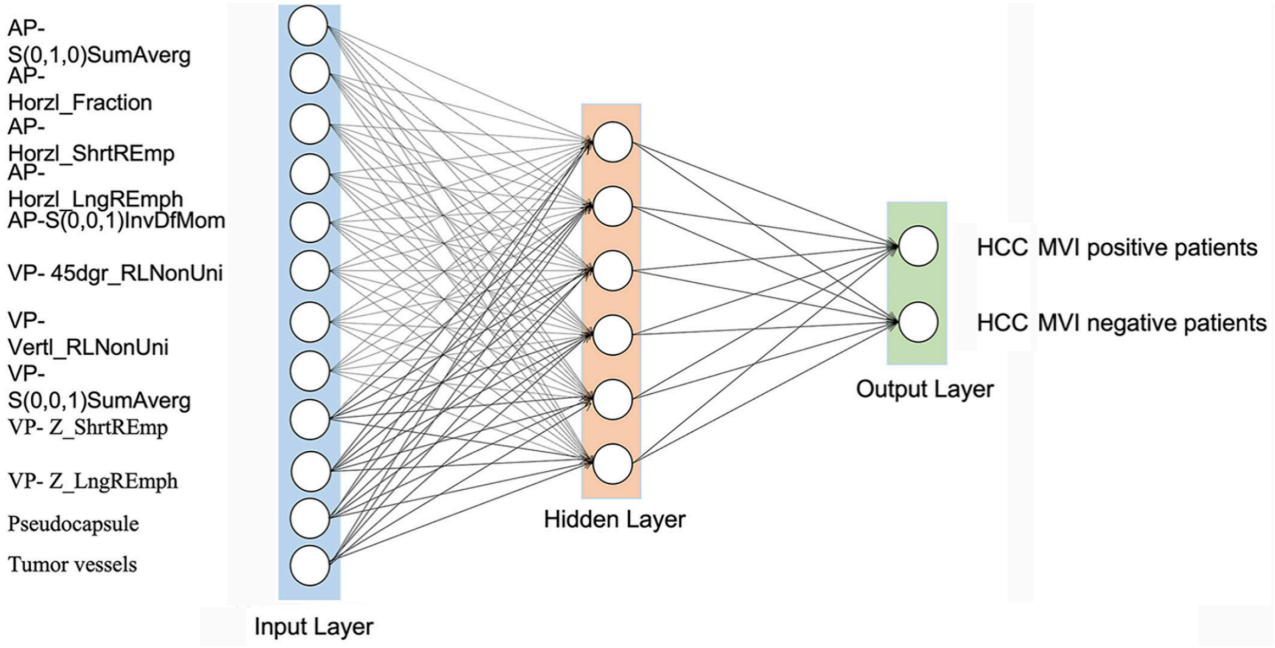

Figure 5 Schematic diagram of the combined group artificial neural network model structure. AP: Arterial phases; VP: Venous phase; MVI: Microvascular invasion; HCC: Hepatocellular carcinoma.

difference between MVI positive and negative cases, however without being an independent risk factor for predicting MVI status. Cirrhosis is an important indicator of poor prognosis in HCC[29], and some studies have reported the presence of cirrhosis as an independent risk factor for MVI in HCC patients. In contrast to these previous finding, our study did not establish a correlation between the occurrence of MVI in HCC patients and a history of cirrhosis.

MVI prediction with ANN models constructed on MRI texture features

Tumors are heterogeneous entities that encompass diverse scales[30], and invasive biopsy-based detection methods have limitations and often fail to capture the overall biological characteristics of a tumor. Tumor texture features mainly include characteristics derived from gray-level histograms, gray-level co-occurrence matrices, gray-level gradients, and long-run matrices, which can reflect subtle texture changes that are challenging to detect with the naked eye. Some of these features may have significant implications for the tumor and its surrounding microenvironment[12,31]. In this study, similar to the research of Zhang *et al*[32] and Meng *et al*[33], 3D VOI image data analysis was used. Previous studies have established that variations in contrast agents, slice thickness, and machine acquisition parameters can affect the repeatability and variability of radiomics[12,34], leading to inconsistencies in pixel or voxel size, gray-level number and range. These factors may affect the performance of texture features, interfering with the texture analysis model's applications in other centers. Therefore, it is essential to perform preprocessing with image resampling and/or gray-level normalization before texture features extractions. In this study, the images were gray-level standardized, minimizing the bias of texture features. Zhu *et al*[35] performed dimensionality reduction on the texture features of MRI AP and VP images and obtained four MR texture features of AP images and five texture features for portal venous phase (PP) images. They established individual logistic regression models utilizing texture features to predict MVI. In the ROC analysis, the AP texture model demonstrated superior diagnostic performance compared to the PP model in the validation cohort, with an AUC of 0.773 *vs* 0.62, which is similar to the AUC value of the ANN model constructed in this study based on AP image texture features. Zhu *et al*[35] focused merely on the texture features of arterial and portal VP, neglecting the predictive value of T2WI and DP image texture features, which have also been routinely used for preoperative MVI prediction. Previous studies[36,37] have shown that diffusion-weighted imaging (DWI)/T2WI mismatch and apparent diffusion coefficient (ADC) measurements are not particularly reliable for predicting MVI, so this study did not incorporate DWI/T2WI mismatch and ADC. Studies by Zhang *et al*[32], Guo *et al*[12], and Zhu *et al*[35] have demonstrated that texture analysis prediction models based on the MRI AP are superior to other single sequence models. Given that HCC increasingly receives blood supply from the hepatic artery, which ultimately predominates, the AP images are believed to more accurately reflect tumor heterogeneity and, consequently, better assess MVI. In this study, the ANN models constructed on single sequence MRI (T2WI/AP/VP/DP) and AP + VP dominant texture features had no statistically significant. This lack of significance may be attributed to variations in the dimensionality reduction methods applied to the texture features, as well as differences in the model construction approaches. Further studies with an increased sample size are necessary to confirm these findings and to determine whether the texture feature values obtained from routine MRI scans are comparable to those derived from enhanced image sources. It is worth mentioning that Nebbia *et al*[38] found that when tumor and margin radiomics features were combined, the performance of the model decreased, indicating that the information obtained from the margin and the tumor itself are not complementary (and might even be conflicting). Similarly, in this study, the prediction performance of the ANN model constructed on AP + VP dominant texture features for HCC MVI did not provide statistically significant additional value to the ANN model constructed on single sequence MRI dominant features. Xu *et al*[39] focused on the CT radiographic features around the tumor according to the MVI definition, but it was not superior to the features obtained from the tumor itself in terms of predicting MVI. Therefore, this study only used the entire tumor texture features to predict MVI and systematically evaluated the predictive performance of T2WI and three phase enhanced MRI images for MVI, all of which exhibited certain predictive capabilities for MVI status.

ANN model constructed on multiparametric MRI texture features combined with radiological signs for MVI prediction

Currently, there is an ongoing debate regarding the extent to which the combination of texture features or radiomics features with radiological signs can enhance the predictive performance of HCC MVI. In this study, the ANN model constructed using the dominant features from the combined group (pseudo-capsule status + tumor blood vessels + AP + VP) achieved a MCR, sensitivity, specificity, and AUC of 13.40%, 80.70%, 97.50%, and 0.891, respectively, for the high-expression group of HCC MVI. The accuracy rate of the test set data for HCC MVI prediction was 0.774 ± 0.335, with a loss function value of 0.647 ± 0.061, indicating good model stability. The differences between this model and the ANN models constructed on single sequence or AP+VP dominant features were statistically significant ($P < 0.05$ for both). In the ANN model, the pseudocapsule status and tumor blood vessels provided statistically significant additional value for the prediction of MVI based on texture features. Lu *et al*[40] studied the preoperative radiomics prediction of HCC MVI based on gadolinium ethoxybenzyl diethylenetriamine pentaacetic acid (Gd-EOB-DTPA)-enhanced MRI and established a combined model using tumor margin, peritumoral low intensity, and seven radiomics features. This combined model demonstrated superior performance compared to both the radiomics model and the clinical radiology model, achieving the highest sensitivity of 90.89% in the validation set. The AUC values for the combined model, radiomics model, and clinical radiology model were 0.826, 0.755, and 0.708, respectively. The AUC of the combined ANN model for predicting MVI in this study was slightly higher than that reported by Lu *et al*[40], Zhang *et al*[13], based on CT enhancement images of radiomics features in 637 patients, established a logistic regression radiomics model to predict MVI status after dimensionality reduction using the LASSO method. The AUCs of the combined radiomics model, including age and alpha-fetoprotein levels, in the training, testing, and independent validation cohorts were 0.806, 0.803, and 0.796, respectively. These results indicate that CT and MRI exhibit comparable predictive performance for MVI in solitary HCC. Furthermore, Meng *et al*[33] demonstrated that MRI radiomics analysis outperformed CT in predicting MVI for HCC tumors larger than 2 cm and up to 5 cm. Despite the reported advancements, various studies employ differing methods for the extraction of texture features or radiomics features, as well as for dimensionality reduction. Additionally, the lack of complete standardization in imaging presents a significant challenge. Furthermore, the variability in combined radiological signs and laboratory indicators is a critical factor contributing to the biases observed in the results. For HCC,

dynamic contrast-enhanced MRI of the liver has become the preferred technology for clinical detection, diagnosis, staging and efficacy evaluation. It has advantages over dynamic contrast-enhanced CT in evaluating whether the portal vein, main hepatic vein and its branches are invaded. Therefore, this study mainly focuses on multiple Modal MRI studies. The ANN model can better analyze complex nonlinear relationships than traditional radiomics models (such as support vector machines, random forests, *etc.*), and is widely used in disease diagnosis, classification, prediction, and survival analysis[41,42]. In this study, the ANN model constructed by combining the dominant features of the group (pseudo-capsule + tumor blood vessels + AP + VP) has higher prediction performance for MVI status. This model is an automatic classification prediction with strong operability and stability. It is good and provides a theoretical basis for clinical prediction of HCC recurrence and metastasis. It has great clinical application value. Therefore, it can be recommended as a non-invasive method to predict the MVI status of HCC before surgery.

Clinical application of ANN model for HCC

Previous retrospective study had developed an ANN model to predict post-hepatectomy early recurrence in HCC patients without macroscopic vascular invasion and achieved satisfactory discriminatory and calibration capacities in both the derivation and validation cohorts with greater prediction capacity than a Cox proportional hazards model, some preexisting recurrence models, and commonly used staging systems[42]. Other studies have shown that ANN diagnostic blueprint established by feature genes showcased robust and transferrable prognostic potentialities, portending to alleviate patient encumbrance and elevate life quality[43], and that the ANN model has better diagnostic capabilities than other commonly used models and scoring systems in assessing liver cirrhosis risk in patients with hepatitis B virus-related HCC[44]. Moreover, it was reported that the ANN model was more accurate in predicting 5-year mortality compared to the conventional logistic regression model for HCC[45]. In our present study, we found that in the ANN models based on the relevant radiological signs can improve the performance of texture features in predicting HCC MVI, which can be recommended as a non-invasive method for preoperative prediction of HCC MVI status. have been designed to attain superior classification accuracy through automated extraction of features from images, as well as to enhance the precision in forecasting biological traits and outcomes, including MVI and the likelihood of tumor recurrence [46]. Nonetheless, significant obstacles, particularly regarding interpretability, have impeded their application in clinical environments. To facilitate the effective integration of these models into clinical practice, additional studies are essential to confirm their efficacy and improve their interpretability. Extensive, large-scale, multi-center validation is necessary prior to real-world clinical use.

Limitations and future directions

(1) This is a retrospective, single-center study with a relatively small sample size. Many patients who were clinically considered "high risk" but did not receive surgical treatment were excluded, which may lead to potential selection bias affecting the repeatability and comparability of the results. Further external validation and prospective data validation are thus needed; (2) The construction of the ANN models in this study was completed using MaZda 4.6 in a one-stop manner, with a single reader involved, rendering it impossible to assess the consistency between different readers; and (3) More comprehensive clinical data such as relevant laboratory indicators were not included in the analysis, and the interpretability of the model was not discussed. This is also the direction for further exploration.

CONCLUSION

In summary, in the ANN models of this study, the relevant radiological signs can improve the performance of texture features in predicting HCC MVI to some extent. The ANN model constructed on texture features of multiparametric MRI combined with radiological signs can be recommended as a non-invasive method for preoperative prediction of HCC MVI status. This model is automated for classification prediction, highly operable, and stable. Our findings also suggest that current computer technology applications in disease diagnosis and treatment should not overly rely on the prediction results obtained solely from primary lesion image information by artificial intelligence.

FOOTNOTES

Author contributions: Nong HY, Ding K, Liu MR, Cen YY and Lu SJ carried out the studies, participated in collecting data, and drafted the manuscript; Ding K, Liu MR, Nong HY and Cen YY performed the statistical analysis and participated in its design; Huang RS, Chen Q, Huang LF, Huang JN, Wei X and Li L helped to draft the manuscript; All authors read and approved the final manuscript.

Supported by the National Natural Science Foundation of China, No. 81560278; the Health Commission of Guangxi Zhuang Autonomous Region, No. Z20200953, No. G201903023, and No. Z-A20221157; and Scientific Research and Technology Development Project of Nanning, No. 20213122.

Institutional review board statement: Adhering to the ethical principles of the Declaration of Helsinki, a retrospective analysis of 97 patients with hepatocellular carcinoma confirmed by surgical pathology at our hospital from January 2019 to July 2022 was conducted, with approval from our Institutional Review Board and completion of all patients' informed consent (approved number: 2015-02-28-1).

Informed consent statement: Informed consent was obtained from all patients.

Conflict-of-interest statement: The authors declare that they have no conflict of interest.

Data sharing statement: The datasets used and/or analyzed during the current study are available from the corresponding author on reasonable request.

Country of origin: China

ORCID number: Ke Ding 0000-0002-8987-1704.

S-Editor: Fan M
L-Editor: A
P-Editor: Zhang XD

REFERENCES

1 **Gordan JD**, Kennedy EB, Abou-Alfa GK, Beg MS, Brower ST, Gade TP, Goff L, Gupta S, Guy J, Harris WP, Iyer R, Jaiyesimi I, Jhawer M, Karippot A, Kaseb AO, Kelley RK, Knox JJ, Kortmansky J, Leaf A, Remak WM, Shroff RT, Sohal DPS, Taddei TH, Venepalli NK, Wilson A, Zhu AX, Rose MG. Systemic Therapy for Advanced Hepatocellular Carcinoma: ASCO Guideline. *J Clin Oncol* 2020; **38**: 4317-4345 [PMID: 33197225 DOI: 10.1200/JCO.20.02672]

2 **Brenet Defour L**, Mulé S, Tenenhaus A, Piardi T, Sommacale D, Hoeffel C, Thiéfin G. Hepatocellular carcinoma: CT texture analysis as a predictor of survival after surgical resection. *Eur Radiol* 2019; **29**: 1231-1239 [PMID: 30159621 DOI: 10.1007/s00330-018-5679-5]

3 **Nitta H**, Allard MA, Sebagh M, Ciacio O, Pittau G, Vibert E, Sa Cunha A, Cherqui D, Castaing D, Bismuth H, Guettier C, Lewin M, Samuel D, Baba H, Adam R. Prognostic Value and Prediction of Extratumoral Microvascular Invasion for Hepatocellular Carcinoma. *Ann Surg Oncol* 2019; **26**: 2568-2576 [PMID: 31054040 DOI: 10.1245/s10434-019-07365-0]

4 **Chen ZH**, Zhang XP, Wang H, Chai ZT, Sun JX, Guo WX, Shi J, Cheng SQ. Effect of microvascular invasion on the postoperative long-term prognosis of solitary small HCC: a systematic review and meta-analysis. *HPB (Oxford)* 2019; **21**: 935-944 [PMID: 30871805 DOI: 10.1016/j.hpb.2019.02.003]

5 **Shah SA**, Cleary SP, Wei AC, Yang I, Taylor BR, Hemming AW, Langer B, Grant DR, Greig PD, Gallinger S. Recurrence after liver resection for hepatocellular carcinoma: risk factors, treatment, and outcomes. *Surgery* 2007; **141**: 330-339 [PMID: 17349844 DOI: 10.1016/j.surg.2006.06.028]

6 **Sun R**, Zhao S, Jiang H, Jiang H, Dai Y, Zhang C, Wang S. Imaging Tool for Predicting Renal Clear Cell Carcinoma Fuhrman Grade: Comparing R.E.N.A.L. Nephrometry Score and CT Texture Analysis. *Biomed Res Int* 2021; **2021**: 1821876 [PMID: 34977234 DOI: 10.1155/2021/1821876]

7 **Feng M**, Zhang M, Liu Y, Jiang N, Meng Q, Wang J, Yao Z, Gan W, Dai H. Texture analysis of MR images to identify the differentiated degree in hepatocellular carcinoma: a retrospective study. *BMC Cancer* 2020; **20**: 611 [PMID: 32605628 DOI: 10.1186/s12885-020-07094-8]

8 **López-Gómez C**, Ortiz-Ramón R, Mollá-Olmos E, Moratal D; Alzheimer's Disease Neuroimaging Initiative. ALTEA: A Software Tool for the Evaluation of New Biomarkers for Alzheimer's Disease by Means of Textures Analysis on Magnetic Resonance Images. *Diagnostics (Basel)* 2018; **8** [PMID: 30029524 DOI: 10.3390/diagnostics8030047]

9 **Giganti F**, Antunes S, Salerno A, Ambrosi A, Marra P, Nicoletti R, Orsenigo E, Chiari D, Albarello L, Staudacher C, Esposito A, Del Maschio A, De Cobelli F. Gastric cancer: texture analysis from multidetector computed tomography as a potential preoperative prognostic biomarker. *Eur Radiol* 2017; **27**: 1831-1839 [PMID: 27553932 DOI: 10.1007/s00330-016-4540-y]

10 **Li Y**, Xu X, Weng S, Yan C, Chen J, Ye R. CT Image-Based Texture Analysis to Predict Microvascular Invasion in Primary Hepatocellular Carcinoma. *J Digit Imaging* 2020; **33**: 1365-1375 [PMID: 32968880 DOI: 10.1007/s10278-020-00386-2]

11 **Liu SC**, Lai J, Huang JY, Cho CF, Lee PH, Lu MH, Yeh CC, Yu J, Lin WC. Predicting microvascular invasion in hepatocellular carcinoma: a deep learning model validated across hospitals. *Cancer Imaging* 2021; **21**: 56 [PMID: 34627393 DOI: 10.1186/s40644-021-00425-3]

12 **Guo D**, Gu D, Wang H, Wei J, Wang Z, Hao X, Ji Q, Cao S, Song Z, Jiang J, Shen Z, Tian J, Zheng H. Radiomics analysis enables recurrence prediction for hepatocellular carcinoma after liver transplantation. *Eur J Radiol* 2019; **117**: 33-40 [PMID: 31307650 DOI: 10.1016/j.ejrad.2019.05.010]

13 **Zhang X**, Ruan S, Xiao W, Shao J, Tian W, Liu W, Zhang Z, Wan D, Huang J, Huang Q, Yang Y, Yang H, Ding Y, Liang W, Bai X, Liang T. Contrast-enhanced CT radiomics for preoperative evaluation of microvascular invasion in hepatocellular carcinoma: A two-center study. *Clin Transl Med* 2020; **10**: e111 [PMID: 32567245 DOI: 10.1002/ctm2.111]

14 **Ni M**, Zhou X, Lv Q, Li Z, Gao Y, Tan Y, Liu J, Liu F, Yu H, Jiao L, Wang G. Radiomics models for diagnosing microvascular invasion in hepatocellular carcinoma: which model is the best model? *Cancer Imaging* 2019; **19**: 60 [PMID: 31455432 DOI: 10.1186/s40644-019-0249-x]

15 **Ma X**, Wei J, Gu D, Zhu Y, Feng B, Liang M, Wang S, Zhao X, Tian J. Preoperative radiomics nomogram for microvascular invasion prediction in hepatocellular carcinoma using contrast-enhanced CT. *Eur Radiol* 2019; **29**: 3595-3605 [PMID: 30770969 DOI: 10.1007/s00330-018-5985-y]

16 **Strzelecki M**, Szczypinski P, Materka A, Klepaczko A. A software tool for automatic classification and segmentation of 2D/3D medical images. *Nucl Instrum Meth A* 2013; **702**: 137-140 [DOI: 10.1016/j.nima.2012.09.006]

17 **Li M**, Yin Z, Hu B, Guo N, Zhang L, Zhang L, Zhu J, Chen W, Yin M, Chen J, Ehman RL, Wang J. MR Elastography-Based Shear Strain Mapping for Assessment of Microvascular Invasion in Hepatocellular Carcinoma. *Eur Radiol* 2022; **32**: 5024-5032 [PMID: 35147777 DOI: 10.1007/s00330-022-08578-w]

18 **Rao C**, Wang X, Li M, Zhou G, Gu H. Value of T1 mapping on gadoxetic acid-enhanced MRI for microvascular invasion of hepatocellular carcinoma: a retrospective study. *BMC Med Imaging* 2020; **20**: 43 [PMID: 32345247 DOI: 10.1186/s12880-020-00433-y]

19 **Mao WB**, Lyu JY, Vaishnani DK, Lyu YM, Gong W, Xue XL, Shentu YP, Ma J. Application of artificial neural networks in detection and diagnosis of gastrointestinal and liver tumors. *World J Clin Cases* 2020; **8**: 3971-3977 [PMID: 33024753 DOI: 10.12998/wjcc.v8.i18.3971]

20 **Rodríguez-Perálvarez M**, Luong TV, Andreana L, Meyer T, Dhillon AP, Burroughs AK. A systematic review of microvascular invasion in hepatocellular carcinoma: diagnostic and prognostic variability. *Ann Surg Oncol* 2013; **20**: 325-339 [PMID: 23149850 DOI: 10.1245/s10434-012-2513-1]

21 **National Cancer Center**, National Tumor Quality Control Center; Liver Cancer Quality Control Expert Committee. [Standardized Diagnosis and Treatment Quality Control Indicators for Chinese Primary Hepatocellular Carcinoma (2022 Edition)]. *Gan'ai Dianzi Zazhi* 2022; **9**: 1-11

22 **Cong WM**, Wu MC. The biopathologic characteristics of DNA content of hepatocellular carcinomas. *Cancer* 1990; **66**: 498-501 [PMID: 1694717 DOI: 10.1002/1097-0142(19900801)66:3<498::aid-cncr2820660316>3.0.co;2-2]

23 **Huang M**, Liao B, Xu P, Cai H, Huang K, Dong Z, Xu L, Peng Z, Luo Y, Zheng K, Peng B, Li ZP, Feng ST. Prediction of Microvascular Invasion in Hepatocellular Carcinoma: Preoperative Gd-EOB-DTPA-Dynamic Enhanced MRI and Histopathological Correlation. *Contrast Media Mol Imaging* 2018; **2018**: 9674565 [PMID: 29606926 DOI: 10.1155/2018/9674565]

24 **Kim KA**, Kim MJ, Jeon HM, Kim KS, Choi JS, Ahn SH, Cha SJ, Chung YE. Prediction of microvascular invasion of hepatocellular carcinoma: usefulness of peritumoral hypointensity seen on gadoxetate disodium-enhanced hepatobiliary phase images. *J Magn Reson Imaging* 2012; **35**: 629-634 [PMID: 22069244 DOI: 10.1002/jmri.22876]

25 **Chou CT**, Chen RC, Lin WC, Ko CJ, Chen CB, Chen YL. Prediction of microvascular invasion of hepatocellular carcinoma: preoperative CT and histopathologic correlation. *AJR Am J Roentgenol* 2014; **203**: W253-W259 [PMID: 25148181 DOI: 10.2214/AJR.13.10595]

26 **Chong HH**, Yang L, Sheng RF, Yu YL, Wu DJ, Rao SX, Yang C, Zeng MS. Multi-scale and multi-parametric radiomics of gadoxetate disodium-enhanced MRI predicts microvascular invasion and outcome in patients with solitary hepatocellular carcinoma ≤ 5 cm. *Eur Radiol* 2021; **31**: 4824-4838 [PMID: 33447861 DOI: 10.1007/s00330-020-07601-2]

27 **Renzulli M**, Brocchi S, Cucchetti A, Mazzotti F, Mosconi C, Sportoletti C, Brandi G, Pinna AD, Golfieri R. Can Current Preoperative Imaging Be Used to Detect Microvascular Invasion of Hepatocellular Carcinoma? *Radiology* 2016; **279**: 432-442 [PMID: 26653683 DOI: 10.1148/radiol.2015150998]

28 **Yang J**, Zhu S, Yong J, Xia L, Qian X, Yang J, Hu X, Li Y, Wang C, Peng W, Zhang L, Deng M, Pan W. A Nomogram for Preoperative Estimation of Microvascular Invasion Risk in Hepatocellular Carcinoma: Single-Center Analyses With Internal Validation. *Front Oncol* 2021; **11**: 616976 [PMID: 33747929 DOI: 10.3389/fonc.2021.616976]

29 **Zhao H**, Hua Y, Lu Z, Gu S, Zhu L, Ji Y, Qiu Y, Dai T, Jin H. Prognostic value and preoperative predictors of microvascular invasion in solitary hepatocellular carcinoma ≤ 5 cm without macrovascular invasion. *Oncotarget* 2017; **8**: 61203-61214 [PMID: 28977857 DOI: 10.18632/oncotarget.18049]

30 **Gerlinger M**, Rowan AJ, Horswell S, Math M, Larkin J, Endesfelder D, Gronroos E, Martinez P, Matthews N, Stewart A, Tarpey P, Varela I, Phillimore B, Begum S, McDonald NQ, Butler A, Jones D, Raine K, Latimer C, Santos CR, Nohadani M, Eklund AC, Spencer-Dene B, Clark G, Pickering L, Stamp G, Gore M, Szallasi Z, Downward J, Futreal PA, Swanton C. Intratumor heterogeneity and branched evolution revealed by multiregion sequencing. *N Engl J Med* 2012; **366**: 883-892 [PMID: 22397650 DOI: 10.1056/NEJMoa1113205]

31 **Xu T**, Ren L, Liao M, Zhao B, Wei R, Zhou Z, He Y, Zhang H, Chen D, Chen H, Liao W. Preoperative Radiomics Analysis of Contrast-Enhanced CT for Microvascular Invasion and Prognosis Stratification in Hepatocellular Carcinoma. *J Hepatocell Carcinoma* 2022; **9**: 189-201 [PMID: 35340666 DOI: 10.2147/JHC.S356573]

32 **Zhang Y**, Shu Z, Ye Q, Chen J, Zhong J, Jiang H, Wu C, Yu T, Pang P, Ma T, Lin C. Preoperative Prediction of Microvascular Invasion in Hepatocellular Carcinoma *via* Multi-Parametric MRI Radiomics. *Front Oncol* 2021; **11**: 633596 [PMID: 33747956 DOI: 10.3389/fonc.2021.633596]

33 **Meng XP**, Wang YC, Zhou JY, Yu Q, Lu CQ, Xia C, Tang TY, Xu J, Sun K, Xiao W, Ju S. Comparison of MRI and CT for the Prediction of Microvascular Invasion in Solitary Hepatocellular Carcinoma Based on a Non-Radiomics and Radiomics Method: Which Imaging Modality Is Better? *J Magn Reson Imaging* 2021; **54**: 526-536 [PMID: 33622022 DOI: 10.1002/jmri.27575]

34 **Wu TH**, Hatano E, Yamanaka K, Seo S, Taura K, Yasuchika K, Fujimoto Y, Nitta T, Mizumoto M, Mori A, Okajima H, Kaido T, Uemoto S. A non-smooth tumor margin on preoperative imaging predicts microvascular invasion of hepatocellular carcinoma. *Surg Today* 2016; **46**: 1275-1281 [PMID: 26983710 DOI: 10.1007/s00595-016-1320-x]

35 **Zhu YJ**, Feng B, Wang S, Wang LM, Wu JF, Ma XH, Zhao XM. Model-based three-dimensional texture analysis of contrast-enhanced magnetic resonance imaging as a potential tool for preoperative prediction of microvascular invasion in hepatocellular carcinoma. *Oncol Lett* 2019; **18**: 720-732 [PMID: 31289547 DOI: 10.3892/ol.2019.10378]

36 **Lee S**, Kim SH, Lee JE, Sinn DH, Park CK. Preoperative gadoxetic acid-enhanced MRI for predicting microvascular invasion in patients with single hepatocellular carcinoma. *J Hepatol* 2017; **67**: 526-534 [PMID: 28483680 DOI: 10.1016/j.jhep.2017.04.024]

37 **Wang WT**, Yang L, Yang ZX, Hu XX, Ding Y, Yan X, Fu CX, Grimm R, Zeng MS, Rao SX. Assessment of Microvascular Invasion of Hepatocellular Carcinoma with Diffusion Kurtosis Imaging. *Radiology* 2018; **286**: 571-580 [PMID: 28937853 DOI: 10.1148/radiol.2017170515]

38 **Nebbia G**, Zhang Q, Arefan D, Zhao X, Wu S. Pre-operative Microvascular Invasion Prediction Using Multi-parametric Liver MRI Radiomics. *J Digit Imaging* 2020; **33**: 1376-1386 [PMID: 32495126 DOI: 10.1007/s10278-020-00353-x]

39 **Xu X**, Zhang HL, Liu QP, Sun SW, Zhang J, Zhu FP, Yang G, Yan X, Zhang YD, Liu XS. Radiomic analysis of contrast-enhanced CT predicts microvascular invasion and outcome in hepatocellular carcinoma. *J Hepatol* 2019; **70**: 1133-1144 [PMID: 30876945 DOI: 10.1016/j.jhep.2019.02.023]

40 **Lu XY**, Zhang JY, Zhang T, Zhang XQ, Lu J, Miao XF, Chen WB, Jiang JF, Ding D, Du S. Using pre-operative radiomics to predict microvascular invasion of hepatocellular carcinoma based on Gd-EOB-DTPA enhanced MRI. *BMC Med Imaging* 2022; **22**: 157 [PMID: 36057576 DOI: 10.1186/s12880-022-00855-w]

41 **Mao Y**, Wang J, Zhu Y, Chen J, Mao L, Kong W, Qiu Y, Wu X, Guan Y, He J. Gd-EOB-DTPA-enhanced MRI radiomic features for predicting histological grade of hepatocellular carcinoma. *Hepatobiliary Surg Nutr* 2022; **11**: 13-24 [PMID: 35284527 DOI: 10.21037/hbsn-19-870]

42 **Mai RY**, Zeng J, Meng WD, Lu HZ, Liang R, Lin Y, Wu GB, Li LQ, Ma L, Ye JZ, Bai T. Artificial neural network model to predict post-hepatectomy early recurrence of hepatocellular carcinoma without macroscopic vascular invasion. *BMC Cancer* 2021; **21**: 283 [PMID: 33726693 DOI: 10.1186/s12885-021-07969-4]

43 **Zhang S**, Jiang C, Jiang L, Chen H, Huang J, Gao X, Xia Z, Tran LJ, Zhang J, Chi H, Yang G, Tian G. Construction of a diagnostic model for hepatitis B-related hepatocellular carcinoma using machine learning and artificial neural networks and revealing the correlation by immunoassay. *Tumour Virus Res* 2023; **16**: 200271 [PMID: 37774952 DOI: 10.1016/j.tvr.2023.200271]

44 **Mai RY**, Zeng J, Mo YS, Liang R, Lin Y, Wu SS, Piao XM, Gao X, Wu GB, Li LQ, Ye JZ. Artificial Neural Network Model for Liver Cirrhosis Diagnosis in Patients with Hepatitis B Virus-Related Hepatocellular Carcinoma. *Ther Clin Risk Manag* 2020; **16**: 639-649 [PMID: 32764948 DOI: 10.2147/TCRM.S257218]

45 **Shi HY**, Lee KT, Wang JJ, Sun DP, Lee HH, Chiu CC. Artificial neural network model for predicting 5-year mortality after surgery for hepatocellular carcinoma: a nationwide study. *J Gastrointest Surg* 2012; **16**: 2126-2131 [PMID: 22878787 DOI: 10.1007/s11605-012-1986-3]

46 **Xia T**, Zhao B, Li B, Lei Y, Song Y, Wang Y, Tang T, Ju S. MRI-Based Radiomics and Deep Learning in Biological Characteristics and Prognosis of Hepatocellular Carcinoma: Opportunities and Challenges. *J Magn Reson Imaging* 2024; **59**: 767-783 [PMID: 37647155 DOI: 10.1002/jmri.28982]

World Journal of Gastrointestinal Oncology

Submit a Manuscript: https://www.f6publishing.com

World J Gastrointest Oncol 2025 January 15; 17(1): 96822

DOI: 10.4251/wjgo.v17.i1.96822

ISSN 1948-5204 (online)

ORIGINAL ARTICLE

Retrospective Study

Dihydropyrimidine dehydrogenase polymorphisms in patients with gastrointestinal malignancies and their impact on fluoropyrimidine tolerability: Experience from a single Italian institution

Mariarosaria D'Amato, Gennaro Iengo, Nicola Massa, Chiara Carlomagno

Specialty type: Oncology

Provenance and peer review: Unsolicited article; Externally peer reviewed.

Peer-review model: Single blind

Peer-review report's classification

Scientific Quality: Grade B, Grade C

Novelty: Grade C, Grade C

Creativity or Innovation: Grade B, Grade C

Scientific Significance: Grade B, Grade D

P-Reviewer: Yang ZY

Received: May 15, 2024

Revised: August 14, 2024

Accepted: August 28, 2024

Published online: January 15, 2025

Processing time: 210 Days and 14.6 Hours

Mariarosaria D'Amato, Department of Oncology, Ospedale San Rocco ASL Caserta, Sessa Aurunca 81037, Campania, Italy

Gennaro Iengo, Nicola Massa, Chiara Carlomagno, Department of Clinical Medicine and Surgery, University of Naples Federico II, Naples 80131, Campania, Italy

Corresponding author: Mariarosaria D'Amato, MD, Doctor, Department of Oncology, Ospedale San Rocco ASL Caserta, Via XXI Luglio, Sessa Aurunca 81037, Campania, Italy.
mariar.damato@gmail.com

Abstract

BACKGROUND

Fluoropyrimidines are metabolized in the liver by the enzyme dihydropyrimidine dehydrogenase (DPD), encoded by the *DPYD* gene. About 7% of the European population is a carrier of *DPYD* gene polymorphisms associated with reduced DPD enzyme activity.

AIM

To assess the prevalence of *DPYD* polymorphisms and their impact on fluoropyrimidine tolerability in Italian patients with gastrointestinal malignancies.

METHODS

A total of 300 consecutive patients with a diagnosis of gastrointestinal malignancy and treated with a fluoropyrimidine-based regimen were included in the analysis and divided into two cohorts: (1) 149 patients who started fluoropyrimidines after *DPYD* testing; and (2) 151 patients treated without *DPYD* testing. Among the patients in cohort A, 15% tested only the *DPYD2A* polymorphism, 19% tested four polymorphisms (*DPYD*2A, HapB3, c.2846A>T, and *DPYD*13), and 66% tested five polymorphisms including *DPYD*6.

RESULTS

Overall, 14.8% of patients were found to be carriers of a *DPYD* variant, the most common being *DPYD*6 (12.1%). Patients in cohort A reported ≥ G3 toxicities (P = 0.00098), particularly fewer nonhematological toxicities (P = 0.0028) compared with cohort B, whereas there was no statistically significant difference between the two cohorts in hematological toxicities (P = 0.6944). Significantly fewer che-

motherapy dose reductions (P = 0.00002) were observed in cohort A compared to cohort B, whereas there was no statistically significant differences in chemotherapy delay.

CONCLUSION

Although this study had a limited sample size, it provides additional information on the prevalence of *DPYD* polymorphisms in the Italian population and highlights the role of pharmacogenetic testing to prevent severe toxicity.

Key Words: Dihydropyrimidine dehydrogenase; *DPYD* polymorphisms; Fluoropyrimidine; Caucasian population; Gastrointestinal cancers

Core Tip: In this retrospective study, we report the prevalence of *DPYD* polymorphisms in a real-world population of patients treated for gastrointestinal malignancies and their impact on fluoropyrimidine tolerability. Furthermore, we demonstrate that the presence of polymorphisms in the *DPYD* gene, which encodes dihydropyrimidine dehydrogenase, leads to an increased risk of G3/G4 nonhematologic toxicity and more frequent dose reductions. We did not find a significant difference in chemotherapy delay.

Citation: D'Amato M, Iengo G, Massa N, Carlomagno C. Dihydropyrimidine dehydrogenase polymorphisms in patients with gastrointestinal malignancies and their impact on fluoropyrimidine tolerability: Experience from a single Italian institution. *World J Gastrointest Oncol* 2025; 17(1): 96822

URL: https://www.wjgnet.com/1948-5204/full/v17/i1/96822.htm

DOI: https://dx.doi.org/10.4251/wjgo.v17.i1.96822

INTRODUCTION

5-Fluorouracil (5-FU) was introduced into clinical practice about 60 years ago[1], and still represents the backbone of therapy for early and metastatic gastrointestinal tumors. Furthermore, its oral prodrug (capecitabine) is widely used for the treatment of gastrointestinal, breast, and head and neck cancers[2]. After intravenous administration, 5-FU is converted to fluorodeoxyuridine monophosphate, which binds and inhibits thymidylate synthase, resulting in reduced DNA and RNA synthesis[3]. After rapid intestinal absorption, the oral 5-FU prodrug, capecitabine, is converted in the liver to 5'-deoxy-5-fluorocytidine, which is transformed to 5'-deoxy-5-fluorouridine and finally converted to 5-FU[4]. 5-FU is metabolized in the liver by the enzyme dihydropyrimidine dehydrogenase (DPD) encoded by the gene *DPYD*, which has several polymorphisms, some of which cause decreased enzyme activity[5]. The ability to eliminate fluoropyrimidines can be assessed at different time points, from the gene encoding the DPD enzyme to the 5-FU catabolic pathway (different ways to analyze fluoropyrimidine metabolism): (1) The detection of relevant *DPYD* gene single nucleotide polymorphisms; (2) The level of *DPYD* mRNA expression; (3) The evaluation of DPD activity in peripheral blood mononuclear cells with radioenzymatic techniques; (4) The measurement of uracil, a natural substrate of DPD, in plasma or urine; (5) The uracil ratio in plasma, *i.e.* the ratio of catabolite (dihydrouracil) to substrate (uracil) of DPD; and (6) The more recent (2-C13) uracil breath test[6,7].

The most commonly used method is the evaluation of polymorphisms of the *DPYD* gene due to large availability, affordable costs, and well-defined risk and dose adjustments for variant carriers[6]. The most studied *DPYD* variants associated with reduced DPD activity are c.1905+1G>A (rs3918290, *DPYD*2A), c.1679T>G (rs55886062, *DPYD*13), c.2846A>T (rs67376798, p.D949V), and c.1129–5923C>G (rs75017182, HapB3)[8]. Furthermore, other variants such as c.2194G>A (rs1801160, *DPYD*6) are associated with moderate reductions of the enzyme activity[9]. Hematological toxicity, nausea, vomiting, diarrhea, mucositis, and hand-foot syndrome are the most common adverse events associated with fluoropyrimidines[10] and polymorphisms that cause reduced DPD activity may increase these toxicities[8,11]. Two prospective studies have shown that adjusting the dose of fluoropyrimidines based on the presence of *DPYD* variants can significantly reduce the incidence of serious toxicities and deaths, as well as save costs of adverse event management[12,13]. In 2020, the European Medicines Agency (EMA) recommended that DPD activity be assessed before the administration of 5-FU, capecitabine, or tegafur, an oral prodrug of 5-FU used primarily in Asia. Soon afterwards, the Associazione Italiana di Oncologia Medica (AIOM) recommended *DPYD* polymorphisms testing before systemic fluoropyrimidine therapy initiation, and a dose reduction if variants are detected. According to the Clinical Pharmacogenetics Implementation Consortium, approximately 7% of the European population carries at least one variant conferring reduced DPD activity, and the most common polymorphism is *DPYD*-HapB3[14]. In Italy, several papers have reported the results of *DPYD* variants testing in selected populations, mainly in clinical trials, but data on the real-world prevalence of the *DPYD* polymorphism are still limited.

The aim of the present study was to evaluate the prevalence of the most common *DPYD* polymorphisms in patients treated with 5-FU or capecitabine (alone or in combination with radiotherapy or other drugs) for gastrointestinal cancer at our institution. We also assessed the association between *DPYD* testing and grade 3 or higher adverse events, dose reductions, and treatment delays.

MATERIALS AND METHODS

This retrospective analysis included 300 patients, older than 18 years, Caucasian race, who were consecutively referred at our Institution from January 2016 to July 2023. Patients should have a histological diagnosis of a gastrointestinal malignancy, requiring chemotherapy with a fluoropyrimidine-based regimen (5-FU or capecitabine), either as monotherapy or in combination with radiotherapy or other agents. The whole population was divided into two cohorts: Cohort A, including patients treated after *DPYD* testing; and cohort B, including patients treated without *DPYD* testing. *DPYD* assessment was performed in several accredited laboratories in our region, according to the patient's residence. The initial dose of fluoropyrimidine was calculated according to the patient's body surface, and reductions were applied based on age, comorbidities, and renal function, which was estimated by the creatinine clearance calculated using the Cockcroft-Gault formula[15]. In case of the presence of a *DPYD* polymorphism, the appropriate dose of fluoropyrimidine was calculated according to the AIOM recommendations. Descriptive statistics were used to show the demographic and clinical characteristics of the study population and the prevalence of the *DPYD* gene polymorphism in patients in cohort A. Hematological and non-hematological adverse events were assessed after each cycle of chemotherapy and graduated according to the National Cancer Institute Common Terminology Criteria for Adverse Events version 4. We estimated the correlation between pharmacogenetic testing and toxicity by comparing the occurrence of grade ≥ 3 adverse events in cohort A and cohort B using the χ^2 test (or Fisher's exact test, if necessary), with α error defined as 0.05.

RESULTS

Three hundred consecutive patients treated at our institution from January 2016 to July 2023 were enrolled (Table 1). Cohort A included 149 patients, treated after publication of the EMA recommendations for *DPYD* testing. Cohort B included 151 patients, treated without *DPYD* testing, before EMA recommendations. Levene's test was applied to evaluate the variability between cohorts A and B, obtaining $P > 0.05$ (0.58371), confirming that the patients' characteristics were well-balanced between the two cohorts (Table 1). About half of the patients were male (165/300, 55%); most patients had large bowel tumors, 55.7% colon, and 26% had rectal adenocarcinoma. About two-thirds of the patients had an early-stage neoplasm with a slightly higher prevalence in cohort A (70%) compared to cohort B (63%). Overall, the number of patients with metastatic disease was 45 (30%) in cohort A and 56 (37%) in cohort B, with 35 (23.5%) and 43 (28.5%) patients with liver metastases in cohorts A and B, respectively. None of the patients with liver metastases had liver impairment greater than grade 1. Fluoropyrimidines were administered as monotherapy in 14% of cases, in combination with radiotherapy in 18%, and doublet with another chemotherapeutic agent in 61.7% of the patients. Patients who received chemoradiotherapy were 20 of 149 in cohort A, and 34 of 151 in cohort B. However, only 1 patient in cohort B received doublet chemotherapy in combination with radiotherapy, in contrast to cohort A in which 7 patients received doublet chemotherapy in combination with radiotherapy. All patients in cohort A were tested for *DPYD*2A (c.1905+1G>A) polymorphism; 23/149 (15%) patients were only tested for *DPYD*2A, 28/149 (19%) patients were tested for the four main polymorphisms (*DPYD*2A, *DPYD*13, HapB3, c.2846A>T), and 98/149 (66%) patients were tested for *DPYD*6 in addition to the four main polymorphisms (Figure 1). *DPYD* testing was performed in various accredited external laboratories, which has progressively implemented this analysis after publication of the EMA and AIOM recommendations[13,14], thereby explaining the variability in the number of polymorphisms analyzed, ranging from a minimum of one polymorphism to a maximum of five polymorphisms. In cohort A, 127/149 patients (85.2%) were wild-type, 2/149 (1.3%) were heterozygous for HapB3 variant, 1/149 (0.7%) was heterozygous for *DPYD*2A, 1/149 (0.7%) was heterozygous for c.28496A>T, 17/149 (11.4%) were heterozygous for *DPYD*6, and 1/149 (0.7%) was homozygous for *DPYD*6 (Table 2). The prevalence of the four main variants was 2.7%, while it raised to 14.8% if *DPYD*6 was considered. The most detected variant was *DPYD*6, followed by HapB3, whereas no *DPYD*13 variant was found. Table 3 summarizes the worst toxicity reported during the treatment. Overall, 39/149 patients in cohort A (26.17%) and 67/151 in cohort B (44.37%) had at least one grade 3 or higher (≥ G3) adverse event, with a statistically significant difference between the two cohorts ($P = 0.00098$). Hematologic toxicities had a similar incidence in both cohorts: 26/149 (17.4%) patients in cohort A and 29/151 (19.2%) patients in cohort B. Non-hematologic toxicities were much more common in cohort B, 20/151 (13.2%), compared to cohort A, 5/149 (3.4%). In total, 33/149 patients in cohort A (22.15%) and 69/151 in cohort B (45.7%) required fluoropyrimidine dose reduction, with a statistically significant difference ($P = 0.00002$). In cohort B, the main cause for dose reductions during treatment was G ≥ 3 non-hematologic toxicity (42/151 [27.8%]), while 16/151 (10.6%) patients had grade 3 or higher hematologic toxicities. In cohort A, the dose was reduced because of hematologic toxicities in 17/149 (11.4%) patients and the same was for non-hematologic toxicities. At least one cycle of chemotherapy was delayed in 38/149 (25.5%) patients in cohort A and 52/151 (34.44%) in cohort B, with a non-statistically significant difference ($P = 0.09136$). Chemotherapy cycles were delayed for toxicities of any grade, predominantly for hematologic ones in both cohorts. Specifically, in cohort A, 29/149 (19.5%) patients required chemotherapy delay because of hematologic toxicities, 8/149 (5.4%) for non-hematologic toxicities, and 8/149 (5.4%) for both types of toxicities. In cohort B, 22/151 (14.6%) patients required chemotherapy delay due to hematologic toxicity, 20/151 (13.2%) due to non-

Table 1 Demographic and clinical characteristics

Characteristic	*DPYD* testing, *n* = 149	No *DPYD* testing, *n* = 151	Total, *n* = 300
Median age	66 (84-33)	65 (85-34)	65 (85-33)
ECOG PS			
0	133 (89)	143 (95)	276 (92)
1	16 (11)	8 (5)	24 (8)
Sex			
Male	79 (53)	86 (57)	165 (55)
Female	70 (47)	65 (43)	135 (45)
Type of cancer			
Colon	80 (54)	87 (58)	167 (55.7)
Rectal	32 (21)	46 (30)	78 (26)
Gastric	29 (19)	16 (11)	45 (15)
Esophageal	1 (1)	0 (0)	1 (0.3)
Anal	7 (5)	1 (1)	8 (2.7)
Appendiceal	0 (0)	1 (1)	1 (0.3)
Stage of disease			
Localized	104 (70)	95 (63)	199 (66.3)
Metastatic	45 (30)	56 (37)	101 (33.7)
Type of treatment			
Monotherapy	23 (15)	20 (13)	43 (14)
Monotherapy + RT	20 (13)	34 (23)	54 (18)
Doublet	97 (65)	88 (58)	185 (61.7)
Triplet	9 (6)	9 (6)	18 (6)

Data are *n* (%). ECOG: Eastern cooperative oncology group; PS: Performance Status; RT: Radiotherapy.

Table 2 Prevalence of *DPYD* polymorphisms

DPYD variant	Number detected (%)
HapB3	2 (1.3)[1]
*DPYD*2A	1 (0.7)[1]
c.2846A>T	1 (0.7)[1]
*DPYD*13	0 (0)
*DPYD*6	18 (12.1)[2]
Wild-type	127 (85.2)
All polymorphisms	22 (14.8)
All polymorphisms except *DPYD*6	4 (2.7)

[1]All in heterozygosity.
[2]All in heterozygosity except 1 in homozygosity.
Data are *n* (%).

Table 3 Correlation between *DPYD* polymorphisms and toxicity

Parameter	Cohort A, *n* = 149	Cohort B, *n* = 151	*P* value
Patients with any AEs ≥ G3	39 (26.17)	67 (44.37)	0.00098
Patients with FP dose reduction	33 (22.15)	69 (45.7)	0.00002
Patients with ChT delay for any grade AEs	38 (25.5)	52 (34.44)	0.09136
Patients with hematological AEs ≥ G3	26 (17.4)	29 (19.3)	0.6944
Patients with non-hematological AEs ≥ G3	5 (3.4)	20 (13.3)	0.0028

Data are *n* (%). AEs: Adverse events; ChT: Chemotherapy; FP: Fluoropyrimidine.

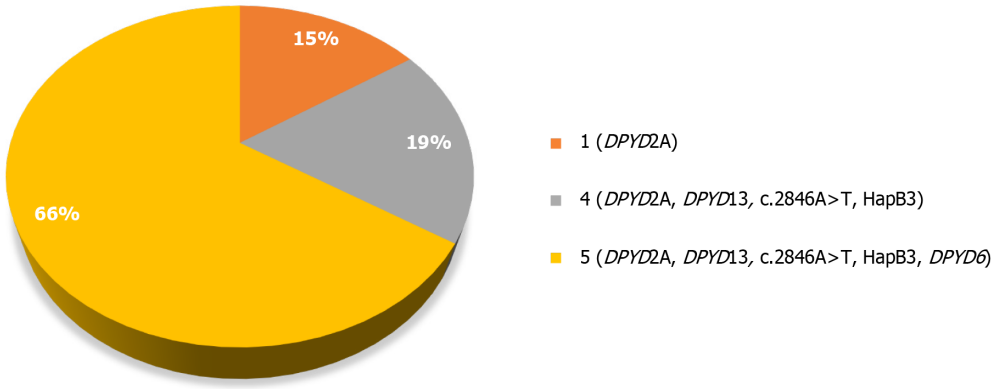

Figure 1 Polymorphisms analyzed.

hematologic toxicity, and 4/151 (2.6%) due to both types of toxicity. In cohort A, 17/149 (11.4%) patients required chemotherapy delay due to at least grade 3 hematologic toxicity, and 2/149 (1.3%) due to at least grade 3 non-hematologic toxicity. In cohort B, 3/151 (2%) patients had chemotherapy delay due to both hematologic and non-hematologic toxicity, 21/151 (13.9%) due to hematologic toxicity, and 5/151 (2%) due to non-hematologic toxicity. In some cases, toxicities of any grade resulted in a reduction in fluoropyrimidine dose without chemotherapy delay need, as they recovered or improved to a lower grade by the end of the cycle. Specifically, 19/149 (12.8%) patients in cohort A and 27/151 (17.9%) patients in cohort B received dose reduction due to non-hematologic toxicities without the need to delay chemotherapy. In total, 1/149 (0.7%) patient in cohort A and 1/151 (0.7%) patient in cohort B received dose reduction due to hematologic toxicities, with no need to delay chemotherapy; and 1/149 (0.7%) patient in cohort A and 5/151 (3.3%) patients in cohort B received dose reduction without chemotherapy delay for both hematologic and non-hematologic toxicities.

DISCUSSION

EMA recommendations raised awareness about the benefits of pharmacogenetic testing among oncologists and national health services. The survey by de With *et al*[16] showed that in Europe, before 2020, *DPYD* testing was difficult to perform routinely, due to a lack of reimbursability, lack of knowledge of the clinical relevance of the test, and lack of clear and unambiguous guidelines. In Italy, there was a progressive increase in the analysis of *DPYD* polymorphisms following the publication of EMA and AIOM recommendations and reimbursement of the test by the National Health Service. Thus, the laboratories progressively implemented the number of polymorphisms tested, from one (*DPYD*2A) to five (*DPYD*2A, HapB3, c.2846A>T, *DPYD*13, *DPYD*6). This is the reason why in our study, 23/149 (15%) patients were tested for only one polymorphism, *DPYD*2A, which was the first polymorphism to be investigated and whose relevance in clinical practice is known[12]. In our study population, the prevalence of the four most common variants of the *DPYD* gene, namely, *DPYD*2A (c.1905+1G>A), c.2846A>T, *DPYD*13 (c.1679T>G), and c.1236G>A/HapB3, was 2.7%. These data were consistent with those reported in several studies including European populations (Table 4): 4.8% in Spain[17], 7.5% in Denmark[18], 4.65% in France[19], and 8% in Netherlands[13]. To the best of our knowledge, few data are available on the prevalence of *DPYD* gene polymorphisms in the Italian real-world population, as most information is derived from retrospective analyses of patients with gastrointestinal cancers enrolled in clinical trials. The most representative series are those recruited for the TOSCA Phase 3 trial (randomized trial investigating the role of oxaliplatin, fluorouracil and leucovorin calcium-4 regimen duration [3 months *vs* 6 months] and bevacizumab as adjuvant therapy for patients with stage 2/3 colon cancer) and the TRIBE Phase 3 trial (randomized trial of oxaliplatin, irinotecan, fluorouracil, and

Table 4 Prevalence of *DPYD* polymorphisms in European populations

Polymorphism	Photo *DPYD* Spain[17], *n* = 8054	Paulsen Denmark[18], *n* = 4215	Pallet France[19], *n* = 3680	Henricks Netherland[13], *n* = 1103
*DPYD*2A	55 (0.7)	43 (1)	25 (0.67)	16 (1)
*DPYD*13	15 (0.2)	8 (0.2)	4 (0.1)	1 (< 1)
Hap3B	209 (2.6)	208 (4.9)	109 (2.96)	51 (5)
c.2846A>T	105 (1.3)	57 (1.4)	34 (0.92)	17 (2)
Total	384 (4.8)	316 (7.5)	172 (4.65)	85 (8)

Data are *n* (%).

leucovorin calcium + bevacizumab *vs* irinotecan, fluorouracil, and leucovorin calcium + bevacizumab as first-line treatment for metastatic colorectal cancer) and a single institution population analysis (Table 5). In the ancillary pharmacogenetic analysis of the TOSCA trial, which enrolled patients candidate to adjuvant chemotherapy after radical resection of high-risk stage 2/3 colon cancer, a total of 10 *DPYD* variants were retrospectively analyzed. Considering only the four variants recommended by the AIOM guidelines (c.1905+1G>A [rs3918290, *DPYD*2A], c.1679T>G [rs55886062, *DPYD*13], c.2846A>T [rs67376798, p.D949V], and c.1129–5923C>G [rs75017182, HapB3]), 19/508 (3.7%) patients were carriers of a variant in heterozygosity, while 5/508 (1%) patients were carriers of a variant in homozygosity. When the c.2194G>A (rs1801160, *DPYD*6) polymorphism was also included, a total of 84/508 (16.5%) patients were found to be carriers of at least one variant in heterozygosity[20]. In the TRIBE trial, which enrolled patients with metastatic colorectal cancer for first-line treatment, only the three *DPYD* variants mostly affecting DPD activity were tested (c.1905+1G>A [rs3918290, *DPYD*2A], c.2846A>T [rs67376798, p.D949V], and c.1679T>G [rs55886062, *DPYD*13]), and 10/439 (2.3%) patients resulted in heterozygous carriers, 5/439 (1.1%) of the c.2846A>T variant and 5/439 (1.1%) of the *DPYD*2A variant, respectively. No carrier of *DPYD* c.1679T>G (rs55886062, *DPYD*13) was identified, as it occurred in our series[21]. In a single Italian institution analysis, five polymorphisms were tested in 1000 patients with gastrointestinal malignancies, candidates for fluoropyrimidines. The variants tested were those recommended by AIOM (c.1905+1G>A [rs3918290, *DPYD*2A], c.1679T>G [rs55886062, *DPYD*13], c.2846A>T [rs67376798, p.D949V], and c.1129–5923C>G [rs75017182, HapB3]), plus c.2194G>A (rs1801160, *DPYD*6). When only four polymorphisms were considered, 39/1000 (3.9%) patients were carriers of a variant in heterozygosity, while no carriers of a variant in homozygosity were found. If all five polymorphisms were included, 180/1000 (18%) patients were heterozygous carriers, and 5/1000 (0.5%) patients resulted in homozygous carriers of the *DPYD*6 variant[22]. Overall, the results of our series are very consistent with those of the other Italian study, confirming that the evaluation of the *DPYD* gene polymorphism is very a reproducible and reliable analysis when performed by quality controlled laboratories. Regarding toxicity, the present study confirmed the role of *DPYD* testing in reducing the risk of developing serious adverse events, as we observed a statistically significant difference in terms of ≥ G3 toxicity and the occurrence of chemotherapy dose reduction between cohort A (*DPYD* test) and cohort B (no *DPYD* test). In our series, patients who started fluoropyrimidine-based therapy after *DPYD* testing experienced less severe toxicity (particularly, less hand-foot syndrome and mucositis) and required fewer dosage adjustments during treatment. There was no statistically significant difference in the delay of therapy due to toxicity between the two cohorts, even though the number of delays was numerically greater in the untested group. A possible explanation for the occurrence of dose reduction without treatment delay is that many severe toxicities in cohort B resolved by the end of the cycle without causing a chemotherapy delay. In addition, the chemotherapy delay was also due to less than grade 3 toxicities. TOSCA and TRIBE retrospective analyses also evaluated the association between the presence of *DPYD* variants and the occurrence of severe toxicity, with similar results. In the TOSCA trial, a statistically significant association was found between the presence of the c.2194G>A (rs1801160, *DPYD*6) polymorphism and the development of severe toxicities[20]. Furthermore, the variants rs181160, rs2297595, and rs3918290 were also correlated to a shorter time-to-toxicity, underlining not only the occurrence of severe adverse events but also the shorter time to toxicity onset in patients carrying *DPYD* polymorphisms[20]. In the TRIBE study, 8 of the 10 patients with polymorphisms (80%) developed at least one ≥ G3 toxicity, mainly neutropenia and stomatitis[21]. In conclusion, the present study, although conducted with a limited sample size, provides additional information about the prevalence of *DPYD* gene polymorphisms in the Italian population and confirms the importance of performing pharmacogenetic testing to prevent severe fluoropyrimidine toxicities. Studies with larger sample sizes may provide more accurate data on the prevalence of the different polymorphisms in the different populations and more accurate information on the role of each *DPYD* variant on the fluoropyrimidine-induced toxicity, to better tailor the *DPYD* testing before fluoropyrimidine treatment in the Italian patients.

CONCLUSION

Although the sample size was limited and the analysis was retrospective, this analysis provides additional information on the prevalence of *DPYD* polymorphisms in the Italian population. Furthermore, this analysis highlights the role of

Table 5 *DPYD* polymorphisms analysis in Italian cancer patients

Feature	TOSCA trial[20]	TRIBE trial[21]	IRCCS Pascale[22]
Setting	Colon cancer high-risk stage 2 or stage 3	Colo-rectal cancer stage 4	Gastrointestinal malignancies
Treatment	FOLFOX/CAPOX	FOLFOXIRI/FOLFIRI + bevacizumab	Patients candidates for fluoropyrimidines
Patients	508	439	1000
Total number of tested variants	10	3	5
Prevalence of the four recommended variants in heterozygosity	19/508 (3.7)	10/439 (2.3)[1]	39/1000 (3.9)
Prevalence of the four recommended variants + *DPYD*6 in heterozygosity	84/508 (16.5)	0/439 (0)[2]	180/1000 (18)
Prevalence of the four recommended variants + *DPYD*6 in homozygosity	5/508 (1.0)[3]	0/439 (0)[2]	5/1000 (0.5)[3]

[1]HapB3 not analyzed.
[2]HapB3 and *DPYD*6 not analyzed.
[3]All *DPYD*6.
Data are *n* (%). TOSCA: A randomized trial investigating the role of oxaliplatin, fluorouracil and leucovorin calcium-4 regimen duration (3 months *vs* 6 months) and bevacizumab as adjuvant therapy for patients with stage 2/3 colon cancer; TRIBE: Phase 3 randomized trial of oxaliplatin, irinotecan, fluorouracil, and leucovorin calcium + bevacizumab *vs* irinotecan, fluorouracil, and leucovorin calcium + bevacizumab as first-line treatment for metastatic colorectal cancer. CAPOX: Capecitabine and oxaliplatin; FOLFIRI: Irinotecan, fluorouracil, and leucovorin calcium; FOLFOX: Oxaliplatin, fluorouracil, and leucovorin calcium; FOLFOXIRI: Oxaliplatin, irinotecan, fluorouracil, and leucovorin calcium; IRCCS: Scientific institute for research, hospitalization and healthcare.

pharmacogenetic testing before treatment with fluoropyrimidines to prevent severe toxicity.

FOOTNOTES

Author contributions: D'Amato M and Carlomagno C participated in the conception and design of the study, analyzed the data, and wrote the original manuscript; D'Amato M collected the data; D'Amato M, Iengo G, Massa N, and Carlomagno C critically reviewed and provided final approval of the manuscript; D'Amato M, Iengo G, Massa N, and Carlomagno C were responsible for the decision to submit the manuscript for publication.

Institutional review board statement: The investigation was approved by the panel of scientists proposing the research and by all the collaborators who participated in the research.

Informed consent statement: The need for patient consent was waived due to the retrospective nature of the study.

Conflict-of-interest statement: The authors have no conflicts of interest to declare.

Data sharing statement: No additional data are available.

Country of origin: Italy

ORCID number: Mariarosaria D'Amato 0009-0007-0257-7718.

S-Editor: Fan M
L-Editor: Filipodia
P-Editor: Zhang L

REFERENCES

1 **Heidelberger C**, Chaudhuri NK, Danneberg P, Mooren D, Griesbach L, Duschinsky R, Schnitzer RJ, Pleven E, Scheiner J. Fluorinated pyrimidines, a new class of tumour-inhibitory compounds. *Nature* 1957; **179**: 663-666 [PMID: 13418758 DOI: 10.1038/179663a0]

2 **Koo K**, Pasternak AL, Henry NL, Sahai V, Hertz DL. Survey of US Medical Oncologists' Practices and Beliefs Regarding DPYD Testing Before Fluoropyrimidine Chemotherapy. *JCO Oncol Pract* 2022; **18**: e958-e965 [PMID: 35239419 DOI: 10.1200/OP.21.00874]

3 **Glimelius B**, Stintzing S, Marshall J, Yoshino T, de Gramont A. Metastatic colorectal cancer: Advances in the folate-fluoropyrimidine chemotherapy backbone. *Cancer Treat Rev* 2021; **98**: 102218 [PMID: 34015686 DOI: 10.1016/j.ctrv.2021.102218]

4 **Lam SW**, Guchelaar HJ, Boven E. The role of pharmacogenetics in capecitabine efficacy and toxicity. *Cancer Treat Rev* 2016; **50**: 9-22 [PMID: 27569869 DOI: 10.1016/j.ctrv.2016.08.001]

5 **Del Re M**, Restante G, Di Paolo A, Crucitta S, Rofi E, Danesi R. Pharmacogenetics and Metabolism from Science to Implementation in Clinical Practice: The Example of Dihydropyrimidine Dehydrogenase. *Curr Pharm Des* 2017; **23**: 2028-2034 [PMID: 28128059 DOI: 10.2174/1381612823666170125155530]

6 **Diasio RB**, Offer SM. Testing for Dihydropyrimidine Dehydrogenase Deficiency to Individualize 5-Fluorouracil Therapy. *Cancers (Basel)* 2022; **14** [PMID: 35804978 DOI: 10.3390/cancers14133207]

7 **Villalvazo P**, Marzal-Alfaro B, García-Alfonso P, Revuelta-Herrero JL, Thomas F, López-Tarruella S, García-González X, Calvo A, Yakoubi M, Salvador-Martín S, López-López F, Aguilar I, Sanjurjo-Sáez M, Martín M, López-Fernández LA. DPYD Exome, mRNA Expression and Uracil Levels in Early Severe Toxicity to Fluoropyrimidines: An Extreme Phenotype Approach. *J Pers Med* 2021; **11** [PMID: 34442436 DOI: 10.3390/jpm11080792]

8 **Meulendijks D**, Henricks LM, Sonke GS, Deenen MJ, Froehlich TK, Amstutz U, Largiadèr CR, Jennings BA, Marinaki AM, Sanderson JD, Kleibl Z, Kleiblova P, Schwab M, Zanger UM, Palles C, Tomlinson I, Gross E, van Kuilenburg AB, Punt CJ, Koopman M, Beijnen JH, Cats A, Schellens JH. Clinical relevance of DPYD variants c.1679T>G, c.1236G>A/HapB3, and c.1601G>A as predictors of severe fluoropyrimidine-associated toxicity: a systematic review and meta-analysis of individual patient data. *Lancet Oncol* 2015; **16**: 1639-1650 [PMID: 26603945 DOI: 10.1016/S1470-2045(15)00286-7]

9 **Del Re M**, Cinieri S, Michelucci A, Salvadori S, Loupakis F, Schirripa M, Cremolini C, Crucitta S, Barbara C, Di Leo A, Latiano TP, Pietrantonio F, Di Donato S, Simi P, Passardi A, De Braud F, Altavilla G, Zamagni C, Bordonaro R, Butera A, Maiello E, Pinto C, Falcone A, Mazzotti V, Morganti R, Danesi R. DPYD*6 plays an important role in fluoropyrimidine toxicity in addition to DPYD*2A and c.2846A>T: a comprehensive analysis in 1254 patients. *Pharmacogenomics J* 2019; **19**: 556-563 [PMID: 30723313 DOI: 10.1038/s41397-019-0077-1]

10 **Barin-Le Guellec C**, Lafay-Chebassier C, Ingrand I, Tournamille JF, Boudet A, Lanoue MC, Defossez G, Ingrand P, Perault-Pochat MC, Etienne-Grimaldi MC. Toxicities associated with chemotherapy regimens containing a fluoropyrimidine: A real-life evaluation in France. *Eur J Cancer* 2020; **124**: 37-46 [PMID: 31715555 DOI: 10.1016/j.ejca.2019.09.028]

11 **Johnson MR**, Diasio RB. Importance of dihydropyrimidine dehydrogenase (DPD) deficiency in patients exhibiting toxicity following treatment with 5-fluorouracil. *Adv Enzyme Regul* 2001; **41**: 151-157 [PMID: 11384742 DOI: 10.1016/s0065-2571(00)00011-x]

12 **Deenen MJ**, Meulendijks D, Cats A, Sechterberger MK, Severens JL, Boot H, Smits PH, Rosing H, Mandigers CM, Soesan M, Beijnen JH, Schellens JH. Upfront Genotyping of DPYD*2A to Individualize Fluoropyrimidine Therapy: A Safety and Cost Analysis. *J Clin Oncol* 2016; **34**: 227-234 [PMID: 26573078 DOI: 10.1200/JCO.2015.63.1325]

13 **Henricks LM**, Lunenburg CATC, de Man FM, Meulendijks D, Frederix GWJ, Kienhuis E, Creemers GJ, Baars A, Dezentjé VO, Imholz ALT, Jeurissen FJF, Portielje JEA, Jansen RLH, Hamberg P, Ten Tije AJ, Droogendijk HJ, Koopman M, Nieboer P, van de Poel MHW, Mandigers CMPW, Rosing H, Beijnen JH, Werkhoven EV, van Kuilenburg ABP, van Schaik RHN, Mathijssen RHJ, Swen JJ, Gelderblom H, Cats A, Guchelaar HJ, Schellens JHM. DPYD genotype-guided dose individualisation of fluoropyrimidine therapy in patients with cancer: a prospective safety analysis. *Lancet Oncol* 2018; **19**: 1459-1467 [PMID: 30348537 DOI: 10.1016/S1470-2045(18)30686-7]

14 **Amstutz U**, Henricks LM, Offer SM, Barbarino J, Schellens JHM, Swen JJ, Klein TE, McLeod HL, Caudle KE, Diasio RB, Schwab M. Clinical Pharmacogenetics Implementation Consortium (CPIC) Guideline for Dihydropyrimidine Dehydrogenase Genotype and Fluoropyrimidine Dosing: 2017 Update. *Clin Pharmacol Ther* 2018; **103**: 210-216 [PMID: 29152729 DOI: 10.1002/cpt.911]

15 **Cockcroft DW**, Gault MH. Prediction of creatinine clearance from serum creatinine. *Nephron* 1976; **16**: 31-41 [PMID: 1244564 DOI: 10.1159/000180580]

16 **de With M**, Sadlon A, Cecchin E, Haufroid V, Thomas F, Joerger M, van Schaik RHN, Mathijssen RHJ, Largiadèr CR; 'The Working Group on the Implementation of DPD-deficiency Testing in Europe'. Implementation of dihydropyrimidine dehydrogenase deficiency testing in Europe. *ESMO Open* 2023; **8**: 101197 [PMID: 36989883 DOI: 10.1016/j.esmoop.2023.101197]

17 **Miarons M**, Manzaneque Gordón A, Riera P, Gutiérrez Nicolás F; RedDPYD Research Group with the Spanish Society of Hospital Pharmacy (SEFH). Allelic Frequency of DPYD Genetic Variants in Patients With Cancer in Spain: The PhotoDPYD Study. *Oncologist* 2023; **28**: e304-e308 [PMID: 37014829 DOI: 10.1093/oncolo/oyad077]

18 **Paulsen NH**, Qvortrup C, Vojdeman FJ, Plomgaard P, Andersen SE, Ramlov A, Bertelsen B, Rossing M, Nielsen CG, Hoffmann-Lücke E, Greibe E, Spangsberg Holm H, Nielsen HH, Lolas IBY, Madsen JS, Bergmann ML, Mørk M, Fruekilde PBN, Bøttger P, Petersen PC, Nissen PH, Feddersen S, Bergmann TK, Pfeiffer P, Damkier P. Dihydropyrimidine dehydrogenase (DPD) genotype and phenotype among Danish cancer patients: prevalence and correlation between DPYD-genotype variants and P-uracil concentrations. *Acta Oncol* 2022; **61**: 1400-1405 [PMID: 36256873 DOI: 10.1080/0284186X.2022.2132117]

19 **Pallet N**, Hamdane S, Garinet S, Blons H, Zaanan A, Paillaud E, Taieb J, Laprevote O, Loriot MA, Narjoz C. A comprehensive population-based study comparing the phenotype and genotype in a pretherapeutic screen of dihydropyrimidine dehydrogenase deficiency. *Br J Cancer* 2020; **123**: 811-818 [PMID: 32595208 DOI: 10.1038/s41416-020-0962-z]

20 **Ruzzo A**, Graziano F, Galli F, Galli F, Rulli E, Lonardi S, Ronzoni M, Massidda B, Zagonel V, Pella N, Mucciarini C, Labianca R, Ionta MT, Bagaloni I, Veltri E, Sozzi P, Barni S, Ricci V, Foltran L, Nicolini M, Biondi E, Bramati A, Turci D, Lazzarelli S, Verusio C, Bergamo F, Sobrero A, Frontini L, Menghi M, Magnani M. Dihydropyrimidine dehydrogenase pharmacogenetics for predicting fluoropyrimidine-related toxicity in the randomised, phase III adjuvant TOSCA trial in high-risk colon cancer patients. *Br J Cancer* 2017; **117**: 1269-1277 [PMID: 29065426 DOI: 10.1038/bjc.2017.289]

21 **Cremolini C**, Del Re M, Antoniotti C, Lonardi S, Bergamo F, Loupakis F, Borelli B, Marmorino F, Citi V, Cortesi E, Moretto R, Ronzoni M, Tomasello G, Zaniboni A, Racca P, Buonadonna A, Allegrini G, Ricci V, Di Donato S, Zagonel V, Boni L, Falcone A, Danesi R. DPYD and UGT1A1 genotyping to predict adverse events during first-line FOLFIRI or FOLFOXIRI plus bevacizumab in metastatic colorectal cancer. *Oncotarget* 2018; **9**: 7859-7866 [PMID: 29487697 DOI: 10.18632/oncotarget.23559]

22 **Cardone C**, Facchini S, Collina F, Brogna M, Daniele A, Casaretti R, Cassata A, De Stefano A, Nappi A, Foschini F, Silvestro L, Romano C, Zanaletti N, Tatangelo F, De Franciscis S, Belli A, Izzo F, Ferrara G, Delrio P, Avallone A. 1753P Universal DPYD genotyping in patients with gastrointestinal malignancies: Real-world data from a single institution in Italy. *Ann Oncol* 2023; **34**: S948-S949 [DOI: 10.1016/j.annonc.2023.09.2707]

World Journal of Gastrointestinal Oncology

Submit a Manuscript: https://www.f6publishing.com

World J Gastrointest Oncol 2025 January 15; 17(1): 98725

DOI: 10.4251/wjgo.v17.i1.98725

ISSN 1948-5204 (online)

ORIGINAL ARTICLE

Retrospective Study

Coagulation indices and fibrinogen degradation products as predictive biomarkers for tumor-node-metastasis staging and metastasis in gastric cancer

Yi-Qing Shen, Qiu-Wan Wei, Yi-Ren Tian, Yun-Zhi Ling, Min Zhang

Specialty type: Gastroenterology and hepatology

Provenance and peer review: Unsolicited article; Externally peer reviewed.

Peer-review model: Single blind

Peer-review report's classification

Scientific Quality: Grade B, Grade C

Novelty: Grade B, Grade B

Creativity or Innovation: Grade B, Grade C

Scientific Significance: Grade C, Grade C

P-Reviewer: Park CH; Pourbagher-Shahri AM

Received: August 28, 2024

Revised: September 30, 2024

Accepted: November 1, 2024

Published online: January 15, 2025

Processing time: 106 Days and 0.8 Hours

Yi-Qing Shen, Qiu-Wan Wei, Yi-Ren Tian, Yun-Zhi Ling, Clinical Laboratory, Civil Aviation Shanghai Hospital, Gubei Branch of Ruijin Hospital Affiliated to Shanghai Jiao Tong University School of Medicine, Shanghai 200000, China

Min Zhang, Clinical Laboratory, Tongji Hospital of Tongji University, Shanghai 200000, China

Co-corresponding authors: Yun-Zhi Ling and Min Zhang.

Corresponding author: Yun-Zhi Ling, MM, Technician, Clinical Laboratory, Civil Aviation Shanghai Hospital, Gubei Branch of Ruijin Hospital Affiliated to Shanghai Jiao Tong University School of Medicine, No. 398 Hongbaoshi Road, Changning District, Shanghai 200000, China. lyz19840126@163.com

Abstract

BACKGROUND

Gastric cancer (GC) is a prevalent malignancy with a substantial health burden and high mortality rate, despite advances in prevention, early detection, and treatment. Compared with the global average, Asia, notably China, reports disproportionately high GC incidences. The disease often progresses asymptomatically in the early stages, leading to delayed diagnosis and compromised outcomes. Thus, it is crucial to identify early diagnostic biomarkers and enhance treatment strategies to improve patient outcomes and reduce mortality.

AIM

To investigate coagulation and fibrinogen products in GC tumor-node-metastasis (TNM) stage and metastasis correlation.

METHODS

Retrospectively analyzed the clinical data of 148 patients with GC treated at the Civil Aviation Shanghai Hospital between December 2022 and December 2023. The associations of coagulation indices - partial thromboplastin time (APTT), prothrombin time (PT), thrombin time (TT), fibrinogen, fibrinogen degradation products (FDP), fasting blood glucose, and D-dimer (D-D) with TNM stage and distant metastasis were examined.

RESULTS
Prolongation of APTT, PT, and TT was significantly correlated with the GC TNM stage. Hence, abnormal coagulation system activation was closely related to disease progression. Elevated FDP and D-D were significantly associated with distant metastasis in GC ($P < 0.05$), suggesting that increased fibrinolytic activity contributes to increased metastatic risk.

CONCLUSION
Our Results reveal coagulation indices, FDPs as GC biomarkers, reflecting abnormal coagulation/fibrinolysis, aiding disease progression, metastasis prediction, and helping clinicians assess thrombotic risk for early intervention and personalized treatment plans.

Key Words: Coagulation indexes; Fibrinogen degradation products; Gastric cancer; Tumor-node-metastasis staging; Distant metastasis

Core Tip: Coagulation indices (associations of coagulation indices - partial thromboplastin time, prothrombin time, thrombin time) and fibrinogen degradation products (FDP and D-dimer) are significantly correlated with tumor-node-metastasis stage and distant metastasis in gastric cancer. These biomarkers are indicative of abnormal coagulation and fibrinolytic states and provide essential insights into disease progression. Understanding these associations will enhance diagnostic precision and facilitate the development of personalized treatment strategies for patients with gastric cancer.

Citation: Shen YQ, Wei QW, Tian YR, Ling YZ, Zhang M. Coagulation indices and fibrinogen degradation products as predictive biomarkers for tumor-node-metastasis staging and metastasis in gastric cancer. *World J Gastrointest Oncol* 2025; 17(1): 98725
URL: https://www.wjgnet.com/1948-5204/full/v17/i1/98725.htm
DOI: https://dx.doi.org/10.4251/wjgo.v17.i1.98725

INTRODUCTION

Gastric cancer (GC), a gastrointestinal cancer with a high global incidence, poses a crucial health challenge worldwide[1-3]. China is one of the countries with the highest incidence of GC globally, accounting for approximately 50% of GC cases [4]. In China, GC is the second most common cancer in men and the third most common cancer in women. Furthermore, its mortality rate is the second highest among cancer-related deaths worldwide[5].

Owing to the lack of specific clinical symptoms, signs, and highly sensitive diagnostic methods in the early stages of GC, metastatic tendencies and microscopic metastatic lesions cannot be detected in a timely manner. Hence, most patients are diagnosed at advanced or locally advanced stages, which is the optimal time to undergo radical surgery. However, advanced GC is typically accompanied by metastases from other sites, adding significant complexity and challenges to clinical treatment[6]. Therefore, early diagnosis and preoperative risk assessment are the key issues in GC management.

Clinically, it has been found that prothrombin time (PT), partial thromboplastin time (APTT), FBG, D-dimer (D-D), and antithrombin-III (AT-III) are of great significance for evaluating the risk of thrombosis in patients and guiding treatment. At present, the relationship between coagulation index and cancer progression is not clear, which may involve various pathophysiological mechanisms. Tumor cells can disrupt the dynamic balance of the coagulation-fibrinolytic system *via* multiple pathways, affecting coagulation and anticoagulation, thereby leading to abnormalities in coagulation functions in patients. Tumors, especially those with concurrent hyperfibrinogenemia, often exhibit a hyperfibrinolytic system and a hypercoagulable state[7]. Blood hypercoagulability is a pathological state in which blood is highly susceptible to clotting due to an imbalance in the coagulation, hemostasis, anticoagulation, and fibrinolytic systems caused by various factors [8]. The hypercoagulable state in patients with malignant tumors is multifactorial and includes direct expression of tissue factors and tumor procoagulant proteins, alterations in the fibrinolytic system, cytokine secretion, vascular endothelial growth factor release, and endothelial cell damage due to tumor-cell-blood-cell interactions[9]. Collectively, these mechanisms result in abnormal coagulation and elevated FBG levels. In this study, APTT, PT, and TT levels were significantly correlated with tumor-node-metastasis (TNM) stage and distant metastasis in patients with GC. PT primarily reflects the common pathway of the coagulation cascade and the exogenous coagulation pathway, whereas APTT primarily reflects the common pathway of the coagulation cascade and the endogenous coagulation pathway. TT primarily reflects FBG conversion to fibrin[10].

Coagulation activation may cause thrombosis and promote tumor growth and metastasis through various mechanisms. GC is often associated with varying degrees of coagulation abnormalities, including hyperfibrinolysis and hypercoagulable states[11]. The mechanisms by which GC leads to abnormal coagulation indices are multifaceted. Tumor cells release procoagulant substances, such as tissue factors and cancer procoagulants, which can directly activate the coagulation system and lead to blood coagulation. In addition, GC cells can also promote intravascular coagulation by interacting with and activating platelets and enhancing their adhesion ability. This triggers a hypercoagulable state,

which not only increases the risk of thrombosis but also accelerates tumor progression and metastasis and may also affect the therapeutic strategy and prognosis. Collectively, these mechanisms result in abnormal coagulation and elevated FBG levels.

For patients with advanced GC, anticoagulant therapy may help to improve hypercoagulability, reduce tumor metastasis, and possibly improve patient survival. The study aims to delve deeper into these mechanisms and explore the specific ways in which coagulation indices and fibrinogen degradation products (FDP) interact with the TNM stage and distant metastasis. Unlike previous studies that may have focused on individual coagulation factors or limited aspects of the disease, adopting a comprehensive approach to analyze multiple coagulation indices simultaneously. This study is of great significance for optimizing diagnostic methods and developing individualized treatment plans.

MATERIALS AND METHODS

General information

A retrospective analysis was performed to select 148 patients with GC who were treated at the Civil Aviation Shanghai Hospital from December 2022 to December 2023, and general data and clinical indices of the patients were collected. The inclusion criteria were as follows: (1) Initial pathological diagnosis of primary GC; and (2) No previous history of radiotherapy. Exclusion criteria were as follows: (1) Previous history of other tumors; (2) A combination of functional coagulation diseases or the use of coagulation drugs in the last six months; and (3) A combination of multiple organ functional disorders. This study was reviewed and approved by the Institutional Review Board of the Civil Aviation Shanghai Hospital.

Observation indices

General data, past medical history, and clinical indicators of patients were collected. Gastroscopy was performed to examine the tumor sites, including the cardia, fundus, gastric body, gastric sinus, pylorus, and whole stomach. In the early morning of the preoperative period, 2 mL of venous blood was collected from patients on an empty stomach. Electrochemical hemagglutination analyzer (Model: OGE-101, manufacturer: Hunan Wandeshan Biotechnology Co., LTD.) for the detection of PT, APTT, TT, AT-III, D-D, FDP, and FBG. TNM staging was performed according to the eighth edition of the American Joint Committee on Cancer GC staging criteria[12]. GC was divided into stages I, II, III, and IV: T stage: Unknown (Tx), carcinoma in situ (Tis), submucosal (T1), intrinsic muscular layer (T2), plasma layer (T3), and extra-plasma membrane (T4). N stage: Unknown (Nx), none (N0), 1-2 (N1), 3-6 (N2), 7 or more (N3). M stage: Unknown (Mx), absent (M0), and present (M1).

Statistical analysis

Statistical software SPSS26.0 was used for statistical analysis. When the data were normally distributed, the mean standard deviation (mean ± SD) was used to represent the measurement data. An independent samples *t*-test was used for analysis between groups, whereas one-way ANOVA test was used for comparison between multiple groups. The sample size (percentage) [*n* (%)] indicated the counting data, and χ^2 test was used for the analysis of one-way factors. Pearson's correlation analysis was used for the normally distributed data. For multivariate analyses, a logistic regression model was used to adjust for potential confounders, such as age, sex, and comorbidities. To assess the correlation between TNM stages and coagulation and FDP, as well as the correlation of distant metastasis with these factors, Pearson's correlation analysis was used. The correlation coefficients (*r*) and corresponding *P* values were calculated to determine the strength and significance of the correlations. A logistic regression model was built, including variables such as age, sex, and comorbidities, to adjust for their effects on the relationship between coagulation indices, FDP, TNM stage, and distant metastasis. The results of the multivariate analysis were presented as odds ratios (ORs) with 95%CI. All differences were considered statistically significant at $P < 0.05$.

RESULTS

Baseline information

In this study, 148 patients with primary GC were included and were diagnosed at the following stages: 13 with TNM stage I, 38 with stage II, 40 with stage III, 57 with stage IV, and 57 with distant metastasis, with a distant metastasis rate of 38.51%. No statistically significant difference was noted between the baseline data of patients with GC with and without distant metastases ($P < 0.05$; Table 1).

Comparison of TNM staging with coagulation function and FDP

There was no significant difference in APTT and PT time between the two groups ($P > 0.05$). TT time did not differ significantly between patients with TNM stage I and those with TNM stages II and III ($P > 0.05$). In contrast, the four groups of GC patients with different TNM stages exhibited statistically significant differences in coagulation function APTT ($F = 11.626$, $P < 0.001$), PT ($F = 14.733$, $P < 0.001$), and TT time ($F = 7.991$, $P < 0.001$). No significant difference was observed between AT-III and TNM stages ($F = 1.346$, $P = 0.736 > 0.05$), as illustrated in Figure 1.

Table 1 Comparison of baseline data of patients with gastric cancer, *n* (%)

Group		Metastases (*n* = 57)	Absence of metastases (*n* = 91)	t/χ^2	*P* value
Age (years), mean ± SD		48.61 ± 12.99	48.39 ± 12.16	0.110	0.912
Sex	Male	30 (52.63)	44 (48.35)	0.287	0.591
	Female	27 (47.37)	47 (51.65)		
BMI (kg/m^2), mean ± SD		22.61 ± 2.13	22.42 ± 2.25	0.236	0.814
A family history of malignancy		3 (5.26)	5 (5.49)	0.004	0.952
Present with hypertension		7 (12.28)	12 (13.19)	0.026	0.873
Hyperglycemia		4 (7.02)	10 (10.99)	0.641	0.423
Hyperlipidemia		5 (8.77)	8 (8.79)	< 0.001	0.997
History of alcohol use		12 (19.30)	16 (17.58)	0.273	0.601
Endoscopic tumor site	Cardia (of stomach)	8 (14.04)	17 (18.68)	4.830	0.395
	Fundus of stomach	7 (12.28)	10 (10.99)		
	Body of stomach	12 (21.05)	16 (17.58)		
	Antrum of stomach	26 (45.61)	47 (51.65)		
	Pylorus	2 (3.51)	1 (1.10)		
	Whole stomach	2 (3.51)	0 (0.00)		
^{14}C-urea breath test	Masculine	48 (84.21)	72 (79.12)	0.592	0.442
	Feminine character	9 (15.79)	19 (20.88)		

BMI: Body mass index.

In patients with TNM stages I and II, there was no significant difference between the D-D groups ($P > 0.05$). Furthermore, there was no significant difference between FBG and FDP groups in patients with TNM stage II and III ($P > 0.05$). However, there were statistically significant differences in fibrin and FDP FBG ($F = 6.892$, $P < 0.001$), D-D ($F = 19.836$, $P < 0.001$), and FDP ($F = 177.027$, $P < 0.001$) among the four groups of GC patients with different TNM stages ($P < 0.001$), as shown in Figure 2.

Comparison of the presence or absence of distant metastases with coagulation function and FDP

(APTT, PT, and TT time) between patients with GC at different TNM stages ($P < 0.001$). No significant differences were observed between AT-III and TNM stages ($P = 0.050$), as shown in Figure 3. However, statistically significant differences were observed in fibrin and FDP (FBG, D-D, and FDP) between groups of patients with GC with different TNM stages ($P < 0.001$; Figure 4).

Correlation between TNM stages and coagulation and FDP

A significant positive correlation was observed between APTT, PT, TT, FDP, D-D, FBG, and TNM in patients with GC ($P < 0.001$); however, no significant positive correlation was observed between AT-III and TNM ($P = 0.062$), as shown in Table 2.

Correlation of distant metastasis with coagulation function and FDP

A significant positive correlation was observed between APTT, PT, TT, FDP, D-D, and FBG and the onset of distant metastasis in patients with GC ($P < 0.05$), whereas no significant positive correlation was observed between AT-III and the onset of distant metastasis ($P > 0.05$), as shown in Table 3.

DISCUSSION

Clinically, APTT, PT, TT, and AT-III are commonly used coagulation indices that reflect a patient's coagulation status to a certain extent[13]. The HYPERCAN study conducted in Italy highlighted the importance of hypercoagulation screening as an innovative tool for assessing cancer risk, early diagnosis, and prognosis prediction[14]. Abnormal coagulation contributes to maintaining a hypercoagulable state in the body, increasing the risk of thrombosis, which can lead to tumor cell migration, invasion, and lymph node metastasis[15]. This not only exacerbates the condition of a patient but also increases the likelihood of complications, thereby intensifying the patient's suffering. FDP is a collective term used for various degradation fragments and complexes formed by fibrin breakdown under the action of fibrinolytic enzymes. It is

Table 2 Analysis of the correlation of tumor node metastasis stage with coagulation function and fibrinogen degradation products

Index	APTT		PT		TT		AT-III		FDP		D-D		FBG	
	r	*P* value	*r*	*P* value	*r*	*P* value	*r*	*P* value	*r*	*P* value	*r*	*P* value	*r*	*P* value
TNM staging	0.368	< 0.001	0.437	< 0.001	0.373	< 0.001	0.162	0.050	0.780	< 0.001	0.530	< 0.001	0.329	< 0.001

APTT: Activated partial thromboplastin time; AT-III: Antithrombin III; TT: Thrombin time; PT: Prothrombin time; TNM: Tumor node metastasis; D-D: D-Dimer; FBG: Fibrinogen; FDP: Fibrinogen degradation product.

Table 3 Analysis of the correlation of distant metastasis with coagulation function and fibrinogen degradation products

Index	APTT		PT		TT		AT-III		FDP		D-D		FBG	
	r	*P* value	*r*	*P* value	*r*	*P* value	*r*	*P* value	*r*	*P* value	*r*	*P* value	*r*	*P* value
Distant metastasis of gastric cancer	0.330	< 0.001	0.451	< 0.001	0.335	< 0.001	0.154	0.062	0.883	< 0.001	0.471	< 0.001	0.316	< 0.001

APTT: Activated partial thromboplastin time; AT-III: Antithrombin III; TT: Thrombin time; PT: Prothrombin time; TNM: Tumor node metastasis; D-D: D-Dimer; FBG: Fibrinogen; FDP: Fibrinogen degradation product.

used to assess the activity of the fibrinolytic system of the body and is often measured in conjunction with D-D levels to collectively reflect the state of the coagulation and fibrinolytic systems[16]. Previous studies have found that the progression of endometrial cancer and breast cancer is related to coagulation indexes[17,18]. Research examining the correlation between the TNM stage, distant metastasis, and coagulation indices in patients with GC is limited. This study investigated the correlation of coagulation indexes and FDP with TNM stage and distant metastasis in GC patients, aiming to provide theoretical basis for clinical identification of high-risk patients. Abnormal coagulation parameters (APTT, PT, TT) and FDP were significantly associated with an increased risk of late and distant metastasis of TNM ($P < 0.05$). The results of this study suggest that these indicators not only reflect dysregulation of the coagulation and fibrinolysis systems but also provide insights into disease progression and prognosis in patients with GC. One possible factor is inflammation; Inflammatory processes often accompany cancer and can activate the clotting system. Tumor cells can release inflammatory cytokines that stimulate the expression of tissue factors and other pro-coagulant molecules, resulting in an imbalance of the clotting and fibrinolytic systems. At the same time, inflammation damages the endothelium of blood vessels, further promoting clotting. Another aspect to consider is the immune response; The immune system plays a complex role in the development of cancer and can interact with the clotting system. Immune cells can release mediators that affect blood clotting, and changes in the clotting system can also affect immune cell function. Hypercoagulation may impair the transport and function of immune cells, creating a favorable environment for tumor growth and metastasis.

Changes in coagulation indices, such as APTT, PT, and TT, in patients with GC reflect an imbalance in the coagulation and fibrinolytic systems. GC cells release tissue factors that activate both endogenous and exogenous coagulation pathways, leading to prolonged APTT and PT, indicating abnormal activation of the coagulation system[19]. Meanwhile, the hyperfibrinolytic system increases FDP, exacerbating blood hypercoagulability and thrombosis risk[20]. Additionally, advanced GC is often accompanied by liver function impairment, impacting coagulation factor synthesis and worsening abnormal coagulation function[21]. These changes are closely related to the clinical stage and prognosis of GC and may promote hematogenous tumor cell metastasis, constituting a high-risk state for thrombosis. Therefore, APTT, PT, and TT are crucial biomarkers that can be used to assess the risk of thrombosis in patients with GC and guide personalized treatment strategies.

Xing *et al*[22] demonstrated that FBG levels ≥ 3.495 g/L are an independent risk factor for primary stage I-II GC. During infiltration and metastasis, malignant tumor cells contribute to excessive tissue factor release, coagulation system activation, and thrombin generation. This process converts FBG into fibrin, thereby inducing a hypercoagulable state and increasing the risk[14].

Ji *et al*[23] reported elevated levels of FDP in patients with GC. Patients with a disease in stages III-IV disease exhibited higher FDP levels than those with stage I-II disease, and a combined analysis using four or six indicators showed enhanced diagnostic sensitivity and specificity, consistent with our findings. In our study, FBG, D-D, and FDP levels in patients with GC significantly correlated with TNM stage and distant metastasis. GC progression often involves abnormal activation of the coagulation system, which increases the risk of thrombosis. Elevated FBG levels indicate enhanced coagulation activity, likely due to the tumor-induced secretion of FBG activators by vascular endothelial cells, stimulating the increased synthesis of FBG and fibrin degradation products. Elevated FBG levels promote tumor cell adhesion to the vascular endothelium, facilitating metastasis[24]. Increased FDP levels may reflect hyperfibrinolytic activity, with D-D serving as a specific indicator of FBG degradation, which is crucial for assessing coagulation status and identifying hypercoagulability and thrombosis[25]. Patients with malignant tumors typically exhibit elevated fibrinolytic enzyme levels, and tumor cells secrete significant FBG activators[26]. Abnormal levels of these indicators correlate with

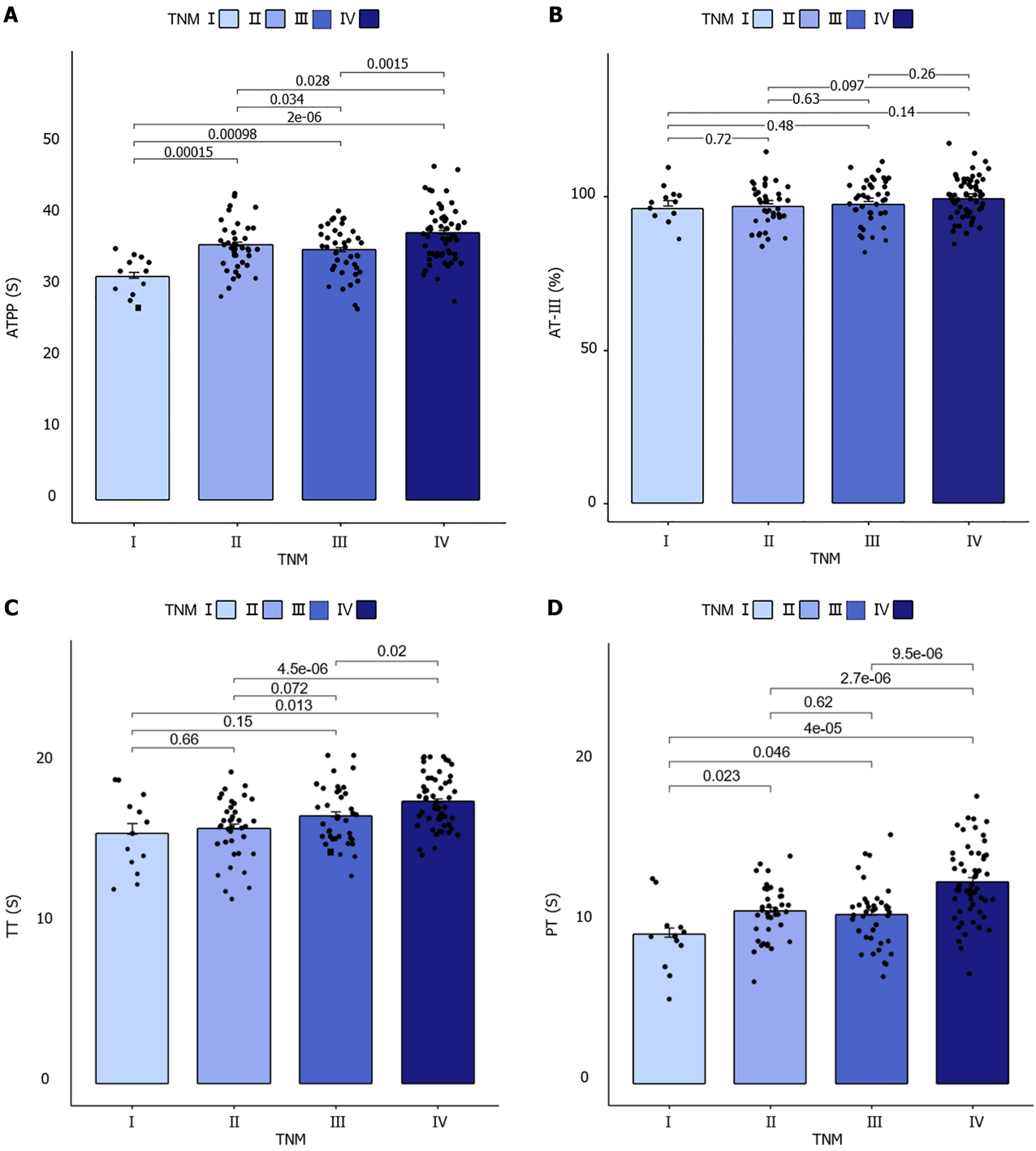

Figure 1 Comparison of tumor node metastasis staging and coagulation function. A: Comparison of activated partial thromboplastin times in patients with different tumor node metastasis (TNM) stages; B: Comparison of Antithrombin-III in patients with different TNM stages; C: Comparison of thrombin times in patients with different TNM stages; D: Comparison of prothrombin time in patients with different TNM stages. APTT: Activated partial thromboplastin time; AT-III: Antithrombin III; TT: Thrombin time; PT: Prothrombin time; TNM: Tumor node metastasis.

increased tumor burden and invasiveness and are closely aligned with the pathobiological characteristics of GC and its impact on host blood environments. Therefore, FBG, D-D, and FDP serve not only as essential blood biochemical markers for coagulation abnormalities in GC patients with GC but also provide a robust biological foundation for disease staging and prognosis assessment. This study's limitations include: First, the retrospective study design may introduce inherent biases, including selective bias and the possibility of difficulty in establishing a causal relationship between abnormal coagulation and GC disease outcomes. Second, being a single-center study limits the generalization of the findings to a wider population with different demographic characteristics and treatment options. In addition, while the sample size was sufficient to detect a significant association, future studies are needed with larger, multicentre studies to verify applicability across different GC patient populations and in different healthcare Settings. Despite these limitations, the findings have important implications for future clinical practice and research. The correlation of coagulation markers and fibrin degradation product levels with TNM staging and remote metastasis observed in this study suggests that these

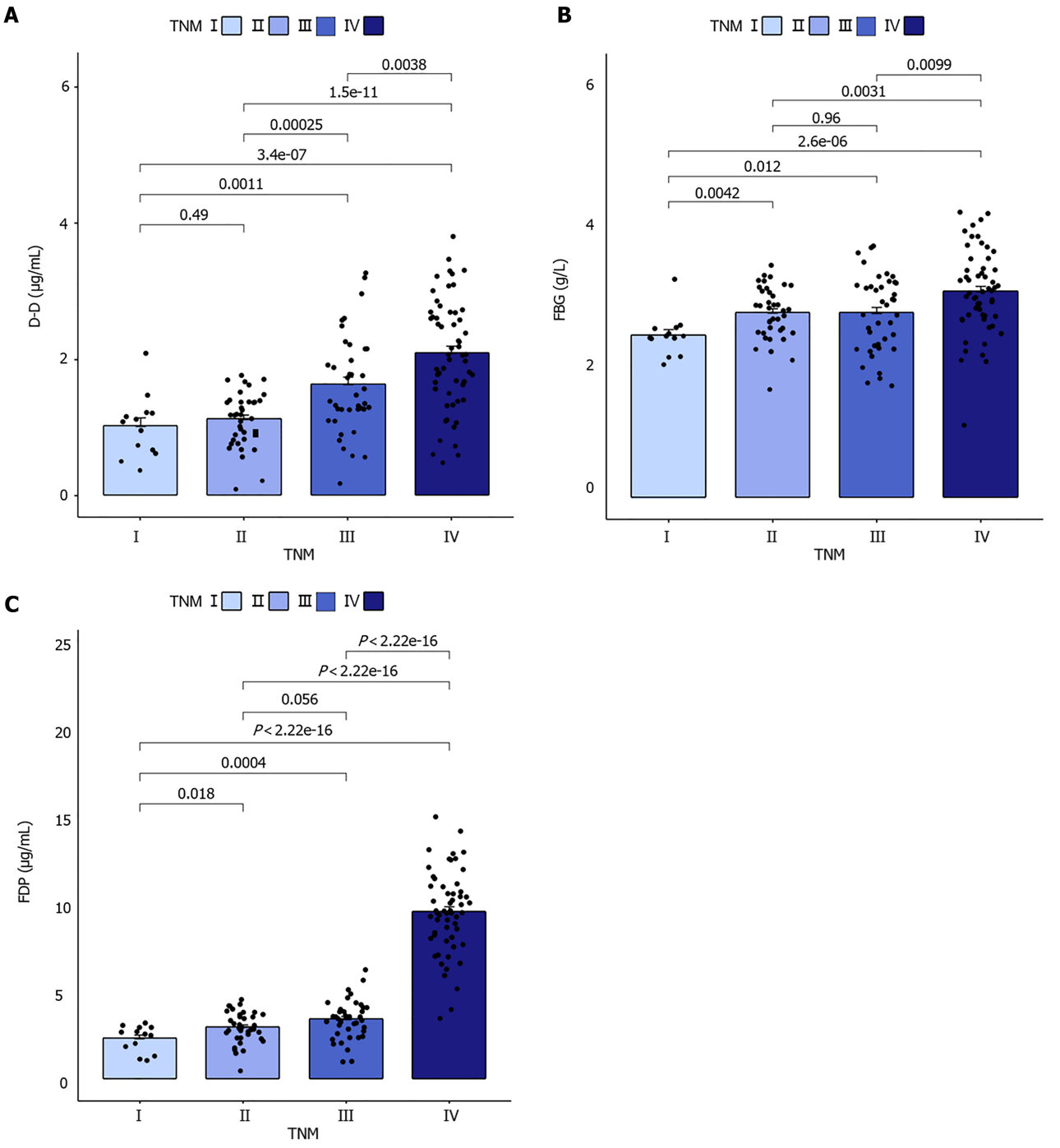

Figure 2 Comparison of tumor node metastasis staging and fibrinogen degradation products. A: A comparison of D-Dimer in patients with different tumor node metastasis (TNM) stages; B: Comparison of fibrinogen in patients with different TNM stages; C: Comparison of fibrinogen degradation products in patients with different TNM stages. D-D: D-Dimer; FBG: Fibrinogen; FDP: Fibrinogen degradation product; TNM: Tumor node metastasis.

biomarkers may be valuable prognostic indicators for GC. Integrating clotting measures with FDP measures into daily assessments helps stratify patients' risk and guide personalized treatment strategies, potentially improving patient outcomes. Future studies should focus on addressing the limitations of this study and investigating the mechanisms of coagulation abnormalities in GC patients, exploring how GC cells interact with the clotting and fibrinolysis system, paving the way for the development of targeted therapies and personalized medicine approaches. In addition, prospective multicenter studies should be conducted to validate the clinical utility of these biomarkers in different patient populations and treatment regimens.

CONCLUSION

In summary, coagulation function and indices were significantly associated with TNM staging and distant metastasis in

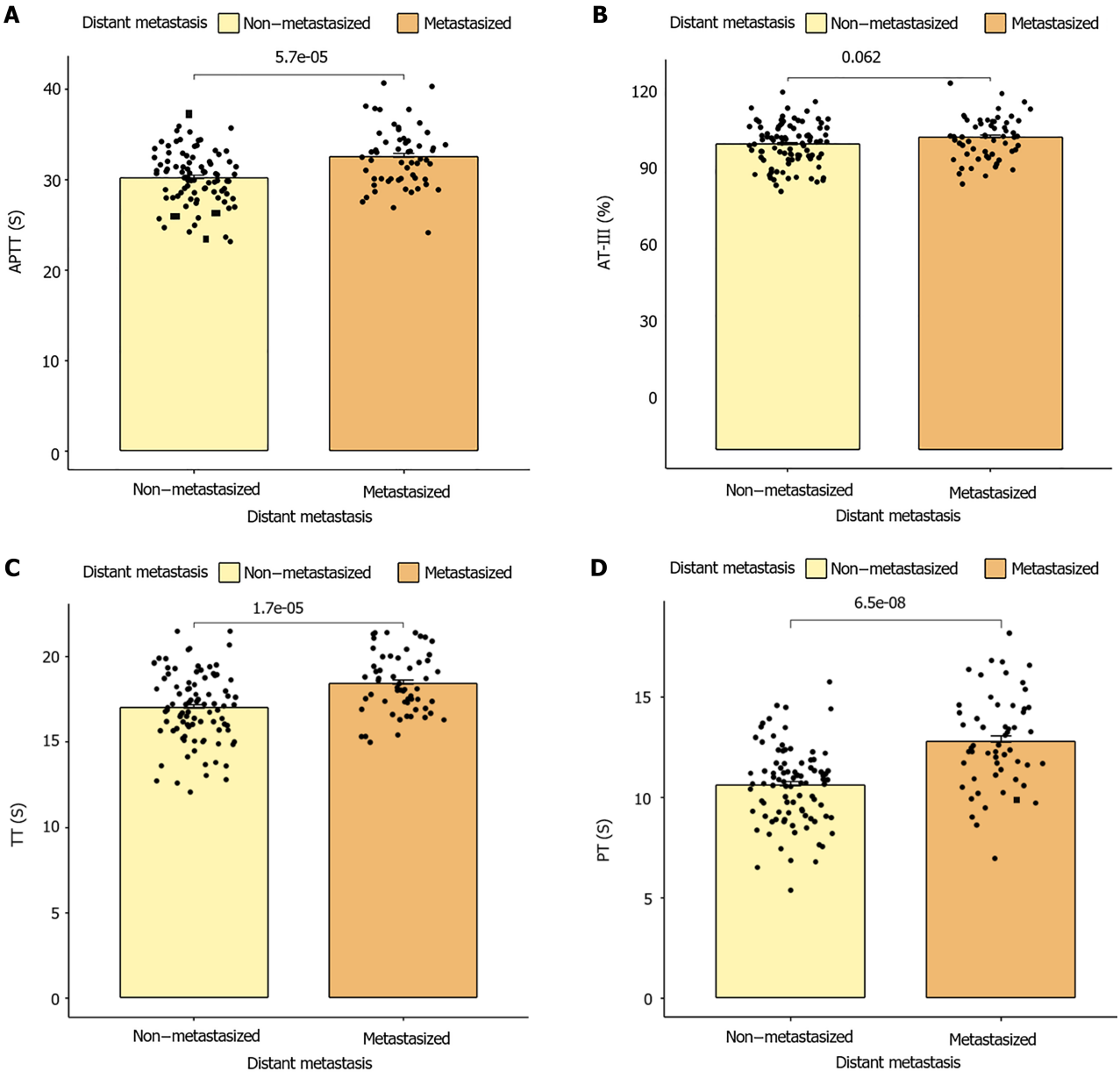

Figure 3 Comparison of distant metastasis and coagulation function. A: Comparison of activated partial thromboplastin time times in patients with or without distant metastasis; B: Comparison of antithrombin-III in patients with or without distant metastasis; C: Comparison of thrombin time times in patients with or without distant metastasis; D: Comparison of prothrombin time times in patients with or without distant metastasis. APTT: Activated partial thromboplastin time; AT-III: Antithrombin III; TT: Thrombin time; PT: Prothrombin time; TNM: Tumor node metastasis.

patients with GC. In clinical practice, coagulation indicators and FDP such as APTT, PT, TT, FDP, D-D, and FBG should be monitored as part of the routine examination of GC patients to gain a comprehensive understanding of the patient's condition and identify high-risk patients with disease progression and metastasis. This allows for early intervention and personalized treatment plans, which are integrated into diagnostic algorithms to improve the accuracy of disease staging and prognosis prediction. At the same time, GC patients should reasonably plan a healthy diet and regular exercise to reduce the risk of inflammation and improve blood clotting. In the future, it could help to develop guidelines for the use of clotting biomarkers in the diagnosis and treatment of GC, ensure consistent, evidence-based approaches in different healthcare settings, and conduct additional research to verify the applicability of these biomarkers in different GC patient populations and treatment regimens, and further explore their mechanisms of action. Prospective multi-center studies are conducted to further validate its clinical efficacy, explore its combination with other clinical indicators, and develop new therapeutic targets and personalized medicines based on a deeper understanding of the mechanism of blood coagulation abnormalities to improve treatment outcomes and quality of life in patients with GC.

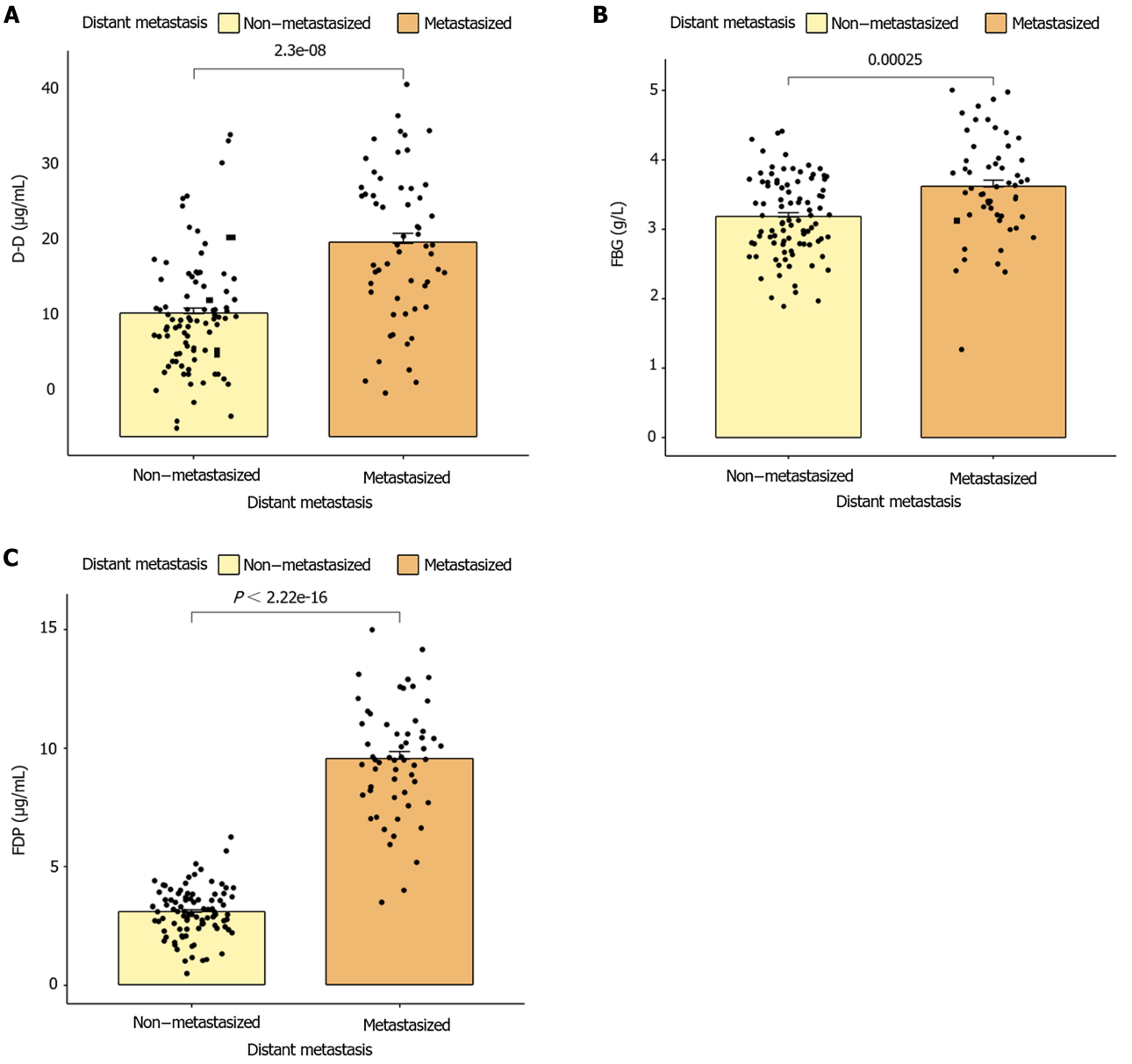

Figure 4 Comparison of distant metastasis and fibrinogen degradation products. A: Comparison of D-Dimer in patients with or without distant metastasis; B: Comparison of fibrinogen in patients with or without distant metastasis; C: Comparison of fibrinogen degradation product times in patients with or without distant metastasis. D-D: D-Dimer; FBG: Fibrinogen; FDP: Fibrinogen degradation product; TNM: Tumor node metastasis.

FOOTNOTES

Author contributions: Shen YQ wrote the manuscript, Wei QW and Tian YR collected and organized data, Ling YZ and Zhang M Designed this research and provided critical feedback on this study. Ling YZ and Zhang M contributed equally to this work and are the co-corresponding authors. First, the research was performed as a collaborative effort, and the designation of co-corresponding authorship accurately reflects the distribution of responsibilities and burdens associated with the time and effort required to complete the study and the resultant paper. This also ensures effective communication and management of post-submission matters, ultimately enhancing the paper's quality and reliability. Second, Ling YZ and Zhang M contributed efforts of equal substance throughout the research process. The choice of these researchers as co-corresponding authors acknowledges and respects this equal contribution, while recognizing the spirit of teamwork and collaboration of this study. In summary, we believe that designating Ling YZ and Zhang M as co-corresponding authors is fitting for our manuscript as it accurately reflects our team's collaborative spirit, equal contributions, and diversity.

Institutional review board statement: This study was reviewed and approved by the Institutional Review Board of the Civil Aviation Shanghai Hospital.

Informed consent statement: All study participants or their legal guardians provided written informed consent for personal and medical data collection before study enrolment.

Conflict-of-interest statement: All the authors report no relevant conflicts of interest for this article.

Data sharing statement: The data used in this study can be obtained from the corresponding author upon request at lyz19840126@163.com.

Country of origin: China

ORCID number: Yi-Qing Shen 0009-0007-2319-2120; Qiu-Wan Wei 0009-0000-8023-1420; Yi-Ren Tian 0009-0003-7386-9807; Yun-Zhi Ling 0009-0006-4934-2601; Min Zhang 0009-0003-2402-463X.

S-Editor: Li L
L-Editor: A
P-Editor: Yu HG

REFERENCES

1 **Smyth EC**, Nilsson M, Grabsch HI, van Grieken NC, Lordick F. Gastric cancer. *Lancet* 2020; **396**: 635-648 [PMID: 32861308 DOI: 10.1016/S0140-6736(20)31288-5]
2 **López MJ**, Carbajal J, Alfaro AL, Saravia LG, Zanabria D, Araujo JM, Quispe L, Zevallos A, Buleje JL, Cho CE, Sarmiento M, Pinto JA, Fajardo W. Characteristics of gastric cancer around the world. *Crit Rev Oncol Hematol* 2023; **181**: 103841 [PMID: 36240980 DOI: 10.1016/j.critrevonc.2022.103841]
3 **Petryszyn P**, Chapelle N, Matysiak-Budnik T. Gastric Cancer: Where Are We Heading? *Dig Dis* 2020; **38**: 280-285 [PMID: 32062657 DOI: 10.1159/000506509]
4 **Guan WL**, He Y, Xu RH. Gastric cancer treatment: recent progress and future perspectives. *J Hematol Oncol* 2023; **16**: 57 [PMID: 37245017 DOI: 10.1186/s13045-023-01451-3]
5 **Wang Z**, Han W, Xue F, Zhao Y, Wu P, Chen Y, Yang C, Gu W, Jiang J. Nationwide gastric cancer prevention in China, 2021-2035: a decision analysis on effect, affordability and cost-effectiveness optimisation. *Gut* 2022; **71**: 2391-2400 [PMID: 35902213 DOI: 10.1136/gutjnl-2021-325948]
6 **Xu H**, Li W. Early detection of gastric cancer in China: progress and opportunities. *Cancer Biol Med* 2022; **19**: 1622-1628 [PMID: 36514907 DOI: 10.20892/j.issn.2095-3941.2022.0655]
7 **Zhang L**, Qin S, Chen H, Hu Z, Li S. Diagnostic Values of the Prealbumin-to-Fibrinogen, Albumin-to-Fibrinogen, and Monocyte-to-Lymphocyte Ratios in Gastric Cancer. *Ann Clin Lab Sci* 2021; **51**: 385-392 [PMID: 34162569]
8 **Ding P**, Zheng C, Cao G, Gao Z, Lei Y, Deng P, Hou B, Li K. Combination of preoperative plasma fibrinogen and AJCC staging improves the accuracy of survival prediction for patients with stage I-II gastric cancer after curative gastrectomy. *Cancer Med* 2019; **8**: 2919-2929 [PMID: 31050218 DOI: 10.1002/cam4.2086]
9 **Liu X**, Shi B. Progress in research on the role of fibrinogen in lung cancer. *Open Life Sci* 2020; **15**: 326-330 [PMID: 33817221 DOI: 10.1515/biol-2020-0035]
10 **Wada H**, Shiraki K, Matsumoto T, Shimpo H, Shimaoka M. Clot Waveform Analysis for Hemostatic Abnormalities. *Ann Lab Med* 2023; **43**: 531-538 [PMID: 37387486 DOI: 10.3343/alm.2023.43.6.531]
11 **Repetto O**, De Re V. Coagulation and fibrinolysis in gastric cancer. *Ann N Y Acad Sci* 2017; **1404**: 27-48 [PMID: 28833193 DOI: 10.1111/nyas.13454]
12 **Lin JX**, Desiderio J, Lin JP, Wang W, Tu RH, Li P, Xie JW, Wang JB, Lu J, Chen QY, Cao LL, Lin M, Zheng CH, Zhou ZW, Parisi A, Huang CM. Multicenter Validation Study of the American Joint Commission on Cancer (8th Edition) for Gastric Cancer: Proposal for a Simplified and Improved TNM Staging System. *J Cancer* 2020; **11**: 3483-3491 [PMID: 32284744 DOI: 10.7150/jca.36891]
13 **Suzuki T**, Shimada H, Nanami T, Oshima Y, Yajima S, Ito M, Washizawa N, Kaneko H. Hyperfibrinogenemia is associated with inflammatory mediators and poor prognosis in patients with gastric cancer. *Surg Today* 2016; **46**: 1394-1401 [PMID: 27160890 DOI: 10.1007/s00595-016-1339-z]
14 **Nataraj A**, Govindan S, Ramani P, Subbaiah KA, Sathianarayanan S, Venkidasamy B, Thiruvengadam M, Rebezov M, Shariati MA, Lorenzo JM, Pateiro M. Antioxidant, Anti-Tumour, and Anticoagulant Activities of Polysaccharide from Calocybe indica (APK2). *Antioxidants (Basel)* 2022; **11**: 1694 [PMID: 36139769 DOI: 10.3390/antiox11091694]
15 **Hosoya Y**, Matsumura M, Madoiwa S, Zuiki T, Matsumoto S, Nunomiya S, Lefor A, Sata N, Yasuda Y. Acquired hemophilia A caused by factor VIII inhibitors: report of a case. *Surg Today* 2013; **43**: 670-674 [PMID: 22890583 DOI: 10.1007/s00595-012-0290-x]
16 **Chen L**, Lin J, Chen Y, Yu J, Wang X. Clinicopathologic features and prognosis of 71 patients with gastric cancer and disseminated intravascular coagulation. *PeerJ* 2023; **11**: e16527 [PMID: 38034872 DOI: 10.7717/peerj.16527]
17 **Wang Y**, Guan W, Zhang Y, Wang Y, Shi B, Liu J, Zhang S. Using heart rate variability to evaluate the association between the autonomic nervous system and coagulation function in patients with endometrial cancer. *Oncol Lett* 2024; **28**: 499 [PMID: 39211300 DOI: 10.3892/ol.2024.14632]
18 **Peng Q**, Zhu J, Ren X. Thromboelastogram and coagulation function index: relevance for female breast cancer. *Front Oncol* 2024; **14**: 1342439 [PMID: 39087022 DOI: 10.3389/fonc.2024.1342439]
19 **Zhang L**, Ye J, Luo Q, Kuang M, Mao M, Dai S, Wang X. Prediction of Poor Outcomes in Patients with Colorectal Cancer: Elevated Preoperative Prothrombin Time (PT) and Activated Partial Thromboplastin Time (APTT). *Cancer Manag Res* 2020; **12**: 5373-5384 [PMID: 32753955 DOI: 10.2147/CMAR.S246695]
20 **Zeng ZY**, Chen XS. [Impact of hemocoagulase on coagulatory function and deep venous thrombosis after abdominal surgery]. *Zhonghua Wei*

Chang Wai Ke Za Zhi 2012; **15**: 353-356 [PMID: 22539379]

21 **Stoencheva SS**, Popov VG, Grudeva-Popova ZG, Deneva TI. Markers of activation of coagulation in cancer patients. *Bratisl Lek Listy* 2023; **124**: 29-35 [PMID: 36519604 DOI: 10.4149/BLL_2023_004]

22 **Xing X**, Zhang Y, Wang Y, Li M. NLR in combination with plasma FIB and RDW is a useful predictor for the diagnosis of early gastric cancer. *Asian J Surg* 2023; **46**: 2219-2220 [PMID: 36509597 DOI: 10.1016/j.asjsur.2022.11.110]

23 **Ji Y**, Qin Y, Tan Q, Qiu Y, Han S, Qi X. Development of a chemiluminescence assay for tissue plasminogen activator inhibitor complex and its applicability to gastric cancer. *BMC Biotechnol* 2024; **24**: 30 [PMID: 38720310 DOI: 10.1186/s12896-024-00850-9]

24 **Ge W**, Zheng LM, Chen G. The Combination of Seven Preoperative Markers for Predicting Patients with Gastric Cancer to Be Either Stage IV or Non-Stage IV. *Gastroenterol Res Pract* 2018; **2018**: 3450981 [PMID: 29967637 DOI: 10.1155/2018/3450981]

25 **Zhang X**, Wang X, Li W, Dang C, Diao D. Effectiveness of managing suspected metastasis using plasma D-dimer testing in gastric cancer patients. *Am J Cancer Res* 2022; **12**: 1169-1178 [PMID: 35411224]

26 **Wu ZJ**, Xu H, Wang R, Bu LJ, Ning J, Hao JQ, Sun GP, Ma T. Cumulative Score Based on Preoperative Fibrinogen and Pre-albumin Could Predict Long-term Survival for Patients with Resectable Gastric Cancer. *J Cancer* 2019; **10**: 6244-6251 [PMID: 31772657 DOI: 10.7150/jca.35157]

World Journal of Gastrointestinal Oncology

Submit a Manuscript: https://www.f6publishing.com

World J Gastrointest Oncol 2025 January 15; 17(1): 99153

DOI: 10.4251/wjgo.v17.i1.99153

ISSN 1948-5204 (online)

ORIGINAL ARTICLE

Retrospective Study

Retrospective analysis of pathological types and imaging features in pancreatic cancer: A comprehensive study

Yang-Gang Luo, Mei Wu, Hong-Guang Chen

Specialty type: Oncology

Provenance and peer review: Unsolicited article; Externally peer reviewed.

Peer-review model: Single blind

Peer-review report's classification

Scientific Quality: Grade B, Grade C

Novelty: Grade B, Grade C

Creativity or Innovation: Grade B, Grade C

Scientific Significance: Grade B, Grade B

P-Reviewer: Tanaka S; Tawara S

Received: August 26, 2024

Revised: September 23, 2024

Accepted: October 15, 2024

Published online: January 15, 2025

Processing time: 108 Days and 0.8 Hours

Yang-Gang Luo, Mei Wu, Hong-Guang Chen, Pathology Department, Xuanhan County People's Hospital, Dazhou 636150, Sichuan Province, China

Corresponding author: Yang-Gang Luo, Associate Chief Physician, Department of Imaging, Xuanhan County People's Hospital, No. 579 Jiefang Middle Road, Dazhou 636150, Sichuan Province, China. lygxuanhan@163.com

Abstract

BACKGROUND

Pancreatic cancer remains one of the most lethal malignancies worldwide, with a poor prognosis often attributed to late diagnosis. Understanding the correlation between pathological type and imaging features is crucial for early detection and appropriate treatment planning.

AIM

To retrospectively analyze the relationship between different pathological types of pancreatic cancer and their corresponding imaging features.

METHODS

We retrospectively analyzed the data of 500 patients diagnosed with pancreatic cancer between January 2010 and December 2020 at our institution. Pathological types were determined by histopathological examination of the surgical specimens or biopsy samples. The imaging features were assessed using computed tomography, magnetic resonance imaging, and endoscopic ultrasound. Statistical analyses were performed to identify significant associations between pathological types and specific imaging characteristics.

RESULTS

There were 320 (64%) cases of pancreatic ductal adenocarcinoma, 75 (15%) of intraductal papillary mucinous neoplasms, 50 (10%) of neuroendocrine tumors, and 55 (11%) of other rare types. Distinct imaging features were identified in each pathological type. Pancreatic ductal adenocarcinoma typically presents as a hypodense mass with poorly defined borders on computed tomography, whereas intraductal papillary mucinous neoplasms present as characteristic cystic lesions with mural nodules. Neuroendocrine tumors often appear as hypervascular lesions in contrast-enhanced imaging. Statistical analysis revealed significant correlations between specific imaging features and pathological types ($P < 0.001$).

CONCLUSION
This study demonstrated a strong association between the pathological types of pancreatic cancer and imaging features. These findings can enhance the accuracy of noninvasive diagnosis and guide personalized treatment approaches.

Key Words: Pancreatic cancer; Pathological types; Imaging features; Retrospective analysis; Diagnostic accuracy

Core Tip: Understanding the correlation between the pathological types of pancreatic cancer and their corresponding imaging features is crucial for early detection and treatment planning. Different types of pancreatic cancers exhibit distinct imaging characteristics, such as hypodense masses with poorly defined borders for pancreatic ductal adenocarcinoma, cystic lesions with mural nodules for intraductal papillary mucinous neoplasm, and hypervascular lesions for neuroendocrine tumors. Utilization of a combination of computed tomography, magnetic resonance imaging, and endoscopic ultrasound can aid in an accurate diagnosis. This knowledge can significantly improve diagnostic accuracy, inform personalized treatment strategies, and potentially enhance outcomes in patients with pancreatic cancer.

Citation: Luo YG, Wu M, Chen HG. Retrospective analysis of pathological types and imaging features in pancreatic cancer: A comprehensive study. *World J Gastrointest Oncol* 2025; 17(1): 99153
URL: https://www.wjgnet.com/1948-5204/full/v17/i1/99153.htm
DOI: https://dx.doi.org/10.4251/wjgo.v17.i1.99153

INTRODUCTION

Pancreatic cancer is one of the most formidable challenges in oncology and is the seventh leading cause of cancer-related deaths globally[1]. Despite advancements in medical technologies and treatment modalities, the prognosis of pancreatic cancer remains poor, with a 5-year survival rate of only 9%[2]. This dismal outlook is largely attributed to late-stage diagnosis, when the cancer has often metastasized or has become locally advanced, limiting treatment options and efficacy[3].

The pancreas is a vital organ with both exocrine and endocrine functions. Various types of neoplasms can arise from the pancreas. Pancreatic ductal adenocarcinoma (PDAC) accounts for approximately 85%-90% of all pancreatic cancers, while other types such as intraductal papillary mucinous neoplasms (IPMN), neuroendocrine tumors (NET), and rarer forms constitute the remaining cases[4]. Each pathological type exhibits distinct biological behavior, clinical presentation, and response to treatment, underscoring the importance of accurate diagnosis for optimal patient management[5].

Imaging plays a pivotal role in the diagnosis, staging, and treatment planning of pancreatic cancer. Various imaging modalities, including computed tomography (CT), magnetic resonance imaging (MRI), and endoscopic ultrasound (EUS), have been used to visualize and characterize pancreatic lesions[6]. However, the interpretation of these imaging studies can be challenging owing to the complex anatomy of the pancreas and subtle differences in appearance among various pancreatic pathologies[7].

Recent studies have suggested that certain imaging features correlate with specific pathological types of pancreatic cancer. Yamada *et al*[8] reported that PDAC typically presents as a hypodense mass with irregular borders on CT, whereas IPMNs often appear as cystic lesions with mural nodules. Similarly, Jeon *et al*[9] found that NETs frequently demonstrate hypervascular enhancement on contrast-enhanced imaging. These observations suggest the potential for the noninvasive differentiation of pancreatic cancer types based on imaging characteristics.

Despite these promising findings, a comprehensive analysis of the relationship between the pathological types and imaging features of pancreatic cancer, encompassing a large patient cohort and multiple imaging modalities, is lacking. Such analysis could potentially enhance diagnostic accuracy, facilitate earlier detection, and inform personalized treatment strategies. The present study aimed to address this gap by conducting a retrospective analysis of 500 pancreatic cancer cases and correlating the pathological findings with imaging features observed on CT, MRI, and EUS.

MATERIALS AND METHODS

Study design and patient selection

This retrospective study was conducted at Xuanhan County People's Hospital, a tertiary referral center for pancreatic diseases in Sichuan Province, China. The study protocol was approved by the Institutional Review Board (No. 2021-LL-092), and the requirement for informed consent was waived due to the retrospective nature of the study.

We reviewed the medical records of patients diagnosed with pancreatic cancer between January 1, 2010 and December 31, 2020. The inclusion criteria were as follows: (1) Histopathologically confirmed diagnosis of pancreatic cancer; (2) Availability of pre-treatment CT, MRI, and EUS imaging studies; and (3) Age ≥ 18 years. Exclusion criteria included: (1) History of prior pancreatic surgery or neoadjuvant therapy; (2) Presence of other concurrent malignancies; and (3) Incomplete medical records or imaging studies. A total of 500 patients met these criteria and were included in the final analysis.

Pathological examination

All pathological specimens were obtained *via* surgical resection (n = 320) or image-guided biopsy (n = 180). Specimens were fixed in 10% neutral buffered formalin, embedded in paraffin, and sectioned at 4 μm thickness. All sections were stained with hematoxylin and eosin. Two experienced pathologists independently reviewed all the slides. Any discrepancies were resolved by consensus. Immunohistochemical staining was performed when necessary for a definitive diagnosis. The tumors were classified according to the World Health Organization Classification of Tumors of the Digestive System, 5th Edition (2019).

Imaging protocols

CT: All CT examinations were performed using a 64-slice multi-detector CT scanner. The scanning protocol was as follows: (1) Non-contrast phase; (2) Pancreatic parenchymal phase (40 seconds after contrast injection); and (3) Portal venous phase (70 seconds after contrast injection). Contrast medium (iohexol, 350 mg/mL) was administered intravenously at a rate of 3-4 mL/s, with the total volume based on body weight (1.5 mL/kg). The scanning parameters were as follows: 120 kVp, 150-300 mAs, a slice thickness of 3 mm, and a reconstruction interval of 2 mm.

MRI: MRI was performed using a 3.0 Tesla system (Ingenia Elition 3.0T; Philips Healthcare, Eindhoven, The Netherlands) with a phased-array body coil. The protocol included: (1) T1-weighted in-phase and out-of-phase sequences; (2) T2-weighted fast spin-echo sequences; (3) Diffusion-weighted imaging (b values: 0, 500, 1000 s/mm²); and (4) Dynamic contrast-enhanced T1-weighted 3D gradient-echo sequences (pre-contrast, arterial, portal venous, and delayed phases). A gadolinium-based contrast agent (gadoteridol, 0.1 mmol/kg) was administered intravenously at a rate of 2 mL/s.

EUS: Experienced endosonographers performed EUS (> 500 pancreatic EUS procedures each) using a linear array echoendoscope (Olympus GF-UCT180; Olympus Medical Systems Corp, Tokyo, Japan). B-mode imaging and color Doppler were used to evaluate pancreatic lesions. Fine-needle aspiration was performed as clinically indicated.

Image analysis

Two radiologists (Luo YG and Wu M, with 10 and 12 years of experience in abdominal imaging, respectively) independently reviewed all imaging studies and were blinded to the pathological diagnosis. Any disagreements were resolved by consensus. The following imaging features were assessed: (1) Tumor location (head/uncinate, body, tail); (2) Tumor size (maximum diameter in cm); (3) Tumor margin (well-defined, ill-defined); (4) Tumor density/signal intensity (compared to normal pancreatic parenchyma); (5) Enhancement pattern; (6) Presence of cystic components; (7) Main pancreatic duct dilatation; (8) Vascular invasion; (9) Lymph node involvement; and (10) Distant metastases. Additional MRI features, such as diffusion restriction and apparent diffusion coefficient were evaluated.

Statistical analysis

Statistical analysis was performed using SPSS software (version 25.0; IBM Corp., Armonk, NY, United States). Continuous variables are expressed as mean ± SD or median (interquartile range), depending on the distribution. Categorical variables are presented as frequencies and percentages. The normality of continuous variables was assessed using the Shapiro-Wilk test. For continuous variables with normal distribution, one-way analysis of variance (ANOVA) was used to compare differences among pathological types. For non-normally distributed continuous variables, the Kruskal-Wallis test was used. *Post hoc* analyses were performed using Tukey's HSD test for normally distributed variables and Dunn's test for non-normally distributed variables. The χ^2 test or Fisher's exact test was used to compare categorical variables between the different pathological types. To identify imaging features that were significantly associated with specific pathological types, multinomial logistic regression analysis was performed. The odds ratios (ORs) with 95% confidence intervals (CIs) were calculated.

Interobserver agreement for the assessment of imaging features was evaluated using the Cohen's kappa coefficient for categorical variables and the intraclass correlation coefficient for continuous variables. The strength of agreement was interpreted as follows: Poor (κ < 0.20), fair (κ = 0.21-0.40), moderate (κ = 0.41-0.60), substantial (κ = 0.61-0.80), and excellent (κ > 0.80). Statistical significance was set at P < 0.05 for all analyses. All statistical tests were two-tailed.

RESULTS

Patient demographics and clinical characteristics

In total, 500 patients with pancreatic cancer were included in this study. The mean age of the patients was 62.7 ± 11.3 years (range: 28-89 years), with a slight male predominance (54%, n = 270). The most common symptoms were abdominal pain (68%; n = 340), weight loss (52%; n = 260), and jaundice (35%; n = 175). Table 1 summarizes the baseline characteristics of the study population.

Table 1 Baseline characteristics of the study population

Characteristic	Value
Age (years), mean ± SD	62.7 ± 11.3
Gender, *n* (%)	
Male	270 (54)
Female	230 (46)
Presenting symptoms, *n* (%)	
Abdominal pain	340 (68)
Weight loss	260 (52)
Jaundice	175 (35)
Nausea/vomiting	125 (25)
Diabetes mellitus (new onset)	75 (15)

Distribution of pathological types

The distribution of pancreatic cancer types based on histopathological examination is shown in Table 2.

Imaging features associated with pathological types

PDAC: PDAC most commonly presents as a hypodense mass on CT and hypointense on T1-weighted MRI. The key imaging features are listed in Table 3.

IPMN: IPMN demonstrated distinct imaging features, as shown in Table 4. Of the 75 IPMN cases, 45 (60%) were classified as branch-duct type, 20 (26.7%) as main-duct type, and 10 (13.3%) as mixed-type. The mean size of the cystic lesions was 3.2 ± 1.5 cm (range: 1.0-7.5 cm). Mural nodules were present in 45 cases (60%), with a mean size of 5.3 ± 3.2 mm (range: 2-15 mm). Contrast enhancement of the mural nodules was observed in 41 patients (54.7%). Main pancreatic duct dilatation (> 5 mm) was noted in 49 cases (65.3%), with a mean duct diameter of 7.8 ± 3.5 mm (range: 5.5-22 mm).

NET: The characteristics of the NETs are summarized in Table 5. Among the 50 NET cases, 30 (60%) were classified as G1, 15 (30%) as G2, and 5 (10%) as G3, based on the World Health Organization 2017 grading system. The mean tumor size was 2.8 ± 1.9 cm (range: 0.8-9.5 cm). Arterial-phase hyperenhancement was observed in 40 cases (80%), with the enhancement pattern becoming more heterogeneous in tumors > 2 cm in size (18/30 cases, 60%). Calcifications were present in 12 cases (24%) and were more common in G2 and G3 tumors (9/20, 45%) than in G1 tumors (3/30, 10%; P = 0.006). On MRI, NETs were typically hyperintense on T2-weighted images (85%; n = 42) and showed restricted diffusion (90%; n = 45).

Other rare types: Imaging features varied among the rare types: Acinar cell carcinomas are large well-defined masses with heterogeneous enhancement (Figure 1A). Solid pseudopapillary neoplasms are well-encapsulated masses with heterogeneous solid and cystic components (Figure 1B). Mucinous cystic neoplasms: Unilocular or multilocular cystic lesions with enhanced septation (Figure 1C).

Statistical analysis of imaging-pathology correlations

Multinomial logistic regression analysis revealed several imaging features that were significantly associated with specific pathological types (P < 0.001). Ill-defined borders (OR = 15.3, 95%CI: 9.2-25.4) and hypoenhancement (OR = 22.1, 95%CI: 13.5-36.2) were strongly associated with PDAC. Cystic lesions communicating with the pancreatic duct (OR = 185.7, 95%CI: 78.3-440.2) were highly predictive of IPMN. Arterial phase hyperenhancement (OR = 28.6, 95%CI: 14.9-54.8) and well-defined borders (OR = 12.4, 95%CI: 6.7-22.9) were significantly associated with NET. Table 6 summarizes the key imaging features and their associations with the pathological types.

Interobserver agreement

The interobserver agreement for the assessment of imaging features is shown in Table 7. Interobserver agreement was substantial to excellent for all evaluated imaging features. The highest agreement was observed for tumor size (intraclass correlation coefficient = 0.92, 95%CI: 0.90-0.94) and vascular invasion (κ = 0.88, 95%CI: 0.84-0.92). The lowest, yet still substantial, agreement was noted for enhancement pattern assessment (κ = 0.79, 95%CI: 0.75-0.83).

DISCUSSION

This comprehensive retrospective study of 500 pancreatic cancer cases provides valuable insights into the relationship between the pathological types and imaging features of pancreatic neoplasms. Our findings demonstrate distinct imaging

Table 2 Distribution of pathological types

Pathological type	Cases	Percentage
Pancreatic ductal adenocarcinoma	320	64%
Intraductal papillary mucinous neoplasms	75	15%
Neuroendocrine tumors	50	10%
Other rare types	55	11%
Acinar cell carcinoma	20	4%
Solid pseudopapillary neoplasm	15	3%
Mucinous cystic neoplasm	12	2.4%
Pancreatoblastoma	5	1%
Miscellaneous	3	0.6%

Table 3 Imaging features of pancreatic ductal adenocarcinoma

Imaging feature	Percentage	Number of cases
Hypodense mass on CT	92%	294
Hypointense on T1-weighted MRI	95%	304
Ill-defined borders	85%	272
Pancreatic duct dilatation	78%	250
Hypoenhancement in all phases	88%	282
Vascular invasion	45%	144
Lymph node involvement	60%	192
Hypoechoic mass with irregular margins on EUS	90%	288

CT: Computed tomography; MRI: Magnetic resonance imaging; EUS: Endoscopic ultrasound.

Table 4 Imaging features of intraductal papillary mucinous neoplasms

Imaging feature	Percentage	Number of cases
Cystic lesions communicating with pancreatic duct	100%	75
Mural nodules	60%	45
Main pancreatic duct dilatation	65%	49
Enhancement of mural nodules on contrast-enhanced CT/MRI	55%	41

CT: Computed tomography; MRI: Magnetic resonance imaging.

characteristics associated with different pathological types, which could potentially enhance the accuracy of noninvasive diagnosis and inform treatment strategies[10].

Our results confirmed and extended previous observations regarding the imaging features of PDAC. The high frequency of ill-defined borders (85%) and hypoenhancement (88%) in our cohort aligned with that in earlier studies[11, 12]. However, our study provided a more precise quantification of these features in a larger cohort. The strong association between these imaging characteristics and PDAC (OR = 15.3, ill-defined borders; OR = 22.1, hypoenhancement) suggests that these features could serve as important radiological markers of PDAC[13].

The high prevalence of pancreatic duct dilatation (78%) in PDAC in our study is particularly noteworthy. This finding supports the "double duct sign"[14] as a potential early indicator of pancreatic head tumors. Our results suggest that this sign may be more common than previously reported, emphasizing its diagnostic value. The imaging features of IPMN in our study, particularly the universal presence of cystic lesions communicating with the pancreatic duct, corroborated the findings of Lee *et al*[15]. However, our observation of mural nodules in 60% of the IPMN cases was higher than the 45% reported in a previous study[16]. This discrepancy may be due to the improved resolution of the current imaging

Table 5 Imaging features of neuroendocrine tumors

Imaging feature	Percentage	Number of cases
Hyperenhancement in the arterial phase	80%	40
Well-defined borders	90%	45
Heterogeneous enhancement in larger tumors (> 2 cm)	60%	30
Calcifications	25%	12
Hyperintense on T2-weighted MRI	85%	42
Restricted diffusion on MRI	90%	45

MRI: Magnetic resonance imaging.

Table 6 Association between imaging features and pathological types

Imaging feature	PDAC	IPMN	NET	*P* value
Ill-defined borders	85%	10%	10%	< 0.001
Hypoenhancement	88%	5%	15%	< 0.001
Cystic components	15%	100%	10%	< 0.001
Arterial hyperenhancement	5%	15%	80%	< 0.001
Pancreatic duct dilatation	78%	65%	15%	< 0.001

PDAC: Pancreatic ductal adenocarcinoma; IPMN: Intraductal papillary mucinous neoplasms; NET: Neuroendocrine tumors.

Table 7 Interobserver agreement for imaging features

Imaging feature	Agreement measure	Value	95%CI
Tumor size	ICC	0.92	0.90-0.94
Tumor margin	κ	0.85	0.81-0.89
Enhancement pattern	κ	0.79	0.75-0.83
Vascular invasion	κ	0.88	0.84-0.92
Lymph node involvement	κ	0.82	0.78-0.86

ICC: Intraclass correlation coefficient; CI: Confidence interval.

techniques or differences in patient populations[17].

The strong association between cystic lesions communicating with the pancreatic duct and IPMN (OR = 185.7) underscores the diagnostic significance of this feature. This finding could aid in differentiating IPMN from other cystic pancreatic lesions, potentially reducing the need for unnecessary invasive procedures[18]. Our findings regarding NET imaging features, particularly the high frequency of arterial-phase hyperenhancement (80%) and well-defined borders (90%), were consistent with those reported by Zhang *et al*[19]. However, our study provided additional quantitative data on the strength of these associations (OR = 28.6; arterial hyperenhancement; OR = 12.4; well-defined borders). These data may be valuable for developing more precise imaging criteria for the diagnosis of pancreatic NETs[20].

The observation of calcification in 25% of NETs in our study is a novel finding that warrants further investigation. This feature could serve as an additional diagnostic marker for NETs, especially in cases where other imaging characteristics are equivocal. The strong association between specific imaging features and the pathological types demonstrated in this study has several important clinical implications. First, our findings could contribute to the development of more accurate imaging-based diagnostic algorithms for pancreatic cancer, potentially reducing the need for invasive diagnostic procedures, particularly for IPMN and NET. Second, the imaging features identified in our study could aid in the risk stratification of pancreatic lesions. For instance, the presence of mural nodules in IPMN has been associated with a higher risk of malignant transformation. The high detection rate of mural nodules (60%) in our study suggests that careful evaluation of this feature could improve risk assessment in patients with IPMN. Third, the ability to predict the pathological types based on imaging features can inform treatment decisions. For example, the identification of imaging features suggestive of NET might prompt the consideration of targeted therapies or more conservative management

Figure 1 Typical computed tomography image of acinar cell carcinomas, solid pseudopapillary neoplasms, and mucinous cystic neoplasms. A: Typical computed tomography image of acinar cell carcinomas; B: Typical computed tomography image of solid pseudopapillary neoplasms; C: Typical computed tomography image of mucinous cystic neoplasms.

approaches than those typically used for PDAC. Finally, our findings regarding early signs of pancreatic cancer, such as the high prevalence of pancreatic duct dilatation in PDAC, could inform the development of more effective screening and surveillance protocols for high-risk individuals.

Our study has several strengths, including large sample size, comprehensive imaging evaluation using multiple modalities, and robust statistical analysis. The high inter-observer agreement for key imaging features supports the reliability and reproducibility of our findings. Our study also has several limitations. First, the retrospective nature of our study introduced potential selection bias and limited our ability to control for all confounding factors. The data collected were based on clinical records and imaging studies performed as part of routine care, which may have led to inconsistencies in imaging protocols or reporting. Second, as our findings are based on data from a single tertiary care center, generalizability to other settings or patient populations may be limited. Different institutions may have varying patient demographics, risk factors, or prevalence of pancreatic cancer subtypes, which could influence the imaging-pathology correlations we observed. Third, given the 10-year span of our study, advances in imaging technology may have influenced the detection and characterization of certain features. The evolution of CT and MRI scanners as well as improvements in imaging protocols could have affected the consistency of our imaging data over time. Fourth, we did not have access to genetic information that could have provided additional insights into the relationship between imaging features, pathological types, and underlying genetic alterations. The integration of genomic data with imaging and pathological findings is an important area for future research. Fifth, our study design did not allow for subgroup analyses of specific pancreatic cancer types, such as different PDAC variants or IPMN grades. Such analyses could potentially reveal additional patterns and refine our understanding of imaging-pathology correlations. Sixth, we did not incorporate newer imaging techniques such as PET/CT or advanced MRI sequences (*e.g.*, diffusion-weighted imaging and dynamic contrast-enhanced MRI) in our analysis. These modalities can provide more valuable information for the characterization of pancreatic lesions. Seventh, our study lacked a longitudinal component to track the changes in imaging features over time. which could provide insights into disease progression and treatment response that were not captured in our cross-sectional analysis. Finally, although our inter-observer agreement for imaging features was high, the subjective nature of some imaging assessments could not be completely eliminated. The use of computer-aided diagnostic tools or radiomics approaches in future studies could potentially reduce this subjectivity.

Although our retrospective study provides valuable insights, we acknowledge the need for prospective studies to further validate our findings and assess their clinical impact. Future prospective, multicenter studies with standardized imaging protocols and pathological assessments would be instrumental in confirming the reliability and generalizability of the identified imaging-pathology correlations. Such studies could also evaluate the impact of these correlations on clinical decision-making, patient outcomes, and potential early detection strategies for pancreatic cancer.

An important area for future research is the longitudinal tracking of imaging features to understand disease progression and treatment responses. Such studies could provide valuable insights into the dynamic changes in imaging characteristics over time, potentially allowing earlier detection of disease progression or treatment resistance. This approach could be particularly valuable in monitoring patients with premalignant lesions, such as IPMN, or in assessing the treatment response in patients with advanced pancreatic cancer. Incorporating radiomics and artificial intelligence techniques into these longitudinal studies could further enhance our ability to detect subtle changes in imaging features that may have prognostic or predictive value.

CONCLUSION

Our comprehensive analysis of the relationship between pathological types and imaging features of pancreatic cancer provides valuable insights that could significantly impact clinical practice. By enhancing our ability to non-invasively characterize pancreatic lesions, these findings have the potential to improve early diagnosis, guide personalized treatment strategies, and ultimately improve outcomes in patients with pancreatic cancer.

FOOTNOTES

Author contributions: Luo YG and Wu M proposed the concept of this study, participated in the data collection, participated in this study, validated it, and jointly reviewed and edited the manuscript; Luo YG drafted the initial draft and guided the research, methodology, and visualization of the manuscript; Chen HG contributed to the formal analysis of this study. All authors critically reviewed and provided final approval of the manuscript; and all authors were responsible for the decision to submit the manuscript for publication.

Institutional review board statement: This study has been approved and reviewed by the Ethics Committee of Xuanhan County People's Hospital, No. 2021-LL-092.

Informed consent statement: Due to the retrospective nature of the study, informed consent was waived.

Conflict-of-interest statement: All the authors report no relevant conflicts of interest for this article.

Data sharing statement: No available data.

Country of origin: China

ORCID number: Yang-Gang Luo 0009-0004-7374-8543.

S-Editor: Wang JJ
L-Editor: A
P-Editor: Cai YX

REFERENCES

1 **Siegel RL**, Miller KD, Jemal A. Cancer statistics, 2018. *CA Cancer J Clin* 2018; **68**: 7-30 [PMID: 29313949 DOI: 10.3322/caac.21442]
2 **Rawla P**, Sunkara T, Gaduputi V. Epidemiology of Pancreatic Cancer: Global Trends, Etiology and Risk Factors. *World J Oncol* 2019; **10**: 10-27 [PMID: 30834048 DOI: 10.14740/wjon1166]
3 **Kamisawa T**, Wood LD, Itoi T, Takaori K. Pancreatic cancer. *Lancet* 2016; **388**: 73-85 [PMID: 26830752 DOI: 10.1016/S0140-6736(16)00141-0]
4 **Younan G**. Pancreas Solid Tumors. *Surg Clin North Am* 2020; **100**: 565-580 [PMID: 32402301 DOI: 10.1016/j.suc.2020.02.008]
5 **Mizrahi JD**, Surana R, Valle JW, Shroff RT. Pancreatic cancer. *Lancet* 2020; **395**: 2008-2020 [PMID: 32593337 DOI: 10.1016/S0140-6736(20)30974-0]
6 **Rana SS**. Evaluating the role of endoscopic ultrasound in pancreatitis. *Expert Rev Gastroenterol Hepatol* 2022; **16**: 953-965 [PMID: 36263489 DOI: 10.1080/17474124.2022.2138856]
7 **McKinney M**, Griffin MO, Tolat PP. Multimodality Imaging for the Staging of Pancreatic Cancer. *Surg Oncol Clin N Am* 2021; **30**: 621-637 [PMID: 34511186 DOI: 10.1016/j.soc.2021.06.006]
8 **Yamada Y**, Mori H, Matsumoto S, Kiyosue H, Hori Y, Hongo N. Pancreatic adenocarcinoma versus chronic pancreatitis: differentiation with triple-phase helical CT. *Abdom Imaging* 2010; **35**: 163-171 [PMID: 19771464 DOI: 10.1007/s00261-009-9579-7]
9 **Jeon SK**, Lee JM, Joo I, Lee ES, Park HJ, Jang JY, Ryu JK, Lee KB, Han JK. Nonhypervascular Pancreatic Neuroendocrine Tumors: Differential Diagnosis from Pancreatic Ductal Adenocarcinomas at MR Imaging-Retrospective Cross-sectional Study. *Radiology* 2017; **284**: 77-87 [PMID: 28092495 DOI: 10.1148/radiol.2016160586]
10 **Singhi AD**, Koay EJ, Chari ST, Maitra A. Early Detection of Pancreatic Cancer: Opportunities and Challenges. *Gastroenterology* 2019; **156**: 2024-2040 [PMID: 30721664 DOI: 10.1053/j.gastro.2019.01.259]
11 **Lee SM**, Katz MH, Liu L, Sundar M, Wang H, Varadhachary GR, Wolff RA, Lee JE, Maitra A, Fleming JB, Rashid A, Wang H. Validation of a Proposed Tumor Regression Grading Scheme for Pancreatic Ductal Adenocarcinoma After Neoadjuvant Therapy as a Prognostic Indicator for Survival. *Am J Surg Pathol* 2016; **40**: 1653-1660 [PMID: 27631521 DOI: 10.1097/PAS.0000000000000738]
12 **Srisajjakul S**, Prapaisilp P, Bangchokdee S. CT and MR features that can help to differentiate between focal chronic pancreatitis and pancreatic cancer. *Radiol Med* 2020; **125**: 356-364 [PMID: 31933064 DOI: 10.1007/s11547-019-01132-7]
13 **Gillies RJ**, Kinahan PE, Hricak H. Radiomics: Images Are More than Pictures, They Are Data. *Radiology* 2016; **278**: 563-577 [PMID: 26579733 DOI: 10.1148/radiol.2015151169]
14 **Sinha R**, Gardner T, Padala K, Greenaway JR, Joy D. Double-Duct Sign in the Clinical Context. *Pancreas* 2015; **44**: 967-970 [PMID: 26087354 DOI: 10.1097/MPA.0000000000000372]
15 **Lee JH**, Kim Y, Choi JW, Kim YS. KRAS, GNAS, and RNF43 mutations in intraductal papillary mucinous neoplasm of the pancreas: a meta-analysis. *Springerplus* 2016; **5**: 1172 [PMID: 27512631 DOI: 10.1186/s40064-016-2847-4]
16 **Hashimoto D**, Satoi S, Yamamoto T, Yamaki S, Ishida M, Hirooka S, Shibata N, Boku S, Ikeura T, Sekimoto M. Long-term outcomes of patients with multifocal intraductal papillary mucinous neoplasm following pancreatectomy. *Pancreatology* 2022; **22**: 1046-1053 [PMID: 35871123 DOI: 10.1016/j.pan.2022.07.004]
17 **Ohtsuka T**, Fernandez-Del Castillo C, Furukawa T, Hijioka S, Jang JY, Lennon AM, Miyasaka Y, Ohno E, Salvia R, Wolfgang CL, Wood

LD. International evidence-based Kyoto guidelines for the management of intraductal papillary mucinous neoplasm of the pancreas. *Pancreatology* 2024; **24**: 255-270 [PMID: 38182527 DOI: 10.1016/j.pan.2023.12.009]

18 **Attiyeh MA**, Fernández-Del Castillo C, Al Efishat M, Eaton AA, Gönen M, Batts R, Pergolini I, Rezaee N, Lillemoe KD, Ferrone CR, Mino-Kenudson M, Weiss MJ, Cameron JL, Hruban RH, D'Angelica MI, DeMatteo RP, Kingham TP, Jarnagin WR, Wolfgang CL, Allen PJ. Development and Validation of a Multi-institutional Preoperative Nomogram for Predicting Grade of Dysplasia in Intraductal Papillary Mucinous Neoplasms (IPMNs) of the Pancreas: A Report from The Pancreatic Surgery Consortium. *Ann Surg* 2018; **267**: 157-163 [PMID: 28079542 DOI: 10.1097/SLA.0000000000002015]

19 **Zhang L**, Sanagapalli S, Stoita A. Challenges in diagnosis of pancreatic cancer. *World J Gastroenterol* 2018; **24**: 2047-2060 [PMID: 29785074 DOI: 10.3748/wjg.v24.i19.2047]

20 **Klimstra DS**, Modlin IR, Coppola D, Lloyd RV, Suster S. The pathologic classification of neuroendocrine tumors: a review of nomenclature, grading, and staging systems. *Pancreas* 2010; **39**: 707-712 [PMID: 20664470 DOI: 10.1097/MPA.0b013e3181ec124e]

World Journal of Gastrointestinal Oncology

Submit a Manuscript: https://www.f6publishing.com

World J Gastrointest Oncol 2025 January 15; 17(1): 100204

DOI: 10.4251/wjgo.v17.i1.100204

ISSN 1948-5204 (online)

ORIGINAL ARTICLE

Retrospective Study

Lipid levels and insulin resistance markers in patients with colorectal cancer: Propensity score matching analysis

Ren-Hao Hu, Dong-Yi Yan, Ke-Hui Zhang, Di Zhang, Xi-Mao Cui, Xiao-Hua Jiang, Shun Zhang

Specialty type: Oncology

Provenance and peer review: Unsolicited article; Externally peer reviewed.

Peer-review model: Single blind

Peer-review report's classification

Scientific Quality: Grade C
Novelty: Grade C
Creativity or Innovation: Grade B
Scientific Significance: Grade C

P-Reviewer: Zhao L

Received: August 9, 2024
Revised: October 16, 2024
Accepted: October 29, 2024
Published online: January 15, 2025
Processing time: 124 Days and 17.9 Hours

Ren-Hao Hu, Dong-Yi Yan, Ke-Hui Zhang, Di Zhang, Xi-Mao Cui, Xiao-Hua Jiang, Shun Zhang, Department of Gastrointestinal Surgery, Shanghai East Hospital, School of Medicine, Tongji University, Shanghai 200120, China

Dong-Yi Yan, Ke-Hui Zhang, School of Medicine, Tongji University, Shanghai 200092, China

Di Zhang, Department of Emergency Medicine, Shanghai East Hospital, School of Medicine, Tongji University, Shanghai 200120, China

Co-first authors: Ren-Hao Hu and Dong-Yi Yan.

Co-corresponding authors: Xiao-Hua Jiang and Shun Zhang.

Corresponding author: Shun Zhang, MD, PhD, Assistant Professor, Department of Gastrointestinal Surgery, Shanghai East Hospital, School of Medicine, Tongji University, No. 1800 Yuntai Road, Pudong New District, Shanghai 200120, China. v2zs@hotmail.com

Abstract

BACKGROUND

Colorectal cancer (CRC) is a prevalent malignant neoplasm characterized by subtle early manifestations.

AIM

To investigate the correlation among serum lipid profiles, the triglyceride-glucose (TyG) index, and the atherosclerotic index (AI) in patients with CRC. Furthermore, it explored the clinical diagnostic utility of combining serum lipids with cancer antigens in the context of CRC.

METHODS

A retrospective analysis encompassed 277 patients with CRC and 1034 healthy individuals.

RESULTS

Following propensity score matching, patients with CRC exhibited significantly reduced levels of serum triglyceride (TG), total cholesterol (TC), high-density lipoprotein cholesterol, and low-density lipoprotein cholesterol (LDL-C), as well as a diminished TyG index. Conversely, they displayed elevated AI levels compared to their healthy counterparts. Patients in advanced stages exhibited lower serum levels of TG, TC, and LDL-C compared to those in early stages.

Patients with positive lymph node metastasis demonstrated reduced levels of TG, LDL-C, and the TyG index. Receiver operating characteristic analysis revealed that the combination of the TyG index, carcinoembryonic antigen, and carbohydrate antigen 19-9 yielded the highest positive prediction rate for CRC at 75.3%.

CONCLUSION

Preoperative serum lipid profiles exhibit a robust association with patients with CRC. The concurrent assessment of multiple serum lipids and cancer antigens effectively enhances the diagnostic accuracy for CRC.

Key Words: Colorectal cancer; Serum lipids; Triglyceride-glucose index; Atherosclerotic index; Diagnostic marker

Core Tip: Timely identification of colorectal cancer (CRC) is essential in lowering both the occurrence and death rates linked to the illness. It has been shown that serum lipids and insulin resistance (IR) markers can be useful biomarkers for detecting CRC in patients. This article retrospectively analyzed 277 patients with CRC and investigated the clinical diagnostic value of a combination of IR indicators, including the triglyceride-glucose index and atherosclerotic index, with cancer antigens as a novel diagnostic marker for CRC.

Citation: Hu RH, Yan DY, Zhang KH, Zhang D, Cui XM, Jiang XH, Zhang S. Lipid levels and insulin resistance markers in patients with colorectal cancer: Propensity score matching analysis. *World J Gastrointest Oncol* 2025; 17(1): 100204
URL: https://www.wjgnet.com/1948-5204/full/v17/i1/100204.htm
DOI: https://dx.doi.org/10.4251/wjgo.v17.i1.100204

INTRODUCTION

Colorectal cancer (CRC) is one of the most common malignant tumors in the world, with 1.9 million new cases per year, and ranking as the second most commonly diagnosed cancer. The prognosis of CRC critically hinges upon the cancer stage determined during diagnosis[1]. Timely detection of CRC is imperative to reduce both its incidence and mortality rates associated with the disease.

Several methods are currently being proposed and used to identify the location of tumors. These methods include the fecal occult blood test, colonoscopy, and computed tomography. Currently, the most widely used diagnostic approach for CRC is colonoscopy, which has high sensitivity and specificity for identifying polyps and cancers[2]. However, it is an invasive, high-cost, and time-consuming procedure that requires complex implementation. Blood-based biomarkers such as carcinoembryonic antigen (CEA) and carbohydrate antigen 19-9 (CA 19-9) have been recognized and accepted as noninvasive diagnostic procedures established to detect CRC[3].

Metabolic syndrome, consisting of impaired glucose tolerance, dyslipidemia, obesity, and hypertension, is associated with insulin resistance (IR)[4]. Dyslipidemia is an integral part of metabolic syndrome and is characterized by an alteration of serum lipids. In recent years, growing evidence has shown that serum lipids play an important role in tumor development and progression[5]. In particular, it has been shown that serum lipids can be a useful biomarker for detecting CRC in patients[6,7]. However, the limited knowledge of the relationship between serum lipids and the clinical parameters of CRC has obstructed the optimized use for serum lipids when obtaining more accurate and meaningful information for CRC diagnosis and treatment outcomes. Furthermore, there has been no research conducted using propensity score matching (PSM) to investigate the relationship between serum lipids and CRC.

Current evidence has confirmed that IR is a relevant risk factor for the morbidity and mortality of various cancers, including CRC[8,9]. Recently, the triglyceride-glucose (TyG) index and the atherosclerotic index (AI [TC−HDLC]/HDLC]), which are closely related to IR, diabetes, and metabolic syndrome, have attracted extensive attention and medical research. Previous studies have demonstrated that the TyG index may serve as a marker of CRC[7,10]. However, the role of the TyG index in cancer risk remains controversial, and its relationship has not been demonstrated in patients with CRC[11]. The AI is widely regarded as a predictor of cardiovascular disease. However, the association between AI and CRC still needs further exploration.

Therefore, we retrospectively analyzed 277 patients with CRC and investigated the clinical diagnostic value of a combination of IR indicators, including the TyG index and AI, with cancer antigens as a novel diagnostic marker for CRC.

MATERIALS AND METHODS

Study population

Patients with histologically confirmed CRC at the Department of Gastrointestinal Surgery of Shanghai East Hospital (Shanghai, China) between 2021 and 2022 were retrospectively reviewed. To evaluate the link between CRC and the lipid

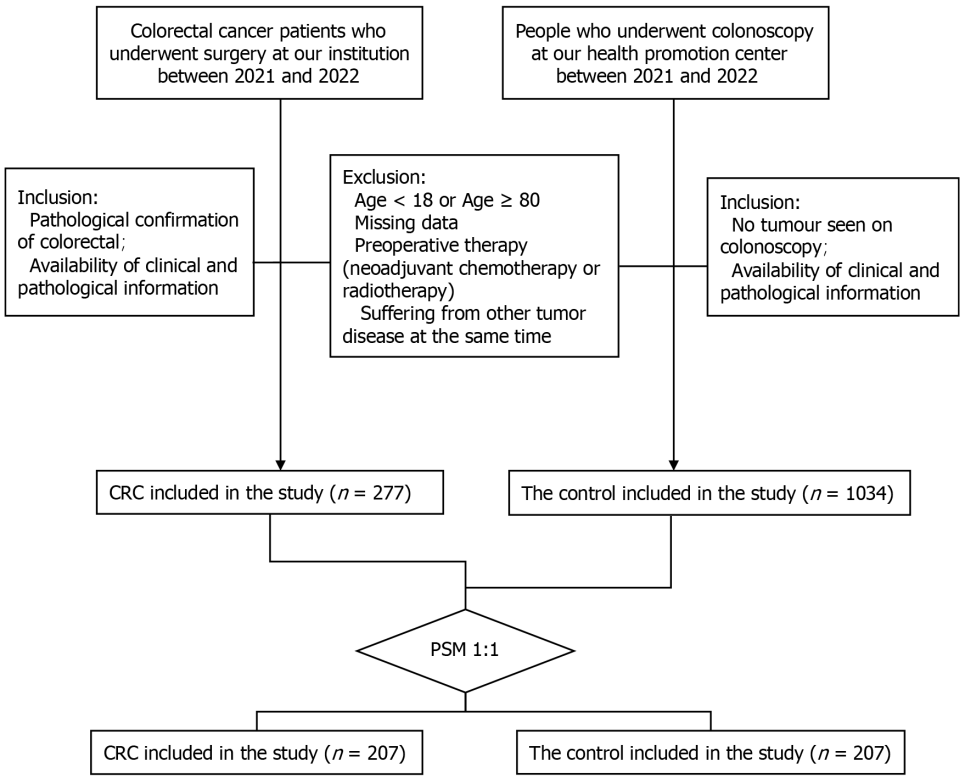

Figure 1 Flow of included participants. CRC: Colorectal cancer; PSM: Propensity score matching.

profile found in the serum, a control group was retrospectively examined from a cohort initially collected at the health promotion center. Patients had a previous history of malignancy. Participants who did not undergo lipid profile assessment in the laboratory or were lost during the follow-up period were excluded from the study. Ultimately, a total of 277 individuals diagnosed with CRC and 1034 healthy control subjects were included in the analysis (Figure 1). All participants provided written informed consent. The methods used in this study were conducted in compliance with the Declaration of Helsinki and other applicable guidelines. The study was approved by the Human Research Ethics Committee of Shanghai East Hospital.

Data collection

The participants in the study were required to fill out a questionnaire that collected information regarding any current or previous illnesses, both acute and chronic, as well as any medications they were currently taking. Peripheral blood was collected for routine hematological tests and cancer antigens such as CEA and CA19-9. The clinicopathological classification of CRC was performed according to the 8th American Joint Committee on Cancer tumor-node-metastasis (TNM) staging system. The serum lipid profiles of all subjects were measured in the study. The levels of serum lipids, such as triglyceride (TG), total cholesterol (TC), high-density lipoprotein cholesterol (HDL-C), and low-density lipoprotein cholesterol (LDL-C), were assessed utilizing the Roche Cobas e801 chemistry analyzer (Roche Diagnostics, Mannheim, Germany). The TyG index was calculated as Ln (fasting TG [mg/dL] × fasting plasma glucose [mg/dL]/2). AI was analytically calculated from (TC-HDL-C)/HDL-C.

Statistical analyses

The data are expressed as the mean ± standard deviation in cases of normal distribution, and as the median with the interquartile range for nonparametric distribution. To analyze categorical variables, χ^2 or Fisher exact tests were employed, while continuous variables were assessed using the Student's *t*-test or one-way analysis of variance. To evaluate the discriminatory ability of the variables in predicting the incidence of CRC, a receiver operating characteristic (ROC) curve was constructed. We calculated the corresponding area under the curve, along with its 95% confidence interval (CI). The statistical software Statistical Package for the Social Sciences (version 26.0; IBM, Armonk, NY, United States) was utilized for data analysis, with statistical significance defined as $P < 0.05$ (two-sided). The effect of serum lipids was evaluated by one-to-one PSM to adjust for factors including sex, body mass index (BMI), coronary heart disease, cerebral infarction, and hypertension.

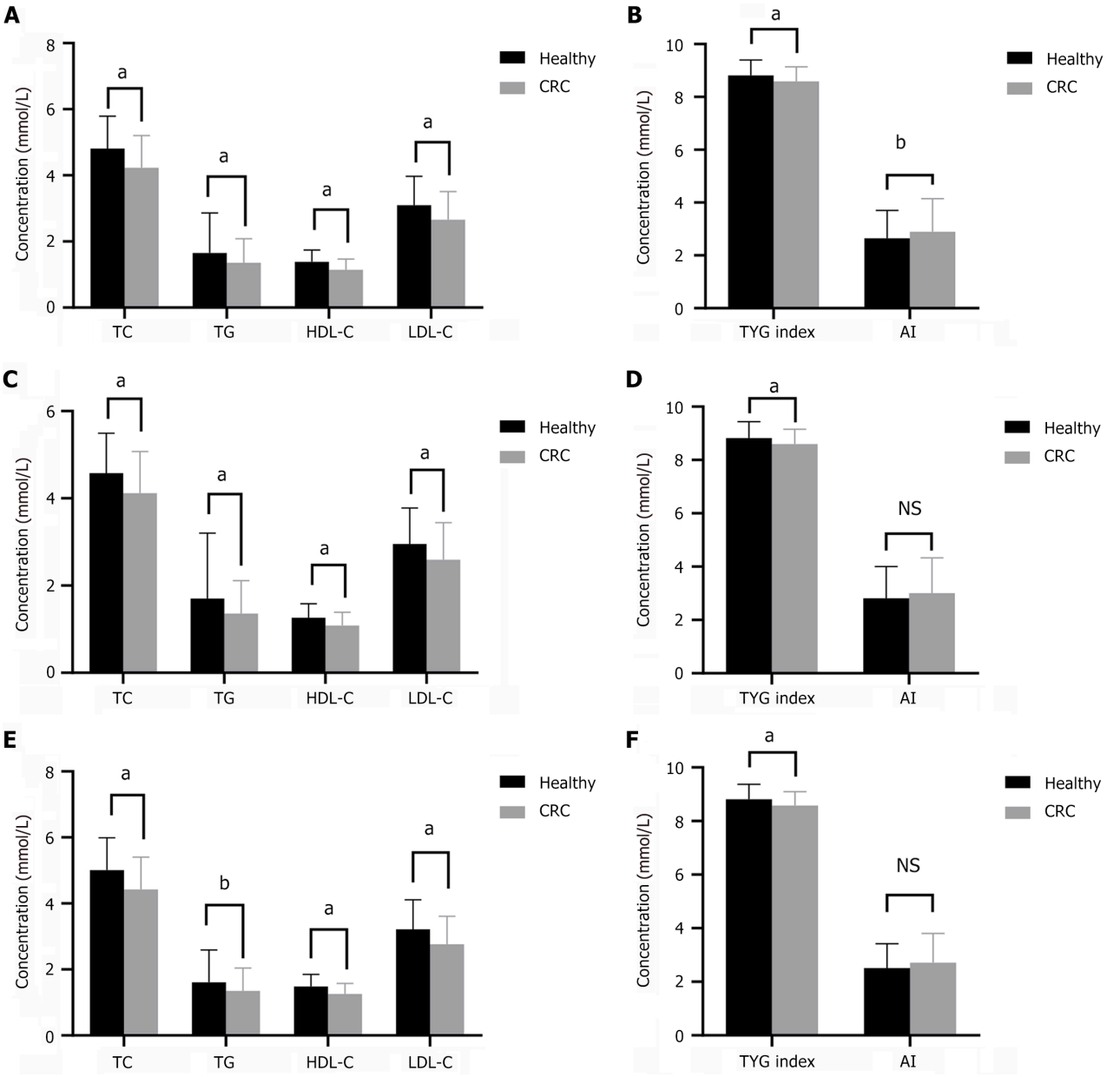

Figure 2 Serum lipid, triglyceride-glucose index, and atherosclerotic index in patients with colorectal cancer and healthy participants. A: Serum lipids including total cholesterol (TC), triglyceride (TG), high-density lipoprotein cholesterol (HDL-C), and low-density lipoprotein cholesterol (LDL-C); B: Triglyceride-glucose (TyG) index and atherosclerotic index (AI) in all research subjects; C: Serum lipids; D: TyG index and AI in male subjects; E and F: Serum lipids; TyG index, and AI in female subjects. Data are presented as the mean ± standard deviation and analyzed by the Student's *t*-test. $^{a}P < 0.05$; $^{b}P < 0.01$; $^{c}P < 0.001$. CRC: Colorectal cancer.

RESULTS

Serum lipid levels, TyG, and AI are strongly associated with CRC before and after PSM

We identified 277 patients with CRC and 1034 healthy participants. Table 1 presents the fundamental data of the patients with CRC. There were significant differences between groups in terms of BMI, white blood cells, red blood cells, hemoglobin, and platelets (Table 2). The serum levels of TG, TC, HDL-C, and LDL-C, and the TyG index were significantly lower in patients with CRC than in healthy participants ($P < 0.01$), whereas AI was significantly higher in patients with CRC than in healthy participants ($P < 0.01$) (Figure 2A and B). The patients with CRC and healthy participants were subsequently divided into two subgroups depending on sex. Our results indicated that TG, TC, HDL-C, LDL-C, and TyG index were also significantly lower in both male and female patients compared with the same sex group in healthy participants (Figure 2C-F).

Based on these findings, we implemented PSM using a modified 1:1 ratio. We achieved successful matching of 414 participants, evenly distributed with 207 individuals in each group. Post PSM, both groups demonstrated robust balance across all variables. Analysis of matched patients showed similar results (Figure 3).

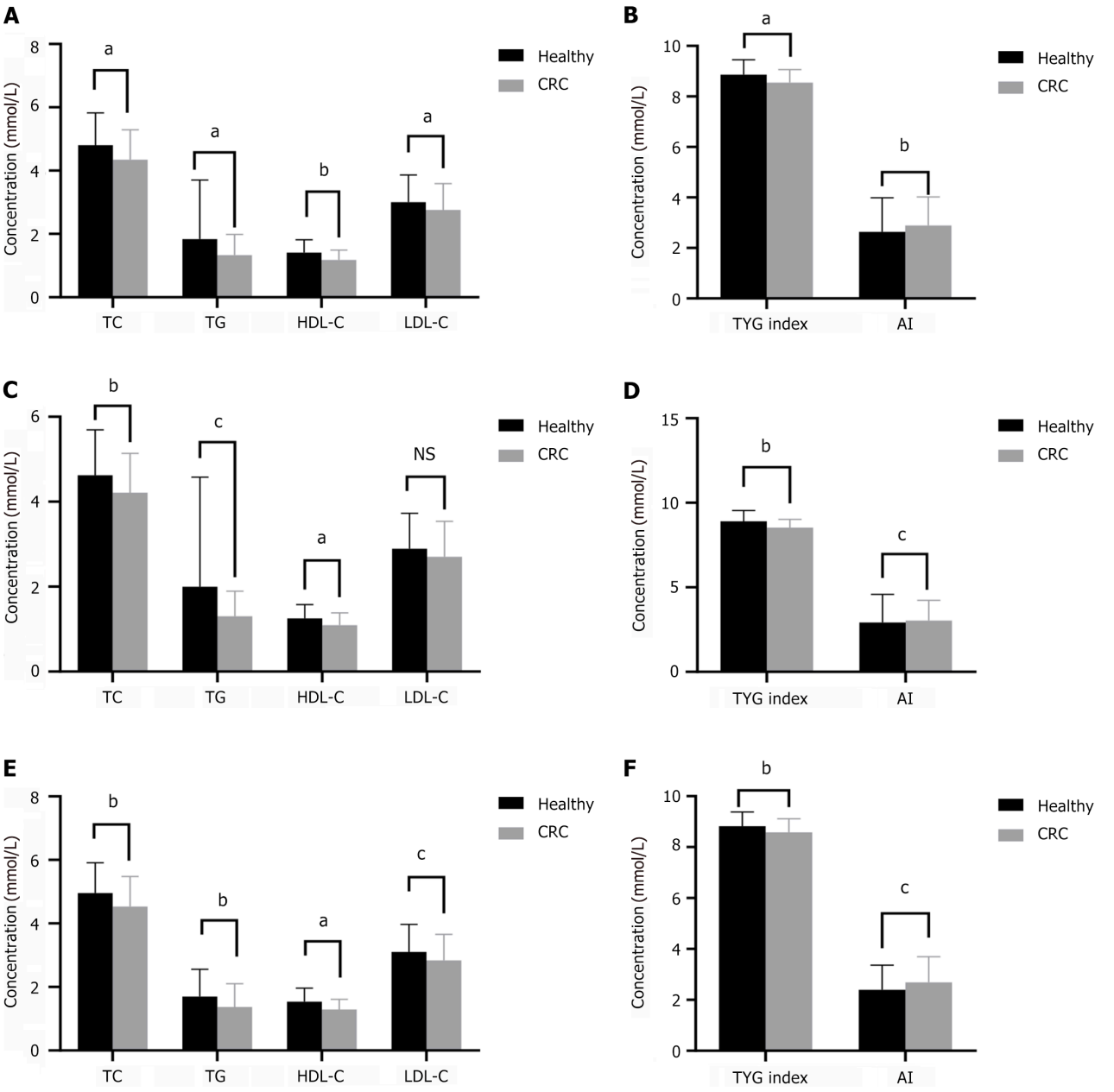

Figure 3 Serum lipid, triglyceride-glucose index, and atherosclerotic index in patients with colorectal cancer and healthy participants after propensity score matching. A and B: Serum lipids, triglyceride-glucose (TyG) index and atherosclerotic index (AI) in all research subjects after propensity score matching (PSM); C and D: Serum lipids, TyG index, and AI in male subjects after PSM; E and F: Serum lipids, TyG index, and AI in female subjects after PSM. Data are presented as the mean ± standard deviation and analyzed by the Student's *t*-test. $^{a}P < 0.05$; $^{b}P < 0.01$; $^{c}P < 0.001$. CRC: Colorectal cancer; HDL-C: High-density lipoprotein cholesterol; LDL-C: Low-density lipoprotein cholesterol; TC: Total cholesterol; TG: Triglyceride.

Relationships between serum lipid levels and the malignancy and invasiveness of CRC

To evaluate the relationship between serum lipids and tumor stage, all patients were stratified into two groups: those with relatively early-stage tumors (stages I and II) and those with advanced-stage tumors (stages III and IV). We found that TC and LDL-C were significantly lower in patients with advanced-stage tumors (Figure 4A and B). The levels of TG and LDL-C and the TyG index in patients with CRC with lymph node metastasis were significantly lower than those in patients without lymph node metastasis (Figure 4C and D). The levels of TG and the TyG index were associated with poor differentiation in patients with CRC (Figure 4E and F).

Relationships between serum lipid levels and tumor location

Of the 277 patients with CRC, 152 (54.9%) had CRC and 125 (45.1%) had rectal cancer. The serum HDL-C level in patients with CRC was significantly lower than that in patients with rectal cancer ($P < 0.01$) (Figure 5A and B). We divided patients with CRC into right-sided CRC (RSCC) and left-sided CRC (LSCC) subgroups. The serum TC level in patients with RSCC was significantly lower than that in patients with LSCC ($P < 0.05$) (Figure 5C and D).

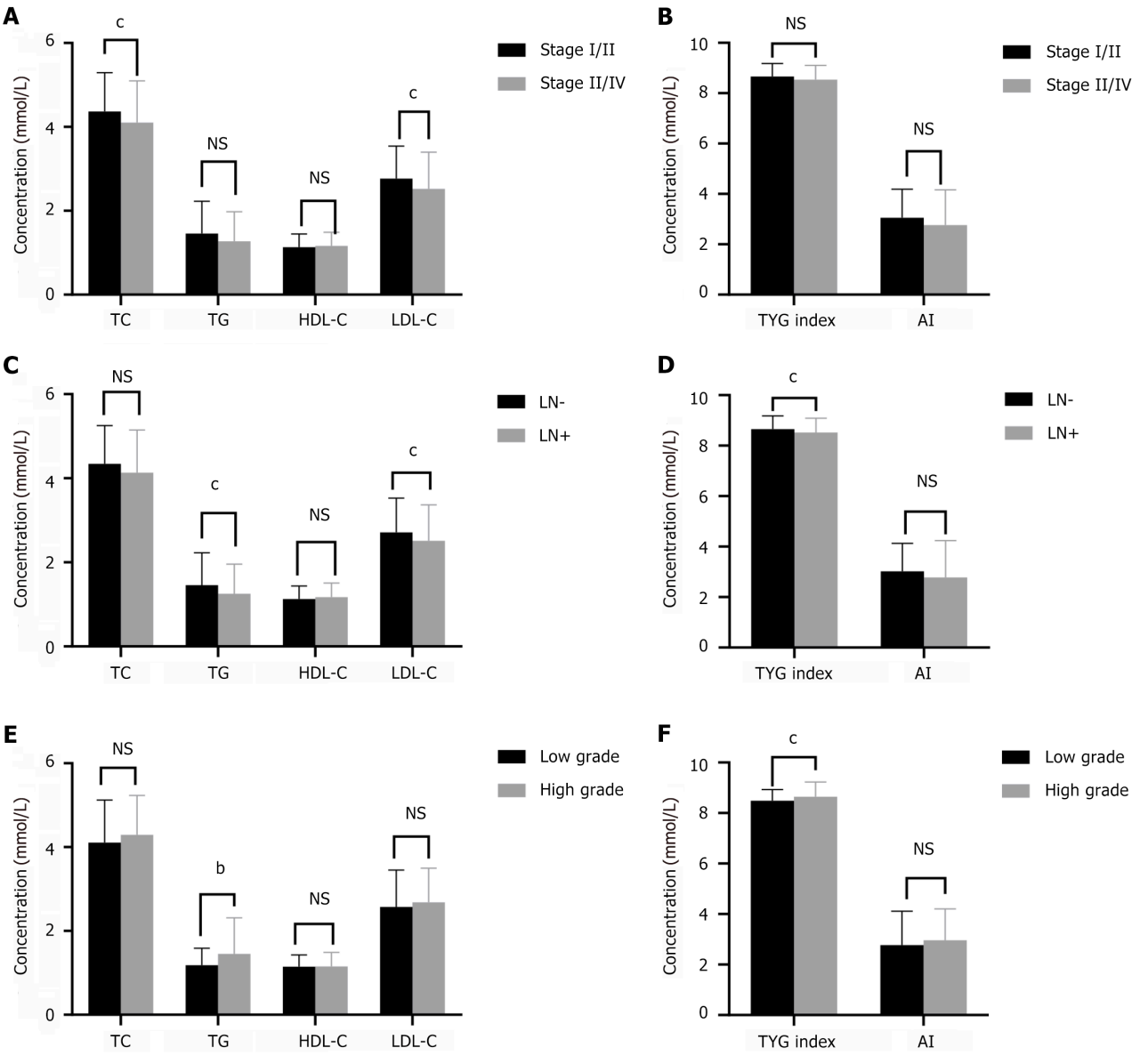

Figure 4 Relationships between serum lipid levels and the malignancy and invasiveness of colorectal cancer. A and B: Serum lipids, triglyceride-glucose (TyG) index, and atherosclerotic index (AI) in different tumor stage of colorectal cancer (CRC); C and D: Serum lipids, TyG index, and AI in patients with CRC with or without with lymph node metastasis; E and F: Serum lipids, TyG index, and AI in patients with CRC with different differentiations. Data are presented as the mean ± standard deviation and analyzed by the Student's *t*-test. $^{a}P < 0.05$; $^{b}P < 0.01$; $^{c}P < 0.001$. HDL-C: High-density lipoprotein cholesterol; LDL-C: Low-density lipoprotein cholesterol; TC: Total cholesterol; TG: Triglyceride.

Serum lipid levels in patents with CRC with normal CEA and CA19-9 levels

Of all patients with CRC, 136 had normal preoperative serum CEA and CA19-9 levels. Serum lipid levels were associated with CRC with normal CEA and CA19-9 levels. The levels of TG, TC, HDL-C, and LDL-C and the TyG index in the CRC group were significantly lower than those in healthy participants, whereas AI was higher in the CRC group (Figure 6A and B). After PSM, analysis of matched patients showed similar results (Figure 6C and D).

Enhanced diagnostic value of serum lipid levels and serum cancer antigens in patients with CRC

Given the abnormal rates of serum lipid levels and serum cancer antigens in patients with CRC, the TyG index, CEA, and CA19-9 were combined to examine whether the combination can enhance the diagnostic rate in patients with CRC. Our results showed that the combination of the TyG index and cancer antigens can be used as a new diagnostic marker for CRC (Figure 7). The combination of the TyG index, CEA, and CA19-9 had the highest positive prediction rate for CRC (75.3%) by ROC analysis. The remaining serum lipids and cancer antigens are shown in Table 3. Based on this candidate model, we developed a nomogram to visualize CRC diagnosis. Utilizing the patient's blood lipids, CEA, CA19-9, and TyG index, we can predict the likelihood of the patient having CRC (Figure 8).

Table 1 Basic information of patients with colorectal cancer before and after propensity score matching

Characteristics	All CRC, *n* = 277	Propensity-matched CRC, *n* = 207
Ascending colon	55 (11.4)	42 (8.7)
Transverse colon	11 (2.3)	8 (1.7)
Descending colon	18 (3.7)	14 (2.9)
Sigmoid colon	68 (14)	49 (10.1)
Rectum	125 (25.8)	94 (19.4)
T. stage		
T1	28 (5.8)	23 (4.8)
T2	36 (7.4)	25 (5.2)
T3	196 (40.5)	148 (30.6)
T4	17 (3.5)	11 (2.3)
N. stage		
N0	156 (32.2)	119 (24.6)
N1	71 (14.7)	53 (11)
N2	50 (10.3)	35 (7.2)
M. stage		
M0	251 (51.9)	190 (39.3)
M1	26 (5.4)	17 (3.5)
Blood vessels		
-	199 (41.1)	150 (31)
+	78 (16.1)	57 (11.8)
Nerve		
-	210 (43.4)	159 (32.9)
+	67 (13.8)	48 (9.9)
Size, median (IQR)	4 (3, 5)	4 (3, 5)
Differentiation		
Low grade	94 (19.4)	69 (14.3)
High grade	183 (37.8)	138 (28.5)
Stage		
I	55 (11.4)	41 (8.2)
II	95 (19.6)	72 (14.9)
III	100 (20.7)	73 (15.1)
IV	27 (5.6)	19 (3.9)

Data are *n* (%) unless otherwise indicated. CRC: Colorectal cancer; IQR: Interquartile range.

DISCUSSION

Identifying simple, feasible, and low-cost markers of CRC is of great significance for the treatment and prognosis of patients with CRC. However, due to the absence of distinct symptoms and restricted detection techniques, CRC is frequently misdiagnosed, resulting in the disease being detected in its advanced stages when noticeable symptoms emerge. The present retrospective study analyzed the relationship between dyslipidemia and CRC. We also explored whether the combination of serum lipids or the TyG index and AI can enhance the diagnostic rate of CRC. Of interest, our results showed that preoperative serum lipids were significantly lower in patients with CRC than in healthy participants, even after PSM. In addition, the TyG index and AI as IR markers were associated with CRC. Our study found that various factors such as lymphatic metastasis, vascular invasion, nerve infiltration, and pathologic TNM stage can impact

Table 2 Characteristics of study participants

Characteristics	All patients			Propensity-matched patients		
	Control, *n* = 1034	CRC, *n* = 277	*P* value	Controls, *n* = 207	CRC, *n* = 207	*P* value
Age in years	66.53 ± 7.41	66.54 ± 10.91	0.989	68.89 ± 5.53	65.58 ± 11.12	0.053
Sex as male/female	466/568	176/101	< 0.001	96/111	122/85	0.010
Hypertension in %	10.25	43.68	< 0.001	34.78	28.99	0.206
Diabetes in %	1.64	14.80	< 0.001	7.73	5.80	0.434
Coronary heart disease or Cerebral infarction in %	0.48%	12.64	< 0.001	2.24	2.24	1
BMI	25.09 ± 5.25	23.78 ± 3.27	< 0.001	24.40 ± 3.77	23.84 ± 3.29	0.106
WBC as × 10^9/L	6.49 ± 1.58	6.16 ± 1.84	0.003	6.64 ± 1.66	6.14 ± 1.84	0.004
RBC as × 10^9/L	4.70 ± 0.43	4.19 ± 0.61	< 0.001	4.66 ± 0.40	4.21 ± 0.58	< 0.001
Hb in g/L	143.23 ± 13.24	120.63 ± 25.73	< 0.001	141.89 ± 12.61	121.47 ± 25.08	< 0.001
PLT as × 10^9/L	216.94 ± 52.78	240.59 ± 83.72	< 0.001	224.17 ± 51.69	240.94 ± 78.97	0.011
ALT in U/L	21.36 ± 7.75	18.50 ± 31.60	0.144	20.33 ± 7.63	17.65 ± 18.27	0.057
AST in U/L	21.40 ± 12.65	21.24 ± 35.77	0.908	19.36 ± 12.60	19.73 ± 11.93	0.758
TC in mmol/L	4.81 ± 0.98	4.23 ± 0.97	< 0.001	4.80 ± 1.02	4.34 ± 0.94	< 0.001
TG in mmol/L	1.65 ± 1.21	1.35 ± 0.73	< 0.001	1.84 ± 1.87	1.33 ± 0.65	< 0.001
HDL-C in mmol/L	1.38 ± 0.36	1.14 ± 0.32	< 0.001	1.41 ± 0.41	1.17 ± 0.32	< 0.001
LDL-C in mmol/L	3.10 ± 0.87	2.66 ± 0.85	< 0.001	3.01 ± 0.86	2.76 ± 0.83	0.003
UA in mmol/L	319.84 ± 77.29	315.62 ± 81.37	0.430	324.75 ± 80.97	312.42 ± 78.70	0.121
SCR in mmol/L	74.63 ± 22.89	76.67 ± 21.08	0.190	78.29 ± 26.10	73.84 ± 19.89	0.056
CEA in ng/mL	1.91 ± 1.51	35.67 ± 176.15	0.002	2.80 ± 1.54	26.62 ± 95.89	0.001
CA199 in U/mL	11.26 ± 7.64	176.16 ± 1013.41	0.009	12.00 ± 8.77	159.62 ± 929.85	0.027
AI	2.65 ± 1.05	35.67 ± 176.15	0.002	2.64 ± 1.35	2.89 ± 1.14	0.042
TyG index	8.81 ± 0.58	8.58 ± 0.55	< 0.001	8.86 ± 0.59	8.55 ± 0.51	< 0.001

AI: Atherosclerotic index; ALT: Alanine aminotransferase; AST: Aspartate transaminase; BMI: Body mass index; CEA: Carcinoembryonic antigen; CRC: Colorectal cancer; Hb: Hemoglobin; HDL-C: High-density lipoprotein cholesterol; LDL-C: Low-density lipoprotein cholesterol; PLT: Platelet; RBCs: Red blood cells; SCR: Serum creatinine; TC: Total cholesterol; TG: Triglyceride; TyG: Triglyceride-glucose; UA: Uric acid; WBCs: White blood cells.

the levels of serum lipids. Therefore, we suggest that measuring serum lipid levels, along with the TyG index and AI, can serve as biomarkers for both diagnosing CRC and predicting its characteristics such as lymph node metastasis, vascular invasion, neural infiltration, and staging. These findings highlight the potential of utilizing these biomarkers for improved understanding and management of CRC. Moreover, the use of these biomarkers can contribute to early detection and intervention strategies, ultimately enhancing outcomes for patients with CRC. Moreover, detection of the TyG index and cancer antigens can effectively improve the diagnosis of CRC.

The routine lipid panel consists of TG, TC, HDL-C, and LDL-C. Accumulating evidence suggests that lipid imbalance may contribute to CRC risk through inflammation, oxidative stress, IR, and protein function alteration[12]. A recent study suggested that serum lipids may serve as a potential marker for CRC[5,12]. However, no research has been conducted on the association of the lipid derivative TyG index and AI with patients with CRC, especially by using PSM analysis. Several studies have demonstrated the association of serum lipid levels and cardiovascular diseases. In recent years, evidence has shown that serum lipid components are associated with the occurrence and development of various types of cancer and thus can be used to evaluate cancer. However, data on the relationship of serum lipid levels with CRC are contradictory[13,14]. PSM analysis is a statistical technique designed to address confounding bias and mimic a randomized clinical trial, improving the level of evidence in studies[15]. It was found that the CRC group had lower serum lipid levels before and after PSM. It is hypothesized that the association of low serum lipids and lipoproteins with CRC results from the metabolic, competitive, and rapid consumption of nutrients by cancer cells, rather than increased levels as a protective factor.

Recent epidemiological and clinical evidence points to a strong association of IR with cancer risk[8]. The TyG index, which relies on fasting levels of TGs and glucose, is gaining recognition as a credible and straightforward proxy for IR. The TyG index is associated with an increased risk of cancers of the digestive system. Limited research has explored the

Table 3 Various combined diagnostic indicators for patients with colorectal cancer

Indicator	AUC	95%CI	Cut-off value	*P* value
TC	0.6243	0.5709-0.6777	4.325	< 0.0001
TG	0.6406	0.5873-0.6938	1.345	< 0.0001
HDL-C	0.6802	0.6292-0.7311	1.165	< 0.0001
LDL-C	0.5812	0.5263-0.6360	3.035	0.0043
CEA	0.6429	0.5882-0.6976	5.15	< 0.0001
CA19-9	0.5623	0.5057-0.6190	23.225	0.0305
AI	0.5748	0.5199-0.6298	2.655	0.0085
TyG index	0.6572	0.6048-0.7097	8.635	< 0.0001
CEA + CA199 + TYG index	0.7525	0.7052-0.7997		< 0.0001

AI: Atherosclerotic index; AUC: Area under the curve; CEA: Carcinoembryonic antigen; CI: Confidence interval; HDL-C: High-density lipoprotein cholesterol; LDL-C: Low-density lipoprotein cholesterol; SCR: Serum creatinine; TG: Triglyceride; TC: Total cholesterol; TyG: Triglyceride-glucose.

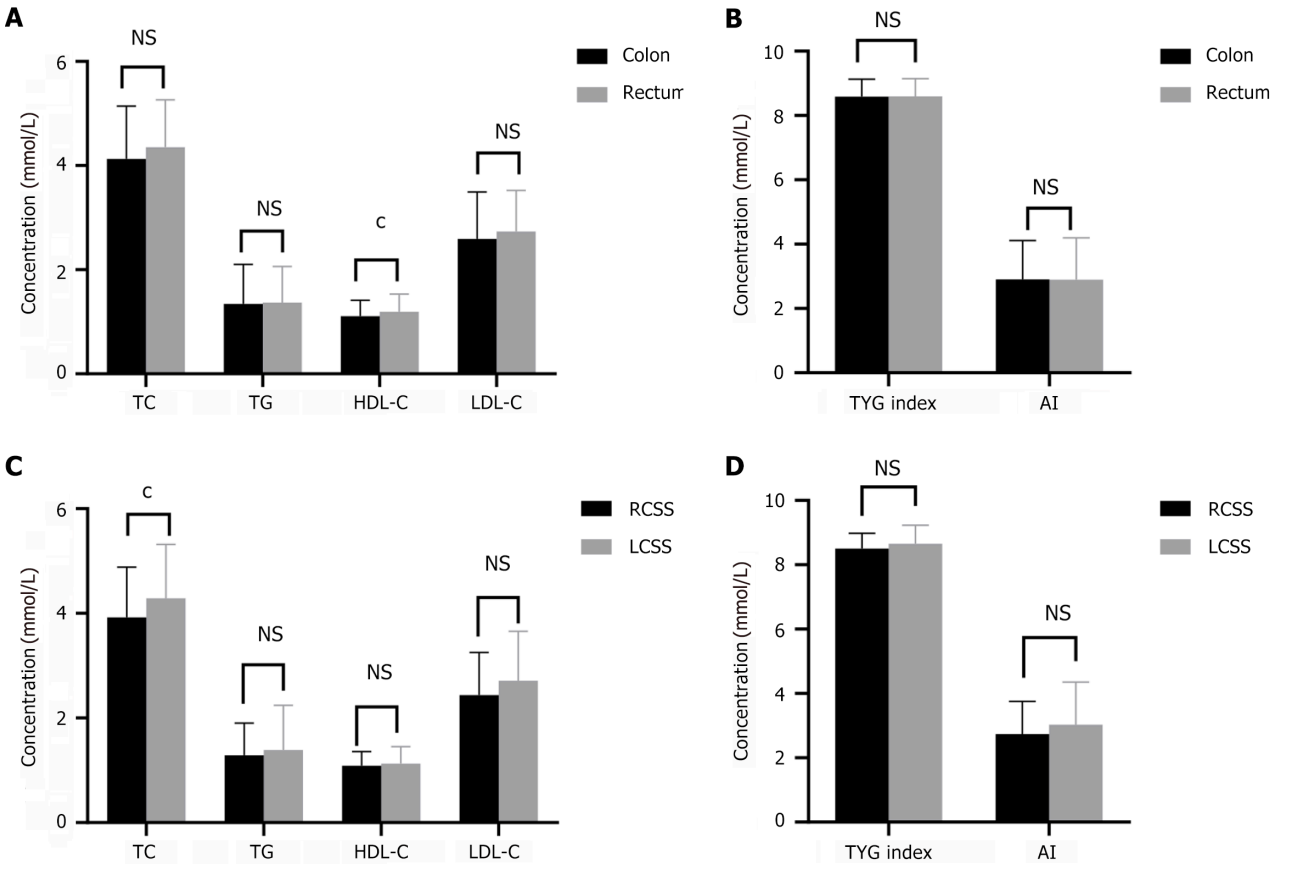

Figure 5 Relationships between serum lipid levels and tumor location. A and B: Serum lipids, triglyceride-glucose (TyG) index, and atherosclerotic index (AI) in patients with colorectal cancer (CRC) and rectal cancer; C and D: Serum lipids, TyG index, and AI in patients with right-sided CRC (RCSS) and left-sided CRC (LCSS). Data are presented as the mean ± standard deviation and analyzed by the Student's *t*-test. $^{a}P < 0.05$; $^{b}P < 0.01$; $^{c}P < 0.001$. HDL-C: High-density lipoprotein cholesterol; LDL-C: Low-density lipoprotein cholesterol; TC: Total cholesterol; TG: Triglyceride.

correlation between patients with CRC and the TyG index. Our investigation, however, reveals noteworthy findings: The TyG index maintains a significant correlation with patients with CRC, persisting even after PSM. This study found that as the TyG index decreased, the tumor stage of CRC increased, suggesting that the TyG index may be a valuable marker for predicting CRC. ROC analysis results indicated that the area under the ROC of the TyG index was 0.657, further supporting its potential as a reliable diagnostic tool for CRC. AI is also closely related to IR, diabetes, and metabolic syndrome. Compared to previous studies, we demonstrated for the first time that both the TyG index and AI are reliable blood-based biomarkers for patients with CRC.

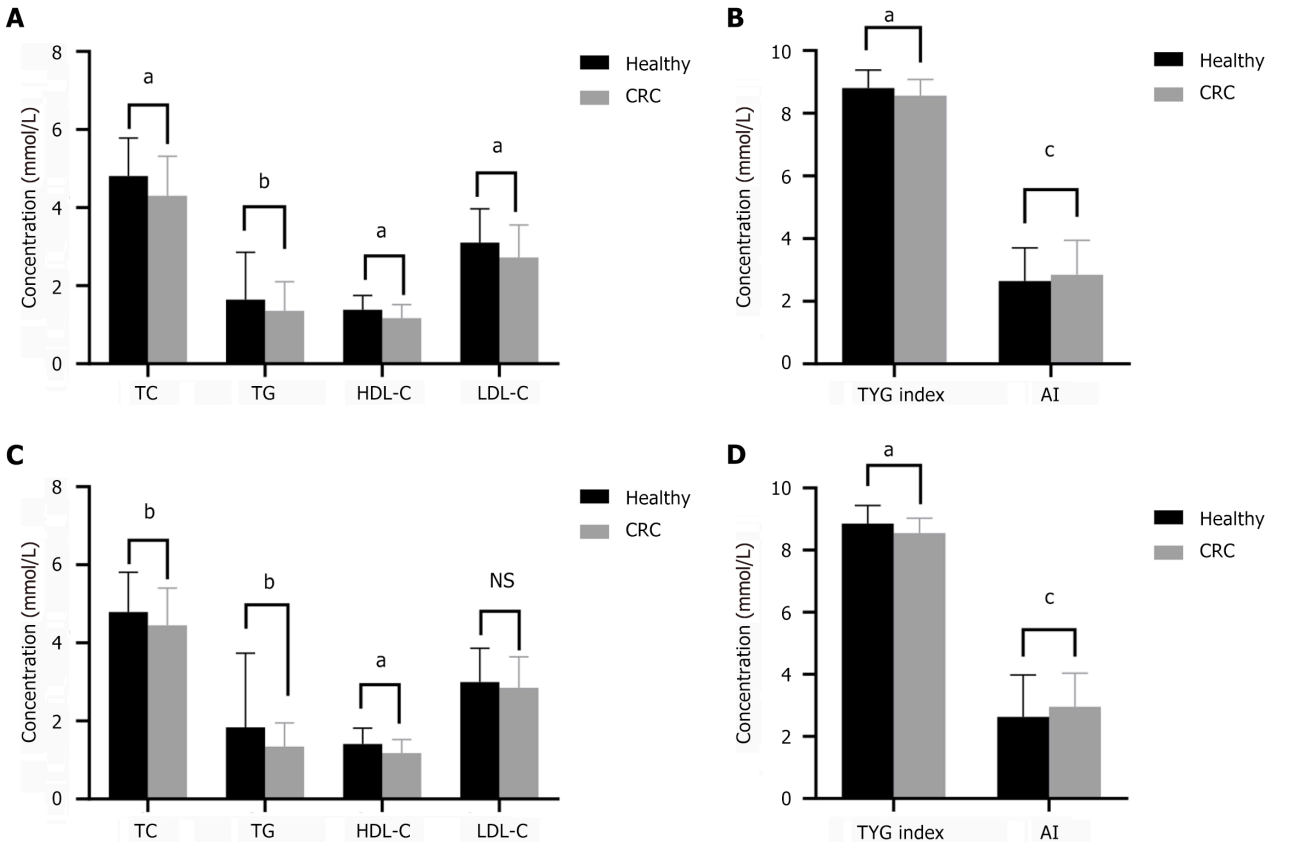

Figure 6 Serum lipid levels in patients with colorectal cancer with normal carcinoembryonic antigen and carbohydrate antigen 19-9. A and B: Serum lipids, triglyceride-glucose (TyG) index, and atherosclerotic index (AI) in patients with colorectal cancer (CRC) with normal carcinoembryonic antigen (CEA) and carbohydrate antigen 19-9 before propensity score matching (PSM); C and D: Serum lipids, TyG index, and AI in patients with CRC with normal CEA and CA19-9 after PSM. Data are presented as the mean ± standard deviation and analyzed by the Student's *t*-test. $^{a}P < 0.05$; $^{b}P < 0.01$; $^{c}P < 0.001$. HDL-C: High-density lipoprotein cholesterol; LDL-C: Low-density lipoprotein cholesterol; TC: Total cholesterol; TG: Triglyceride.

Tumor location plays a vital role in determining the progression of the disease, prognosis, and the appropriate management. Various factors, such as the embryonic origin of the tumor, its vascular and nervous supplies, as well as its microbiotic burden, contribute to these differences[16]. When analyzed by anatomical site, the results indicated a positive and significant association between HDL-C and rectal cancer. At a physiological level, RSCC is more likely to exhibit advanced tumor stage and increased lymphovascular invasion[17] with poor prognosis and overall survival compared with LSCC[18]. When subgroup analysis was stratified by the left and right colons, TC levels were much lower in patients with RSCC than in those with LSCC.

Over the years, researchers have pursued tumor markers capable of detecting early stages of malignant cell transformation. These biomarkers, typically proteins associated with cancer, hold promise for clinical applications in patients with cancer. Several indicators of CRC, including CEA, CA 19-9, tissue polypeptide-specific antigen, tumor-associated glycoprotein 72, and hematopoietic growth factors, are widely established and routinely used in clinical practice[19]. Nevertheless, these assessments often lack outstanding diagnostic accuracy. Individual marker analyses for disease detection and prognosis are frequently limited by the modest sensitivity and specificity of conventional medical protocols. A more effective strategy involves simultaneous evaluation of multiple markers to improve diagnostic efficacy. The tumor markers CEA and CA19-9 are widely used for real-world opportunistic cancer screening, treatment response assessment, and recurrence monitoring in CRC. However, both tumor markers do not necessarily increase in all cases; sometimes none or only one of the two tumor markers increases. It is possible that patients with advanced stages may not exhibit elevated serum levels of CEA or CA19-9. A recent study suggested that serum lipids may serve as biomarkers for CRC. Nonetheless, there is a dearth of investigations that have delved into the possibility of utilizing serum lipids to diagnose patients with CRC displaying normal levels of CEA and CA19-9[6]. Our results showed that even in patients with normal CEA and CA19-9, serum lipids, TyG index, and AI had a strong association with CRC, even after PMS.

Due to the highly heterogeneous nature of CRC, a single tumor marker is unlikely to have sufficient sensitivity or specificity for use in diagnostic tests. Moreover, combinations of two or more types of biomarkers are often used in clinical practice to improve the accuracy and efficiency of disease diagnosis. In our study, combining serum lipids and tumor markers improved clinical sensitivity for the detection of CRC and could be a more effective marker.

Our study had several limitations. Initially, it should be noted that this study was conducted retrospectively at a solitary institution, which introduces the possibility of selection bias. To adequately assess the diagnostic efficacy of serum lipids, it is imperative to conduct prospective studies spanning multiple institutions. Additionally, due to the limited number of patients with CRC, our dataset cannot be split into separate training and test sets for statistical

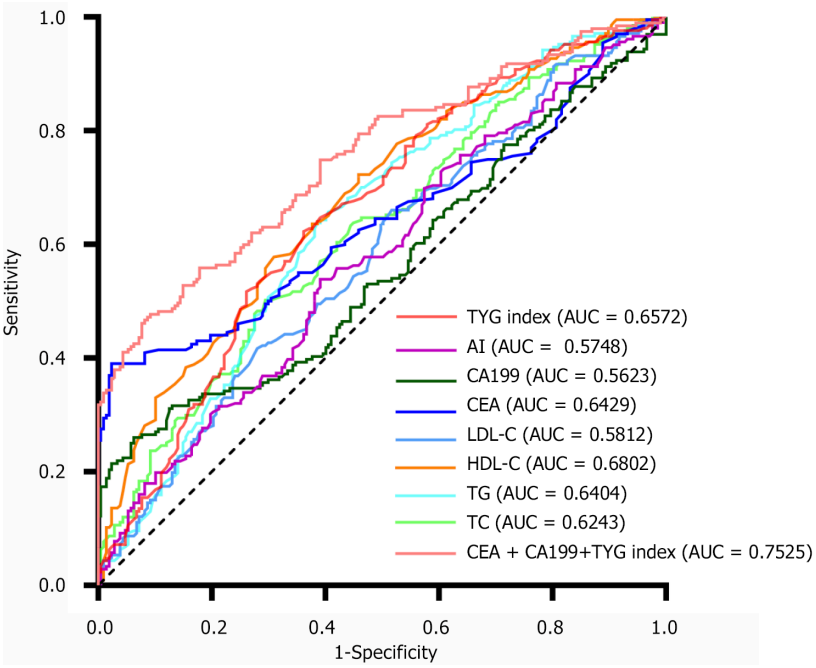

Figure 7 Various combined diagnostic indicators for patients with colorectal cancer. AI: Atherosclerotic index; AUC: Area under the curve; CEA: Carcinoembryonic antigen; HDL-C: High-density lipoprotein cholesterol; LDL-C: Low-density lipoprotein cholesterol; TC: Total cholesterol; TG: Triglyceride; TyG: Triglyceride-glucose.

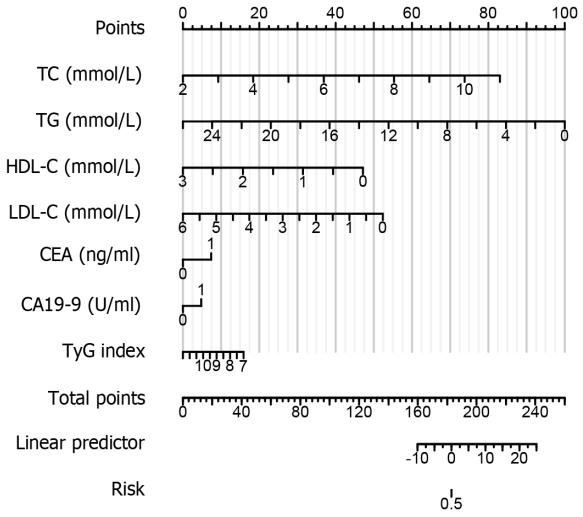

Figure 8 Nomogram for colorectal cancer diagnosis. AUC: Area under the curve; CEA: Carcinoembryonic antigen; HDL-C: High-density lipoprotein cholesterol; LDL-C: Low-density lipoprotein cholesterol; TC: Total cholesterol; TG: Triglyceride; TyG: Triglyceride-glucose.

validation. The lack of a validation cohort hampers a thorough confirmation of our findings. Moving forward, we plan to collect additional data to facilitate validation efforts. Additionally, we failed to assess treatment response or perform survival analysis based on serum lipid levels. Nevertheless, our findings convincingly demonstrate that the amalgamation of serum lipids and tumor markers holds substantial diagnostic capability for patients with CRC.

CONCLUSION

In conclusion, the results of our study suggest that the serum lipids have strong association with CRC. The detection of TyG index and cancer antigens can effectively improve the diagnosis of CRC.

FOOTNOTES

Author contributions: Hu RH, Yan DY, Zhang KH, Cui XM, and Zhang S performed material preparation, data collection, and analysis; Zhang S and Jiang XH wrote the first draft of the manuscript; Yan DY aided in the manuscript writing and finalized the manuscript; Zhang S and Jiang XH discussed the content and critically reviewed the manuscript draft; All authors contributed to the study conception and design, and read and approved the final manuscript. Hu RH and Yan DY contributed equally to this work as co-first authors. Jiang XH and Zhang S were appointed for this paper. First, the two professors participated in the design of the research study, provided research ideas, and made important revisions to the paper during the writing process, and finally finalized the manuscript. Second, these two professors played a significant role in project management and team collaboration. Therefore, both corresponding authors have made important and equal contributions to the article. For this reason, the article designates these two as co-corresponding authors.

Supported by Pudong New Area Science and Technology Development Fund for Livelihood Research Special Project, No. PKJ2023-Y38.

Institutional review board statement: The study was approved by the Human Research Ethics Committee of Shanghai East Hospital.

Informed consent statement: All participants signed the informed consent.

Conflict-of-interest statement: The authors have no conflicts of interests to declare.

Data sharing statement: The datasets used and/or analyzed during the current study are available from the corresponding author on reasonable request.

Country of origin: China

ORCID number: Shun Zhang 0000-0002-3493-1247.

Corresponding Author's Membership in Professional Societies: Chinese Society of Clinical Oncology, No. 18621896856.

S-Editor: Qu XL
L-Editor: Filipodia
P-Editor: Zhang XD

REFERENCES

1 **Pang X**, Xu B, Lian J, Wang R, Wang X, Shao J, Tang S, Lu H. Real-world survival of colon cancer after radical surgery: A single-institutional retrospective analysis. *Front Oncol* 2022; **12**: 914076 [PMID: 36185216 DOI: 10.3389/fonc.2022.914076]
2 **Bretthauer M**, Løberg M, Wieszczy P, Kalager M, Emilsson L, Garborg K, Rupinski M, Dekker E, Spaander M, Bugajski M, Holme Ø, Zauber AG, Pilonis ND, Mroz A, Kuipers EJ, Shi J, Hernán MA, Adami HO, Regula J, Hoff G, Kaminski MF; NordICC Study Group. Effect of Colonoscopy Screening on Risks of Colorectal Cancer and Related Death. *N Engl J Med* 2022; **387**: 1547-1556 [PMID: 36214590 DOI: 10.1056/NEJMoa2208375]
3 **Gao Y**, Wang J, Zhou Y, Sheng S, Qian SY, Huo X. Evaluation of Serum CEA, CA19-9, CA72-4, CA125 and Ferritin as Diagnostic Markers and Factors of Clinical Parameters for Colorectal Cancer. *Sci Rep* 2018; **8**: 2732 [PMID: 29426902 DOI: 10.1038/s41598-018-21048-y]
4 **O'Neill S**, O'Driscoll L. Metabolic syndrome: a closer look at the growing epidemic and its associated pathologies. *Obes Rev* 2015; **16**: 1-12 [PMID: 25407540 DOI: 10.1111/obr.12229]
5 **Fang Z**, He M, Song M. Serum lipid profiles and risk of colorectal cancer: a prospective cohort study in the UK Biobank. *Br J Cancer* 2021; **124**: 663-670 [PMID: 33139801 DOI: 10.1038/s41416-020-01143-6]
6 **Li T**, Zhou Y, Wang J, Xiao S, Duan Y, Li C, Gao Y, An H, Tao N. Association of triglyceride-glucose index with the risk of prostate cancer: a retrospective study. *PeerJ* 2023; **11**: e16313 [PMID: 37953784 DOI: 10.7717/peerj.16313]
7 **Liu T**, Zhang Q, Wang Y, Ma X, Zhang Q, Song M, Cao L, Shi H. Association between the TyG index and TG/HDL-C ratio as insulin resistance markers and the risk of colorectal cancer. *BMC Cancer* 2022; **22**: 1007 [PMID: 36138391 DOI: 10.1186/s12885-022-10100-w]
8 **Arcidiacono B**, Iiritano S, Nocera A, Possidente K, Nevolo MT, Ventura V, Foti D, Chiefari E, Brunetti A. Insulin resistance and cancer risk: an overview of the pathogenetic mechanisms. *Exp Diabetes Res* 2012; **2012**: 789174 [PMID: 22701472 DOI: 10.1155/2012/789174]
9 **Yamamoto S**, Nakagawa T, Matsushita Y, Kusano S, Hayashi T, Irokawa M, Aoki T, Korogi Y, Mizoue T. Visceral fat area and markers of insulin resistance in relation to colorectal neoplasia. *Diabetes Care* 2010; **33**: 184-189 [PMID: 19837793 DOI: 10.2337/dc09-1197]
10 **Li W**, Liu T, Qian L, Wang Y, Ma X, Cao L, Zhang Q, Qu J. Insulin resistance and inflammation mediate the association of abdominal obesity with colorectal cancer risk. *Front Endocrinol (Lausanne)* 2022; **13**: 983160 [PMID: 36407320 DOI: 10.3389/fendo.2022.983160]
11 **Wang H**, Yan F, Cui Y, Chen F, Wang G, Cui W. Association between triglyceride glucose index and risk of cancer: A meta-analysis. *Front Endocrinol (Lausanne)* 2022; **13**: 1098492 [PMID: 36714554 DOI: 10.3389/fendo.2022.1098492]
12 **Yang Z**, Tang H, Lu S, Sun X, Rao B. Relationship between serum lipid level and colorectal cancer: a systemic review and meta-analysis. *BMJ Open* 2022; **12**: e052373 [PMID: 35732386 DOI: 10.1136/bmjopen-2021-052373]
13 **Chung YW**, Han DS, Park YK, Son BK, Paik CH, Lee HL, Jeon YC, Sohn JH. Association of obesity, serum glucose and lipids with the risk

of advanced colorectal adenoma and cancer: a case-control study in Korea. *Dig Liver Dis* 2006; **38**: 668-672 [PMID: 16790371 DOI: 10.1016/j.dld.2006.05.014]

14 **Yamada K**, Araki S, Tamura M, Sakai I, Takahashi Y, Kashihara H, Kono S. Relation of serum total cholesterol, serum triglycerides and fasting plasma glucose to colorectal carcinoma in situ. *Int J Epidemiol* 1998; **27**: 794-798 [PMID: 9839735 DOI: 10.1093/ije/27.5.794]

15 **Lonjon G**, Boutron I, Trinquart L, Ahmad N, Aim F, Nizard R, Ravaud P. Comparison of treatment effect estimates from prospective nonrandomized studies with propensity score analysis and randomized controlled trials of surgical procedures. *Ann Surg* 2014; **259**: 18-25 [PMID: 24096758 DOI: 10.1097/SLA.0000000000000256]

16 **Mukund K**, Syulyukina N, Ramamoorthy S, Subramaniam S. Right and left-sided colon cancers - specificity of molecular mechanisms in tumorigenesis and progression. *BMC Cancer* 2020; **20**: 317 [PMID: 32293332 DOI: 10.1186/s12885-020-06784-7]

17 **Narayanan S**, Gabriel E, Attwood K, Boland P, Nurkin S. Association of Clinicopathologic and Molecular Markers on Stage-specific Survival of Right Versus Left Colon Cancer. *Clin Colorectal Cancer* 2018; **17**: e671-e678 [PMID: 30108021 DOI: 10.1016/j.clcc.2018.07.001]

18 **Yahagi M**, Okabayashi K, Hasegawa H, Tsuruta M, Kitagawa Y. The Worse Prognosis of Right-Sided Compared with Left-Sided Colon Cancers: a Systematic Review and Meta-analysis. *J Gastrointest Surg* 2016; **20**: 648-655 [PMID: 26573851 DOI: 10.1007/s11605-015-3026-6]

19 **Jelski W**, Mroczko B. Biochemical Markers of Colorectal Cancer - Present and Future. *Cancer Manag Res* 2020; **12**: 4789-4797 [PMID: 32606968 DOI: 10.2147/CMAR.S253369]

World Journal of Gastrointestinal Oncology

Submit a Manuscript: https://www.f6publishing.com

World J Gastrointest Oncol 2025 January 15; 17(1): 98168

DOI: 10.4251/wjgo.v17.i1.98168

ISSN 1948-5204 (online)

ORIGINAL ARTICLE

Observational Study

Pretreatment red blood cell distribution width as a predictive marker for postoperative complications after laparoscopic pancreatoduodenectomy

Xian-Rang Cao, Yin-Long Xu, Jia-Wei Chai, Kai Zheng, Jun-Jie Kong, Jun Liu, Shun-Zhen Zheng

Specialty type: Gastroenterology and hepatology

Provenance and peer review: Unsolicited article; Externally peer reviewed.

Peer-review model: Single blind

Peer-review report's classification

Scientific Quality: Grade C

Novelty: Grade B

Creativity or Innovation: Grade B

Scientific Significance: Grade B

P-Reviewer: Lin WJ

Received: June 19, 2024

Revised: September 10, 2024

Accepted: October 29, 2024

Published online: January 15, 2025

Processing time: 175 Days and 22.5 Hours

Xian-Rang Cao, Yin-Long Xu, Kai Zheng, Jun-Jie Kong, Jun Liu, Shun-Zhen Zheng, Department of Liver Transplantation and Hepatobiliary Surgery, Shandong Provincial Hospital Affiliated to Shandong First Medical University, Jinan 250021, Shandong Province, China

Jia-Wei Chai, Department of Breast and Thyroid Surgery, Shandong Provincial Maternal and Child Health Care Hospital, Jinan 250014, Shandong Province, China

Corresponding author: Shun-Zhen Zheng, MD, PhD, Professor, Department of Liver Transplantation and Hepatobiliary Surgery, Shandong Provincial Hospital Affiliated to Shandong First Medical University, No. 324 Jingwu Weiqi Road, Jinan 250021, Shandong Province, China. zsz5512920@hotmail.com

Abstract

BACKGROUND

Red blood cell distribution width (RDW) is associated with the development and progression of various diseases.

AIM

To explore the association between pretreatment RDW and short-term outcomes after laparoscopic pancreatoduodenectomy (LPD).

METHODS

A total of 804 consecutive patients who underwent LPD at our hospital between March 2017 and November 2021 were retrospectively analyzed. Correlations between pretreatment RDW and clinicopathological characteristics and short-term outcomes were investigated.

RESULTS

Patients with higher pretreatment RDW were older, had higher Eastern Cooperative Oncology Group scores and were associated with poorer short-term outcomes than those with normal RDW. High pretreatment RDW was an independent risk factor for postoperative complications (POCs) (hazard ratio = 2.973, 95% confidence interval: 2.032-4.350, $P < 0.001$) and severe POCs of grade IIIa or higher (hazard ratio = 3.138, 95% confidence interval: 2.042-4.824, $P < 0.001$) based on the Clavien-Dino classification system. Subgroup analysis showed that high pretreatment RDW was an independent risk factor for Clavien-Dino classi-

fication grade IIIb or higher POCs, a comprehensive complication index score ≥ 26.2, severe postoperative pancreatic fistula, severe bile leakage and severe hemorrhage. High pretreatment RDW was positively associated with the neutrophil-to-lymphocyte ratio and platelet-to-lymphocyte ratio and was negatively associated with albumin and the prognostic nutritional index.

CONCLUSION

Pretreatment RDW was a special parameter for patients who underwent LPD. It was associated with malnutrition, severe inflammatory status and poorer short-term outcomes. RDW could be a surrogate marker for nutritional and inflammatory status in identifying patients who were at high risk of developing POCs after LPD.

Key Words: Biomarker; Laparoscopic pancreatoduodenectomy; Postoperative complication; Red blood cell distribution width; Short-term outcomes

Core Tip: Pretreatment red blood cell distribution width was a special parameter for patients who underwent laparoscopic pancreatoduodenectomy. It was associated with malnutrition, severe inflammatory status and poorer short-term outcomes. Pretreatment red blood cell distribution width could be a surrogate marker for nutritional and inflammatory status in identifying patients who were at high risk of developing postoperative complications after laparoscopic pancreatoduodenectomy.

Citation: Cao XR, Xu YL, Chai JW, Zheng K, Kong JJ, Liu J, Zheng SZ. Pretreatment red blood cell distribution width as a predictive marker for postoperative complications after laparoscopic pancreatoduodenectomy. *World J Gastrointest Oncol* 2025; 17(1): 98168
URL: https://www.wjgnet.com/1948-5204/full/v17/i1/98168.htm
DOI: https://dx.doi.org/10.4251/wjgo.v17.i1.98168

INTRODUCTION

With the development of laparoscopic instruments and the accumulation and progress of surgical experience, laparoscopic pancreatoduodenectomy (LPD) has been widely performed in high-volume medical centers[1-3]. However, as one of the most challenging abdominal surgeries with high complexity, LPD is associated with a high incidence of postoperative complications (POCs), and the incidence of POCs after LPD ranges from 30% to 50%[1,3,4]. POCs could lead to higher costs and longer hospital stays for patients undergoing surgery[5,6]. Meanwhile, recent studies have demonstrated that POCs have a negative impact on the long-term outcomes of patients with malignant tumors, including hepatocellular carcinoma[7] and colorectal liver metastasis[8]. Consequently, increased attention has been placed on identifying risk factors for the development of POCs in efforts to improve both the short- and long-term outcomes for patients undergoing surgery.

Traditionally, operation-related parameters, such as pancreas texture and blood loss, are considered risk factors for POCs after pancreatoduodenectomy[9,10]. In recent studies, nutritional and inflammatory factors such as prognostic nutritional index (PNI), neutrophil-to-lymphocyte ratio (NLR) and platelet-to-lymphocyte ratio (PLR) have been found to be associated with the development of POCs after surgery[11-13]. Malnutrition and systemic inflammatory responses play crucial roles in the development of POCs by causing tissue friability, decreasing the production of proinflammatory molecules and weakening the blood vessel wall, thereby impacting the immune response and wound healing after surgery[14,15].

Red blood cell distribution width (RDW) is a parameter reflecting the degree of heterogeneity of erythrocyte volume and is used for estimating the pathogenesis of anemia[16]. Recent studies revealed that RDW could be an indicator of malnutrition and systemic inflammation and was associated with the development of many disorders[17-19]. For instance, higher RDW was found to be associated with critical illness for patients with coronavirus disease 2019 infection [20]. Recent studies revealed that high RDW was associated with the development of POCs after operation, including esophagectomy[21] and cardiac surgery[22]. However, no previous studies have reported the relationship between high pretreatment RDW and short-term outcomes in patients undergoing LPD. This study aimed to explore the association between high pretreatment RDW and short-term outcomes and identify risk factors for POCs after LPD. In addition, the correlation between high pretreatment RDW and malnutrition and immune response was investigated to reveal how high RDW reflects the frequent incidence of POCs after LPD.

MATERIALS AND METHODS

Patients

Between March 2017 and November 2021, a total of 832 consecutive patients who underwent LPD at Shandong Provincial Hospital Affiliated to Shandong First Medical University were initially identified and enrolled in this study. Of these, 11 patients who were aged < 18 or > 80 years old and 17 patients with insufficient clinical data [3 for RDW pretreatment data, 2 for C-reactive protein (CRP), 5 for prothrombin time (PT), 3 for operative time and 4 for total lymphocyte count] were excluded. Eventually, 804 patients were included in this study. This study obtained ethics approval from the ethics committee of Shandong Provincial Hospital Affiliated to Shandong First Medical University and was performed in accordance with the Declaration of Helsinki (as revised in 2013). Written informed consent was obtained from each participant in the study.

Data collection

The clinicopathological profiles of the 804 patients were collected, including age, sex, body mass index (BMI), smoking and alcohol consumption history, comorbidities (diabetes mellitus, hypertension and pancreatitis), Eastern Cooperative Oncology Group (ECOG) score, up-abdominal operation history, preoperative biliary drainage, pathology, American Society of Anesthesiologists physical status, preoperative laboratory data, surgery-related parameters and postoperative outcomes. Preoperative laboratory data included alanine aminotransferase (ALT), aspartate aminotransferase (AST), alkaline phosphatase (ALP), γ-glutamyl transferase (GGT), hemoglobin, RDW, platelet count, neutrophil cell count, lymphocyte count, total bilirubin (TBIL), albumin, CRP and PT. Surgery-related parameters included operative time, blood loss and intraoperative blood transfusion. Postoperative outcomes included POCs, postoperative pancreatic fistula (POPF), bile leakage (BL), hemorrhage, intra-abdominal infection and delayed gastric emptying (DGE). Patients were divided into two groups according to the institutional standard value of pretreatment RDW: High (> 15.4) and normal (≤ 15.4) RDW groups.

Definition of POCs

POCs were graded according to the Clavien-Dino classification (CDc) system[23]. The comprehensive complication index was also used for assessing POCs[24]. POPF was defined according to the criteria provided by the International Study Group of Pancreatic Surgery. DGE and hemorrhage were defined according to the International Study Group of Pancreatic Surgery criteria[25,26]. The diagnosis of BL was determined according to the definitions provided by the International Study Group of Liver Surgery[27].

Statistical analysis

Categorical variables are expressed as numbers (n) and proportions (%), and continuous variables are expressed as the mean ± SD. The χ^2 test and Fisher's exact test were used to compare categorical variables between two groups. The Mann-Whitney U test was used for continuous variables. Logistic regression analysis was used to identify risk factors for POCs. Variables with $P < 0.1$ in the univariate analysis were regarded as potential risk factors and were included in the multivariate analysis. The odds ratios (ORs) with 95% confidence intervals (95%CIs) were recorded. The NLR, PLR, and PNI were calculated as follows: NLR = absolute neutrophil count/absolute lymphocyte count; PLR = absolute platelet count/absolute lymphocyte count[28]; PNI = 10 × serum albumin (g/dL) + 0.005 × total lymphocyte count in peripheral blood (/mm^3)[29]. Finally, Pearson's correlation coefficients were calculated to evaluate the relationship between RDW and nutritional (albumin and PNI) and inflammatory (NLR and PLR) factors. All statistical tests were two-sided, and $P < 0.05$ was defined as statistically significant. SPSS version 26.0 (SPSS Inc., Chicago, IL, United States) was employed in the statistical analysis.

RESULTS

Association between pretreatment RDW and clinical features for patients who underwent LPD

Out of 804 patients, 231 (28.7%) had a higher pretreatment RDW level (≥ 15.4), including 146 males and 85 females. The clinicopathological data of the patients are shown in Table 1. Compared with those with normal pretreatment RDW, patients in the high RDW group were significantly older and had a higher ECOG score and more preoperative biliary drainage (all $P < 0.05$). Meanwhile, higher RDW was associated with lower BMI and more malignant tumors (all $P < 0.05$). There were no significant differences in sex, alcohol consumption, smoking, comorbidities, upper-abdominal operation history or American Society of Anesthesiologists status between the two groups (all $P > 0.05$). For the laboratory data, compared with those with normal pretreatment RDW, patients in the high RDW group had higher preoperative ALT, AST, ALP, GGT, TBIL, CRP, leucocyte count, platelet level, NLR, and PLR (all $P > 0.05$). Meanwhile, higher RDW was associated with lower albumin, leucocyte and lymphocyte counts, hemoglobin levels and PNI (all $P < 0.05$). There were no significant differences in PT between the two groups ($P > 0.05$).

Intra- and postoperative outcomes

The average operative time was 329.14 ± 91.77 minutes. Patients in the high RDW group had more cases of blood transfusion ($P < 0.05$), and there were no significant differences in operative time and blood loss between the two groups (Table 2, all $P > 0.05$). The postoperative outcomes were shown in Table 2. A total of 383 (47.6%) patients developed

Table 1 Baseline characteristics of patients who underwent laparoscopic pancreaticoduodenectomy, *n* (%)

Variables	Total (*n* = 804)	Red blood cell distribution width		*P* value
		< 15.4 (*n* = 573)	≥ 15.4 (*n* = 231)	
Age, years				
< 65	478 (59.5)	353 (61.6)	125 (54.1)	0.050
≥ 65	326 (40.5)	220 (38.4)	106 (45.9)	
Sex				0.325
Male	529 (65.8)	383 (66.8)	146 (63.2)	
Female	275 (34.2)	190 (33.2)	85 (36.8)	
Body mass index, kg/m^2				
< 25	500 (62.2)	341 (59.5)	159 (68.8)	0.014
≥ 25	304 (37.8)	232 (40.5)	72 (31.2)	
Drinking				0.489
No	553 (68.8)	390 (68.1)	163 (70.6)	
Yes	251 (31.2)	183 (31.9)	68 (29.4)	
Smoking				0.983
No	526 (65.4)	375 (65.4)	151 (65.4)	
Yes	278 (34.6)	198 (34.6)	80 (34.6)	
ECOG score				0.029
0-1	734 (91.3)	531 (92.7)	203 (87.9)	
2	70 (8.7)	42 (7.3)	28 (12.1)	
Comorbidity				
Hypertension	218 (27.1)	156 (27.2)	62 (26.8)	0.911
Pancreatitis	65 (8.1)	52 (9.1)	13 (5.6)	0.105
Diabetes mellitus	157(19.5)	119 (20.8)	38 (16.5)	0.162
Upper-abdominal operation history				0.717
No	759 (94.4)	542 (94.6)	217 (93.9)	
Yes	45 (5.6)	31 (5.4)	14 (6.1)	
Preoperative biliary drainage				0.009
No	682 (84.8)	498 (86.9)	184 (79.7)	
Yes	122 (15.2)	75 (13.1)	47 (20.3)	
Pathology				< 0.001
Malignant tumor	618 (76.9)	414 (72.3)	204 (88.3)	
Benign tumor	186 (23.1)	159 (27.7)	27 (11.7)	
ASA physical status				0.083
II	514 (63.9)	377 (65.8)	137 (59.3)	
III	290 (36.1)	196 (34.2)	94 (40.7)	
ALT, U/L, mean ± SD	134.91 ± 144.16	122.26 ± 134.32	166.31 ± 162.17	< 0.001
< 40	257 (32.0)	214 (37.3)	43 (18.6)	< 0.001
≥ 40	547 (68.0)	359 (62.7)	188 (81.4)	
AST, U/L, mean ± SD	104.40 ± 134.09	92.11 ± 128.77	134.89 ± 142.22	< 0.001
< 35	549 (68.3)	349 (60.9)	31 (13.4)	< 0.001
≥ 35	255 (31.7)	224 (39.1)	200 (86.6)	

ALP, U/L, mean ± SD	345.49 ± 305.36	287.75 ± 263.95	488.72 ± 351.25	< 0.001
< 140	268 (33.3)	239 (41.7)	29 (12.6)	< 0.001
≥ 140	536 (66.7)	334 (58.3)	202 (87.4)	
GGT, U/L, mean ± SD	511.57 ± 559.77	115.90 ± 529.70	667.70 ± 601.57	< 0.001
< 54	217 (27.0)	195 (34.0)	22 (9.5)	< 0.001
≥ 54	587 (73.0)	378 (66.0)	209 (90.5)	
TBIL, μmol/L, mean ± SD	125.95 ± 141.75	87.95 ± 109.20	220.19 ± 167.27	< 0.001
< 235.0	547 (68.0)	449 (78.4)	98 (42.4)	< 0.001
≥ 235.0	257 (32.0)	124 (21.6)	133 (57.6)	
Albumin, g/L, mean ± SD	39.55 ± 5.65	40.74 ± 5.28	36.60 ± 5.47	< 0.001
< 35	152 (18.9)	60 (10.5)	92 (39.8)	< 0.001
≥ 35	652 (81.1)	513 (89.5)	139 (60.2)	
CRP, mg/L, mean ± SD	12.72 ± 21.03	12.14 ± 21.65	14.14 ± 19.39	< 0.001
< 10	564 (70.1)	425 (74.2)	139 (60.2)	< 0.001
≥ 10	240 (29.9)	148 (25.8)	92 (39.8)	
PT, second, mean ± SD	12.32 ± 1.39	12.26 ± 1.32	12.47 ± 1.54	0.105
< 14	730 (90.8)	523 (91.3)	207 (89.6)	0.460
≥ 14	74 (9.2)	50 (8.7)	24 (10.4)	
Hemoglobin, g/L, mean ± SD	126.52 ± 18.88	131.65 ± 16.46	113.80 ± 18.49	< 0.001
< 115	192 (23.9)	79 (13.8)	113 (48.9)	< 0.001
≥ 115	612 (76.1)	494 (86.2)	118 (51.1)	
Leucocytes, 10^9/L, mean ± SD	6.37 ± 2.64	6.13 ± 2.43	6.96 ± 3.03	< 0.001
< 9.5	722 (89.8)	521 (90.9)	201 (87.0)	
≥ 9.5	82 (10.2)	52 (9.1)	30 (13.0)	0.097
Lymphocyte, 10^9/L, mean ± SD	1.55 ± 0.60	1.64 ± 0.59	1.33 ± 0.57	< 0.001
< 3.2	797 (99.1)	567 (99.0)	230 (99.6)	0.680 (F)
≥ 3.2	7 (0.9)	6 (1.0)	1 (0.4)	
Platelet, 10^9/L, mean ± SD	258.893 ± 88.76	249.92 ± 75.82	281.27 ± 111.84	< 0.001
< 350	698 (86.8)	518 (90.4)	180 (77.9)	< 0.001
≥ 350	106 (13.2)	55 (9.6)	51 (22.1)	
NLR, mean ± SD	3.23 ± 2.94	2.70 ± 2.46	4.54 ± 3.56	< 0.001
PLR, mean ± SD	197.51 ± 101.20	187.46 ± 95.80	222.45 ± 109.82	< 0.001
PNI, mean ± SD	46.94 ± 6.766	48.26 ± 6.35	43.69 ± 6.64	< 0.001

ECOG: Eastern Cooperative Oncology Group; ASA: American Society of Anesthesiologists; ALT: Alanine aminotransferase; AST: Aspartate aminotransferase; ALP: Alkaline phosphatase; GGT: γ-glutamyl transferase; TBIL: Total bilirubin; CRP: C-reactive protein; PT: Prothrombin time; NLR: Neutrophil-to-lymphocyte ratio; PLR: Platelet-to-lymphocyte ratio; PNI: Prognostic nutritional index.

POCs, 166 (20.6%) patients had severe POCs (CDc grade ≥ IIIa) and the postoperative mortality was 1.7% (14 patients). The average comprehensive complication index (CCI) score was 20.0 ± 25.5. Patients in the high RDW group had a higher incidence of POCs, more severe POCs, higher CCI scores and longer hospital stay (all $P < 0.05$). In addition, high RDW was associated with a higher incidence of BL, hemorrhage, POPF, intra-abdominal infection and longer hospital stay (all $P < 0.05$). There was no significant difference in DGE between the two groups ($P > 0.05$).

Risk factors for POCs after LPD and subgroup analysis

The risk factors for POCs after LPD were further explored. For any CDc grade POCs, univariate analysis showed that preoperative biliary drainage, intraoperative blood transfusion, RDW, platelet level, AST, ALT, GGT, ALP, TBIL, albumin, and CRP were potential risk factors (all $P < 0.05$, Table 3). Multivariate analysis indicated that the independent

Table 2 Surgical details and short-term outcomes of patients who underwent laparoscopic pancreatoduodenectomy, *n* (%)

Variables	Total (*n* = 804)	Red blood cell distribution		*P* value
		< 15.4 (*n* = 573)	≥ 15.4 (*n* = 231)	
Operative time, minute, mean ± SD	329.14 ± 91.77	325.39 ± 92.03	338.44 ± 90.65	0.068
Blood loss, mL, mean ± SD	156.20 ± 155.38	155.13 ± 160.75	158.85 ± 141.47	0.759
Blood transfusion				< 0.001
No	576 (71.6)	454 (79.2)	122 (52.8)	
Yes	228 (28.4)	119 (20.8)	109 (47.2)	
Postoperative morbidity				< 0.001
No	421 (52.4)	327 (57.1)	94 (40.7)	
Yes	383 (47.6)	246 (42.9)	137 (59.3)	
Any POPF	213 (26.5)	132 (23.0)	81 (35.1)	< 0.001
POPF, grade B/C	83 (10.3)	44 (7.7)	39 (16.9)	< 0.001
BL	119 (14.8)	70 (12.2)	49 (21.2)	0.001
BL, grade B/C	89 (11.1)	40 (7.0)	49 (21.2)	< 0.001
DGE	185 (23.0)	126 (22.0)	59 (25.5)	0.279
DGE, grade B/C	62 (7.7)	43 (7.5)	19 (8.2)	0.729
Hemorrhage	113 (14.1)	69 (12.0)	44 (19.0)	0.010
Hemorrhage, B/C	82 (10.2)	47 (8.2)	35 (15.2)	0.003
Intra-abdominal infection	140 (17.4)	90 (15.7)	50 (21.6)	0.045
Clavien-Dino classification				< 0.001
0	421 (52.4)	327 (57.1)	94 (40.7)	
I	53 (6.6)	38 (6.6)	15 (6.5)	
II	164 (20.4)	102 (17.8)	62 (26.8)	
IIIa	117 (14.6)	80 (14.0)	37 (16.0)	
IIIb	12 (1.5)	8 (1.4)	4 (1.7)	
IVa	16 (2.0)	11 (1.9)	5 (2.2)	
IVb	7 (0.9)	3 (0.5)	4 (1.7)	
V	14 (1.7)	4 (0.7)	10 (4.3)	
CCI score, mean ± SD	20.0 ± 25.5	17.2 ± 23.5	26.9 ± 28.9	< 0.001
< 26.2	519 (64.6)	396 (69.1)	123 (53.2)	< 0.001
≥ 26.2	285 (35.4)	177 (30.9)	108 (46.8)	
Hospital stay, day, mean ± SD	13.65 ± 11.98	13.13 ± 10.44	14.93 ± 15.09	0.027

POPF: Postoperative pancreatic fistula; BL: Bile leakage; DGE: Delayed gastric emptying; CCI: Comprehensive complication index.

risk factors for POCs were preoperative biliary drainage [hazard ratio (HR) = 2.160, 95%CI: 1.387-3.364, P = 0.001], ALP (HR = 1.979, 95%CI: 1.130-3.464, P = 0.017), RDW (HR = 2.973, 95%CI: 2.032-4.350, P < 0.001) and albumin (HR = 1.735, 95%CI: 1.130-2.662, P = 0.012) (Table 3). Furthermore, for CDc grade IIIa or higher POCs, univariate analysis showed that sex, age, ECOG score, diabetes mellitus, intraoperative blood transfusion, RDW, hemoglobin, leucocytes, AST, ALT, GGT, TBIL, albumin, and CRP were potential risk factors (all P < 0.05, Table 3). Multivariate analysis indicated that the independent risk factors for POCs were diabetes mellitus (HR = 1.773, 95%CI: 1.054-2.983, P = 0.031) and RDW (HR = 3.138 95%CI: 2.042-4.824, P < 0.001) (Table 3).

In subgroup analysis (Table 4), we found that RDW was still an independent risk factor for CDc grade IIIb or higher POCs (HR = 2.127, 95%CI: 1.116-4.055, P = 0.022) and CCI score ≥ 26.2 (HR = 1.680, 95%CI: 1.185-2.382, P = 0.004). In addition, RDW was found to be risk factors for severe BL (HR = 3.401, 95%CI: 1.979-5.845, P < 0.001), severe POPF (HR = 2.246, 95%CI: 1.320-3.820, P = 0.003) and severe hemorrhage (HR = 1.794, 95%CI: 1.050-3.063, P = 0.032). RDW was not an independent risk factor for intra-abdominal infection (HR = 1.201, 95%CI: 0.793-1.817, P = 0.387) or severe DGE (HR =

Table 3 Logistic analysis for exploration of risk factors of any postoperative complications of patients who underwent laparoscopic pancreatoduodenectomy

Variables	Univariate analysis[1]		Multivariate analysis[1]		Univariate analysis[2]		Multivariate analysis[2]	
	OR (95%CI)	*P* value	OR (95%CI)	*P* value	OR (95%CI)	*P* value	OR (95%CI)	*P* value
Sex		0.766				0.095		0.528
Male	1.000				1.000		1.000	
Female	0.957 (0.714-1.281)				0.729 (0.502-1.057)		0.872 (0.570-1.334)	
Age		0.268				0.046		0.209
< 65	1.000				1.000		1.000	
≥ 65	1.173 (0.885-1.555)				1.417 (1.006-1.998)		1.266 (0.876-1.829)	
Pathology		0.203				0.117		
Benign tumors	1.000				1.000			
Malignant tumors	1.239 (0.891-1.723)				1.411 (0.918-2.169)			
ECOG score		0.245				0.010		0.107
0-1	1.000				1.000		1.000	
2	1.339 (0.819-2.190)				2.005 (1.179-3.410)		1.637 (0.898-2.982)	
Preoperative biliary drainage		0.047				0.419		
Yes	1.000		1.000	0.001	1.000			
No	1.488 (1.005-2.205)		2.160 (1.387-3.364)		1.227 (0.747-2.017)			
Hypertension		0.510				0.802		
No	1.000				1.000			
Yes	1.110 (0.813-1.516)				1.051 (0.714-1.545)			
Diabetes mellitus		0.568				0.012		0.031
No	1.000				1.000		1.000	
Yes	1.107 (0.781-1.569)				1.887 (1.150-3.096)		1.773 (1.054-2.983)	
Pancreatitis		0.194				0.633		
No	1.000				1.000			
Yes	1.402 (0.842-2.335)				1.159 (0.633-2.119)			
Abdominal surgery history		0.276				0.170		
No	1.000				1.000			
Yes	1.400(0.765-2.564)				1.596 (0.818-3.144)			
Smoking		0.511				0.253		
No	1.000				1.000			
Yes	1.103 (0.824-1.476)				1.228 (0.863-1.747)			
Alcohol consumption		0.258				0.272		
No	1.000				1.000			
Yes	1.188 (0.881-1.602)				1.224 (0.854-1.756)			

BMI		0.115				0.271		
< 25	1.000				1.000			
≥ 25	1.259 (0.945-1.676)				1.222 (0.855-1.747)			
Operation time	1.001 (0.999-1.002)	0.484			1.001 (0.999-1.003)	0.408		
Blood loss	1.000 (0.999-1.001)	0.956			1.000 (0.998-1.001)	0.533		
Intraoperative blood transfusion		0.004		0.890		0.096		0.660
No	1.000		1.000		1.000		1.000	
Yes	1.572 (1.154-2.140)		1.025 (0.722-1.455)		1.364 (0.946-1.966)		1.102 (0.715-1.700)	
ASA score		0.475				0.496		
II	1.000				1.000			
III	1.111 (0.833-1.481)				1.130 (0.795-1.606)			
RDW		< 0.001		< 0.001		< 0.001		< 0.001
< 15.4	1.000		1.000		1.000		1.000	
≥ 15.4	3.537 (2.553-4.900)		2.973 (2.032-4.350)		3.603 (2.525-5.141)		3.138 (2.042-4.824)	
Hemoglobin, g/L		0.212				0.024		0.426
< 115	1.000				1.000		1.000	
≥ 115	0.813 (0.588-1.125)				0.647 (0.443-0.944)		0.823 (0.509-1.331)	
Leucocytes, 10^9/L		0.250				0.047		0.533
< 9.5	1.000				1.000		1.000	
≥ 9.5	1.308 (0.827-2.068)				1.675 (1.006-2.789)		1.198 (0.679-2.113)	
Platelet, 10^9/L		0.003		0.093		0.996		
< 350	1.000		1.000		1.000			
≥ 350	1.894 (1.247-2.878)		1.493 (0.935-2.383)		1.001 (0.605-1.657)			
Lymphocyte, 10^9/L		0.225				0.612		
< 3.2	1.000				1.000			
≥ 3.2	2.771 (0.534-14.368)				1.532 (0.295-7.968)			
AST, U/L		0.002		0.190		0.016		0.649
< 35	1.000		1.000		1.000		1.000	
≥ 35	1.610 (1.191-2.177)		1.617 (0.788-3.320)		1.618 (1.094-2.393)		1.229 (0.505-2.991)	
ALT, U/L		0.042		0.731		0.035		0.651
< 40	1.000		1.000		1.000		1.000	
≥ 40	1.363 (1.011-1.837)		1.140 (0.541-2.403)		1.516 (1.031-2.231)		1.226 (0.508-2.959)	
GGT, U/L		0.004		0.186		0.006		0.454
< 45	1.000		1.000		1.000		1.000	
≥ 45	1.601 (1.166-2.199)		1.511 (0.820-2.785)		1.809 (1.182-2.770)		1.335 (0.626-2.848)	
ALP, U/L		0.058		0.017		0.220		

< 140	1.000		1.000		1.000			
≥ 140	1.330 (0.990-1.787)		1.979 (1.130-3.464)		1.262 (0.871-1.829)			
TBIL, umol/L		0.002		0.624		< 0.001		0.152
< 235	1.000		1.000		1.000		1.000	
≥ 235	1.605 (1.191-2.163)		1.099 (0.754-1.601)		2.172 (1.531-3.082)		1.551 (0.850-2.829)	
Albumin, g/L		< 0.001		0.012		< 0.001		0.149
≥ 35	1.000		1.000		1.000		1.000	
< 35	2.598 (1.794-3.764)		1.735 (1.130-2.662)		2.628 (1.781-3.879)		1.417 (0.883-2.274)	
CRP, mg/L		0.002		0.197		0.001		0.205
< 10	1.000		1.000		1.000		1.000	
≥ 10	1.599 (1.180-2.168)		1.265 (0.885-1.807)		1.797 (1.260-2.564)		1.308 (0.863-1.983)	
PT, second		0.760				0.277		
< 14	1.000				1.000			
≥ 14	0.928 (0.574-1.499)				0.736 (0.424-1.278)			

[1]Any morbidity, Clavien-Dino classification grade I or higher.

[2]Severe morbidity, Clavien-Dino classification grade IIIa or higher.

OR: Odds ratio; CI: Confidence interval; ECOG: Eastern Cooperative Oncology Group; BMI: Body mass index; ASA: American Society of Anesthesiologists; RDW: Red blood cell distribution width; ALT: Alanine aminotransferase; AST: Aspartate aminotransferase; ALP: Alkaline phosphatase; GGT: γ-glutamyl transferase; TBIL: Total bilirubin; CRP: C-reactive protein; PT: Prothrombin time.

1.130, 95%CI: 0.573-2.226, P = 0.725).

Relationship between red blood cell width distribution and nutritional and inflammatory factors

Previous studies demonstrated that RDW was an indicator of inflammation and malnutrition. We postulated that systemic inflammation and malnutrition might be involved in the high RDW of these patients. Consequently, the relationship between RDW and PNI, albumin, NLR and PLR was analyzed. As shown in Figure 1, higher RDW was positively associated with NLR (r^2 = 0.258, P < 0.001) and PLR (r^2 = 0.359, P < 0.001) and was negatively associated with albumin (r^2 = -0.440, P < 0.001) and PNI (r^2 = -0.442, P < 0.001).

DISCUSSION

The high incidence of POCs after LPD is one of the main concerns of surgeons, and exploring the risk factors for POCs is thus vitally important. In this study, we found that higher RDW at the time of admission was associated with poorer short-term outcomes after LPD. In the subgroup analysis, high pretreatment RDW was still an independent risk factor for severe POCs and specific types of POCs. In addition, RDW was found to be associated with nutritional and inflammatory markers, including PNI, albumin, PLR, and NLR, which indicated that it could be a surrogate biomarker for nutritional and inflammatory markers in predicting the development of POCs after surgery.

RDW, reflecting the degree of heterogeneity of erythrocyte volume, is a simple and easily obtained parameter that is conventionally used in estimating the pathogenesis of anemia[16]. Nevertheless, recent evidence revealed that RDW was associated with the development and progression of multiple diseases[16]. RDW was associated with mortality of cardiovascular diseases, including coronary artery disease, coronary artery ectasia, atrial fibrillation, *etc.*[30]. RDW could be a prognostic factor for various gastrointestinal cancers, including colorectal cancer[31], pancreatic cancer[32] and gastric cancer[33]. However, only a few studies have focused on the relationship between RDW and short-term outcomes after surgery. Aali-Rezaie *et al*[34] revealed that a higher preoperative RDW was associated with mortality, any in-hospital medical complications and readmission following revision arthroplasty. Higher RDW was also found to be associated with a higher prevalence of systemic morbidity after laryngectomy[35]. For gastrointestinal surgery, higher pretreatment RDW was reported to be a risk factor for POCs after esophagectomy[21] and hepatectomy[36], and no earlier studies have reported the association between high pretreatment RDW and short-term outcomes after LPD. In this study, using a large cohort of patients, we demonstrated that higher pretreatment RDW was associated with poorer short-term outcomes after LPD.

Table 4 Subgroup analysis of risk factors for the development of postoperative complications of grades IIIa or higher, grades IIIb or higher according to the Clavien-Dino classification, and specific types of postoperative complications, including severe bile leakage, severe postoperative pancreatic fistula, delayed gastric emptying, hemorrhage, and intra-abdominal infection in patients who underwent laparoscopic pancreatoduodenectomy

POCs	Variables	Univariate analysis		Multivariate analysis	
		OR (95%CI)	*P* value	OR (95%CI)	*P* value
CDc grade IIIb or higher	ECOG score, 2 *vs* 0-1	3.415 (1.659-7.028)	0.001	4.169 (1.895-9.174)	< 0.001
	Preoperative biliary drainage, yes *vs* no	0.225 (0.054-0.940)	0.041	0.138 (0.032-0.600)	0.008
	Smoking, yes *vs* no	1.735 (0.970-3.101)	0.063	1.496 (0.727-3.079)	0.274
	Drinking, yes *vs* no	1.712 (0.952-3.078)	0.072	1.650 (0.791-3.440)	0.182
	ALP, ≥ 140 U/L *vs* < 140 U/L	1.783 (0.896-3.546)	0.099	1.614 (0.717-3.634)	0.247
	RDW, ≥ 15.4 *vs* < 15.4	2.326 (1.298-4.169)	0.005	2.127 (1.116-4.055)	0.022
	Lymphocyte, ≥ 3.2 × 10^9/L *vs* < 3.2 × 10^9/L	6.383 (1.206-33.775)	0.029	6.536 (1.068-39.978)	0.042
	CRP, ≥ 10 mg/L *vs* < 10 mg/L	1.836 (1.020-3.302)	0.043	1.400 (0.741-2.646)	0.300
Severe POPF (grade B and C)	Age, ≥ 65 years *vs* < 65 years	1.756 (1.113-2.772)	0.016	1.435 (0.889-2.316)	0.139
	ECOG score, 2 *vs* 0-1	2.671 (1.433-4.981)	0.002	2.878 (1.435-5.774)	0.003
	Operative time	0.997 (0.994-1.000)	0.026	0.996 (0.993-0.999)	0.006
	RDW, ≥ 15.4 *vs* < 15.4	2.442 (1.539-3.875)	< 0.001	2.246 (1.320-3.820)	0.003
	Hemoglobin, ≥ 115 g/L *vs* < 115 g/L	0.544 (0.335-0.882)	0.014	0.856 (0.495-1.481)	0.579
	Leucocytes, ≥ 9.5 × 10^9/L *vs* < 9.5 × 10^9/L	1.755 (0.924-3.334)	0.086	1.609 (0.815-3.177)	0.170
	Albumin, < 35 g/L *vs* ≥ 35 g/L	1.885 (1.130-3.143)	0.015	1.153 (0.641-2.074)	0.643
	PT, ≥ 14 seconds *vs* < 14 seconds	0.343 (0.106-1.115)	0.075	0.229 (0.067-0.783)	0.019
Severe BL	Diabetes mellitus, yes *vs* no	3.110 (1.408-6.870)	0.005	2.484 (1.105-5.583)	0.028
	Smoking, yes *vs* no	2.010 (1.289-3.133)	0.002	1.660 (0.959-2.874)	0.070
	Drinking, yes *vs* no	1.580 (1.005-2.484)	0.048	1.200 (0.687-2.097)	0.522
	BMI ≥ 24 kg/m^2 *vs* < 24 kg/m^2	2.442 (1.439-4.143)	0.001	1.988 (1.143-3.456)	0.015
	Intra-operative blood transfusion, yes *vs* no	1.660 (1.050-2.625)	0.030	1.210 (0.707-2.072)	0.487
	RDW, ≥ 15.4 *vs* < 15.4	3.587 (2.287-5.628)	< 0.001	3.401 (1.979-5.845)	< 0.001
	Hemoglobin, ≥ 115 g/L *vs* < 115 g/L	0.648 (0.401-1.048)	0.077	0.824 (0.448-1.515)	0.533
	TBIL, ≥ 235 μmol/L *vs* < 235 μmol/L	2.188 (1.402-3.417)	0.001	1.326 (0.776-2.264)	0.302
	Albumin, < 35 g/L *vs* ≥ 35 g/L	2.326 (1.434-3.774)	0.001	1.290 (0.721-2.309)	0.391
	CRP, ≥ 10 mg/L *vs* < 10 mg/L	1.527 (0.967-2.413)	0.069	1.138 (0.679-1.907)	0.623
Severe hemorrhage	ECOG score, 2 *vs* 0-1	2.715 (1.455-5.066)	0.002	2.832 (1.447-5.540)	0.002
	Smoking, yes *vs* no	1.937 (1.223-3.068)	0.005	1.437 (0.820-2.517)	0.206
	Drinking, yes *vs* no	2.064 (1.299-3.278)	0.002	1.858 (1.047-3.297)	0.034
	RDW, ≥ 15.4 *vs* < 15.4	1.998 (1.252-3.189)	0.004	1.794 (1.050-3.063)	0.032
	GGT, ≥ 45 U/L *vs* < 45 U/L	1.735 (0.969-3.108)	0.064	1.215 (0.640-2.307)	0.551
	Albumin, < 35 g/L *vs* ≥ 35 g/L	1.792 (1.067-3.008)	0.027	1.022 (0.559-1.869)	0.944
	CRP, ≥ 10 mg/L *vs* < 10 mg/L	1.582 (0.986-2.536)	0.057	1.181 (0.699-1.997)	0.534

Intra-abdominal infection	Age, ≥ 65 *vs* < 65	1.539 (1.067-2.220)	0.021	1.363 (0.928-2.001)	0.114
	ECOG score, 2 *vs* 0-1	1.887 (1.076-3.310)	0.027	1.725 (0.957-3.109)	0.070
	Hypertension, yes *vs* no	1.577 (1.069-2.326)	0.022	1.365 (0.909-2.052)	0.134
	Drinking, yes *vs* no	1.603 (1.100-2.338)	0.014	1.556 (1.052-2.301)	0.027
	RDW, ≥ 15.4 *vs* < 15.4	1.483 (1.008-2.180)	0.045	1.201 (0.793-1.817)	0.387
	Leucocytes, ≥ 9.5 × 10^9/L *vs* < 9.5 × 10^9/L	1.618 (0.942-2.779)	0.081	1.247 (0.703-1.817)	0.450
	TBIL, ≥ 235 μmol/L *vs* < 235 μmol/L	1.426 (0.977-2.081)	0.066	1.585 (1.027-2.446)	0.038
	CRP, ≥ 10 mg/L *vs* < 10 mg/L	1.675 (1.147-2.448)	0.008	1.304 (0.868-1.960)	0.202
Severe DGE	Pathology, malignant tumors *vs* benign tumors	1.652 (0.944-2.892)	0.079	1.058 (0.548-2.042)	0.886
	Preoperative biliary drainage, yes *vs* no	0.365 (0.130-1.024)	0.055	0.421 (0.144-1.236)	0.155
	Pancreatitis, yes *vs* no	2.748 (1.354-5.578)	0.005	2.555 (1.158-5.639)	0.020
	Intra-operative blood transfusion, yes *vs* no	1.931 (1.137-3.279)	0.015	1.667 (0.901-3.082)	0.103
	ASA, III *vs* I-II	1.683 (0.935-3.031)	0.083	1.893 (1.028-3.487)	0.041
	RDW, ≥ 15.4 *vs* < 15.4	1.105 (0.629-1.940)	0.729	1.130 (0.573-2.226)	0.725
	Operative time	1.003 (1.000-1.005)	0.028	1.002 (0.999-1.005)	0.212
	Lymphocyte, ≥ 3.2 × 10^9/L *vs* < 3.2 × 10^9/L	4.913 (0.933-25.861)	0.060	4.019 (0.696-23.193)	0.120
	ALP, ≥ 140 U/L *vs* < 140 U/L	2.131 (1.265-3.588)	0.004	2.913 (1.538-5.518)	0.001
	Albumin, < 35 g/L *vs* ≥ 35 g/L	2.201 (1.251-3.871)	0.006	3.065 (1.568-5.992)	0.001
CCI ≥ 26.2	Intra-operative blood transfusion, yes *vs* no	1.489(1.087-2.041)	0.013	1.150 (0.816-1.621)	0.425
	Preoperative biliary drainage, yes *vs* no	0.695 (0.456-1.060)	0.091	0.573 (0.368-0.891)	0.014
	RDW, ≥ 15.4 *vs* < 15.4	1.964 (1.436-2.687)	< 0.001	1.680 (1.185-2.382)	0.004
	Leucocytes, ≥ 9.5 × 10^9/L *vs* < 9.5 × 10^9/L	1.854 (1.171-2.936)	0.008	1.740 (1.076-2.815)	0.024
	Albumin, < 35 g/L *vs* ≥ 35 g/L	1.918 (1.341-2.743)	< 0.001	1.511 (1.017-2.244)	0.041
	Platelet, ≥ 350 × 10^9/L *vs* 350 × 10^9/L	1.472 (0.973-2.229)	0.067	1.241 (0.798-1.930)	0.337

POCs: Postoperative complications; OR: Odds ratio; CI: Confidence interval; CDc: Clavien-Dino classification; ECOG: Eastern Cooperative Oncology Group; BMI: Body mass index; ASA: American Society of Anesthesiologists; RDW: Red blood cell distribution width; ALT: Alanine aminotransferase; AST: Aspartate aminotransferase; ALP: Alkaline phosphatase; GGT: γ-glutamyl transferase; TBIL: Total bilirubin; CRP: C-reactive protein; PT: Prothrombin time; POPF: Postoperative pancreatic fistula; BL: Bile leakage; DGE: Delayed gastric emptying; CCI: Comprehensive complication index.

The underlying mechanisms of the negative impact of RDW on short-term outcomes after surgery have not been fully elucidated. Actually, it is not clear whether RDW is a "cause" or just an "effect" of POCs. Several factors could lead to higher RDW, including nutritional deficiencies, shortening of telomere length, oxidative stress, inflammation, venous thromboembolism and increased erythrocyte mechanical fragility. Some of these conditions were also risk factors for the development of POCs after surgery. Malnutrition, such as iron and folic acid deficiency, could induce increased RDW by impairing the production and survival of erythrocytes[37]. Inflammation could lead to higher RDW by inhibiting the synthesis or activity of erythropoietin, lowering erythrocyte survival and impairing iron metabolism[16]. Short or critically short telomeres could induce increased RDW by causing cell senescence of the hematopoietic progenitors, which could lead to impaired maturation and increased replicative stress of the erythroid lineage[38]. Recently, the impact of red blood cell biology on the development of nonhematological disorders has also been reported, especially in cardiovascular disorders. It was reported that anisocytosis could accelerate atherogenesis by promoting the expansion of the lipid core and the ulceration of the fibrous cap, inhibiting endothelium-dependent nitric oxide-mediated vasodilation, increasing blood viscosity and impairing blood flow[39-41]. However, few studies have reported the potential causal association between anisocytosis and other noncardiovascular disorders, and the pathophysiological mechanisms for the impact of RDW on the development of these disorders cannot be fully explained at this point in time. Further studies are

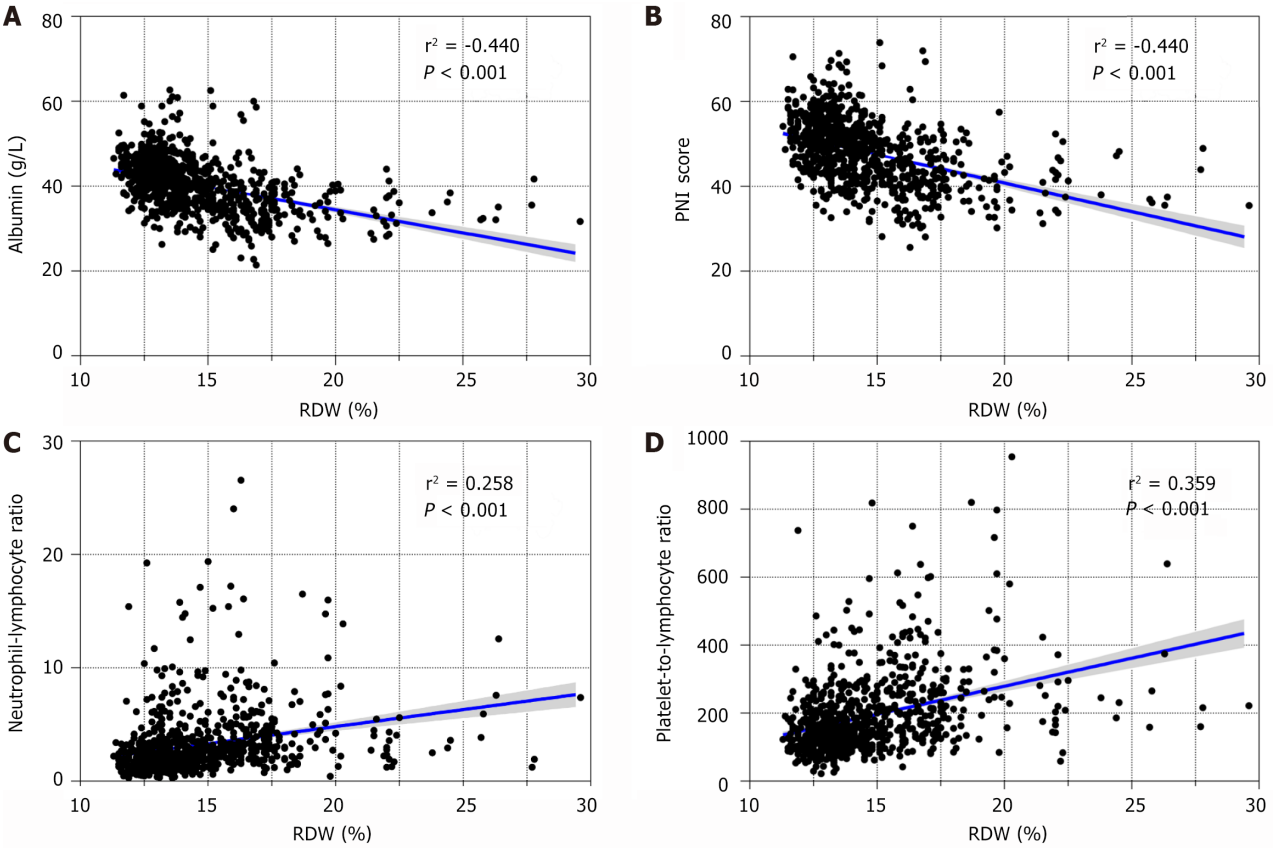

Figure 1 Relationship between pretreatment red blood cell distribution width and nutritional and inflammatory status. A-D: Negative correlation between pretreatment red cell distribution width and albumin (r^2 = -0.440, P < 0.001) (A) and prognostic nutritional index (r^2 = -0.442, P < 0.001) (B); and positive correlation between pretreatment red cell distribution width and neutrophil-to-lymphocyte ratio (r^2 = 0.258, P < 0.001) (C) and platelet-to-lymphocyte ratio (r^2 = 0.359, P < 0.001) (D) in peripheral blood in patients who underwent laparoscopic pancreatoduodenectomy. RDW: Red cell distribution width; PNI: Prognostic nutritional index.

needed to elucidate the potential mechanisms.

Nutritional (*e.g.*, albumin level, BMI and PNI) and inflammatory factors (*e.g.*, PLR, NLR, and CRP) have been demonstrated to be closely associated with the development of POCs after operation and could be predictive markers for POCs[42-44]. RDW was considered to be a general health status and could be a reflection of nutritional and inflammatory status. Consequently, the association between RDW and nutritional and inflammatory status was further explored in our study. We found that higher RDW was associated with higher preoperative CRP, platelet level, NLR and PLR, while it was associated with lower albumin and hemoglobin level. Meanwhile, line regression analysis showed that higher pretreatment RDW was associated with malnutrition (lower albumin and PNI) and severe inflammatory status (higher NLR and PLR). These results support that RDW could be a reflection of patients' preoperative nutritional and inflammatory status and affect short-term outcomes after LPD. Consequently, RDW may be regarded as a surrogate marker of nutritional and inflammatory factors in selecting patients who are at high risk of developing POCs after surgery.

The strength of our study was its large sample size of patients who underwent LPD. However, our study has several limitations worth noting. First, this was a retrospective study from a single institution. Although comprehensive statistical analysis was performed to improve the reliability of our findings, the results may still be influenced by selection bias, and there was a lack of external validation for them. In addition, the patients included in this study were selected from a relatively long study period, and the improvement of treatment strategy and perioperative management could lead to a historical bias.

CONCLUSION

In conclusion, this study found that elevated pretreatment RDW was a special parameter for patients who underwent LPD. It was associated with malnutrition, severe inflammatory status and poorer short-term outcomes. RDW could be a surrogate marker for nutritional and inflammatory status in identifying patients who were at high risk of developing POCs after LPD. However, further multi-institution, international studies with a larger cohort should be conducted to consolidate our findings.

FOOTNOTES

Author contributions: Liu J and Zheng SZ conceived the article; Cao XR, Xu YL, and Chai JW performed all the operations; Zheng K collected the data; Zheng K and Kong JJ provided data management and analysis support. All authors contributed to the article and approved the submitted version.

Supported by the National Natural Science Foundation of China, No. 81302124.

Institutional review board statement: This study obtained ethics approval from the ethics committee of Shandong Provincial Hospital Affiliated to Shandong First Medical University and was performed in accordance with the Declaration of Helsinki (No. 2024-498). All patients signed an informed consent form.

Informed consent statement: Patients were not required to give informed consent to the study because the analysis used anonymous data that were obtained after each patient agreed to treatment by written consent.

Conflict-of-interest statement: All the authors report no relevant conflicts of interest for this article.

Data sharing statement: No additional data are available.

STROBE statement: The authors have read the STROBE Statement-checklist of items, and the manuscript was prepared and revised according to the STROBE Statement-checklist of items.

Country of origin: China

ORCID number: Jun Liu 0000-0003-4707-7286; Shun-Zhen Zheng 0000-0002-3028-3430.

S-Editor: Wang JJ
L-Editor: A
P-Editor: Zhang XD

REFERENCES

1 **Wang M**, Li D, Chen R, Huang X, Li J, Liu Y, Liu J, Cheng W, Chen X, Zhao W, Li J, Tan Z, Huang H, Li D, Zhu F, Qin T, Ma J, Yu G, Zhou B, Zheng S, Tang Y, Han W, Meng L, Ke J, Feng F, Chen B, Yin X, Chen W, Ma H, Xu J, Liu Y, Lin R, Dong Y, Yu Y, Liu J, Zhang H, Qin R; Minimally Invasive Treatment Group in the Pancreatic Disease Branch of China's International Exchange and Promotion Association for Medicine and Healthcare (MITG-P-CPAM). Laparoscopic versus open pancreatoduodenectomy for pancreatic or periampullary tumours: a multicentre, open-label, randomised controlled trial. *Lancet Gastroenterol Hepatol* 2021; **6**: 438-447 [PMID: 33915091 DOI: 10.1016/S2468-1253(21)00054-6]

2 **Lof S**, Vissers FL, Klompmaker S, Berti S, Boggi U, Coratti A, Dokmak S, Fara R, Festen S, D'Hondt M, Khatkov I, Lips D, Luyer M, Manzoni A, Rosso E, Saint-Marc O, Besselink MG, Abu Hilal M; European consortium on Minimally Invasive Pancreatic Surgery (E-MIPS). Risk of conversion to open surgery during robotic and laparoscopic pancreatoduodenectomy and effect on outcomes: international propensity score-matched comparison study. *Br J Surg* 2021; **108**: 80-87 [PMID: 33640946 DOI: 10.1093/bjs/znaa026]

3 **Song KB**, Kim SC, Lee W, Hwang DW, Lee JH, Kwon J, Park Y, Lee SJ, Park G. Laparoscopic pancreaticoduodenectomy for periampullary tumors: lessons learned from 500 consecutive patients in a single center. *Surg Endosc* 2020; **34**: 1343-1352 [PMID: 31214805 DOI: 10.1007/s00464-019-06913-9]

4 **Wang M**, Peng B, Liu J, Yin X, Tan Z, Liu R, Hong D, Zhao W, Wu H, Chen R, Li D, Huang H, Miao Y, Liu Y, Liang T, Wang W, Cai Y, Xing Z, Cheng W, Zhong X, Zhao Z, Zhang J, Yang Z, Li G, Shao Y, Lin G, Jiang K, Wu P, Jia B, Ma T, Jiang C, Peng S, Qin R. Practice Patterns and Perioperative Outcomes of Laparoscopic Pancreaticoduodenectomy in China: A Retrospective Multicenter Analysis of 1029 Patients. *Ann Surg* 2021; **273**: 145-153 [PMID: 30672792 DOI: 10.1097/SLA.0000000000003190]

5 **Werdelin L**, Boysen G, Jensen TS, Mogensen P. Immunosuppressive treatment of patients with amyotrophic lateral sclerosis. *Acta Neurol Scand* 1990; **82**: 132-134 [PMID: 2256442 DOI: 10.1111/j.1600-0404.1990.tb01602.x]

6 **Nathan H**, Atoria CL, Bach PB, Elkin EB. Hospital volume, complications, and cost of cancer surgery in the elderly. *J Clin Oncol* 2015; **33**: 107-114 [PMID: 25422483 DOI: 10.1200/JCO.2014.57.7155]

7 **Kong J**, Li G, Chai J, Yu G, Liu Y, Liu J. Impact of Postoperative Complications on Long-Term Survival After Resection of Hepatocellular Carcinoma: A Systematic Review and Meta-Analysis. *Ann Surg Oncol* 2021; **28**: 8221-8233 [PMID: 34160708 DOI: 10.1245/s10434-021-10317-2]

8 **Fernández-Moreno MC**, Dorcaratto D, Garcés-Albir M, Muñoz E, Arvizu R, Ortega J, Sabater L. Impact of type and severity of postoperative complications on long-term outcomes after colorectal liver metastases resection. *J Surg Oncol* 2020; **122**: 212-225 [PMID: 32335938 DOI: 10.1002/jso.25946]

9 **Braga M**, Capretti G, Pecorelli N, Balzano G, Doglioni C, Ariotti R, Di Carlo V. A prognostic score to predict major complications after pancreaticoduodenectomy. *Ann Surg* 2011; **254**: 702-7; discussion 707 [PMID: 22042466 DOI: 10.1097/SLA.0b013e31823598fb]

10 **Joliat GR**, Petermann D, Demartines N, Schäfer M. Prediction of Complications After Pancreaticoduodenectomy: Validation of a

Postoperative Complication Score. *Pancreas* 2015; **44**: 1323-1328 [PMID: 26465955 DOI: 10.1097/MPA.0000000000000399]

11 **Matsuda T**, Umeda Y, Matsuda T, Endo Y, Sato D, Kojima T, Sui K, Inagaki M, Ota T, Hioki M, Oishi M, Kimura M, Murata T, Ishido N, Yagi T, Fujiwara T. Preoperative prognostic nutritional index predicts postoperative infectious complications and oncological outcomes after hepatectomy in intrahepatic cholangiocarcinoma. *BMC Cancer* 2021; **21**: 708 [PMID: 34130648 DOI: 10.1186/s12885-021-08424-0]

12 **Shiihara M**, Higuchi R, Izumo W, Yazawa T, Uemura S, Furukawa T, Yamamoto M. Impact of the controlling nutritional status score on severe postoperative complications of pancreaticoduodenectomy for pancreatic cancer. *Langenbecks Arch Surg* 2021; **406**: 1491-1498 [PMID: 33791827 DOI: 10.1007/s00423-021-02151-7]

13 **Dan Zeng CD**, Tong YX, Xiao AT, Gao C, Zhang S. Peripheral Lymphocyte Subsets Absolute Counts as Feasible Clinical Markers for Predicting Surgical Outcome in Gastric Cancer Patients After Laparoscopic D2 Gastrectomy: A Prospective Cohort Study. *J Inflamm Res* 2021; **14**: 5633-5646 [PMID: 34744447 DOI: 10.2147/JIR.S335847]

14 **Nishida Y**, Kato Y, Kudo M, Aizawa H, Okubo S, Takahashi D, Nakayama Y, Kitaguchi K, Gotohda N, Takahashi S, Konishi M. Preoperative Sarcopenia Strongly Influences the Risk of Postoperative Pancreatic Fistula Formation After Pancreaticoduodenectomy. *J Gastrointest Surg* 2016; **20**: 1586-1594 [PMID: 27126054 DOI: 10.1007/s11605-016-3146-7]

15 **Lee B**, Han HS, Yoon YS, Cho JY, Lee JS. Impact of preoperative malnutrition, based on albumin level and body mass index, on operative outcomes in patients with pancreatic head cancer. *J Hepatobiliary Pancreat Sci* 2021; **28**: 1069-1075 [PMID: 33128839 DOI: 10.1002/jhbp.858]

16 **Salvagno GL**, Sanchis-Gomar F, Picanza A, Lippi G. Red blood cell distribution width: A simple parameter with multiple clinical applications. *Crit Rev Clin Lab Sci* 2015; **52**: 86-105 [PMID: 25535770 DOI: 10.3109/10408363.2014.992064]

17 **Li N**, Zhou H, Tang Q. Red Blood Cell Distribution Width: A Novel Predictive Indicator for Cardiovascular and Cerebrovascular Diseases. *Dis Markers* 2017; **2017**: 7089493 [PMID: 29038615 DOI: 10.1155/2017/7089493]

18 **Hong N**, Kim CO, Youm Y, Choi JY, Kim HC, Rhee Y. Elevated Red Blood Cell Distribution Width Is Associated with Morphometric Vertebral Fracture in Community-Dwelling Older Adults, Independent of Anemia, Inflammation, and Nutritional Status: The Korean Urban Rural Elderly (KURE) Study. *Calcif Tissue Int* 2019; **104**: 26-33 [PMID: 30159752 DOI: 10.1007/s00223-018-0470-9]

19 **Moreno-Torres V**, Royuela A, Múñez-Rubio E, Gutierrez-Rojas Á, Mills-Sánchez P, Ortega A, Tejado-Bravo S, García-Sanz J, Muñoz-Serrano A, Calderón-Parra J, Fernández-Cruz A, Ramos-Martínez A. Red blood cell distribution width as prognostic factor in sepsis: A new use for a classical parameter. *J Crit Care* 2022; **71**: 154069 [PMID: 35667275 DOI: 10.1016/j.jcrc.2022.154069]

20 **Wang ZH**, Fu BQ, Lin YW, Wei XB, Geng H, Guo WX, Yuan HQ, Liao YW, Qin TH, Li F, Wang SH. Red blood cell distribution width: A severity indicator in patients with COVID-19. *J Med Virol* 2022; **94**: 2133-2138 [PMID: 35048392 DOI: 10.1002/jmv.27602]

21 **Yoshida N**, Horinouchi T, Toihata T, Harada K, Eto K, Sawayama H, Iwatsuki M, Nagai Y, Ishimoto T, Baba Y, Miyamoto Y, Baba H. Clinical Significance of Pretreatment Red Blood Cell Distribution Width as a Predictive Marker for Postoperative Morbidity After Esophagectomy for Esophageal Cancer: A Retrospective Study. *Ann Surg Oncol* 2022; **29**: 606-613 [PMID: 34467503 DOI: 10.1245/s10434-021-10719-2]

22 **Poz D**, De Falco E, Pisano C, Madonna R, Ferdinandy P, Balistreri CR. Diagnostic and Prognostic Relevance of Red Blood Cell Distribution Width for Vascular Aging and Cardiovascular Diseases. *Rejuvenation Res* 2019; **22**: 146-162 [PMID: 30132390 DOI: 10.1089/rej.2018.2094]

23 **Clavien PA**, Barkun J, de Oliveira ML, Vauthey JN, Dindo D, Schulick RD, de Santibañes E, Pekolj J, Slankamenac K, Bassi C, Graf R, Vonlanthen R, Padbury R, Cameron JL, Makuuchi M. The Clavien-Dindo classification of surgical complications: five-year experience. *Ann Surg* 2009; **250**: 187-196 [PMID: 19638912 DOI: 10.1097/SLA.0b013e3181b13ca2]

24 **Slankamenac K**, Nederlof N, Pessaux P, de Jonge J, Wijnhoven BP, Breitenstein S, Oberkofler CE, Graf R, Puhan MA, Clavien PA. The comprehensive complication index: a novel and more sensitive endpoint for assessing outcome and reducing sample size in randomized controlled trials. *Ann Surg* 2014; **260**: 757-62; discussion 762 [PMID: 25379846 DOI: 10.1097/SLA.0000000000000948]

25 **Wente MN**, Bassi C, Dervenis C, Fingerhut A, Gouma DJ, Izbicki JR, Neoptolemos JP, Padbury RT, Sarr MG, Traverso LW, Yeo CJ, Büchler MW. Delayed gastric emptying (DGE) after pancreatic surgery: a suggested definition by the International Study Group of Pancreatic Surgery (ISGPS). *Surgery* 2007; **142**: 761-768 [PMID: 17981197 DOI: 10.1016/j.surg.2007.05.005]

26 **Wente MN**, Veit JA, Bassi C, Dervenis C, Fingerhut A, Gouma DJ, Izbicki JR, Neoptolemos JP, Padbury RT, Sarr MG, Yeo CJ, Büchler MW. Postpancreatectomy hemorrhage (PPH): an International Study Group of Pancreatic Surgery (ISGPS) definition. *Surgery* 2007; **142**: 20-25 [PMID: 17629996 DOI: 10.1016/j.surg.2007.02.001]

27 **Koch M**, Garden OJ, Padbury R, Rahbari NN, Adam R, Capussotti L, Fan ST, Yokoyama Y, Crawford M, Makuuchi M, Christophi C, Banting S, Brooke-Smith M, Usatoff V, Nagino M, Maddern G, Hugh TJ, Vauthey JN, Greig P, Rees M, Nimura Y, Figueras J, DeMatteo RP, Büchler MW, Weitz J. Bile leakage after hepatobiliary and pancreatic surgery: a definition and grading of severity by the International Study Group of Liver Surgery. *Surgery* 2011; **149**: 680-688 [PMID: 21316725 DOI: 10.1016/j.surg.2010.12.002]

28 **Buettner S**, Spolverato G, Kimbrough CW, Alexandrescu S, Marques HP, Lamelas J, Aldrighetti L, Gamblin TC, Maithel SK, Pulitano C, Weiss M, Bauer TW, Shen F, Poultsides GA, Marsh JW, IJzermans JNM, Koerkamp BG, Pawlik TM. The impact of neutrophil-to-lymphocyte ratio and platelet-to-lymphocyte ratio among patients with intrahepatic cholangiocarcinoma. *Surgery* 2018; **164**: 411-418 [PMID: 29903509 DOI: 10.1016/j.surg.2018.05.002]

29 **Kubota K**, Ito R, Narita N, Tanaka Y, Furudate K, Akiyama N, Chih CH, Komatsu S, Kobayashi W. Utility of prognostic nutritional index and systemic immune-inflammation index in oral cancer treatment. *BMC Cancer* 2022; **22**: 368 [PMID: 35392843 DOI: 10.1186/s12885-022-09439-x]

30 **Xanthopoulos A**, Giamouzis G, Dimos A, Skoularigki E, Starling RC, Skoularigis J, Triposkiadis F. Red Blood Cell Distribution Width in Heart Failure: Pathophysiology, Prognostic Role, Controversies and Dilemmas. *J Clin Med* 2022; **11** [PMID: 35407558 DOI: 10.3390/jcm11071951]

31 **Cheng KC**, Lin YM, Liu CC, Wu KL, Lee KC. High Red Cell Distribution Width Is Associated with Worse Prognosis in Early Colorectal Cancer after Curative Resection: A Propensity-Matched Analysis. *Cancers (Basel)* 2022; **14** [PMID: 35205691 DOI: 10.3390/cancers14040945]

32 **Dang C**, Wang M, Qin T, Qin R. Clinical importance of preoperative red-cell volume distribution width as a prognostic marker in patients undergoing radical surgery for pancreatic cancer. *Surg Today* 2022; **52**: 465-474 [PMID: 34524510 DOI: 10.1007/s00595-021-02374-7]

33 **Saito H**, Shimizu S, Shishido Y, Miyatani K, Matsunaga T, Fujiwara Y. Prognostic significance of the combination of preoperative red cell distribution width and platelet distribution width in patients with gastric cancer. *BMC Cancer* 2021; **21**: 1317 [PMID: 34879841 DOI: 10.1186/s12885-021-09043-5]

34 **Aali-Rezaie A**, Alijanipour P, Shohat N, Vahedi H, Foltz C, Parvizi J. Red Cell Distribution Width: An Unacknowledged Predictor of

Mortality and Adverse Outcomes Following Revision Arthroplasty. *J Arthroplasty* 2018; **33**: 3514-3519 [PMID: 30072185 DOI: 10.1016/j.arth.2018.06.035]

35 **Marcus K**, Sullivan CB, Al-Qurayshi Z, Buchakjian MR. Can Red Blood Cell Distribution Width Predict Laryngectomy Complications or Survival Outcomes? *Ann Otol Rhinol Laryngol* 2022; **131**: 1102-1108 [PMID: 34715735 DOI: 10.1177/00034894211056117]

36 **Chen Q**, Mao R, Zhao J, Bi X, Li Z, Huang Z, Zhang Y, Zhou J, Zhao H, Cai J. Nomograms incorporating preoperative RDW level for the prediction of postoperative complications and survival in colorectal liver metastases after resection. *Ann Palliat Med* 2021; **10**: 4143-4158 [PMID: 33832316 DOI: 10.21037/apm-20-2418]

37 **Sun H**, Weaver CM. Decreased Iron Intake Parallels Rising Iron Deficiency Anemia and Related Mortality Rates in the US Population. *J Nutr* 2021; **151**: 1947-1955 [PMID: 33834234 DOI: 10.1093/jn/nxab064]

38 **Xi H**, Li C, Ren F, Zhang H, Zhang L. Telomere, aging and age-related diseases. *Aging Clin Exp Res* 2013; **25**: 139-146 [PMID: 23739898 DOI: 10.1007/s40520-013-0021-1]

39 **Rezende SM**, Lijfering WM, Rosendaal FR, Cannegieter SC. Hematologic variables and venous thrombosis: red cell distribution width and blood monocyte count are associated with an increased risk. *Haematologica* 2014; **99**: 194-200 [PMID: 23894011 DOI: 10.3324/haematol.2013.083840]

40 **Virmani R**, Kolodgie FD, Burke AP, Finn AV, Gold HK, Tulenko TN, Wrenn SP, Narula J. Atherosclerotic plaque progression and vulnerability to rupture: angiogenesis as a source of intraplaque hemorrhage. *Arterioscler Thromb Vasc Biol* 2005; **25**: 2054-2061 [PMID: 16037567 DOI: 10.1161/01.ATV.0000178991.71605.18]

41 **Kim-Shapiro DB**, Schechter AN, Gladwin MT. Unraveling the reactions of nitric oxide, nitrite, and hemoglobin in physiology and therapeutics. *Arterioscler Thromb Vasc Biol* 2006; **26**: 697-705 [PMID: 16424350 DOI: 10.1161/01.ATV.0000204350.44226.9a]

42 **Lee DU**, Hastie DJ, Fan GH, Addonizio EA, Lee KJ, Han J, Karagozian R. Effect of malnutrition on the postoperative outcomes of patients undergoing pancreatectomy for pancreatic cancer: Propensity score-matched analysis of 2011-2017 US hospitals. *Nutr Clin Pract* 2022; **37**: 117-129 [PMID: 34994482 DOI: 10.1002/ncp.10816]

43 **Bora Makal G**, Yıldırım O. Are the C-reactive protein/albumin ratio (CAR), neutrophil-to-lymphocyte ratio (NLR), and platelet-to-lymphocyte ratio (NLR) novel inflammatory biomarkers in the early diagnosis of postoperative complications after laparoscopic sleeve gastrectomy? *Obes Res Clin Pract* 2020; **14**: 467-472 [PMID: 32807712 DOI: 10.1016/j.orcp.2020.07.003]

44 **Nakazawa N**, Sohda M, Yamaguchi A, Watanabe T, Saito H, Ubukata Y, Kuriyama K, Sano A, Sakai M, Ogawa H, Shirabe K, Saeki H. Preoperative Risk Factors and Prognostic Impact of Postoperative Complications Associated with Total Gastrectomy. *Digestion* 2022; **103**: 397-403 [PMID: 35724642 DOI: 10.1159/000525356]

World Journal of Gastrointestinal Oncology

Submit a Manuscript: https://www.f6publishing.com

World J Gastrointest Oncol 2025 January 15; 17(1): 96686

DOI: 10.4251/wjgo.v17.i1.96686

ISSN 1948-5204 (online)

ORIGINAL ARTICLE

Prospective Study

Development of a nomogram for overall survival in patients with esophageal carcinoma: A prospective cohort study in China

Shi-Shi Yu, Xi Zheng, Xiao-Sheng Li, Qian-Jie Xu, Wei Zhang, Zhong-Li Liao, Hai-Ke Lei

Specialty type: Oncology

Provenance and peer review: Unsolicited article; Externally peer reviewed.

Peer-review model: Single blind

Peer-review report's classification

Scientific Quality: Grade C, Grade C

Novelty: Grade B, Grade B

Creativity or Innovation: Grade B, Grade B

Scientific Significance: Grade B, Grade B

P-Reviewer: Sun X

Received: May 13, 2024

Revised: September 2, 2024

Accepted: September 9, 2024

Published online: January 15, 2025

Processing time: 213 Days and 1.1 Hours

Shi-Shi Yu, Xi Zheng, Zhong-Li Liao, Department of Gastroenterology, Chongqing University Cancer Hospital, Chongqing 400030, China

Xiao-Sheng Li, Wei Zhang, Hai-Ke Lei, Chongqing Cancer Multi-omics Big Data Application Engineering Research Center, Chongqing University Cancer Hospital, Chongqing 400030, China

Qian-Jie Xu, Department of Health Statistics, School of Public Health, Chongqing Medical University, Chongqing 400016, China

Co-first authors: Shi-Shi Yu and Xi Zheng.

Co-corresponding authors: Zhong-Li Liao and Hai-Ke Lei.

Corresponding author: Hai-Ke Lei, Doctor, Associate Professor, Chongqing Cancer Multi-omics Big Data Application Engineering Research Center, Chongqing University Cancer Hospital, No. 181 Hanyu Road, Shapingba District, Chongqing 400030, China.
tohaike@163.com

Abstract

BACKGROUND

Esophageal carcinoma (EC) presents a significant public health issue in China, with its prognosis impacted by myriad factors. The creation of a reliable prognostic model for the overall survival (OS) of EC patients promises to greatly advance the customization of treatment approaches.

AIM

To create a more systematic and practical model that incorporates clinically significant indicators to support decision-making in clinical settings.

METHODS

This study utilized data from a prospective longitudinal cohort of 3127 EC patients treated at Chongqing University Cancer Hospital between January 1, 2018, and December 12, 2020. Utilizing the least absolute shrinkage and selection operator regression alongside multivariate Cox regression analyses helped pinpoint pertinent variables for constructing the model. Its efficacy was assessed by concordance index (C-index), area under the receiver operating characteristic curve (AUC), calibration curves, and decision curve analysis (DCA).

RESULTS
Nine variables were determined to be significant predictors of OS in EC patients: Body mass index (BMI), Karnofsky performance status, TNM stage, surgery, radiotherapy, chemotherapy, immunotherapy, platelet-to-lymphocyte ratio, and albumin-to-globulin ratio (ALB/GLB). The model demonstrated a C-index of 0.715 (95%CI: 0.701-0.729) in the training cohort and 0.711 (95%CI: 0.689-0.732) in the validation cohort. In the training cohort, AUCs for 1-year, 3-year, and 5-year OS predictions were 0.773, 0.787, and 0.750, respectively; in the validation cohort, they were 0.772, 0.768, and 0.723, respectively, illustrating the model's precision. Calibration curves and DCA verified the model's predictive accuracy and net benefit.

CONCLUSION
A novel prognostic model for determining the OS of EC patients was successfully developed and validated to help clinicians in devising individualized treatment schemes for EC patients.

Key Words: Esophageal carcinoma; High-risk factors; Prognosis; Overall survival; Prediction model

Core Tip: In this study, we identified nine key independent risk factors associated with esophageal carcinoma patients. These factors span clinical characteristics (body mass index, Karnofsky performance status), the TNM stage, treatment approaches (surgery, radiotherapy, chemotherapy, and immunotherapy), and laboratory markers (platelet-to-lymphocyte ratio, albumin-to-globulin ratio). And then, a novel prognostic model was successfully developed and validated. It could be considered as a more systematic and practical model that incorporates clinically significant indicators to support decision-making in clinical settings.

Citation: Yu SS, Zheng X, Li XS, Xu QJ, Zhang W, Liao ZL, Lei HK. Development of a nomogram for overall survival in patients with esophageal carcinoma: A prospective cohort study in China. *World J Gastrointest Oncol* 2025; 17(1): 96686
URL: https://www.wjgnet.com/1948-5204/full/v17/i1/96686.htm
DOI: https://dx.doi.org/10.4251/wjgo.v17.i1.96686

INTRODUCTION

Esophageal carcinoma (EC) stands as one of the predominant malignant tumors globally[1]. Data from global cancer statistics in 2020 indicate that there were 604000 new EC cases, with nearly half originating from China[2,3]. The five-year overall survival (OS) rate for those diagnosed with EC is a mere 21%[4]. Early diagnosis and comprehensive treatment strategies are currently the most effective means of improving patient outcomes. Identifying high-risk factors is crucial for crafting multidisciplinary treatment plans. However, the widely-used TNM staging system falls short of providing an accurate survival prognosis for EC patients due to its omission of clinical traits, treatment options, and laboratory data. Recent studies have identified several significant independent risk factors for EC, including body mass index (BMI), Karnofsky performance status (KPS), TNM stage, treatment modalities, the platelet-to-lymphocyte ratio (PLR), and the albumin-to-globulin ratio (ALB/GLB)[5-11]. Despite the advances, genetic research integrating factors like CDK8, ARID1A, and certain autophagy-related lncRNAs into prognostic models has been hindered by the high costs and complexity of gene testing, which adds to patient financial strain[12,13]. Additionally, the absence of valuable laboratory predictors has diminished the precision of some models[14]. This highlights the need for a more scientifically robust, systematic, and practical model that incorporates clinically significant indicators to support decision-making in clinical settings.

Moreover, Chongqing has been identified as a region with a notably high incidence of EC in China, where early detection rates are below 10%[15-17]. The vast majority of EC cases are diagnosed at advanced stages, resulting in poor survival outcomes. Thus, creating a more dependable prognostic model is crucial for guiding clinicians towards more effective anti-cancer treatment strategies, ultimately aiming to enhance the survival rates of patients with EC. In light of this, our study has pinpointed 9 high-risk factors linked to EC and constructed an accessible online predictive model.

MATERIALS AND METHODS

Subjects

Chongqing is recognized as a region with a notably high rate of EC in China. In our study, we gathered data from patients diagnosed with EC at the Chongqing University Cancer Hospital over a period spanning from January 1, 2018, to December 12, 2020. Eligibility criteria for inclusion in this study were set as follows: (1) Being 18 years or older; (2) Receiving a new EC diagnosis confirmed by pathology; (3) Undergoing and completing the prescribed course of

treatment, which included options such as surgery, radiotherapy, chemotherapy, immunotherapy, or targeted therapy; and (4) Having a complete set of baseline clinical data and follow-up records. On the other hand, patients were excluded if they lacked follow-up records or had received treatment for cancer prior to this study. The methodology and progression of the study are illustrated in Figure 1.

Clinical evaluations

We collected a comprehensive set of data including demographic information (age and gender), clinical characteristics (KPS, BMI, pathological type, and TNM staging), treatment modalities (surgery, radiotherapy, chemotherapy, immunotherapy, and targeted therapy), laboratory markers (β2-microglobulin, neutrophil-lymphocyte ratio, lymphocyte-monocyte ratio, PLR, ALB/GLB, and the CD4/CD8 ratio), as well as follow-up details. The laboratory tests were conducted at the Chongqing University Cancer Hospital's laboratory. We excluded patients who were exclusively undergoing traditional Chinese medicine treatments due to the challenges associated with analyzing their incomplete or missing data.

The primary objective of this study was to assess the 1-year, 3-year, and 5-year OS rates. OS was measured from the date of EC diagnosis to the date of death or the last known follow-up. Follow-ups were conducted semiannually for the first two years post-diagnosis and annually thereafter until the demise of the subject. The study was concluded on December 31, 2023, with a one-month follow-up period acting as the cut-off point.

Statistical analysis

Continuous variables are presented as the mean ± SD, whereas categorical variables are shown as frequencies and percentages. To compare demographic and clinical variables between the training and validation cohorts, we utilized the Pearson χ^2 test for categorical data. All statistical procedures were carried out using R software version 4.2.1 (Institute for Statistics and Mathematics, Vienna, Austria). The dataset was split into training and validation groups in a 7:3 ratio. We employed least absolute shrinkage and selection operator (LASSO) regression to identify risk factors, which were then evaluated through univariate Cox regression analysis.

Construction and validation of the prognostic prediction model

To develop an effective clinical prognostic model, we meticulously selected and identified variables for the prediction model through a two-step process. Initially, LASSO regression was applied to sift through patient characteristics within the training cohort. We determined the optimal parameter (λ) for LASSO regression *via* cross-validation, selecting crucial variables based on the minimum λ principle. Subsequent to this, we conducted both univariate and multivariate Cox regression analyses on these variables (Figure 2). Recognizing that the clinical relevance of these variables during the selection process is not solely based on their statistical significance, we ultimately pinpointed 9 predictors: BMI, KPS, TNM stage, surgery, radiotherapy, chemotherapy, immunotherapy, the PLR, and the ALB/GLB ratio. These 9 risk factors were incorporated into the prediction model, with each factor being allocated a score. This score can be derived from the illustrated ruler, allowing for the prediction of 1-, 3-, and 5-year OS rates by overlaying it onto the subsequent ruler.

The model's capability to forecast survival outcomes was further appraised in the validation cohort by examining both its discrimination and calibration. The concordance index (C-index) was utilised to articulate the model's proficiency in predicting the survival of patients whose prognoses have been objectively verified. To assess the model's prediction accuracy and discriminative power, a calibration curve was plotted. Additionally, a receiver operating characteristic (ROC) curve was employed to confirm the model's generalization potential.

RESULTS

Demographic characteristics

A cohort of 3127 patients diagnosed with EC participated in the study and were systematically divided into two groups for analysis: A training group consisting of 2189 patients (approximately 70%) and a validation group comprising 938 patients (around 30%), following a 7:3 distribution ratio. According to statistical analysis, no significant differences were observed between the training and validation groups, as presented in Table 1. For the entire cohort, the median survival time was recorded at 27.50 months, with a range spanning from 0.10 to 60.45 months. Within the training cohort, there were 1267 fatalities over a median duration of 27.40 months (ranging from 0.10 to 61.10 months). In the validation group, 391 patients succumbed, with a median survival time extending to 28.00 months, also within a broad range of 0.10 to 59.30 months.

Univariate and multivariate logistic regression results

The univariate logistic regression analysis revealed nine prognostic factors linked to patient outcomes, including KPS (HR 0.98, 95%CI: 0.97-0.99, $P < 0.001$), BMI (< 18.5: HR 1.29, 95%CI: 1.11-1.49, $P = 0.001$), TNM (II: HR 2.16, 95%CI: 1.56-2.98, $P < 0.001$; III: HR 3.04, 95%CI: 2.22-4.18, $P < 0.001$; IV: HR 4.12, 95%CI: 2.98-5.70, $P < 0.001$), surgery (HR 0.56, 95%CI: 0.49-0.64, $P < 0.001$), radiotherapy (HR 0.72, 95%CI: 0.64-0.81, $P < 0.001$), chemotherapy (HR 0.74, 95%CI: 0.65-0.84, $P < 0.001$), immunotherapy (HR 0.73, 95%CI: 0.54-0.98, $P = 0.033$), and PLR (HR 0.81, 95%CI: 0.67-0.98, $P = 0.034$), and ALB/GLB (HR 1.01, 95%CI: 1.01-1.01, $P < 0.001$) (Table 2).

Table 1 Patient demographics and clinical characteristics

Characteristics	Overall (*n* = 3127)	Training cohort (*n* = 2189)	Validation cohort (*n* = 938)	*P* value
Age[1]	65.30 ± 8.59	65.35 ± 8.65	65.19 ± 8.46	0.620
KPS[1]	83.75 ± 8.11	83.74 ± 7.97	83.78 ± 8.43	0.910
Sex, *n* (%)				
Male	2549 (81.52)	1789 (81.73)	760 (81.02)	0.679
Female	578 (18.48)	400 (18.27)	178 (18.98)	
BMI, *n* (%)				
18.5-23.9	1931 (61.75)	1350 (61.67)	581 (61.94)	0.357
≥ 24	720 (23.03)	494 (22.57)	226 (24.09)	
< 18.5	476 (15.22)	345 (15.76)	131 (13.97)	
Base disease, *n* (%)				
No	2521 (80.62)	1757 (80.26)	764 (81.45)	0.472
Yes	606 (19.38)	432 (19.74)	174 (18.55)	
Pathological, *n* (%)				
SCC	3021 (96.61)	2121 (96.89)	900 (95.95)	0.219
Others	106 (3.39)	68 (3.11)	38 (4.05)	
TNM, *n* (%)				
I	226 (7.23)	162 (7.40)	64 (6.82)	0.703
II	780 (24.94)	536 (24.49)	244 (26.01)	
III	1230 (39.33)	858 (39.20)	372 (39.66)	
IV	891 (28.49)	633 (28.92)	258 (27.51)	
Radiotherapy, *n* (%)				
No	1918 (61.34)	1345 (61.44)	573 (61.09)	0.883
Yes	1209 (38.66)	844 (38.56)	365 (38.91)	
Chemotherapy, *n* (%)				
No	1804 (57.69)	1265 (57.79)	539 (57.46)	0.897
Yes	1323 (42.31)	924 (42.21)	399 (42.54)	
Surgery, *n* (%)				
No	1644 (52.57)	1156 (52.81)	488 (52.03)	0.716
Yes	1483 (47.43)	1033 (47.19)	450 (47.97)	
Immunotherapy, *n* (%)				
No	2901 (92.77)	2029 (92.69)	872 (92.96)	0.846
Yes	226 (7.23)	160 (7.31)	66 (7.04)	
Targeted, *n* (%)				
No	3019 (96.55)	2117 (96.71)	902 (96.16)	0.507
Yes	108 (3.45)	72 (3.29)	36 (3.84)	
LDH[1]	202.19 ± 155.15	202.47 ± 143.90	201.53 ± 178.76	0.877
β2. Microglobulin[1]	2.59 ± 1.19	2.58 ± 1.15	2.61 ± 1.28	0.472
CD4/CD8[1]	1.81 ± 1.06	1.80 ± 1.05	1.85 ± 1.09	0.163
ALB/GLB[1]	1.37 ± 0.32	1.37 ± 0.31	1.38 ± 0.32	0.707
PLR[1]	168.66 ± 113.61	168.01 ± 111.13	170.17 ± 119.24	0.625
LMR[2]	3.33 [2.36, 4.65]	3.32 [2.36, 4.61]	3.37 [2.41, 4.79]	0.147

NLR[2]	2.74 [1.94, 4.09]	2.74 [1.92, 4.12]	2.74 [1.97, 4.02]	0.714

[1]Expressed as mean ± SD.
[2]Expressed as median[P25, P75].
PLR: Platelet-to-lymphocyte ratio; BMI: Body mass index; KPS: Karnofsky performance status; LDH: Lactic dehydrogenase; SCC: Esophageal squamous cell carcinoma; LMR: Lymphocyte-monocyte ratio; NLR: Neutrophil-lymphocyte ratio.

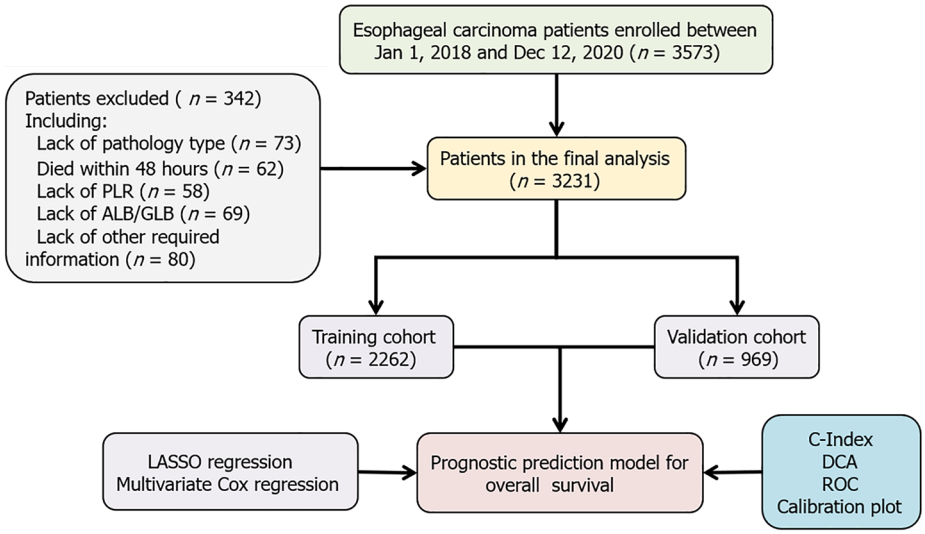

Figure 1 Flow diagram of study design. PLR: Platelet-to-lymphocyte ratio; ALB/GLB: Albumin-to-globulin ratio; LASSO: Least absolute shrinkage and selection operator; DCA: Decision curve analysis; ROC: Receiver operating characteristic.

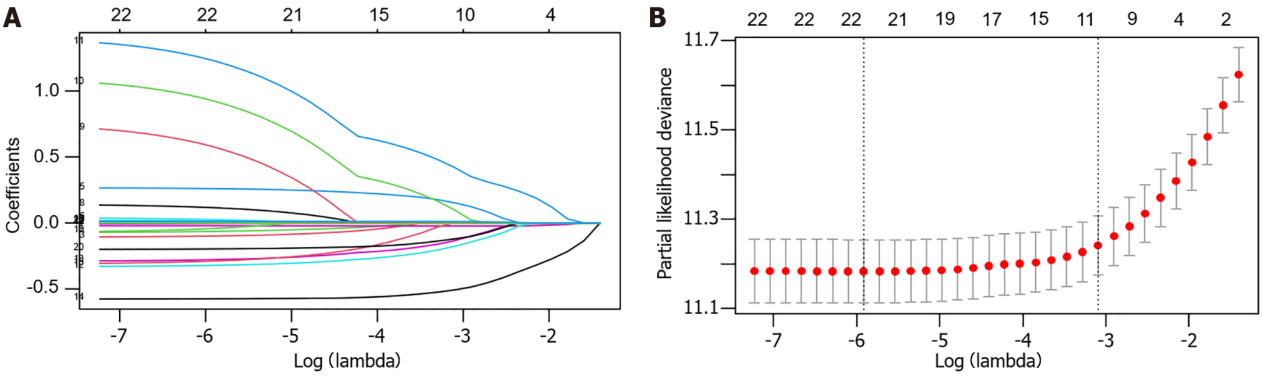

Figure 2 Variable selection by least absolute shrinkage and selection operator Cox regression model. A coefficient profile plot was produced against the log (lambda) sequence. A: 22 variables with nonzero coefficients were selected by optimal lambda; B: By verifying the optimal parameter (lambda) in the least absolute shrinkage and selection operator model, the partial likelihood deviance (binomial deviance) curve was plotted *vs* log (lambda) and dotted vertical lines were drawn based on 1 standard error criteria.

Prognostic prediction model performance and validation

In the developed prognostic prediction model, each identified risk factor was assigned a corresponding score, using a method where scores are derived from an upper ruler and superimposed onto a lower ruler for the prediction of 1-, 3-, and 5-year OS rates (as shown in Figure 3). Additionally, an online calculator was developed based on this predictive model (available at https://cqchprognosis.shinyapps.io/esophagus/) to estimate the long-term OS for patients with EC. Illustratively, for a patient with stage III EC, a BMI of 25 kg/m^2, a KPS score of 85, a PLR of 193, ALB/GLB ratio of 2, without undergoing radiotherapy and immunotherapy, treated with surgery and chemotherapy, the model estimates a 5-year OS probability of 44%.

The model's C-index for OS was found to be 0.715 (with a 95%CI of 0.701-0.729) in the training cohort, and 0.711 (95%CI: 0.689-0.732) in the validation cohort. In terms of the ROC values within the training cohort, the prediction capabilities for 1-, 3-, and 5-year OS stood at 0.773, 0.787, and 0.750, respectively (Figure 4A); for the validation cohort, these values were 0.772, 0.768, and 0.723, respectively (Figure 4B). Additionally, the calibration curves illustrated good agreement between the predicted and observed probabilities for 1-, 3-, and 5-year OS in both the training (Figure 4C) and

Table 2 Univariate and multivariate analysis for overall survival of the training cohort

Characteristics	HR (univariable)	HR (multivariable)
Age	1.02 (1.01-1.02, $P < 0.001$)	
KPS	0.95 (0.94-0.95, $P < 0.001$)	0.98 (0.97-0.99, $P < 0.001$)
Gender (%)		
Male		
Female	0.85 (0.74-0.99, $P = 0.033$)	
BMI (%)		
18.5-23.9		
≥ 24	0.76 (0.66-0.88, $P < 0.001$)	0.94 (0.82-1.09, $P = 0.428$)
< 18.5	1.68 (1.45-1.94, $P < 0.001$)	1.29 (1.11-1.49, $P = 0.001$)
Base disease (%)		
No		
Yes	1.04 (0.91-1.20, $P = 0.578$)	
Pathological (%)		
SCC		
Others	1.41 (1.03-1.92, $P = 0.032$)	
TNM (%)		
I		
II	2.10 (1.52-2.90, $P < 0.001$)	2.16 (1.56-2.98, $P < 0.001$)
III	3.13 (2.29-4.28, $P < 0.001$)	3.04 (2.22-4.18, $P < 0.001$)
IV	5.51 (4.03-7.54, $P < 0.001$)	4.12 (2.98-5.70, $P < 0.001$)
Radiotherapy (%)		
No		
Yes	0.74 (0.66-0.83, $P < 0.001$)	0.72 (0.64-0.81, $P < 0.001$)
Chemotherapy (%)		
No		
Yes	0.72 (0.64-0.81, $P < 0.001$)	0.74 (0.65-0.84, $P < 0.001$)
Surgery (%)		
No		
Yes	0.41 (0.37-0.46, $P < 0.001$)	0.56 (0.49-0.64, $P< 0.001$)
Immunotherapy (%)		
No		
Yes	0.54 (0.41-0.72, $P < 0.001$)	0.73 (0.54-0.98, $P = 0.033$)
Targeted (%)		
No		
Yes	0.78 (0.57-1.07, $P = 0.120$)	
LDH	1.01 (1.00-1.01, $P = 0.057$)	
β2. microglobulin	1.14 (1.09-1.19, $P < 0.001$)	
CD4/CD8	0.93 (0.88-0.99, $P = 0.018$)	
ALB/GLB	0.43 (0.35-0.52, $P < 0.001$)	0.81 (0.67-0.98, $P = 0.034$)
PLR	1.01 (1.01-1.01, $P < 0.001$)	1.01 (1.01-1.01, $P < 0.001$)
LMR	0.99 (0.99-1.00, $P = 0.120$)	

NLR	1.06 (1.05-1.07, $P < 0.001$)

PLR: Platelet-to-lymphocyte ratio; BMI: Body mass index; KPS: Karnofsky performance status; LDH: Lactic dehydrogenase; SCC: Esophageal squamous cell carcinoma; LMR: Lymphocyte-monocyte ratio; NLR: Neutrophil-lymphocyte ratio.

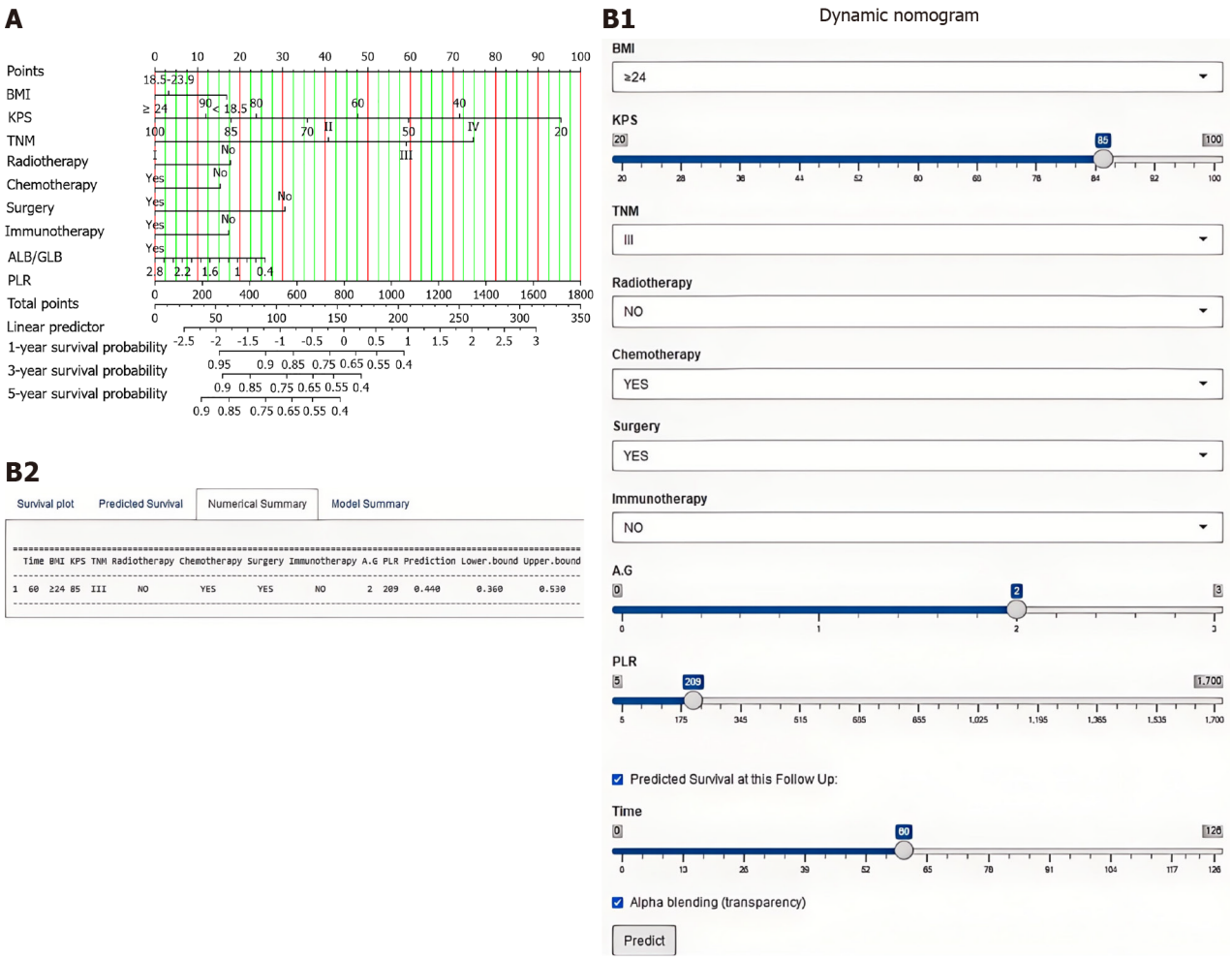

Figure 3 Prediction model for predicting 1-, 3- and 5-year overall survival of patients with Esophageal carcinoma. A: Nomogram model; B: The interface of the web-based nomogram. PLR: Platelet-to-lymphocyte ratio; ALB/GLB: Albumin-to-globulin ratio; BMI: Body mass index; KPS: Karnofsky performance status.

validation cohorts (Figure 4D), according to the predictive model.

Moreover, decision curve analysis (DCA) was employed to evaluate the model's predictive performance, showing that the model yielded a positive net benefit in both training (Figure 5A) and validation cohorts (Figure 5B). Utilizing this newly established model, we grouped patients from both the training set (Figure 5C) and the validation set (Figure 5D) into high or low risk categories. The findings underscored the model's robust capability to distinguish between patients at high and low risk ($P < 0.05$).

DISCUSSION

In this study, we utilized both univariate and multivariate Cox regression analyses to identify nine key independent risk factors associated with EC. These factors include clinical characteristics (BMI and KPS), TNM stage, treatment approaches (surgery, radiotherapy, chemotherapy, and immunotherapy), and laboratory markers (PLR, ALB/GLB). Leveraging these factors, we developed a prognostic risk prediction model to predict OS rates in EC patients. This model exhibited high reliability and reproducibility, as evidenced by its calibration curve and C-index. Furthermore, DCA demonstrated that this model more accurately predicted EC outcomes than the TNM stage. The key findings of our research include the integration of a broader scope of independent risk factors into our predictive model than that incorporated by previously utilized models, which improved prognostic risk assessment in EC patients. These factors, which align with findings from prior studies, encompass clinical characteristics, treatment methods, and particular laboratory indicators linked to

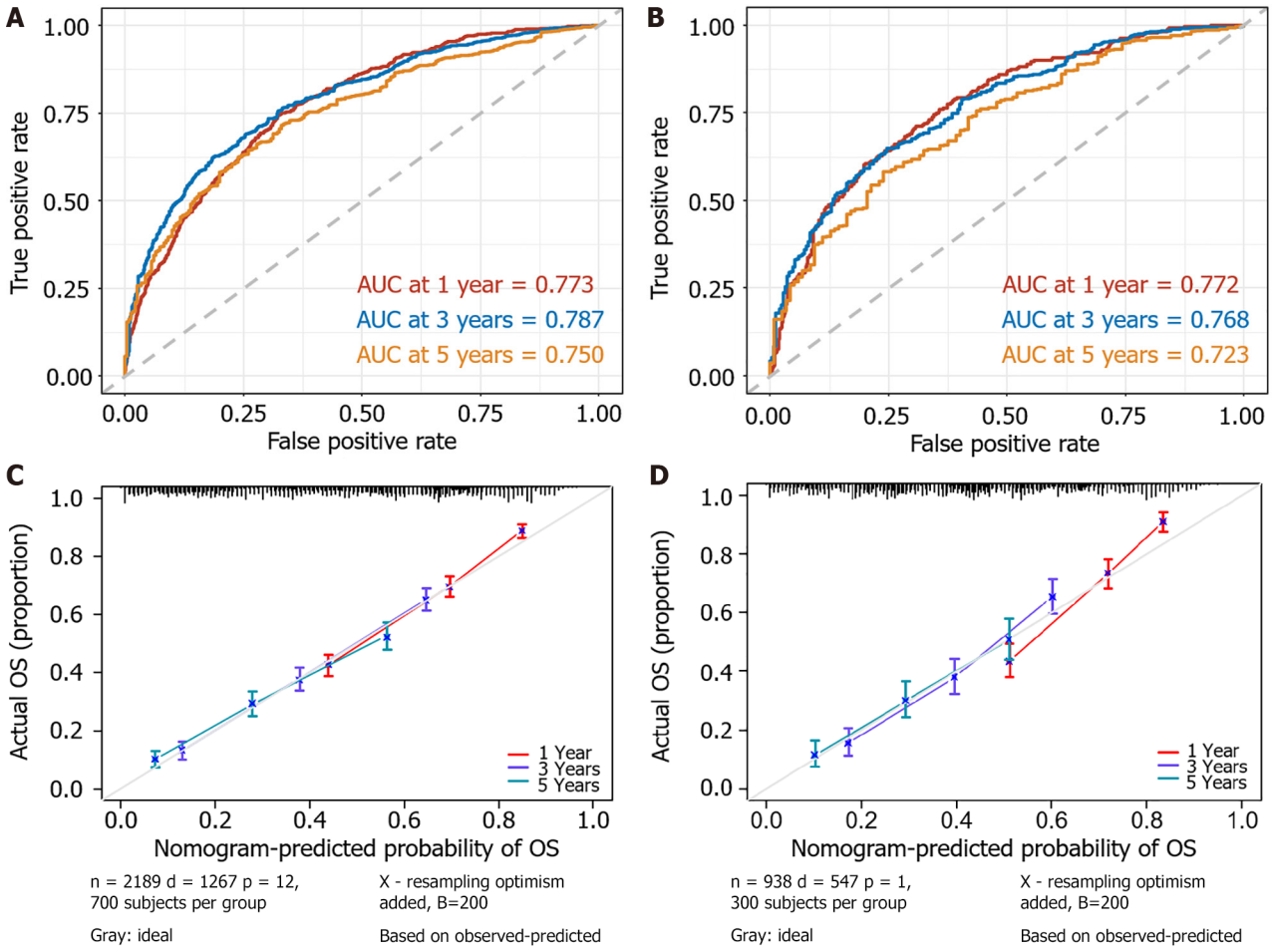

Figure 4 Receiver operating characteristic and calibration curves of the prediction model for 1-, 3- and 5-year overall survival prediction.
A: Receiver operating characteristic (ROC) in the training cohort; B: ROC in the validation cohort; C: Calibration plot in the training cohort; D: Calibration plot in the validation cohort. AUC: Area under the receiver operating characteristic curve; OS: Overall survival.

systemic inflammation[18,19]. Notably, our model underscores the significance of comprehensive treatment and monitoring strategies over reliance solely on the TNM stage, highlighting factors such as low BMI and KPSs, types of treatment received, and specific biomarkers as integral to predicting patient outcomes[20-26].

The traditional KPS is an important tool in oncology for assessing functional performance and aiding in prognosis. It has high reliability and adaptability across various scenarios and serves as a crucial prognostic factor in most prognostic models[27]. A study by Freeman *et al*[28] revealed that KPSs are closely associated with progression-free survival in patients with breast cancer that has metastasized to the brain and can effectively reflect the quality of life of these patients. Similarly, Bao *et al*[29] reported that a lower KPS was significantly associated with shorter OS in a study of prognostic indicators for glioma, suggesting that the KPS can be a powerful indicator for investigating the prognosis of patients with glioma. Although the KPS is widely recognized for its application in oncology, some argue that it may not fully capture the complexity of patient function in different rehabilitation environments[30], indicating the need for supplementary assessment tools. Therefore, our nomogram model additionally incorporates other clinical feature variables as predictive factors, which significantly improved the model's predictive accuracy and generalizability.

The clinical relationship between the BMI and the risk of EC has long been ambiguous. Some studies suggest that a high BMI is associated with an increased risk of EC[31], whereas others find that a low BMI is related to a greater risk of developing EC[32]. Recently, a meta-analysis based on evidence from 25 observational studies indicated that being underweight, compared with a normal weight, is significantly associated with an increased risk of EC (RR = 1.78, 95%CI: 1.48-2.14; $P < 0.001$). Additionally, being overweight or obese was found to increase the risk of esophageal adenocarcinoma (RR = 1.56, 95%CI: 1.42-1.71, $P < 0.001$; RR = 2.34, 95%CI: 2.02-2.70, $P < 0.001$) while simultaneously decreasing the risk of esophageal squamous cell carcinoma (RR = 0.71, 95%CI: 0.60-0.84, $P < 0.001$; RR = 0.63, 95%CI: 0.60-0.84, $P = 0.002$) [33]. In our study, a BMI of less than 18 was associated with the highest risk of EC compared with other BMI levels. Interestingly, overweight individuals demonstrated a lower risk of EC, which we speculate is because our selected EC patients were predominantly those with esophageal squamous cell carcinoma.

The TNM staging system, an important indicator for assessing tumor progression, also reflects patient survival chances to a certain extent. Recent studies have shown that incorporating the TNM stage as a predictive factor in conventional tumor prognostic models can significantly increase the predictive accuracy of these models[34]. In our research, TNM stage emerged as a crucial predictor of OS in EC patients, showing substantial predictive value in the nomogram plot.

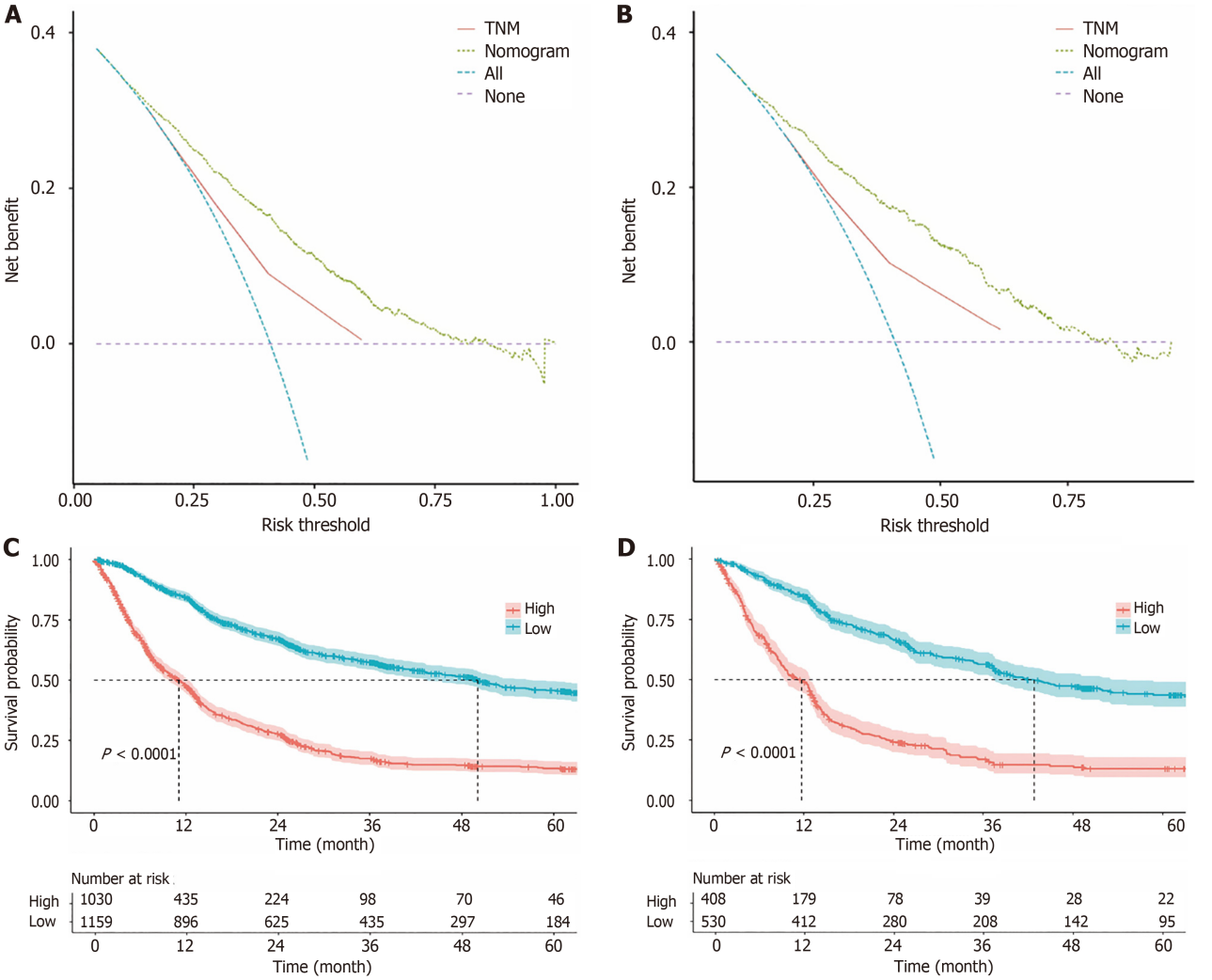

Figure 5 Decision curve analysis for the prediction model's ability to predict overall survival in Esophageal carcinoma patients and the prediction model distinguished the risk of Esophageal carcinoma patients. A: Decision curve analysis (DCA) in the training cohort; B: DCA validation cohort; C: The prediction model in the training cohort; D: The prediction model in the validation cohort.

Recent studies have shown that the presence of systemic inflammation is associated with poorer survival rates in patients with EC. In this study, patients with a higher PLR often had worse survival rates, indicating that the PLR is a risk factor. Zheng *et al*[35] investigated the prognostic value of the PLR in EC patients and reported that a high PLR is significantly associated with poorer disease-free survival, which suggested that the PLR can serve as a predictive factor for quality of life in EC patients. Similarly, a lower ALB/GLB ratio has been associated with poorer prognosis[36], which is consistent with our study. Surgery, radiotherapy, chemotherapy and immunotherapy are the primary clinical treatments for EC. A recent review noted that surgical treatment remains the primary therapeutic approach for patients with EC[37]. Consequently, in our study, patients who did not undergo surgical treatment had poorer prognoses. Notably, other treatment modalities, such as immunotherapy, chemotherapy, and radiotherapy, can also effectively prolong survival time and improve the quality of life of patients. Moreover, targeted therapy had a limited influence on the OS of EC patients in our study and warrants further investigation.

Because all of the above factors are easily measured in the clinical setting, our model is clinically practical. Another practical contribution of our model is the creation of an accessible online calculator designed to aid clinicians in tailoring treatment plans through dynamic survival predictions at various time points. This tool aims to minimize the economic burden on patients while maximizing the model's utility in clinical settings.

However, our work is not without limitations. The exclusive use of data from a single medical institution and the absence of a broader prospective cohort study underline the need for further validation through larger-scale, multicenter research. Furthermore, the lack of imaging data in our study points to an area for future enhancement, potentially increasing the robustness of our findings.

CONCLUSION

In conclusion, our comprehensive predictive model for EC patients, supported by an easy-to-use online calculator,

presents a novel approach to improving patient outcomes through personalized interventions.

FOOTNOTES

Author contributions: Yu SS conceived and designed the study; Zheng X wrote initial drafts of the paper; Li XS handled the data collection and statistical analysis; Xu QJ, Zhang W, performed analysis and interpretation of statistics; Liao ZL and Lei HK designed the study, revised the article and final approval of the version to be published. All authors collectively designed the methods and experiments, read, and approved the final manuscript. Yu SS and Zheng X contributed equally to this work as co-first authors. Liao ZL works at Department of Gastroenterology, Chongqing University Cancer Hospital and found there was need for a more scientifically robust, systematic, and practical model that incorporates clinically significant indicators to support decision-making. Lei HK works at Chongqing Cancer Multi-omics Big Data Application Engineering Research Center, Chongqing University Cancer Hospital and is mainly responsible for follow-up of cancer patients. For this reason, Liao ZL and Lei HK designed the study, revised the article and final approval of the version to be published. They are designated as co-corresponding authors.

Institutional review board statement: The study was reviewed and approved by the Ethics Committee of Chongqing University Tumor Hospital (Approval No. CZLS2023338-A).

Informed consent statement: All study participants, or their legal guardian, provided informed written consent prior to study enrollment.

Conflict-of-interest statement: We have no financial relationships to disclose.

Data sharing statement: The datasets used and/or analyzed during the current study are available from the corresponding author on reasonable request.

CONSORT 2010 statement: The authors have read the CONSORT 2010 Statement, and the manuscript was prepared and revised according to the CONSORT 2010 Statement.

Country of origin: China

ORCID number: Zhong-Li Liao 0000-0001-7818-0126; Hai-Ke Lei 0000-0003-0284-2052.

S-Editor: Qu XL
L-Editor: A
P-Editor: Yu HG

REFERENCES

1 **Abnet CC**, Arnold M, Wei WQ. Epidemiology of Esophageal Squamous Cell Carcinoma. *Gastroenterology* 2018; **154**: 360-373 [PMID: 28823862 DOI: 10.1053/j.gastro.2017.08.023]
2 **Sung H**, Ferlay J, Siegel RL, Laversanne M, Soerjomataram I, Jemal A, Bray F. Global Cancer Statistics 2020: GLOBOCAN Estimates of Incidence and Mortality Worldwide for 36 Cancers in 185 Countries. *CA Cancer J Clin* 2021; **71**: 209-249 [PMID: 33538338 DOI: 10.3322/caac.21660]
3 **Arnold M**, Abnet CC, Neale RE, Vignat J, Giovannucci EL, McGlynn KA, Bray F. Global Burden of 5 Major Types of Gastrointestinal Cancer. *Gastroenterology* 2020; **159**: 335-349.e15 [PMID: 32247694 DOI: 10.1053/j.gastro.2020.02.068]
4 **Siegel RL**, Miller KD, Wagle NS, Jemal A. Cancer statistics, 2023. *CA Cancer J Clin* 2023; **73**: 17-48 [PMID: 36633525 DOI: 10.3322/caac.21763]
5 **Koyanagi YN**, Matsuo K, Ito H, Wang C, Tamakoshi A, Sugawara Y, Tsuji I, Ono A, Tsugane S, Sawada N, Wada K, Nagata C, Takeuchi T, Kitamura T, Utada M, Sakata R, Mizoue T, Abe SK, Inoue M; Research Group for the Development and Evaluation of Cancer Prevention Strategies in Japan. Body mass index and esophageal and gastric cancer: A pooled analysis of 10 population-based cohort studies in Japan. *Cancer Sci* 2023; **114**: 2961-2972 [PMID: 37013939 DOI: 10.1111/cas.15805]
6 **Ogawa K**, Toita T, Sueyama H, Fuwa N, Kakinohana Y, Kamata M, Adachi G, Saito A, Yoshii Y, Murayama S. Brain metastases from esophageal carcinoma: natural history, prognostic factors, and outcome. *Cancer* 2002; **94**: 759-764 [PMID: 11857310 DOI: 10.1002/cncr.10271]
7 **Liu Y**, Bao Y, Yang X, Sun S, Yuan M, Ma Z, Zhang W, Zhai Y, Wang Y, Men Y, Qin J, Xue L, Wang J, Hui Z. Efficacy and safety of neoadjuvant immunotherapy combined with chemoradiotherapy or chemotherapy in esophageal cancer: A systematic review and meta-analysis. *Front Immunol* 2023; **14**: 1117448 [PMID: 36761760 DOI: 10.3389/fimmu.2023.1117448]
8 **Deng J**, Zhang P, Sun Y, Peng P, Huang Y. Prognostic and clinicopathological significance of platelet to lymphocyte ratio in esophageal cancer: a meta-analysis. *J Thorac Dis* 2018; **10**: 1522-1531 [PMID: 29707302 DOI: 10.21037/jtd.2018.02.58]
9 **Zhang F**, Sun P, Wang ZQ, Wang de S, Wang Y, Zhang DS, Wang FH, Fu JH, Xu RH, Li YH. Low preoperative albumin-globulin score

predicts favorable survival in esophageal squamous cell carcinoma. *Oncotarget* 2016; **7**: 30550-30560 [PMID: 27105522 DOI: 10.18632/oncotarget.8868]
10 **Turati F**, Tramacere I, La Vecchia C, Negri E. A meta-analysis of body mass index and esophageal and gastric cardia adenocarcinoma. *Ann Oncol* 2013; **24**: 609-617 [PMID: 22898040 DOI: 10.1093/annonc/mds244]
11 **Coia LR**, Minsky BD, Berkey BA, John MJ, Haller D, Landry J, Pisansky TM, Willett CG, Hoffman JP, Owen JB, Hanks GE. Outcome of patients receiving radiation for cancer of the esophagus: results of the 1992-1994 Patterns of Care Study. *J Clin Oncol* 2000; **18**: 455-462 [PMID: 10653860 DOI: 10.1200/JCO.2000.18.3.455]
12 **Deng J**, Weng X, Chen W, Zhang J, Ma L, Zhao K. A nomogram and risk classification model predicts prognosis in Chinese esophageal squamous cell carcinoma patients. *Transl Cancer Res* 2022; **11**: 3128-3140 [PMID: 36237263 DOI: 10.21037/tcr-22-915]
13 **Zhao X**, Wang Y, Meng F, Liu Z, Xu B. Risk Stratification and Validation of Eleven Autophagy-Related lncRNAs for Esophageal Squamous Cell Carcinoma. *Front Genet* 2022; **13**: 894990 [PMID: 35832188 DOI: 10.3389/fgene.2022.894990]
14 **Shao CY**, Liu XL, Yao S, Li ZJ, Cong ZZ, Luo J, Dong GH, Yi J. Development and validation of a new clinical staging system to predict survival for esophageal squamous cell carcinoma patients: Application of the nomogram. *Eur J Surg Oncol* 2021; **47**: 1473-1480 [PMID: 33349524 DOI: 10.1016/j.ejso.2020.12.004]
15 **Chen W**, Zheng R, Zhang S, Zeng H, Xia C, Zuo T, Yang Z, Zou X, He J. Cancer incidence and mortality in China, 2013. *Cancer Lett* 2017; **401**: 63-71 [PMID: 28476483 DOI: 10.1016/j.canlet.2017.04.024]
16 **Islami F**, Boffetta P, Ren JS, Pedoeim L, Khatib D, Kamangar F. High-temperature beverages and foods and esophageal cancer risk--a systematic review. *Int J Cancer* 2009; **125**: 491-524 [PMID: 19415743 DOI: 10.1002/ijc.24445]
17 **Chen ZM**, Xu Z, Collins R, Li WX, Peto R. Early health effects of the emerging tobacco epidemic in China. A 16-year prospective study. *JAMA* 1997; **278**: 1500-1504 [PMID: 9363969 DOI: 10.1001/jama.278.18.1500]
18 **Huang B**, Ding F, Li Y. A practical recurrence risk model based on Lasso-Cox regression for gastric cancer. *J Cancer Res Clin Oncol* 2023; **149**: 15845-15854 [PMID: 37672074 DOI: 10.1007/s00432-023-05346-1]
19 **Wang Y**, Xiao L, Zhang J, Lv X, Cao F, Zhao M, Wu F, Jing S, Wang J. Clinicopathological characteristics and prognosis of brain metastases in elderly patients with esophageal carcinoma. *Thorac Cancer* 2021; **12**: 3005-3010 [PMID: 34581508 DOI: 10.1111/1759-7714.14167]
20 **Amin MB**, Greene FL, Edge SB, Compton CC, Gershenwald JE, Brookland RK, Meyer L, Gress DM, Byrd DR, Winchester DP. The Eighth Edition AJCC Cancer Staging Manual: Continuing to build a bridge from a population-based to a more "personalized" approach to cancer staging. *CA Cancer J Clin* 2017; **67**: 93-99 [PMID: 28094848 DOI: 10.3322/caac.21388]
21 **Smyth EC**, Lagergren J, Fitzgerald RC, Lordick F, Shah MA, Lagergren P, Cunningham D. Oesophageal cancer. *Nat Rev Dis Primers* 2017; **3**: 17048 [PMID: 28748917 DOI: 10.1038/nrdp.2017.48]
22 **Rogers JE**, Sewastjanow-Silva M, Waters RE, Ajani JA. Esophageal cancer: emerging therapeutics. *Expert Opin Ther Targets* 2022; **26**: 107-117 [PMID: 35119973 DOI: 10.1080/14728222.2022.2036718]
23 **Aoyama T**, Kazama K, Maezawa Y, Hara K. Usefulness of Nutrition and Inflammation Assessment Tools in Esophageal Cancer Treatment. *In Vivo* 2023; **37**: 22-35 [PMID: 36593006 DOI: 10.21873/invivo.13051]
24 **Oki S**, Toiyama Y, Okugawa Y, Shimura T, Okigami M, Yasuda H, Fujikawa H, Okita Y, Yoshiyama S, Hiro J, Kobayashi M, Ohi M, Araki T, Inoue Y, Mohri Y, Kusunoki M. Clinical burden of preoperative albumin-globulin ratio in esophageal cancer patients. *Am J Surg* 2017; **214**: 891-898 [PMID: 28460738 DOI: 10.1016/j.amjsurg.2017.04.007]
25 **Aoyama T**, Ju M, Komori K, Tamagawa H, Tamagawa A, Onodera A, Morita J, Hashimoto I, Ishiguro T, Endo K, Cho H, Onuma S, Fukuda M, Oshima T, Yukawa N, Rino Y. The Platelet-to-Lymphocyte Ratio Is an Independent Prognostic Factor for Patients With Esophageal Cancer Who Receive Curative Treatment. *In Vivo* 2022; **36**: 1916-1922 [PMID: 35738628 DOI: 10.21873/invivo.12912]
26 **Yao Y**, Cai C, Sun F, Gong W. A New Index AGR-PLR Score (APS) for Patients with Esophageal Squamous Cell Carcinoma Undergoing Radical Esophagectomy. *Cancer Manag Res* 2021; **13**: 6129-6139 [PMID: 34385842 DOI: 10.2147/CMAR.S325219]
27 **Terret C**, Albrand G, Moncenix G, Droz JP. Karnofsky Performance Scale (KPS) or Physical Performance Test (PPT)? That is the question. *Crit Rev Oncol Hematol* 2011; **77**: 142-147 [PMID: 20185330 DOI: 10.1016/j.critrevonc.2010.01.015]
28 **Freeman M**, Ennis M, Jerzak KJ. Karnofsky Performance Status (KPS) ≤60 Is Strongly Associated With Shorter Brain-Specific Progression-Free Survival Among Patients With Metastatic Breast Cancer With Brain Metastases. *Front Oncol* 2022; **12**: 867462 [PMID: 35965535 DOI: 10.3389/fonc.2022.867462]
29 **Bao H**, Wang H, Sun Q, Wang Y, Liu H, Liang P, Lv Z. The involvement of brain regions associated with lower KPS and shorter survival time predicts a poor prognosis in glioma. *Front Neurol* 2023; **14**: 1264322 [PMID: 38111796 DOI: 10.3389/fneur.2023.1264322]
30 **Pochettino F**, Visconti G, Godoy D, Rivarola P, Crivelli A, Puga M, González HF, Fernández A. Association between Karnofsky performance status and outcomes in cancer patients on home parenteral nutrition. *Clin Nutr ESPEN* 2023; **54**: 211-214 [PMID: 36963865 DOI: 10.1016/j.clnesp.2023.01.020]
31 **Li W**, Wang W. Contribution of High Body Mass Index to the Global Burden of Esophageal Cancer: A Population-Based Study from 1990 to 2019. *Dig Dis Sci* 2024; **69**: 1125-1134 [PMID: 38433126 DOI: 10.1007/s10620-024-08290-3]
32 **Saadaat R**, Abdul-Ghafar J, Haidary AM, Atta N, Ali TS. Esophageal Carcinoma and Associated Risk Factors: A Case-control Study in Two Tertiary Care Hospitals of Kabul, Afghanistan. *Cancer Manag Res* 2022; **14**: 2445-2456 [PMID: 35975105 DOI: 10.2147/CMAR.S372883]
33 **Tian J**, Zuo C, Liu G, Che P, Li G, Li X, Chen H. Cumulative evidence for the relationship between body mass index and the risk of esophageal cancer: An updated meta-analysis with evidence from 25 observational studies. *J Gastroenterol Hepatol* 2020; **35**: 730-743 [PMID: 31733067 DOI: 10.1111/jgh.14917]
34 **Engholm G**, Lundberg FE, Kønig SM, Ólafsdóttir E, Johannesen TB, Pettersson D, Mørch LS, Johansson ALV, Friis S. Influence of various assumptions for the individual TNM components on the TNM stage using Nordic cancer registry data. *Acta Oncol* 2023; **62**: 215-222 [PMID: 36961761 DOI: 10.1080/0284186X.2023.2189528]
35 **Zheng Z**, Yang C, Cai C, Zhu H. The Preoperative Neutrophil Lymphocyte Ratio and Platelet Lymphocyte Ratio Predicts Disease-Free Survival in Resectable Esophageal Squamous Cell Carcinoma. *Cancer Manag Res* 2021; **13**: 7511-7516 [PMID: 34621132 DOI: 10.2147/CMAR.S321326]
36 **Feng JF**, Wang L, Yang X. The preoperative hemoglobin, albumin, lymphocyte and platelet (HALP) score is a useful predictor in patients with resectable esophageal squamous cell carcinoma. *Bosn J Basic Med Sci* 2021; **21**: 773-781 [PMID: 33974528 DOI: 10.17305/bjbms.2021.5666]
37 **He S**, Xu J, Liu X, Zhen Y. Advances and challenges in the treatment of esophageal cancer. *Acta Pharm Sin B* 2021; **11**: 3379-3392 [PMID: 34900524 DOI: 10.1016/j.apsb.2021.03.008]

World Journal of Gastrointestinal Oncology

Submit a Manuscript: https://www.f6publishing.com

World J Gastrointest Oncol 2025 January 15; 17(1): 99272

DOI: 10.4251/wjgo.v17.i1.99272

ISSN 1948-5204 (online)

ORIGINAL ARTICLE

Randomized Controlled Trial

Effects of Shenqi Xiangyi granules in advanced gastric cancer chemotherapy

Xiao-Jing Shi, Yu Song, Xue-Xue Liang, Ting Chen, Huang-Yu Hao, Xue Han, Ya-Nan Chen

Specialty type: Oncology

Provenance and peer review: Unsolicited article; Externally peer reviewed.

Peer-review model: Single blind

Peer-review report's classification

Scientific Quality: Grade B, Grade C

Novelty: Grade B, Grade B

Creativity or Innovation: Grade B, Grade C

Scientific Significance: Grade C, Grade C

P-Reviewer: Krishan A; Shin HJ

Received: August 28, 2024

Revised: September 21, 2024

Accepted: October 18, 2024

Published online: January 15, 2025

Processing time: 106 Days and 0.6 Hours

Xiao-Jing Shi, Yu Song, Xue-Xue Liang, Ting Chen, Huang-Yu Hao, Xue Han, Ya-Nan Chen, Department of Oncology, Zhangjiagang First People's Hospital, Suzhou 215600, Jiangsu Province, China

Co-first authors: Xiao-Jing Shi and Yu Song.

Corresponding author: Ya-Nan Chen, MMed, Doctor, Department of Oncology, Zhangjiagang First People's Hospital, No. 68 Jiyang West Road, Zhangjiagang, Suzhou 215600, Jiangsu Province, China. chenyanan@126.com

Abstract

BACKGROUND

Owing to the absence of specific symptoms in early-stage gastric cancer, most patients are diagnosed at intermediate or advanced stages. As a result, treatment often shifts from surgery to other therapies, with chemotherapy and targeted therapies being the primary options for advanced gastric cancer treatment.

AIM

To investigate both treatment efficacy and immune modulation.

METHODS

A total of 116 patients with advanced gastric cancer, admitted from January 2021 to December 2023, were selected and divided into two groups of 58 each using the random number table method. The control group received FOLFOX4 chemotherapy (oxaliplatin + calcium + folinate + 5-fluorouracil) combined with intravenous sindilizumab. The observation group received the same treatment as the control group, supplemented by oral administration of Senqi Shiyiwei granules. Both groups underwent treatment cycles of 3 weeks, with a minimum of two cycles. The therapeutic efficacy, immune mechanisms, and treatment-related toxicity and side effects were compared between the groups.

RESULTS

The objective remission rate in the observation group (55.17%) was higher than that of the control group (36.21%) ($P < 0.05$). After two treatment cycle, CD3+, CD4+, and CD4+/CD8+ levels were higher in the observation group compared to the control group, while CD8+, regulatory T cells, and natural killer cells were lower ($P < 0.05$). Additionally, the incidence of leukopenia, nausea, and vomiting was lower in observed group ($P < 0.05$). No significant differences were observed

in the incidence of other adverse reactions ($P > 0.05$).

CONCLUSION
Adjuvant therapy with Shenqixian granules may enhance the efficacy of simudizumab combined with FOLFOX4 chemotherapy in advanced gastric cancer and the immune function by increasing immune cell counts, making it a valuable option in clinical treatment.

Key Words: Sindilizumab; FOLFOX4 chemotherapy; Advanced gastric cancer; Ginseng Qi Xiangyi granule; Clinic treatment

Core Tip: Reasonable and effective treatment with traditional Chinese medicine is crucial for patients with advanced cancer, especially those receiving chemotherapy and targeted therapy.

Citation: Shi XJ, Song Y, Liang XX, Chen T, Hao HY, Han X, Chen YN. Effects of Shenqi Xiangyi granules in advanced gastric cancer chemotherapy. *World J Gastrointest Oncol* 2025; 17(1): 99272
URL: https://www.wjgnet.com/1948-5204/full/v17/i1/99272.htm
DOI: https://dx.doi.org/10.4251/wjgo.v17.i1.99272

INTRODUCTION

Gastric cancer is a highly prevalent malignant tumor worldwide, characterized by incidence, morbidity, and mortality rates. Statistical investigations have shown that the survival and cure rates of patients with gastric cancer are closely associated with the tumor stage, pathological type, treatment method, and the patient's overall health status. For patients with early-stage gastric cancer, the 5-year survival rate can reach 95% or > 98% after surgery[1]. However, because of the insidious onset of gastric cancer in its early stages and the lack of significant clinical symptoms, patients are diagnosed at advanced stages, making treatment more challenging. Chemotherapy-based integrated programs are the treatment of choice for patients with advanced gastric cancer.

Chemotherapy is a cornerstone in the clinical management of advanced gastric cancer, with the FOLFOX4 regimen (oxaliplatin + calcium folinic acid + 5-fluorouracil) being a commonly used protocol. However, it is associated with adverse reactions, negatively affecting the patient's immune function, and prolonged use can lead to resistance[2]. Recently, targeted drugs have been widely utilized in cancer treatment, with sindilizumab being a commonly used agent to enhance the body's immune system and exert anti-tumor effects. It has demonstrated improved outcomes and has been clinically accepted[3]. However, immunosuppression persists in patients during the treatment. Chemotherapy, targeted therapy, and other therapies can lead to a deficiency positive qi in patients, allowing external evils to invade the body and block the meridians. This results in a deficiency of qi and blood, ultimately weakening of organs[4]. Therefore, based on the basic patho-mechanism of positive qi deficiency and blood stasis obstruction in patients with advanced gastric cancer, the treatment approach emphasizing strengthening the spleen, tonifying qi, and promoting blood circulation is proposed.

Ginseng astragalus 11 flavor granules are a kind of Chinese herbal preparation with significant therapeutic effects on various cancers. They tonify the spleen and enhance qi, primarily used in clinical practice to address the symptoms of weakness, particularly limb weakness resulting from the spleen and qi deficiency[5]. Recent studies have demonstrated the effectiveness of Radix astragali decylenic granules. However, the potential of Radix astragali decylenic granules in the adjuvant treatment of advanced gastric cancer to improve patient outcomes and immune function is warrants further clinical investigation. This study analyzed the recent efficacy of adjuvant treatment with Radix Astragali Decima Granules in patients with advanced gastric cancer treated with sindilizumab combined with FOLFOX4 chemotherapy and explored its effect on the immune function. The finding aim to provide theoretical guidance for the use of Traditional Chinese medicine (TCM) in treatment of advanced gastric cancer.

MATERIALS AND METHODS

Participants

A total of 116 patients with advanced gastric cancer admitted to the hospital between January 2021 and December 2023 were selected. This study was double-blinded with medication concealment for treating physicians and patients.

The inclusion criteria were as follows: (1) Patients diagnosed with gastric cancer[6]; (2) Classified as having advanced cancer with predicted survival > 3 months; (3) At least one measurable tumor lesion detectable *via* imaging techniques; and (4) Awareness of the study and signed the consent form. The exclusion criteria were as follows: (1) Extensive systemic metastases; (2) Combined acute and chronic infections; (3) A history of hematopoietic stem cell transplantation and primary immunodeficiency; (4) Other types of malignant tumors; and (5) Allergies to drugs.

Treatment

The control group received FOLFOX4 chemotherapy comprising oxaliplatin (Qilu Pharmaceuticals, State Pharmaceutical Licence H20093127), IV, at a dose of 85 mg/m^2 for 120 minutes, day 1; Calcium folinic acid (Jiangsu Hengrui Pharmaceuticals, State Pharmaceutical Licence H20000584), IV, at a dose of 200 mg/m^2 for 120 minutes, day 1-2; and 5-fluorouracil (Southwest Pharmaceuticals, National Drug Licence H50020128), intravenous push at a dose of 400 mg/m^2 and continuous pumping at a dose of 600 mg/m^2 for 22 hours, day 1-2; this regimen was repeated every 3 weeks as one cycle. Sindilizumab (Xinda Bio-Pharmaceuticals, National Drug Standard S20180016) at a dose of 200 mg/dose was administered intravenously (day 1) every 3 weeks as one cycle. The observation group received the same basic treatment as the control group, with the addition of oral administration of Shenqi Xiangyiwei granules (Jiangxi Shanko Pharmaceuticals, State Pharmaceutical Approval Character Z10980002), 2 g in lukewarm water, three times a day, for 3 weeks for one cycle. Both groups underwent at least two treatment cycles.

Observation indicators

Immediate effects: Efficacy was assessed after two cycles of treatment based on the solid tumor efficacy evaluation criteria[7]: Complete remission (CR): The lesion measurable by imaging had completely disappeared and was maintained for 4 weeks or more; partial remission (PR): The lesion measurable by imaging had shrunk by > 30% compared with the pretreatment period; stable disease (SD): The lesion measurable by imaging shrunk by < 30% or increased by < 20%; progression disease: Did not meet the SD criteria; and the objective remission rate is CR rate + PR rate.

Immune function: Venous blood samples (5 mL) were collected from patients before treatment and after two cycles of treatment, centrifuged for 10 minutes at 3000 r per minute, and the plasma was kept after centrifugation and preserved for examination. Flow cytometry (Beckman Coulter, United States) was used to detect T-lymphocyte sub-populations, including CD3+, CD4+, CD8+, and CD4+/CD8+ ratio. Regulatory T-cells (Tregs) and natural killer cells (NK) were also detected.

Toxic and side effects: According to the toxicity judgment criteria[8], adverse drug reactions were assessed with grades ranging from 1 to 4, including nausea and vomiting, leukocyte reduction, platelet reduction, and liver and kidney function impairments.

Statistical analysis

Statistical analysis of the data within the study was performed using SPSS software (version 26.0). Measurement data were represented as mean ± SD, and independent samples *t*-test was used when they met the normal distribution. Measurement data that did not meet the normal distribution, were represented as median and interquartile spacing (median, interquartile range), and the rank sum test was used. Counting data were expressed as percentage rate (%), and the χ^2 test was performed. A P value < 0.05 was considered statistically significant.

RESULTS

Objective response rates

Both the groups exhibited no significant difference in radiographic lesions (P > 0.05; Table 1).

Immune responses

No difference was observed between the two groups before treatment (P = 0.05). After treatment, the two groups improved, and the improvement was greater in the observation group (P < 0.05), as presented in Table 2 and Table 3.

Poison side reaction

The analysis revealed that the incidence of leukocyte reduction, nausea, and vomiting was lower in the observation group than in the control group (P < 0.05). However, there were no difference in the other indicators (P < 0.05), as shown in Table 4 and Table 5.

DISCUSSION

Chemotherapy is the preferred treatment for advanced gastric cancer, with the FOLFOX4 regimen, in which fluorouracil disrupts the synthesis pathway of tumor cell DNA, blocks mitosis, inhibits the growth of tumor cells, and promotes apoptosis. Oxaliplatin is a non-specific cell cycle drug that impedes tumor cell progression, while leucovoror calcium can improve the anti-tumor effect of fluorouracil, further promoting tumor apoptotic effect[9]. However, chemotherapy alone has toxic effects, and its efficacy cannot meet clinical needs. Sindilizumab is a targeted drug commonly used in clinical practice. It improves the immune system of patients with cancer and enhances the T-cell-mediated killing of tumor cells in the body, promoting tumor cell apoptosis[10]. However, cindilizumab has some adverse effects, and its ability to mitigate chemotherapy-induced side effects is limited. According to TCM, patients with advanced gastric cancer develop heat poisoning and blood stasis due to the decline of visceral function and the deficiency of vital qi, and after a long time, qi, blood, and yang are unbalanced. Consequently, the toxic effects of chemotherapy further weakens body's vital qi,

Table 1 Comparison of the recent effects between the two groups, *n* (%)

Group	CR	PR	SD	PD	Objective mitigation rate
Observation (n = 58)	5 (8.62)	27 (46.55)	23 (39.66)	3 (5.17)	32 (55.17)
Control (n = 58)	1 (1.72)	20 (34.48)	29 (50.00)	8 (13.79)	21 (36.21)
χ^2					4.204
P value					0.040

CR: Complete remission; PR: Partial remission; SD: Stable disease; PD: Progression disease.

Table 2 Comparison of immune function indicators between the two groups before treatment (mean ± SD)

Group	$CD3^+$ (%)	$CD4^+$ (%)	$CD8^+$ (%)	$CD4^+/CD8^+$	Treg cell (%)	NK cell (%)
Observation (n = 58)	42.86 ± 4.86	26.95 ± 3.10	31.04 ± 2.08	0.87 ± 0.12	5.80 ± 1.04	30.24 ± 4.85
Control (n = 58)	43.10 ± 4.96	27.05 ± 3.18	30.85 ± 2.12	0.88 ± 0.13	5.76 ± 1.08	29.82 ± 4.90
t	0.263	0.171	0.487	0.430	0.203	0.464
P value	0.793	0.864	0.627	0.668	0.839	0.644

Tregs: Regulatory T-cells; NK cell: Natural killer cells.

Table 3 Comparison of immune function indicators between the two groups after treatment (mean ± SD)

Group	$CD3^+$ (%)	$CD4^+$ (%)	$CD8^+$ (%)	$CD4^+/CD8^+$	Treg cell (%)	NK cell (%)
Observation (n = 58)	61.28 ± 5.84[a]	38.84 ± 3.58[a]	21.58 ± 2.08[a]	1.81 ± 0.18[a]	2.08 ± 0.65[a]	21.26 ± 3.28[a]
Control (n = 58)	52.84 ± 5.80[a]	33.10 ± 3.48[a]	24.63 ± 2.12[a]	1.34 ± 0.14[a]	3.07 ± 0.72[a]	24.95 ± 3.35[a]
t	7.809	8.756	7.821	15.697	7.773	5.994
P value	< 0.001	< 0.001	< 0.001	< 0.001	< 0.001	< 0.001

[a]P < 0.05.
Tregs: Regulatory T-cells; NK cell: Natural killer cells.

Table 4 Comparison of the two toxic groups, *n* (%)

Group	White blood cell reduction		Platelet reduction		Liver and kidney function injury	
	Level 1-2	Level 3-4	Level 1-2	Level 3-4	Level 1-2	Level 3-4
Observation (n = 58)	22 (37.93)	0	18 (31.03)	0	13 (22.41)	0
Control (n = 58)	31 (53.45)	3 (5.17)	20 (34.48)	2 (3.45)	23 (39.66)	0
χ^2	4.971		0.611		4.028	
P value	0.026		0.435		0.045	

exacerbating cancer-induced obstruction of the meridians. Therefore, based on the etiology and pathogenesis, TCM advocates invigorating the spleen and replenishing qi. Shenqi, known for nourishing blood and replenishing marrow-filling essence, has demonstrated significant adjuvant therapeutic effects in cancer treatment.

This study revealed that the recent objective response rate in the observation group was 55.17% higher than in the control group (36.21%; P < 0.05). This indicates that the efficacy of cindilizumab combined with FOLFOX4 chemotherapy can be further improved. The FOLFOX4 chemotherapy regimen inhibits the proliferation of tumor cells, promotes apoptosis, and, when combined with cinalimmab, alleviates the state of immune suppression by activating T cells in the body and then exerting the killing ability of immune cells to tumor cells, improving antitumor effect[11]. Simultaneously,

Table 5 Comparison of the two toxic groups, *n* (%)

Group	Nausea and vomiting		Hand-foot syndrome		Senses the abnormalities in peripheral nerves	
	Level 1-2	Level 3-4	Level 1-2	Level 3-4	Level 1-2	Level 3-4
Control (n = 58)	21 (36.21)	1 (1.72)	3 (5.17)	0	6 (10.34)	0
Observation (n = 58)	33 (56.90)	3 (5.17)	5 (8.62)	0	9 (15.52)	0
χ^2	6.759		0.134		0.689	
P value	0.009		0.714		0.406	

combined with Shenqi granules, Chinese ginseng can replenish qi, invigorate qi, astragalus, nourish yang yi wei, nourish the kidney, nourish blood, angelica, nourish qi and blood, nourish water dampness, heat release, remove turbidity and reduce fat, relieve cold, remove wind, and relieve pain; cassia, barbary wolfberry and kidney, warm antler and kidney yang eliminate blood and swelling; silk, nourish the liver and kidney, solid essence, and reduce urine. Therefore, the prescription emphasizes strengthening the body's constitution and eliminating harmful elements, which helps restore the function of the spleen and stomach and modulate the tumor microenvironment. This synergistic approach can enhance the treatment of advanced gastric cancer and improve short-term therapeutic outcomes.

Tumors arise from dysplasia of normal cell, which invades surrounding tissues and impairs the immune function of patients. In advanced stages, patients often suffer from chronic illness, with reduced spleen and stomach functions, leading to weakened immunity and decreased tolerance to treatment[12]. T lymphocyte subsets are important factors that reflect the human immune system and participate in human immune regulation. Treg cells have the role of maintaining immune tolerance and immune homeostasis, inhibiting the activity of other immune cells, and avoiding excessive reaction of the immune system, as well as antiviral infection and immune regulation, which can identify target cells and kill mediators[13]. Owing to the widespread immunosuppressive state in patients with tumors, immune function is impaired, and the immune regulation system is destroyed, resulting in reduced levels of CD3+ and CD4 and increased CD8+, Treg, and NK cells. Meng *et al*[14] confirmed that Peiyuan Yiqi soup can alleviate the symptoms of gastric cancer and enhance immune function. This indicates that TCM prescriptions are important for improving the immune function of patients with malignant tumors. However, compared with Shenqi Shiyi granules, Chinese medicine decoction is not convenient enough, and some patients cannot bear the taste of the Chinese medicine decoction; therefore, the feasibility of its application in clinical practice was confirmed again.

This study found that after treatment, the improvement of all immune cells in the observation group was higher than that in the control group. Han *et al*[15] reported that the combined chemotherapy regimen of Shenqi can significantly improve the immune function of patients with advanced colorectal cancer. These results indicate that it can improve the immune function of patients with advanced gastric cancer. Sindilimumab can increase the number of immune cells in patients, relieve immunosuppression, and restore immune responses in the human body, thereby improving immune function. However, Chen *et al*[16] revealed that there is no considerable difference between the tumor immune microenvironment and chemotherapy after neoadjuvant cisplatin treatment, which may be attributed to variations in the treatment cycle and individual patient differences. Therefore, the efficacy of cisplatin-based immunotherapy remains debatable.

Modern pharmacological research has shown that ginseng can increase the number of white blood cells, improve immune function, inhibit the proliferation of tumor cells, and promote the apoptosis of tumor cells in the human body. Ratan *et al*[17] revealed that ginseng has the regulation of human immune function and plays antiviral, antibacterial, and other roles. Astragalus has a significant effect on immune disorders, cancer, and other diseases, which can promote the proliferation of hematopoietic stem cells, repair the damage of bone marrow cells, and improve the body's immune function. Sheik *et al*[18] found that astragalus can regulate the immune system during drug treatment; its polysaccharide, methanoside, and other components have significant potential anticancer activity[18,19]. Therefore, treatment with Shenqi Shiyiwei granules can activate the immune response in the human body and inhibit the immune escape of tumor cells, thus improving immune function. Moreover, the study demonstrated that the incidence of leukocyte reduction, nausea, and vomiting was lower in the treatment group than in the control group ($P < 0.05$). Treatment is helpful to further improve the immune response of patients, reduce the tumor load, and regulate the blood system to reduce the toxicity and side effects of drug treatment to a certain extent. Previous studies have demonstrated the therapeutic effects of TCM on gastric cancer. Previous studies demonstrated that the treatment of Yianpi Huayu in patients with gastric cancer effectively improved their quality of life, increased the number of immune cells, and improved their immunotherapy. Treatment with Shenqi Xiangyi granules in this study also exhibited its effects on improving immune function.

This study had some limitations. First, the sample size of 116 patients was relatively small, which may limit the generalizability of the results. Additionally, the follow-up duration was restricted to two treatment cycles. Thus, the study mainly focused on the immediate effects after these two cycles and lacked an assessment of long-term outcomes, such as progression-free survival, overall survival, or long-term immune recovery. Future studies should include longer follow-up periods to capture data on long-term survival and quality of life. Second, although the study reported some toxicity outcomes, such as leukopenia and nausea, it failed to provide a comprehensive toxicity profile. There is a lack of data on other potential side effects, including the impairment of liver and kidney function, fatigue, and gastrointestinal disturbances. A more comprehensive analysis of toxicity would provide a more accurate understanding of the treatment safety profiles. However, it is hoped that these limitations can be compensated for in future studies. Larger sample sizes

and longer follow-up periods can help obtain more accurate and generalizable results. A comprehensive assessment of toxicity can provide a more complete understanding of treatment safety and guide clinical decision-making.

CONCLUSION

When patients with advanced gastric cancer are treated with cintilizumab combined with FOLFOX4 chemotherapy, it can modulate the immune system, improve immune function, enhance recent treatment outcomes, and reduce the toxic side effects of chemotherapy. This has significant implications for promoting the use of TCM in cancer treatment. However, the study had small sample size and only focused on short-term effects through immune mechanism, which may introduce bias results. Therefore, future studies should aim to expand the sample size, extend the observation period, and explore the treatment efficacy from multiple perspectives to provide more comprehensive evidence for the use of Shenqixian granules in advanced gastric cancer.

FOOTNOTES

Author contributions: Shi XJ and Song Y contributed equally to this work; Shi XJ and Song Y designed the study; Shi XJ, Song Y, Liang XX, Chen T, Hao HY, Han X and Chen YN contributed to the analysis of the manuscript; Shi XJ, Song Y, Liang XX, Chen T, Hao HY, Han X and Chen YN involved in the data and writing of this article; Shi XJ and Song Y are jointly responsible for data collection, design research, and have made equal contributions to this article (so designated Shi XJ and Song Y as co first authors); All authors have read and approved the final manuscript.

Institutional review board statement: This study was reviewed and approved by the Institutional Review Board of Zhangjiagang First People's Hospital, No. 2021-Z-1254.

Clinical trial registration statement: The study was registered at the Clinical Trial Center (www.researchregistry.com) with registration number: researchregistry10707.

Informed consent statement: All study participants and their legal guardians provided written informed consent before recruitment.

Conflict-of-interest statement: All the authors report no relevant conflicts of interest for this article.

Data sharing statement: No additional data is available.

CONSORT 2010 statement: The authors have read the CONSORT 2010 Statement, and the manuscript was prepared and revised according to the CONSORT 2010 Statement.

Country of origin: China

ORCID number: Xiao-Jing Shi 0009-0008-6366-0870; Ya-Nan Chen 0009-0001-3071-9425.

S-Editor: Li L
L-Editor: A
P-Editor: Xu ZH

REFERENCES

1 **López MJ**, Carbajal J, Alfaro AL, Saravia LG, Zanabria D, Araujo JM, Quispe L, Zevallos A, Buleje JL, Cho CE, Sarmiento M, Pinto JA, Fajardo W. Characteristics of gastric cancer around the world. *Crit Rev Oncol Hematol* 2023; **181**: 103841 [PMID: 36240980 DOI: 10.1016/j.critrevonc.2022.103841]

2 **Salvatori S**, Marafini I, Laudisi F, Monteleone G, Stolfi C. Helicobacter pylori and Gastric Cancer: Pathogenetic Mechanisms. *Int J Mol Sci* 2023; **24**: 2895 [PMID: 36769214 DOI: 10.3390/ijms24032895]

3 **Zhang Y**, Jiang L, Ouyang J, Du X, Jiang L. Efficacy and safety of traditional Chinese medicine injections combined with FOLFOX4 regimen for gastric cancer: A protocol for systematic review and network meta-analysis. *Medicine (Baltimore)* 2021; **100**: e27525 [PMID: 34731143 DOI: 10.1097/MD.0000000000027525]

4 **Wu H**, Miao X, Liu Y, Zhang S, Li C, Hao J. Clinical Efficacy of Modified Yiwei Shengyang Decoction Combined with FOLFOX4 Chemotherapy Regimen in the Treatment of Advanced Gastric Cancer and Its Effect on Tumor Marker Levels. *Evid Based Complement Alternat Med* 2022; **2022**: 6234032 [PMID: 35571732 DOI: 10.1155/2022/6234032]

5 **Xu J**, Jiang H, Pan Y, Gu K, Cang S, Han L, Shu Y, Li J, Zhao J, Pan H, Luo S, Qin Y, Guo Q, Bai Y, Ling Y, Yang J, Yan Z, Yang L, Tang

Y, He Y, Zhang L, Liang X, Niu Z, Zhang J, Mao Y, Guo Y, Peng B, Li Z, Liu Y, Wang Y, Zhou H; ORIENT-16 Investigators. Sintilimab Plus Chemotherapy for Unresectable Gastric or Gastroesophageal Junction Cancer: The ORIENT-16 Randomized Clinical Trial. *JAMA* 2023; **330**: 2064-2074 [PMID: 38051328 DOI: 10.1001/jama.2023.19918]

6 **Japanese Gastric Cancer Association**. Japanese Gastric Cancer Treatment Guidelines 2021 (6th edition). *Gastric Cancer* 2023; **26**: 1-25 [PMID: 36342574 DOI: 10.1007/s10120-022-01331-8]

7 **Kim JH**. Comparison of the RECIST 1.0 and RECIST 1.1 in patients treated with targeted agents: a pooled analysis and review. *Oncotarget* 2016; **7**: 13680-13687 [PMID: 26885610 DOI: 10.18632/oncotarget.7322]

8 **Basch E**, Becker C, Rogak LJ, Schrag D, Reeve BB, Spears P, Smith ML, Gounder MM, Mahoney MR, Schwartz GK, Bennett AV, Mendoza TR, Cleeland CS, Sloan JA, Bruner DW, Schwab G, Atkinson TM, Thanarajasingam G, Bertagnolli MM, Dueck AC. Composite grading algorithm for the National Cancer Institute's Patient-Reported Outcomes version of the Common Terminology Criteria for Adverse Events (PRO-CTCAE). *Clin Trials* 2021; **18**: 104-114 [PMID: 33258687 DOI: 10.1177/1740774520975120]

9 **Li WW**, Jiao J, Wang ZY, Wei YN, Zhang YF. Clinical efficacy of immunotherapy combined with chemotherapy in patients with advanced gastric cancer, its effect on nutritional status and Changes of peripheral blood T lymphocyte subsets. *Pak J Med Sci* 2021; **37**: 1902-1907 [PMID: 34912415 DOI: 10.12669/pjms.37.7.4347]

10 **Hoy SM**. Sintilimab: First Global Approval. *Drugs* 2019; **79**: 341-346 [PMID: 30742278 DOI: 10.1007/s40265-019-1066-z]

11 **Zhang L**, Wang W, Ge S, Li H, Bai M, Duan J, Yang Y, Ning T, Liu R, Wang X, Ji Z, Wang F, Zhang H, Ba Y, Deng T. Sintilimab Plus Apatinib and Chemotherapy as Second/Third-Line treatment for Advanced Gastric or Gastroesophageal Junction Adenocarcinoma: a prospective, Single-Arm, phase II trial. *BMC Cancer* 2023; **23**: 211 [PMID: 36872337 DOI: 10.1186/s12885-023-10661-4]

12 **Villarroel-Espindola F**, Ejsmentewicz T, Gonzalez-Stegmaier R, Jorquera RA, Salinas E. Intersections between innate immune response and gastric cancer development. *World J Gastroenterol* 2023; **29**: 2222-2240 [PMID: 37124883 DOI: 10.3748/wjg.v29.i15.2222]

13 **Röcken C**. Predictive biomarkers in gastric cancer. *J Cancer Res Clin Oncol* 2023; **149**: 467-481 [PMID: 36260159 DOI: 10.1007/s00432-022-04408-0]

14 **Meng X**, Zhang XQ, Li L, Zhang YR. [Peiyuan Yiqi decoction improves cancer-related fatigue of gastric cancer with deficiency of qi and yin and its effect on immune function]. *Shanxi Zhongyi* 2023; **44**: 174-177 [DOI: 10.3969/j.issn.1000-7369.2023.02.008]

15 **Chen Y**, Ren M, Li B, Meng Y, Wang C, Jiang P, Song T, Yang J, Zhu D, Yu Q. Neoadjuvant sintilimab plus chemotherapy for locally advanced resectable esophageal squamous cell carcinoma: a prospective, single-arm, phase II clinical trial (CY-NICE). *J Thorac Dis* 2023; **15**: 6761-6775 [PMID: 38249875 DOI: 10.21037/jtd-23-1388]

16 **Chen X**, Xu X, Wang D, Liu J, Sun J, Lu M, Wang R, Hui B, Li X, Zhou C, Wang M, Qiu T, Cui S, Sun N, Li Y, Wang F, Liu C, Shao Y, Luo J, Gu Y. Neoadjuvant sintilimab and chemotherapy in patients with potentially resectable esophageal squamous cell carcinoma (KEEP-G 03): an open-label, single-arm, phase 2 trial. *J Immunother Cancer* 2023; **11** [PMID: 36759013 DOI: 10.1136/jitc-2022-005830]

17 **Ratan ZA**, Youn SH, Kwak YS, Han CK, Haidere MF, Kim JK, Min H, Jung YJ, Hosseinzadeh H, Hyun SH, Cho JY. Adaptogenic effects of Panax ginseng on modulation of immune functions. *J Ginseng Res* 2021; **45**: 32-40 [PMID: 33437154 DOI: 10.1016/j.jgr.2020.09.004]

18 **Sheik A**, Kim K, Varaprasad GL, Lee H, Kim S, Kim E, Shin JY, Oh SY, Huh YS. The anti-cancerous activity of adaptogenic herb Astragalus membranaceus. *Phytomedicine* 2021; **91**: 153698 [PMID: 34479785 DOI: 10.1016/j.phymed.2021.153698]

19 **Zhang M**, Cuan J, Wang W, Guo Y, Zhao J. Effects of Yipi Huayu decoction on tumor markers, immune function, and adverse reactions during chemotherapy in gastric cancer patients: a retrospective propensity score-matched study. *Am J Transl Res* 2024; **16**: 3599-3613 [PMID: 39262718 DOI: 10.62347/SRHB1100]

World Journal of Gastrointestinal Oncology

Submit a Manuscript: https://www.f6publishing.com

World J Gastrointest Oncol 2025 January 15; 17(1): 97831

DOI: 10.4251/wjgo.v17.i1.97831

ISSN 1948-5204 (online)

ORIGINAL ARTICLE

Basic Study

Interleukin-17A facilitates tumor progression *via* upregulating programmed death ligand-1 expression in hepatocellular carcinoma

Zhong-Xia Yang, Li-Ting Zhang, Xiao-Jun Liu, Xue-Bin Peng, Xiao-Rong Mao

Specialty type: Gastroenterology and hepatology

Provenance and peer review: Unsolicited article; Externally peer reviewed.

Peer-review model: Single blind

Peer-review report's classification

Scientific Quality: Grade C, Grade D

Novelty: Grade B, Grade C

Creativity or Innovation: Grade B, Grade C

Scientific Significance: Grade B, Grade C

P-Reviewer: Qiao SM; Zhou ST

Received: June 10, 2024

Revised: September 2, 2024

Accepted: October 28, 2024

Published online: January 15, 2025

Processing time: 184 Days and 19.8 Hours

Zhong-Xia Yang, Li-Ting Zhang, Xiao-Rong Mao, The First School of Clinical Medicine, Lanzhou University, Lanzhou 730000, Gansu Province, China

Zhong-Xia Yang, Xue-Bin Peng, Xiao-Rong Mao, Department of Infectious Diseases, The First Hospital of Lanzhou University, Lanzhou 730000, Gansu Province, China

Xiao-Jun Liu, Department of Radiotherapy, Gansu Provincial Hospital, Lanzhou 730000, Gansu Province, China

Corresponding author: Xiao-Rong Mao, Doctor, Chief Physician, Department of Infectious Diseases, The First Hospital of Lanzhou University, No. 1 Donggangxi Road, Chengguan District, Lanzhou 730000, Gansu Province, China. layygrk@126.com

Abstract

BACKGROUND

Hepatocellular carcinoma (HCC) is an inflammation-associated tumor with a dismal prognosis. Immunotherapy has become an important treatment strategy for HCC, as immunity is closely related to inflammation in the tumor microenvironment. Inflammation regulates the expression of programmed death ligand-1 (PD-L1) in the immunosuppressive tumor microenvironment and affects immunotherapy efficacy. Interleukin-17A (IL-17A) is involved in the remodeling of the tumor microenvironment and plays a protumor or antitumor role in different tumors. We hypothesized that IL-17A participates in tumor progression by affecting the level of immune checkpoint molecules in HCC.

AIM

To investigate the effect and mechanism of action of IL-17A on PD-L1 expression and to identify attractive candidates for the treatment of HCC.

METHODS

The upregulation of PD-L1 expression in HCC cells by IL-17A was assessed by reverse transcription PCR, western blotting, and flow cytometry. Mechanistic studies were conducted with gene knockout models and pathway inhibitors. The function of IL-17A in immune evasion was explored through coculture of T cells and HCC cells. The effects of IL-17A on the malignant biological behaviors of HCC cells were evaluated *in vitro*, and the antitumor effects of an IL-17A inhibitor and its synergistic effects with a PD-L1 inhibitor were studied *in vivo*.

RESULTS
IL-17A upregulated PD-L1 expression in HCC cells in a dose-dependent manner, whereas IL-17A receptor knockout or treatment with a small mothers against decapentaplegic 2 inhibitor diminished the PD-L1 expression induced by IL-17A. IL-17A enhanced the survival of HCC cells in the coculture system. IL-17A increased the viability, G2/M ratio, and migration of HCC cells and decreased the apoptotic index. Cyclin D1, *VEGF*, *MMP9*, and *Bcl-1* expression increased after IL-17A treatment, whereas *BAX* expression decreased. The combination of IL-17A and PD-L1 inhibitors showed synergistic antitumor efficacy and increased cluster of differentiation 8 + T lymphocyte infiltration in an HCC mouse model.

CONCLUSION
IL-17A upregulates PD-L1 expression *via* the IL-17A receptor/phosphorylation-small mothers against decapentaplegic 2 signaling pathway in HCC cells. Blocking IL-17A enhances the therapeutic efficacy of PD-L1 antibodies in HCC *in vivo*.

Key Words: Interleukin-17A; Programmed death ligand-1; Interleukin-17A receptor; Small mothers against decapentaplegic 2; Hepatocellular carcinoma; Immunotherapy

Core Tip: Overexpression of programmed death ligand-1 (PD-L1) on tumor cells promotes cancer immune escape through inhibiting T cell function. Interleukin-17A (IL-17A) can increase the expression of PD-L1 in tumor cells and promote tumor progression. However, related research in hepatocellular carcinoma (HCC) is scarce. We clarified a novel mechanism by which IL-17A upregulated PD-L1 expression in HCC cells by the IL-17A receptor/phosphorylation-small mothers against decapentaplegic 2 axis. IL-17A could drive immune escape and promote proliferation, migration, and angiogenesis of HCC cells while inhibiting the apoptosis of HCC cells. IL-17A inhibition enhanced the therapeutic efficacy of the PD-L1 antibody in HCC *in vivo*.

Citation: Yang ZX, Zhang LT, Liu XJ, Peng XB, Mao XR. Interleukin-17A facilitates tumor progression *via* upregulating programmed death ligand-1 expression in hepatocellular carcinoma. *World J Gastrointest Oncol* 2025; 17(1): 97831
URL: https://www.wjgnet.com/1948-5204/full/v17/i1/97831.htm
DOI: https://dx.doi.org/10.4251/wjgo.v17.i1.97831

INTRODUCTION

Hepatocellular carcinoma (HCC) is the fifth most common cancer worldwide[1]. Most patients are diagnosed at an advanced stage, which is associated with a higher mortality rate[1]. The major HCC guidelines recommend immune checkpoint blockade (ICB) as a first- or second-line therapy for the treatment of patients with cancer. However, the effective rates of ICB monotherapy vary only from 15% to 23% and increase to approximately 30% after combined treatment in patients with advanced HCC[2]. The tumor immune microenvironment (TME) aggressively promotes the progression of HCC and adversely affects the efficacy of antitumor therapies. Inflammatory factors and immune checkpoint molecules are two critical components of the TME. Inflammatory factors can facilitate tumor immune evasion and tumor progression[3]. The aberrant activation of some inflammatory pathways is a significant cause of the limited efficacy of ICB in HCC[4].

Programmed death ligand-1 (PD-L1) is typically overexpressed on cancer cells and is correlated with a poor prognosis in patients with HCC[5]. The overexpression of PD-L1 on tumor cells not only promotes cancer cell immune escape by inhibiting T cell function[6] but also promotes tumor development signals[7]. The expression of PD-L1 on HCC cells can be upregulated by inflammatory factors[8], oncogenic pathways[9], and transcriptional regulators[10].

Interleukin-17A (IL-17A) plays a protumor or antitumor role *via* different signaling pathways in various types of TMEs, as shown in previous studies[11-14]. IL-17A is a double-edged sword in the tumor microenvironment. Increasing evidence suggests that IL-17A exerts a tumor-promoting effect through PD-L1. IL-17A may also contribute to creating an immunosuppressive tumor microenvironment by enhancing PD-L1 expression in colon and prostate tumors[15]. IL-17A reduces PD-L1 degradation and promotes tumorigenesis in non-small cell lung cancer[16]. IL-17A elevates PD-L1 levels on mesenchymal stem cells *via* inducible nitric oxide synthase and accelerates tumor development[17]. IL-17A therefore has a protumor effect on HCC. Future studies will explore whether IL-17A promotes HCC progression in a PD-L1-dependent manner.

Growing evidence has shown that the limited efficacy of immunotherapy is closely related to tumor-associated chronic inflammation. Targeting inflammation, including IL-17A, as an adjuvant therapy to increase the therapeutic effectiveness of ICBs is one potential treatment approach. Patients with colorectal cancer could benefit from cancer immunotherapy consisting of anti-IL-17 monoclonal antibodies as an adjuvant therapy[18]. However, Liao *et al*[16] reported conflicting

results that targeting IL-17A and PD-L1 diminishes the therapeutic effect of PD-L1 inhibitors in lung cancer. Other studies reported that IL-17A itself could increase the efficacy of immunotherapy in gastric cancer[19], and breast adenocarcinoma [20]. The results of multiple studies are inconsistent and might be related to the heterogeneity of the TME. IL-17A plays a protumor role in alcohol-induced HCC[21], but its implications for ICB in HCC and the underlying mechanisms remain elusive.

Our previous study revealed a positive correlation between the levels of IL-17A and soluble PD-L1 in the plasma of HCC patients. IL-17A was also associated with tumor load and tumor invasiveness in that study. The specific role of IL-17A in HCC development and the mechanism by which PD-L1 expression is upregulated require further exploration. Given the possible effect of IL-17A on PD-L1, we hypothesized that blocking IL-17A might sensitize HCC cells to ICB. To investigate this hypothesis, we examined the phenotypic changes in HCC cells after IL-17A treatment and the potential signaling pathway by which IL-17A regulates PD-L1 expression. Our study also evaluated the therapeutic efficacy of an IL-17A inhibitor combined with a PD-L1 inhibitor in a syngeneic model.

MATERIALS AND METHODS

Cell culture and reagents

The human HCC cell lines HCCLM3, Huh7, and Hep3B and the mouse HCC cell line Hepa1-6 were purchased from the American Type Culture Collection (Manassas, VA, United States). Cells were cultured in Dulbecco's Modified Eagle's Medium (HyClone, Cytiva, United States) supplemented with 10% fetal bovine serum (HyClone, Cytiva, United States) and 100 U/mL penicillin/streptomycin. All cells were cultured at 37 °C with 5% carbon dioxide in a humidified incubator.

Recombinant human IL-17A (No. 7955-IL-025) was obtained from R and D Systems. Transforming growth factor (TGF)-beta signal pathway inhibitor (ITD-1) (S6713), an IL-17A inhibitor (a2120), and a PD-L1 inhibitor (a2115) were obtained from Selleck Chemicals. Anti-PD-L1 (ab213480) and anti-IL-17A receptor (IL-17RA) (ab263908) antibodies were purchased from Abcam. Anti-GAPDH was purchased from Bioworld, and anti-small mothers against decapentaplegic 2 (SMAD2) (AF1300), anti-phosphorylation-SMAD2 (AF2545), anti-Bcl-2 (AF0060), anti-cyclinD1 (AF1516), anti-Ki67 (AF1738), and 5, 6-carboxyfluorescein diacetate, succinimidyl ester (C1031) were purchased from Beyotime Biotechnology. Anti-BAX (No. 9664) was obtained from Cell Signaling Technology, and anti-VEGF (ET1604-28) and anti-MMP9 (ET1704-69) were purchased from HUABIO. Anti-PD-L1 (mouse, 66248-1), anti-IL-17A (mouse 26163-1-AP), and PD-L1 ELISA kits were obtained from Protein tech. A cell counting kit 8 kit (K1018) was purchased from APExBIO. Annexin V-FITC/PI apoptosis detection kits (E-CK-A211) and anti-PD-L1 (FCM), anti-PD-1 (FCM), anti-cluster of differentiation (CD) 8 (FCM), and IL-17A ELISA kits were purchased from Elabscience Biotechnology. Recombinant human IL-2, anti-human CD3 (317325), and anti-human CD28 (302933) antibodies were obtained from BioLegend.

Mice

C57BL/6J mice (male, 4-5 weeks) were purchased from Cavens, Changzhou, China. The mice were housed in a specific pathogen-free environment at the Animal Research Center of Gansu University of Chinese Medicine and had access to adequate food and water. All mouse studies were performed according to protocols approved by the Animal Research Committee of Gansu University of Chinese Medicine.

Western blotting analysis

The cells were cultured in 6-well plates with or without IL-17A. After 24 h, proteins were extracted in radioimmunoprecipitation assay lysis buffer containing protease and phosphatase inhibitors. Protein concentrations were assayed with a bicinchoninic acid protein assay kit. The proteins were boiled in loading buffer for 10 minutes after which proteins were separated by 10% gradient sodium dodecyl sulfate-polyacrylamide gel electrophoresis, transferred from the gel to polyvinylidene difluoride membranes, and blocked with QuickBlock™ Western for 30 min. The membranes were subsequently incubated with primary antibodies overnight at 4 °C and then incubated with secondary antibodies for 1 hour at room temperature. Protein expression was visualized *via* enhanced chemiluminescence detection reagents and an Amersham Imager 600 system (GE Healthcare, Boston, MA, United States). The results were analyzed using ImageJ2x software.

Establishment of the IL-17RA knockout cell line

The IL-17RA knockout virus was constructed by Genechem Shanghai, and the sequences of the single guide RNAs against the IL-17RA knockout virus were as follows: (1) 5′-CCACAGTTGCTTTGAGCACAT-3′; (2) 5′-GCTGAACAC-CAAtgAACGTTT-3′; and (3) 5′-AGGAGAtgGTGGAGAGCAACT-3′. The viruses were subsequently used to infect Huh7 cells, and the cultured medium was replaced after 12 h. After 48 h, 1 μg/mL puromycin was added to select infected cells. IL-17RA knockout clones were identified by western blotting and quantitative reverse transcription PCR.

RNA extraction and quantitative reverse transcription PCR

The cells were cultured in 6-well plates with or without IL-17A. RNAiso Plus reagent was used to extract total RNA. Then, 1 μg of total RNA was converted into complementary DNA *via* a reverse transcription kit. Quantitative PCR was performed on a CFX96 deep well real-time PCR system (Bio-Rad) with a reaction volume of 35 μL containing 7.7 μL of RNase-free water, 7 μL of complementary DNA, 1.4 μL of forward primer, 1.4 μL of reverse primer, and 17.5 μL of TB

green premix ex-Taq II. The 2-ΔΔct method was used to determine the RNA expression level. PCR primers were purchased from Tsingke Biological Technology (Beijing, China). The sequences of primers used were as follows: (1) *PD-L1*, 5′-GGTGCCGACTACAAGCGAATTAC-3′ (forward), 5′-GGAATTGGTGGTGGTGGTCTTAC-3′ (reverse); (2) *IL-17RA*, 5′-GAAAtgGCATCCAGGTCCATC-3′ (forward), 5′-CCTAAATGGACAGGGCGAGAG-3′ (reverse); and (3) *GAPDH*, 5′-TGTGTCCGTCGTGGATCTGA-3′ (forward), 5′-TTGCTGTTGAAGTCGCAGGAG-3′ (reverse).

T cell coculture assay

Peripheral blood was obtained from healthy volunteers after which peripheral blood mononuclear cells were extracted according to the manufacturer's instructions (TBD Sciences, Tianjin, China). Peripheral blood mononuclear cells were placed in RPMI-1640 medium and incubated for 2 h. Then, the suspended cells were transferred to culture bottles and stimulated with IL-2 (1000 U/mL). Moreover, antibodies against CD3 (1 μg/mL) and CD28 (2 μg/mL) were added to the medium to stimulate T cell activation. The culture medium containing IL-2 (1000 U/mL) was replaced every 3 days. HCCLM3, Huh7, and Hep3B cells were labeled with carboxy fluorescein diacetate succinimidyl ester. Next, activated T cells were seeded into medium containing tumor cells (T cell to tumor cell ratio was 10:1) and cocultured with or without IL-17A (100 ng/mL) for 24 h. Finally, live tumor cells and CD8+ T cells were analyzed by flow cytometry.

Cell viability assay

HCCLM3, Huh7, and Hep3B cells were seeded in 96-well plates (5×10^3 cells/well). IL-17A was diluted to gradient concentrations in serum-free Dulbecco's modified eagle medium. After the cells adhered to the wall, the medium was substituted with the prepared solution, and the cells were cultured for 24 h. Cell viability was tested *via* a cell counting kit 8 assay kit. The absorbance was measured at 450 nm using a microplate reader.

Migration assay

Scratch wound and Transwell assays were used to measure the migration ability of the cells. Different cells were cultured in 6-well plates (5×10^5 cells/well) for the scratch test. The monolayer was scratched, and the detached cells were removed. The cells were cultured with or without IL-17A (100 ng/mL). The cells in each well were photographed at 0 h, 24 h, and 48 h after the scratch was generated. The area of wound healing was calculated according to the formula (migration area (%) = (A0 - An)/A0 × 100%, where A0 represents the initial wound area and An represents the remaining area of the wound at the metering point).

For the Transwell assay, 10×10^5 cells suspended in medium (200 μL) without fetal bovine serum were incubated in the upper chamber, while complete medium (600 μL) with or without IL-17A (100 ng/mL) was added to the lower chamber. After 24 h, the cells were fixed in 4% paraformaldehyde for 20 min and stained with 0.1% crystal violet for 30 min. Nonmigrating cells in the upper chamber were removed with a cotton swab. The number of migrating cells was calculated using ImageJ2x software.

Flow cytometry

For the detection of apoptotic cells, HCC cells were cultured in 6-well plates with or without IL-17A (100 ng/mL). After 24 h, the cells were collected and resuspended in 500 μL of staining buffer containing 5 μL of Annexin VFITC and 5 μL of propidium iodide. The cells were then incubated in the dark for 20 min after which apoptotic cells were detected by flow cytometry (Agilent, United States). The results were evaluated using NovoExpress software.

For cell cycle distribution analysis, HCC cells were collected and washed with PBS. The cells were then incubated with DNA staining solution and permeabilization solution for 30 min in the dark. The cell cycle distribution was determined by flow cytometry, and the data were analyzed using NovoExpress software.

For the detection of PD-L1, HCC cells were cultured in 24-well plates with or without IL-17A (100 ng/mL). After 24 h, the cells were collected and washed with PBS. The cells were then incubated with staining buffer and an anti-PD-L1 antibody for 30 min in the dark. Flow cytometry was used to detect PD-L1 expression on the cells.

For the detection of PD-1, T cells were collected after coculture with tumor cells and resuspended in staining buffer. An anti-PD-1 antibody was added to the buffer after which T cells were incubated for 30 min in the dark. Flow cytometry was used to detect PD-1 expression on the cells.

In vivo efficacy studies

A total of 1×10^6 Hepa1-6 tumor cells were injected subcutaneously into C57BL/6J mice (n = 9/group). When the tumors grew to 50 mm^3 to 100 mm^3 in size, the mice were randomly divided into the following groups: isotype control; the anti-IL-17A; the anti-PD-L1; and the combined groups. The antibodies (100 μg/mouse) were intraperitoneally injected into the mice once every other day for 10 days. The length and width of the tumors were measured using electronic calipers every 2 days. The tumor volume was calculated as length × $width^2/2$. The mice were sacrificed 24 h after the last treatment. The serum was collected by centrifugation at 3000 rpm for 10 min and prepared for ELISA. Tumor tissues were collected for flow cytometry and immunohistochemistry.

ELISA detection

Serums PD-L1 and IL-17A levels were tested using ELISA kits according to the manufacturer's instructions. The standards and test samples were pipetted into 96-well plates and incubated at 37 °C. Biotinylated detection antibodies were added to each well, after which the plates were incubated, and unbound biotinylated antibodies were washed with washing buffer. The horseradish peroxidase-conjugated working solution was pipetted into each well. The plates were incubated, after which the wells were washed, and the substrate stop solution was added. The optical absorbance was

measured at 450 nm in a microplate reader (Thermo Scientific Varioskan Flash, MA, United States). The protein concentration was calculated according to the standard curves.

Immunohistochemistry analysis

Paraffin-embedded tumor tissue was sectioned, and immunohistochemical staining was performed to detect PD-L1, IL-17A, and Ki67. The experimental procedures included deparaffinization, rehydration, antigen retrieval, endogenous peroxidase inactivation, nonspecific protein blocking, incubation with primary antibodies, and incubation with secondary antibodies. The slides were subsequently incubated with horseradish enzyme-labeled streptavidin working solution. Finally, the slides were successively stained with diaminobenzidine solution and hematoxylin. The negative control was performed by omitting the primary antibodies. The positive rate was evaluated ImageJ2x software.

The Cancer Genome Atlas data analysis

RNA-seq data with standard annotations were downloaded from The Cancer Genome Atlas (TCGA), (https://portal.gdc.cancer.gov/). The data were analyzed using TCGA biolinks.

Statistical analysis

Statistical analysis was conducted using statistical product and service solutions (v29.0, Chicago, IL, United States) and Graphpad Prism8.0.2. Comparisons between groups were performed *via t* tests or one-way analysis of variance. Correlation analysis was performed *via* Pearson's test or Spearman's test. $P < 0.05$ indicated statistical significance.

RESULTS

IL-17A upregulated PD-L1 expression in a dose-dependent manner

IL-17A promoted the expression of *PD-L1* mRNA and PD-L1 protein in Hep3B, Huh7, and HCCLM3 cells in a dose-dependent manner (Figure 1A and B). Compared with the 0 ng/mL treatment, the 100 ng/mL treatment for 24 h significantly increased the PD-L1 level. The low doses of IL-17A were insufficient to regulate the transcript and protein levels of PD-L1 in HCC cells. Further verification of this upregulation effect was performed. Flow cytometric analysis also revealed that the expression of PD-L1 was greater in the IL-17A-100 ng/mL group than in the control group (Figure 1C). Therefore, we treated HCC cells with 100 ng/mL IL-17A for 24 h in this study.

IL-17A reduced the killing effect of T cells on HCC cells

It is generally acknowledged that the overexpression of PD-L1 promotes the immune escape of tumor cells. To evaluate the PD-L1 activity induced by IL-17A, we performed a coculture assay, which consistently revealed that IL-17A increased the proliferation ability and decreased the death of tumor cells in the T cell and HCC cell coculture system (Figure 2A). Bar graphs revealed a significant difference between the two groups with or without IL-17A treatment (Figure 2B). The level of PD-1 on T cells was greater in the coculture system than on T cells cultured alone (Figure 2C). IL-17A had no effect on PD-1 levels in cocultured cells (Figure 2C).

IL-17A enhanced PD-L1 protein expression in HCC cells via the IL-17RA/p-SMAD2 signaling pathway

To further explore the possible mechanism by which IL-17A regulates the expression of PD-L1, blocking experiments were performed, and RNA-seq data from liver HCC samples ($n = 374$) and nontumor samples ($n = 50$) from the genomic data common were analyzed. The results of the TCGA database analysis revealed that *IL-17RA* and *SMAD2* expression increased in liver HCC samples compared with normal samples (Figure 3A). To determine the possible effect of IL-17RA on IL-17A-induced PD-L1 expression, we introduced lentivirus-mediated stable silencing of IL-17RA in Huh7 cells. The efficiency of IL-17RA knockdown is shown in Figure 3B and C. We investigated the effect of IL-17RA knockdown on PD-L1 expression. As shown in Figure 3D, the level of PD-L1 was not altered in the IL-17RA-knockdown group compared with the negative control (NC) group. Then, cells in which IL-17RA was stably silenced and control cells were treated with 100 ng/mL IL-17A for 24 h. Western blot analysis demonstrated that IL-17A-induced PD-L1 expression was inhibited by IL-17RA knockdown (Figure 3E). Therefore, the expression of PD-L1 in HCC cells may be regulated by the IL-17A/IL-17RA pathway.

Western blotting revealed that IL-17A notably increased only the level of p-SMAD2 protein but did not affect the level of SMAD2 protein (Figure 3F). The ratio of p-SMAD2 to SMAD2 in the IL-17A-100 ng/mL group was greater than that in the control group (Figure 3F). Subsequent analysis revealed that the IL-17A-induced increase in PD-L1 expression was inhibited by pretreatment with ITD-1 (an inhibitor of Smad2 phosphorylation) (Figure 3G). The dose of ITD was determined according to the cell viability inhibitory concentrations (IC50 values) established by the cell counting kit-8 assay (Supplementary Figure 1). However, further studies are needed to verify whether IL-17A binds to IL-17RA to directly or indirectly regulate p-SMAD2 expression. The cells in the IL-17RA-knockdown and NC groups were treated with IL-17A. The protein levels of SMAD2 and p-SMAD2 were tested *via* western blotting. The ratio of p-SMAD2 to SMAD2 in the IL-17RA-knockdown group was lower than that in the NC group (Figure 3H). Together, these findings suggest that the upregulation of PD-L1 expression by IL-17A may be mediated through the IL-17RA/p-SMAD2 signaling pathway.

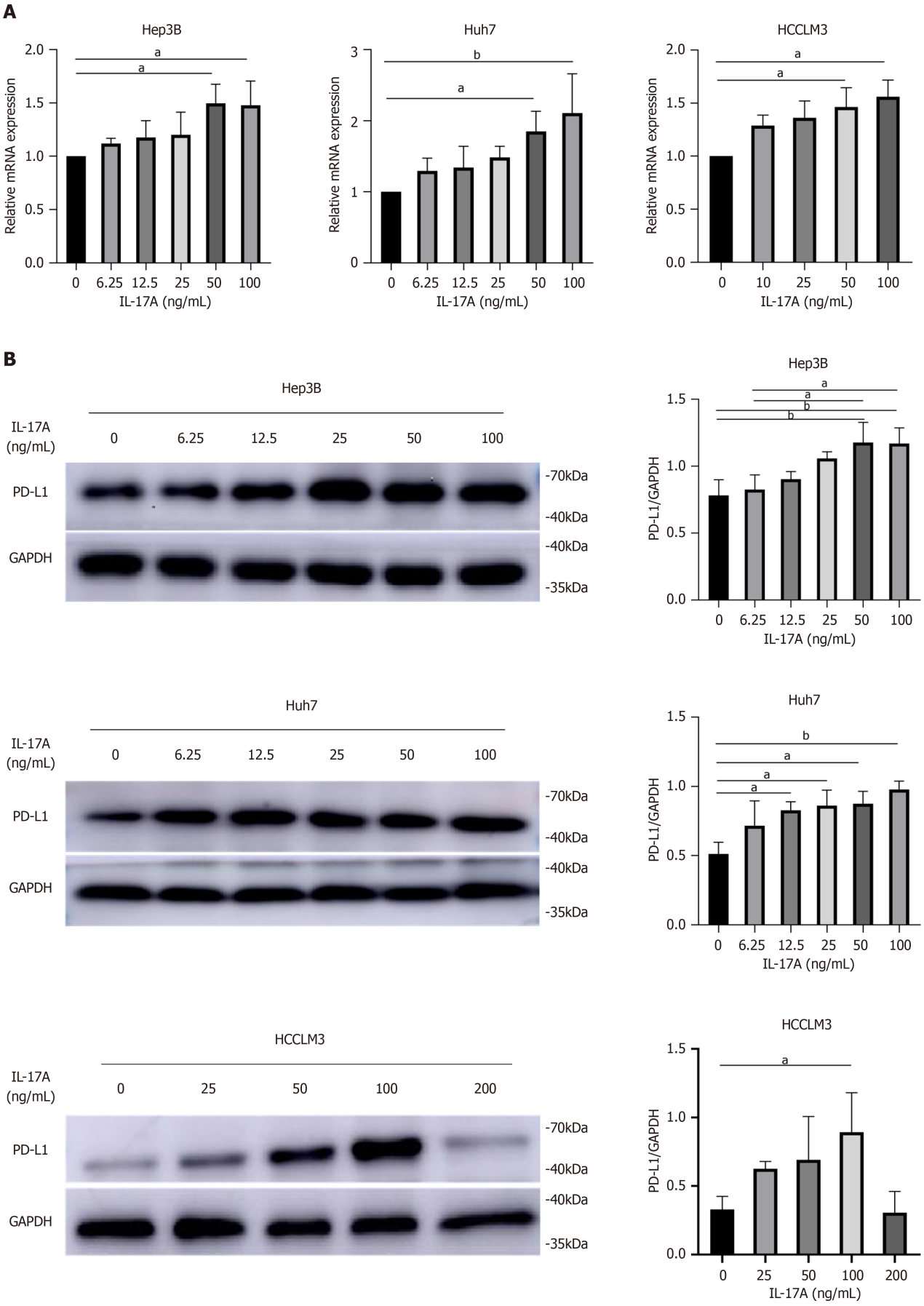
A
Hep3B
Huh7
HCCLM3
Relative mRNA expression
IL-17A (ng/mL)
B
Hep3B
Huh7
HCCLM3
IL-17A (ng/mL)
PD-L1
GAPDH
-70kDa
-40kDa
-35kDa
PD-L1/GAPDH

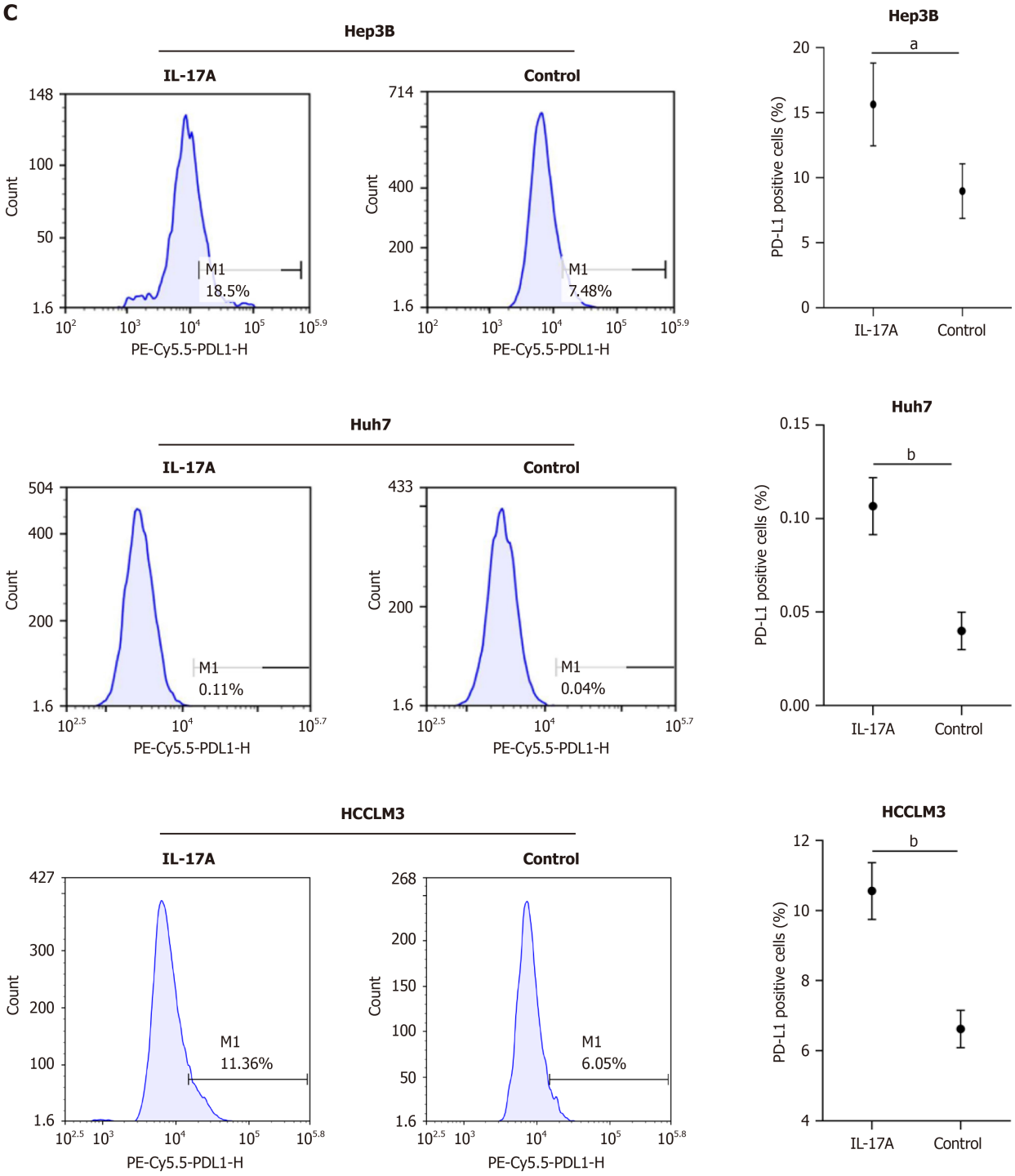

Figure 1 Interleukin-17A regulated programmed cell death ligand-1 expression at the RNA and protein levels in a dose-dependent manner. A: Programmed cell death ligand-1 (*PD-L1*) mRNA levels were detected by reverse transcription PCR in hepatocellular carcinoma (HCC) cells after treatment with different concentrations of interleukin-17A (IL-17A) for 24 h; B: PD-L1 protein levels were determined by western blotting in HCC cells after treatment with different concentrations of IL-17A for 24 h; C: PD-L1 protein levels in HCC cells were tested by flow cytometry after treatment with 100 ng/mL IL-17A for 24 h. $^{a}P < 0.05$; $^{b}P < 0.01$. PE: Phycoerythrin.

IL-17A facilitated HCC cell proliferation, migration, and angiogenesis

The proliferation abilities of the HCC cells were analyzed, and growth curves were generated. The viability of HCC cells increased significantly after IL-17A treatment for 24 h (Figure 4A). Notably, even with prolonged incubation, IL-17A did not exert a sustained effect on the proliferation of HCC cells (Figure 4A). As expected, further experiments confirmed that IL-17A could promote HCC cell proliferation. Flow cytometry analysis revealed that, compared with the control, IL-17A greatly increased the proportion of HCC cells in G2/M phase (Figure 4B). The effect of IL-17A on the protein expression of CyclinD1 in HCCLM3, Huh7, and Hep3B cells was subsequently observed by western blotting. The results revealed that IL-17A increased the level of CyclinD1 in these cells (Figure 4C).

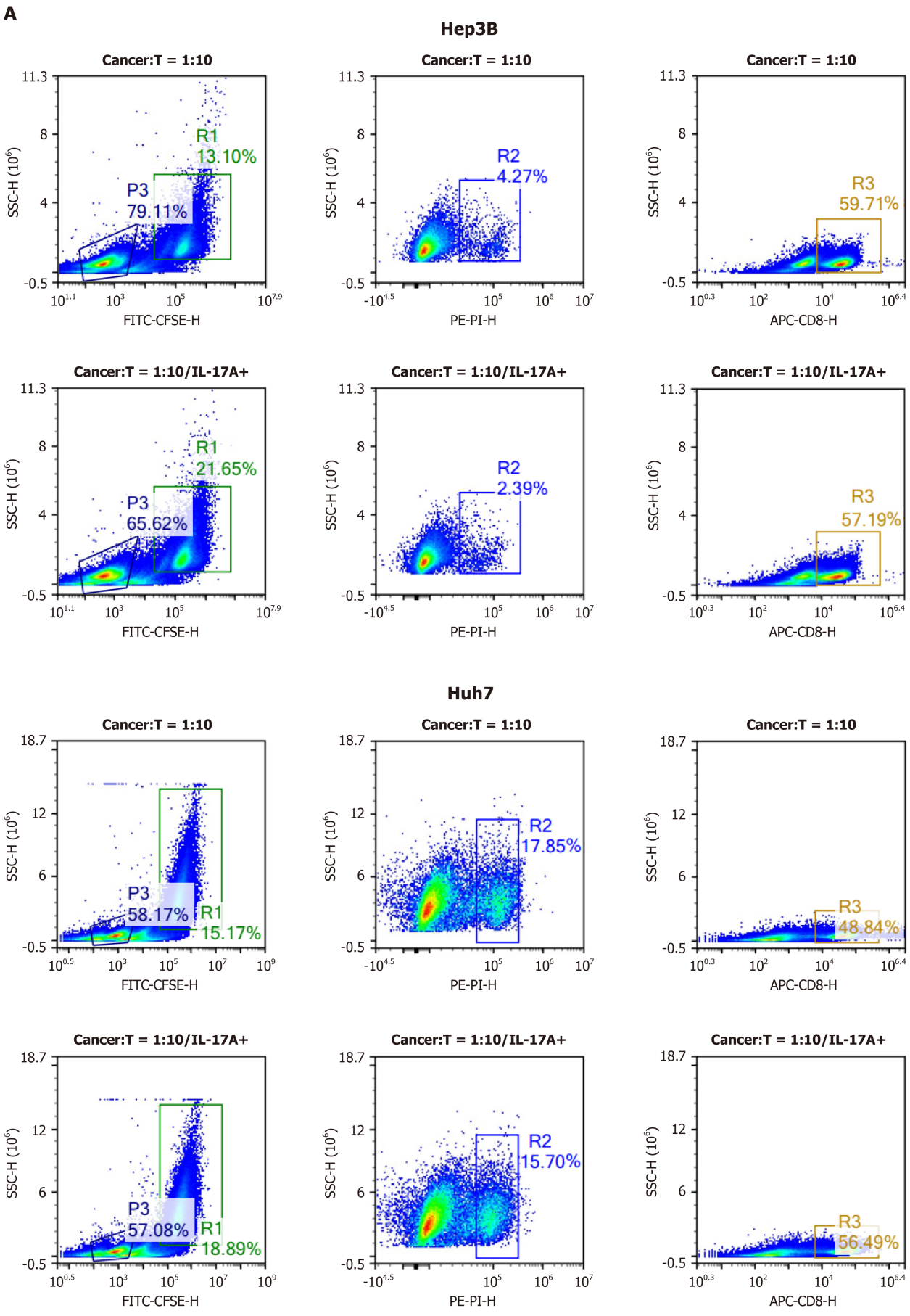
A
Hep3B
Cancer:T = 1:10
R1
13.10%
P3
79.11%
FITC-CFSE-H
SSC-H (10^6)
R2
4.27%
PE-PI-H
R3
59.71%
APC-CD8-H
Cancer:T = 1:10/IL-17A+
R1
21.65%
P3
65.62%
R2
2.39%
R3
57.19%
Huh7
P3
58.17%
R1
15.17%
R2
17.85%
R3
48.84%
P3
57.08%
R1
18.89%
R2
15.70%
R3
56.49%

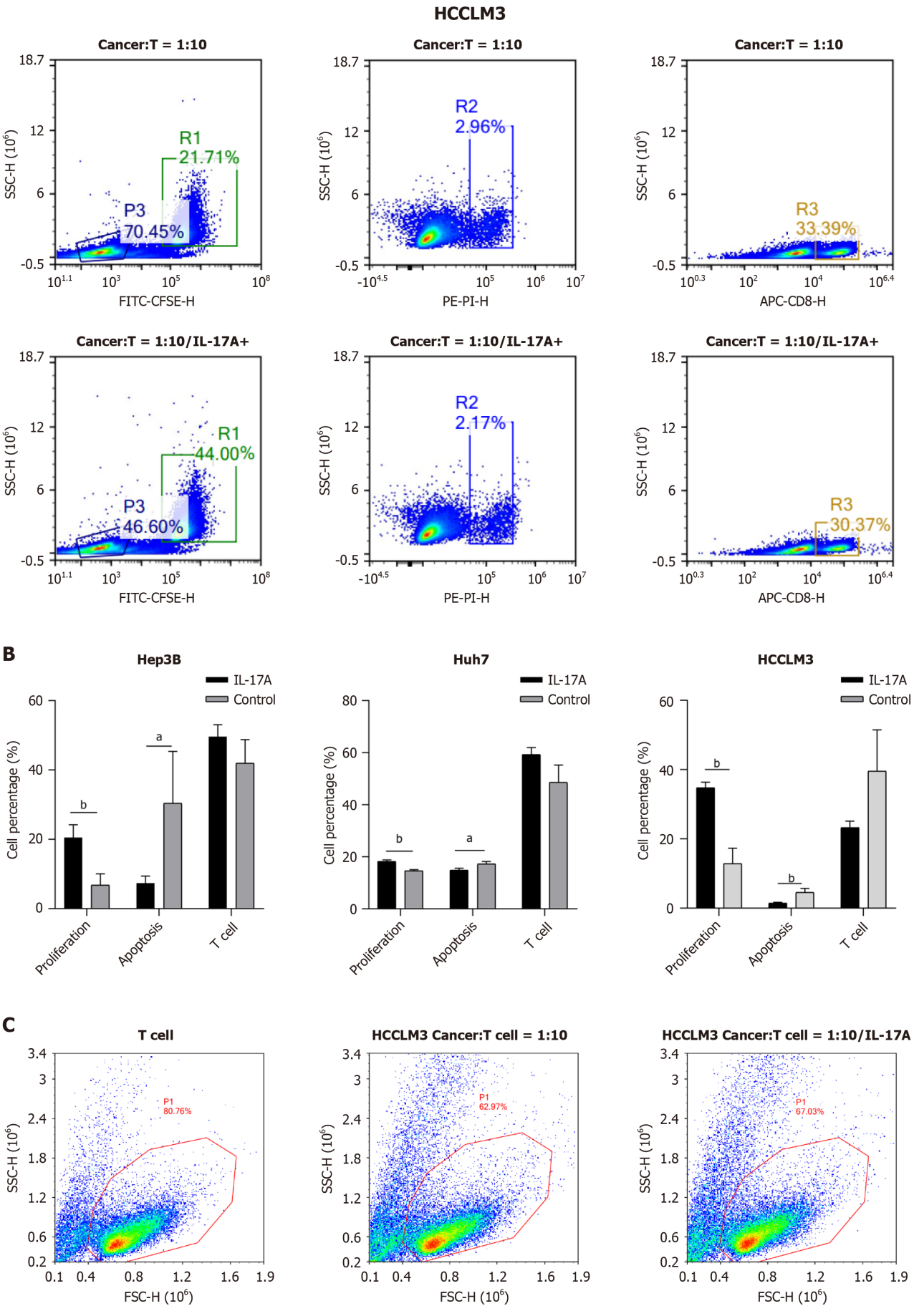
HCCLM3
Cancer:T = 1:10
R1
21.71%
P3
70.45%
FITC-CFSE-H
SSC-H (10^6)
Cancer:T = 1:10
R2
2.96%
PE-PI-H
Cancer:T = 1:10
R3
33.39%
APC-CD8-H
Cancer:T = 1:10/IL-17A+
R1
44.00%
P3
46.60%
Cancer:T = 1:10/IL-17A+
R2
2.17%
Cancer:T = 1:10/IL-17A+
R3
30.37%
B
Hep3B
Huh7
HCCLM3
IL-17A
Control
Cell percentage (%)
Proliferation
Apoptosis
T cell
C
T cell
P1
80.76%
HCCLM3 Cancer:T cell = 1:10
P1
62.97%
HCCLM3 Cancer:T cell = 1:10/IL-17A
P1
67.03%
FSC-H (10^6)

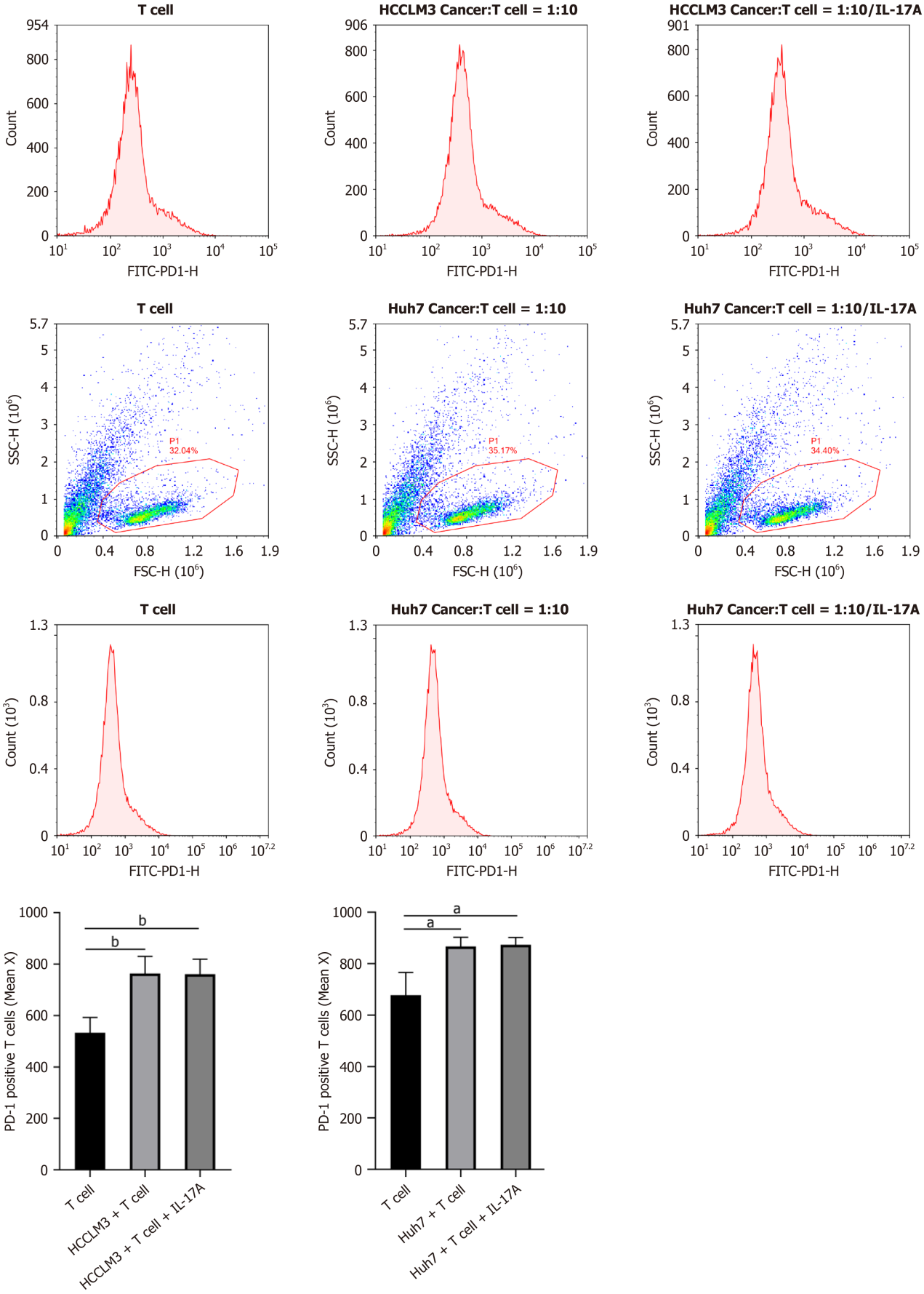

Figure 2 Interleukin-17A weakened the killing effect of T cells on hepatocellular carcinoma cells. A: Hepatocellular carcinoma cell proliferation and apoptosis were tested by flow cytometry after coculture with or without interleukin-17A (IL-17A) for 24 h. The number of T cells was ten times greater than the number of tumor cells; B: Histogram showing the percentage of proliferating and apoptotic hepatocellular carcinoma cells and the percentage of T cells in the coculture model;

C: The expression of programmed death-1 on T cells in coculture models. [a]*P* < 0.05; [b]*P* < 0.01; [c]*P*< 0.001. APC-CD8-H: Allophycocyanin-cluster of differentiation 8-height; FITC-CFSE-H: Fluorescein isothiocyanate-carboxy fluorescein diacetate succinimidyl ester-height; FITC-PD1-H: Fluorescein isothiocyanate-programmed cell death 1-height; FSC-H: Forward scatter-height; PE-PI-H: Phycoerythrin-propidium iodide-height; SSC-H: Side scatter-height.

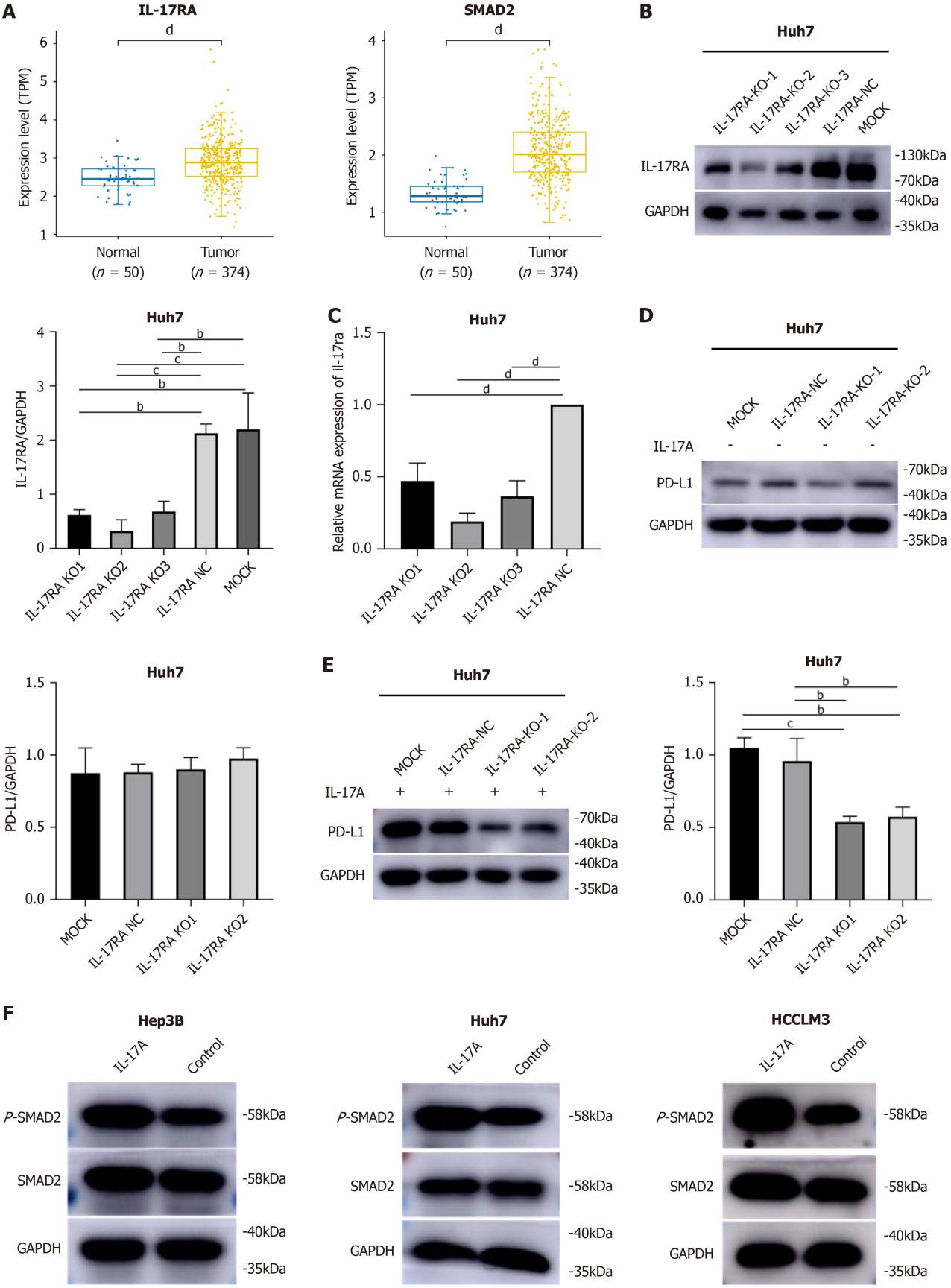

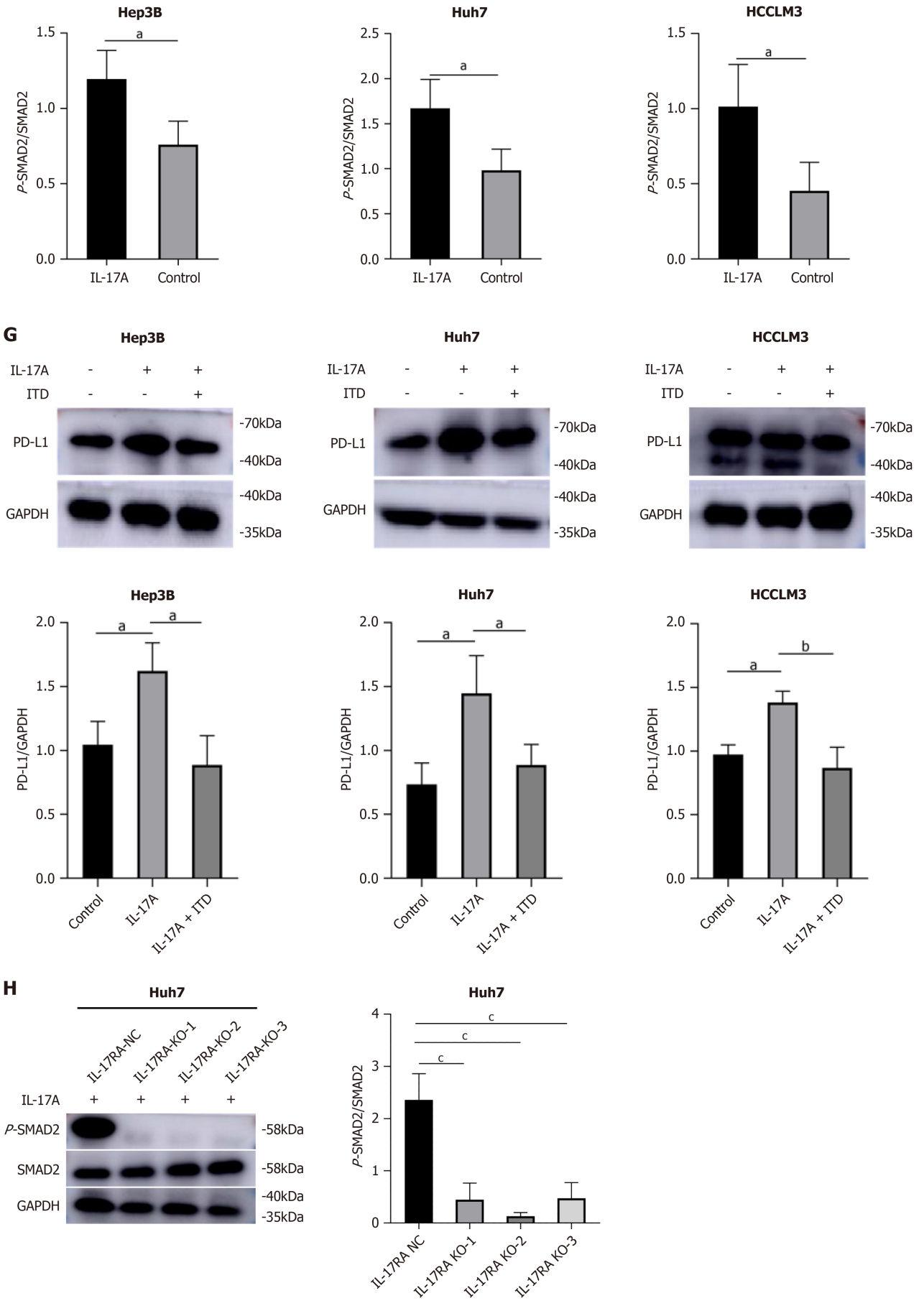

Figure 3 Interleukin-17A upregulated programmed cell death ligand-1 expression *via* the interleukin-17A receptor/p-small mothers against decapentaplegic 2 signaling pathway in hepatocellular carcinoma cells. A: The Cancer Genome Atlas results revealed that interleukin-17A

(IL-17A) and small mothers against decapentaplegic 2 (SMAD2) expression was increased in hepatocellular carcinoma (HCC) samples compared with normal tissue samples; B: Interleukin-17A receptor (IL-17RA) protein expression level after knockout (KO) of *IL-17RA* in Huh7 cells; C: *IL-17RA* mRNA levels after KO of IL-17RA in Huh7 cells; D: *IL-17RA* KO alone did not affect programmed cell death ligand-1 (PD-L1) expression in Huh7 cells; E: IL-17A-induced PD-L1 expression was reversed by *IL-17RA* KO in Huh7 cells; F: IL-17A increased the level of phosphorylated (p)-SMAD2 in HCC cells; G: IL-17A-induced PD-L1 expression was inhibited by pretreatment with transforming growth factor-beta signal pathway inhibitor in HCC cells; H: *IL-17RA* KO sharply reversed IL-17A-induced p-SMAD2 expression in Huh7 cells. $^{a}P < 0.05$; $^{b}P < 0.01$; $^{c}P < 0.001$; $^{d}P < 0.0001$. ITD: TGF-beta signal pathway inhibitor; MOCK: Blank control; NC: Negative control.

The migration abilities of Hep3B, Huh7, and HCCLM3 cells after IL-17A treatment for 24 h were observed by wound healing and Transwell assays, which showed that HCC cell migration was promoted by IL-17A (Figure 4D and E). VEGF plays a crucial role in angiogenesis, and MMP9 promotes angiogenesis indirectly by interacting with VEGF[22]. We also evaluated the effects of IL-17A on VEGF and MMP9 protein expression in HCC cells. The results revealed that the protein levels of VEGF and MMP9 were increased in HCC cells treated with IL-17A compared with those in the control group of HCC cells (Figure 4F). These results indicate that IL-17A can stimulate the proliferation, migration, and angiogenesis of HCC cells.

IL-17A inhibited HCC cell apoptosis

To assess the impact of IL-17A on the apoptosis of Hep3B cells, we cultured the cells with IL-17A for 24 h and tested apoptosis *via* flow cytometry. The results demonstrated that IL-17A reduced the percentage of apoptotic Hep3B cells (Figure 5A). Moreover, we performed western blotting to investigate the role of IL-17A in the expression of BAX and Bcl-2 in Hep3B cells. IL-17A downregulated the protein expression of BAX and upregulated the protein expression of Bcl-2 in the treatment group compared with the control group (Figure 5B). Similar results were observed in Huh7 and HCCLM3 cells (Figure 5A and B). Collectively, these data suggest that IL-17A inhibits HCC cell apoptosis.

Blockade of IL-17A suppressed tumor growth and increased the effect of the PD-L1 antibody in vivo

According to the regulation of PD-L1 expression and the role of IL-17A in malignant cell behavior, we hypothesized that blocking IL-17A might suppress tumor progression and enhance the therapeutic effect of anti-PD-L1 therapy. To test this hypothesis, we subsequently performed a preclinical study using a mouse model. These results indicated that anti-IL-17A antibodies combined with anti-PD-L1 antibodies and anti-IL-17A antibodies alone could inhibit tumor growth. Moreover, the efficacy of this combination was better than that of anti-IL-17A antibody or anti-PD-L1 antibody monotherapy (Figure 6A-C). The effects of different treatments on immune cell recruitment, serum parameters, and pathological parameters were also assessed. The number of infiltrating CD8+ T cells in the combined therapy group was greater than that in the control group and the anti-IL-17A monotherapy group (Figure 6D). The number of infiltrating CD4+ T cells in the combined therapy group was lower than that in the control group (Figure 6D). The serum expression of soluble PD-L1 and IL-17A was lower in the combined therapy group than in the control group (Figure 6E). A positive correlation was observed between the serum expression of soluble PD-L1 and that of IL-17A in the control group (Figure 6E). The expression of Ki67, IL-17A, and PD-L1 in tumor tissues in the combined therapy group was obviously lower than that in the control group (Figure 6F).

DISCUSSION

Several studies have shown that IL-17A can increase the expression of PD-L1 in tumor cells and promote the progression of tumors, including colorectal cancer[23], ovarian cancer[24], pancreatic carcinoma[25], and lung cancer[16]. However, related research in HCC is scarce. To our knowledge, only one study has reported the regulatory effect of IL-17A on PD-L1 in hepatoma stem cells[26]. However, the significance of IL-17A in the regulation of PD-L1 in HCC cells has not been clearly defined. Our previous study indicated that the plasma level of IL-17A was positively correlated with the expression of soluble PD-L1 in HCC patients. Similar results were observed in the mouse model in this study. Furthermore, the results of the present study revealed that IL-17A upregulated the mRNA and protein levels of PD-L1 in a dose-dependent manner in HCC cells. The overexpression of PD-L1 in tumor cells leads to effector T cell exhaustion, which suggests a crucial correlation with tumor invasiveness and postoperative recurrence in HCC[27]. IL-17A also increased the resistance of hepatoma stem cells to cytotoxic T cells *via* the upregulation of PD-L1[26]. Similarly, we performed a coculture assay, and the results revealed that IL-17A could increase the survival of HCC cells. These findings demonstrated that IL-17A could regulate PD-L1 in HCC cells and might play a protumor role partially through the upregulation of PD-L1.

It is important to explore how IL-17A enhances PD-L1 expression in HCC cells. However, the specific mechanism of IL-17A in HCC is unclear. To some extent, this study revealed a novel mechanism by which IL-17A regulates PD-L1 expression in HCC cells. Liver fibrosis, particularly cirrhosis, is closely correlated with the occurrence of HCC. The SMAD pathway is crucial for the origin and development of liver fibrosis. Therefore, many studies on the mechanism of liver cancer progression and invasion have focused on the SMAD pathway. *SOX18* expression is increased by TGF-β1 *via* stimulation of the SMAD2/3 complex, which promotes tumor associated macrophage and regulatory T cell accumulation and HCC development[28]. *KIN17* accelerates the migration ability and invasiveness of HCC cells by activating the TGF-β/SMAD2 pathway[29].

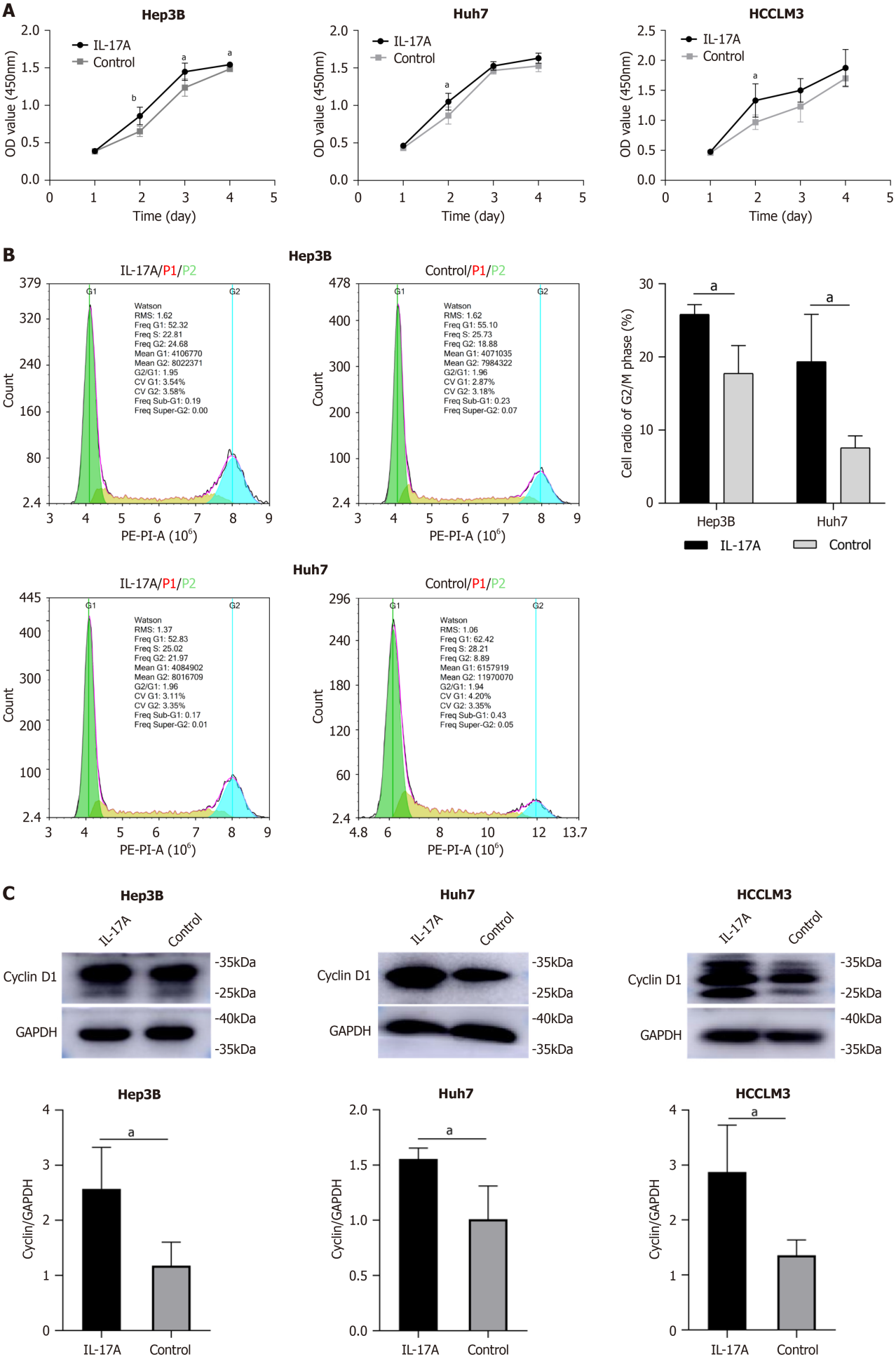
A
Hep3B
Huh7
HCCLM3
IL-17A
Control
OD value (450nm)
Time (day)
B
Hep3B
IL-17A/P1/P2
Control/P1/P2
Watson
RMS: 1.62
Freq G1: 52.32
Freq S: 22.81
Freq G2: 24.68
Mean G1: 4106770
Mean G2: 8022371
G2/G1: 1.95
CV G1: 3.54%
CV G2: 3.58%
Freq Sub-G1: 0.19
Freq Super-G2: 0.00
Freq G1: 55.10
Freq S: 25.73
Freq G2: 18.88
Mean G1: 4071035
Mean G2: 7984322
G2/G1: 1.96
CV G1: 2.87%
CV G2: 3.18%
Freq Sub-G1: 0.23
Freq Super-G2: 0.07
Count
PE-PI-A (10^6)
Cell radio of G2/M phase (%)
Huh7
Watson
RMS: 1.37
Freq G1: 52.83
Freq S: 25.02
Freq G2: 21.97
Mean G1: 4084902
Mean G2: 8016709
G2/G1: 1.96
CV G1: 3.11%
CV G2: 3.35%
Freq Sub-G1: 0.17
Freq Super-G2: 0.01
Watson
RMS: 1.06
Freq G1: 62.42
Freq S: 28.21
Freq G2: 8.89
Mean G1: 6157919
Mean G2: 11970070
G2/G1: 1.94
CV G1: 4.20%
CV G2: 3.35%
Freq Sub-G1: 0.43
Freq Super-G2: 0.05
C
Hep3B
Huh7
HCCLM3
Cyclin D1
GAPDH
-35kDa
-25kDa
-40kDa
Cyclin/GAPDH

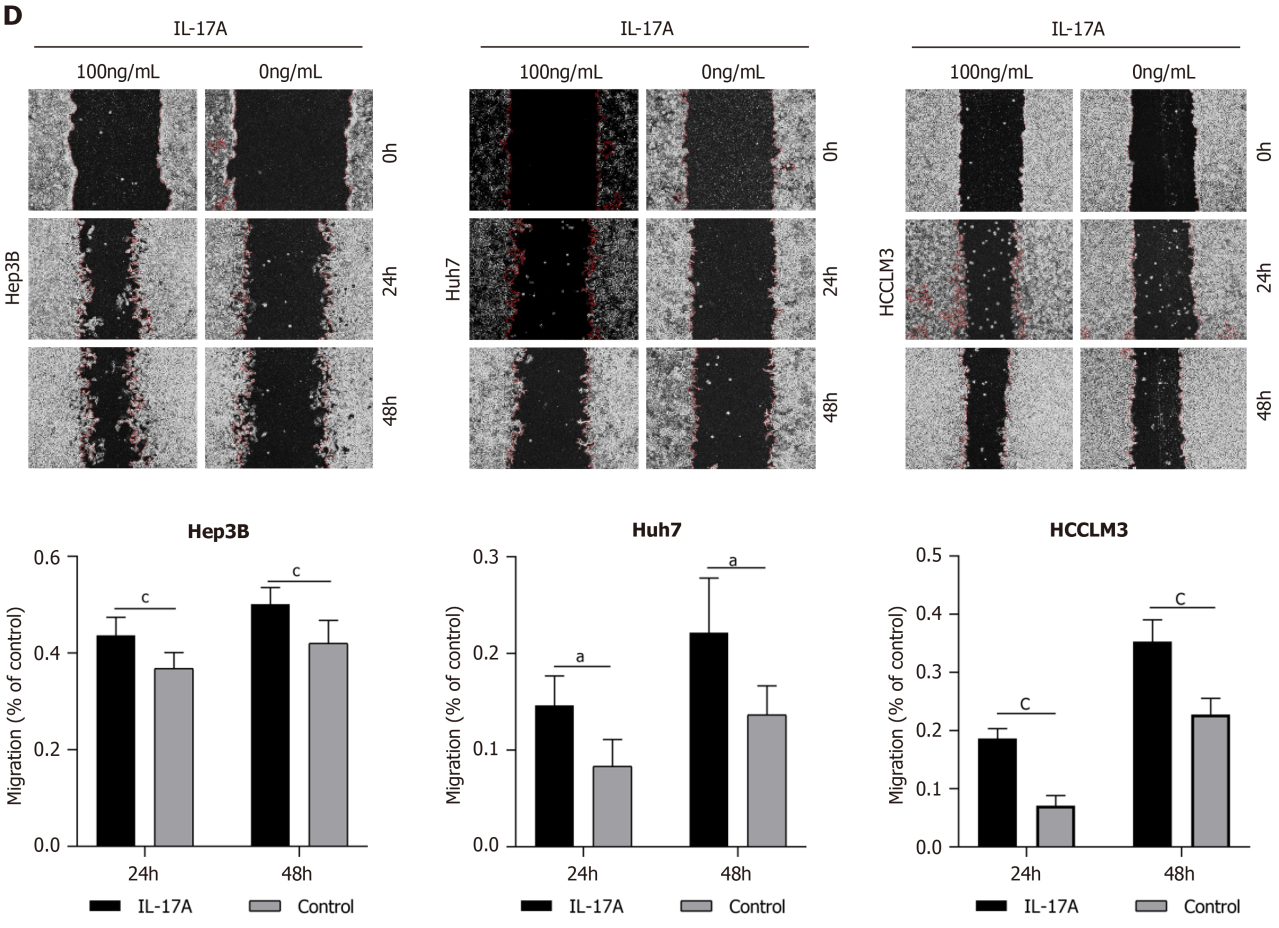
D
IL-17A
100ng/mL
0ng/mL
Hep3B
Huh7
HCCLM3
0h
24h
48h
Hep3B
Huh7
HCCLM3
Migration (% of control)
0.6
0.4
0.2
0.0
0.3
0.1
0.5
c
a
24h
48h
IL-17A
Control

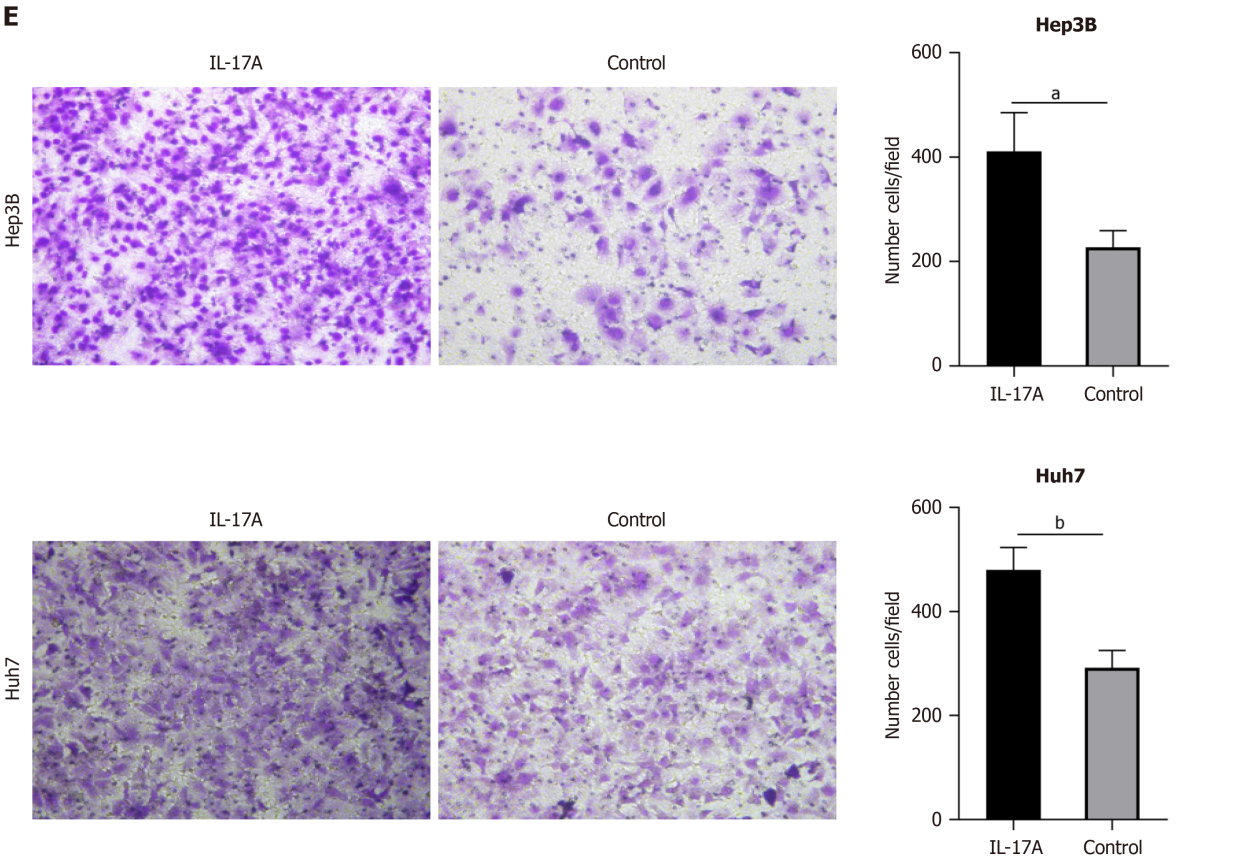
E
IL-17A
Control
Hep3B
Huh7
Number cells/field
600
400
200
0
a
b
IL-17A
Control

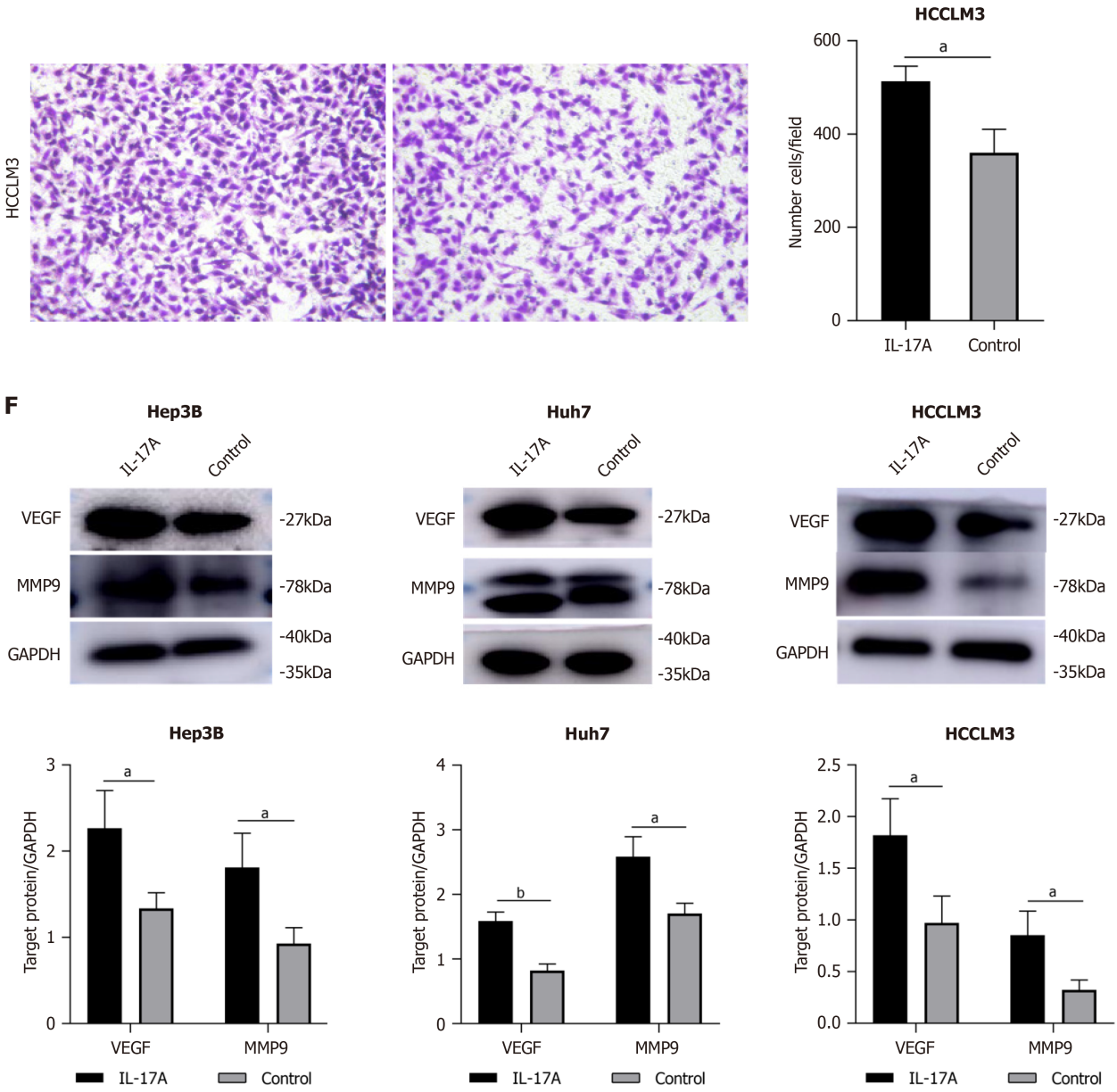

Figure 4 Interleukin-17A promoted hepatocellular carcinoma cell proliferation, migration, and angiogenesis. A: Growth curve showed that interleukin-17A (IL-17A) stimulated cell proliferation, a significant difference that was detected at 24 h after treatment; B: Flow cytometry revealed that, compared with the control, IL-17A significantly increased the proportion of cells in G2/M phase; C: IL-17A elevated cyclinD1 expression in hepatocellular carcinoma (HCC) cells; D and E: Scratch tests and Transwell assays revealed that IL-17A promoted the migration of HCC cells (× 100 magnification); F: IL-17A increased the protein expression of VEGF and MMP9 in HCC cells. $^{a}P < 0.05$; $^{b}P < 0.01$; $^{c}P < 0.001$. PE: Phycoerythrin; PI: Propidium iodide.

Golgi protein 73 promotes epithelial-mesenchymal transition and invasiveness of HCC cells by increasing p-SMAD2 and p-SMAD3 levels[29]. MiR-148a inhibits the development of HCC by decreasing SMAD2 expression[30]. Moreover, the relationship between SMADs and immune checkpoint molecules has been studied in other solid tumors. For example, one study revealed that p-SMAD2 expression was greater in PD-L1-positive *vs* PD-L1-negative non-small cell lung cancer patients[31]. However, whether IL-17A mediates PD-L1 expression through p-SMAD2 has not been reported in HCC. In the present study, we found that SMAD2 expression was increased in HCC samples compared with normal samples according to the TCGA database analysis. Further experiments revealed that IL-17A increased p-SMAD2 levels in HCC cells. Inhibition of p-SMAD2 with the pharmacological inhibitor ITD-1 markedly reduced IL-17A-related PD-L1 expression. Taken together, these results confirm that IL-17A induces PD-L1 expression through the SMAD2 pathway.

Cytokines in the IL-17A family exert their biological effects *via* IL-17 receptors. IL-17A/IL-17RA signaling plays a critical role in tumorigenesis and tumor development[13]. To further verify whether IL-17A regulates PD-L1 expression through IL-17RA in HCC, we silenced *IL-17RA via* gene knockout. The results indicated that specific deletion of *IL-17RA* in HCC cell lines had the opposite effect on IL-17A-induced PD-L1 expression. These findings demonstrated that IL-17A positively regulates PD-L1 protein expression by acting on IL-17RA in HCC. Another study revealed that IL-17RA could regulate the SMAD pathway in the formation of hypertrophic scars[23]. To the best of our knowledge, no study has reported the relationship between IL-17RA and the SMAD2 signaling pathway in tumors. Here, we verified that IL-17A-induced p-SMAD2 expression was reversed by *IL-17RA* knockout, whereas SMAD2 expression was unchanged.

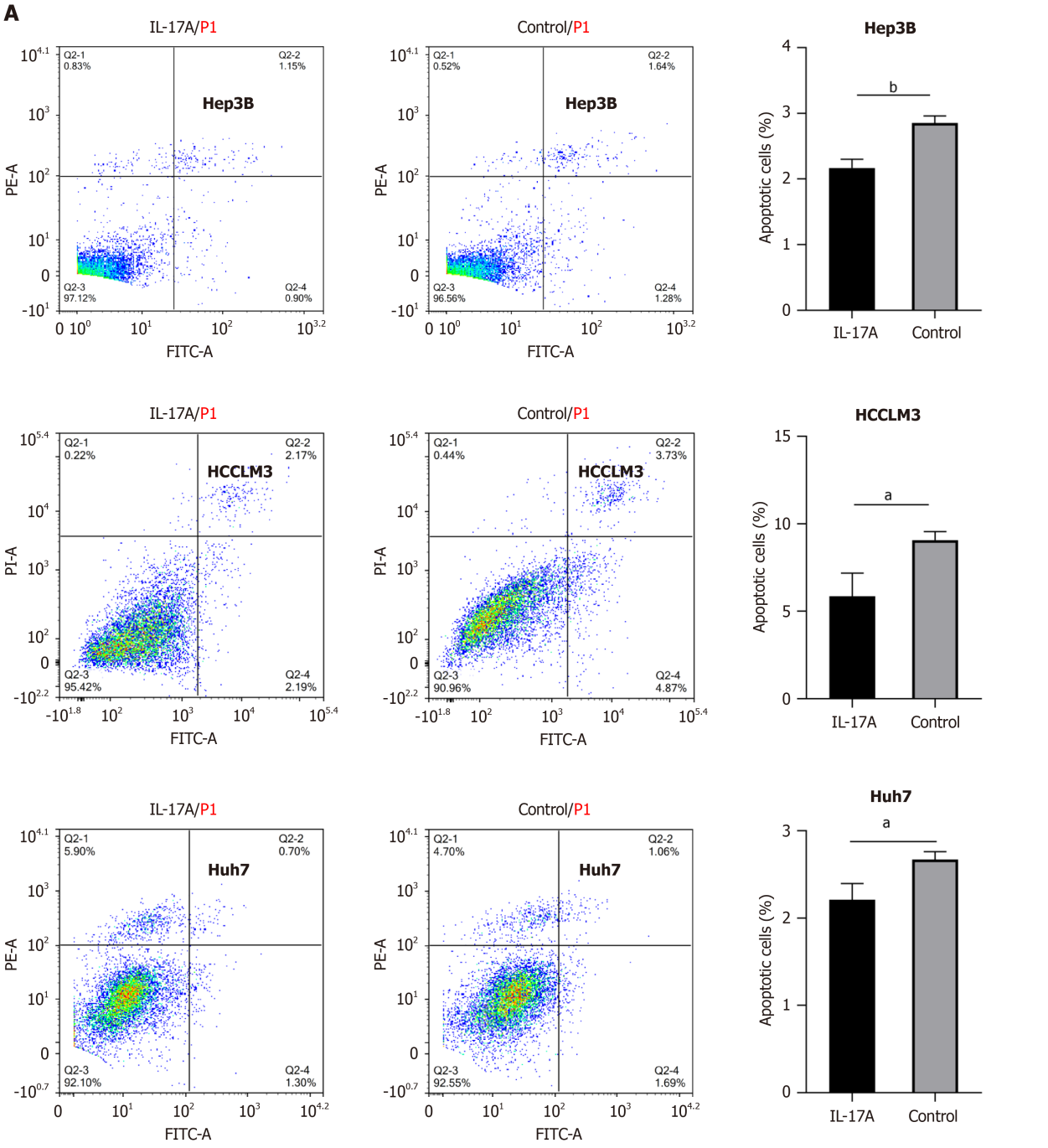
A
IL-17A/P1
Control/P1
Hep3B
Q2-1 0.83%
Q2-2 1.15%
Q2-3 97.12%
Q2-4 0.90%
Q2-1 0.52%
Q2-2 1.64%
Q2-3 96.56%
Q2-4 1.28%
PE-A
FITC-A
Apoptotic cells (%)
b
IL-17A
Control
HCCLM3
Q2-1 0.22%
Q2-2 2.17%
Q2-3 95.42%
Q2-4 2.19%
Q2-1 0.44%
Q2-2 3.73%
Q2-3 90.96%
Q2-4 4.87%
PI-A
a
Huh7
Q2-1 5.90%
Q2-2 0.70%
Q2-3 92.10%
Q2-4 1.30%
Q2-1 4.70%
Q2-2 1.06%
Q2-3 92.55%
Q2-4 1.69%
B
Bax
Bcl-2
GAPDH
-25kDa
-15kDa
-35kDa
-40kDa

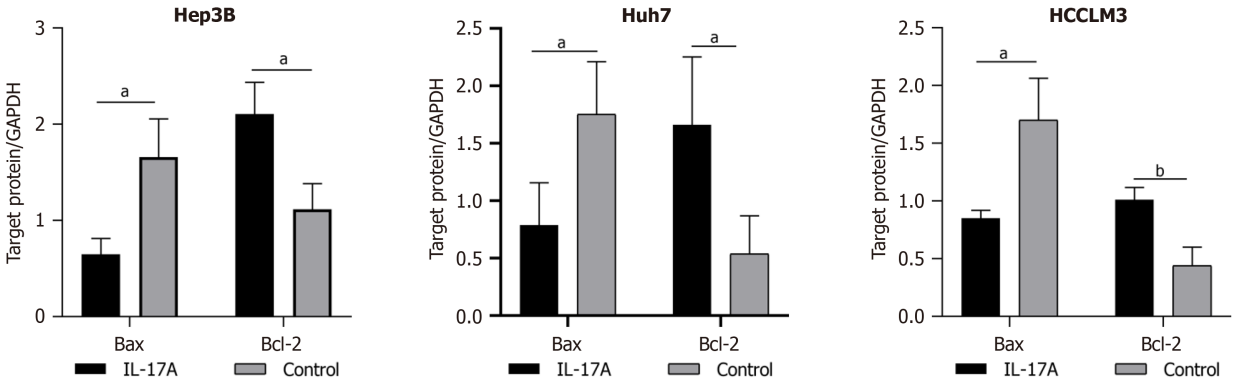

Figure 5 Interleukin-17A inhibited hepatocellular carcinoma cell apoptosis. A: Flow cytometry analysis revealed that interleukin-17A (IL-17A) suppressed hepatocellular carcinoma (HCC) cell apoptosis; B: IL-17A decreased the expression of BAX and increased the expression of Bcl-2 in HCC cells. [a]*P* < 0.05; [b]*P* < 0.01. FITC-A: Fluorescein isothiocyanate-area; PE-A: Phycoerythrin-area.

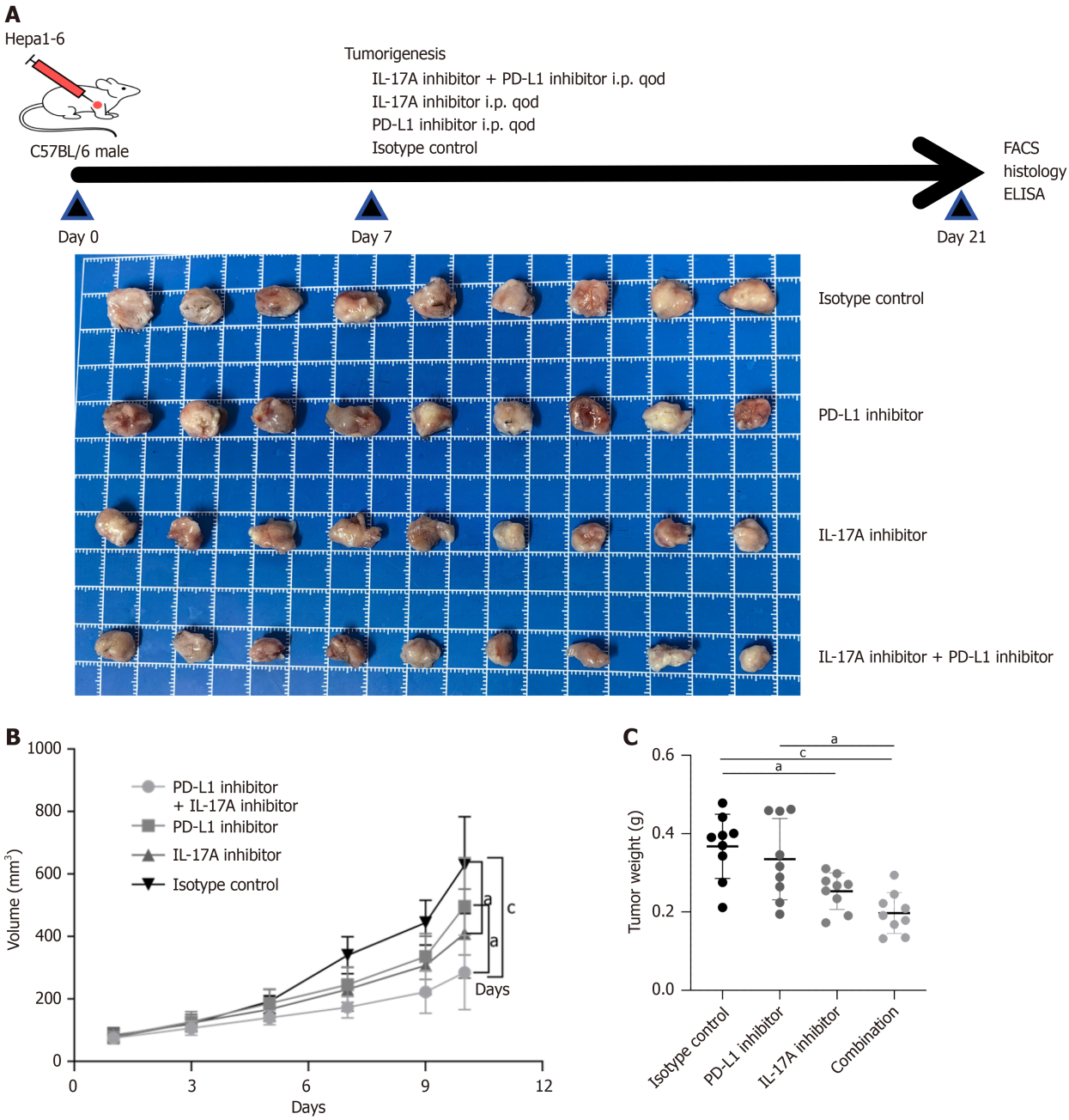

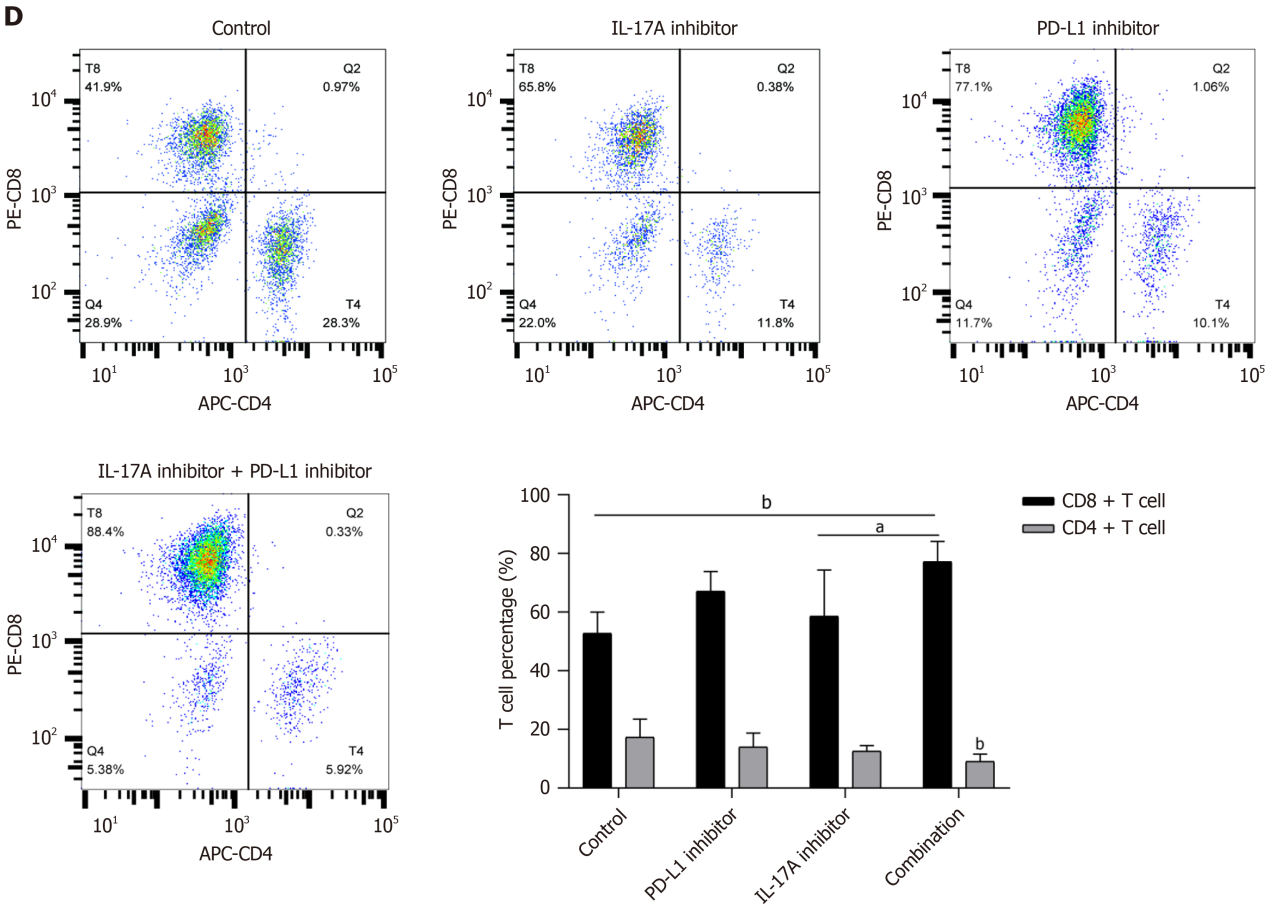
D
Control
IL-17A inhibitor
PD-L1 inhibitor
IL-17A inhibitor + PD-L1 inhibitor
PE-CD8
APC-CD4
T8 41.9%
Q2 0.97%
Q4 28.9%
T4 28.3%
T8 65.8%
Q2 0.38%
Q4 22.0%
T4 11.8%
T8 77.1%
Q2 1.06%
Q4 11.7%
T4 10.1%
T8 88.4%
Q2 0.33%
Q4 5.38%
T4 5.92%
T cell percentage (%)
CD8 + T cell
CD4 + T cell
Control
PD-L1 inhibitor
IL-17A inhibitor
Combination

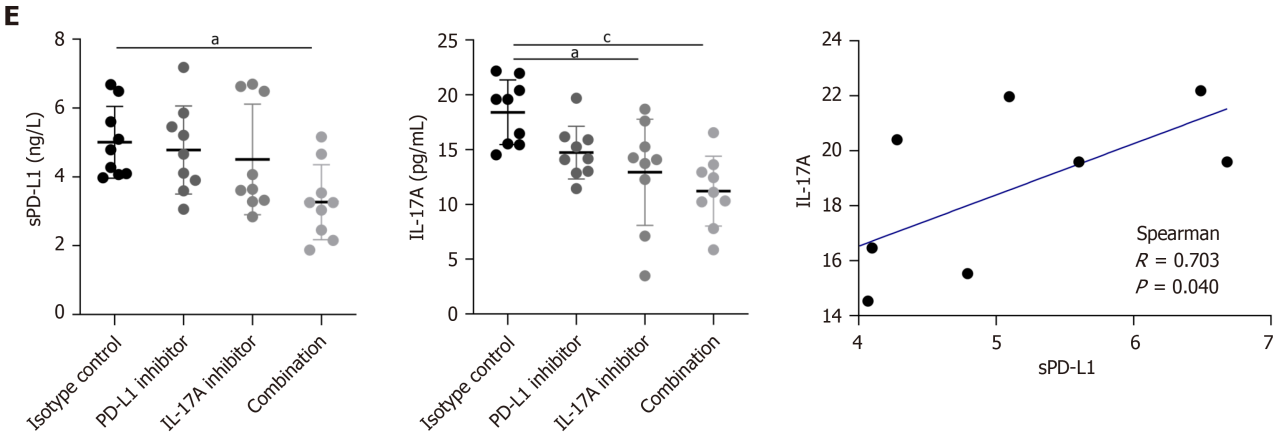
E
sPD-L1 (ng/L)
IL-17A (pg/mL)
IL-17A
sPD-L1
Spearman
R = 0.703
P = 0.040
Isotype control
PD-L1 inhibitor
IL-17A inhibitor
Combination

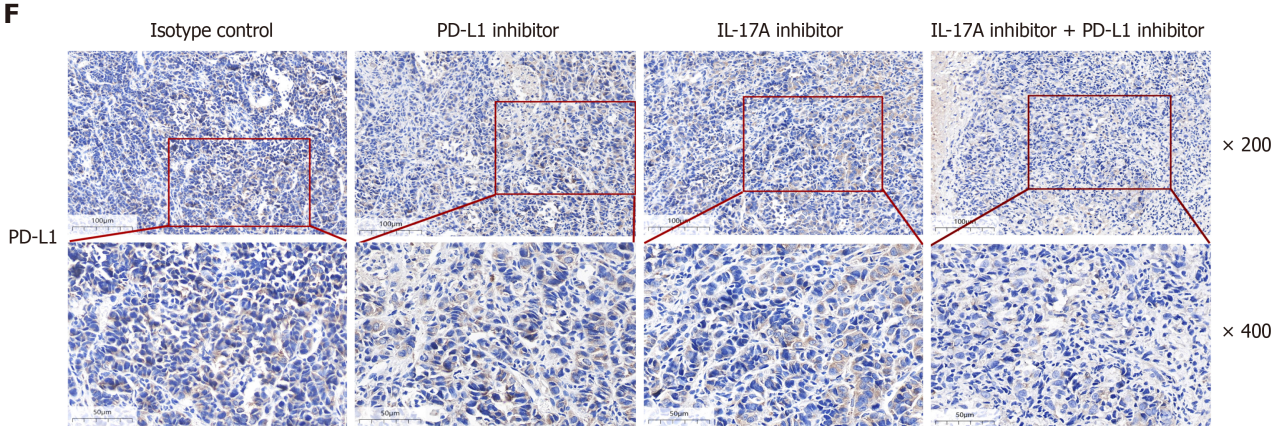
F
Isotype control
PD-L1 inhibitor
IL-17A inhibitor
IL-17A inhibitor + PD-L1 inhibitor
PD-L1
× 200
× 400

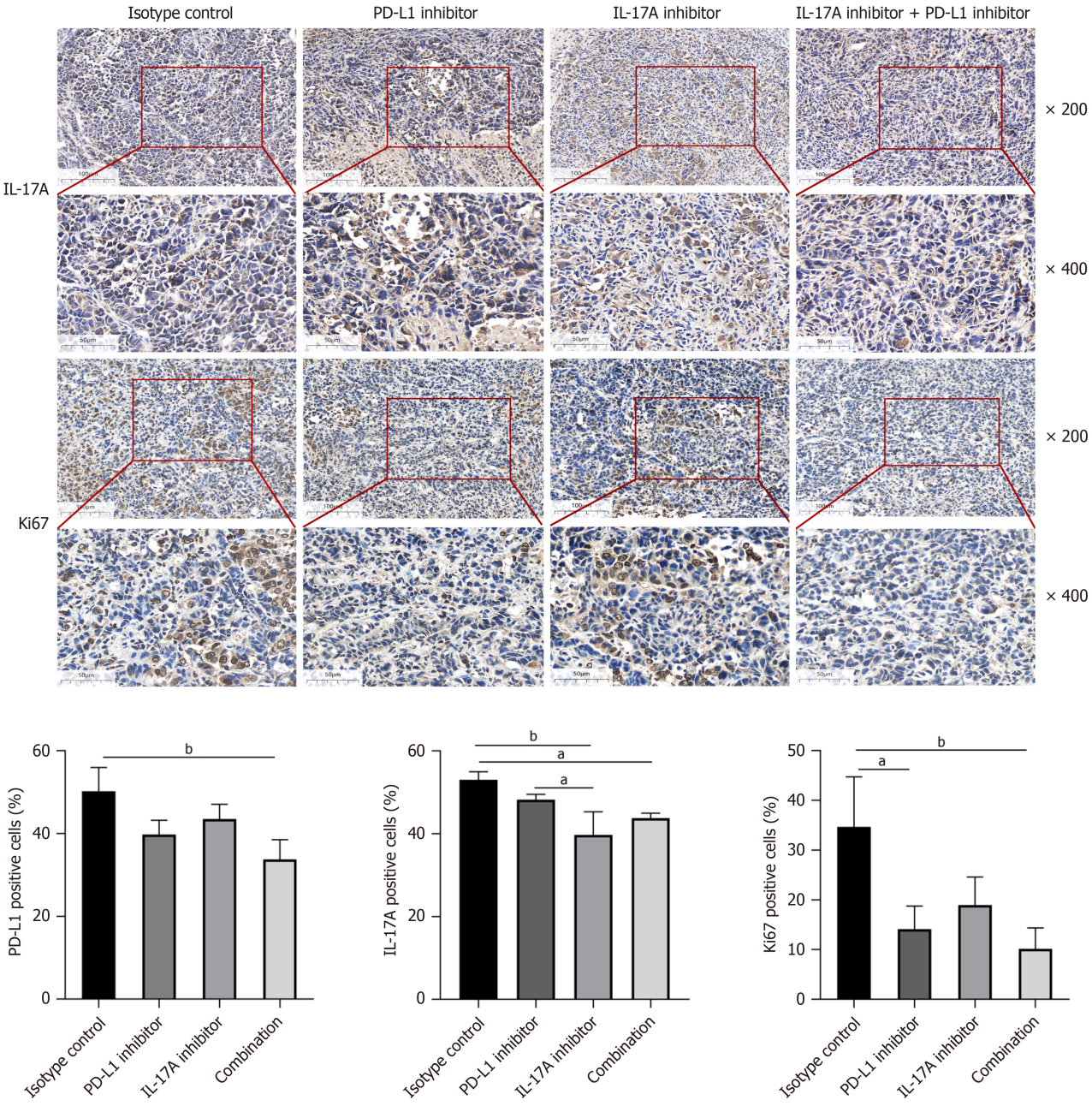

Figure 6 An interleukin-17A inhibitor suppressed tumor growth and enhanced the therapeutic efficacy of an anti-programmed cell death ligand-1 antibody. A: Flow diagram of the construction of the mouse model and treatment scheme for programmed cell death ligand-1 (PD-L1) inhibitors and/or interleukin-17A (IL-17A) inhibitors in mice. Images of the tumors in different treatment groups (the control group, PD-L1 inhibitor group, IL-17A inhibitor group, and combined group) are shown. Each group contained nine mice; B: Tumor growth curves of the mice after PD-L1 inhibitor and/or IL-17A inhibitor treatment. A PD-L1 inhibitor combined with an IL-17A inhibitor demonstrated a much greater antitumor effect on the hepatocellular carcinoma mouse model; C: Tumor weights of mice in the four groups after treatment. The tumor weights of mice in the combined group were significantly lower than those of mice in the control group; D: Flow cytometry analysis of the differences in the infiltration of cluster of differentiation 8+ T cells and cluster of differentiation 4+ T cells in tumor tissues among the four groups; E: The levels of serum soluble (s)PD-L1 and IL-17A were compared among the four groups. The sPD-L1 and IL-17A levels were lower in the combined group than in the control group. The sPD-L1 level was positively correlated with the serum IL-17A level in the control group; F: Immunohistochemical staining revealed the expression of PD-L1, IL-17A, and Ki67 in tumor tissues. Scale bars, 100 μm (× 200) and 50 μm (× 400). The number of positive cells was determined using ImageJ2x software. Boxplots displaying the expression of PD-L1, IL-17A, and Ki67 in the four groups. $^{a}P < 0.05$; $^{b}P < 0.01$; $^{c}P < 0.001$. APC-CD4: Allophycocyanin-cluster of differentiation 4; FACS: Fluorescence-activated cell sorting; PE-CD8: Phycoerythrin-cluster of differentiation 8.

Collectively, these data emphasize that IL-17A induces PD-L1 protein expression in HCC cells *via* the IL-17RA/p-SMAD2 axis.

Atezolizumab in combination with bevacizumab has become the standard first-line therapy for advanced HCC. However, advanced HCC develops primarily from cirrhosis and is always accompanied by esophageal and gastric varices. Therefore, VEGF-neutralizing antibodies may increase the risk of bleeding in these patients. A new methodology is therefore needed to improve the therapeutic sensitivity to anti-PD-L1 antibodies beyond the VEGF-neutralizing antibody. In one study, the combination of an IL-17A inhibitor and a PD-1 inhibitor exhibited better antitumor efficacy

than monotherapy in patients with colorectal cancer[32].

Research has shown that IL-17A contributes to the immune evasion of HCC cells, possibly by upregulating PD-L1 expression. IL-17A also promotes HCC cell proliferation, migration, and angiogenesis and inhibits cell apoptosis. On the basis of these results, it was necessary to assess the therapeutic efficacy of an IL-17A inhibitor in combination with an anti-PD-L1 antibody for the treatment of HCC *in vivo*. We expected that targeting IL-17A could delay carcinoma growth and significantly enhance immune therapeutic efficacy in an HCC mouse model. However, anti-PD-L1 monotherapy was not sufficient to exert a strong antitumor effect. These results are consistent with the idea that combining an IL-17A inhibitor with an anti-PD-L1 antibody has a synergistic antitumor effect on HCC[33], but the dosage and frequency of drug administration in other studies were different from those in our study. Therefore, targeting IL-17A is a potential treatment strategy for optimizing PD-L1 antibodies for the treatment of HCC.

The combination of an IL-17A inhibitor and PD-1 blockade stimulates the infiltration of CD8+, interferon-γ+, CD3+ T cells into tumors and demonstrates significant efficacy in colorectal cancer models[23]. The prognosis of tumor patients is associated with CD8+ T cell enrichment in tumors[25]. IL-17A can recruit CD8+ T cells to infiltrate tumors in cancer models[14]. Clinical studies have shown that CD8+ T cell infiltration is predictive of whether patients with tumors will benefit from ICB treatment[34]. Consistent with previous work, our study also confirmed that the infiltration of CD8+ T cells in the combined treatment group was significantly greater than that in the other groups in HCC models. In addition, the data indicated that the levels of IL-17A and PD-L1 in tumor tissue and serum were lower in the combined treatment group than in the control group. This might partly explain why combination therapy is preferable for HCC.

These results provide a foundation for exploring the role of IL-17A in accelerating HCC progression in a PD-L1-dependent manner. Further clinical studies are needed to estimate the therapeutic efficacy and safety of anti-IL-17A combined with PD-L1 blockade in patients with HCC.

CONCLUSION

This study demonstrated a potential mechanism by which IL-17A upregulates PD-L1 expression through the IL-17RA/p-SMAD2 signaling pathway in HCC cells. Blockade of IL-17A enhances the therapeutic efficacy of PD-L1 antibodies for the treatment of HCC.

ACKNOWLEDGEMENTS

The authors would like to thank the staff of the Medical Frontier Innovation Research Center of the First Hospital of Lanzhou University. The authors thank two anonymous reviewers who provided helpful and constructive comments that improved the manuscript substantially.

FOOTNOTES

Author contributions: Yang ZX, Zhang LT, and Mao XR designed the research study; Yang ZX and Peng XB performed the research; Yang ZX and Liu XJ analyzed the data and wrote the manuscript; Zhang LT and Mao XR critically revised the article.

Supported by the Natural Science Foundation of Gansu Province, No. 21JR7RA373 and No. 24JRRA295.

Institutional review board statement: This study was reviewed and approved by the Ethics Committee of the First Hospital of Lanzhou University, No. LDYYLL2021-319 and No. LDYYLL2024-457.

Institutional animal care and use committee statement: All procedures involving animals were reviewed and approved by the Animal Experimental Ethical Inspection of Gansu University of Chinese Medicine, No. SY2023-766.

Conflict-of-interest statement: The authors declare that they have no conflicts of interest.

Data sharing statement: No additional data are available.

ARRIVE guidelines statement: The authors have read the ARRIVE guidelines, and the manuscript was prepared and revised according to the ARRIVE guidelines.

Country of origin: China

ORCID number: Xiao-Jun Liu 0000-0001-5197-011X; Xiao-Rong Mao 0009-0000-9169-6020.

S-Editor: Fan M
L-Editor: Filipodia
P-Editor: Zhao YQ

REFERENCES

1 **Vogel A**, Meyer T, Sapisochin G, Salem R, Saborowski A. Hepatocellular carcinoma. *Lancet* 2022; **400**: 1345-1362 [PMID: 36084663 DOI: 10.1016/S0140-6736(22)01200-4]
2 **Pinter M**, Jain RK, Duda DG. The Current Landscape of Immune Checkpoint Blockade in Hepatocellular Carcinoma: A Review. *JAMA Oncol* 2021; **7**: 113-123 [PMID: 33090190 DOI: 10.1001/jamaoncol.2020.3381]
3 **Coussens LM**, Werb Z. Inflammation and cancer. *Nature* 2002; **420**: 860-867 [PMID: 12490959 DOI: 10.1038/nature01322]
4 **Mariathasan S**, Turley SJ, Nickles D, Castiglioni A, Yuen K, Wang Y, Kadel EE III, Koeppen H, Astarita JL, Cubas R, Jhunjhunwala S, Banchereau R, Yang Y, Guan Y, Chalouni C, Ziai J, Şenbabaoğlu Y, Santoro S, Sheinson D, Hung J, Giltnane JM, Pierce AA, Mesh K, Lianoglou S, Riegler J, Carano RAD, Eriksson P, Höglund M, Somarriba L, Halligan DL, van der Heijden MS, Loriot Y, Rosenberg JE, Fong L, Mellman I, Chen DS, Green M, Derleth C, Fine GD, Hegde PS, Bourgon R, Powles T. TGFβ attenuates tumour response to PD-L1 blockade by contributing to exclusion of T cells. *Nature* 2018; **554**: 544-548 [PMID: 29443960 DOI: 10.1038/nature25501]
5 **Liao H**, Chen W, Dai Y, Richardson JJ, Guo J, Yuan K, Zeng Y, Xie K. Expression of Programmed Cell Death-Ligands in Hepatocellular Carcinoma: Correlation With Immune Microenvironment and Survival Outcomes. *Front Oncol* 2019; **9**: 883 [PMID: 31572677 DOI: 10.3389/fonc.2019.00883]
6 **Fang W**, Zhou T, Shi H, Yao M, Zhang D, Qian H, Zeng Q, Wang Y, Jin F, Chai C, Chen T. Progranulin induces immune escape in breast cancer *via* up-regulating PD-L1 expression on tumor-associated macrophages (TAMs) and promoting CD8(+) T cell exclusion. *J Exp Clin Cancer Res* 2021; **40**: 4 [PMID: 33390170 DOI: 10.1186/s13046-020-01786-6]
7 **Clark CA**, Gupta HB, Sareddy G, Pandeswara S, Lao S, Yuan B, Drerup JM, Padron A, Conejo-Garcia J, Murthy K, Liu Y, Turk MJ, Thedieck K, Hurez V, Li R, Vadlamudi R, Curiel TJ. Tumor-Intrinsic PD-L1 Signals Regulate Cell Growth, Pathogenesis, and Autophagy in Ovarian Cancer and Melanoma. *Cancer Res* 2016; **76**: 6964-6974 [PMID: 27671674 DOI: 10.1158/0008-5472.CAN-16-0258]
8 **Zong Z**, Zou J, Mao R, Ma C, Li N, Wang J, Wang X, Zhou H, Zhang L, Shi Y. M1 Macrophages Induce PD-L1 Expression in Hepatocellular Carcinoma Cells Through IL-1β Signaling. *Front Immunol* 2019; **10**: 1643 [PMID: 31379842 DOI: 10.3389/fimmu.2019.01643]
9 **Ploeger C**, Schreck J, Huth T, Fraas A, Albrecht T, Charbel A, Ji J, Singer S, Breuhahn K, Pusch S, Köhler BC, Springfeld C, Schirmacher P, Mehrabi A, Goeppert B, Roessler S. STAT1 and STAT3 Exhibit a Crosstalk and Are Associated with Increased Inflammation in Hepatocellular Carcinoma. *Cancers (Basel)* 2022; **14** [PMID: 35267462 DOI: 10.3390/cancers14051154]
10 **Yan Y**, Zheng L, Du Q, Yan B, Geller DA. Interferon regulatory factor 1 (IRF-1) and IRF-2 regulate PD-L1 expression in hepatocellular carcinoma (HCC) cells. *Cancer Immunol Immunother* 2020; **69**: 1891-1903 [PMID: 32377817 DOI: 10.1007/s00262-020-02586-9]
11 **Bian Z**, Wu X, Chen Q, Gao Q, Xue X, Wang Y. Oct4 activates IL-17A to orchestrate M2 macrophage polarization and cervical cancer metastasis. *Cancer Immunol Immunother* 2024; **73**: 73 [PMID: 38430256 DOI: 10.1007/s00262-023-03596-z]
12 **Cui G**, Li Z, Florholmen J, Goll R. Dynamic stromal cellular reaction throughout human colorectal adenoma-carcinoma sequence: A role of TH17/IL-17A. *Biomed Pharmacother* 2021; **140**: 111761 [PMID: 34044278 DOI: 10.1016/j.biopha.2021.111761]
13 **Wang X**, Wu S, Wu W, Zhang W, Li L, Liu Q, Yan Z. Candida albicans Promotes Oral Cancer *via* IL-17A/IL-17RA-Macrophage Axis. *mBio* 2023; **14**: e0044723 [PMID: 37067414 DOI: 10.1128/mbio.00447-23]
14 **Feng WQ**, Zhang YC, Xu ZQ, Yu SY, Huo JT, Tuersun A, Zheng MH, Zhao JK, Zong YP, Lu AG. IL-17A-mediated mitochondrial dysfunction induces pyroptosis in colorectal cancer cells and promotes CD8 + T-cell tumour infiltration. *J Transl Med* 2023; **21**: 335 [PMID: 37211606 DOI: 10.1186/s12967-023-04187-3]
15 **Wang X**, Yang L, Huang F, Zhang Q, Liu S, Ma L, You Z. Inflammatory cytokines IL-17 and TNF-α up-regulate PD-L1 expression in human prostate and colon cancer cells. *Immunol Lett* 2017; **184**: 7-14 [PMID: 28223102 DOI: 10.1016/j.imlet.2017.02.006]
16 **Liao H**, Chang X, Gao L, Ye C, Qiao Y, Xie L, Lin J, Cai S, Dong H. IL-17A promotes tumorigenesis and upregulates PD-L1 expression in non-small cell lung cancer. *J Transl Med* 2023; **21**: 828 [PMID: 37978543 DOI: 10.1186/s12967-023-04365-3]
17 **Wang S**, Wang G, Zhang L, Li F, Liu K, Wang Y, Shi Y, Cao K. Interleukin-17 promotes nitric oxide-dependent expression of PD-L1 in mesenchymal stem cells. *Cell Biosci* 2020; **10**: 73 [PMID: 32509271 DOI: 10.1186/s13578-020-00431-1]
18 **Zhao H**, Wu L, Yan G, Chen Y, Zhou M, Wu Y, Li Y. Inflammation and tumor progression: signaling pathways and targeted intervention. *Signal Transduct Target Ther* 2021; **6**: 263 [PMID: 34248142 DOI: 10.1038/s41392-021-00658-5]
19 **Wang JT**, Li H, Zhang H, Chen YF, Cao YF, Li RC, Lin C, Wei YC, Xiang XN, Fang HJ, Zhang HY, Gu Y, Liu X, Zhou RJ, Liu H, He HY, Zhang WJ, Shen ZB, Qin J, Xu JJ. Intratumoral IL17-producing cells infiltration correlate with antitumor immune contexture and improved response to adjuvant chemotherapy in gastric cancer. *Ann Oncol* 2019; **30**: 266-273 [PMID: 30445581 DOI: 10.1093/annonc/mdy505]
20 **Mattarollo SR**, Loi S, Duret H, Ma Y, Zitvogel L, Smyth MJ. Pivotal role of innate and adaptive immunity in anthracycline chemotherapy of established tumors. *Cancer Res* 2011; **71**: 4809-4820 [PMID: 21646474 DOI: 10.1158/0008-5472.CAN-11-0753]
21 **Ma HY**, Yamamoto G, Xu J, Liu X, Karin D, Kim JY, Alexandrov LB, Koyama Y, Nishio T, Benner C, Heinz S, Rosenthal SB, Liang S, Sun M, Karin G, Zhao P, Brodt P, Mckillop IH, Quehenberger O, Dennis E, Saltiel A, Tsukamoto H, Gao B, Karin M, Brenner DA, Kisseleva T. IL-17 signaling in steatotic hepatocytes and macrophages promotes hepatocellular carcinoma in alcohol-related liver disease. *J Hepatol* 2020; **72**: 946-959 [PMID: 31899206 DOI: 10.1016/j.jhep.2019.12.016]
22 **Bausch D**, Pausch T, Krauss T, Hopt UT, Fernandez-del-Castillo C, Warshaw AL, Thayer SP, Keck T. Neutrophil granulocyte derived MMP-9 is a VEGF independent functional component of the angiogenic switch in pancreatic ductal adenocarcinoma. *Angiogenesis* 2011; **14**: 235-243 [PMID: 21442180 DOI: 10.1007/s10456-011-9207-3]
23 **Liu C**, Liu R, Wang B, Lian J, Yao Y, Sun H, Zhang C, Fang L, Guan X, Shi J, Han S, Zhan F, Luo S, Yao Y, Zheng T, Zhang Y. Blocking IL-17A enhances tumor response to anti-PD-1 immunotherapy in microsatellite stable colorectal cancer. *J Immunother Cancer* 2021; **9** [PMID: 33462141 DOI: 10.1136/jitc-2020-001895]
24 **Aotsuka A**, Matsumoto Y, Arimoto T, Kawata A, Ogishima J, Taguchi A, Tanikawa M, Sone K, Mori-Uchino M, Tsuruga T, Oda K, Kawana

K, Osuga Y, Fujii T. Interleukin-17 is associated with expression of programmed cell death 1 ligand 1 in ovarian carcinoma. *Cancer Sci* 2019; **110**: 3068-3078 [PMID: 31432577 DOI: 10.1111/cas.14174]

25 **Picard FSR**, Lutz V, Brichkina A, Neuhaus F, Ruckenbrod T, Hupfer A, Raifer H, Klein M, Bopp T, Pfefferle PI, Savai R, Prinz I, Waisman A, Moos S, Chang HD, Heinrich S, Bartsch DK, Buchholz M, Singh S, Tu M, Klein L, Bauer C, Liefke R, Burchert A, Chung HR, Mayer P, Gress TM, Lauth M, Gaida M, Huber M. IL-17A-producing CD8(+) T cells promote PDAC *via* induction of inflammatory cancer-associated fibroblasts. *Gut* 2023; **72**: 1510-1522 [PMID: 36759154 DOI: 10.1136/gutjnl-2022-327855]

26 **Wei Y**, Shi D, Liang Z, Liu Y, Li Y, Xing Y, Liu W, Ai Z, Zhuang J, Chen X, Gao Q, Jiang J. IL-17A secreted from lymphatic endothelial cells promotes tumorigenesis by upregulation of PD-L1 in hepatoma stem cells. *J Hepatol* 2019; **71**: 1206-1215 [PMID: 31499129 DOI: 10.1016/j.jhep.2019.08.034]

27 **Gao Q**, Wang XY, Qiu SJ, Yamato I, Sho M, Nakajima Y, Zhou J, Li BZ, Shi YH, Xiao YS, Xu Y, Fan J. Overexpression of PD-L1 significantly associates with tumor aggressiveness and postoperative recurrence in human hepatocellular carcinoma. *Clin Cancer Res* 2009; **15**: 971-979 [PMID: 19188168 DOI: 10.1158/1078-0432.CCR-08-1608]

28 **Chen J**, Feng W, Sun M, Huang W, Wang G, Chen X, Yin Y, Chen X, Zhang B, Nie Y, Fan D, Wu K, Xia L. TGF-β1-Induced SOX18 Elevation Promotes Hepatocellular Carcinoma Progression and Metastasis Through Transcriptionally Upregulating PD-L1 and CXCL12. *Gastroenterology* 2024; **167**: 264-280 [PMID: 38417530 DOI: 10.1053/j.gastro.2024.02.025]

29 **Dai Z**, Huang Q, Huang X, Zhu C, Zahid KR, Liu T, Li Q, Wu C, Peng M, Xiao X, Raza U, Yu N, Zeng T. KIN17 promotes cell migration and invasion through stimulating the TGF-β/Smad2 pathway in hepatocellular carcinoma. *Mol Carcinog* 2023; **62**: 369-384 [PMID: 36468848 DOI: 10.1002/mc.23492]

30 **Huang Z**, Wen J, Yu J, Liao J, Liu S, Cai N, Liang H, Chen X, Ding Z, Zhang B. MicroRNA-148a-3p inhibits progression of hepatocelluar carcimoma by repressing SMAD2 expression in an Ago2 dependent manner. *J Exp Clin Cancer Res* 2020; **39**: 150 [PMID: 32746934 DOI: 10.1186/s13046-020-01649-0]

31 **David JM**, Dominguez C, McCampbell KK, Gulley JL, Schlom J, Palena C. A novel bifunctional anti-PD-L1/TGF-β Trap fusion protein (M7824) efficiently reverts mesenchymalization of human lung cancer cells. *Oncoimmunology* 2017; **6**: e1349589 [PMID: 29123964 DOI: 10.1080/2162402X.2017.1349589]

32 **Li S**, Na R, Li X, Zhang Y, Zheng T. Targeting interleukin-17 enhances tumor response to immune checkpoint inhibitors in colorectal cancer. *Biochim Biophys Acta Rev Cancer* 2022; **1877**: 188758 [PMID: 35809762 DOI: 10.1016/j.bbcan.2022.188758]

33 **Song M**, Wang L, Jiang S, Liang J, Li W, Rao W, Du Q, Liu G, Meng H, Tang L, Li Z, Yang Y, Zhang L, Zhang B. Pathogenic Th17 cell-mediated liver fibrosis contributes to resistance to PD-L1 antibody immunotherapy in hepatocellular carcinoma. *Int Immunopharmacol* 2024; **129**: 111601 [PMID: 38350354 DOI: 10.1016/j.intimp.2024.111601]

34 **Chalabi M**, Fanchi LF, Dijkstra KK, Van den Berg JG, Aalbers AG, Sikorska K, Lopez-Yurda M, Grootscholten C, Beets GL, Snaebjornsson P, Maas M, Mertz M, Veninga V, Bounova G, Broeks A, Beets-Tan RG, de Wijkerslooth TR, van Lent AU, Marsman HA, Nuijten E, Kok NF, Kuiper M, Verbeek WH, Kok M, Van Leerdam ME, Schumacher TN, Voest EE, Haanen JB. Neoadjuvant immunotherapy leads to pathological responses in MMR-proficient and MMR-deficient early-stage colon cancers. *Nat Med* 2020; **26**: 566-576 [PMID: 32251400 DOI: 10.1038/s41591-020-0805-8]

World Journal of Gastrointestinal Oncology

Submit a Manuscript: https://www.f6publishing.com

World J Gastrointest Oncol 2025 January 15; 17(1): 98409

DOI: 10.4251/wjgo.v17.i1.98409

ISSN 1948-5204 (online)

ORIGINAL ARTICLE

Basic Study

Dysregulation of genes involved in the long-chain fatty acid transport in pancreatic ductal adenocarcinoma

Radu Cristian Poenaru, Elena Milanesi, Andrei Marian Niculae, Anastasia-Maria Dobre, Catalina Vladut, Mihai Ciocîrlan, Daniel Vasile Balaban, Vlad Herlea, Maria Dobre, Mihail Eugen Hinescu

Specialty type: Oncology

Provenance and peer review: Unsolicited article; Externally peer reviewed.

Peer-review model: Single blind

Peer-review report's classification
Scientific Quality: Grade B
Novelty: Grade B
Creativity or Innovation: Grade B
Scientific Significance: Grade B

P-Reviewer: Chen YJC

Received: June 25, 2024
Revised: September 17, 2024
Accepted: October 22, 2024
Published online: January 15, 2025
Processing time: 169 Days and 17 Hours

Radu Cristian Poenaru, Elena Milanesi, Andrei Marian Niculae, Anastasia-Maria Dobre, Catalina Vladut, Mihai Ciocîrlan, Daniel Vasile Balaban, Vlad Herlea, Maria Dobre, Mihail Eugen Hinescu, Faculty of Medicine, Carol Davila University of Medicine and Pharmacy, Bucharest 050474, Romania

Elena Milanesi, Department of Radiobiology, Victor Babes National Institute of Pathology, Bucharest 050096, Romania

Andrei Marian Niculae, Maria Dobre, Mihail Eugen Hinescu, Department of Pathology, Victor Babes National Institute of Pathology, Bucharest 050096, Romania

Catalina Vladut, Mihai Ciocîrlan, Department of Gastroenterology, Prof. Dr. Agrippa Ionescu Clinical Emergency Hospital, Bucharest 011356, Romania

Vlad Herlea, Department of Pathology, Fundeni Clinical Institute, Bucharest 022258, Romania

Co-first authors: Radu Cristian Poenaru and Elena Milanesi.

Co-corresponding authors: Andrei Marian Niculae and Maria Dobre.

Corresponding author: Maria Dobre, MSc, PhD, Research Scientist, Department of Pathology, Victor Babes National Institute of Pathology, Splaiul Independentei 99-101, Bucharest 050096, Romania. maria_dobre70@yahoo.com

Abstract

BACKGROUND

Pancreatic ductal adenocarcinoma (PDAC) is an aggressive lethal malignancy with limited options for treatment and a 5-year survival rate of 11% in the United States. As for other types of tumors, such as colorectal cancer, aberrant *de novo* lipid synthesis and reprogrammed lipid metabolism have been suggested to be associated with PDAC development and progression.

AIM

To identify the possible involvement of lipid metabolism in PDAC by analyzing in tumoral and non-tumoral tissues the expression level of the most relevant genes involved in the long-chain fatty acid (FA) import into cell.

METHODS
A gene expression analysis of *FASN*, *CD36*, *SLC27A1*, *SLC27A2*, *SLC27A3*, *SLC27A4*, *SLC27A5*, *ACSL1*, and *ACSL3* was performed by qRT-PCR in 24 tumoral PDAC tissues and 11 samples from non-tumoral pancreatic tissues obtained *via* fine needle aspiration or *via* surgical resection. The genes were considered significantly dysregulated between the groups when the p value was < 0.05 and the fold change (FC) was ≤ 0.5 and ≥ 2.

RESULTS
We found that three FA transporters and two long-chain acyl-CoA synthetases genes were significantly upregulated in the PDAC tissue compared to the non-tumoral tissue: *SLC27A2* (FC = 5.66; *P* = 0.033), *SLC27A3* (FC = 2.68; *P* = 0.040), *SLC27A4* (FC = 3.13; *P* = 0.033), *ACSL1* (FC = 4.10; *P* < 0.001), and *ACSL3* (FC = 2.67; *P* = 0.012). We further investigated any possible association between the levels of the analyzed mRNAs and the specific characteristics of the tumors, including the anatomic location, the lymph node involvement, and the presence of metastasis. A significant difference in the expression of *SLC27A3* (FC = 3.28; *P* = 0.040) was found comparing patients with and without lymph nodes involvement with an overexpression of this transcript in 17 patients presenting tumoral cells in the lymph nodes.

CONCLUSION
Despite the low number of patients analyzed, these preliminary results seem to be promising. Addressing lipid metabolism through a broad strategy could be a beneficial way to treat this malignancy. Future *in vitro* and *in vivo* studies on these genes may offer important insights into the mechanisms linking PDAC with the long-chain FA import pathway.

Key Words: Carcinoma; Pancreatic ductal; Fatty acid transport; Gene expression; Biomarkers

Core Tip: In this original article, we show preliminary results of a case-control study in which we analyzed the expression level of nine relevant genes involved in the long-chain fatty acid (FA) import in pancreatic ductal adenocarcinoma (PDAC). We found that three FA transporters (*SLC27A2*, *SLC27A3*, and *SLC27A4*) and two long-chain acyl-CoA synthetases genes (*ACSL1* and *ACSL3*) were significantly upregulated in the PDAC tissue compared to the non-tumoral tissue. These data suggest that addressing lipid metabolism through a broad strategy that may impact both tumor cells and the tumor microenvironment could be a beneficial way to treat this malignancy.

Citation: Poenaru RC, Milanesi E, Niculae AM, Dobre AM, Vladut C, Ciocîrlan M, Balaban DV, Herlea V, Dobre M, Hinescu ME. Dysregulation of genes involved in the long-chain fatty acid transport in pancreatic ductal adenocarcinoma. *World J Gastrointest Oncol* 2025; 17(1): 98409
URL: https://www.wjgnet.com/1948-5204/full/v17/i1/98409.htm
DOI: https://dx.doi.org/10.4251/wjgo.v17.i1.98409

INTRODUCTION

Lipids are essential biological components that function as building blocks for membranes and are involved in energy metabolism, signaling cascades, and cell transport. The preservation of lipid homeostasis is essential for life, and prolonged exposure to excess lipids may have harmful effects and lead to serious lipid-related illnesses[1]. In particular, reprogramming of lipid metabolism is a characteristic of different types of cancer[2], as tumor cells can increase *de novo* lipogenesis, fatty acid (FA) absorption, and FA oxidation represent mechanisms to produce energy and accumulate lipids for the synthesis of plasma membranes[3].

Dysregulated FA metabolism is driven by specific carcinogenic signaling pathways, including the B-Raf kinase and the epidermal growth factor receptor, and affects the composition and saturation of lipid membranes[4]. This, in turn, modulates cancer cell tolerance to reactive oxygen species, enabling their survival, invasion, and metastasis[5]. Consequently, targeting lipid metabolism using a multifaceted strategy that can affect tumor cells as well as the tumor microenvironment would appear to represent a valuable approach to treat cancer[6]. Notably, alterations in cellular lipid metabolism also play a significant role in tumor drug resistance[7].

One of the most lethal cancers is pancreatic ductal adenocarcinoma (PDAC), an aggressive solid tumor with a 5-year survival rate of 11% in the United States. The poor survival rate is attributed to several characteristics, including aggressive tumor biology, late symptom presentation, tumor localization, difficult surgical care, and an absence of effective systemic drugs[8]. When adjusting for age, countries with the highest projected growth in the number of individuals above 65-years-old are the same as those with the highest rates of pancreatic cancer. Unfortunately, only approximately 15%-20% of patients are diagnosed with surgically resectable PDAC[9]. Thus, as the lifespan increases

worldwide, the overall burden of pancreatic cancer will also increase. Current estimates indicate that pancreatic cancer will become the second leading cause of cancer-related death after lung cancer.

A growing number of studies now indicate a relationship between PDAC and dysregulated lipid metabolism[10-13]. Specialized transporters, such as CD36 or the FA transport protein family [FATPs; often referred to as solute carrier protein family 27 (SLC27)], are necessary for the effective passage of exogenous FAs across the plasma membrane[14].

CD36 (also known as FA translocase) is a cell surface scavenger receptor involved in metastasis, immune evasion, and drug resistance[15]. Kubo *et al*[16] identified elevated CD36 expression as a major adverse prognostic factor in PDAC that affects gemcitabine resistance by influencing anti-apoptosis protein activity. Conversely, a low expression of CD36 in PDAC has been found to be associated with low Tumor, Node, Metastasis (TNM) staging and CA19-9 levels, even in the presence of a large tumor size and a poor prognosis for survival[17].

Another factor that affects several aspects of PDAC is SLC27. It consists of a family of six members, from SLC27A1 through SLC27A6, that are involved in the uptake of long-chain FAs. These transporters are also implicated in the emergence of several malignancies, as they can modify FA metabolism, cell growth, and cell proliferation[18]. For example, while normal cells obtain FAs exogenously, tumor cells obtain FAs both exogenously and by *de novo* synthesis *via* FASN[19]. FASN functions as a major regulator of lipid metabolism, is essential for the development and survival of tumors exhibiting lipogenic characteristics, and is also involved in the metabolism of amino acids and glycolysis in cells [19].

The bioconversion of exogenous or newly generated FAs to fatty acyl-CoA is catalyzed by five distinct long-chain acyl-CoA synthetase (ACSL) isoforms that make up the ACSL family and are implicated in the growth of malignant tumor cells[20,21]. For example, Cai and Ma demonstrated that ACSL1 expression levels were elevated in human prostate cancers, and that ACSL1 enhanced triglyceride production, lipid accumulation in cancer cells, and the manufacture of fatty acyl-CoAs, such as C16: 0-, C18: 0-, C18: 1-, and C18: 2-CoA[22].

In the present study, our aim was to investigate the role of genes involved in long-chain FA transport in PDAC by comparing the gene expression levels of *CD36*, *SLC27A1*, *FASN*, *SLC27A2*, *SLC27A3*, *SLC27A4*, *SLC27A5*, *ACSL1*, and *ACSL3* in 24 PDAC tumoral tissues to the expression levels in 11 pancreatic non-tumoral tissues.

MATERIALS AND METHODS

Sample collection and gene expression analysis

Tumoral pancreatic tissue from 24 patients was obtained *via* fine needle aspiration (n = 19) or surgical resection (n = 5) and were diagnosed with PDAC at the Clinical Emergency Hospital of Bucharest. During surgical resection, 11 samples of non-tumoral pancreatic tissue were also obtained from the peritumoral area of patients with PDAC (n = 6), neuroendocrine tumor (n = 3), and metastasis of colorectal carcinoma (n = 2) as a control group (CTRL). The CTRL tissues were verified by a pathologist and only tissues without tumoral cells were included in the study. The samples were collected between January 2020 and March 2023. Only adults aged 18 years or older with a diagnosis of PDAC were included in the study; patients who underwent chemotherapy before sample collection were excluded. When possible, information on the lifestyle habits, presence of diabetes, and months of survival after PDAC diagnosis, were collected (Table 1). All patients provided written informed consent to participate in the study.

For the gene expression analysis, we selected the most relevant genes involved in long-chain FA import into cells (GO: 0044539), which included *CD36*, *SLC27A1*, *FASN*, *SLC27A2*, *SLC27A3*, *SLC27A4*, *SLC27A5*, *ACSL1*, and *ACSL3*. *IPO8* was used as the reference gene for qRT-PCR, as a previous study demonstrated its stability in human pancreatic cancer[23].

The miRNeasy Mini Kit (Qiagen, Hilden, Germany) was used to isolate the total RNA and the RT2 First Strand Kit (Qiagen) to reverse transcribe 300 ng of total RNA. PCR was performed in a volume of 25 µL on an ABI-7500 fast instrument (Thermo Scientific, Waltham, MA, United States) using 12.5 µL of RT2 SYBR® Green qPCR Mastermix (Qiagen), 2 µL of cDNA, 9.5 µL of RNase free water, and 1 µL of primer (RT2 qPCR Primer Assay 200 Cat. No./ID: 330001). The primers were purchased at Qiagen and the Gene Globe IDs were PPH01356A, (*CD36*, NM_000072) PPH17902A (*SLC27A1*, NM_198580), PPH07803A (*SLC27A2*, NM_003645), PPH20806A (*SLC27A3*, NM_024330), PPH00471A (*SLC27A4*, NM_005094), PPH16732B (*SLC27A5*, NM_012254), PPH19272A (*ACSL1*, NM_001995), PPH15368F (*ACSL3*, NM_004457), and PPH16835A (*IPO8*, NM_006390). The mRNA expression data are reported both as $2^{-\Delta CT}$ values for each group and as fold change (FC = $2^{-\Delta\Delta CT}$; Table 2, Figure 1 and Figure 2), and were calculated as previously described by Livak and Schmittgen[24]. A gene was considered differentially expressed between the groups when FC > 2 or FC < 0.5 and P < 0.05.

In silico validation of gene expression results

Genes that showed significant dysregulation in our comparison of the 24 PDAC and 11 CTRL tissues were searched in public databases that report RNA-seq data from large case-control studies. Data from the TCGA database, including 178 patients with pancreatic adenocarcinoma and 200 controls (obtained from GTEx study), were downloaded from OncoDB (http://oncodb.org/index.html) and analyzed with Student's t-test.

Statistical analysis

Differences in categorical variables (sex, lifestyle habits, and presence of diabetes) and continuous variables between the groups were assessed using the χ^2 test and Student's t-test, respectively. The normality of the gene expression data (in terms of $2^{-\Delta CT}$) was evaluated using the Shapiro–Wilk test. Because the gene expression data were not normally distributed (Shapiro–Wilk test, P < 0.05), the nonparametric Mann–Whitney test was used to assess the statistical

Table 1 Sociodemographic data, lifestyle habits, and presence of diabetes in pancreatic ductal adenocarcinoma patients and controls

Parameter	PDAC, *n* = 24	CTRL, *n* = 11	*P* value
Age	64.75 ± 10.17	58.00 ± 13.94	0.115
Sex as %	54.2 (F), 45.3 (M)	54.5 (F), 45.5 (M)	0.983
Smokers as %	25	33.3[1]	0.632
Coffee consumers as %	63.2[2]	55.5[1]	0.700
Alcohol consumers as %	4.1	0[1]	0.557
Diabetes as %	20.8	0[1]	0.160
Survival in months	4.81 ± 3.25[3]		

[1]Available for 9 control group patients.
[2]Available for 19 pancreatic ductal adenocarcinoma patients.
[3]Available for 16 pancreatic ductal adenocarcinoma patients.
CTRL: Control group; PDAC: Pancreatic ductal adenocarcinoma.

Table 2 Gene expression results

Gene	Our study (24 PDAC *vs* 11 NT)				OncoDB (200 PDAC *vs* 178 normal)	
	PDAC ($2^{-\Delta CT}$ ± SEM)	NT ($2^{-\Delta CT}$ ± SEM)	FC	*P* value[1]	FC	*P* value[2]
CD36	0.527 ± 0.004	0.499 ± 0.009	1.06	0.001	2.893	< 0.001
SLC27A1	0.462 ± 0.003	0.462 ± 0.002	1.00	ns	2.836	< 0.001
FASN	1.325 ± 0.233	0.986 ± 0.222	1.34	ns	1.86	< 0.001
SLC27A2	0.763 ± 0.252	0.135 ± 0.036	5.66	0.033	3.689	< 0.001
SLC27A3	2.384 ± 0.548	0.888 ± 0.168	2.68	0.04	2.948	< 0.001
SLC27A4	0.996 ± 0.367	0.318 ± 0.059	3.13	0.033	2.366	< 0.001
SLC27A5	0.087 ± 0.026	0.045 ± 0.010	1.94	ns	2.385	< 0.001
ACSL1	14.063 ± 2.103	3.424 ± 0.725	4.10	< 0.001	19.043	ns
ACSL3	6.925 ± 1.397	2.593 ± 0.651	2.67	0.012	7.242	< 0.001

[1]Mann–Whitney test.
[2]*t*-test Student mean.
FC: Fold change; NT: Non-tumoral; PDAC: Pancreatic ductal adenocarcinoma; SEM: Standard error of the mean.

differences between the two groups. The statistical analyses were performed using SPSS version 20.0, and the graphs were generated using GraphPad Prism 8.4.3.

RESULTS

The groups of patients and controls were age-matched ($P = 0.115$) and sex-matched ($P = 0.983$). No difference between patients and controls was found in terms of number of smokers ($P = 0.632$), coffee consumers ($P = 0.700$), alcohol consumers ($P = 0.557$), and presence of diabetes ($P = 0.160$; Table 1).

Most of the patients presented PDAC localized in the head of the pancreas ($n = 18$, 75%), followed by 2 in the body (8.3%), 2 in the body-tail (8.3%), 1 patient in the neck (4.2%), and 1 patient in the tail of the pancreas (4.2%). At the time of sample retrieval, 17 of 24 patients presented with lymph node involvement, 9 patients had hepatic metastasis, and 3 patients had lung metastasis.

The gene expression analysis showed that five of the nine investigated genes were significantly dysregulated within the PDAC tissue compared to the CTRL. The dysregulated genes belonged to two categories: FA transporters and Long-Chain ACSL. Our gene expression results obtained by qRT-PCR and those obtained by RNA-seq available in OncoDB are reported in Table 2.

The five genes that showed significant differences in expression between the groups were *SLC27A2*, *SLC27A3*, *SLC27-A4*, *ACSL1*, and *ACSL3*. All five genes were upregulated (FC > 2 and $P < 0.05$) in the pathological condition: *SLC27A2* (FC = 5.66; $P = 0.033$), *SLC27A3* (FC = 2.68; $P = 0.040$), *SLC27A4* (FC = 3.13; $P = 0.033$), *ACSL1* (FC = 4.10; $P < 0.001$), and *ACSL3*

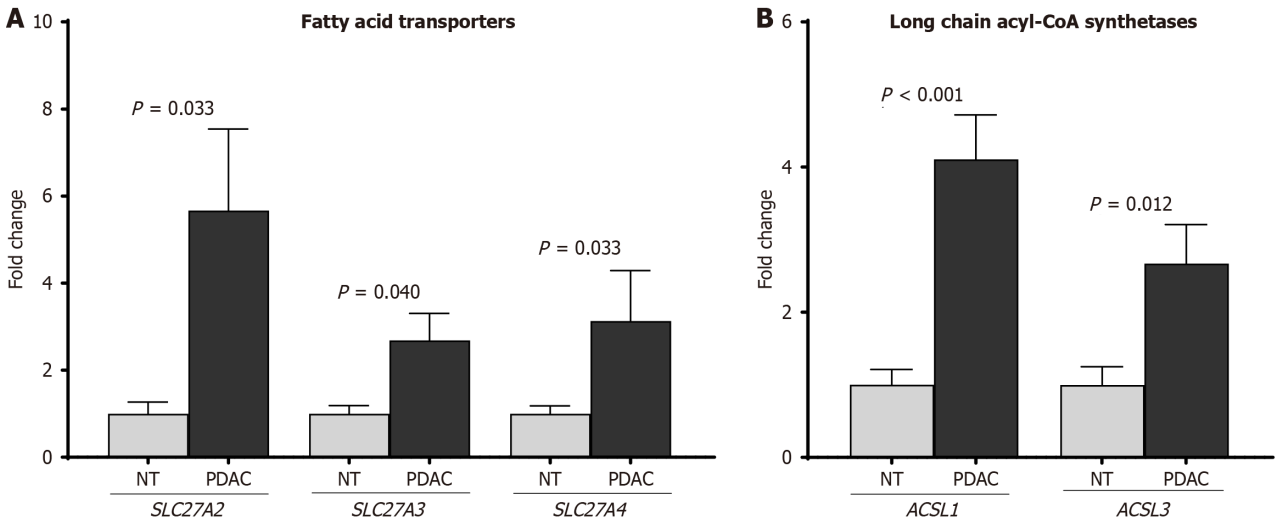

Figure 1 Gene expression results. A and B: Genes found differentially expressed between non-tumoral pancreatic tissue and pancreatic ductal adenocarcinoma tissue, comprising fatty acid transporters (A) and long-chain acyl-CoA synthetases (B). Bars indicate the mean ± standard error. NT: Non-tumoral; PDAC: Pancreatic ductal adenocarcinoma.

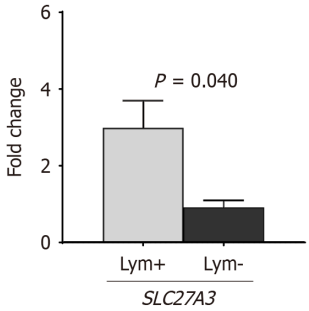

Figure 2 Expression difference of SLC27A3 between pancreatic ductal adenocarcinoma tissue with lymph nodes invasion (Lym+) and pancreatic ductal adenocarcinoma tissue without (Lym-). Bars indicate the mean ± standard error.

(FC = 2.67; P = 0.012); (Figure 1).

We further investigated any possible association between the levels of the analyzed mRNAs and the specific characteristics of the tumors, including the anatomic location, the lymph node involvement, and the presence of metastasis. A significant difference in the expression of *SLC27A3* was found comparing patients with and without lymph nodes involvement with an overexpression of this transcript in 17 patients presenting tumoral cells in the lymph nodes (FC = 3.27; P = 0.040; Figure 2). When correlating the expression levels of the analyzed genes with the patient's survival, we observed a significant negative correlation between the months of survival and the *FASN* expression (P = 0.035, r = -0.528).

DISCUSSION

In this study, we report a general upregulation of key genes involved in long-chain FA import in PDAC. We found that three FA transporters and two long-chain ACSLs genes were significantly upregulated in the tumoral tissue compared to the non-tumoral pancreatic tissue. Specifically, we found upregulation of *SLC27A2*, *SLC27A3*, and *SLC27A4*, as well as *ACSL1* and *ACSL3*.

The *SLC27A2*, *SLC27A3*, and *SLC27A4* genes encode FATP2, FATP3, and FATP4, respectively. FATP2 and FATP4 transport exogenous FAs into the cell[25,26], whereas FATP3 does not have a transporter function, but instead acts as an acyl-CoA ligase, facilitating the ATP-dependent formation of fatty acyl-CoA[27]. The existing literature indicates that FATPs contribute to the development of various cancers by altering FA metabolism.

FATP2 plays a role in reprogramming neutrophils in cancer to mediate the acquisition of immunosuppressive activity [28]. In the kidneys, FATP2 regulates proximal tubule lipoapoptosis[29], and its upregulation suppresses the proliferation and invasion of renal cancer[30]. In lung cancer, reduced levels of FATP2 induce cisplatin resistance and are correlated with poor patient survival[31]. In thyroid cancer, high levels of FATP2 promote tumor proliferation and migration[32].

FATP3 expression is involved in glioblastoma, where it supports glioblastoma stem cell maintenance and tumorigenicity[33]. FATP3 expression is increased in lung cancer[27], and our research group has observed similar increases in FATP3 expression in colorectal cancer[34], as well as upregulation of FATP4.

Elevated levels of FATP4 have also been associated with tumorigenesis and tumor progression in clear cell renal cell carcinoma[35], and with tumor progression in non-muscle-invasive bladder cancer[36].

To our knowledge, our study is the first to report upregulation of expression of genes encoding these three transporters in PDAC tissue. Moreover, we also found higher levels of *SLC27A3* (FATP3) in the tumors from patients with lymph node involvement than in those without. This upregulation is not surprising since FATP3 can mediate the levels of long-chain FAs that have been found to accumulate in metastatic sites. Targeting this mechanism to reduce this accumulation has been suggested to improve anti-tumor immune responses[37].

We also found that *ACSL1* and *ACSL3* were upregulated in PDAC tissue compared to non-tumoral pancreatic tissue. The ACSL family enzymes, which comprise ACSL1 and ACSL3-6, play key roles in activating free FAs to form fatty acyl-CoAs, which are needed for FA incorporation into phospholipids.

ACSLs are involved in endoplasmic reticulum stress, ferroptosis, drug resistance, and in perpetuating the tumor inflammatory microenvironment[38]. In liver cancer, ACSL1 promotes tumor growth[39], and its upregulation in hepatocellular carcinoma induces intracellular lipid accumulation[40]. In colorectal cancer, ACSL1 is considered a prognostic biomarker because its high expression is associated with poor clinical outcomes in stage-II cancer[41] and with promotion of tumor invasion in ovarian cancer[42].

ACSL3 expression is also associated with different cancers and shows an involvement in the metastasis of melanoma [43] and prostate cancer, where it also promotes tumor growth and proliferation[44]. In lung cancer, ACSL3 seems to promote tumor survival and chemosensitivity, and its high expression correlates with worse outcome in patients[45].

In pancreatic cancer, evidence linking ACSL family members has come from studies that investigated ACSL3, ACSL4, and ACLS5. In line with our findings, Sebastiano *et al*[46] found that *ACSL3* mRNA levels were higher in primary ductal adenocarcinomas and metastasis than in healthy epithelium, and their results were confirmed by interrogating public databases analyzing PDAC human samples. The authors, conducting a study in mice, also demonstrated that ACSL3 deletion delayed PDAC progression and reduced fibrosis[46].

Another study showed that depletion of extracellularly derived lipids by restriction of *ACSL3* could trigger autophagy and reduce PDAC cell proliferation[47]. For ACSL4, most studies indicate that it has an oncogenic function in most cancers; however, in pancreatic cancer ACSL4 expression appears to facilitate cell sensitivity to chemotherapy[48]. For ACSL5, progression-free survival is significantly shorter in patients with low expression than with high expression[49].

In the present study, although we identified an association between PDAC and the expression of three FA transporters and two long-chain ACSLs, our results cannot explain the molecular mechanism underpinning this relation. We can hypothesize that, as for other cancers, the overexpression of these transporters induces the elevated uptake of exogenous FAs that are subsequently stored as lipid droplets and ultimately undergo β-oxidation to generate ATP. This mechanism may produce enough ATP to support the enhanced growth and progression of tumor cells. The limitations of our study included its relatively small sample size and our investigation of our panel of genes only at the mRNA level, without confirming expression at the protein level.

CONCLUSION

The results reported in this article highlight the involvement of genes implicated in long-chain FA import in PDAC. We identified five transcripts (*SLC27A2*, *SLC27A3*, *SLC27A4*, *ACSL1*, and *ACSL3*) that were differentially expressed between PDAC and non-tumoral pancreatic tissue, with significant upregulation observed in the pathological condition. Despite the small number of patients analyzed, the preliminary results are promising. Future *in vitro* and *in vivo* studies on these genes may offer important insights into the mechanisms linking PDAC with the long-chain FA import pathway.

FOOTNOTES

Author contributions: Poenaru RC and Milanesi E contributed equally to this work as co-first authors; Niculae AM and Dobre M contributed equally to this work as co-corresponding authors; Poenaru RC, Milanesi E, Niculae AM, Dobre M, and Dobre AM contributed to methodology, formal analysis, data extraction, writing, reviewing, and editing; Vladut C, Ciocîrlan M, Balaban VD, Herlea V were involved in acquisition and data interpretation; Hinescu ME was involved in supervision; All authors contributed to the interpretation of the study and approved the final version to be published.

Supported by Romanian Ministry of Research, Innovation and Digitization, No. PN23.16.02.04 and No. 31PFE/30.12.2021.

Institutional review board statement: The study was conducted in accordance with the Declaration of Helsinki and was approved by the Ethics Committee of Clinical Emergency Hospital Bucharest (registration number 1960, 28 February 2019) and the Ethics Committee of the "Victor Babes" National Institute of Pathology (approval number 78, 3 December 2019).

Informed consent statement: All the patients signed the written informed consent.

Conflict-of-interest statement: All the authors report having no relevant conflicts of interest for this article.

Data sharing statement: The dataset used during the current study is available from the corresponding author on reasonable request.

Country of origin: Romania

ORCID number: Elena Milanesi 0000-0003-2753-3395; Mihai Ciocîrlan 0000-0002-6363-0320; Daniel Vasile Balaban 0000-0003-3436-8041; Vlad Herlea 0000-0002-0125-7815; Maria Dobre 0000-0002-1376-4021; Mihail Eugen Hinescu 0000-0002-7740-9336.

S-Editor: Lin C
L-Editor: Filipodia
P-Editor: Zhang L

REFERENCES

1 **Yoon H**, Shaw JL, Haigis MC, Greka A. Lipid metabolism in sickness and in health: Emerging regulators of lipotoxicity. *Mol Cell* 2021; **81**: 3708-3730 [PMID: 34547235 DOI: 10.1016/j.molcel.2021.08.027]
2 **Beloribi-Djefaflia S**, Vasseur S, Guillaumond F. Lipid metabolic reprogramming in cancer cells. *Oncogenesis* 2016; **5**: e189 [PMID: 26807644 DOI: 10.1038/oncsis.2015.49]
3 **Broadfield LA**, Pane AA, Talebi A, Swinnen JV, Fendt SM. Lipid metabolism in cancer: New perspectives and emerging mechanisms. *Dev Cell* 2021; **56**: 1363-1393 [PMID: 33945792 DOI: 10.1016/j.devcel.2021.04.013]
4 **Bi J**, Ichu TA, Zanca C, Yang H, Zhang W, Gu Y, Chowdhry S, Reed A, Ikegami S, Turner KM, Zhang W, Villa GR, Wu S, Quehenberger O, Yong WH, Kornblum HI, Rich JN, Cloughesy TF, Cavenee WK, Furnari FB, Cravatt BF, Mischel PS. Oncogene Amplification in Growth Factor Signaling Pathways Renders Cancers Dependent on Membrane Lipid Remodeling. *Cell Metab* 2019; **30**: 525-538.e8 [PMID: 31303424 DOI: 10.1016/j.cmet.2019.06.014]
5 **Ladanyi A**, Mukherjee A, Kenny HA, Johnson A, Mitra AK, Sundaresan S, Nieman KM, Pascual G, Benitah SA, Montag A, Yamada SD, Abumrad NA, Lengyel E. Adipocyte-induced CD36 expression drives ovarian cancer progression and metastasis. *Oncogene* 2018; **37**: 2285-2301 [PMID: 29398710 DOI: 10.1038/s41388-017-0093-z]
6 **Jin HR**, Wang J, Wang ZJ, Xi MJ, Xia BH, Deng K, Yang JL. Lipid metabolic reprogramming in tumor microenvironment: from mechanisms to therapeutics. *J Hematol Oncol* 2023; **16**: 103 [PMID: 37700339 DOI: 10.1186/s13045-023-01498-2]
7 **Germain N**, Dhayer M, Boileau M, Fovez Q, Kluza J, Marchetti P. Lipid Metabolism and Resistance to Anticancer Treatment. *Biology (Basel)* 2020; **9** [PMID: 33339398 DOI: 10.3390/biology9120474]
8 **Siegel RL**, Miller KD, Fuchs HE, Jemal A. Cancer statistics, 2022. *CA Cancer J Clin* 2022; **72**: 7-33 [PMID: 35020204 DOI: 10.3322/caac.21708]
9 **Stoffel EM**, Brand RE, Goggins M. Pancreatic Cancer: Changing Epidemiology and New Approaches to Risk Assessment, Early Detection, and Prevention. *Gastroenterology* 2023; **164**: 752-765 [PMID: 36804602 DOI: 10.1053/j.gastro.2023.02.012]
10 **Sunami Y**, Rebelo A, Kleeff J. Lipid Metabolism and Lipid Droplets in Pancreatic Cancer and Stellate Cells. *Cancers (Basel)* 2017; **10** [PMID: 29295482 DOI: 10.3390/cancers10010003]
11 **Li JT**, Wang YP, Yin M, Lei QY. Metabolism remodeling in pancreatic ductal adenocarcinoma. *Cell Stress* 2019; **3**: 361-368 [PMID: 31832601 DOI: 10.15698/cst2019.12.205]
12 **Li Y**, Amrutkar M, Finstadsveen AV, Dalen KT, Verbeke CS, Gladhaug IP. Fatty acids abrogate the growth-suppressive effects induced by inhibition of cholesterol flux in pancreatic cancer cells. *Cancer Cell Int* 2023; **23**: 276 [PMID: 37978383 DOI: 10.1186/s12935-023-03138-8]
13 **Yin X**, Xu R, Song J, Ruze R, Chen Y, Wang C, Xu Q. Lipid metabolism in pancreatic cancer: emerging roles and potential targets. *Cancer Commun (Lond)* 2022; **42**: 1234-1256 [PMID: 36107801 DOI: 10.1002/cac2.12360]
14 **Koundouros N**, Poulogiannis G. Reprogramming of fatty acid metabolism in cancer. *Br J Cancer* 2020; **122**: 4-22 [PMID: 31819192 DOI: 10.1038/s41416-019-0650-z]
15 **Feng WW**, Zuppe HT, Kurokawa M. The Role of CD36 in Cancer Progression and Its Value as a Therapeutic Target. *Cells* 2023; **12** [PMID: 37371076 DOI: 10.3390/cells12121605]
16 **Kubo M**, Gotoh K, Eguchi H, Kobayashi S, Iwagami Y, Tomimaru Y, Akita H, Asaoka T, Noda T, Takeda Y, Tanemura M, Mori M, Doki Y. Impact of CD36 on Chemoresistance in Pancreatic Ductal Adenocarcinoma. *Ann Surg Oncol* 2020; **27**: 610-619 [PMID: 31605325 DOI: 10.1245/s10434-019-07927-2]
17 **Jia S**, Zhou L, Shen T, Zhou S, Ding G, Cao L. Down-expression of CD36 in pancreatic adenocarcinoma and its correlation with clinicopathological features and prognosis. *J Cancer* 2018; **9**: 578-583 [PMID: 29483963 DOI: 10.7150/jca.21046]
18 **Acharya R**, Shetty SS, Kumari N S. Fatty acid transport proteins (FATPs) in cancer. *Chem Phys Lipids* 2023; **250**: 105269 [PMID: 36462545 DOI: 10.1016/j.chemphyslip.2022.105269]
19 **Fhu CW**, Ali A. Fatty Acid Synthase: An Emerging Target in Cancer. *Molecules* 2020; **25** [PMID: 32872164 DOI: 10.3390/molecules25173935]
20 **Yan S**, Yang XF, Liu HL, Fu N, Ouyang Y, Qing K. Long-chain acyl-CoA synthetase in fatty acid metabolism involved in liver and other diseases: an update. *World J Gastroenterol* 2015; **21**: 3492-3498 [PMID: 25834313 DOI: 10.3748/wjg.v21.i12.3492]
21 **Ma Y**, Zha J, Yang X, Li Q, Zhang Q, Yin A, Beharry Z, Huang H, Huang J, Bartlett M, Ye K, Yin H, Cai H. Long-chain fatty acyl-CoA synthetase 1 promotes prostate cancer progression by elevation of lipogenesis and fatty acid beta-oxidation. *Oncogene* 2021; **40**: 1806-1820 [PMID: 33564069 DOI: 10.1038/s41388-021-01667-y]

22 **Cai H**, Ma Y. Biosynthesis of acyl-CoAs sustains prostate cancer progression. *FASEB J* 2018; **32**: 811.1 [DOI: 10.1096/fasebj.2018.32.1_supplement.811.1]

23 **Ge WL**, Shi GD, Huang XM, Zong QQ, Chen Q, Meng LD, Miao Y, Zhang JJ, Jiang KR. Optimization of internal reference genes for qPCR in human pancreatic cancer research. *Transl Cancer Res* 2020; **9**: 2962-2971 [PMID: 35117652 DOI: 10.21037/tcr.2020.02.48]

24 **Livak KJ**, Schmittgen TD. Analysis of relative gene expression data using real-time quantitative PCR and the 2(-Delta Delta C(T)) Method. *Methods* 2001; **25**: 402-408 [PMID: 11846609 DOI: 10.1006/meth.2001.1262]

25 **Pohl J**, Ring A, Hermann T, Stremmel W. Role of FATP in parenchymal cell fatty acid uptake. *Biochim Biophys Acta* 2004; **1686**: 1-6 [PMID: 15522816 DOI: 10.1016/j.bbalip.2004.06.004]

26 **Doege H**, Stahl A. Protein-mediated fatty acid uptake: novel insights from in vivo models. *Physiology (Bethesda)* 2006; **21**: 259-268 [PMID: 16868315 DOI: 10.1152/physiol.00014.2006]

27 **Pei Z**, Fraisl P, Shi X, Gabrielson E, Forss-Petter S, Berger J, Watkins PA. Very long-chain acyl-CoA synthetase 3: overexpression and growth dependence in lung cancer. *PLoS One* 2013; **8**: e69392 [PMID: 23936004 DOI: 10.1371/journal.pone.0069392]

28 **Veglia F**, Tyurin VA, Blasi M, De Leo A, Kossenkov AV, Donthireddy L, To TKJ, Schug Z, Basu S, Wang F, Ricciotti E, DiRusso C, Murphy ME, Vonderheide RH, Lieberman PM, Mulligan C, Nam B, Hockstein N, Masters G, Guarino M, Lin C, Nefedova Y, Black P, Kagan VE, Gabrilovich DI. Fatty acid transport protein 2 reprograms neutrophils in cancer. *Nature* 2019; **569**: 73-78 [PMID: 30996346 DOI: 10.1038/s41586-019-1118-2]

29 **Khan S**, Cabral PD, Schilling WP, Schmidt ZW, Uddin AN, Gingras A, Madhavan SM, Garvin JL, Schelling JR. Kidney Proximal Tubule Lipoapoptosis Is Regulated by Fatty Acid Transporter-2 (FATP2). *J Am Soc Nephrol* 2018; **29**: 81-91 [PMID: 28993506 DOI: 10.1681/ASN.2017030314]

30 **Xu N**, Xiao W, Meng X, Li W, Wang X, Zhang X, Yang H. Up-regulation of SLC27A2 suppresses the proliferation and invasion of renal cancer by down-regulating CDK3-mediated EMT. *Cell Death Discov* 2022; **8**: 351 [PMID: 35927229 DOI: 10.1038/s41420-022-01145-8]

31 **Su J**, Wu S, Tang W, Qian H, Zhou H, Guo T. Reduced SLC27A2 induces cisplatin resistance in lung cancer stem cells by negatively regulating Bmi1-ABCG2 signaling. *Mol Carcinog* 2016; **55**: 1822-1832 [PMID: 26513225 DOI: 10.1002/mc.22430]

32 **Feng K**, Ma R, Li H, Yin K, Du G, Chen X, Liu Z, Yin D. Upregulated SLC27A2/FATP2 in differentiated thyroid carcinoma promotes tumor proliferation and migration. *J Clin Lab Anal* 2022; **36**: e24148 [PMID: 34854499 DOI: 10.1002/jcla.24148]

33 **Sun P**, Xia S, Lal B, Shi X, Yang KS, Watkins PA, Laterra J. Lipid metabolism enzyme ACSVL3 supports glioblastoma stem cell maintenance and tumorigenicity. *BMC Cancer* 2014; **14**: 401 [PMID: 24893952 DOI: 10.1186/1471-2407-14-401]

34 **Niculae AM**, Dobre M, Herlea V, Vasilescu F, Ceafalan LC, Trandafir B, Milanesi E, Hinescu ME. Lipid Handling Protein Gene Expression in Colorectal Cancer: CD36 and Targeting miRNAs. *Life (Basel)* 2022; **12** [PMID: 36556492 DOI: 10.3390/life12122127]

35 **Kim YS**, Jung J, Jeong H, Lee JH, Oh HE, Lee ES, Choi JW. High Membranous Expression of Fatty Acid Transport Protein 4 Is Associated with Tumorigenesis and Tumor Progression in Clear Cell Renal Cell Carcinoma. *Dis Markers* 2019; **2019**: 5702026 [PMID: 31089396 DOI: 10.1155/2019/5702026]

36 **Jeong H**, Oh HE, Kim H, Lee JH, Lee ES, Kim YS, Choi JW. Upregulation of Fatty Acid Transporters is Associated With Tumor Progression in Non-Muscle-Invasive Bladder Cancer. *Pathol Oncol Res* 2021; **27**: 594705 [PMID: 34257543 DOI: 10.3389/pore.2021.594705]

37 **Edwards DN**, Wang S, Song W, Kim LC, Ngwa VM, Hwang Y, Ess KC, Boothby MR, Chen J. Regulation of fatty acid delivery to metastases by tumor endothelium. *bioRxiv* 2024 [PMID: 38617241 DOI: 10.1101/2024.04.02.587724]

38 **Quan J**, Bode AM, Luo X. ACSL family: The regulatory mechanisms and therapeutic implications in cancer. *Eur J Pharmacol* 2021; **909**: 174397 [PMID: 34332918 DOI: 10.1016/j.ejphar.2021.174397]

39 **Yang G**, Wang Y, Feng J, Liu Y, Wang T, Zhao M, Ye L, Zhang X. Aspirin suppresses the abnormal lipid metabolism in liver cancer cells *via* disrupting an NFκB-ACSL1 signaling. *Biochem Biophys Res Commun* 2017; **486**: 827-832 [PMID: 28359761 DOI: 10.1016/j.bbrc.2017.03.139]

40 **Dongiovanni P**, Crudele A, Panera N, Romito I, Meroni M, De Stefanis C, Palma A, Comparcola D, Fracanzani AL, Miele L, Valenti L, Nobili V, Alisi A. β-Klotho gene variation is associated with liver damage in children with NAFLD. *J Hepatol* 2020; **72**: 411-419 [PMID: 31655133 DOI: 10.1016/j.jhep.2019.10.011]

41 **Sánchez-Martínez R**, Cruz-Gil S, García-Álvarez MS, Reglero G, Ramírez de Molina A. Complementary ACSL isoforms contribute to a non-Warburg advantageous energetic status characterizing invasive colon cancer cells. *Sci Rep* 2017; **7**: 11143 [PMID: 28894242 DOI: 10.1038/s41598-017-11612-3]

42 **Zhang Q**, Zhou W, Yu S, Ju Y, To SKY, Wong AST, Jiao Y, Poon TCW, Tam KY, Lee LTO. Metabolic reprogramming of ovarian cancer involves ACSL1-mediated metastasis stimulation through upregulated protein myristoylation. *Oncogene* 2021; **40**: 97-111 [PMID: 33082557 DOI: 10.1038/s41388-020-01516-4]

43 **Ubellacker JM**, Tasdogan A, Ramesh V, Shen B, Mitchell EC, Martin-Sandoval MS, Gu Z, McCormick ML, Durham AB, Spitz DR, Zhao Z, Mathews TP, Morrison SJ. Lymph protects metastasizing melanoma cells from ferroptosis. *Nature* 2020; **585**: 113-118 [PMID: 32814895 DOI: 10.1038/s41586-020-2623-z]

44 **Migita T**, Takayama KI, Urano T, Obinata D, Ikeda K, Soga T, Takahashi S, Inoue S. ACSL3 promotes intratumoral steroidogenesis in prostate cancer cells. *Cancer Sci* 2017; **108**: 2011-2021 [PMID: 28771887 DOI: 10.1111/cas.13339]

45 **Fernández LP**, Merino M, Colmenarejo G, Moreno-Rubio J, Sánchez-Martínez R, Quijada-Freire A, Gómez de Cedrón M, Reglero G, Casado E, Sereno M, Ramírez de Molina A. Metabolic enzyme ACSL3 is a prognostic biomarker and correlates with anticancer effectiveness of statins in non-small cell lung cancer. *Mol Oncol* 2020; **14**: 3135-3152 [PMID: 33030783 DOI: 10.1002/1878-0261.12816]

46 **Rossi Sebastiano M**, Pozzato C, Saliakoura M, Yang Z, Peng RW, Galiè M, Oberson K, Simon HU, Karamitopoulou E, Konstantinidou G. ACSL3-PAI-1 signaling axis mediates tumor-stroma cross-talk promoting pancreatic cancer progression. *Sci Adv* 2020; **6** [PMID: 33127675 DOI: 10.1126/sciadv.abb9200]

47 **Saliakoura M**, Sebastiano MR, Nikdima I, Pozzato C, Konstantinidou G. Restriction of extracellular lipids renders pancreatic cancer dependent on autophagy. *J Exp Clin Cancer Res* 2022; **41**: 16 [PMID: 34998392 DOI: 10.1186/s13046-021-02231-y]

48 **Ye Z**, Hu Q, Zhuo Q, Zhu Y, Fan G, Liu M, Sun Q, Zhang Z, Liu W, Xu W, Ji S, Yu X, Xu X, Qin Y. Abrogation of ARF6 promotes RSL3-induced ferroptosis and mitigates gemcitabine resistance in pancreatic cancer cells. *Am J Cancer Res* 2020; **10**: 1182-1193 [PMID: 32368394]

49 **Ma W**, Li T, Wu S, Li J, Wang X, Li H. LOX and ACSL5 as potential relapse markers for pancreatic cancer patients. *Cancer Biol Ther* 2019; **20**: 787-798 [PMID: 30712446 DOI: 10.1080/15384047.2018.1564565]

World Journal of Gastrointestinal Oncology

Submit a Manuscript: https://www.f6publishing.com

World J Gastrointest Oncol 2025 January 15; 17(1): 98410

DOI: 10.4251/wjgo.v17.i1.98410

ISSN 1948-5204 (online)

ORIGINAL ARTICLE

Basic Study

Correlations of the expression of Cx43, SCF^{FBXW7}, p-cyclin E1 (Ser73), p-cyclin E1 (Thr77) and p-cyclin E1 (Thr395) in colon cancer tissues

Rong-Gang Luan, Ming-Da Liu, Zi-Feng Deng, Cong-Lan Lu, Mei-Ling Yu, Ming-Yu Zhang, Rong Liu, Ran An, You-Liang Yao, Dong-Bei Guo, Yong-Xing Zhang, Lei Zhao

Specialty type: Oncology

Provenance and peer review: Unsolicited article; Externally peer reviewed.

Peer-review model: Single blind

Peer-review report's classification

Scientific Quality: Grade C

Novelty: Grade B

Creativity or Innovation: Grade B

Scientific Significance: Grade B

P-Reviewer: Zhang Z

Received: June 25, 2024

Revised: October 13, 2024

Accepted: October 28, 2024

Published online: January 15, 2025

Processing time: 169 Days and 16.7 Hours

Rong-Gang Luan, Department of Gastrointestinal Surgery, Air Force Hospital of Eastern Theater, Anhui Medical University, Nanjing 230032, Jiangsu Province, China

Ming-Da Liu, Zi-Feng Deng, Rong Liu, Ran An, You-Liang Yao, Dong-Bei Guo, Yong-Xing Zhang, State Key Laboratory of Molecular Vaccinology and Molecular Diagnostics, School of Public Health, Xiamen University, Xiamen 361102, Fujian Province, China

Cong-Lan Lu, Mei-Ling Yu, Ming-Yu Zhang, Trauma Surgery, Air Force Hospital of Eastern Theater, Anhui Medical University, Nanjing 230032, Jiangsu Province, China

Lei Zhao, Department of Orthopaedics, Air Force Hospital of Eastern Theater, Anhui Medical University, Nanjing 230032, Jiangsu Province, China

Co-corresponding authors: Yong-Xing Zhang and Lei Zhao.

Corresponding author: Lei Zhao, MD, PhD, Attending Doctor, Surgeon, Department of Orthopaedics, Air Force Hospital of Eastern Theater, Anhui Medical University, No. 1 Changfu Road, Malu Road, Nanjing 230032, Jiangsu Province, China. 18742583975@163.com

Abstract

BACKGROUND

Previous cellular studies have demonstrated that elevated expression of Cx43 promotes the degradation of cyclin E1 and inhibits cell proliferation through ubiquitination. Conversely, reduced expression results in a loss of this capacity to facilitate cyclin E degradation. The ubiquitination and degradation of cyclin E1 may be associated with phosphorylation at specific sites on the protein, with Cx43 potentially enhancing this process by facilitating the phosphorylation of these critical residues.

AIM

To investigate the correlation between expression of Cx43, SKP1/Cullin1/F-box (SCF)^{FBXW7}, p-cyclin E1 (ser73, thr77, thr395) and clinicopathological indexes in colon cancer.

METHODS

Expression levels of Cx43, SCF^{FBXW7}, p-cyclin E1 (ser73, thr77, thr395) in 38 clinical colon cancer samples were detected by immunohistochemistry and were analyzed

by statistical methods to discuss their correlations.

RESULTS

Positive rate of Cx43, SCF^{FBXW7}, p-cyclin E1(Ser73), p-cyclin E1 (Thr77) and p-cyclin E1 (Thr395) in detected samples were 76.32%, 76.32%, 65.79%, 5.26% and 55.26% respectively. Positive expressions of these proteins were not related to the tissue type, degree of tissue differentiation or lymph node metastasis. Cx43 and SCF^{FBXW7}(r = 0.749), p-cyclin E1 (Ser73) (r = 0.667) and p-cyclin E1 (Thr395) (r = 0.457), SCF^{FBXW7} and p-cyclin E1 (Ser73) (r = 0.703) and p-cyclin E1 (Thr395) (0.415) were correlated in colon cancer (P < 0.05), and expressions of the above proteins were positively correlated in colon cancer.

CONCLUSION

Cx43 may facilitate the phosphorylation of cyclin E1 at the Ser73 and Thr195 sites through its interaction with SCF^{FBXW7}, thereby influencing the ubiquitination and degradation of cyclin E1.

Key Words: Colon cancer; Cx43; SCF^{FBXW7}; Phosphorylation of cyclin E1; Sites of cyclin E1; Correlation analysis

Core Tip: In this study, we found that SKP1/Cullin1/F-box (SCF)^{FBXW7} exhibited a positive correlation with cyclin E1 expression at positions ser73 and thr395 in colon cancer tissues, suggesting that SCF^{FBXW7} may facilitate phosphorylation-dependent degradation by interacting with cyclin E1 at these specific sites. Furthermore, the expressions of Cx43 and SCF^{FBXW7} were positively correlated, as well as their association with the levels at positions ser73 and thr395. This indicates that Cx43 may enhance the phosphorylation of these two sites through its interaction with SCF^{FBXW7}, thereby promoting the ubiquitination and degradation of cyclin E1.

Citation: Luan RG, Liu MD, Deng ZF, Lu CL, Yu ML, Zhang MY, Liu R, An R, Yao YL, Guo DB, Zhang YX, Zhao L. Correlations of the expression of Cx43, SCF^{FBXW7}, p-cyclin E1 (Ser73), p-cyclin E1 (Thr77) and p-cyclin E1 (Thr395) in colon cancer tissues. *World J Gastrointest Oncol* 2025; 17(1): 98410
URL: https://www.wjgnet.com/1948-5204/full/v17/i1/98410.htm
DOI: https://dx.doi.org/10.4251/wjgo.v17.i1.98410

INTRODUCTION

Colon cancer is the third most commonly diagnosed cancer and the second leading cause of cancer-related mortality[1]. Despite significant advancements in recent years with chemotherapeutic agents targeting colon cancer, severe side effects, toxicity, and drug resistance remain major clinical challenges[2]. Therefore, it is imperative to identify additional therapeutic targets for colon cancer treatment to mitigate these adverse effects.

Cx43 is a crucial component of cell gap junctions, regulating cell proliferation and differentiation through intercellular communication *via* gap junctions[3]. Cx43 plays a significant role in modulating the cell cycle of tumor cells, and its abnormal expression is often associated with tumorigenesis[3,4-6]. Our previous studies have demonstrated that Cx43 expression is reduced in various cancer tissues, including lung and esophageal cancers[7-9].

Our previous study has indicated that AKAP95 and Cx43, functioning as a pair of molecular switches, influence the cell cycle by regulating the expression of cyclin Ds and cyclin Es, as well as the expression and activity of their associated cyclin-dependent kinases[10,11]. In lung cancer, Cx43 down-regulates cyclin E1 expression, thereby inhibiting Rb phosphorylation and E2F activation, which hinders cell cycle progression through competitive bindings to cyclin E1 with AKAP95[10]. Furthermore, Cx43 can negate the protective effect of AKAP95 on cyclin Es[10].

Ubiquitination is a crucial and widespread mechanism of protein degradation within cells. This pathway is catalyzed by ubiquitin-activating enzyme (E1), ubiquitin-conjugating enzyme (E2), and ubiquitin ligase (E3)[12-14]. Among the family of E3 Ligases, SCF has garnered significant attention in recent years. SCF^{FBXW7} has been identified as a specific ubiquitin ligase for cyclin E1, mediating its ubiquitination and subsequent degradation[15-17]. The SCF protein complex contains phosphate-binding domains that recognize and bind to phosphorylated sites on substrates, thereby facilitating substrate reactions[18]. We hypothesize that phosphorylation of cyclin E1 is a prerequisite for its ubiquitination and degradation; thus, we examined the expression levels of Cx43, SCF^{FBXW7}, and the phosphorylation status at various sites of cyclin E1 in 38 clinical colon cancer tissues while analyzing correlations among these proteins.

MATERIALS AND METHODS

Sample sources

Thirty-eight colon cancer tissue samples were all surgical specimens from colon cancer patients in Air Force Hospital of Eastern Theater during 2015-2020. The age range of the patients was 30-94, with an average of 67.3 years. The pathological diagnosis of patient samples was clear, including 1 case of T1N0M0, 1 case of T1N1aM1a, 5 cases of T2N0M0, 1 case of T2N1aM0, 2 cases of T3N0M0, 16 cases of T4aN0M0, 1 case of T4aN0M1a, 3 cases of T4aN1bM0, 1 case of T4aN1bM1a, 3 cases of T4aN1cM0, 2 cases of T4aN1cM1a, 1 case of T4aN2bM0 and 1 case of TisN0M0 (TNM typing).

Reagents and antibodies

General two-step immunohistochemical kit (PV-9000) and DAB chromogenic solution were purchased from Fuzhou Maxim Biotechnology Development Co., Ltd; Hematoxylin dye was purchased from Solarbio Co., Ltd; Anti-rabbit Cx43 (AF0137), FBXW7(DF12400), p-cyclin E1 (Ser73) (AF4413), and p-cyclin E1 (Thr395) (AF3235) were purchased from Affinity Biosciences (Ohio, United States). Anti-rabbit p-cyclin E1 (Thr77) (ET1612-31) was purchased from Hangzhou HuaAn Biotechnoloy Co., Ltd (Hangzhou, China).

Immunohistochemical assay

The specimens were fixed in 10% neutral formaldehyde and embedded in paraffin, and then 4 μm serial sections were cut. After hydration with xylene and gradient ethanol, the sections were placed in citric acid/ sodium citrate buffer for thermal repair. After blocking endogenous peroxidase, the primary antibody was incubated overnight (8 hours) and then the reaction enhancer and horseradish peroxidase labeled secondary antibody were incubated successively. After incubating DAB reagent, slides were put into hematoxylin staining solution to stain the nucleus, and dehydrate the slides after cleaning.

Positive criteria

Brownish yellow in cancer tissues was considered as protein positive expression under the light microscope. Each tissue slide was randomly observed in 10 different visual fields, and 200 tumor cells were counted in each visual field. The ratio of the number of positive cells to the total number of counted cells and the positive intensity were taken as the judgment criteria. Under the light microscope, no brownish yellow in the field of vision or proportion of positive cells was less than 10% would be record as '-'; proportion of positive cells was ≥ 10% and < 30% would be recorded as '+'; proportion of positive cells was ≥ 30% and < 50% would be recorded as '++'; proportion of positive cells was ≥ 50% would be recorded as '+++. '-' was regarded as negative results while '+', '++' and '+++' were regarded as positive results. The slides were read by different experimenters for 3 times, and the average results were taken for statistical analysis.

Statistical analysis

IBM SPSS statistical was used for statistical analysis. χ^2 test was used for rate comparison, Spearman rank correlation analysis was used for correlation analysis, and test level $\alpha = 0.05$.

RESULTS

Expression of Cx43, SCF^{FBXW7} and p-cyclin E1(Ser73, Thr77, Thr395) in colon cancer tissues

In 38 cases of colon cancer, positive expression of Cx43 and SCF^{FBXW7} were 29 and 29 cases respectively, and their positive rates were 76.32% and 76.32%; positive expression of phosphorylation site Ser73, Thr77 and Thr395 of cyclin E1 were 25, 2 and 21 cases, and positive rates were 65.79%, 5.26% and 55.26% respectively (Table 1).

Positive rates of expression of Cx43, SCF^{FBXW7}, p-cyclin E1 (Ser73) and p-cyclin E1 (Thr395) were significantly higher than p-cyclin E1 (Thr77). Cx43, SCF^{FBXW7}, p-cyclin E1 (Ser73) and p-cyclin E1 (Thr395) were expressed in both nucleus and cytoplasm (Figure 1).

Correlation analysis of SCF^{FBXW7}, p-cyclin E1(Ser73, Thr77, Thr395)

Tables 2, 3, and 4 showed analysis results of correlation between expression of SCF^{FBXW7} and p-cyclin E1 (Ser73), SCF^{FBXW7} and p-cyclin E1 (Thr77), and SCF^{FBXW7} and p-cyclin E1 (Thr395) in 38 colon cancer tissue cases. The expression of SCF^{FBXW7} and p-cyclin E1 (ser73), SCF^{FBXW7} and p-cyclin E1 (Thr395) were statistically significant ($P < 0.05$) and their spearman correlation coefficient were 0.703 and 0.415 respectively. The results showed that there were positive correlations between the expression of SCF^{FBXW7} and p-cyclin E1 (ser73), and SCF^{FBXW7} and p-cyclin E1 (thr395) in colon cancer. No correlation between SCF^{FBXW7} and p-cyclin E1 (Thr77) was detected this time.

Correlation analysis of Cx43, SCF^{FBXW7}, p-cyclin E1(Ser73), p-cyclin E1(Thr77) and p-cyclin E1(Thr395)

Tables 5, 6, 7, and 8 showed analysis results of correlation between expression of Cx43 and SCF^{FBXW7}, Cx43 and p-cyclin E1 (Ser73), Cx43 and p-cyclin E1 (Thr77), and Cx43 and p-cyclin E1 (Thr395) in 38 colon cancer tissue cases. The expression of Cx43 and SCF^{FBXW7}, Cx43 and p-cyclin E1 (ser73), Cx43 and p-cyclin E1 (Thr395) were statistically significant ($P < 0.05$) and their spearman correlation coefficient were 0.749, 0.667 and 0.457 respectively. The results showed that there were positive correlations between the expression of Cx43 and SCF^{FBXW7}, Cx43 and p-cyclin E1 (ser73), and Cx43 and p-cyclin E1 (Thr395) in colon cancer while there was no correlation between Cx43 and p-cyclin E1 (Thr77).

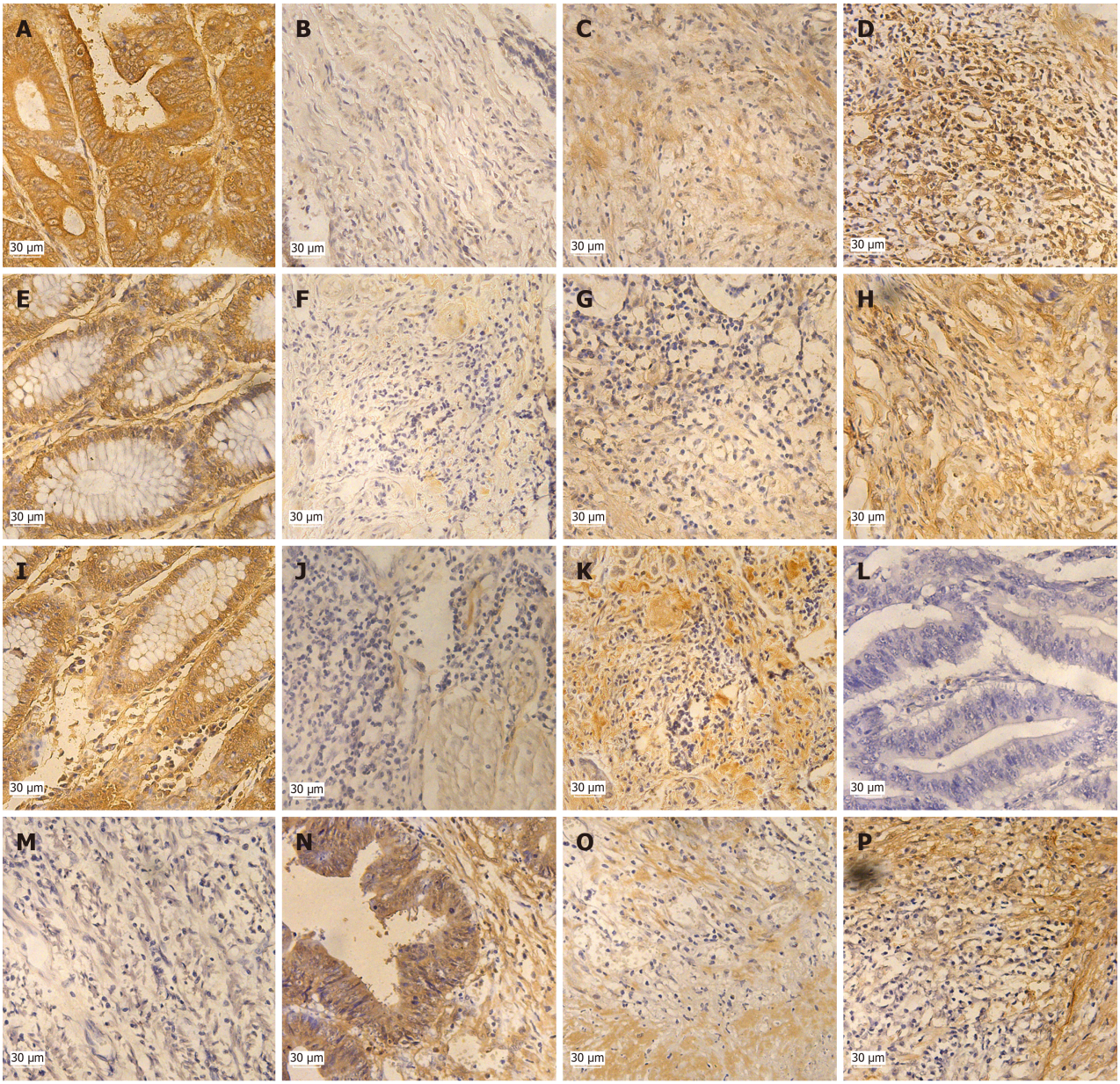

Figure 1 Expression of Cx43, Skp1-Cullin1-F-box (SCF)^{FBXW7}, Phosphorylation of cyclin E1 (p-cyclin E1) (Ser73, Thr77, Thr395) in 38 colon cancer tissue cases. A: High expression of Cx43 in normal tissues; B: Low expression of Cx43 in colon cancer tissues; C: Medium expression of Cx43 in colon cancer tissues; D: High expression of Cx43 in colon cancer tissues; E: High expression of SCF^{FBXW7} in normal tissues; F: Low expression of SCF^{FBXW7} in colon cancer tissues; G: Medium expression of SCF^{FBXW7}in colon cancer tissues; H: High expression of SCF^{FBXW7}in colon cancer tissues; I: High expression of p-cyclin E1 (Ser73) in normal tissues; J: Low expression of p-cyclin E1(Ser73) in colon cancer tissues; K: High expression of p-cyclin E1 (Ser73) in colon cancer tissues; L: Negative expression of p-cyclin E1 (Thr77) in normal tissues; M: Negative expression of p-cyclin E1 (Thr77) in colon cancer tissues; N: High expression of p-cyclin E1(Thr395) in normal tissues; O: Medium expression of p-cyclin E1(Thr395) in colon cancer tissues; P: High expression of p-cyclin E1 (Thr395) in colon cancer tissues.

DISCUSSION

Our long-term studies have showed that AKAP95 and Cx43 are a pair of "molecular switches", regulating the progress of cell cycle by affecting the expression of cyclin Es[7-11,19]. AKAP95 and Cx43 could competitively bind to cyclin Ds and cyclin Es, regulating degradation of them: AKAP95 could bind to cyclin Ds and cyclin Es, preventing them from degradation, on the one hand, and inhibiting Cx43 promoting degradation of cyclin Ds and cyclin Es by binding to Cx43; Cx43, on the contrary to AKAP95, could accelerate the degradation of cyclin Ds and cyclin Es[10].

Ubiquitination is an important way of protein hydrolysis in cells. To discuss whether Cx43 affects the degradation of cyclin E1 and its expression level by regulating cyclin E1's ubiquitination, we further detected the expression of Cx43 and SCF^{FBXW7} and their correlation in clinical colon cancer tissues this time. Our data showed that there was a positive correlation between expression of Cx43 and SCF^{FBXW7}, which was in line with the relevant report of 'Cx43 promote the degradation of cyclin E1/2 and hinder the progress of cell cycle'[15-17].

Protein ubiquitination and degradation mediated by SCFs are related to the phosphorylation of substrate molecules [18]. For instance, phosphorylation of Thr286 site of cyclin D1 has been reported to be a necessary condition for cyclin

Table 1 Expressions of proteins in colon cancer tissues (*n* = 38)

	Cx43	SCF^{FBW7}	p-cyclin E1 (Ser73)	p-cyclin E1 (Thr77)	p-cyclin E1 (Thr395)
Positive	29	29	25	2	21
Negative	9	9	13	36	17
Positive rate (%)	76.32	76.32	65.79	5.26	55.26

Table 2 Correlation analysis between FBXW7 and p-cyclin E1 (Ser73) in colon cancer tissues

FBXW7	Ser73(-)	Ser73(+)	Ser73(++)	Ser73(+++)	*r*	*P* value
-	7	2	0	0	0.703	0.001
+	5	7	2	2		
++	1	1	4	2		
+++	0	0	2	3		

Table 3 Correlation analysis between FBXW7 and p-cyclin E1 (Thr77) in colon cancer tissues

FBXW7	Thr77(-)	Thr77(+)	Thr77(++)	Thr77(+++)	*r*	*P* value
-	9	0	0	0	0.079	0.638
+	15	0	0	0		
++	9	0	0	0		
+++	5	0	0	0		

Table 4 Correlation analysis between FBXW7 and p-cyclin E1 (Thr395) in colon cancer tissues

FBXW7	Thr395(-)	Thr395(+)	Thr395(++)	Thr395(+++)	*r*	*P* value
-	5	3	0	0	0.415	0.010
+	8	5	2	1		
++	4	2	3	0		
+++	0	1	2	2		

Table 5 Correlation analysis between Cx43 and FBXW7 in colon cancer tissues

Cx43	FBXW7(-)	FBXW7(+)	FBXW7(++)	FBXW7(+++)	*r*	*P* value
-	6	3	0	0	0.749	0.001
+	3	6	3	0		
++	0	6	4	1		
+++	0	0	2	5		

D1's ubiquitination and degradation[20]. However, there is still a lack of researches on the relationship between ubiquitination and phosphorylation of related site and of cyclin E1. We detected correlation between ubiquitination and three phosphorylation sites of cyclin E1 this time, and our data showed that phosphorylation of sites Ser73 and Thr395 of cyclin E1 was positively correlated with SCF^{FBXW7} and Cx43 respectively, and Cx43 and SCF^{FBXW7} were also positively correlated as well, suggesting that ubiquitination and degradation of cyclin E1 might be related to the phosphorylation of sites Ser73 and Thr395 of cyclin E1, and Cx43 might promote the ubiquitination and degradation of cyclin E1 by promoting the phosphorylation of these two sites.

Low positive rate of phosphorylation level of sites Thr77 of cyclin E1 was detected and no correlation between expression levels of Cx43 or SCF^{FBXW7} showed this time, suggesting that the phosphorylation of site Thr77 might not be related to ubiquitination and degradation of cyclin E1, and Cx43 did not affect its phosphorylation.

Table 6 Correlation analysis between Cx43 and p-cyclin E1 (Ser73) in colon cancer tissues

Cx43	Ser73(-)	Ser73(+)	Ser73(++)	Ser73(+++)	*r*	*P* value
-	8	1	0	0	0.667	0.001
+	2	7	2	1		
++	3	2	3	3		
+++	0	0	3	3		

Table 7 Correlation analysis between Cx43 and p-cyclin E1 (Thr77) in colon cancer tissues

Cx43	Thr77(-)	Thr77(+)	Thr77(++)	Thr77(+++)	*r*	*P* value
-	9	0	0	0	0.262	0.112
+	12	0	0	0		
++	11	0	0	0		
+++	6	0	0	0		

Table 8 Correlation analysis between Cx43 and p-cyclin E1(Thr395) in colon cancer tissues

Cx43	Thr395(-)	Thr395(+)	Thr395(++)	Thr395(+++)	*r*	*P* value
-	5	3	0	1	0.457	0.004
+	8	3	1	0		
++	4	4	3	0		
+++	0	1	3	2		

In general, our results of 38 clinical colon cancer samples preliminarily showed that ubiquitination and degradation of cyclin E1 were related to phosphorylation of site Ser73 and Thr395, but further experimental verification was still needed. In addition, Cx43 might affect degradation of cyclin E1 by affecting its phosphorylation and the expression of SCF^{FBXW7}.

CONCLUSION

It is postulated that Cx43 might facilitate the phosphorylation of cyclin E1 at the Ser73 and Thr395 sites *via* its interaction with SCF^{FBXW7}, thereby exerting an impact on the ubiquitination and degradation of cyclin E1.

FOOTNOTES

Author contributions: Zhang YX and Zhao L designed the research study; Luan RG, Liu MD and Deng ZF performed the research; Lu CL, Zhang MY, Liu R and Yu ML analyzed the data; Zhao L contributed of pathological tissues; Luan RG wrote the manuscript; An R, Yao YL and Guo DB gave administrative support. All authors have read and approved the final manuscript. Professor Zhang YX and Zhao L jointly designed the experiment. Professor Zhang YX provided most of the experimental platforms and techniques, while Zhao L provided pathological tissues and annotated corresponding general conditions and clinical stages. Subsequent to the initial drafting phase, Professor Zhang YX and Zhao L have contributed equally to the iterative revisions of the manuscript. Following a comprehensive deliberation involving all co-authors, it has been mutually agreed that Professor Zhang YX and Dr. Zhao L be designated as co-corresponding authors.

Supported by Innovative Practice Platform for Undergraduate Students, School of Public Health Xiamen University, No. 2021001.

Institutional review board statement: The experimental design and protocol of this study fully consider the principles of safety and fairness, and its research content will not cause harm or risk to the research subjects. The research subject belongs to the principle of voluntariness, the right to know is guaranteed, and the rights and privacy of the research subject will be maximally protected.

Conflict-of-interest statement: The authors have no conflicts of interest to declare.

Data sharing statement: All original slices are kept by our laboratory. Please contact z63y94x@xmu.edu.cn for relevant data.

Country of origin: China

ORCID number: Lei Zhao 0000-0001-8823-2487.

S-Editor: Qu XL
L-Editor: A
P-Editor: Xu ZH

REFERENCES

1 **Torp SH**, Solheim O, Skjulsvik AJ. The WHO 2021 Classification of Central Nervous System tumours: a practical update on what neurosurgeons need to know-a minireview. *Acta Neurochir (Wien)* 2022; **164**: 2453-2464 [PMID: 35879477 DOI: 10.1007/s00701-022-05301-y]
2 **Hammond WA**, Swaika A, Mody K. Pharmacologic resistance in colorectal cancer: a review. *Ther Adv Med Oncol* 2016; **8**: 57-84 [PMID: 26753006 DOI: 10.1177/1758834015614530]
3 **Lezcano V**, Bellido T, Plotkin LI, Boland R, Morelli S. Role of connexin 43 in the mechanism of action of alendronate: dissociation of anti-apoptotic and proliferative signaling pathways. *Arch Biochem Biophys* 2012; **518**: 95-102 [PMID: 22230328 DOI: 10.1016/j.abb.2011.12.022]
4 **Decrock E**, De Vuyst E, Vinken M, Van Moorhem M, Vranckx K, Wang N, Van Laeken L, De Bock M, D'Herde K, Lai CP, Rogiers V, Evans WH, Naus CC, Leybaert L. Connexin 43 hemichannels contribute to the propagation of apoptotic cell death in a rat C6 glioma cell model. *Cell Death Differ* 2009; **16**: 151-163 [PMID: 18820645 DOI: 10.1038/cdd.2008.138]
5 **Bruzzone R**. Learning the language of cell-cell communication through connexin channels. *Genome Biol* 2001; **2**: REPORTS4027 [PMID: 11737941 DOI: 10.1186/gb-2001-2-11-reports4027]
6 **Johnstone SR**, Best AK, Wright CS, Isakson BE, Errington RJ, Martin PE. Enhanced connexin 43 expression delays intra-mitotic duration and cell cycle traverse independently of gap junction channel function. *J Cell Biochem* 2010; **110**: 772-782 [PMID: 20512937 DOI: 10.1002/jcb.22590]
7 **Liu W**, Hua S, Dai Y, Yuan Y, Yang J, Deng J, Huo Y, Chen X, Teng B, Yu X, Zhang Y. Roles of Cx43 and AKAP95 in ovarian cancer tissues in G1/S phase. *Int J Clin Exp Pathol* 2015; **8**: 14315-14324 [PMID: 26823747]
8 **Wang S**, Wang K, Deng Z, Jiang Z, Wang D, Yao Y, Guo D, Kong X, Guan Z, Zhang Y. Correlation between the protein expression levels of A-kinase anchor protein95, p-retinoblastoma (Ser780), cyclin D2/3, and cyclin E2 in esophageal cancer tissues. *Asia Pac J Clin Oncol* 2019; **15**: e162-e166 [PMID: 30990963 DOI: 10.1111/ajco.13146]
9 **Guan Z**, Zhuang W, Lei H, Wang D, Yao Y, Guo D, Sun Q, Chen Y, Chen X, Lin H, Teng B, Zhang Y. Epac1, PDE4, and PKC protein expression and their correlation with AKAP95 and Cx43 in esophagus cancer tissues. *Thorac Cancer* 2017; **8**: 572-576 [PMID: 28771997 DOI: 10.1111/1759-7714.12479]
10 **Chen R**, Chen Y, Yuan Y, Zou X, Sun Q, Lin H, Chen X, Liu M, Deng Z, Yao Y, Guo D, Zhang Y. Cx43 and AKAP95 regulate G1/S conversion by competitively binding to cyclin E1/E2 in lung cancer cells. *Thorac Cancer* 2020; **11**: 1594-1602 [PMID: 32338437 DOI: 10.1111/1759-7714.13435]
11 **Chen X**, Kong X, Zhuang W, Teng B, Yu X, Hua S, Wang S, Liang F, Ma D, Zhang S, Zou X, Dai Y, Yang W, Zhang Y. Dynamic changes in protein interaction between AKAP95 and Cx43 during cell cycle progression of A549 cells. *Sci Rep* 2016; **6**: 21224 [PMID: 26880274 DOI: 10.1038/srep21224]
12 **Hochstrasser M**. Biochemistry. All in the ubiquitin family. *Science* 2000; **289**: 563-564 [PMID: 10939967 DOI: 10.1126/science.289.5479.563]
13 **Cardozo T**, Pagano M. The SCF ubiquitin ligase: insights into a molecular machine. *Nat Rev Mol Cell Biol* 2004; **5**: 739-751 [PMID: 15340381 DOI: 10.1038/nrm1471]
14 **Li Y**, Jin K, Bunker E, Zhang X, Luo X, Liu X, Hao B. Structural basis of the phosphorylation-independent recognition of cyclin D1 by the SCF(FBXO31) ubiquitin ligase. *Proc Natl Acad Sci U S A* 2018; **115**: 319-324 [PMID: 29279382 DOI: 10.1073/pnas.1708677115]
15 **Reiterer V**, Figueras-Puig C, Le Guerroue F, Confalonieri S, Vecchi M, Jalapothu D, Kanse SM, Deshaies RJ, Di Fiore PP, Behrends C, Farhan H. The pseudophosphatase STYX targets the F-box of FBXW7 and inhibits SCFFBXW7 function. *EMBO J* 2017; **36**: 260-273 [PMID: 28007894 DOI: 10.15252/embj.201694795]
16 **Shiba-Ishii A**, Hong J, Hirokawa T, Kim Y, Nakagawa T, Sakashita S, Sakamoto N, Kozuma Y, Sato Y, Noguchi M. Stratifin Inhibits SCF(FBW7) Formation and Blocks Ubiquitination of Oncoproteins during the Course of Lung Adenocarcinogenesis. *Clin Cancer Res* 2019; **25**: 2809-2820 [PMID: 30728155 DOI: 10.1158/1078-0432.CCR-18-3631]
17 **Sailo BL**, Banik K, Girisa S, Bordoloi D, Fan L, Halim CE, Wang H, Kumar AP, Zheng D, Mao X, Sethi G, Kunnumakkara AB. FBXW7 in Cancer: What Has Been Unraveled Thus Far? *Cancers (Basel)* 2019; **11** [PMID: 30791487 DOI: 10.3390/cancers11020246]
18 **Cenciarelli C**, Chiaur DS, Guardavaccaro D, Parks W, Vidal M, Pagano M. Identification of a family of human F-box proteins. *Curr Biol* 1999; **9**: 1177-1179 [PMID: 10531035 DOI: 10.1016/S0960-9822(00)80020-2]
19 **Kong XY**, Zhang DC, Zhuang WX, Hua SH, Dai Y, Yuan YY, Feng LL, Huang Q, Teng BG, Yu XY, Liu WZ, Zhang YX. AKAP95 promotes cell cycle progression *via* interactions with cyclin E and low molecular weight cyclin E. *Am J Transl Res* 2016; **8**: 811-826 [PMID: 27158371]
20 **Jia L**, Sun Y. F-box proteins FBXO31 and FBX4 in regulation of cyclin D1 degradation upon DNA damage. *Pigment Cell Melanoma Res* 2009; **22**: 518-519 [PMID: 19645770 DOI: 10.1111/j.1755-148X.2009.00611.x]

World Journal of Gastrointestinal Oncology

Submit a Manuscript: https://www.f6publishing.com

World J Gastrointest Oncol 2025 January 15; 17(1): 99376

DOI: 10.4251/wjgo.v17.i1.99376

ISSN 1948-5204 (online)

ORIGINAL ARTICLE

Basic Study

BIBR1532 inhibits proliferation and metastasis of esophageal squamous cancer cells by inducing telomere dysregulation

Qin Wang, Qing-Rong Li, Lei Xu, Zi-Chun Yuan, Xiao Liu, Mao-Ju Tang, Man Luo, Xiao-Wu Zhong, Qiang Ma, Xiao-Lan Guo

Specialty type: Oncology

Provenance and peer review: Unsolicited article; Externally peer reviewed.

Peer-review model: Single blind

Peer-review report's classification

Scientific Quality: Grade A

Novelty: Grade A

Creativity or Innovation: Grade A

Scientific Significance: Grade A

P-Reviewer: Nirenberg A

Received: July 21, 2024

Revised: October 5, 2024

Accepted: November 1, 2024

Published online: January 15, 2025

Processing time: 144 Days and 0 Hours

Qin Wang, Qing-Rong Li, Zi-Chun Yuan, Man Luo, Xiao-Wu Zhong, Qiang Ma, Xiao-Lan Guo, Department of Clinical Laboratory, Affiliated Hospital of North Sichuan Medical College, Nanchong 637000, Sichuan Province, China

Qin Wang, Qing-Rong Li, Lei Xu, Zi-Chun Yuan, Xiao Liu, Mao-Ju Tang, Man Luo, Xiao-Wu Zhong, Qiang Ma, Xiao-Lan Guo, School of Laboratory Medicine & Translational Medicine Research Center, North Sichuan Medical College, Nanchong 637000, Sichuan Province, China

Co-first authors: Qin Wang and Qing-Rong Li.

Co-corresponding authors: Qiang Ma and Xiao-Lan Guo.

Corresponding author: Xiao-Lan Guo, MD, PhD, Professor, Department of Clinical Laboratory, Affiliated Hospital of North Sichuan Medical College, No. 1 South Maoyuan Road, Shunqing District, Nanchong 637000, Sichuan Province, China. alan5200@hotmail.com

Abstract

BACKGROUND

Esophageal squamous cell carcinoma (ESCC) is a malignant tumor with high morbidity and mortality, and easy to develop resistance to chemotherapeutic agents. Telomeres are DNA-protein complexes located at the termini of chromosomes in eukaryotic cells, which are unreplaceable in maintaining the stability and integrity of genome. Telomerase, an RNA-dependent DNA polymerase, play vital role in telomere length maintain, targeting telomerase is a promising therapeutic strategy for cancer.

AIM

To investigate the efficacy and underlying mechanisms of BIBR1532, a telomerase inhibitor, in ESCC.

METHODS

KYSE150 and KYSE410 cells were cultured and exposed to various concentrations of BIBR1532. Cell viability was assessed at 48 hours and 72 hours to determine the IC_{50} values. The effects of BIBR1532 on ESCC cell proliferation, migration, and cellular senescence were evaluated using the cell counting kit-8 assay, plate colony formation assay, scratch assay, transwell assay, and β-galactosidase staining, respectively. Western blotting was performed to detect the expression of

proteins in BIBR1532-treated ESCC cells, such as human telomerase reverse transcriptase (hTERT), key molecules involved in DNA damage response (DDR) or cellular senescence, as well as telomere-binding proteins. Additionally, a tumor-bearing nude mouse model was established to evaluate the anti-cancer effect of BIBR1532 *in vivo*.

RESULTS

The IC_{50} values for KYSE150 and KYSE410 cells after 48 hours of BIBR1532 exposure were 48.53 μM and 39.59 μM, respectively. These values decreased to 37.22 μM and 22.71 μM, respectively, following a longer exposure of 72 hours. BIBR1532 exhibited dose-dependent effects on KYSE150 and KYSE410 cells, including decreased hTERT expression, inhibition of proliferation and metastasis, and induction of cellular senescence. Mechanistically, BIBR1532 upregulated the expression of the DDR protein, γ-H2AX, and activated the ataxia telangiectasia and Rad3-related protein (ATR)/ check point kinase 1 (CHK-1) and ataxia-telangiectasia mutated gene (ATM)/CHK2 pathways. BIBR1532 downregulated the expression of telomere-binding proteins, including telomeric-repeat binding factor 1 (TRF1), TRF2, protection of telomeres 1, and TIN2-interacting protein 1. In a nude mouse xenograft model, BIBR1532 significantly suppressed tumor growth, reduced hTERT expression, and increased γ-H2AX protein levels. Hematoxylin and eosin staining of various organs, including the heart, liver, spleen, lungs, and kidneys, revealed no apparent adverse effects.

CONCLUSION

BIBR1532 exerts anti-cancer effects on ESCC by inducing DDR through the ATR/CHK1 and ATM/CHK2 pathways and downregulating the expression of telomere-binding proteins.

Key Words: Esophageal squamous cell carcinoma; BIBR1532; Human telomerase reverse transcriptase; DNA damage response; Telomere-binding proteins

Core Tip: BIBR1532 inhibited proliferation and metastasis of esophageal squamous cell carcinoma (ESCC) cells in a dose-dependent manner, which also effectively blocked the growth of ESCC in tumor-bearing nude mouse model. Mechanistically, BIBR1532 downregulated the expression of telomere-binding proteins, upregulated the expression of phosphorylated histone H2AX, ataxia telangiectasia and Rad3-related protein/check point kinase 1 (CHK-1) and ataxia-telangiectasia mutated gene/CHK2 pathways. The *in vitro* and *in vivo* studies showed that BIBR1532 is a potential chemotherapeutic drug for ESCC.

Citation: Wang Q, Li QR, Xu L, Yuan ZC, Liu X, Tang MJ, Luo M, Zhong XW, Ma Q, Guo XL. BIBR1532 inhibits proliferation and metastasis of esophageal squamous cancer cells by inducing telomere dysregulation. *World J Gastrointest Oncol* 2025; 17(1): 99376
URL: https://www.wjgnet.com/1948-5204/full/v17/i1/99376.htm
DOI: https://dx.doi.org/10.4251/wjgo.v17.i1.99376

INTRODUCTION

Esophageal cancer (EC) is one of the most frequently occurring malignant tumors worldwide, ranking seventh in terms of incidence and sixth in terms of mortality[1]. Approximately 600000 new cases of EC are reported globally each year, and over half of these occur in China. Esophageal squamous cell carcinoma (ESCC) is the predominant histological variety, constituting more than 90% of cases[1-3]. The incidence of ESCC has been correlated with various dietary and lifestyle factors, including the consumption of very hot food and drinks, alcohol intake, and cigarette smoking. Additional risk factors include the consumption of mold-contaminated food, food preparation methods involving charring or smoking, drinking water quality, soil composition, and environmental microbial communities[4]. According to the EC Diagnosis and Treatment Guidelines (version 2022), ESCC treatment modalities include surgery, radiotherapy, chemotherapy, targeted therapy, immunotherapy, and combination therapies[4]. However, the initial stages of EC are often asymptomatic and a significant number of patients present with advanced local disease or distant metastases upon diagnosis. This precludes surgical intervention and necessitates systemic drug therapy to manage the disease[4]. ESCC has been documented to develop resistance to radiotherapy and chemotherapy due to heterogeneity in histology, molecular characteristics, and etiology[5]. Immunotherapy and targeted therapy, although promising, may present with severe side effects or offer uncertain efficacy[6,7]. The current standard first-line chemotherapy regimen typically comprises paclitaxel combined with cisplatin, or cisplatin in combination with fluorouracil or capecitabine. However, side effects of these treatments are often undesirable. Despite advances in ESCC treatment, the prognosis remains poor, with an overall five-year survival rate of < 30%[8]. This highlights the urgent need to identify novel and safe anti-EC agents.

Telomeres are DNA-protein complexes located at the termini of chromosomes in eukaryotic cells. They consist of short repetitive sequences of telomeric DNA (5′-TTAGGG-3′) and associated proteins [telomeric-repeat binding factor 1 (TRF1), TRF2, TIN2-interacting protein 1 (TPP1), protection of telomeres 1 (POT1), TRF1-interacting nuclear protein 2 (TIN2), and repressor activation protein 1 (RAP1)]. The primary role of telomeres is to shield chromosome ends from degradation or aberrant recombination[9,10]. Telomere length homeostasis depends on cellular division and telomerase activity. Telomerase is an RNA-dependent DNA polymerase comprising RNA molecules with telomeric template sequences and a protein catalytic subunit telomerase reverse transcriptase (TERT)[11]. Several studies have identified human TERT (hTERT) as a key regulator of telomerase activity[12]. Although telomerase remains transcriptionally inactive in most somatic cells, it is reactivated in over 85% of human cancers, primarily through upregulation of the typically silent hTERT gene[13]. Our previous study demonstrated that the expression of hTERT mRNA in ESCC tissues is significantly upregulated and that hTERT overexpression substantially enhances the proliferation and metastatic potential of cancer cells[14]. These findings suggest that hTERT contributes to ESCC progression and is a potential therapeutic target in afflicted patients.

For nearly two decades, targeting telomerase has been the focus of cancer research. Therapeutic strategies include immunotherapy, small-molecule telomerase inhibitors, oligonucleotide inhibitors, and plant compounds[15]. Among these, the small molecule inhibitor BIBR1532 is a non-nucleoside, non-competitive antagonist that selectively inhibits hTERT[16]. Lavanya *et al*[17] demonstrated that BIBR1532 dose-dependently curtails telomerase activity in human glioblastoma LN18 cells, inducing apoptosis through downregulation of telomerase at both the transcriptional and translational levels. Ding *et al*[18] revealed that lower concentrations of BIBR1532 effectively suppress telomerase activity and exacerbate radiation-induced telomeric dysfunction, compromising chromosome stability and inhibiting the ataxia-telangiectasia mutated gene (ATM)/check point kinase 1 (CHK-1) pathway, thereby impeding DNA damage response (DDR). Another study indicated that telomerase inhibition could regulate epithelial-mesenchymal transition (EMT) in breast cancer, suggesting that telomerase inhibitors primarily eradicate breast cancer stem cells, constrain cellular migration and invasiveness, and ultimately prevent breast cancer cell metastasis[19]. Collectively, these studies imply that BIBR1532 may function as a broad-spectrum anti-cancer agent. However, the effects of BIBR1532 on ESCC have yet to be reported. This study aimed to decipher the biological impact and molecular mechanisms of the telomerase inhibitor BIBR1532 in ESCC cells and provide data for its future clinical use as a potential therapeutic agent for ESCC.

MATERIALS AND METHODS

Reagents and antibodies

RPMI 1640 medium was obtained from Gibco (Grand Island, NY, United States). Fetal bovine serum (FBS) was purchased from OPCEL (Inner Mongolia, China). Penicillin and Streptomycin were procured from SolarBio (Beijing, China). BIBR1532 was obtained from Pottery (Shanghai, China). Cell counting kit-8 (CCK-8) and β-galactosidase (β-gal) detection kits were obtained from Beyotime Biotechnology (Shanghai, China). The cell cycle detection kit was provided by KeyGen Biotech (Nanjing, Jiangsu Province, China). Immunohistochemistry (IHC) kit was purchased from BOSTER (Wuhan, Hubei Province, China). Antibodies against GAPDH, CHK1, CHK2, phosphorylated histone H2AX (γ-H2AX), phosphorylated ataxia telangiectasia and Rad3-related protein (p-ATR), phosphorylated ATM, hTERT, and goat anti-rabbit IgG were purchased from Cell Signaling Technology (Beverly, CA, United States). Goat anti-rabbit IgG antibody was purchased from BOSTER (Wuhan, Hubei Province, China).

Cell culture

The human ESCC cell lines KYSE150 and KYSE410 were obtained from the Translational Medicine Research Center of the North Sichuan Medical College. All the cells were cultured in DMEM supplemented with 10% FBS at 37 °C in a humidified atmosphere containing 5% CO_2.

CCK-8 assay

CCK-8 assay was performed to assess the viability of KYSE150 and KYSE410 cells. Briefly, the cells were seeded in 96-well plates at a density of 3×10^3 cells/well and incubated at 37 °C in 5% CO_2. After 24 hours, cells were treated with DMSO (vehicle control) or a series of BIBR1532 concentrations (25 μM, 50 μM, 75 μM, and 100 μM) for 48 hours or 72 hours. At the indicated time points, 10 μL of the CCK-8 reagent was added to each well. The plates were incubated for 2 hours in the dark, and the absorbance (A) was measured at 450 nm using a microplate reader.

Plate colony formation assay

KYSE150 and KYSE410 cells were seeded in six-well plates at a density of 2×10^3 cells/well. After 24 hours of incubation, cells were treated with either DMSO or different concentrations of BIBR1532 (25 μM, 50 μM, and 75 μM). Cells were cultured for 1-2 weeks until visible clones emerged in control wells. Subsequently, cells were fixed with methanol for 10 minutes and stained with crystal violet for 10 minutes. Finally, plates were washed, air-dried, and imaged.

Wound healing assay

KYSE150 and KYSE410 cells were seeded in six-well plates at a density of 5×10^5 cells/well. When the cell monolayer reached approximately 90% confluence, two parallel scratches were created across the cell layer by using a sterile pipette tip. The plates were washed three times with PBS and fresh culture medium was added. Initial images (0 hour) were

captured, and the cells were treated with either DMSO or a series of BIBR1532 concentrations (25 μM, 50 μM, and 75 μM). After 24 hours, images of the same locations were obtained using an optical microscope to assess the wound closure.

Transwell assay

KYSE150 and KYSE410 cells were cultured, trypsinized (0.25% w/v), and resuspended in serum-free RPMI 1640. The cell density was adjusted to 5 × 10^5 cells/mL. Subsequently, 500 μL of RPMI 1640 medium containing 10% FBS was added to the lower chamber of a 12-well plate, and 200 μL of the cell suspension was added to the upper chamber of the Transwell insert. The cells were then treated with DMSO or different concentrations of BIBR1532 (25 μM, 50 μM, and 75 μM). After 24 hours, the non-migrated cells on the upper surface of the membrane were removed, and the migrated cells on the lower surface were fixed with methanol for 10 minutes and stained with crystal violet for 20 minutes. Images were captured using an optical microscope.

Cell senescence assay

KYSE150 and KYSE410 cells were seeded into six-well plates at a density of 1 × 10^5 cells/well and treated with either DMSO or different concentrations of BIBR1532 (25 μM, 50 μM, and 75 μM). After treatment, cells were washed twice with PBS and fixed at room temperature for 15 minutes. Subsequently, the cells were washed three times with PBS and incubated overnight at 37 °C in β-gal staining solution. The plates were sealed with plastic wrap to prevent evaporation, and the senescent cells were observed under an optical microscope.

Tumor-bearing nude mice model construction and treatment

Male 6-week-old BALB/c nude mice (approximately 20 g) were purchased from Beijing Laboratory Animal Research Center (Beijing, China). Animal care and experiments were performed with the approval of the Animal Ethics Committee of North Sichuan Medical College. KYSE150 cells in the logarithmic phase of growth were harvested and adjusted to a density of 1 × 10^7 cells/mL. Subsequently, 100 μL of the cell suspension was subcutaneously implanted into the upper right flank of each mouse. When the tumor volume reached approximately 100 mm^3, mice were randomly divided into two groups (n = 4 per group). The treatment group received intraperitoneal injections of BIBR1532 (50 mg/kg), whereas the control group received an equal volume of DMSO. Injections were administered every two days. Tumor dimensions were measured using a Vernier caliper every two days, and tumor volumes were calculated using the following formula: Volume (mm^3) = length × $width^2$/2. On day 20, all mice were euthanized and tumor tissues were collected and fixed in 4% paraformaldehyde solution for 24 hours. Fixed tissues were embedded in paraffin for further analysis.

Immunohistochemical staining

Paraffin-embedded xenograft tissues were sectioned and subjected to immunohistochemical staining. Briefly, sections were deparaffinized, rehydrated, and subjected to antigen retrieval using sodium citrate buffer. The sections were incubated with primary antibodies against hTERT, Ki-67, and γ-H2AX at 4 °C overnight. Subsequently, the sections were stained using an immunostaining kit (BOSTER, Wuhan, Hubei Province, China), according to the manufacturer's instructions.

Hematoxylin and eosin staining of the tissue specimens

Paraffin-embedded tissue sections were deparaffinized and rehydrated. The nuclei were stained with hematoxylin, and the cytoplasm was counterstained with eosin. Finally, the sections were dehydrated, cleared, mounted, and observed under a microscope.

Western blotting

Tissue samples were homogenized, and total proteins were extracted using RIPA buffer. Proteins were separated using SDS-PAGE and electrophoretically transferred to polyvinylidene difluoride (PVDF) membranes. The PVDF membranes were washed and blocked with 5% skimmed milk for 1 hour at room temperature. Subsequently, the membranes were incubated with the primary antibodies overnight at 4 °C. After washing, membranes were incubated with secondary antibodies for 1 hour at room temperature. Finally, the protein bands were detected using an enhanced chemiluminescence system (VILBER FUSION FX7, France).

Statistical analysis

The experimental data were analyzed using the GraphPad Prism 8 software. Data are presented as mean ± SD of three independent experiments. Comparisons between two groups were performed using the Student's t-test, and comparisons between multiple groups were performed using analysis of variance (ANOVA). Differences were considered statistically significant at $P < 0.05$.

RESULTS

IC50 of BIBR1532 in ESCC Cells

To assess the potential toxicity of BIBR1532 in ESCC cells, KYSE150 and KYSE410 cells were treated with various concentrations of BIBR1532 (25 μM, 50 μM, 75 μM, and 100 μM) for 48 hours or 72 hours. Cell viability was evaluated, and the half-maximal inhibitory concentration (IC50) values were calculated. Our results indicated a significant dose-dependent

decrease in the viability of both KYSE150 and KYSE410 cells post-treatment at both time points, the IC50 of BIBR1532 was 48.53 μM and 39.59 μM in KYSE150 and KYSE410 cells treated for 48 hours, and 37.22 μM and 22.71 μM in abovementioned two cell lines treated for 72 hours (Figure 1). Based on these findings, BIBR1532 concentrations of 25 μM, 50 μM, and 75 μM and a 48-hour treatment duration were selected for subsequent experiments.

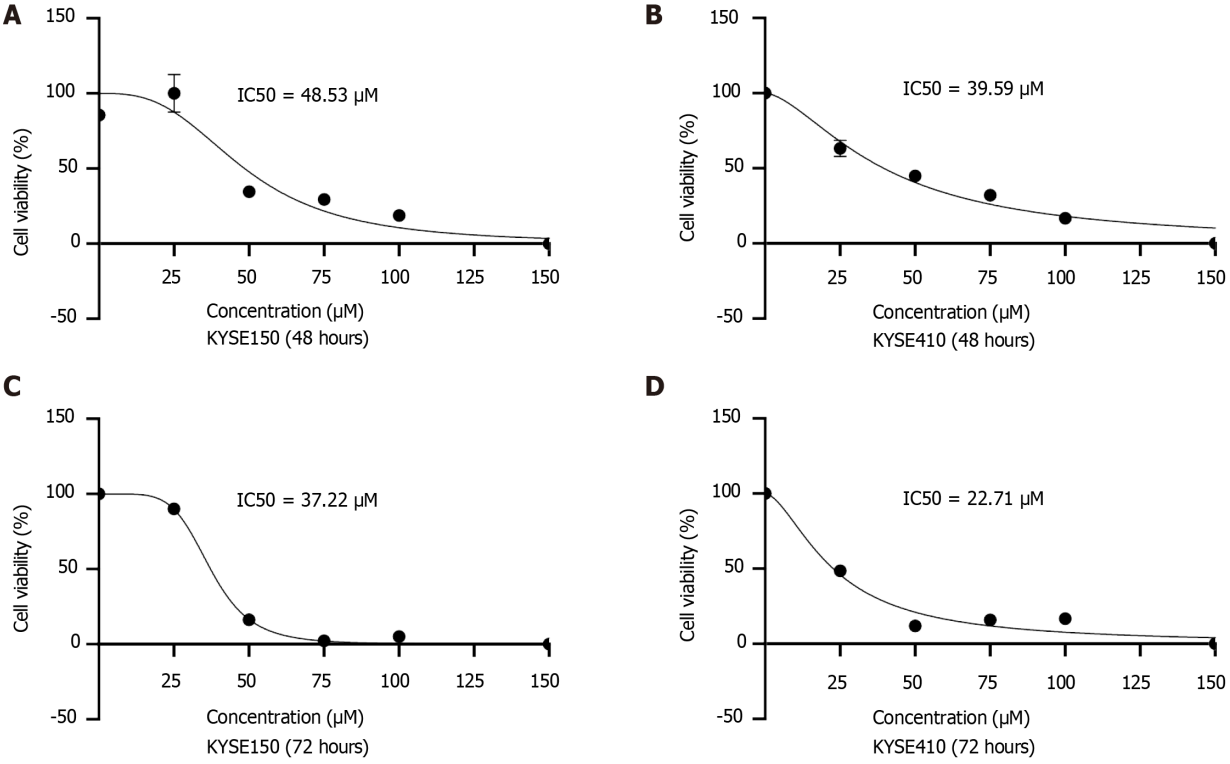

Figure 1 IC_{50} determination of BIBR1532 in esophageal squamous cell carcinoma cells. A and B: Viability of KYSE150 (A) and KYSE410 (B) cells after treatment with the indicated concentrations of BIBR1532 for 48 hours; C and D: Viability of KYSE150 (C) and KYSE410 (D) cells after treatment with the indicated concentrations of BIBR1532 for 72 hours.

BIBR1532 inhibits ESCC proliferation

Since BIBR1532 is a telomerase inhibitor, we first evaluated whether it regulates the expression of hTERT, a core catalytic subunit of telomerase. The results showed that BIBR1532 significantly downregulated the expression of hTERT in KYSE150 and KYSE410 cells in a dose-dependent manner (Figure 2A). Subsequently, we evaluated the effect of BIBR1532 on the proliferation of KYSE150 and KYSE410 cells. As shown in Figure 2B, BIBR1532 significantly inhibited the viability of both the cell lines. The inhibitory effect on cell viability increased gradually with higher concentrations of BIBR1532 and longer incubation times, in a time- and dose-dependent manner. Plate colony formation assays further confirmed the ability of BIBR1532 to inhibit proliferation of KYSE150 and KYSE410 cells (Figure 2C).

BIBR1532 inhibits the migration ability of ESCC

To explore whether BIBR1532 regulates the migration capacity of EC cells, scratch and transwell assays were used to evaluate the migration of KYSE150 and KYSE410 cells after exposure to BIBR1532. The results showed that the migration distance of KYSE150 and KYSE410 cells in the BIBR1532-treated group was significantly shorter than that in the DMSO control group, in a dose-dependent manner (Figure 3A). Similarly, transwell assays revealed that the number of migrated cells in the BIBR1532-treated group was significantly lower than that in the DMSO group (Figure 3B). These results suggested that BIBR1532 significantly inhibits the migration of EC cells.

BIBR1532 induces senescence in ESCC

Because BIBR1532 is a telomerase inhibitor, we investigated whether it induced cellular senescence. β-gal staining assay was employed to detect the effect of BIBR1532 on the senescence of KYSE150 and KYSE410 cells. The number of senescent cells in the BIBR1532-treated group was significantly higher than that in the DMSO control group (Figure 4A). In addition, the senescent marker P53 was evidently upregulated after BIBR1532 exposure (Figure 4B). These results showed that BIBR1532 induces senescence in ESCC.

BIBR1532 inhibits the proliferation and migration of ESCC through downregulation of hTERT

To determine whether BIBR1532 exerted its anti-cancer effect on ESCC cells by downregulating hTERT expression, we treated the cells with BIBR1532 (50 μM) combined with hTERT overexpression. The results showed that BIBR1532

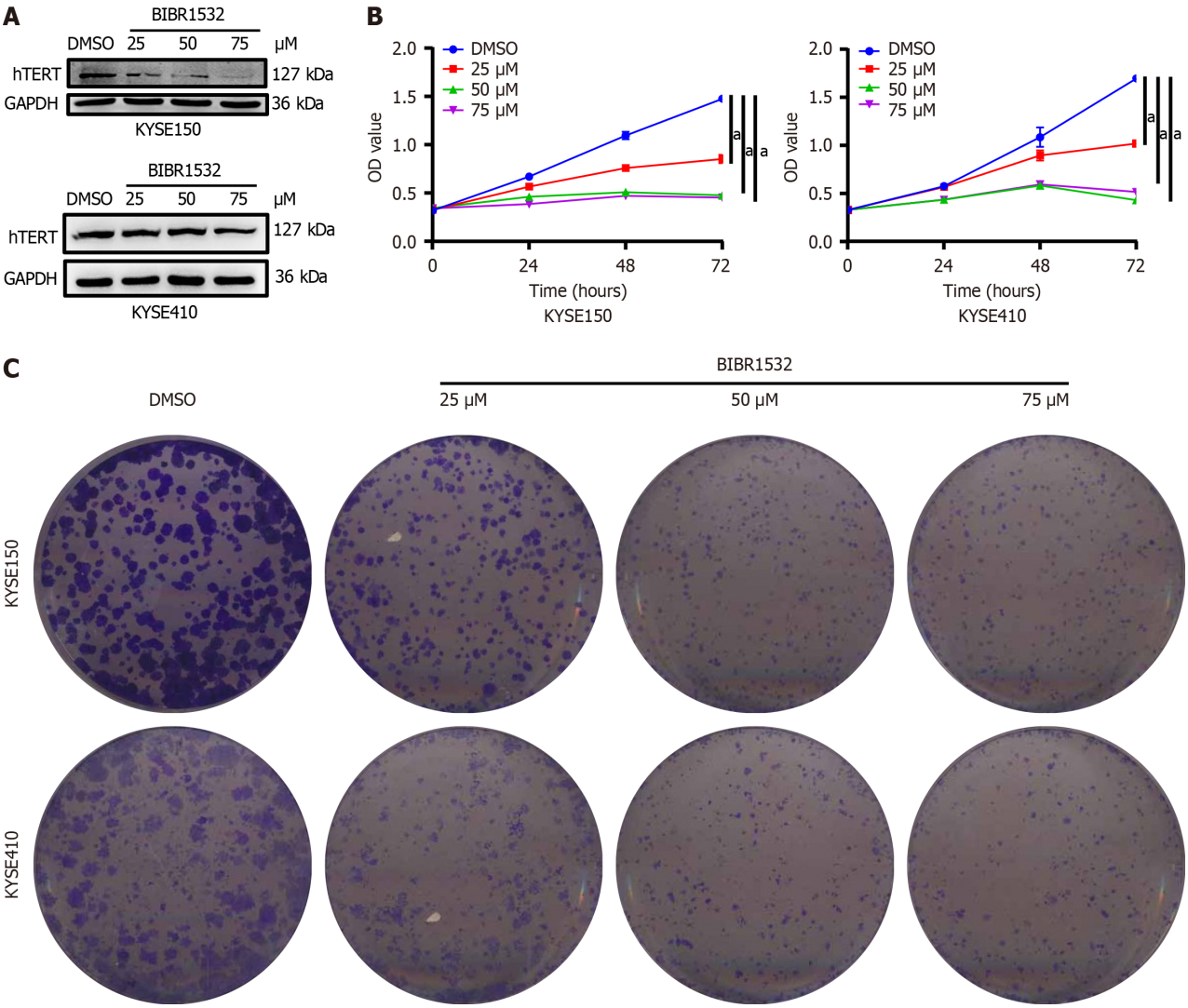

Figure 2 Effect of BIBR1532 on the proliferation of KYSE150 and KYSE410 cells. A: Human telomerase reverse transcriptase expression in KYSE150 and KYSE410 cells after exposure to a series of BIBR1532 concentrations; B: Viability of KYSE150 and KYSE410 cells after treatment with various concentrations of BIBR1532 at the indicated time points; C: Plate colony formation by KYSE150 and KYSE410 cells after treatment with various concentrations of BIBR1532 at the indicated time points. $^{a}P < 0.05$ was compared with the control group respectively. $P < 0.05$ was considered statistically significant. hTERT: Human telomerase reverse transcriptase.

inhibited the proliferation and migration of KYSE150 cells. Moreover, hTERT overexpression in KYSE150 cells promoted ESCC cell proliferation and migration. Importantly, hTERT overexpression alleviated the tumor-suppressive effects of BIBR1532 in KYSE150 cells (Figure 5). These results indicated that BIBR1532 exerts anti-cancer effects on ESCC by downregulating hTERT expression.

BIBR1532 downregulates the expression of telomere protective proteins in EC cells

Studies have demonstrated that BIBR1532 is cytotoxic and can cause direct damage to telomere structure, leading to the loss of TRF2 binding, thereby inducing telomere dysfunction[20]. To investigate whether BIBR1532 regulated the expression of other telomere protection proteins, the expression of shelterin proteins (TRF1, TRF2, TPP1, POT1, TIN2, and RAP1) was evaluated in KYSE150 and KYSE410 cells treated with BIBR1532. The results showed that BIBR1532 significantly downregulated the expression of TRF1, TRF2, TPP1, and POT1 in both cell lines, but had no significant effect on the expression of TIN2 and RAP1 (Figure 6A and B). These results indicated that BIBR1532 may lead to the dysregulation of telomere structure and function.

BIBR1532 regulates the DDR of EC cells through the ATM/ATR signaling pathway

The main function of telomere protection proteins is to protect DNA ends from being recognized as double-strand breaks that trigger DDR[15]. Excessive lengthening or shortening of telomeres results in an imbalance in genome homeostasis, ultimately inducing DDR. Given that BIBR1532 inhibits the expression of hTERT and the telomere protection proteins TRF1, TRF2, TPP1, and POT1, we hypothesized that BIBR1532 can induce DDR in ESCC cells. As shown in Figure 6C and D, the expression of γ-H2AX in KYSE150 and KYSE410 cells was significantly upregulated after treatment with the indicated concentrations of BIBR1532. ATM- and ATR-mediated protein expression levels of CHK2 and CHK1, which are

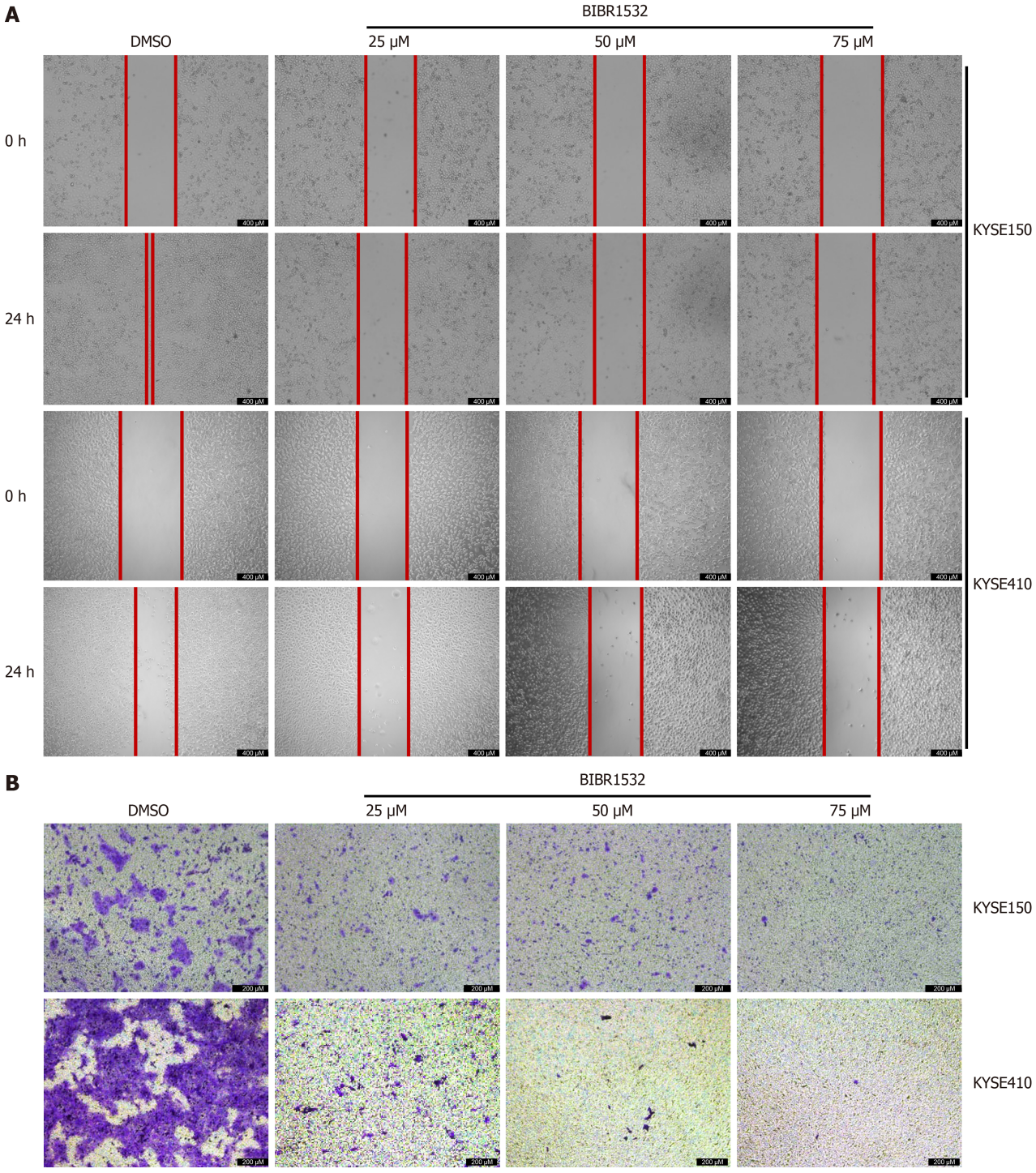

Figure 3 Effect of BIBR1532 on the migration of KYSE150 and KYSE410 cells. A: Migration of KYSE150 and KYSE410 cells after treatment with various concentrations of BIBR1532 for 24 hours, as evaluated by scratch assay; B: Migration of KYSE150 and KYSE410 cells after treatment with various concentrations of BIBR1532 for 24 hours, as evaluated by the transwell assay.

important downstream regulators of the DNA damage repair pathway, were also upregulated. These results suggested that BIBR1532 may induce DDR in ESCC cells through the ATM-CHK2 and ATR-CHK1 pathways.

BIBR1532 inhibits tumor growth in ESCC xenograft mouse model

To further investigate the anti-cancer effect of BIBR1532 *in vivo*, nude mouse xenograft models were constructed by subscapular injection of KYSE150 cells. The results showed that tumor growth was inhibited in xenograft mice after treatment with BIBR1532 (Figure 7A and B). Moreover, the tumor weight was significantly lower in BIBR1532-treated mice than in DMSO-treated controls (Figure 7C). Furthermore, IHC results showed that the expression of hTERT and Ki-67 was reduced, whereas that of γ-H2AX was increased in tumor tissues treated with BIBR1532 (Figure 7D). Consistent with the IHC results, western blot analysis confirmed that the expression of hTERT was significantly downregulated, whereas that of γ-H2AX was upregulated in tumors treated with BIBR1532 (Figure 7E). Importantly, macroscopic images

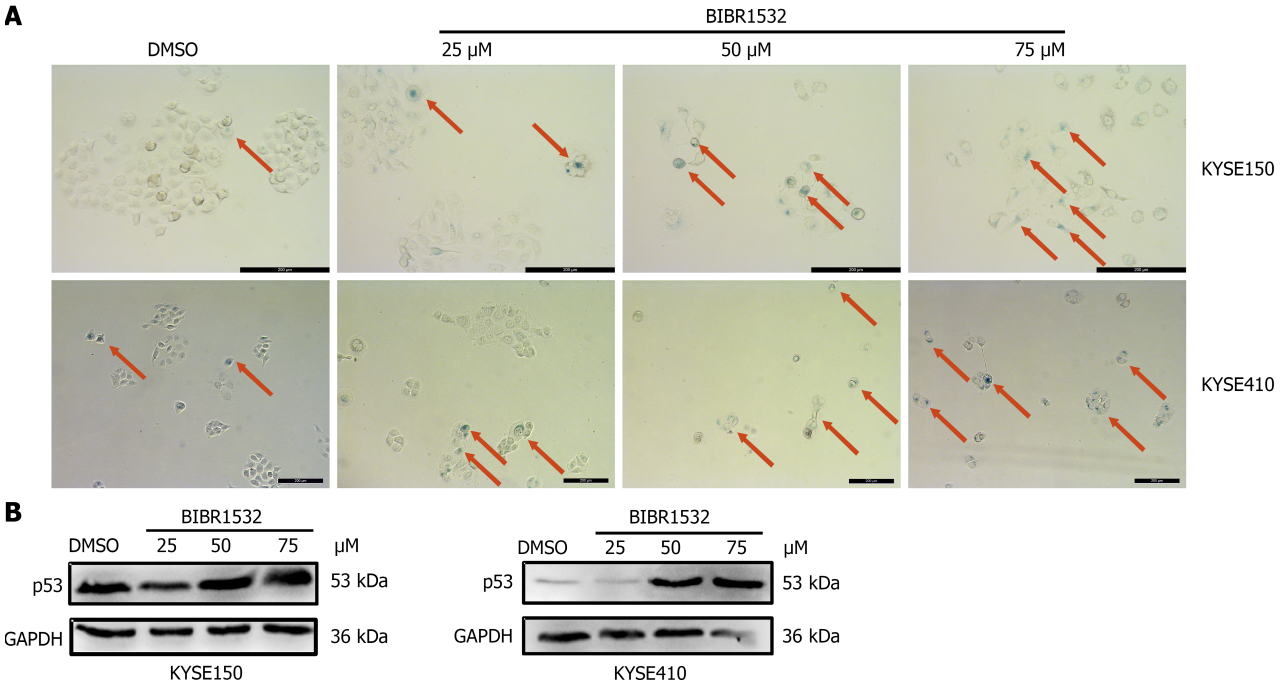

Figure 4 Effect of BIBR1532 on the senescence of KYSE150 and KYSE410 cells. A: Senescence of KYSE150 and KYSE410 cells after treatment with various concentrations of BIBR1532 for 48 hours; B: Expression of the cell senescence biomarker p53 in KYSE150 and KYSE410 cells after treatment with various BIBR1532 concentrations for 48 hours.

and hematoxylin and eosin (H&E) staining of the heart, liver, spleen, lungs, and kidneys of mice showed no obvious differences between the BIBR1532-treated group and the DMSO group (Figure 7F and G). Taken together, these data demonstrated that BIBR1532 inhibits ESCC growth *in vivo* without apparent toxicity.

DISCUSSION

Telomerase, an enzyme comprising catalytic proteins and RNA templates, is responsible for telomere elongation in cells. Normally, telomerase expression is suppressed in somatic cells, resulting in telomere shortening after cell division[21]. During the malignant transformation of cells, telomerase is reactivated, promoting uncontrolled cell growth. Studies have shown that telomerase maintains tumor cell proliferation capacity and promotes tumor development by regulating telomere length[22]. Previous research has demonstrated that hTERT is highly expressed in various tumors, including ESCC[23-25]. Our previous studies also confirmed that hTERT overexpression promotes the proliferation and metastasis of EC cells[14]. Therefore, targeting hTERT holds great potential for EC treatment.

Various telomerase inhibitors have been developed as potential therapeutic agents. Among them, BIBR1532 is a selective non-competitive inhibitor that primarily impairs DNA substrate extension after extending to the 5′ end of the template, reducing the number of TTAGGG repeats, and inhibiting long reactant formation[26]. BIBR1532 inhibits the proliferation, migration, and invasion of endometrial cells in patients with endometriosis by reducing the cascade reaction of telomerase activity and the MAPK signaling pathway[27]. In addition to benign diseases, BIBR1532 is primarily used in cancer therapy. For instance, it inhibits proliferation and migration, while inducing apoptosis in anaplastic thyroid cancer SW1736 cells[28]. Consistent with previous studies, we found that BIBR5132 downregulated hTERT expression and inhibited ESCC cell proliferation in a dose-dependent manner. Moreover, BIBR1532 significantly inhibited EC cell migration in a dose-dependent manner. Next, we explored the *in vivo* anti-EC effect of BIBR1532. These results demonstrated that BIBR1532 inhibited the growth of transplanted tumors in nude mice. H&E staining of the heart, liver, spleen, lung, and kidney tissues showed that BIBR1532 did not cause obvious microscopic changes in the key organs of nude mice, indicating its low toxicity *in vivo*. These findings further demonstrated that BIBR1532 is a potential therapeutic drug for ESCC.

Telomeres play a crucial role in the maintenance of chromosomal integrity. In eukaryotic cells, telomeres are protected by the telomere protection protein complex to prevent chromosome end DNA molecules from being recognized as broken double-stranded DNA, which induces ATM- and ATR-dependent DDR[29,30]. When DNA is damaged, upstream ATM and/or ATR protein kinases are activated, subsequently activating downstream signal transduction kinases, CHK1 and/or CHK2, as well as a series of receptors (BRCA1, MDC1, and 53BP1). These kinase cascades enhance DNA damage signals and initiate different response systems through the effectors CDC25, p53, and SMC1, ultimately leading to cell cycle arrest, activation of DNA damage repair pathways, and cell apoptosis and/or senescence[31]. In this study, we found that the expression of telomere protection proteins (TRF1, TRF2, TPP1, and POT1) was downregulated in BIBR1532 treated EC cells KYSE150 and KYSE410. Concurrently, the expression of the DNA damage-related response proteins γ-

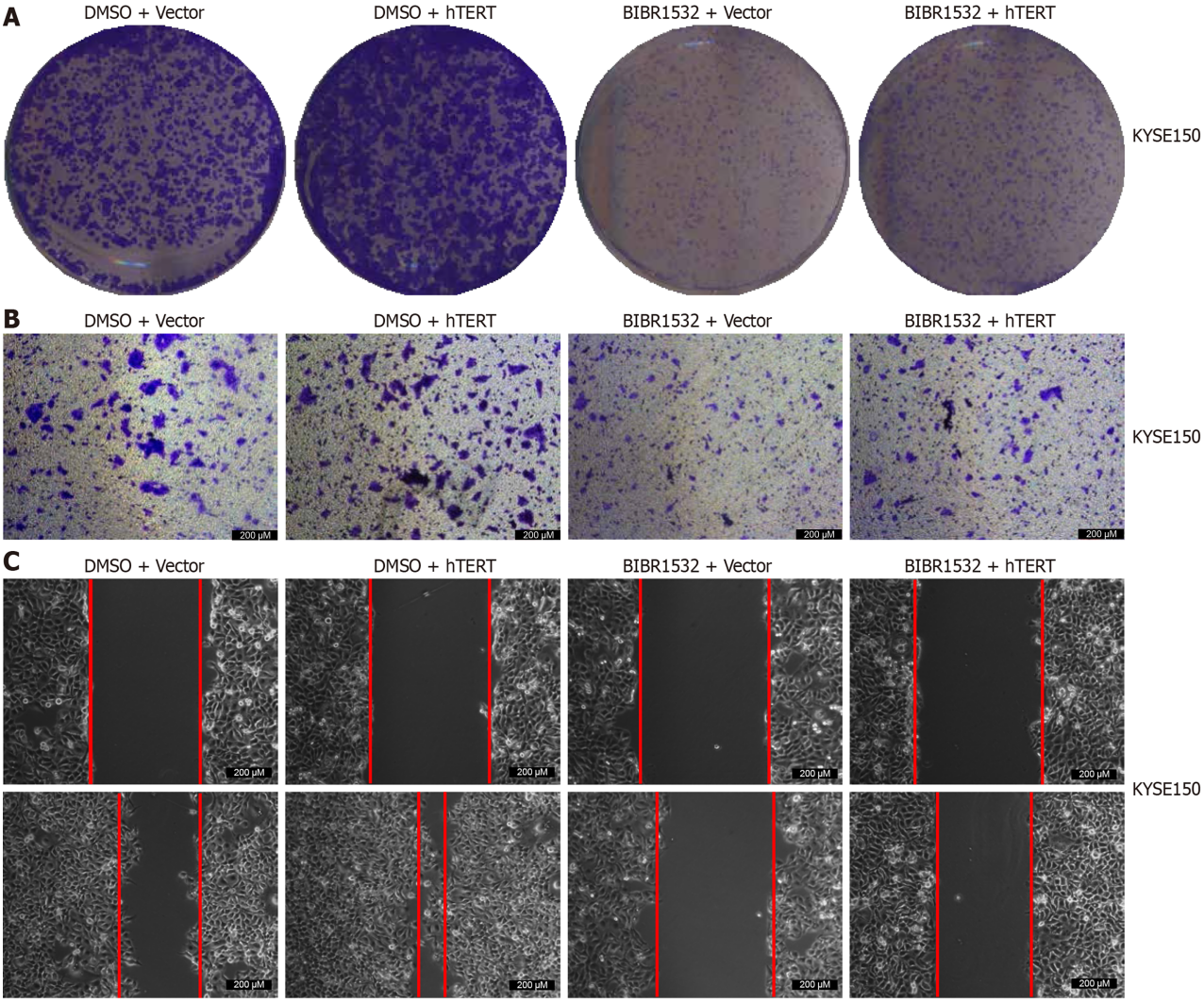

Figure 5 Proliferation and migration of KYSE150 cells after treatment with BIBR1532 combined with human telomerase reverse transcriptase overexpression. A: Plate colony formation by KYSE150 cells after treatment with BIBR1532 (50 μM) and/or human telomerase reverse transcriptase (hTERT) overexpression for 48 hours; B: Migration evaluated by transwell assay of KYSE150 cells after treatment with BIBR1532 (50 μM) and/or hTERT overexpression for 48 hours; C: Migration evaluated by the scratch assay of KYSE150 cells after treatment with BIBR1532 (50 μM) and/or hTERT overexpression for 48 hours. hTERT: Human telomerase reverse transcriptase.

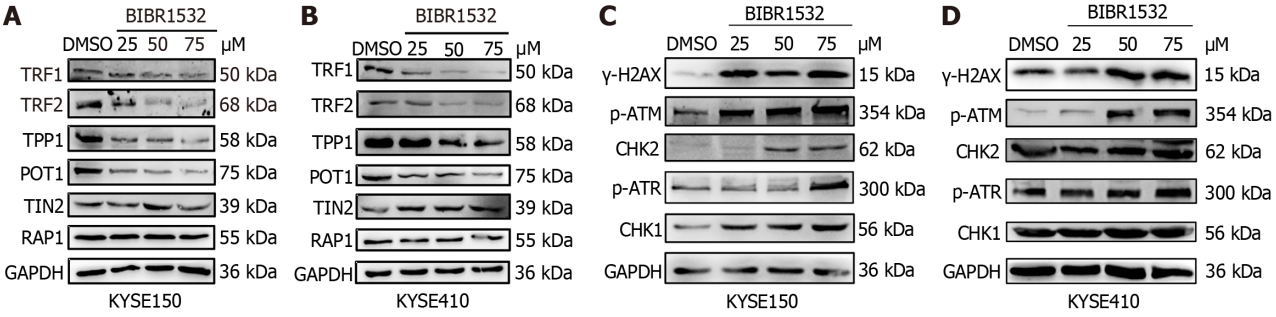

Figure 6 Effect of BIBR1532 on shelterin protein and key proteins in the DNA damage response pathway expression in KYSE150 and KYSE410 cells. A and B: Expression of telomeric-repeat binding factor 1 (TRF1), TRF2, TIN2-interacting protein 1, protection of telomeres 1, TIN2, and repressor activation protein 1 in KYSE150 (A) and KYSE410 (B) cells after treatment with indicated concentrations of BIBR1532 for 48 hours; C and D: Expression of γ-H2AX, p-ATM, CHK2, p-ATR, and CHK1 in KYSE150 (C) and KYSE410 (D) cells after treatment with the indicated concentrations of BIBR1532 for 48 hours. TRF1: Telomeric-repeat binding factor 1; TRF2: Telomeric-repeat binding factor 2; TPP1: TIN2-interacting protein 1; POT1: Protection of telomeres 1; TIN2: TRF1-interacting nuclear protein 2; RAP1: Repressor activation protein 1; γ-H2AX: Phosphorylated histone H2AX; p-ATM: Phosphorylated ataxia-telangiectasia mutated gene; p-ATR: Phosphorylated ataxia telangiectasia and Rad3-related protein; CHK2: Check point kinase 2; CHK1: Check point kinase 1.

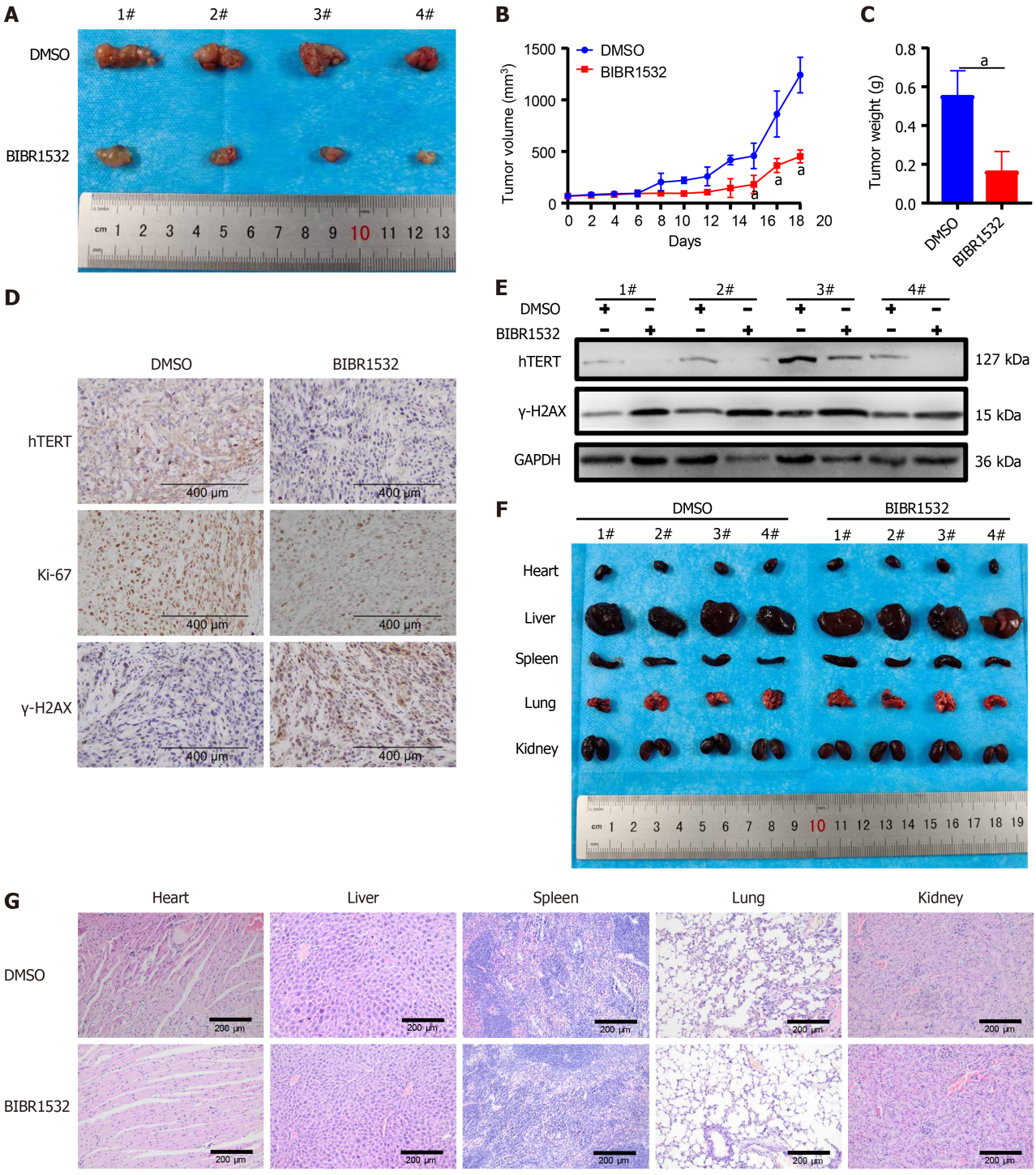

Figure 7 Anti-cancer effect of BIBR1532 in an esophageal squamous cell carcinoma xenograft mouse model. A-C: Tumor images (A), growth curves (B), and tumor weights (C) obtained from xenograft tumors derived from KYSE150 cells treated with BIBR1532 (50 mg/kg); D and E: Expression of human telomerase reverse transcriptase, Ki-67, and γ-H2AX in xenografted tumor tissues evaluated by immunohistochemistry (D) and Western blotting (E); F: Macroscopic images of the heart, liver, spleen, lungs, and kidneys of nude mice treated with BIBR1532 or DMSO; G: Hematoxylin and eosin staining of the heart, liver, spleen, lung, and kidney tissues from nude mice treated with BIBR1532 or DMSO. $^{a}P < 0.05$ was compared with the control group respectively. $P < 0.05$ was considered statistically significant. hTERT: Human telomerase reverse transcriptase; γ-H2AX: Phosphorylated histone H2AX.

H2AX, p-ATM, CHK1, p-ATR, and CHK2 was significantly upregulated. These findings indicate that BIBR1532 inhibits telomerase activity and downregulates the expression of telomere protection proteins, inducing DDR and activating the ATM/ATR signaling pathway in EC cells. Our findings are consistent with those of a previous study showing that the knockdown of TPP1 induces DDR in EC cells[32]. Additionally, we observed that BIBR1532 induced cellular senescence in a concentration-dependent manner and upregulated the expression of the senescence marker P53, which is consistent with a series of reactions following telomere attrition, such as triggering the DDR pathway, cellular senescence, and apoptosis[33,34].

CONCLUSION

In summary, we found that BIBR1532 inhibited the proliferation and migration of ESCC cells, which is likely associated with the activation of DDR and the ATM/ATR signaling pathway, ultimately leading to telomere dysregulation and cellular senescence. Although this study presents novel findings, it has several limitations. First, we were unable to uncover the detailed mechanisms by which BIBR1532 downregulates hTERT expression, or whether it affects telomerase activity. Second, the mechanism by which BIBR1532 downregulates the expression of the four telomere protective proteins remains unclear. In the near future, we will further investigate the role of BIBR1532 in ESCC to provide more information regarding its potential therapeutic application. This may include exploring the direct effects of BIBR1532 on telomerase activity, elucidating the molecular pathways involved in the downregulation of telomere-protective proteins, and investigating potential combination therapies to enhance its anti-cancer effects.

FOOTNOTES

Author contributions: Guo XL and Ma Q contributed to conceptualization; Yuan ZC, Liu X, and Zhong XW contributed to investigation; Wang Q, Li QR, Xu L, Yuan ZC, Liu X, Tang MJ, Luo M, and Zhong XW contributed to methodology; Wang Q, Li QR, and Ma Q contributed to writing-original draft; Guo XL contributed to writing-review and editing; and all authors have read and approved the manuscript.

Supported by the Scientific Research Development Plan Project or the Scientific Research Foundation for Advanced Talents, Affiliated Hospital of North Sichuan Medical College, No. 2023MPZK017, No. 2023ZD001, No. 2023-2ZD002, and No. 2023GC009; Science and Technology Support Program of Nanchong, No. 22SXQT0001; Youth Medical Innovation Research Project, or Medical Research Project of Sichuan Province, No. Q23047 and No. S23020; and Development of a Scientific Research Plan for the Doctoral Scientific Research Foundation of the North Sichuan Medical College, No. CBY22-ZDA03.

Institutional animal care and use committee statement: The studies involving animals were reviewed and approved by the Ethics Committee of the North Sichuan Medical College (approval No. 2023033).

Conflict-of-interest statement: The authors declared that there are no conflicts of interest.

Data sharing statement: The data supporting the findings of this study are available from the corresponding author upon reasonable request.

ARRIVE guidelines statement: The authors have read the ARRIVE guidelines, and the manuscript was prepared and revised according to the ARRIVE guidelines.

Country of origin: China

ORCID number: Qin Wang 0009-0003-3446-4241; Lei Xu 0009-0000-9783-1385; Zi-Chun Yuan 0000-0002-5522-6977; Xiao-Wu Zhong 0000-0002-6643-4624; Qiang Ma 0000-0002-5326-5809; Xiao-Lan Guo 0000-0003-4591-0676.

S-Editor: Chen YL
L-Editor: A
P-Editor: Zhao S

REFERENCES

1 **Sung H**, Ferlay J, Siegel RL, Laversanne M, Soerjomataram I, Jemal A, Bray F. Global Cancer Statistics 2020: GLOBOCAN Estimates of Incidence and Mortality Worldwide for 36 Cancers in 185 Countries. *CA Cancer J Clin* 2021; **71**: 209-249 [PMID: 33538338 DOI: 10.3322/caac.21660]

2 **Abnet CC**, Arnold M, Wei WQ. Epidemiology of Esophageal Squamous Cell Carcinoma. *Gastroenterology* 2018; **154**: 360-373 [PMID: 28823862 DOI: 10.1053/j.gastro.2017.08.023]

3 **Uhlenhopp DJ**, Then EO, Sunkara T, Gaduputi V. Epidemiology of esophageal cancer: update in global trends, etiology and risk factors. *Clin J Gastroenterol* 2020; **13**: 1010-1021 [PMID: 32965635 DOI: 10.1007/s12328-020-01237-x]

4 **National Health Commission of the People's Republic of China Medical Administration and Medical Administration**. [Standardization for diagnosis and treatment of esophageal cancer (2022 edition)]. *Zhonghua Xiaohua Waike Zazhi* 2022; **21**: 1247-1268 [DOI: 10.3760/cma.j.cn115610-20220726-00433]

5 **Ajani JA**, Barthel JS, Bentrem DJ, D'Amico TA, Das P, Denlinger CS, Fuchs CS, Gerdes H, Glasgow RE, Hayman JA, Hofstetter WL, Ilson DH, Keswani RN, Kleinberg LR, Korn WM, Lockhart AC, Mulcahy MF, Orringer MB, Osarogiagbon RU, Posey JA, Sasson AR, Scott WJ,

Shibata S, Strong VE, Varghese TK Jr, Warren G, Washington MK, Willett C, Wright CD; National Comprehensive Cancer Network. Esophageal and esophagogastric junction cancers. *J Natl Compr Canc Netw* 2011; **9**: 830-887 [PMID: 21900218 DOI: 10.6004/jnccn.2011.0072]

6 **Shoji Y**, Koyanagi K, Kanamori K, Tajima K, Ogimi M, Ninomiya Y, Yamamoto M, Kazuno A, Nabeshima K, Nishi T, Mori M. Immunotherapy for esophageal cancer: Where are we now and where can we go. *World J Gastroenterol* 2024; **30**: 2496-2501 [PMID: 38817664 DOI: 10.3748/wjg.v30.i19.2496]

7 **Jiang HF**, Wang MS. [Current status of targeted therapy for esophageal cancer]. *Shijie Linchuang Yaowu* 2015; **36**: 378-383 [DOI: 10.13683/j.wph.2015.06.004]

8 **Malhotra GK**, Yanala U, Ravipati A, Follet M, Vijayakumar M, Are C. Global trends in esophageal cancer. *J Surg Oncol* 2017; **115**: 564-579 [PMID: 28320055 DOI: 10.1002/jso.24592]

9 **Blackburn EH**. Structure and function of telomeres. *Nature* 1991; **350**: 569-573 [PMID: 1708110 DOI: 10.1038/350569a0]

10 **Zakian VA**. Structure and function of telomeres. *Annu Rev Genet* 1989; **23**: 579-604 [PMID: 2694944 DOI: 10.1146/annurev.ge.23.120189.003051]

11 **Blackburn EH**, Collins K. Telomerase: an RNP enzyme synthesizes DNA. *Cold Spring Harb Perspect Biol* 2011; **3** [PMID: 20660025 DOI: 10.1101/cshperspect.a003558]

12 **Leão R**, Apolónio JD, Lee D, Figueiredo A, Tabori U, Castelo-Branco P. Mechanisms of human telomerase reverse transcriptase (hTERT) regulation: clinical impacts in cancer. *J Biomed Sci* 2018; **25**: 22 [PMID: 29526163 DOI: 10.1186/s12929-018-0422-8]

13 **Shay JW**. Role of Telomeres and Telomerase in Aging and Cancer. *Cancer Discov* 2016; **6**: 584-593 [PMID: 27029895 DOI: 10.1158/2159-8290.CD-16-0062]

14 **Li Q**, Ma Q, Xu L, Gao C, Yao L, Wen J, Yang M, Cheng J, Zhou X, Zou J, Zhong X, Guo X. Human Telomerase Reverse Transcriptase as a Therapeutic Target of Dihydroartemisinin for Esophageal Squamous Cancer. *Front Pharmacol* 2021; **12**: 769787 [PMID: 34744749 DOI: 10.3389/fphar.2021.769787]

15 **Jäger K**, Walter M. Therapeutic Targeting of Telomerase. *Genes (Basel)* 2016; **7** [PMID: 27455328 DOI: 10.3390/genes7070039]

16 **Chen X**, Tang WJ, Shi JB, Liu MM, Liu XH. Therapeutic strategies for targeting telomerase in cancer. *Med Res Rev* 2020; **40**: 532-585 [PMID: 31361345 DOI: 10.1002/med.21626]

17 **Lavanya C**, Venkataswamy MM, Sibin MK, Srinivas Bharath MM, Chetan GK. Down regulation of human telomerase reverse transcriptase (hTERT) expression by BIBR1532 in human glioblastoma LN18 cells. *Cytotechnology* 2018; **70**: 1143-1154 [PMID: 29546682 DOI: 10.1007/s10616-018-0205-9]

18 **Ding X**, Cheng J, Pang Q, Wei X, Zhang X, Wang P, Yuan Z, Qian D. BIBR1532, a Selective Telomerase Inhibitor, Enhances Radiosensitivity of Non-Small Cell Lung Cancer Through Increasing Telomere Dysfunction and ATM/CHK1 Inhibition. *Int J Radiat Oncol Biol Phys* 2019; **105**: 861-874 [PMID: 31419512 DOI: 10.1016/j.ijrobp.2019.08.009]

19 **Kusoglu A**, Goker Bagca B, Ozates Ay NP, Gunduz C, Biray Avci C. Telomerase inhibition regulates EMT mechanism in breast cancer stem cells. *Gene* 2020; **759**: 145001 [PMID: 32738420 DOI: 10.1016/j.gene.2020.145001]

20 **Gao J**, Pickett HA. Targeting telomeres: advances in telomere maintenance mechanism-specific cancer therapies. *Nat Rev Cancer* 2022; **22**: 515-532 [PMID: 35790854 DOI: 10.1038/s41568-022-00490-1]

21 **Blasco MA**. Telomeres and human disease: ageing, cancer and beyond. *Nat Rev Genet* 2005; **6**: 611-622 [PMID: 16136653 DOI: 10.1038/nrg1656]

22 **Mizukoshi E**, Kaneko S. Telomerase-Targeted Cancer Immunotherapy. *Int J Mol Sci* 2019; **20** [PMID: 31013796 DOI: 10.3390/ijms20081823]

23 **Pal J**, Gold JS, Munshi NC, Shammas MA. Biology of telomeres: importance in etiology of esophageal cancer and as therapeutic target. *Transl Res* 2013; **162**: 364-370 [PMID: 24090770 DOI: 10.1016/j.trsl.2013.09.003]

24 **Yang R**, Han Y, Guan X, Hong Y, Meng J, Ding S, Long Q, Yi W. Regulation and clinical potential of telomerase reverse transcriptase (TERT/hTERT) in breast cancer. *Cell Commun Signal* 2023; **21**: 218 [PMID: 37612721 DOI: 10.1186/s12964-023-01244-8]

25 **Zalewska-Ziob M**, Dobija-Kubica K, Biernacki K, Adamek B, Kasperczyk J, Bruliński K, Ostrowska Z. Clinical and prognostic value of hTERT mRNA expression in patients with non-small-cell lung cancer. *Acta Biochim Pol* 2017; **64**: 641-646 [PMID: 29141053 DOI: 10.18388/abp.2017_1618]

26 **Pascolo E**, Wenz C, Lingner J, Hauel N, Priepke H, Kauffmann I, Garin-Chesa P, Rettig WJ, Damm K, Schnapp A. Mechanism of human telomerase inhibition by BIBR1532, a synthetic, non-nucleosidic drug candidate. *J Biol Chem* 2002; **277**: 15566-15572 [PMID: 11854300 DOI: 10.1074/jbc.M201266200]

27 **Zhao X**, Luo D, Liu T, Zhang H, Xie Y, Kong W. BIBR1532 Affects Endometrial Cell Proliferation, Migration, and Invasion in Endometriosis *via* Telomerase Inhibition and MAPK Signaling. *Gynecol Obstet Invest* 2023; **88**: 226-239 [PMID: 37429261 DOI: 10.1159/000530460]

28 **Turkmen E**, Sogutlu F, Erdogan M, Biray Avci C. Evaluation of the anticancer effect of telomerase inhibitor BIBR1532 in anaplastic thyroid cancer in terms of apoptosis, migration and cell cycle. *Med Oncol* 2023; **40**: 196 [PMID: 37284891 DOI: 10.1007/s12032-023-02063-0]

29 **Matsuoka S**, Ballif BA, Smogorzewska A, McDonald ER 3rd, Hurov KE, Luo J, Bakalarski CE, Zhao Z, Solimini N, Lerenthal Y, Shiloh Y, Gygi SP, Elledge SJ. ATM and ATR substrate analysis reveals extensive protein networks responsive to DNA damage. *Science* 2007; **316**: 1160-1166 [PMID: 17525332 DOI: 10.1126/science.1140321]

30 **Li Z**, Pearlman AH, Hsieh P. DNA mismatch repair and the DNA damage response. *DNA Repair (Amst)* 2016; **38**: 94-101 [PMID: 26704428 DOI: 10.1016/j.dnarep.2015.11.019]

31 **d'Adda di Fagagna F**, Reaper PM, Clay-Farrace L, Fiegler H, Carr P, Von Zglinicki T, Saretzki G, Carter NP, Jackson SP. A DNA damage checkpoint response in telomere-initiated senescence. *Nature* 2003; **426**: 194-198 [PMID: 14608368 DOI: 10.1038/nature02118]

32 **Wen J**, Zhong X, Gao C, Yang M, Tang M, Yuan Z, Wang Q, Xu L, Ma Q, Guo X, Fang L. TPP1 Inhibits DNA Damage Response and Chemosensitivity in Esophageal Cancer. *Crit Rev Eukaryot Gene Expr* 2023; **33**: 77-91 [PMID: 37606165 DOI: 10.1615/CritRevEukaryotGeneExpr.2023048720]

33 **Engin AB**, Engin A. The Connection Between Cell Fate and Telomere. *Adv Exp Med Biol* 2021; **1275**: 71-100 [PMID: 33539012 DOI: 10.1007/978-3-030-49844-3_3]

34 **Frias C**, Pampalona J, Genesca A, Tusell L. Telomere dysfunction and genome instability. *Front Biosci (Landmark Ed)* 2012; **17**: 2181-2196 [PMID: 22652771 DOI: 10.2741/4044]

World Journal of Gastrointestinal Oncology

Submit a Manuscript: https://www.f6publishing.com

World J Gastrointest Oncol 2025 January 15; 17(1): 98433

DOI: 10.4251/wjgo.v17.i1.98433

ISSN 1948-5204 (online)

CASE REPORT

Complete response of gallbladder cancer treated with gemcitabine and cisplatin chemotherapy combined with durvalumab: A case report and review of literature

Kai Chen, Xu Feng, Yuan Shi, Xin-Lin Li, Zheng-Rong Shi, Xiang Lan

Specialty type: Oncology

Provenance and peer review: Unsolicited article; Externally peer reviewed.

Peer-review model: Single blind

Peer-review report's classification

Scientific Quality: Grade B

Novelty: Grade B

Creativity or Innovation: Grade B

Scientific Significance: Grade B

P-Reviewer: Rusman RD

Received: June 26, 2024

Revised: October 10, 2024

Accepted: November 4, 2024

Published online: January 15, 2025

Processing time: 169 Days and 5.1 Hours

Kai Chen, Xu Feng, Yuan Shi, Xin-Lin Li, Zheng-Rong Shi, Xiang Lan, Department of Hepatobiliary Surgery, The First Affiliated Hospital of Chongqing Medical University, Chongqing 400016, China

Corresponding author: Xiang Lan, PhD, Chief Doctor, Department of Hepatobiliary Surgery, The First Affiliated Hospital of Chongqing Medical University, Youyi Road, Yuzhong District, Chongqing 400016, China. lanxiang_tmmu@163.com

Abstract

BACKGROUND

Gallbladder cancer (GBC) is the most common and aggressive subtype of biliary tract cancer (BTC) and has a poor prognosis. A newly developed regimen of gemcitabine, cisplatin, and durvalumab shows promise for the treatment of advanced BTC. However, the efficacy of this treatment for GBC remains unclear.

CASE SUMMARY

In this report, we present a case in which the triple-drug regimen exhibited marked effectiveness in treating locally advanced GBC, thus leading to a long-term survival benefit. A 68-year-old man was diagnosed with locally advanced GBC, which rendered him ineligible for curative surgery. Following three cycles of therapy, a partial response was observed. After one year of combined therapy, a clinical complete response was successfully achieved. Subsequent maintenance therapy with durvalumab monotherapy resulted in a disease-free survival of 9 months for the patient. The patient experienced tolerable toxicities of reversible grade 2 nausea and fatigue. Tolerable adverse events were observed in the patient throughout the entirety of the treatment.

CONCLUSION

The combination of gemcitabine and cisplatin chemotherapy with durvalumab was proven to be an effective treatment approach for advanced GBC, with manageable adverse events. Further research is warranted to substantiate the effectiveness of the combined regimen in the context of GBC.

Key Words: Gallbladder cancer; Chemotherapy; Immunotherapy; Durvalumab; Complete response; Case report

Core Tip: This study presents a significant case of a patient with locally advanced gallbladder cancer (GBC) who achieved a clinical complete response following treatment with a novel regimen combining gemcitabine, cisplatin, and durvalumab (GC-D). Despite the notorious resistance of GBC to conventional therapies, the positive outcomes observed in this case suggest potential benefits of immunotherapy in this context. These findings highlight the need for further research to validate the efficacy of the GC-D regimen and to explore its implications for future treatment protocols in GBC.

Citation: Chen K, Feng X, Shi Y, Li XL, Shi ZR, Lan X. Complete response of gallbladder cancer treated with gemcitabine and cisplatin chemotherapy combined with durvalumab: A case report and review of literature. *World J Gastrointest Oncol* 2025; 17(1): 98433
URL: https://www.wjgnet.com/1948-5204/full/v17/i1/98433.htm
DOI: https://dx.doi.org/10.4251/wjgo.v17.i1.98433

INTRODUCTION

Gallbladder cancer (GBC) is a rare but invasive malignant tumor, accompanied by high mortality (median 5-year overall survival of 18%)[1]. In its early stage, GBC often remains asymptomatic, thus leading to frequent negligence. Based on the GLOBOCAN 2018 data, 43% of GBCs are diagnosed with concurrent liver and lymph node metastases, which eliminates the chance for curative surgical resection[2].More than half of the GBC patients suffer from tumor recurrence after undergoing radical surgery[3].

Traditionally, gemcitabine and cisplatin (GC) are widely regarded as being first-line therapies for locally advanced biliary tract cancer (BTC), but their effectiveness is limited[4].

In recent years, the emergence of immunotherapy has revolutionized the treatment approach for solid tumors, thus leading to substantial improvements in patient survival. The success of the double-blind phase III TOPAZ-1 study, which has explored the effects of a combined regimen of gemcitabine, cisplatin, and durvalumab (GC-D) in combination with GC, has marked the beginning of a new era in immunotherapy for BTC[5]. Research has indicated that patients who are given GC-D have notably increased median overall survival (OS; 12.8 *vs* 11.5 months), 24-month OS rate (24.9% *vs* 10.4%), and progression-free survival (7.2 *vs* 5.7 months), with comparable adverse events being reported[6]. This triple therapy regimen is recommended as first-line treatment for BTC, according to the 2023 National Comprehensive Cancer Network guidelines. However, compared with other types of BTC, GBC has distinct biological characteristics, including unique genetic mutations and a more immunosuppressive microenvironment, which contributes to its aggressive nature and poor response to standard therapies[7,8]. Unlike cholangiocarcinoma or pancreatic cancer, GBC is frequently diagnosed at advanced stages because of its asymptomatic nature, thus leading to a more dismal prognosis. Given the unique biological characteristics and clinical behavior of GBC, investigations of the treatment responses within this specific context are crucial. Moreover an understanding of these nuances can provide insights into optimizing therapeutic strategies and improving patient outcomes.

Herein, we report a case in which GC-D was significantly effective for locally advanced GBC, with a clinical complete response (CR) eventually achieved. This case is particularly noteworthy, as it highlights the potential for improved outcomes in a patient population that is typically characterized by poor prognosis, thus contributing valuable insights into the treatment landscape for GBC.

CASE PRESENTATION

Chief complaints

A 68-year-old man presented with right upper abdominal pain that has persisted for 7 days.

History of present illness

Seven days earlier, the patient experienced intermittent mild pain in the right upper abdomen, which was tolerable and lasted for several hours before subsiding on its own. There were no accompanying symptoms such as fever, nausea, vomiting, or diarrhea. The patient's abdominal pain worsened after meals, prompting the patient to seek medical attention at a local hospital, where an ultrasound examination indicated cholecystitis.

History of past illness

No significant past medical history was reported.

Personal and family history
The patient's personal and family medical histories were unremarkable.

Physical examination
Physical examination revealed tenderness in the right upper quadrant, with no signs of jaundice or masses.

Laboratory examinations
Laboratory examinations revealed a total white blood cell count of 12.32 × 10^9/L, with a neutrophil percentage of 80.3%. Additionally, the CA19-9 level was 28.7 U/mL, which was slightly elevated above normal limits and other routine blood tests were within normal limits.

Imaging examinations
Multiphasic contrast-enhanced computed tomography (MCCT) indicated gallbladder enlargement, wall thickening, and potential cholecystitis, in addition to swollen hepatoduodenal mesenteric lymph nodes and a lower density lesion in the S4 segment of the liver, thus suggesting possible metastasis (Figure 1).

FINAL DIAGNOSIS
The preoperative diagnosis was unclear, thus raising the possibility of either cholecystitis or GBC.

TREATMENT
Given the unclear preoperative diagnosis, laparoscopic examination was performed. Thickening and hardening of the cystic duct were intraoperatively observed. A cholecystectomy was initially performed, and the proximal end of the cystic duct was sent for intraoperative frozen sectioning, which revealed the presence of tumor cells accompanied by necrosis. Further exploration revealed the presence of multiple enlarged lymph nodes at the hepatic hilum, with some nodes fused together, as well as involvement of the lower segment of the common bile duct. If radical resection had been performed, the performance of hepatopancreatoduodenectomy would have entailed significant surgical trauma and extensive resection, thus possibly resulting in a variety of postoperative complications. After communicating the corresponding risks with the patient's family, they refused to have the patient undergo radical surgical resection and opted for later systemic treatment instead, thus eliminating the need for the operation. The patient received GC-D therapy (gemcitabine: 1000 mg/m^2, days 1 and 8; cisplatin: 25 mg/m^2, days 1 and 8; durvalumab: 1500mg, days 1; 1 course for 21 days).

OUTCOME AND FOLLOW-UP
The patient experienced tolerable toxicities of reversible grade 2 nausea and fatigue. These symptoms occurred in approximately 60% of the treatment cycles and were effectively managed with tropisetron prior to chemotherapy. After 3 cycles of therapy, the CA19-9 level decreased to 11.4 U/mL. MCCT revealed a reduction in the number of hepatoduodenal mesenteric lymph nodes and a lower-density lesion in the S4 segment of the liver (Figure 2). Due to the positive outcomes, the patient proceeded with the ongoing treatment regimen. Six months after the start of GC-D therapy, the tumor marker level remained relatively low. MCCT revealed a significant reduction in the number of hepatoduodenal mesenteric lymph nodes and the disappearance of lower- density lesions in the S4 segment of the liver (Figure 3). An objective response of partial response (PR) was assessed. As a result of the favourable treatment effects, the patient was able to continue with the initial therapeutic regimen despite experiencing increased nausea and fatigue two days after chemotherapy. One year after beginning therapy, MCCT revealed the disappearance of the hepatoduodenal mesenteric lymph nodes, with his tumor marker levels remaining within normal range. A clinical CR was assessed. When considering the adverse effects of chemotherapy, the patient chose maintenance therapy with durvalumab monotherapy. The entire clinical course is displayed in Figure 4. He returned to his normal daily life, and the ultimate goal of treatment, which was to prolong the patient's quality of life, was achieved. Given the significant CR, we plan to conduct follow-up studies to track the patient's long-term survival, recurrence rates, and overall quality of life over several years, to assess the durability of the GC-D regimen for GBC patients.

DISCUSSION
GBC is a highly malignant tumor. Due to its insensitivity to chemotherapy, its therapeutic efficacy is limited[9-11]. Despite ongoing efforts and exploration, progress in treating GBC has been limited over a prolonged period of time[12-14]. TOPAZ-1 represents a silver lining that illuminates the path for treating TBC[5]. However, the extent to which GBC patients can derive any survival benefits from triple treatment remains uncertain. This aspect has rarely been addressed in previous studies. In this study, a triple combined regimen of gemcitabine, cisplatin and durvalumab achieved a clinical

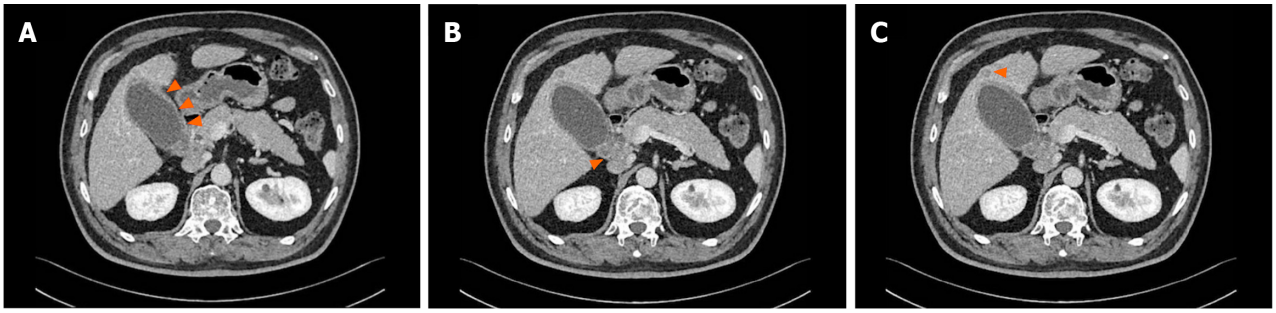

Figure 1 Multiphasic contrast-enhanced computed tomography findings. A: Gallbladder enlargement and wall thickening; B: Swollen hepatoduodenal mesenteric lymph nodes; C: A slightly lower density lesion.

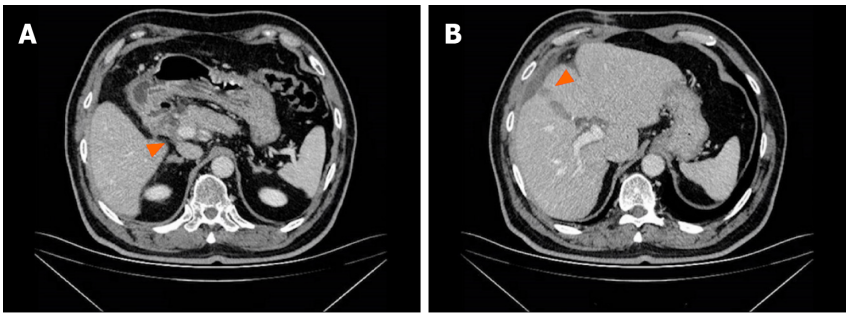

Figure 2 Multiphasic contrast-enhanced computed tomography findings after 3 cycles of therapy. A: The shrunken hepatoduodenal mesenteric lymph nodes; B: The shrunken lower density lesion.

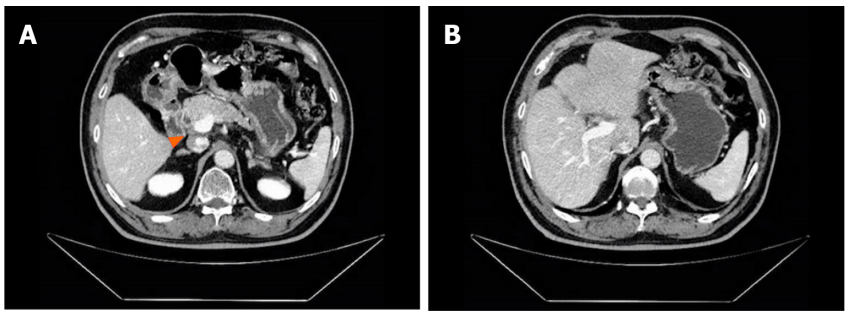

Figure 3 Multiphasic contrast-enhanced computed tomography findings after 6 months of therapy. A: The significantly shrunken hepatoduodenal mesenteric lymph nodes; B: The disappeared lower density lesion.

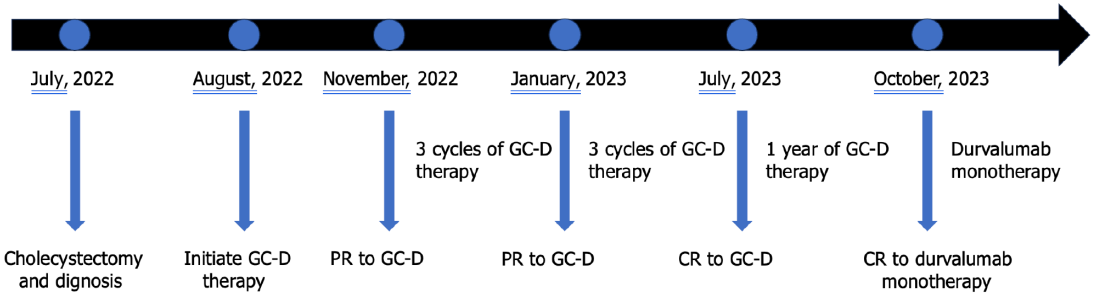

Figure 4 The timeline of the entire clinical course. GC-D: Gemcitabine, cisplatin, and durvalumab; PR: Partial response; CR: Complete response.

CR in a patient with locally advanced GBC, which is an encouraging outcome. Consequently, the present case demonstrates considerable clinical value.

Given the atypical clinical presentation of early-stage GBC, it is challenging to determine the presence of the tumor through preoperative examinations. Intraoperative laparoscopy and frozen section biopsy serve as effective modalities for elucidating the histopathological characteristics of tumors[15-17]. In this study, the malignancy of the gallbladder tumor was intraoperatively confirmed through laparoscopic exploration and frozen section biopsy following cholecystectomy. Furthermore, the tumor was assessed as being in a locally advanced stage, thus rendering curative resection infeasible. Hepatopancreatoduodenectomy may potentially achieve curative resection of the tumor, but it is associated with significant trauma to the patient and the possibility of severe postoperative complications[18,19]. Therefore, full respect should be given to the viewpoints of patients' family members, while actively engaging in communication to avert potential doctor-patient discord.

Multiple studies have suggested that immune checkpoint inhibitors (ICIs) have a profound impact on the treatment of BTC. In a previous phase 1 trial of nivolumab treatment alone or in combination with cisplatin plus gemcitabine for unresectable BTC, Ueno *et al*[20] reported that 40% of patients achieved a PR in the combination therapy group, whereas no patient achieved a CR. Findings from another research endeavor involving pembrolizumab in advanced biliary adenocarcinoma demonstrated an objective response rate (ORR) of 5.8% (with all 6 out of 104 patients displaying a PR) [21]. A real-world study investigating the treatment of advanced biliary tract tumors with the combination of durvalumab and the GC regimen revealed an ORR of 34.5%, with a CR rate of 4.8% and a PR rate of 29.6%[22]. Unfortunately, none of the abovementioned studies conducted subgroup analyses specifically for GBC. Therefore, further research to validate the efficacy of the combination of durvalumab and the GC regimen in the context of GBC is warranted.

The mechanism underlying the combination of chemotherapy and immunotherapy in GBC remains a complex and debated topic. Programmed death-1 (PD-1) protein is a checkpoint protein that, when engaged, inhibits T-cell activation and proliferation[23]. In GBC, tumor cells can upregulate PD-1 expression in response to chemotherapy, thus promoting an immune-evasive environment. This upregulation may hinder the effectiveness of immunotherapy by reducing the activity of cytotoxic T cells against tumor cells[24]. However, the combination of chemotherapy and immunotherapy can counteract this effect, thus restoring T-cell function and enhancing antitumor immunity[25]. Additionally, GBC is characterized by a unique microenvironment that is often immunosuppressive. Chemotherapy may induce changes in the tumor microenvironment, thus potentially decreasing the levels of immunosuppressive factors and thereby enhancing the efficacy of ICIs. This synergistic effect may improve patient outcomes by promoting a more favorable immune response against the tumor[26]. Furthermore, chemotherapy can induce cellular stress responses that increase the expression of tumor-associated antigens on cancer cells, thereby enhancing antigen presentation. Improved antigen presentation can lead to increased recognition and attack by the immune system, particularly when combined with PD-1 blockade[27,28]. This dual approach may help to overcome the tumor's mechanisms of immune evasion. Overall, the combination of chemotherapy and immunotherapy may create a synergistic effect in which chemotherapy sensitizes tumors to immune attack. By inducing immunogenic cell death, chemotherapy may enhance the effectiveness of subsequent immunotherapy, thus leading to better overall responses[23,29]. This mechanism could justify further exploration of combination regimens in clinical trials.

The most commonly observed adverse events associated with GC treatment include fatigue, anemia, neutropenia, thrombocytopenia, and other conditions[9,11,22,30]. In our study, only mild nausea and fatigue were observed, with no additional immune-related adverse events being identified. This discrepancy could be attributed to several individual patient factors, such as age, overall health status, and genetic variations that influence drug metabolism. Additionally, the specific dosing regimen may have played a role in mitigating these adverse effects, thus suggesting a potential avenue for future research into optimizing treatment protocols to increase tolerability.

Some studies have shown that curative resection is performed after effective conversion therapy for initially unresectable GBC[31-33]. With the advent of the immunotherapy era, a series of questions have arisen. For example, there is a question regarding if surgery is still warranted for patients achieving CR through immunotherapy combined with chemotherapy. Additionally, there are questions regarding the extent of targeted resection, as well as the optimal timing for surgery. These inquiries all necessitate further research efforts to offer definitive answers.

This case provides critical insights into the potential efficacy of the GC-D regimen for GBC patients, particularly in achieving a clinically CR. These findings encourage clinicians to consider the role of immunotherapy in GBC treatment protocols. Furthermore, these findings underscore the need for larger-scale clinical trials to confirm these findings and to explore the optimal integration of immunotherapy in the management of GBC.

CONCLUSION

The combination of GC chemotherapy with durvalumab has proven to be an effective treatment approach for advanced GBC, with manageable adverse events. Further research is warranted to substantiate the effectiveness of the combined regimen in the context of GBC.

FOOTNOTES

Author contributions: Chen K conducted the literature review and contributed to manuscript drafting and data interpretation; Feng X collected all clinical data and evaluated the examination results; Shi Y assisted in data collection and analysis; Li XL was responsible for

revising the manuscript for important intellectual content; Shi ZR contributed to the study design and methodology; Lan X served as the corresponding author, overseeing the overall direction and final approval of the manuscript for submission and publication.

Supported by General Project of Natural Science Foundation of Chongqing, China, No. cstc2021jcyj-msxmX0604; and Chongqing Doctoral "Through Train" Research Program, China, No. CSTB2022BSXM-JCX0045.

Informed consent statement: All study participants, or their legal guardian, provided informed written consent prior to study enrollment.

Conflict-of-interest statement: The authors declare no conflict of interest.

CARE Checklist (2016) statement: The authors have read the CARE Checklist (2016), and the manuscript was prepared and revised according to the CARE Checklist (2016).

Country of origin: China

ORCID number: Kai Chen 0000-0003-1083-073X; Xu Feng 0000-0003-4579-8557; Zheng-Rong Shi 0000-0003-4950-3613; Xiang Lan 0000-0002-5626-0106.

S-Editor: Lin C
L-Editor: A
P-Editor: Zhang XD

REFERENCES

1 **Goetze TO**. Gallbladder carcinoma: Prognostic factors and therapeutic options. *World J Gastroenterol* 2015; **21**: 12211-12217 [PMID: 26604631 DOI: 10.3748/wjg.v21.i43.12211]
2 **Rawla P**, Sunkara T, Thandra KC, Barsouk A. Epidemiology of gallbladder cancer. *Clin Exp Hepatol* 2019; **5**: 93-102 [PMID: 31501784 DOI: 10.5114/ceh.2019.85166]
3 **Baiu I**, Visser B. Gallbladder Cancer. *JAMA* 2018; **320**: 1294 [PMID: 30264121 DOI: 10.1001/jama.2018.11815]
4 **Valle J**, Wasan H, Palmer DH, Cunningham D, Anthoney A, Maraveyas A, Madhusudan S, Iveson T, Hughes S, Pereira SP, Roughton M, Bridgewater J; ABC-02 Trial Investigators. Cisplatin plus gemcitabine versus gemcitabine for biliary tract cancer. *N Engl J Med* 2010; **362**: 1273-1281 [PMID: 20375404 DOI: 10.1056/NEJMoa0908721]
5 **Oh D**, He AR, Qin S, Chen L, Okusaka T, Vogel A, Kim JW, Suksomboon charoen T, Lee MA, Kitano M, Burris Iii HA, Bouattour M, Tanasanvimon S, Zaucha R, Avallone A, Cundom J, Rokutanda N, Xiong J, Cohen G, Valle JW. A phase 3 randomized, double-blind, placebo-controlled study of durvalumab in combination with gemcitabine plus cisplatin (GemCis) in patients (pts) with advanced biliary tract cancer (BTC): TOPAZ-1. *J Clin Oncol* 2022; **40**: 378-378 [DOI: 10.1200/jco.2022.40.4_suppl.378]
6 **Oh DY**, Ruth He A, Qin S, Chen LT, Okusaka T, Vogel A, Kim JW, Suksomboon charoen T, Ah Lee M, Kitano M, Burris H, Bouattour M, Tanasanvimon S, McNamara MG, Zaucha R, Avallone A, Tan B, Cundom J, Lee CK, Takahashi H, Ikeda M, Chen JS, Wang J, Makowsky M, Rokutanda N, He P, Kurland JF, Cohen G, Valle JW. Durvalumab plus Gemcitabine and Cisplatin in Advanced Biliary Tract Cancer. *NEJM Evid* 2022; **1**: EVIDoa2200015 [PMID: 38319896 DOI: 10.1056/EVIDoa2200015]
7 **Hirosawa T**, Ishida M, Ishii K, Kanehara K, Kudo K, Ohnuma S, Kamei T, Motoi F, Naitoh T, Selaru FM, Unno M. Loss of BAP1 expression is associated with genetic mutation and can predict outcomes in gallbladder cancer. *PLoS One* 2018; **13**: e0206643 [PMID: 30395583 DOI: 10.1371/journal.pone.0206643]
8 **Kuipers H**, de Bitter TJJ, de Boer MT, van der Post RS, Nijkamp MW, de Reuver PR, Fehrmann RSN, Hoogwater FJH. Gallbladder Cancer: Current Insights in Genetic Alterations and Their Possible Therapeutic Implications. *Cancers (Basel)* 2021; **13** [PMID: 34771420 DOI: 10.3390/cancers13215257]
9 **Abdel-Rahman O**, Elsayed Z, Elhalawani H. Gemcitabine-based chemotherapy for advanced biliary tract carcinomas. *Cochrane Database Syst Rev* 2018; **4**: CD011746 [PMID: 29624208 DOI: 10.1002/14651858.CD011746.pub2]
10 **Kim ST**, Kang JH, Lee J, Lee HW, Oh SY, Jang JS, Lee MA, Sohn BS, Yoon SY, Choi HJ, Hong JH, Kim MJ, Kim S, Park YS, Park JO, Lim HY. Capecitabine plus oxaliplatin versus gemcitabine plus oxaliplatin as first-line therapy for advanced biliary tract cancers: a multicenter, open-label, randomized, phase III, noninferiority trial. *Ann Oncol* 2019; **30**: 788-795 [PMID: 30785198 DOI: 10.1093/annonc/mdz058]
11 **Morizane C**, Okusaka T, Mizusawa J, Katayama H, Ueno M, Ikeda M, Ozaka M, Okano N, Sugimori K, Fukutomi A, Hara H, Mizuno N, Yanagimoto H, Wada K, Tobimatsu K, Yane K, Nakamori S, Yamaguchi H, Asagi A, Yukisawa S, Kojima Y, Kawabe K, Kawamoto Y, Sugimoto R, Iwai T, Nakamura K, Miyakawa H, Yamashita T, Hosokawa A, Ioka T, Kato N, Shioji K, Shimizu K, Nakagohri T, Kamata K, Ishii H, Furuse J; members of the Hepatobiliary and Pancreatic Oncology Group of the Japan Clinical Oncology Group (JCOG-HBPOG). Combination gemcitabine plus S-1 versus gemcitabine plus cisplatin for advanced/recurrent biliary tract cancer: the FUGA-BT (JCOG1113) randomized phase III clinical trial. *Ann Oncol* 2019; **30**: 1950-1958 [PMID: 31566666 DOI: 10.1093/annonc/mdz402]
12 **Tan S**, Yu J, Huang Q, Zhou N, Gou H. PD-1 inhibitors plus nab-paclitaxel-containing chemotherapy for advanced gallbladder cancer in a second-line setting: A retrospective analysis of a case series. *Front Oncol* 2022; **12**: 1006075 [PMID: 36465365 DOI: 10.3389/fonc.2022.1006075]
13 **Conci S**, Catalano G, Roman D, Zecchetto C, Lucin E, De Bellis M, Tripepi M, Guglielmi A, Milella M, Ruzzenente A. Current Role and

Future Perspectives of Immunotherapy and Circulating Factors in Treatment of Biliary Tract Cancers. *Int J Med Sci* 2023; **20**: 858-869 [PMID: 37324191 DOI: 10.7150/ijms.82008]

14 **Noji T**, Nagayama M, Imai K, Kawamoto Y, Kuwatani M, Imamura M, Okamura K, Kimura Y, Hirano S. Conversion surgery for initially unresectable biliary malignancies: a multicenter retrospective cohort study. *Surg Today* 2020; **50**: 1409-1417 [PMID: 32468112 DOI: 10.1007/s00595-020-02031-5]

15 **Cavallaro A**, Piccolo G, Di Vita M, Zanghì A, Cardì F, Di Mattia P, Barbera G, Borzì L, Panebianco V, Di Carlo I, Cavallaro M, Cappellani A. Managing the incidentally detected gallbladder cancer: algorithms and controversies. *Int J Surg* 2014; **12** Suppl 2: S108-S119 [PMID: 25182380 DOI: 10.1016/j.ijsu.2014.08.367]

16 **Cavallaro A**, Piccolo G, Panebianco V, Lo Menzo E, Berretta M, Zanghì A, Di Vita M, Cappellani A. Incidental gallbladder cancer during laparoscopic cholecystectomy: managing an unexpected finding. *World J Gastroenterol* 2012; **18**: 4019-4027 [PMID: 22912553 DOI: 10.3748/wjg.v18.i30.4019]

17 **Sun J**, Xie TG, Ma ZY, Wu X, Li BL. Current status and progress in laparoscopic surgery for gallbladder carcinoma. *World J Gastroenterol* 2023; **29**: 2369-2379 [PMID: 37179580 DOI: 10.3748/wjg.v29.i16.2369]

18 **Yamamoto Y**, Sugiura T, Okamura Y, Ito T, Ashida R, Uemura S, Miyata T, Kato Y, Uesaka K. Is combined pancreatoduodenectomy for advanced gallbladder cancer justified? *Surgery* 2016; **159**: 810-820 [PMID: 26506566 DOI: 10.1016/j.surg.2015.09.009]

19 **Yamamoto Y**, Sugiura T, Ashida R, Okamura Y, Ito T, Uesaka K. Indications for major hepatectomy and combined procedures for advanced gallbladder cancer. *Br J Surg* 2017; **104**: 257-266 [PMID: 27864927 DOI: 10.1002/bjs.10401]

20 **Ueno M**, Ikeda M, Morizane C, Kobayashi S, Ohno I, Kondo S, Okano N, Kimura K, Asada S, Namba Y, Okusaka T, Furuse J. Nivolumab alone or in combination with cisplatin plus gemcitabine in Japanese patients with unresectable or recurrent biliary tract cancer: a non-randomised, multicentre, open-label, phase 1 study. *Lancet Gastroenterol Hepatol* 2019; **4**: 611-621 [PMID: 31109808 DOI: 10.1016/S2468-1253(19)30086-X]

21 **Bang Y**, Ueno M, Malka D, Chung HC, Nagrial A, Kelley RK, Piha-paul SA, Ros W, Italiano A, Nakagawa K, Rugo HS, De Braud FG, Varga AI, Hansen AR, Gao C, Krishnan S, Norwood K, Doi T. Pembrolizumab (pembro) for advanced biliary adenocarcinoma: Results from the KEYNOTE-028 (KN028) and KEYNOTE-158 (KN158) basket studies. *J Clin Oncol* 2019; **37**: 4079 [DOI: 10.1200/jco.2019.37.15_suppl.4079]

22 **Rimini M**, Fornaro L, Lonardi S, Niger M, Lavacchi D, Pressiani T, Lucchetti J, Giordano G, Pretta A, Tamburini E, Pirrone C, Rapposelli IG, Diana A, Martinelli E, Garajová I, Simionato F, Schirripa M, Formica V, Vivaldi C, Caliman E, Rizzato MD, Zanuso V, Nichetti F, Angotti L, Landriscina M, Scartozzi M, Ramundo M, Pastorino A, Daniele B, Cornara N, Persano M, Gusmaroli E, Cerantola R, Salani F, Ratti F, Aldrighetti L, Cascinu S, Rimassa L, Antonuzzo L, Casadei-Gardini A. Durvalumab plus gemcitabine and cisplatin in advanced biliary tract cancer: An early exploratory analysis of real-world data. *Liver Int* 2023; **43**: 1803-1812 [PMID: 37452505 DOI: 10.1111/liv.15641]

23 **Mahoney KM**, Rennert PD, Freeman GJ. Combination cancer immunotherapy and new immunomodulatory targets. *Nat Rev Drug Discov* 2015; **14**: 561-584 [PMID: 26228759 DOI: 10.1038/nrd4591]

24 **Pardoll DM**. The blockade of immune checkpoints in cancer immunotherapy. *Nat Rev Cancer* 2012; **12**: 252-264 [PMID: 22437870 DOI: 10.1038/nrc3239]

25 **Gong K**, Gong ZJ, Lu PX, Ni XL, Shen S, Liu H, Wang JW, Zhang DX, Liu HB, Suo T. PLAC8 overexpression correlates with PD-L1 upregulation and acquired resistance to chemotherapies in gallbladder carcinoma. *Biochem Biophys Res Commun* 2019; **516**: 983-990 [PMID: 31272718 DOI: 10.1016/j.bbrc.2019.06.121]

26 **Fridman WH**, Dieu-Nosjean MC, Pagès F, Cremer I, Damotte D, Sautès-Fridman C, Galon J. The immune microenvironment of human tumors: general significance and clinical impact. *Cancer Microenviron* 2013; **6**: 117-122 [PMID: 23108700 DOI: 10.1007/s12307-012-0124-9]

27 **Hou J**, Greten TF, Xia Q. Immunosuppressive cell death in cancer. *Nat Rev Immunol* 2017; **17**: 401 [PMID: 28480899 DOI: 10.1038/nri.2017.46]

28 **Galluzzi L**, Buqué A, Kepp O, Zitvogel L, Kroemer G. Immunogenic cell death in cancer and infectious disease. *Nat Rev Immunol* 2017; **17**: 97-111 [PMID: 27748397 DOI: 10.1038/nri.2016.107]

29 **Khalil DN**, Smith EL, Brentjens RJ, Wolchok JD. The future of cancer treatment: immunomodulation, CARs and combination immunotherapy. *Nat Rev Clin Oncol* 2016; **13**: 273-290 [PMID: 26977780 DOI: 10.1038/nrclinonc.2016.25]

30 **You MS**, Ryu JK, Choi YH, Choi JH, Huh G, Paik WH, Lee SH, Kim YT. Therapeutic outcomes and prognostic factors in unresectable gallbladder cancer treated with gemcitabine plus cisplatin. *BMC Cancer* 2019; **19**: 10 [PMID: 30611225 DOI: 10.1186/s12885-018-5211-y]

31 **Miura Y**, Ashida R, Sugiura T, Ohgi K, Yamada M, Otsuka S, Todaka A, Uesaka K. Pathological complete response achieved by gemcitabine plus cisplatin therapy for initially unresectable advanced gallbladder cancer: a case report. *Surg Case Rep* 2022; **8**: 20 [PMID: 35079922 DOI: 10.1186/s40792-022-01375-z]

32 **Kato A**, Shimizu H, Ohtsuka M, Yoshidome H, Yoshitomi H, Furukawa K, Takeuchi D, Takayashiki T, Kimura F, Miyazaki M. Surgical resection after downsizing chemotherapy for initially unresectable locally advanced biliary tract cancer: a retrospective single-center study. *Ann Surg Oncol* 2013; **20**: 318-324 [PMID: 23149849 DOI: 10.1245/s10434-012-2312-8]

33 **Tsuyuki H**, Maruo H, Shimizu Y, Shibasaki Y, Nakamura K, Higashi Y, Shoji T, Hirayama K, Yamazaki M. [A Case of Advanced Gallbladder Cancer with Paraaortic Lymph Node Metastases Successfully Treated by Chemotherapy and Conversion Surgery]. *Gan To Kagaku Ryoho* 2018; **45**: 2117-2119 [PMID: 30692303]

World Journal of Gastrointestinal Oncology

Submit a Manuscript: https://www.f6publishing.com

World J Gastrointest Oncol 2025 January 15; 17(1): 100210

DOI: 10.4251/wjgo.v17.i1.100210

ISSN 1948-5204 (online)

CASE REPORT

Multiple liver metastases of unknown origin: A case report

Ying-Jin Wang, Ze-Chuan Liu, Jian Wang, Yin-Mo Yang

Specialty type: Oncology

Provenance and peer review: Unsolicited article; Externally peer reviewed.

Peer-review model: Single blind

Peer-review report's classification

Scientific Quality: Grade B, Grade B, Grade C, Grade C, Grade D

Novelty: Grade B, Grade B, Grade B, Grade B, Grade B

Creativity or Innovation: Grade B, Grade B, Grade B, Grade C, Grade C

Scientific Significance: Grade A, Grade A, Grade B, Grade B, Grade B

P-Reviewer: Du Y; Jankovic K; Yuan T

Received: August 9, 2024

Revised: October 17, 2024

Accepted: November 7, 2024

Published online: January 15, 2025

Processing time: 124 Days and 14.8 Hours

Ying-Jin Wang, Yin-Mo Yang, Department of Hepatobiliary Pancreatic Surgery, Peking University First Hospital, Beijing 100034, China

Ze-Chuan Liu, Jian Wang, Department of Interventional and Vascular Surgery, Peking University First Hospital, Beijing 100034, China

Co-first authors: Ying-Jin Wang and Ze-Chuan Liu.

Corresponding author: Yin-Mo Yang, MD, Department of Hepatobiliary Pancreatic Surgery, Peking University First Hospital, No. 8 Xishiku Street, Xicheng District, Beijing 100034, China. yangyinmosci@163.com

Abstract

BACKGROUND

The liver is the most common site of digestive system tumor metastasis, but not all liver metastases can be traced back to the primary lesions. Although it is unusual, syphilis can impact the liver, manifesting as syphilitic hepatitis with inflammatory nodules, which might be misdiagnosed as metastasis.

CASE SUMMARY

This case report involves a 46-year-old female who developed right upper abdominal pain and intermittent low fever that persisted for more than three months. No definitive diagnosis of a tumor had been made in the past decades, but signs of multiple liver metastases were recognized after a computed tomography scan without evidence of primary lesions. With positive serological tests for syphilis and a biopsy of the liver nodules, a diagnosis of hepatic syphilis was made and confirmed with follow-up nodule reduction after anti-syphilis therapy.

CONCLUSION

Clinicians must be aware of the possibility that syphilis can cause hepatic inflammatory masses, especially when liver metastasis is suspected without evidence of primary lesions. A definitive diagnosis should be established in conjunction with a review of the patient's medical history for accurate therapeutic intervention.

Key Words: Syphilitic hepatitis; Liver nodules; Liver metastasis; Treponema pallidum; Case report

Core Tip: The liver is the most common metastasis site of digestive system tumor, while not all liver metastases could be traced back to the primary lesions. Syphilis is unusual and impacts the liver manifesting syphilitic hepatitis with inflammatory nodules, which might be misdiagnosed as metastasis. We presented a case showing that when multiple hepatic nodules with primary lesions are confronted, focusing on infectious or self-immune diseases based on the patient's history might help to answer the final question.

Citation: Wang YJ, Liu ZC, Wang J, Yang YM. Multiple liver metastases of unknown origin: A case report. *World J Gastrointest Oncol* 2025; 17(1): 100210
URL: https://www.wjgnet.com/1948-5204/full/v17/i1/100210.htm
DOI: https://dx.doi.org/10.4251/wjgo.v17.i1.100210

INTRODUCTION

The liver is the most common metastasis site of digestive system tumors, with malignant colorectal tumors accounting for approximately 70% of metastatic lesions[1]. Incidental identification of single or multiple solid liver lesions is not uncommon in general surgery practice, and it is important to locate the primary tumor or prevent the recurrence of previously treated lesions[2]. However, not all liver metastases can be traced back to the primary lesions. It is essential to exclude inflammatory lesions caused by viruses, bacteria, and special pathogens. Caused by the *Treponema pallidum*, the syphilis spirochete has reemerged as a significant public health concern[3]. If untreated, it progresses through various stages of infection. Several weeks to months following infection, a subset of patients developed secondary syphilis, which is characterized by a distinctive rash affecting the palms and soles, lymphadenopathy, and systemic symptoms[4]. Syphilis can impact the liver during the secondary stage as syphilitic hepatitis and during the tertiary stage as gumma. The diagnosis of syphilitic hepatitis relies on the presence of abnormal liver tests in conjunction with other indications of systemic syphilis, particularly the characteristic rash[3]. Herein, we present a case of syphilis that manifested as a hepatic mass, which was initially suspected to be a malignant tumor, given the absence of a primary lesion.

CASE PRESENTATION

Chief complaints

The patient's main complaints were right upper abdominal pain and intermittent low fever persisting for more than three months.

History of present illness

Three months earlier, a 46-year-old female experienced right upper abdominal pain without any obvious cause. It was occasionally accompanied by a slight increase in body temperature, but there were no symptoms of nausea, vomiting, jaundice, palpitation, chest tightness, or changes in bowel habits.

History of past illness

No definitive diagnosis of the tumor had been made in past decades. The patient denied any previous history of infection.

Personal and family history

The patient's family had no history of tumors.

Physical examination

After admission, the patient's blood pressure was 121 mmHg/75 mmHg, heart rate was 85 beats per minute, and body temperature was 36.8 °C. Tests for abdominal tenderness, rebounding pain, muscle tension, and acute peritonitis were negative. No enlarged lymph nodes were found during the physical examination.

Laboratory examinations

Blood tests revealed mild anemia (hemoglobin: 105 g/L) and an increased neutrophil percentage (82.4%) without an elevated leucocyte count. Total bilirubin was slightly elevated (20.6 μmol/L) according to the results of the biochemical analyses. Coagulation and thyroid function tests were normal. Serum tumor marker levels, including alpha-fetoprotein, carbohydrate antigen 19-9, and carcinoembryonic antigen levels, were also within normal ranges. Infectious screening revealed syphilis antibody positivity, yet results of the rapid plasma reagin test were negative. The relative markers of the hepatitis virus were negative. Infection with severe acute respiratory syndrome coronavirus 2 was also excluded *via* polymerase chain reaction.

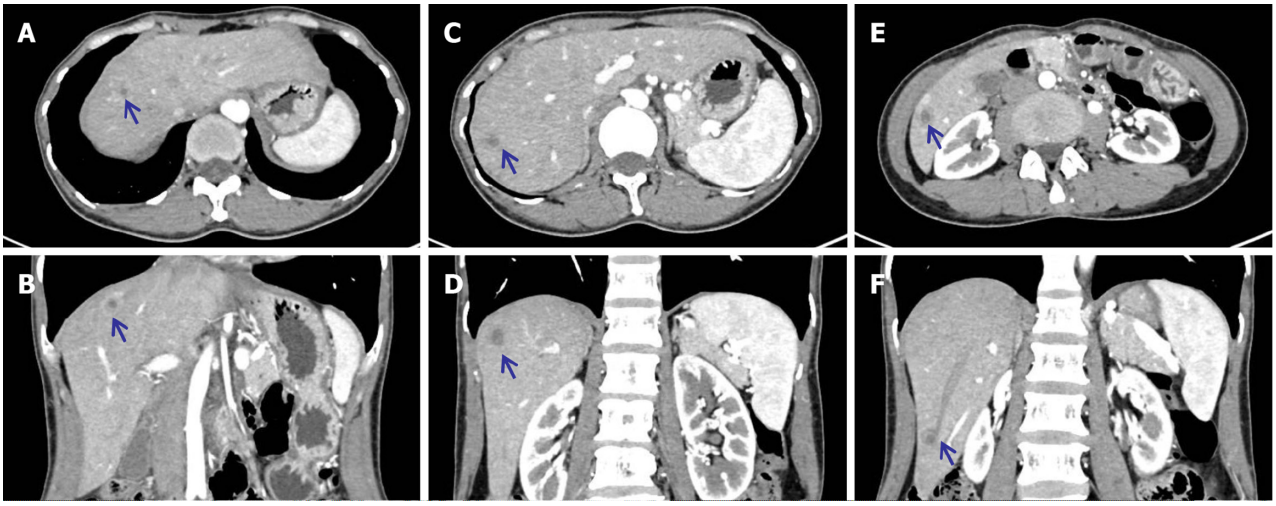

Figure 1 Baseline contrast-enhanced computed tomography revealed multiple liver nodules with a typical bull's eye sign. A and B: Central liver region; C and D: Subcapsular lesion; E and F: Inferior margin lesion. Blue arrow: Abnormal lesions in lateral and coronal sections of computed tomography.

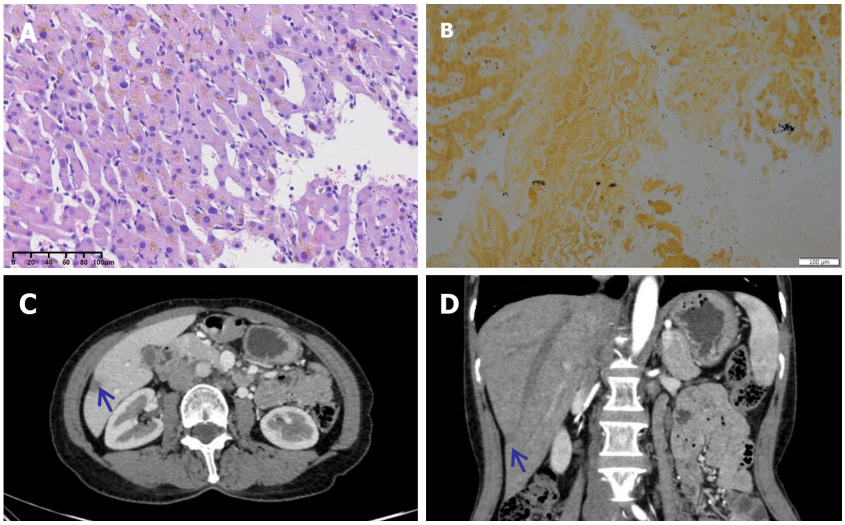

Figure 2 The patient's final diagnosis, outcome, and follow-up. A and B: Pathology results of hematoxylin-eosin and silver-impregnation staining showing hepatitis and *Treponema pallidum*; C and D: After penicillin G treatment, the number of nodules was significantly reduced, and they were well controlled. Blue arrow: Hepatic lesion in inferior margin after treatment.

Imaging examinations

Contrast-enhanced computed tomography (CT) revealed multiple potential liver metastases (Figure 1, bull's eye sign) without certain primary lesions. Due to financial constraints, the patient refused further positron emission tomography/CT scans. Unfortunately, gastrointestinal endoscopy had also been neglected.

FINAL DIAGNOSIS

To inform a definite diagnosis, a percutaneous biopsy of the liver was performed, and radiofrequency ablation was completed incidentally. However, the final pathology was not consistent with the preoperative diagnosis. The results revealed fibrinoid necrosis and eosinophilic infiltration without any evidence of cancerous lesions. Recognizing the history of syphilis, hematoxylin-eosin and silver-impregnation staining were performed to confirm the diagnosis of the lesion, and *Treponema pallidum* was detected (Figure 2A and B).

TREATMENT

Penicillin G was subsequently used to control the progression of the hepatic nodules.

OUTCOME AND FOLLOW-UP

A few months later, some small nodules disappeared, and medium nodules were partially reduced or controlled (Figure 2C and D, compared with the pre-treatment results shown in Figure 1E and F).

DISCUSSION

When confronting multiple liver nodules, especially the typical bull's eye suggested by contrast-enhanced CT, we usually prefer to consider the diagnosis of liver metastases subconsciously. However, doing so may result in unforeseen complications due to a lack of evidence of a primary tumor. Currently, it is vital to review the patient's history of infectious diseases, including those caused by bacteria, viruses, parasites, and other pathogens, such as *Treponema pallidum*. With respect to etiological treatment, multiple liver nodules can be effectively controlled or cured. We reviewed previously reported cases involving multiple hepatic nodules of unknown origin caused by *Treponema pallidum*. In the literature, 12 cases involving five female patients and seven male patients have been reported. The characteristics of these patients are summarized in Table 1. Their average age was 50 years, and the primary symptom was right upper quadrant abdominal pain. The majority of syphilis patients are in stage III and are diagnosed with mucosal damage and gumma. It was evident that male patients tended to carry human immunodeficiency virus (HIV), especially those with a history of sex with men. For treatment, penicillin G was the main therapeutic regimen, and doxycycline was also used. Common outcomes of interest were a reduction in or disappearance of liver nodules and recovery of liver function.

Table 1 Characteristics of previously reported cases of hepatic nodules caused by syphilis

Ref.	Country	Gender	Age	Primary symptoms	Radiologic or ultrasonic findings	Stage of syphilis	HIV infection	Treatment	Outcome
Maincent *et al*[5], 1997	France	Female	56	Right upper quadrant abdominal pain	Several low-density nodules with no contrast uptake	III	No	Penicillin G (daily for five days and weekly for six weeks)	The abdominal pain subsided, and the liver nodules disappeared
Peeters *et al* [13], 2005	/	Female	47	Vision problems, pain in the right hypochondrium, one enlarged submandibular lymph node	Two hepatic lesions	III	No	Doxycyclin	The sedimentation rate and liver tests normalized, and the hepatic lesions disappeared. However, vision problems remained
Mahto *et al* [6], 2006	United Kingdom	Male	44	Fever, severe persistent upper abdominal pain, weight loss, and a desquamating rash on the palms and soles	Mildly enlarged liver with multiple ill-defined hypoechoic lesions	II	Yes	Doxycycline twice daily for a month	Repeat CT at one month showed that the largest mass decreased in size, and at two months, there was near-complete resolution of the liver masses
Shim[7], 2010	South Korea	Female	65	Intermittent abdominal pain and distension	Ascites and two hepatic nodules with peripheral enhancement	III	No	In the beginning, platinumbased combination chemotherapy for six months; after recurrence, penicillin was used	Complete response after six cycles of chemotherapy but recurrence after nine months; liver nodules disappeared followed by penicillin application
Hagen *et al* [3], 2014	United States	Male	51	Follow-up with liver lesions during chemotherapy for Burkitt lymphoma	Two liver lesions on PET	I	Yes	Penicillin G for 2-3 weeks	Resolution of liver test abnormalities and 50% reduction of the liver masses size
		Male	53	Right upper quadrant abdominal pain and weight loss	Multiple enhancing lesions in the liver and spleen, up to 5.7 cm	I	Yes		Liver tests resolved, but follow-up imaging was not performed
		Male	47	Fatigue, left lower chest wall pain,	Over 50 enhancing lesions in the liver, the	I	Yes		The liver test abnormalities

				fever, chills, intermittent diarrhea, and nausea	largest measuring 2.6 cm				resolved, and virtually complete resolution of the hepatic lesions was achieved
Gaslightwala *et al*[11], 2014	United States	Male	59	Persistent fevers, chills, night sweats, and weight loss	Multiple intensely hypermetabolic hepatic lesions on PET/CT	III	No	Penicillin G	None
Desilets *et al* [14], 2019	Canada	Male	54	General deterioration, posterior rib pain, progressive weight loss	PET-scan showed multiple hypermetabolic liver nodules	II	Yes	Penicillin G	Complete interval resolution of hypermetabolic osteomedullary and liver lesions
Al Dallal *et al* [15], 2021	United States	Female	36	Unresponsive with convulsions of all extremities and fever	Multiple hypoenhancing lesions	III	No	Penicillin G for only four days due to patient refusal	Liver function improved, but follow-up imaging was not performed
Smith *et al* [16], 2022	Australia	Male	39	Right upper quadrant and several weeks of fluctuating tenesmus and diarrhea	Short segmental, irregular rectal wall thickening, bilateral mesorectal lymphadenopathy, and multiple hypoattenuating liver lesions	III	Yes	Penicillin G	Significant reduction in the size of a dominant lesion in the right anterior liver section, with no other appreciable lesions
Otsuka *et al* [8], 2023	Japan	Female	50	Low-grade fever and nausea	Three nodules in the S3, S4, and S5 of the liver with round ring enhancement at the portal phase	III	No	Sulbactam sodium and ampicillin sodium	Marked downsizing of liver nodules

HIV: Human immunodeficiency virus; CT: Computed tomography; PET: Positron emission tomography.

In 1997, Maincent *et al*[5] reported the first case in which a 56-year-old female presented with right upper quadrant abdominal pain and several low-density liver nodules with no primary origin. Based on the patient's history of syphilis, serum tests, and pathological evidence from biopsy, hepatic syphilis gumma was diagnosed. The patient was prescribed penicillin G daily for five days and then weekly for six weeks. As a result, not only did her abdominal pain subside but also her liver nodules disappeared. In 2006, Mahto *et al*[6] reported a case involving a male patient with syphilis who was coinfected with HIV. However, the diagnostic process is not always straightforward. In 2010, Shim[7] described a patient who was initially diagnosed with primary peritoneal serous carcinoma and achieved complete remission following six cycles of platinum-based chemotherapy. Two hepatic nodules subsequently developed during the follow-up period and were originally labeled hepatic metastases. Nevertheless, the pathological examination of resected hepatic nodules did not support the initial diagnosis, underscoring the importance of considering tertiary syphilis in the differential diagnosis of space-occupying lesions, even in the presence of a preexisting cancer diagnosis. Otsuka *et al*[8] reported a similar case in 2023, adding that syphilitic hepatitis was difficult to identify, especially because it manifested as multiple hepatic nodules with a bull's eye sign. In terms of radiological features, the hepatic nodules caused by syphilitic hepatitis are similar to those caused by metastatic tumors. Consequently, the special abscesses and tertiary hepatic syphilis should be considered in the differential diagnosis of metastatic tumors.

The manifestations of syphilis, including intermittent low-grade fever, abdominal pain, headache, weight loss, sore throat, arthralgia, splenomegaly, lymphadenopathy, and uveitis, are always non-specific[9,10]. The tertiary stage of syphilis occurs in approximately one-third of untreated patients. Whereas any organ can be affected, the most common manifestations of tertiary disease include gummatous lesions, cardiovascular syphilis, and neurosyphilis[4]. Syphilis can impact the liver during both the secondary and the tertiary stages of the disease. Secondary hepatic syphilis typically develops within a few weeks to a few months following the appearance of the primary chancre[7,11]. Localized gummas may form in the liver during the tertiary stage, typically arising 1 to 10 years after the initial infection[3,6,9]. Hepatic syphilis is unusual but is reported somewhat more frequently among men who have sex with men and in patients with HIV[12]. Notably, we reported a female patient with syphilis and a relatively healthy immune system. Accordingly, we speculate that the strength of the patient's immunity might not be critical to pathogenesis and that delayed treatment with standardized anti-syphilis agents might induce multiple system injuries, including hepatic syphilis, especially inflammatory nodules.

CONCLUSION

We presented a case showing that when multiple hepatic nodules with primary lesions are confronted, focusing on

infectious or self-immune diseases based on the patient's history might help to answer the final question. A definite diagnosis should be made in conjunction with a medical history review for accurate therapeutic intervention.

FOOTNOTES

Author contributions: Wang YJ and Liu ZC collected the patient data and drafted the manuscript, they contributed equally to this article, they are the co-first authors of this manuscript; Wang J and Yang YM revised the manuscript; and all the authors read and approved the final manuscript.

Informed consent statement: Informed consent was obtained in writing from the patient to publish this report and any accompanying images. This case has been approved by the patient.

Conflict-of-interest statement: All the authors report no relevant conflicts of interest for this article.

CARE Checklist (2016) statement: The authors have read the CARE Checklist (2016), and the manuscript was prepared and revised according to the CARE Checklist (2016).

Country of origin: China

ORCID number: Ying-Jin Wang 0000-0002-9166-0009; Yin-Mo Yang 0000-0002-5887-7935.

S-Editor: Bai Y
L-Editor: A
P-Editor: Zhang XD

REFERENCES

1 **Clark AM**, Ma B, Taylor DL, Griffith L, Wells A. Liver metastases: Microenvironments and ex-vivo models. *Exp Biol Med (Maywood)* 2016; **241**: 1639-1652 [PMID: 27390264 DOI: 10.1177/1535370216658144]
2 **Rashidian N**, Alseidi A, Kirks RC. Cancers Metastatic to the Liver. *Surg Clin North Am* 2020; **100**: 551-563 [PMID: 32402300 DOI: 10.1016/j.suc.2020.02.005]
3 **Hagen CE**, Kamionek M, McKinsey DS, Misdraji J. Syphilis presenting as inflammatory tumors of the liver in HIV-positive homosexual men. *Am J Surg Pathol* 2014; **38**: 1636-1643 [PMID: 24921640 DOI: 10.1097/PAS.0000000000000264]
4 **Baughn RE**, Musher DM. Secondary syphilitic lesions. *Clin Microbiol Rev* 2005; **18**: 205-216 [PMID: 15653827 DOI: 10.1128/CMR.18.1.205-216.2005]
5 **Maincent G**, Labadie H, Fabre M, Novello P, Derghal K, Patriarche C, Licht H. Tertiary hepatic syphilis. A treatable cause of multinodular liver. *Dig Dis Sci* 1997; **42**: 447-450 [PMID: 9052534 DOI: 10.1023/a:1018855011180]
6 **Mahto M**, Mohammed F, Wilkins E, Mason J, Haboubi NY, Khan AN. Pseudohepatic tumour associated with secondary syphilis in an HIV-positive male. *Int J STD AIDS* 2006; **17**: 139-141 [PMID: 16464282 DOI: 10.1258/095646206775455702]
7 **Shim HJ**. Tertiary syphilis mimicking hepatic metastases of underlying primary peritoneal serous carcinoma. *World J Hepatol* 2010; **2**: 362-366 [PMID: 21161022 DOI: 10.4254/wjh.v2.i9.362]
8 **Otsuka Y**, Minaga K, Watanabe T. An Overlooked Cause of Multiple Liver Nodules Exhibiting the Bull's-Eye Sign. *Gastroenterology* 2023; **165**: 548-551 [PMID: 36804603 DOI: 10.1053/j.gastro.2023.02.018]
9 **Huang J**, Lin S, Wang M, Wan B, Zhu Y. Syphilitic hepatitis: a case report and review of the literature. *BMC Gastroenterol* 2019; **19**: 191 [PMID: 31744461 DOI: 10.1186/s12876-019-1112-z]
10 **Mullick CJ**, Liappis AP, Benator DA, Roberts AD, Parenti DM, Simon GL. Syphilitic hepatitis in HIV-infected patients: a report of 7 cases and review of the literature. *Clin Infect Dis* 2004; **39**: e100-e105 [PMID: 15546070 DOI: 10.1086/425501]
11 **Gaslightwala I**, Khara HS, Diehl DL. Syphilitic gummas mistaken for liver metastases. *Clin Gastroenterol Hepatol* 2014; **12**: e109-e110 [PMID: 24793023 DOI: 10.1016/j.cgh.2014.04.022]
12 **Manavi K**, Dhasmana D, Cramb R. Prevalence of hepatitis in early syphilis among an HIV cohort. *Int J STD AIDS* 2012; **23**: e4-e6 [PMID: 22930309 DOI: 10.1258/ijsa.2009.009386]
13 **Peeters L**, Van Vaerenbergh W, Van der Perre C, Lagrange W, Verbeke M. Tertiary syphilis presenting as hepatic bull's eye lesions. *Acta Gastroenterol Belg* 2005; **68**: 435-439 [PMID: 16432997]
14 **Desilets A**, Arsenault F, Laskine M. HIV-Infected Patient Diagnosed With Osteomedullary and Hepatic Syphilis on Positron Emission Tomography: A Case Report. *J Clin Med Res* 2019; **11**: 301-304 [PMID: 30937122 DOI: 10.14740/jocmr3756]
15 **Al Dallal HA**, Narayanan S, Alley HF, Eiswerth MJ, Arnold FW, Martin BA, Shandiz AE. Case Report: Syphilitic Hepatitis-A Rare and Underrecognized Etiology of Liver Disease With Potential for Misdiagnosis. *Front Med (Lausanne)* 2021; **8**: 789250 [PMID: 34912834 DOI: 10.3389/fmed.2021.789250]
16 **Smith MJ**, Ong M, Maqbool A. Tertiary syphilis mimicking metastatic rectal cancer. *J Surg Case Rep* 2022; **2022**: rjac093 [PMID: 35355571 DOI: 10.1093/jscr/rjac093]

World Journal of Gastrointestinal Oncology

Submit a Manuscript: https://www.f6publishing.com

World J Gastrointest Oncol 2025 January 15; 17(1): 100757

DOI: 10.4251/wjgo.v17.i1.100757

ISSN 1948-5204 (online)

CASE REPORT

Targeted gene sequencing and bioinformatics analysis of patients with gallbladder neuroendocrine carcinoma: A case report

Yun-Chuan Yang, Zhi-Tao Chen, Da-Long Wan, Hui Tang, Mu-Lin Liu

Specialty type: Medicine, research and experimental

Provenance and peer review: Unsolicited article; Externally peer reviewed.

Peer-review model: Single blind

Peer-review report's classification
Scientific Quality: Grade B
Novelty: Grade A
Creativity or Innovation: Grade B
Scientific Significance: Grade B

P-Reviewer: Guo Z

Received: August 26, 2024
Revised: September 26, 2024
Accepted: October 30, 2024
Published online: January 15, 2025
Processing time: 108 Days and 21.1 Hours

Yun-Chuan Yang, Mu-Lin Liu, Department of Medical College, Jinan University, Guangzhou 510000, Guangdong Province, China

Yun-Chuan Yang, Mu-Lin Liu, Department of General Surgery, The First Affiliated Hospital of Bengbu Medical University, Bengbu 233000, Anhui Province, China

Zhi-Tao Chen, Department of Hepatobiliary Surgery, Shulan (Hangzhou) Hospital Affiliated to Zhejiang Shuren University Shulan International Medical College, Hangzhou 310022, Zhejiang Province, China

Da-Long Wan, Department of Hepatobiliary and Pancreatic Surgery, The First Affiliated Hospital, College of Medicine, Zhejiang University, Hangzhou 310003, Zhejiang Province, China

Hui Tang, Department of Pathology, The First Affiliated Hospital of Medical School of Zhejiang University, Hangzhou 310000, Zhejiang Province, China

Corresponding author: Mu-Lin Liu, PhD, Chief Doctor, Department of General Surgery, The First Affiliated Hospital of Bengbu Medical University, No. 287 Changhuai Road, Longzihu District, Bengbu 233000, Anhui Province, China. liumulin66@aliyun.com

Abstract

BACKGROUND

Gallbladder neuroendocrine carcinoma (NEC) represents a subtype of gallbladder malignancies characterized by a low incidence, aggressive nature, and poor prognosis. Despite its clinical severity, the genetic alterations, mechanisms, and signaling pathways underlying gallbladder NEC remain unclear.

CASE SUMMARY

This case study presents a rare instance of primary gallbladder NEC in a 73-year-old female patient, who underwent a radical cholecystectomy with hepatic hilar lymphadenectomy and resection of liver segments IV-B and V. Targeted gene sequencing and bioinformatics analysis tools, including STRING, GeneMANIA, Metascape, TRRUST, Sangerbox, cBioPortal and GSCA, were used to analyze the biological functions and features of mutated genes in gallbladder NEC. Twelve mutations (*APC*, *ARID2*, *IFNA6*, *KEAP1*, *RB1*, *SMAD4*, *TP53*, *BTK*, *GATA1*, *GNAS*, and *PRDM3*) were identified, and the tumor mutation burden was determined to be 9.52 muts/Mb *via* targeted gene sequencing. A protein-protein interaction network showed significant interactions among the twelve mutated genes. Gene

Ontology and Kyoto Encyclopedia of Genes and Genomes analyses were used to assess mutation functions and pathways. The results revealed 40 tumor-related pathways. A key regulatory factor for gallbladder NEC-related genes was identified, and its biological functions and features were compared with those of gallbladder carcinoma.

CONCLUSION
Gallbladder NEC requires standardized treatment. Comparisons with other gallbladder carcinomas revealed clinical phenotypes, molecular alterations, functional characteristics, and enriched pathways.

Key Words: Gallbladder neuroendocrine carcinoma; Targeted-gene sequencing; Bioinformatics analysis; case report; Immunocytochemistry; Case report

Core Tip: Gallbladder neuroendocrine carcinoma (NEC) is a rare and aggressive malignancy with unclear genetic alterations and mechanisms. Our case study of a 73-year-old female with gallbladder NEC revealed 12 mutated genes (*APC*, *ARID2*, *IFNA6*, *KEAP1*, *RB1*, *SMAD4*, *TP53*, *BTK*, *GATA1*, *GNAS*, *JAK2*, *PRDM3*) and a high tumor mutation burden. Bioinformatic analysis identified significant protein-protein interactions and tumor-related functions/pathways, highlighting key regulatory factors. Gallbladder NEC exhibits distinct molecular profiles compared to other gallbladder carcinomas, emphasizing the need for tailored therapeutic strategies and further research to unravel its underlying biology.

Citation: Yang YC, Chen ZT, Wan DL, Tang H, Liu ML. Targeted gene sequencing and bioinformatics analysis of patients with gallbladder neuroendocrine carcinoma: A case report. *World J Gastrointest Oncol* 2025; 17(1): 100757
URL: https://www.wjgnet.com/1948-5204/full/v17/i1/100757.htm
DOI: https://dx.doi.org/10.4251/wjgo.v17.i1.100757

INTRODUCTION

Neuroendocrine carcinoma (NEC) predominantly affects the digestive and respiratory tracts, including the stomach, intestines, pancreas, and lung, accounting for approximately 97% of all NEC cases[1]. However, the occurrence of gallbladder NEC is rare in clinical practice[2]. Owing to a lack of specific guidelines or consensus, treatment for gallbladder NEC often follows protocols for gallbladder adenocarcinoma[3]. Notably, gallbladder NEC exhibits aggressive traits distinct from those of other gallbladder malignancies[4]. However, due to limited research, the clinicopathological, genetic, and molecular characteristics of gallbladder NEC are poorly understood. Therefore, gaining a deeper insight into its genetic and molecular features is essential. Comprehensive gene mutation profiling and molecular analysis could clarify the mechanisms underlying tumorigenesis and progression, offering key insights for formulating future research, clinical diagnosis, and treatment strategies.

This case report describes an instance of gallbladder NEC in a 73-year-old female patient, incorporating targeted gene sequencing with standard histopathological evaluation. Notably, the mutational spectrum, regulatory factors, functional interactions, and enriched pathways of mutated genes in gallbladder NEC have not been studied thoroughly. This study aimed to explore the clinical profiles, genetic features, and clinical management of gallbladder NEC, while comparing its biological characteristics to those of gallbladder adenocarcinoma to obtain crucial insights into this disease. The report follows the CARE checklist for clinical case reporting.

CASE PRESENTATION

Chief complaints

A 73-year-old Chinese female presented with upper abdominal discomfort lasting for one week on December 30, 2019. An initial abdominal ultrasonography revealed a 7 cm hyperechoic focus with ill-defined margins and multiple gallbladder stones in the context of cholecystitis. No edema, anemia, jaundice, hepatomegaly, or splenomegaly were observed on admission. The patient did not experience discomfort, weight loss, fever, or night sweats. A history of hypertension for 5 years and cholelithiasis for 10 years was noted. Levels of tumor markers, including carcinoembryonic antigen, carbohydrate antigen 19-9, and alpha-fetoprotein, were normal. Biochemical tests for aspartate aminotransferase (AST), alanine aminotransferase (ALT), albumin, and bilirubin were also within the normal range. Abdominal contrast-enhanced computed tomography (CT) demonstrated a 7 cm mass in liver segments IVb and V, accompanied by thickening of the gallbladder fundus wall with early and prolonged enhancement. Multiple gallbladder stones were also identified. No pancreatic enlargement or bile duct dilatation was observed (Figure 1). Dynamic contrast-enhanced magnetic resonance imaging (MRI) showed a 6.7 cm mass with low T1 and high T2 signal intensities, along with diffusion-weighted imaging findings (Figure 2). Given the imaging features, gallbladder carcinoma with liver invasion and cholelithiasis was initially

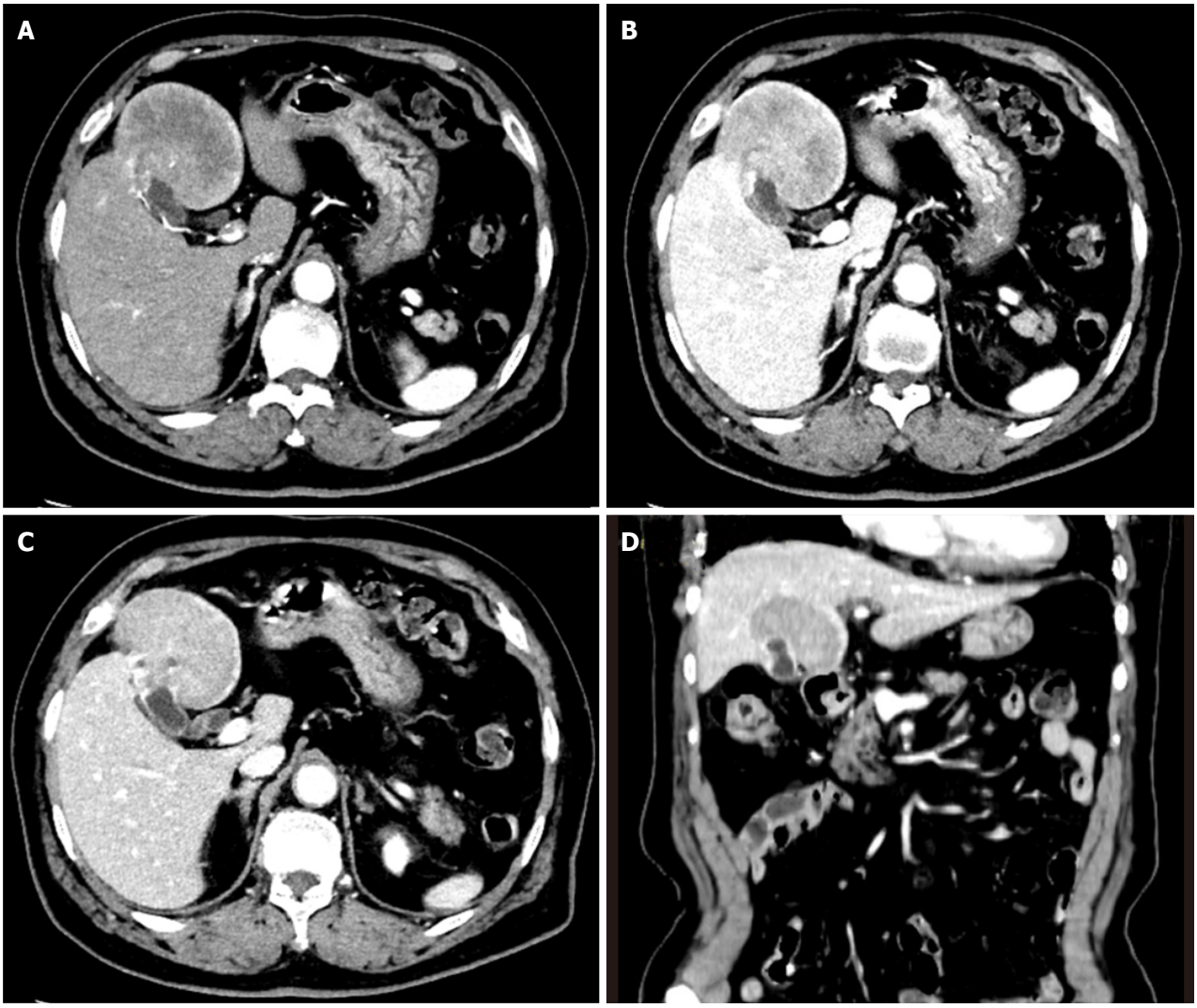

Figure 1 Abdominal contrast-enhanced computed tomography scan reveals a 7 cm mass in liver segments IVb and V, with localized thickening of the gallbladder fundus wall and early-stage enhancement followed by a prolonged contrast effect. A: Arterial phase showed inhomogeneous lesion enhancement; B: The portal venous phase showed a prolonged contrast effect in the mass; C: The delayed phase showed progressive enhancement of the mass; D: The mass invades liver segments IVb and V.

suspected. After discussions with a multidisciplinary team, a diagnosis of extensive gallbladder carcinoma with liver invasion and cholelithiasis was confirmed. Surgical resection was planned prior to chemotherapy, considering the potential complications of cholelithiasis and the patient's refusal to undergo chemotherapy.

A radical cholecystectomy with hepatic hilar lymphadenectomy and resection of liver segments IV-B and V was performed. A 6 cm × 7 cm greyish-yellow globular lesion, largely occupied by multiple yellow stones, was macroscopically identified at the gallbladder fundus (Figure 3). Immunohistochemical analysis revealed a nest-like pattern of heterogeneous tumor cells undergoing necrosis infiltrating the gallbladder and liver. These cells were positive for CK7, CK19, CK (pan), chromogranin A (CgA), and synaptophysin (Syn), while negative results were obtained for CD56, CK5/6, P40, and hepatocytes. Notably, the mitotic count was 24 per 10 high-power fields, along with a Ki-67 index of 70%, indicating a poorly differentiated NEC (Figure 4).

Comprehensive genetic testing was performed on tumor DNA extracted from the gallbladder NEC, encompassing selected introns of 448 cancer-related genes and all exons. As summarized in Table 1, twelve somatic mutations were identified. The tumor mutation burden (TMB) was determined to be 9.52 muts/Mb. An immunohistochemical assay for PD-L1 was performed to predict the response to PD-1/PD-L1 inhibitors, and the results revealed a lack of expression in the gallbladder NEC. Additionally, the tumor proportion score and combined positivity score were calculated to assess the immunohistochemical expression of PD-L1, as depicted in Figure 5.

The patient recovered smoothly and was discharged on the 8th day post-surgery. One month later, six cycles of chemotherapy, consisting of cisplatin (area under the curve of 5 on day 1, repeated every 21 days) and etoposide (80 mg/m^2 on days 1-3, repeated every 21 days), were administered. However, at two months post-discharge, an MRI scan revealed a recurrence in segment VI of the liver. Subsequently, second-line oral chemotherapy was initiated with capecitabine (3 tablets BID, days 1-14) and temozolomide (200 mg, days 10-14), repeated every 3 weeks. After 1 month, multiple recurrences were detected in the liver, leading to disease progression and the patient's demise 15 months post-

Table 1 The information of neuroendocrine carcinoma of gallbladder-related mutated genes

Genes	Original name	Cytoband	Exon count	Variant type	Abundance variation
APC	APC regulator of WNT signaling pathway	5q22.2	20	Copy number variation	CN: 1.2
ARID2	AT-rich interaction domain 2	12q12	22	c.3382C>T (p.Q1128)	77.3%
IFNA6	interferon alpha 6	9p21.3	1	c.53C>G (p.S18)	42.8%
KEAP1	Kelch like ECH associated protein 1	19p13.2	7	c.1408C>T (p.R470C)	87.9%
RB1	RB transcriptional corepressor 1	13q14.2	27	c.772-776del (p.N258Efs1)	76.1%
SMAD4	SMAD family member 4	18q21.2	12	Copy number variation	CN: 1.1
TP53	tumor protein p53	17p13.1	11	Copy number variation	CN: 1.1
				c.574C>T (p.Q192)	81.3%
BTK	Bruton tyrosine kinase	Xq22.1	21	c.574C>T (p.D232V)	48.6%
GATA1	GATA binding protein 1	Xp11.23	6	c.173C>A (p.A58E)	42.5%
GNAS	GNAS complex locus	20q13.32	22	c.1048G>C (p.E350Q)	42.9%
MECOM	MDS1 and EVI1 complex locus	3q26.2	24	c.1161G>T (p.Q387H)	2.4%

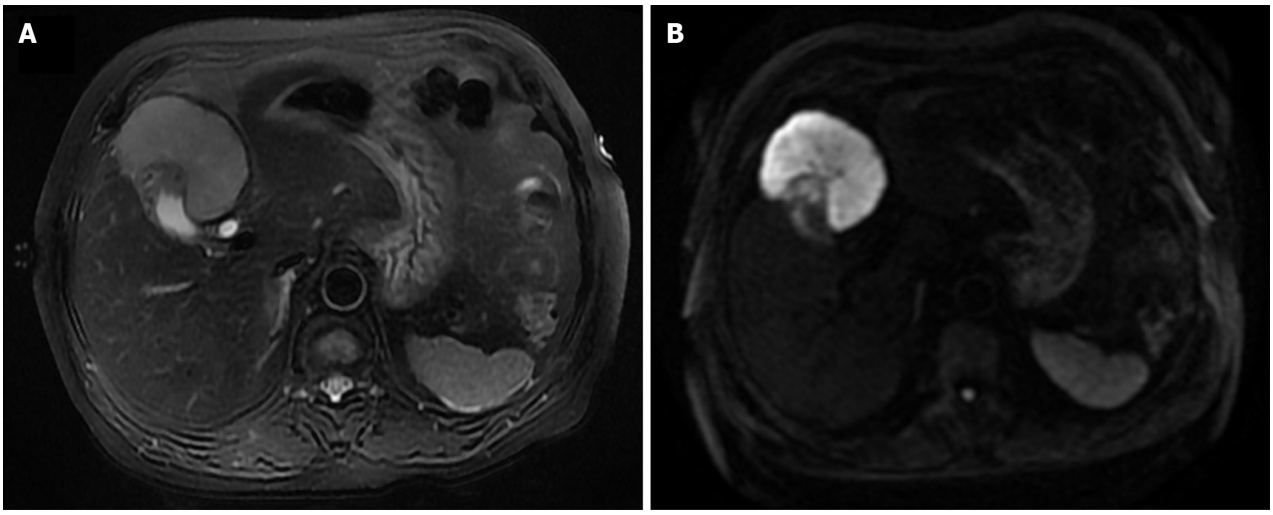

Figure 2 Preoperative magnetic resonance imaging examination of the reported case. A and B: The gallbladder lesion appears slightly hyperintense on T2-weighted imaging (A) and hyperintense on diffusion-weighted imaging (B).

surgery.

History of present illness

A 73-year-old Chinese female presented with upper abdominal discomfort lasting for one week on December 30, 2019. An initial abdominal ultrasonography revealed a 7 cm hyperechoic focus with ill-defined margins and multiple gallbladder stones in the context of cholecystitis. No edema, anemia, jaundice, hepatomegaly, or splenomegaly were observed on admission. The patient did not experience discomfort, weight loss, fever, or night sweats.

History of past illness

A history of hypertension for 5 years and cholelithiasis for 10 years was noted.

Laboratory examinations

Levels of tumor markers, including carcinoembryonic antigen, carbohydrate antigen 19-9, and alpha-fetoprotein, were normal. Biochemical tests for AST, ALT, albumin, and bilirubin were also within the normal range.

Imaging examinations

Abdominal contrast-enhanced CT demonstrated a 7 cm mass in liver segments IVb and V, accompanied by thickening of the gallbladder fundus wall with early and prolonged enhancement. Multiple gallbladder stones were also identified. No pancreatic enlargement or bile duct dilatation was observed (Figure 1). Dynamic contrast-enhanced MRI showed a 6.7 cm

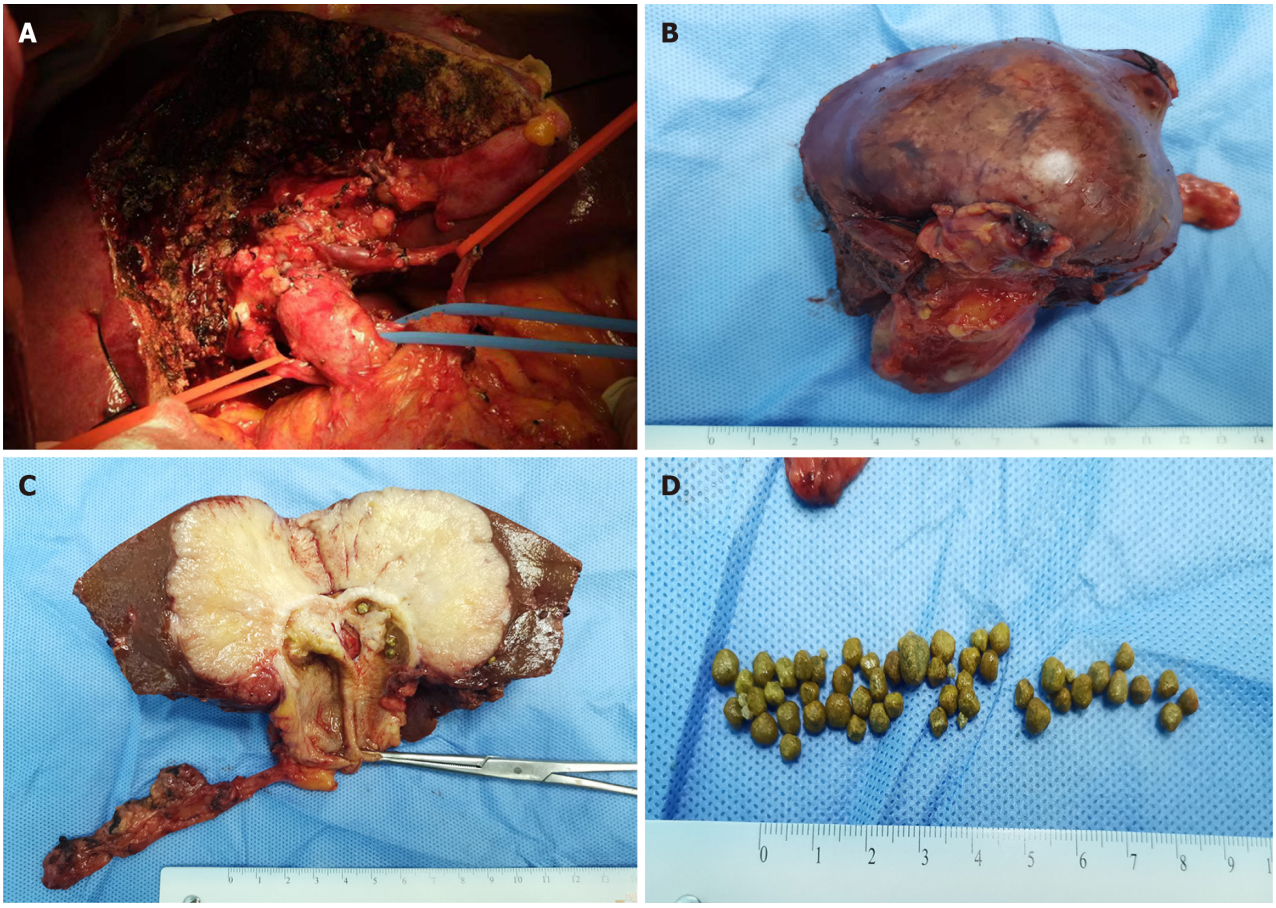

Figure 3 Illustration of the surgical procedure. A: A radical cholecystectomy was performed; B: The gross tumor specimen was displayed; C: Macroscopic analysis revealed a greyish-yellow globular lesion; D: Multiple yellowish stones were identified.

mass with low T1 and high T2 signal intensities, along with diffusion-weighted imaging findings (Figure 2).

MULTIDISCIPLINARY EXPERT CONSULTATION

After discussions with a multidisciplinary team, a diagnosis of extensive gallbladder carcinoma with liver invasion and cholelithiasis was confirmed. Surgical resection was planned prior to chemotherapy, considering the potential complications of cholelithiasis and the patient's refusal to undergo chemotherapy.

FINAL DIAGNOSIS

Given the imaging features, gallbladder carcinoma with liver invasion and cholelithiasis was initially suspected.

TREATMENT

A radical cholecystectomy with hepatic hilar lymphadenectomy and resection of liver segments IV-B and V was performed. A 6 cm × 7 cm greyish-yellow globular lesion, largely occupied by multiple yellow stones, was macroscopically identified at the gallbladder fundus (Figure 3).

OUTCOME AND FOLLOW-UP

The patient recovered smoothly and was discharged on the 8th day post-surgery. One month later, six cycles of chemotherapy, consisting of cisplatin (area under the curve of 5 on day 1, repeated every 21 days) and etoposide (80 mg/m^2 on days 1-3, repeated every 21 days), were administered. However, at two months post-discharge, an MRI scan revealed a recurrence in segment VI of the liver. Subsequently, second-line oral chemotherapy was initiated with

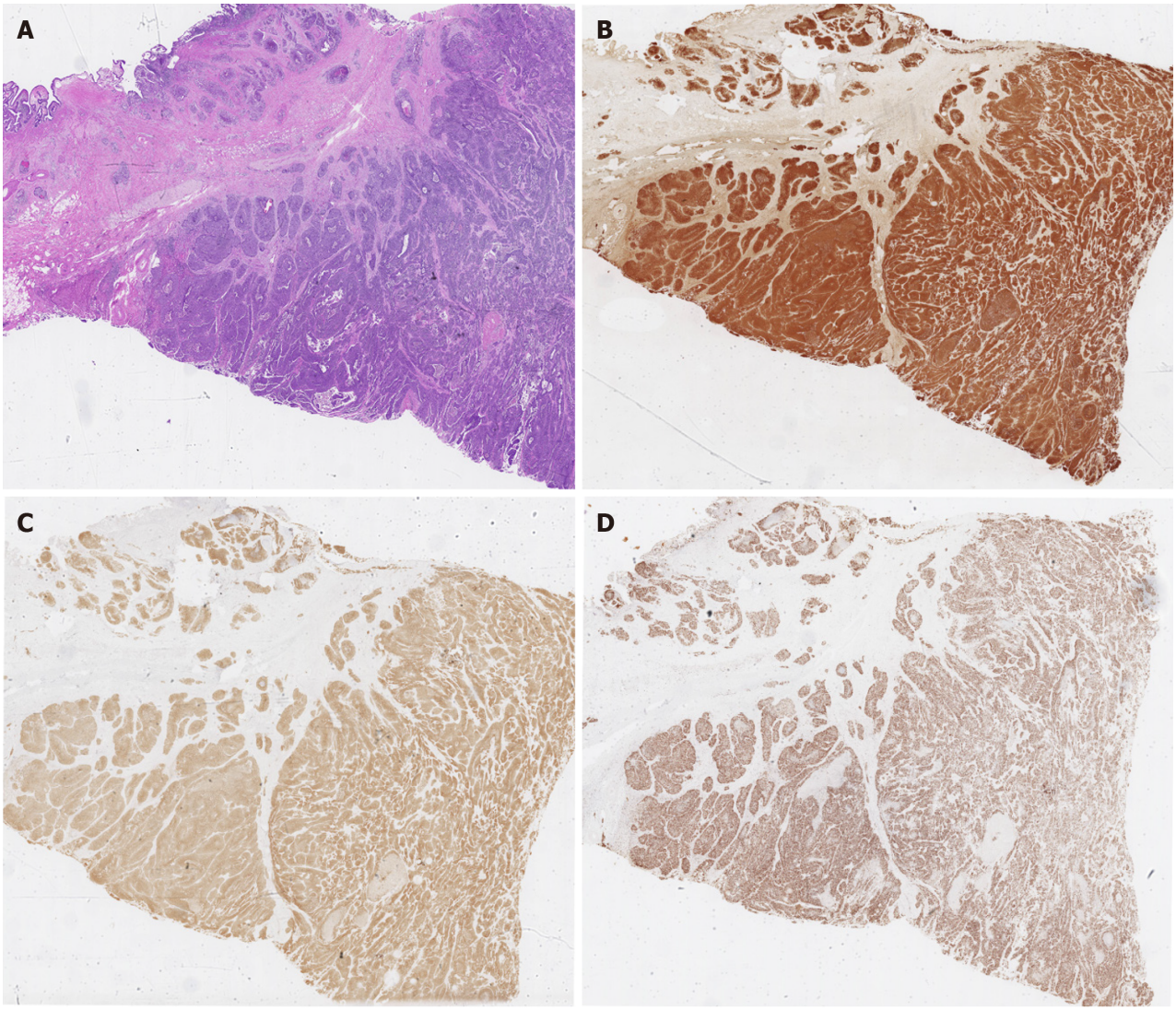

Figure 4 Pathological analysis results. A: Hematoxylin and eosin staining revealed a nest-like arrangement of tumor cells exhibiting marked cellular heterogeneity and visible necrosis; B–D: Immunohistochemical analyses showed positivity for chromogranin A, Ki-67, and synaptophysin, respectively.

capecitabine (3 tablets BID, days 1-14) and temozolomide (200 mg, days 10-14), repeated every 3 weeks. After 1 month, multiple recurrences were detected in the liver, leading to disease progression and the patient's demise 15 months post-surgery.

DISCUSSION

It has been hypothesized that gallbladder NEC evolves from adenocarcinoma, and the interconversion between NET tumors and adenocarcinomas in the gastrointestinal tract has been reported previously[5]. However, our understanding of the differences between gallbladder NEC and gallbladder carcinoma remains limited. This study reviews existing literature and uses bioinformatics analysis to compare the clinicopathologic and genetic characteristics of gallbladder NECs and gallbladder carcinomas.

Targeted gene sequencing helped identify 12 mutations unique to the specimen (Table 1). To understand the biological properties and potential therapeutic targets of this rare tumor more effectively, bioinformatics databases were utilized to explore oncogenic mechanisms. Protein-protein interaction networks (PPIs) were analyzed and visualized using the STRING[6] (version: 11.5, https://string-db.org/) database. The resulting STRING network consisted of 11 nodes and 14 edges, with an average local clustering coefficient of 0.776 (PPI enrichment P value < 0.0001; Figure 6A). GeneMANIA (http://genemania.org/) was used to explore the potential biological mechanisms, and our results[7] revealed that the mutated genes were associated with the transcription regulator complex, ATPase complex, SWI/SNF superfamily-type complex, negative regulation of mitotic cell cycle phase transition, negative regulation of cell cycle phase transition, protein-DNA complex subunit organization, and regulation of metaphase/anaphase transition of cell cycle (Figure 6B). In addition, protein-protein interaction enrichment analysis was performed using the Metascape (https://metascape.org/) database (Figure 6C and D).

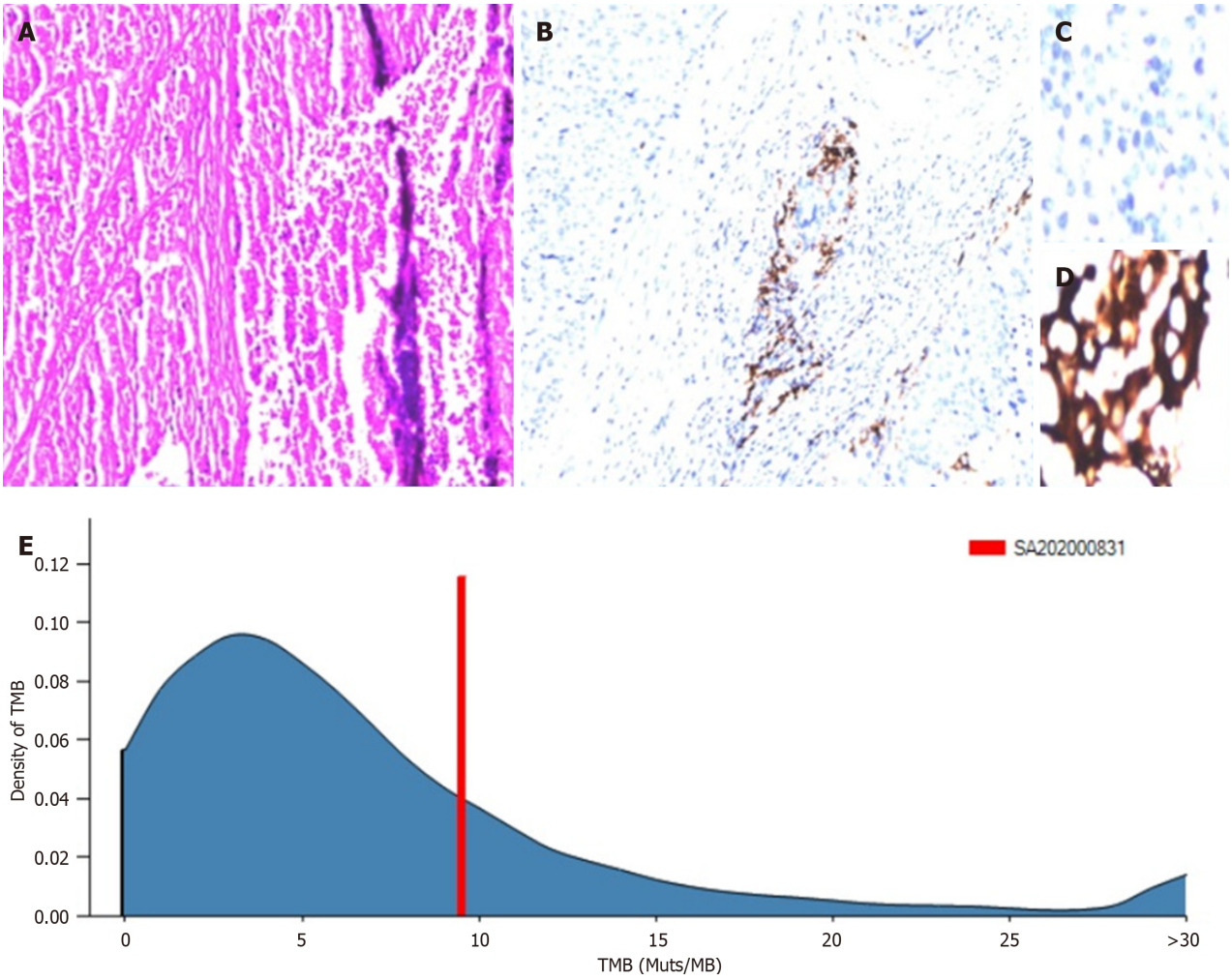

Figure 5 PD-L1 and tumor mutation burden. A and B: Targeted gene sequencing revealed no expression of PD-L1 in gallbladder neuroendocrine carcinoma cells; C and D: Buffer solutions and isotype-matched monoclonal antibodies were used as controls to confirm the specificity of primary antibody binding; E: Targeted gene sequencing also helped quantify the tumor mutation burden. TMB: Tumor mutation burden.

Transcription factors are important regulators of gene expression that play a crucial role in tumor development. The TRRUST[8] (version 2, https://www.grnpedia.org/trrust/) database was used to identify the transcription factors associated with these mutated genes in humans. YY1, KAT2B, PAX5, DNMT1, EZH2, FOS, GATA1, SPI1, MYC, E2F1, and TP53 were identified as pivotal transcription factors linked to these mutations (Table 2). Using the Sangerbox 3.0 (http://vip.sangerbox.com) database, Gene Ontology (GO) and Kyoto Encyclopedia of Genes and Genomes (KEGG) analyses were performed to explore the potential biological functions of these genes. GO analysis of biological processes suggested that these genes might be involved in regulating molecular function (MF) and biological quality, as well as tissue development (Figure 7A). GO analysis of cellular components indicated that these genes were mainly located in the nucleoplasm, transcription factor complex, and chromosomes (Figure 7B). GO analysis of the MF showed enrichment in identical protein binding, transcription factor binding, and proximal promoter sequence-specific DNA binding (Figure 7C). KEGG enrichment analysis revealed potential involvement in cancer pathways, hepatocellular carcinomas, and human papillomavirus infections (Figure 7D). These results are consistent with the findings from the Metascape database (Figure 2E and F).

Sakaki *et al*[9] proposed that gallbladder NEC arises from the metamorphosis of gallbladder adenocarcinoma. A recent study involving the whole exome sequencing analysis of 151 gallbladder cancer patients identified the most common mutated genes as *TP53* (27%), *KMT2C* (11%), *SMAD4* (11%), *PER3* (8%), *ERBB3* (8%), *ARID2* (7%), *ARID1A* (7%), and *ERBB2* (7%), with the ErbB signaling pathway being the most commonly altered pathway[10]. Our findings indicate that the mutational profiles of gallbladder NEC partially overlap with those of gallbladder adenocarcinoma. Therefore, we further analyzed the relationship between these two tumor types.

Tumorigenesis is driven by genetic mutations, making the nucleus a key target for tumor suppression. The cBioPortal (https://www.cbioportal.org/) database was used to explore gene mutation information for gallbladder carcinoma (MSK, Cancer 2018). As shown in Figure 8A, a high mutation rate was observed for *SMAD4* and *TP53* in gallbladder carcinoma patients. Among the 101 sequenced cases, genetic alterations were found in 31% and 58% of 3159 gallbladder carcinoma patients. Meanwhile, these genes showed the highest mutation rates in gallbladder carcinoma (74.76% of 103 cases), followed by cholangiocarcinomas (48.92% of 417 cases) and intrahepatic cholangiocarcinomas (24.03% of 412 cases; Figure 8B). Taken together, these results suggest that the identified mutations may play a crucial role in gallbladder

Table 2 Key regulated factor of neuroendocrine carcinoma of gallbladder-related genes

	Key TF	Description	Overlapped genes	*P* value	FDR
1	YY1	YY1 transcription factor	*APC*, *GNAS*, *TP53*	1.74E-05	1.32E-04
2	KAT2B	K(lysine) acetyltransferase 2B	*RB1*, *SMAD4*	2.40E-05	1.32E-04
3	PAX5	Paired box 5	*RB1*, *TP53*	6.45E-05	2.36E-04
4	DNMT1	DNA (cytosine-5-)-methyltransferase 1	*RB1*, *TP53*	1.42E-04	3.91E-04
5	EZH2	Enhancer of zeste homolog 2 (Drosophila)	*APC*, *TP53*	2.38E-04	5.24E-04
6	FOS	FBJ murine osteosarcoma viral oncogene homolog	*SMAD4*, *TP53*	4.85E-04	7.61E-04
7	GATA1	GATA binding protein 1 (globin transcription factor 1)	*GATA1*, *GNAS*	4.85E-04	7.61E-04
8	SPI1	SFFV proviral integration oncogene spi1	*BTK*, *GATA1*	5.73E-04	7.88E-04
9	MYC	V-myc myelocytomatosis viral oncogene homolog (avian)	*GATA1*, *TP53*	1.48E-03	1.81E-03
10	E2F1	E2F transcription factor 1	*RB1*, *TP53*	2.64E-03	2.90E-03
11	TP53	Tumor protein p53	*RB1*, *TP53*	3.92E-03	3.92E-03

TF: Transcription factor; FDR: False discovery rate; SFFV: Spleen focus forming virus.

carcinoma development.

KEAP1 is an important tumor suppressor gene. Mutations in *KEAP1* reduce its affinity for Nrf2 in the cytoplasm, resulting in Nrf2 accumulation in the nucleus, which promotes tumor occurrence and development[11]. Importantly, *KEAP1* mutations are found in many types of cancer, including gallbladder cancer[12-14]. Genetic mutations serve as targets for precision therapy in cancer treatment. In the present sample, *KEAP1* was the most frequently mutated gene, with a mutation frequency of 87.9%. To identify potential drugs targeting *KEAP1* mutations, the GSCA (http://bioinfo.life.hust.edu.cn/GSCA/) web server was used to explore drug–gene interactions. Figure 8C shows the correlation between *KEAP1* expression and the sensitivity of the top 30 GDSC drugs during pan-cancer analysis.

The genetic and molecular characteristics of gallbladder NECs are poorly understood, and no molecular targeted therapies for gallbladder NEC have been developed for clinical use[15]. There is an urgent clinical need to identify molecular markers that contribute to its pathological progression and develop new therapeutic modalities. While gallbladder NECs and gallbladder adenocarcinomas are distinct entities, they are closely related to each other. However, treatment strategies for gallbladder adenocarcinoma are not entirely applicable to gallbladder neuroendocrine tumors.

The available literature on gallbladder NECs is limited to case reports and case series. Common symptoms include epigastric pain, weight loss, and anorexia, often affecting females over 60[16]. Gallbladder stones and cholecystitis are thought to promote NEC development, as in our case, where gallbladder NECs co-occurred with gallbladder stones. Although imaging modalities, including ultrasound, enhanced CT, and MRI aid in diagnosis, distinguishing NECs from other gallbladder cancers remains challenging. Gallbladder NECs often originate from the deeper layers of the lamina propria or submucosa, which might explain the partial preservation of the gallbladder mucosal epithelium and the linear enhancement seen on CT and MRI. Similar findings have been reported in previous studies on NECs in the gastrointestinal tract[17,18]. In addition, metastatic lymph nodes in gallbladder NECs tend to be larger than those in adenocarcinomas[19], complicating accurate preoperative diagnosis.

A definitive diagnosis of gallbladder NEC necessitates an integrative approach combining pathological and immunohistochemical analyses. Among the array of immunohistochemical markers, CgA, Syn, and neuro-specific enolase (NSE) are widely recognized to be essential for differentiating NECs from other gallbladder pathologies[20]. CgA is a secretory protein found in neural and neuroendocrine tissues, including the adrenal medulla, thyroid C-cells, and certain endocrine tumors. In the context of gallbladder NEC, the detection of CgA through immunohistochemistry analysis indicates the presence of neuroendocrine elements or neuroendocrine differentiation in the necrotic process. Syn, another important biomarker, is a synaptic vesicle protein expressed in neurons and neuroendocrine cells. Its presence in gallbladder NEC tissues is suggestive of neuronal or neuroendocrine differentiation, which further supports disease diagnosis. NSE, also known as gamma-enolase, is an enzyme found primarily in neurons and neuroendocrine cells. Elevated levels of NSE in the context of gallbladder NEC can signify neuronal damage or the presence of neuroendocrine components within necrotic tissues. The combined use of these biomarkers, along with standard pathological examination, significantly enhances the accuracy of diagnosis of gallbladder NEC. Healthcare professionals can make more informed treatment decisions by identifying the presence and distribution of these specific proteins.

In a previous study involving 21 patients with gallbladder NECs, over 80% showed positive staining for CgA and Syn [21]. Another study involving 15 patients with gallbladder NECs reported positive rates of 92.3% and 100% for CgA and Syn, respectively[22]. Consistent with these findings, immunohistochemical results of the patients showed positivity for CgA and Syn. However, the occurrence of NSE was not verified through immunohistochemistry analysis. Additionally, a previous study has reported that an elevated Ki-67 index and high mitotic rate are strongly associated with poor prognosis[21]. Unfortunately, the patients in this study exhibited high Ki-67 index and mitotic indices. Despite postoperative adjuvant chemotherapy, the tumor recurred rapidly and the patient succumbed to the disease 15 months

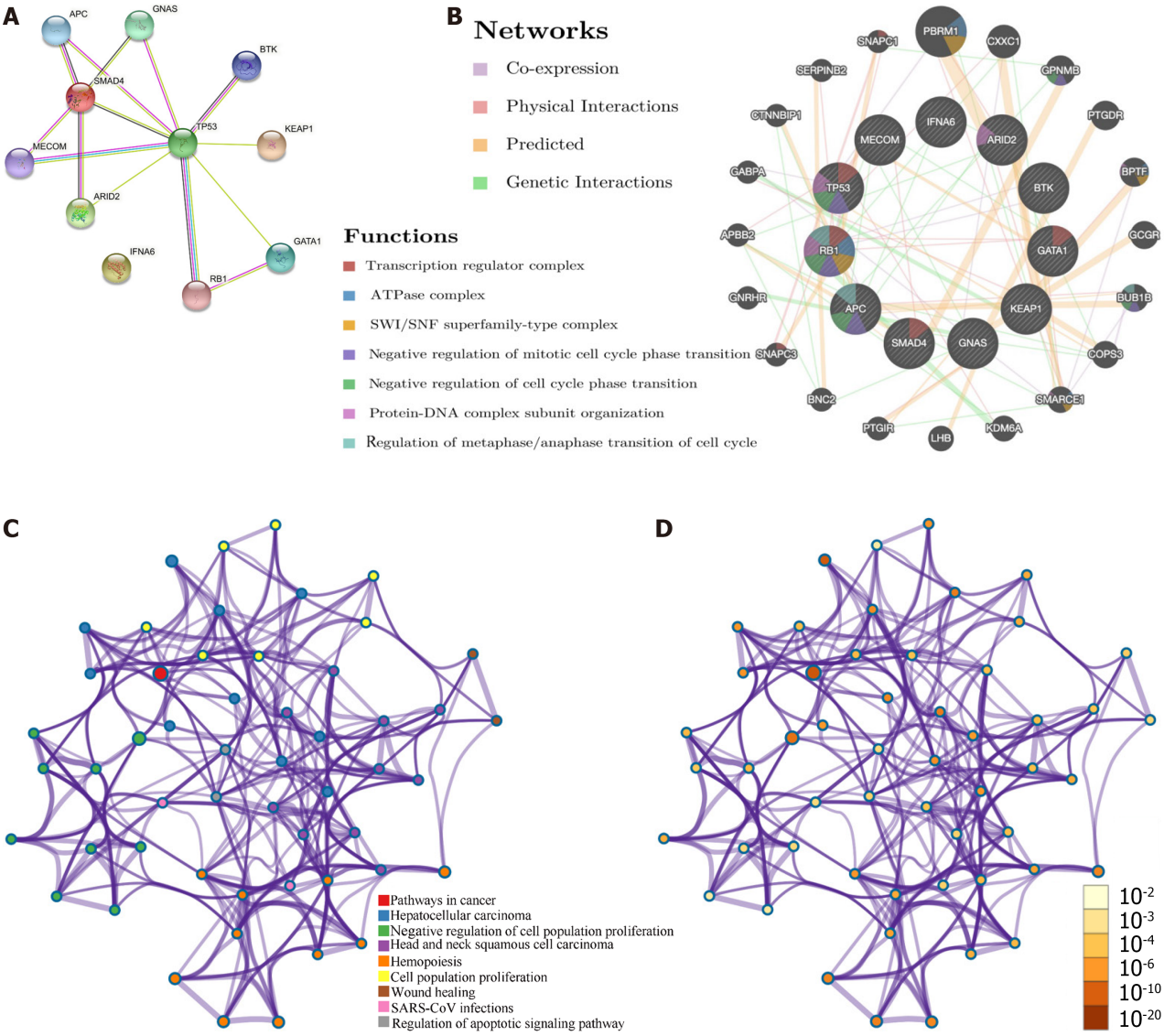

Figure 6 Interaction network analyses. A and B: The protein-protein interaction network was constructed using 12 mutated genes; C and D: Protein-protein interaction enrichment analysis was performed to explore functional relationships between these 12 mutated genes.

after surgery.

Globally, there are no definitive guidelines or consensus on optimal treatment strategies for gallbladder NEC. Treatment options for gallbladder NEC are typically guided by recommendations for gallbladder cancer. In early-stage gallbladder NEC, radical surgery can improve long-term survival, while chemotherapy serves as a palliative treatment modality for advanced cases, though its efficacy remains debatable. Wang *et al*[3] assessed 62 patients with gallbladder NECs and found no significant impact of postoperative adjuvant chemotherapy on overall survival. Similarly, a large multicenter study in China reported no improvement in long-term survival using platinum-based chemotherapy as an adjuvant therapy[16]. However, a Japanese case report enumerated upon a complete response to a combination of cisplatin, irinotecan, and radiotherapy in advanced gallbladder NEC, with no recurrence after 3 years of follow-up[23]. Ayabe *et al*[24] analyzed survival outcomes for patients with gastrointestinal NETs and gallbladder adenocarcinomas using a national database, revealing that gallbladder NECs are associated with the poorest survival among gastrointestinal NETs, although their prognosis is better than that of gallbladder adenocarcinomas.

The dependence of the study on a single case report, albeit justified given the rarity of gallbladder NEC, inherently limits the generalizability of the findings. Although it provides valuable insights into the unique clinical, histopathological, and molecular characteristics of this malignancy, a single case cannot fully reflect the heterogeneity and complexity of the disease across patients. The identified genetic mutations, TMB, and molecular pathways may not be representative of all cases, given the potential for significant variation in the genetic and biological behavior of gallbladder NEC. To address this limitation, future research should aim to expand the sample size by including multiple cases of gallbladder NEC, potentially through multicenter collaborations between different institutions that pool resources and data to conduct larger-scale studies. Such efforts would increase the statistical accuracy of the findings and provide a broader understanding of the commonalities and differences among cases, thereby enhancing the generalizability of the results.

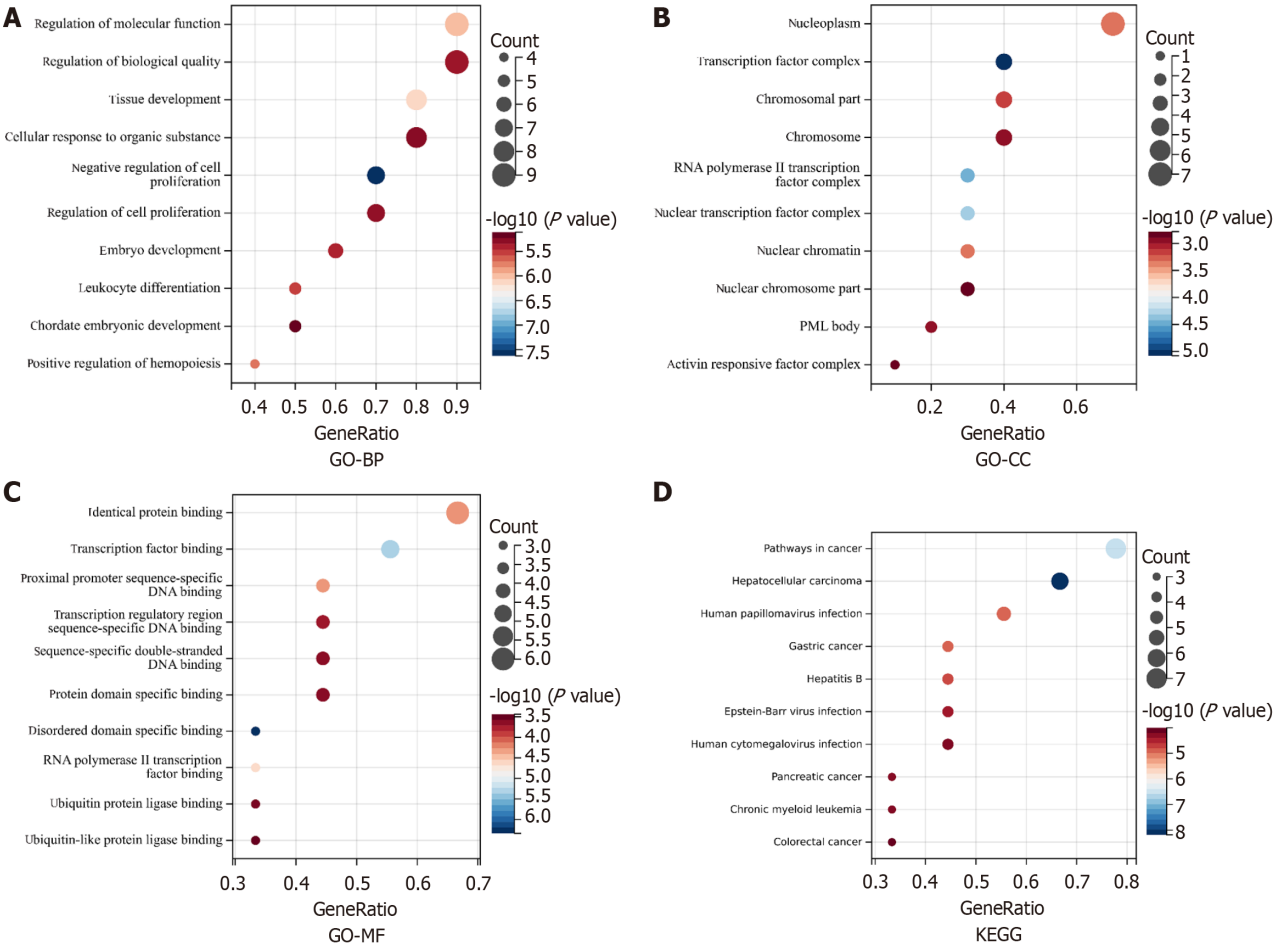

Figure 7 Significantly enriched Gene Ontology terms and Kyoto Encyclopedia of Genes and Genomes pathways for mutated genes. A-D: Gene Ontology analysis of biological processes (A), cellular components (B), molecular function (C), and Kyoto Encyclopedia of Genes and Genomes enrichment analysis (D); E and F: The Metascape database yielded similar results for the mutated genes. GO: Gene Ontology; BP: Biological processes; CC: Cellular

components; MF: Molecular function; KEGG: Kyoto Encyclopedia of Genes and Genomes.

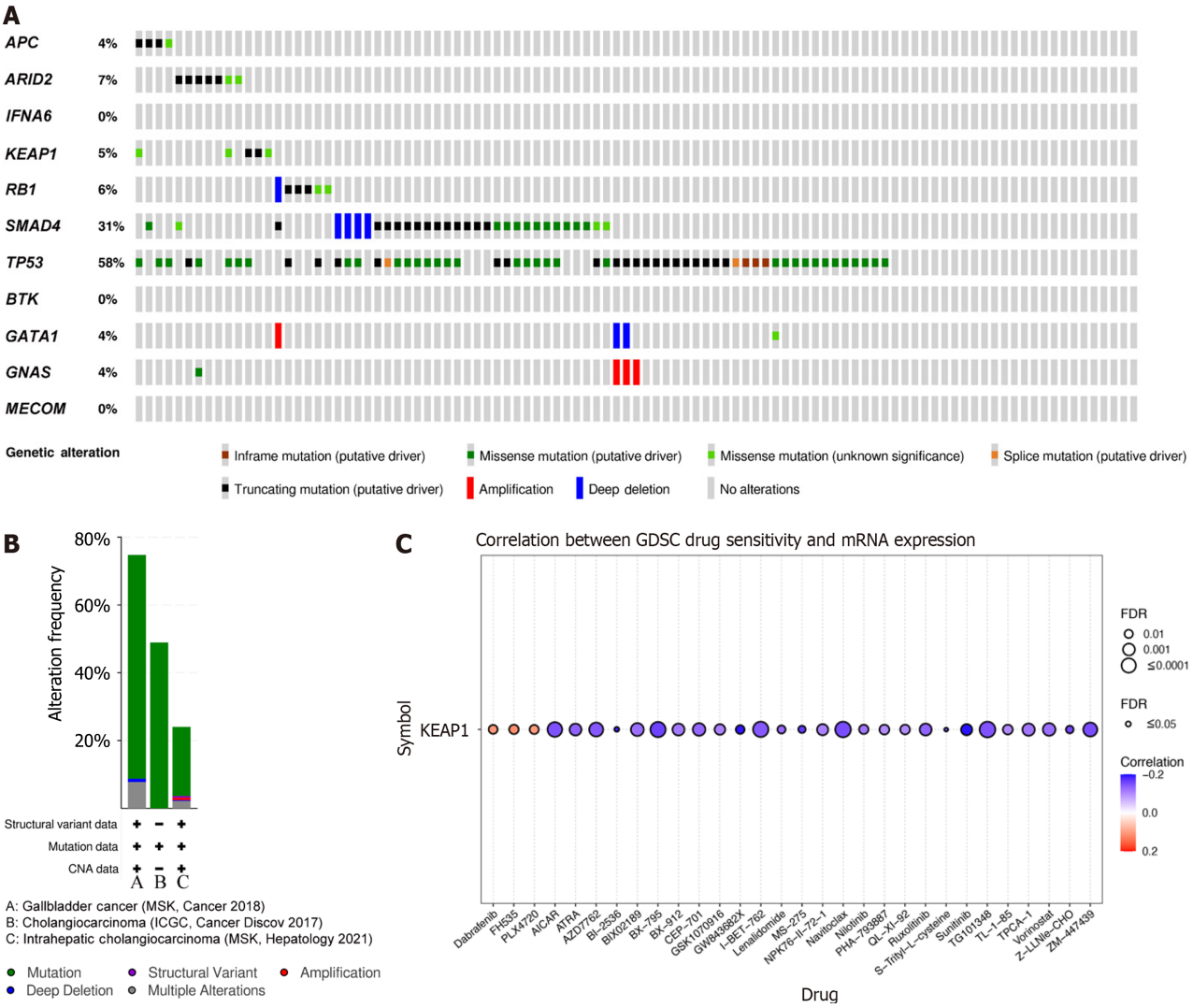

Figure 8 Gene mutations in gallbladder carcinomas. A: A summary of alterations in the 12 queried gene mutations from the cBioPortal database; B: Detailed summary of alterations in the 12 mutated genes; C: The correlation between KEAP1 expression and the sensitivity to GDSC drugs (top 30) in pan-cancer analysis.

CONCLUSION

In summary, a rare case of rare gallbladder NEC was presented, and clinicopathologic and genetic characteristics were discussed. The prognosis of gallbladder NEC was unsatisfactory. Gene sequencing tests may improve clinical management and disease prognosis. Studies involving a higher number of cases are needed to investigate more effective treatments for gallbladder NEC.

FOOTNOTES

Author contributions: Yang YC, Chen ZT, and Wan DL made substantial contributions to the conception and design of the study and critically revised the manuscript; Yang YC and Chen ZT were responsible for data collection, analysis, and manuscript writing; Tang H performed pathological evaluations; Wan DL and Liu ML made critical revisions; all authors assume full responsibility for the integrity and accuracy of the work, ensuring that all relevant queries were appropriately addressed; the final version of the manuscript has been reviewed and approved by all authors.

Supported by School-Level Key Projects at Bengbu Medical College, No. 2021byzd109.

Informed consent statement: Informed written consent was obtained from the patient for the publication of this report and the

accompanying images.

Conflict-of-interest statement: All the authors state that there are no conflicts of interest to declare.

CARE Checklist (2016) statement: The authors have read the CARE Checklist (2016), and the manuscript was prepared and revised according to the CARE Checklist (2016).

Country of origin: China

ORCID number: Yun-Chuan Yang 0009-0001-7541-1192; Zhi-Tao Chen 0000-0001-9469-7176; Da-Long Wan 0000-0001-8912-770X; Mu-Lin Liu 0000-0002-4744-5715.

S-Editor: Lin C
L-Editor: A
P-Editor: Zhao S

REFERENCES

1 **Zhu J**, Xiao W, Li Y. Management of Primary Hepatopancreatobiliary and Ampulla Large Cell Neuroendocrine Carcinoma. *J Laparoendosc Adv Surg Tech A* 2022; **32**: 639-645 [PMID: 34637632 DOI: 10.1089/lap.2021.0482]
2 **Chu H**, Zhang C, Shi Y, Wu W, Hu Z, Zhang J, Huang D. Gallbladder neuroendocrine carcinoma: A single center experience. *Medicine (Baltimore)* 2020; **99**: e21912 [PMID: 32899024 DOI: 10.1097/MD.0000000000021912]
3 **Wang W**, Yang CX, Yu XZ, Zhang SL, Wang J, Wang J. Clinicopathological characteristics and prognostic factors of patients with primary gallbladder neuroendocrine carcinomas. *J Dig Dis* 2022; **23**: 166-173 [PMID: 35187836 DOI: 10.1111/1751-2980.13088]
4 **Li M**, Liu F, Zhang Y, Wu X, Wu W, Wang XA, Zhao S, Liu S, Liang H, Zhang F, Ma Q, Xiang S, Li H, Jiang L, Hu Y, Gong W, Zhang Y, Ma T, Zhang K, Liu Y, Liu Y. Whole-genome sequencing reveals the mutational landscape of metastatic small-cell gallbladder neuroendocrine carcinoma (GB-SCNEC). *Cancer Lett* 2017; **391**: 20-27 [PMID: 28040546 DOI: 10.1016/j.canlet.2016.12.027]
5 **Vortmeyer AO**, Lubensky IA, Merino MJ, Wang CY, Pham T, Furth EE, Zhuang Z. Concordance of genetic alterations in poorly differentiated colorectal neuroendocrine carcinomas and associated adenocarcinomas. *J Natl Cancer Inst* 1997; **89**: 1448-1453 [PMID: 9326914 DOI: 10.1093/jnci/89.19.1448]
6 **Szklarczyk D**, Gable AL, Lyon D, Junge A, Wyder S, Huerta-Cepas J, Simonovic M, Doncheva NT, Morris JH, Bork P, Jensen LJ, Mering CV. STRING v11: protein-protein association networks with increased coverage, supporting functional discovery in genome-wide experimental datasets. *Nucleic Acids Res* 2019; **47**: D607-D613 [PMID: 30476243 DOI: 10.1093/nar/gky1131]
7 **Franz M**, Rodriguez H, Lopes C, Zuberi K, Montojo J, Bader GD, Morris Q. GeneMANIA update 2018. *Nucleic Acids Res* 2018; **46**: W60-W64 [PMID: 29912392 DOI: 10.1093/nar/gky311]
8 **Han H**, Cho JW, Lee S, Yun A, Kim H, Bae D, Yang S, Kim CY, Lee M, Kim E, Lee S, Kang B, Jeong D, Kim Y, Jeon HN, Jung H, Nam S, Chung M, Kim JH, Lee I. TRRUST v2: an expanded reference database of human and mouse transcriptional regulatory interactions. *Nucleic Acids Res* 2018; **46**: D380-D386 [PMID: 29087512 DOI: 10.1093/nar/gkx1013]
9 **Sakaki M**, Hirokawa M, Sano T, Horiguchi H, Wakatsuki S, Ogata S. Gallbladder Adenocarcinoma with Florid Neuroendocrine Cell Nests and Extensive Paneth Cell Metaplasia. *Endocr Pathol* 2000; **11**: 365-371 [PMID: 12114761 DOI: 10.1385/ep:11:4:365]
10 **Li M**, Liu F, Zhang F, Zhou W, Jiang X, Yang Y, Qu K, Wang Y, Ma Q, Wang T, Bai L, Wang Z, Song X, Zhu Y, Yuan R, Gao Y, Liu Y, Jin Y, Li H, Xiang S, Ye Y, Zhang Y, Jiang L, Hu Y, Hao Y, Lu W, Chen S, Gu J, Zhou J, Gong W, Zhang Y, Wang X, Liu X, Liu C, Liu H, Liu Y, Liu Y. Genomic ERBB2/ERBB3 mutations promote PD-L1-mediated immune escape in gallbladder cancer: a whole-exome sequencing analysis. *Gut* 2019; **68**: 1024-1033 [PMID: 29954840 DOI: 10.1136/gutjnl-2018-316039]
11 **Yamamoto M**, Kensler TW, Motohashi H. The KEAP1-NRF2 System: a Thiol-Based Sensor-Effector Apparatus for Maintaining Redox Homeostasis. *Physiol Rev* 2018; **98**: 1169-1203 [PMID: 29717933 DOI: 10.1152/physrev.00023.2017]
12 **Takahashi T**, Sonobe M, Menju T, Nakayama E, Mino N, Iwakiri S, Nagai S, Sato K, Miyahara R, Okubo K, Hirata T, Date H, Wada H. Mutations in Keap1 are a potential prognostic factor in resected non-small cell lung cancer. *J Surg Oncol* 2010; **101**: 500-506 [PMID: 20213688 DOI: 10.1002/jso.21520]
13 **Tian L**, Lu Y, Yang T, Deng Z, Xu L, Yao W, Ma C, Li X, Zhang J, Liu Y, Wang J. aPKCι promotes gallbladder cancer tumorigenesis and gemcitabine resistance by competing with Nrf2 for binding to Keap1. *Redox Biol* 2019; **22**: 101149 [PMID: 30822690 DOI: 10.1016/j.redox.2019.101149]
14 **Shibata T**, Kokubu A, Gotoh M, Ojima H, Ohta T, Yamamoto M, Hirohashi S. Genetic alteration of Keap1 confers constitutive Nrf2 activation and resistance to chemotherapy in gallbladder cancer. *Gastroenterology* 2008; **135**: 1358-1368, 1368.e1 [PMID: 18692501 DOI: 10.1053/j.gastro.2008.06.082]
15 **Liu F**, Li Y, Ying D, Qiu S, He Y, Li M, Liu Y, Zhang Y, Zhu Q, Hu Y, Liu L, Li G, Pan W, Jin W, Mu J, Cao Y, Liu Y. Whole-exome mutational landscape of neuroendocrine carcinomas of the gallbladder. *Signal Transduct Target Ther* 2021; **6**: 55 [PMID: 33563892 DOI: 10.1038/s41392-020-00412-3]
16 **Wang Y**, Huang B, Fu Q, Wang J, Ye M, Hu M, Qu K, Liu K, Hu X, Wei S, Sun K, Xiao W, Zhang B, Li H, Li J, Zhang Q, Liang T. Comprehensive Clinical Analysis of Gallbladder Neuroendocrine Neoplasms: A Large-Volume Multicenter Study During One Decade. *Ann Surg Oncol* 2022; **29**: 7619-7630 [PMID: 35849293 DOI: 10.1245/s10434-022-12107-w]

17 **Kim SH**, Kim SH, Kim MA, Shin CI, Han JK, Choi BI. CT differentiation of poorly-differentiated gastric neuroendocrine tumours from well-differentiated neuroendocrine tumours and gastric adenocarcinomas. *Eur Radiol* 2015; **25**: 1946-1957 [PMID: 25899412 DOI: 10.1007/s00330-015-3600-z]

18 **Bae JS**, Kim SH, Yoo J, Kim H, Han JK. Differential and prognostic MRI features of gallbladder neuroendocrine tumors and adenocarcinomas. *Eur Radiol* 2020; **30**: 2890-2901 [PMID: 32025835 DOI: 10.1007/s00330-019-06588-9]

19 **Faraoun SA**, Guerrache Y, Dautry R, Boudiaf M, Dohan A, Barral M, Hoeffel C, Rousset P, Fohlen A, Soyer P. Computed Tomographic Features of Primary Small Cell Neuroendocrine Tumors of the Gallbladder. *J Comput Assist Tomogr* 2018; **42**: 707-713 [PMID: 29901505 DOI: 10.1097/RCT.0000000000000753]

20 **Klimstra DS**, Modlin IR, Coppola D, Lloyd RV, Suster S. The pathologic classification of neuroendocrine tumors: a review of nomenclature, grading, and staging systems. *Pancreas* 2010; **39**: 707-712 [PMID: 20664470 DOI: 10.1097/MPA.0b013e3181ec124e]

21 **Do MY**, Jang SI, Kang HP, Kim EJ, Lee KJ, Park GE, Lee SJ, Lee DK, Woo SM, Cho JH. Comparison of the Clinical Features and Outcomes of Gallbladder Neuroendocrine Carcinoma with Those of Adenocarcinoma: A Propensity Score-Matched Analysis. *Cancers (Basel)* 2021; **13** [PMID: 34572940 DOI: 10.3390/cancers13184713]

22 **Yan S**, Wang Y, Chen X, Zhang Y, Huang Z, Zhao J, Zhou J, Li Z, Bi X, Luo Z, Cai J, Zhao H. Clinical Analysis of 15 Cases of Gallbladder Neuroendocrine Carcinoma and Comparison with Gallbladder Adenocarcinoma Using a Propensity Score Matching. *Cancer Manag Res* 2020; **12**: 1437-1446 [PMID: 32161496 DOI: 10.2147/CMAR.S227501]

23 **Takeda Y**, Kobayashi N, Kessoku T, Okubo N, Suzuki A, Tokuhisa M, Miwa H, Udaka N, Ichikawa Y. Case reports: chemoradiotherapy for locally advanced neuroendocrine carcinoma of the gallbladder. *Clin J Gastroenterol* 2022; **15**: 803-808 [PMID: 35653037 DOI: 10.1007/s12328-022-01645-1]

24 **Ayabe RI**, Wach M, Ruff S, Martin S, Diggs L, Wiemken T, Hinyard L, Davis JL, Luu C, Hernandez JM. Primary Gallbladder Neuroendocrine Tumors: Insights into a Rare Histology Using a Large National Database. *Ann Surg Oncol* 2019; **26**: 3577-3585 [PMID: 31102094 DOI: 10.1245/s10434-019-07440-6]

World Journal of Gastrointestinal Oncology

Submit a Manuscript: https://www.f6publishing.com

World J Gastrointest Oncol 2025 January 15; 17(1): 99083

DOI: 10.4251/wjgo.v17.i1.99083

ISSN 1948-5204 (online)

LETTER TO THE EDITOR

Advancing treatment strategies: Insights from network meta-analysis of hepatic arterial infusion chemotherapy for advanced hepatocellular carcinoma

Chun-Han Cheng, Wen-Rui Hao, Tzu-Hurng Cheng

Specialty type: Oncology

Provenance and peer review: Invited article; Externally peer reviewed.

Peer-review model: Single blind

Peer-review report's classification

Scientific Quality: Grade B

Novelty: Grade B

Creativity or Innovation: Grade B

Scientific Significance: Grade B

P-Reviewer: Miao YD

Received: July 13, 2024

Revised: September 26, 2024

Accepted: October 23, 2024

Published online: January 15, 2025

Processing time: 152 Days and 1.7 Hours

Chun-Han Cheng, Department of Medical Education, Linkou Chang Gung Memorial Hospital, Taoyuan City 33305, Taiwan

Wen-Rui Hao, Division of Cardiology, Department of Internal Medicine, Shuang Ho Hospital, Ministry of Health and Welfare, Taipei Medical University, New Taipei City 23561, Taiwan

Wen-Rui Hao, Division of Cardiology, Department of Internal Medicine, School of Medicine, College of Medicine, Taipei Medical University, Taipei 11002, Taiwan

Tzu-Hurng Cheng, Department of Biochemistry, School of Medicine, College of Medicine, China Medical University, Taichung City 404328, Taiwan

Co-first authors: Chun-Han Cheng and Wen-Rui Hao.

Corresponding author: Tzu-Hurng Cheng, PhD, Professor, Department of Biochemistry, School of Medicine, College of Medicine, China Medical University, No. 91 Xueshi Road, North District, Taichung City 404328, Taiwan. thcheng@mail.cmu.edu.tw

Abstract

This study examines the pivotal findings of the network meta-analysis of Zhou *et al*, which evaluated the efficacy of hepatic arterial infusion chemotherapy and combination therapies for advanced hepatocellular carcinoma (HCC). This meta-analysis suggests that therapeutic combinations have greater efficacy than do standard treatments. The article highlights the key insights that have the potential to shift current clinical practice and enhance outcomes for patients with advanced HCC. Additionally, this article discusses further research that can be conducted to optimize these treatments and achieve personalized care for patients with HCC.

Key Words: Hepatic arterial infusion chemotherapy; Advanced hepatocellular carcinoma; Combination therapy; Network meta-analysis; Treatment efficacy

Core Tip: This study discusses the comprehensive findings of the network meta-analysis of Zhou *et al* on hepatic arterial infusion chemotherapy (HAIC) and its combination strategies for advanced hepatocellular carcinoma. It highlights the efficacy and comparative benefits of HAIC in improving treatment outcomes and emphasizes its potential as a targeted therapeutic option in clinical practice.

Citation: Cheng CH, Hao WR, Cheng TH. Advancing treatment strategies: Insights from network meta-analysis of hepatic arterial infusion chemotherapy for advanced hepatocellular carcinoma. *World J Gastrointest Oncol* 2025; 17(1): 99083
URL: https://www.wjgnet.com/1948-5204/full/v17/i1/99083.htm
DOI: https://dx.doi.org/10.4251/wjgo.v17.i1.99083

TO THE EDITOR

The study of Zhou *et al*[1] published in the *World Journal of Gastrointestinal Oncology* presents a comprehensive network meta-analysis evaluating the efficacy of hepatic arterial infusion chemotherapy (HAIC) and its combination therapies for advanced hepatocellular carcinoma (HCC). HCC often presents in an advanced stage for which treatment options are limited, rendering treatment challenging. HAIC delivers potent anticancer agents directly to the tumor through the hepatic artery. The meta-analysis of Zhou *et al*[1] compares the effectiveness and safety of HAIC alone and in combination with other treatments. This study contextualizes the findings, explores their clinical implications, and discusses strategies for optimizing therapeutic approaches for managing advanced HCC. Studies such as that of Zuo *et al*[2] have highlighted the potential of combining HAIC with immune checkpoint inhibitors and antiangiogenic agents such as camrelizumab and apatinib to improve outcomes and survival in patients with advanced HCC. Mei *et al*[3] introduced the Assessment for Retreatment with HAIC (ARH) score as a tool to guide retreatment decisions on the basis of treatment response and disease progression. Moreover, Wang *et al*[4] examined the effects of a combination of programmed cell death protein-1 (PD-1) inhibitors, tyrosine kinase inhibitors (TKIs), and HAIC as a first-line treatment of advanced HCC associated with the hepatitis B virus (HBV), and they obtained promising tumor control and survival results. These studies illustrate the ongoing efforts to enhance therapeutic outcomes through innovative combinations and personalized treatment strategies tailored to the clinical profiles of patients with advanced HCC. In summary, the meta-analysis of Zhou *et al*[1] and recent advancements in combination therapies offer critical insights into the evolving role of HAIC in treating advanced HCC. This study provides clinicians with perspectives on current practices and to guide research and improve outcomes for patients who have received a diagnosis of this challenging condition.

Evolution of HAIC

HAIC was developed as a targeted treatment for HCC that utilizes the liver's unique vascular anatomy to deliver concentrated chemotherapy drugs directly to tumor sites, reducing systemic exposure and related toxicities[1]. This approach addresses the challenge of the liver's dual blood supply by enabling selective delivery of therapeutic agents through the hepatic artery, which primarily supplies HCC tumors. Advancements in HAIC have been driven by a deep understanding of HCC's pathophysiology and the need for localized treatment strategies involving high drug efficacy and small adverse effects. The network meta-analysis of Zhou *et al*[1] illustrates the comparative effectiveness of HAIC across therapeutic regimens, emphasizing the role of the treatment in improving survival and tumor response rates in patients with advanced HCC. Furthermore, recent studies have explored combination therapies aiming to enhance the efficacy of HAIC. For example, synergistic effects were found when HAIC was combined with immune checkpoint inhibitors such as camrelizumab and targeted therapies such as apatinib; antitumor immune responses were enhanced, and progression-free survival was extended[2]. Mei *et al*[3] emphasized the importance of personalizing treatment on the basis of a patient's response and disease progression. HAIC is thus a pivotal advancement in the management of HCC that enables tailored therapeutic approaches, maximizing efficacy and minimizing systemic toxicity. Researchers continue to refine HAIC protocols and explore new combinations to optimize outcomes for patients with advanced HCC.

Comparative effectiveness of HAIC and combination therapies

The network meta-analysis of Zhou *et al*[1] provides a comprehensive evaluation of HAIC alone and in combination with various therapeutic agents or modalities for advanced HCC. The meta-analysis provides a comparative assessment of outcomes such as tumor response rate, progression-free survival, and overall survival. Additionally, the meta-analysis indicates the efficacy of HAIC in delivering targeted therapy directly to liver tumors, using the liver's vascular anatomy to achieve high local drug concentrations and to minimize systemic toxicity. Zhou *et al*[1] employed a frequentist approach to compare the efficacy and safety of HAIC and its combination strategies for treating advanced HCC. This method estimates treatment effects by integrating direct and indirect evidence from multiple studies, enhancing the robustness of the comparative outcomes[1]. Zhou *et al*[1] used hazard ratios (HRs) and odds ratios (ORs) with 95% confidence intervals to evaluate overall survival, progression-free survival, the tumor response rate, and adverse events. HRs and ORs provide standardized measures of effect size across studies, enabling comparison of treatments with varying baseline characteristics[1]. Additionally, the *P*-score, which ranks treatments on the basis of the probability they are the best option, was calculated to provide a detailed interpretation of the relative efficacy of various therapeutic combinations[1]. Use of the *P*-score enabled the inclusion of studies that did not directly compare all treatments but

contributed valuable indirect comparisons. This approach is particularly relevant for HAIC, for which direct head-to-head trials are lacking. Combining direct and indirect evidence addresses gaps in the literature to provide a comprehensive understanding of the benefits and risks associated with various HAIC strategies[1]. This article references studies that have employed similar or complementary statistical methods, emphasizing the importance of robust analysis in advancing treatment strategies for HCC. For example, Zuo *et al*[2] employed a similar approach to demonstrate the effectiveness of the combination of HAIC, camrelizumab, and apatinib, validating the findings of Zhou *et al*[1] and highlighting the ability of innovative combination therapies to improve patient outcome. By highlighting the incorporation of detailed statistical methods in the meta-analysis of Zhou *et al*[1], this article underscores the reliability of network meta-analyses in guiding clinical decisions to advance HCC treatment. The methodological rigor of these studies supports this article's conclusions and suggests directions for future research and clinical practice[1]. Zhou *et al*[1] further discussed the synergistic benefits of combining HAIC with therapies such as immune checkpoint inhibitors (camrelizumab) and vascular endothelial growth factor receptor inhibitors (apatinib) that exhibit enhanced antitumor activity and provide long-term disease control in patients with advanced HCC[2,4]. Their findings underscore the focus of research on treating HCC with combination therapies involving HAIC to improve outcomes and patient survival.

Safety and tolerability profiles

Assessing the safety and tolerability of therapeutic regimens is integral to treating HCC. The network meta-analysis of Zhou *et al*[1] provides insights into the safety of HAIC and its combination therapies for advanced HCC. The meta-analysis highlights safety concerns such as hematological and hepatic toxicities and other treatment-related adverse events[1]. For example, when combined with an immunotherapy agent such as camrelizumab and targeted therapy such as apatinib, HAIC has manageable toxicity if a patient is carefully monitored[2]. Additionally, the retrospective study of Wang *et al*[4] highlights the balance that must be struck between efficacy and safety, particularly when integrating immune checkpoint inhibitors and TKIs with HAIC to treat advanced HCC associated with HBV. Managing treatment-related adverse effects is essential to optimizing outcomes and ensuring the feasibility of HAIC-based therapies for advanced HCC.

Clinical implications and future directions

The meta-analysis of Zhou *et al*[1] can inform clinical decision-making and shape research into HCC treatment strategies. Integrating these strategies into clinical practice can enhance outcomes for patients with advanced HCC. For example, combining HAIC with camrelizumab and apatinib may improve the efficacy and tolerability or HAIC[2]. Mei *et al*[3] emphasized the importance of personalized treatment approaches, suggesting the use of tools such as the ARH score to optimize retreatment decisions and manage adverse events. Future research must identify predictive biomarkers with which patient populations receiving tailored treatments can be identified. Additional research is required to develop combination therapies that minimize toxicity and maximize efficacy[4]. However, acknowledging gaps and challenges in the study of Zhou *et al*[1] is essential in examining the limitations of evidence regarding the efficacy of HAIC and its combination therapies. One major limitation is the heterogeneity among studies in the network meta-analysis; variations in design, patient populations, and treatment regimens may have affected the generalizability of the findings. The lack of direct comparisons between therapeutic strategies also complicates the interpretation of the results because indirect comparisons can introduce biases that weaken the conclusions[1]. Another limitation is the inadequate representation of certain combination therapies, particularly those involving novel agents such as immune checkpoint inhibitors. Although HAIC combined with PD-1 inhibitors and TKIs has potential, as noted by Wang *et al*[4], the retrospective nature of the studies and the absence of large-scale randomized controlled trials (RCTs) raise concerns regarding the robustness of the evidence supporting these combinations[1]. Future research must prioritize well-designed RCTs to validate the efficacy and safety of these novel combinations and establish standardized treatment protocols for broader clinical use. However, the literature does not address long-term outcomes or potential late-onset toxicities associated with HAIC and its combination therapies. Studies such as those of Zuo *et al*[2] and Mei *et al*[3] provide insights into short-term efficacy and safety, but more comprehensive studies are required to assess long-term survival, quality of life, and posttreatment complications. Future research must also identify and validate predictive biomarkers to enable personalized treatment approaches tailored to each individual patient's characteristics. Additionally, decision-making tools, such as the ARH score proposed by Mei *et al*[3], need to be refined and validated in larger cohorts to enhance their clinical utility[1]. Personalized treatment strategies must consider individual patient factors, specifically liver function, tumor burden, and molecular profiles, when evaluating the appropriateness of HAIC and its combination therapies. Using predictive biomarkers in clinical decision-making can help tailor treatment plans to maximize efficacy and minimize adverse effects [1]. Nevertheless, combining HAIC with modalities such as PD-1 inhibitors or TKIs must be approached cautiously until validated by large-scale RCTs. Clinicians must weigh the benefits against the risks, particularly for patients with compromised liver function or comorbidities[1]. Monitoring patients undergoing HAIC-based therapies in terms of their long-term outcomes and potential late-onset toxicities is critical; regular follow-ups and comprehensive assessments are required to manage adverse effects and ensure sustained therapeutic benefits[1]. Ongoing clinical trials can provide additional evidence regarding the effectiveness of HAIC and its combinations and enable refinement of treatment protocols and improvement of outcomes[1]. Addressing these limitations and incorporating these recommendations can help researchers and clinicians effectively harness HAIC's potential, improving the prognosis for patients with advanced HCC.

CONCLUSION

The network meta-analysis of Zhou *et al*[1] considerably advances our understanding of HAIC and its combination therapies for treating advanced HCC. Their findings illustrate HAIC's potency as a localized treatment that delivers high concentrations of chemotherapy agents directly to liver tumors and thereby minimizes systemic side effects[1]. This study summarizes the results of the meta-analysis, emphasizing the comparative efficacy of HAIC alone and in combination with other therapies. Additionally, this article examines HAIC's history, mechanistic benefits, and safety profiles highlighted in the analysis. The discussion addresses clinical implications, suggesting methods for optimizing treatment strategies and improving patient outcomes for those with advanced HCC. Future research should refine HAIC protocols, explore novel combinations such as HAIC with immunotherapy and targeted agents (*e.g.*, camrelizumab and apatinib), and identify biomarkers that can enable personalization of treatments[2-4]. These efforts can expand therapeutic options for advanced HCC, improving survival rates and patients' quality of life. In conclusion, the meta-analysis of Zhou *et al*[1] provides critical insights for future HCC treatment, validating the role of HAIC in managing this challenging disease.

FOOTNOTES

Author contributions: Cheng CH and Hao WR contribute equally to this study as co-first authors. Cheng CH and Hao WR wrote the paper; Cheng TH revised the paper; all authors have read and approved the final manuscript.

Conflict-of-interest statement: The authors declare having no conflicts of interest.

Country of origin: Taiwan

ORCID number: Tzu-Hurng Cheng 0000-0002-9155-4169.

S-Editor: Lin C
L-Editor: A
P-Editor: Zhao S

REFERENCES

1 **Zhou SA**, Zhou QM, Wu L, Chen ZH, Wu F, Chen ZR, Xu LQ, Gan BL, Jin HS, Shi N. Efficacy of hepatic arterial infusion chemotherapy and its combination strategies for advanced hepatocellular carcinoma: A network meta-analysis. *World J Gastrointest Oncol* 2024; **16**: 3672-3686 [PMID: 39171172 DOI: 10.4251/wjgo.v16.i8.3672]

2 **Zuo M**, Cao Y, Yang Y, Zheng G, Li D, Shao H, Ma Q, Song P, An C, Li W. Hepatic arterial infusion chemotherapy plus camrelizumab and apatinib for advanced hepatocellular carcinoma. *Hepatol Int* 2024; **18**: 1486-1498 [PMID: 38961006 DOI: 10.1007/s12072-024-10690-6]

3 **Mei J**, Yu C, Shi F, Guan R, Li S, Zhong C, Guo R, Wei W. The ARH score, a practical guide to decision-making for retreatment with hepatic arterial infusion chemotherapy in hepatocellular carcinoma patients. *Int Immunopharmacol* 2024; **138**: 112551 [PMID: 38950459 DOI: 10.1016/j.intimp.2024.112551]

4 **Wang D**, Zhang Z, Yang L, Zhao L, Liu Z, Lou C. PD-1 Inhibitors Combined with Tyrosine Kinase Inhibitors with or without Hepatic Artery Infusion Chemotherapy for the First-Line Treatment of HBV-Related Advanced Hepatocellular Carcinoma: A Retrospective Study. *J Hepatocell Carcinoma* 2024; **11**: 1157-1170 [PMID: 38911293 DOI: 10.2147/JHC.S457527]

World Journal of Gastrointestinal Oncology

Submit a Manuscript: https://www.f6publishing.com

World J Gastrointest Oncol 2025 January 15; 17(1): 99994

DOI: 10.4251/wjgo.v17.i1.99994

ISSN 1948-5204 (online)

LETTER TO THE EDITOR

Gallbladder carcinoma in the era of artificial intelligence: Early diagnosis for better treatment

Ismail AS Burud, Sherreen Elhariri, Nabil Eid

Specialty type: Oncology

Provenance and peer review: Invited article; Externally peer reviewed.

Peer-review model: Single blind

Peer-review report's classification

Scientific Quality: Grade A
Novelty: Grade A
Creativity or Innovation: Grade A
Scientific Significance: Grade A

P-Reviewer: Yang J

Received: August 5, 2024
Revised: October 22, 2024
Accepted: October 24, 2024
Published online: January 15, 2025
Processing time: 129 Days and 6.9 Hours

Ismail AS Burud, Sherreen Elhariri, Department of Surgery, Clinical Campus, IMU University, Seremban 70300, Negeri Sembilan, Malaysia

Nabil Eid, Department of Anatomy, Division of Human Biology, School of Medicine, IMU University, Kuala Lumpur 57000, Kuala Lumpur, Malaysia

Corresponding author: Nabil Eid, MD, PhD, Associate Professor, Senior Lecturer, Department of Anatomy, Division of Human Biology, School of Medicine, IMU University, Bukit Jalil, Kuala Lumpur 57000, Kuala Lumpur, Malaysia. nabilsaleheid@imu.edu.my

Abstract

Gallbladder carcinoma (GBC) is the most common malignant tumor of biliary tract, with poor prognosis due to its aggressive nature and limited therapeutic options. Early detection of GBC is a major challenge, with most GBCs being detected accidentally during cholecystectomy procedures for gallbladder stones. This letter comments on the recent article by Deqing *et al* in the *World Journal of Gastrointestinal Oncology*, which summarized the various current methods used in early diagnosis of GBC, including endoscopic ultrasound (EUS) examination of the gallbladder for high-risk GBC patients, and the use of EUS-guided elastography, contrast-enhanced EUS, trans-papillary biopsy, natural orifice translumenal endoscopic surgery, magnifying endoscopy, choledochoscopy, and confocal laser endomicroscopy when necessary for early diagnosis of GBC. However, there is a need for novel methods for early GBC diagnosis, such as the use of artificial intelligence and non-coding RNA biomarkers for improved screening protocols. Additionally, the use of *in vitro* and animal models may provide critical insights for advancing early detection and treatment strategies of this aggressive tumor.

Key Words: Gallbladder carcinoma; Endoscopic ultrasound; Biopsy; Elastography; Choledochoscopy; Artificial intelligence; Non-coding RNAs; Screening; Animal models; *In vitro* studies

Core Tip: Gallbladder carcinoma is the most common malignant tumor of biliary tract, with poor prognosis due to its aggressive nature and limited therapeutic options. Current methods available for early screening include endoscopic ultrasound (EUS) examination, EUS-guided elastography, contrast-enhanced EUS, trans-papillary biopsy, natural orifice transluminal endoscopic surgery, magnifying endoscopy, choledochoscopy, and confocal laser endomicroscopy. Despite these established modalities, there is a need for innovative diagnostic methods, particularly the use of artificial intelligence and non-coding RNA biomarkers, to improve screening protocols and facilitate earlier disease detection.

Citation: Burud IA, Elhariri S, Eid N. Gallbladder carcinoma in the era of artificial intelligence: Early diagnosis for better treatment. *World J Gastrointest Oncol* 2025; 17(1): 99994
URL: https://www.wjgnet.com/1948-5204/full/v17/i1/99994.htm
DOI: https://dx.doi.org/10.4251/wjgo.v17.i1.99994

TO THE EDITOR

Gallbladder carcinoma (GBC) is the most common biliary malignant tumor with an aggressive nature and poor prognosis [1,2]. The editorial reported by Deqing *et al*[1]: "Endoscopic diagnosis and management of Gallbladder carcinoma in a minimally invasive era: New needs, new models", highlighted various minimally invasive diagnostic and therapeutic procedures in GBC. This editorial written by Deqing *et al*[1] was based on the work published by Pavlidis *et al*[2]: "New Trends in the Diagnosis and Management of Gallbladder Carcinoma". GBC is diagnosed late and has a poor prognosis with a 5-year survival rate of 13%[3].

Imaging, endoscopic and non-endoscopic methods for early detection of GBC

Deqing *et al*[1] emphasized the early detection of GBC and recommended incorporating endoscopic ultrasound (EUS) examination of the gallbladder inner wall as a quality control indicator for high-risk GBC patients. They also advocated using EUS-guided elastography, contrast-enhanced EUS, trans-papillary biopsy, natural orifice transluminal endoscopic surgery, magnifying endoscopy, choledochoscopy, and confocal laser endomicroscopy, when necessary for early diagnosis of GBC[1].

Other new emerging modalities used for differentiating benign and malignant lesions in the liver and breast such as real-time elastography using acoustic radiation force impulse (ARFI) could play an important role in the diagnosis of GBC[4,5]. Routine use of ARFI while doing ultrasonography combined with multidimensional computed tomography (CT) and contrast-enhanced endoscopic ultrasonography can help diagnose and stage early diffuse wall thickening type GBC[6].

The use of dual-time-point 18F-fluoro-2-deoxy-2-D-glucose [(18)F-FDG] positron emission tomography (PET) has also shown encouraging results in predicting gall bladder malignancy in gall bladder polyps. Delayed (18)F-FDG PET is more helpful than early (18)F-FDG PET for evaluating malignant lesions because of increased lesion uptake and increased lesion-to-background contrast, and when combined with the retention index, sensitivity is increased to 100% and specificity to 80%[2,7].

Early diagnosis of GBC using artificial intelligence and non-coding RNAs

Recent investigations have examined the potential of artificial intelligence (AI) in enhancing the detection and early diagnosis of GBC through CT imaging analysis. Deep learning AI algorithms have demonstrated particularly promising results, with improved efficacy and accuracy at early diagnosis of GBC, achieving accuracy rates of 98.35% using deep neural networks and MobileNet architectures. Conventional neural network approaches have shown moderate efficacy, with an area under the curve of 0.81. Despite their considerable promise, several barriers to clinical implementation persist, including regulatory compliance requirements, ethical considerations, as well as the need for validation and integration within existing clinal workflows. Despite these challenges, the integration of AI in CT scan analyses presents a promising method for the early diagnosis of GBC[8].

The early identification of GBC is a major clinical challenge, with most cases being discovered accidentally during cholecystectomy procedures performed for gallbladder stones. At present, there is a lack of effective population- level screening tests for GBC. Traditional tumor markers, including carcinoembryonic antigen and carbohydrate antigen 19-9 demonstrate limited diagnostic ability, particularly in early-stage GBC[9]. As a result, non-coding RNAs have emerged as potential novel biomarkers for early diagnosis and treatment of GBC, given their role in transcriptional regulation of target genes associated with solid tumor development[10,11]. However, there is a need for further research using both *in vitro* systems and experimental animal models to identify and validate new GBC-specific biomarkers[12].

The editorial by Deqing *et al*[1] presents limitations in its analysis, notably omitting crucial economic considerations related to novel GBC diagnostic technologies. A comprehensive evaluation should address the healthcare workforce and time costs, as well as medical insurance reimbursement implications, factors which are essential to assess feasibility of clinical implementation and integration into current systems to enhance the practicality and clinical relevance of their recommendations[13-15].

CONCLUSION

Current diagnosis methods for GBC cover a spectrum of techniques, such as EUS examination, EUS-guided elastography, contrast-enhanced EUS, trans-papillary biopsy, natural orifice transluminal endoscopic surgery, magnifying endoscopy, choledochoscopy, and confocal laser endomicroscopy. Despite the variety of diagnostic techniques available, early detection of GBC remains a major challenge, with most GBCs being detected accidentally during cholecystectomy procedures for gallbladder stones. This challenge has prompted the study of new modalities for early detection of GBC, particularly into AI and non-coding RNA biomarkers to improve screening protocols for GBC. Additionally, further research using *in vitro* systems and animal models of GBC is essential to develop novel diagnostic approaches and detect new biomarkers to assist with early diagnosis and better treatment of this aggressive tumor.

FOOTNOTES

Author contributions: Eid N wrote, revised and approved the final draft of the manuscript; Burud IAS and Elhariri S wrote the manuscript; All authors have read and approved the final manuscript.

Conflict-of-interest statement: All the authors report no relevant conflicts of interest for this article.

Country of origin: Malaysia

ORCID number: Nabil Eid 0000-0002-2938-2618.

S-Editor: Gao CC
L-Editor: A
P-Editor: Xu ZH

REFERENCES

1 **Deqing LC**, Zhang JW, Yang J. Endoscopic diagnosis and management of gallbladder carcinoma in minimally invasive era: New needs, new models. *World J Gastrointest Oncol* 2024; **16**: 4333-4337
2 **Pavlidis ET**, Galanis IN, Pavlidis TE. New trends in diagnosis and management of gallbladder carcinoma. *World J Gastrointest Oncol* 2024; **16**: 13-29 [PMID: 38292841 DOI: 10.4251/wjgo.v16.i1.13]
3 **Lau CSM**, Zywot A, Mahendraraj K, Chamberlain RS. Gallbladder Carcinoma in the United States: A Population Based Clinical Outcomes Study Involving 22,343 Patients from the Surveillance, Epidemiology, and End Result Database (1973-2013). *HPB Surg* 2017; **2017**: 1532835 [PMID: 28638176 DOI: 10.1155/2017/1532835]
4 **Fahey BJ**, Nelson RC, Bradway DP, Hsu SJ, Dumont DM, Trahey GE. In vivo visualization of abdominal malignancies with acoustic radiation force elastography. *Phys Med Biol* 2008; **53**: 279-293 [PMID: 18182703 DOI: 10.1088/0031-9155/53/1/020]
5 **Cho SH**, Lee JY, Han JK, Choi BI. Acoustic radiation force impulse elastography for the evaluation of focal solid hepatic lesions: preliminary findings. *Ultrasound Med Biol* 2010; **36**: 202-208 [PMID: 20018432 DOI: 10.1016/j.ultrasmedbio.2009.10.009]
6 **Vijayakumar A**, Vijayakumar A, Patil V, Mallikarjuna MN, Shivaswamy BS. Early diagnosis of gallbladder carcinoma: an algorithm approach. *ISRN Radiol* 2013; **2013**: 239424 [PMID: 24959553 DOI: 10.5402/2013/239424]
7 **Nishiyama Y**, Yamamoto Y, Fukunaga K, Kimura N, Miki A, Sasakawa Y, Wakabayashi H, Satoh K, Ohkawa M. Dual-time-point 18F-FDG PET for the evaluation of gallbladder carcinoma. *J Nucl Med* 2006; **47**: 633-638 [PMID: 16595497]
8 **Sehrawat A**, Gopi VP, Gupta A. A Systematic Review on Role of Deep Learning in CT scan for Detection of Gall Bladder Cancer. *Arch Computat Methods Eng* 2024; **31**: 3303-3311 [DOI: 10.1007/s11831-024-10073-y]
9 **Roa JC**, García P, Kapoor VK, Maithel SK, Javle M, Koshiol J. Gallbladder cancer. *Nat Rev Dis Primers* 2022; **8**: 69 [PMID: 36302789 DOI: 10.1038/s41572-022-00398-y]
10 **Shahin RK**, Elkady MA, Abulsoud AI, Abdelmaksoud NM, Abdel Mageed SS, El-Dakroury WA, Zewail MB, Elazazy M, Sobhy MH, Nomier Y, Elazazy O, Elballal MS, Mohammed OA, Midan HM, Elrebehy MA, Ziada BO, Doghish AS. miRNAs orchestration of gallbladder cancer - Particular emphasis on diagnosis, progression and drug resistance. *Pathol Res Pract* 2023; **248**: 154684 [PMID: 37454489 DOI: 10.1016/j.prp.2023.154684]
11 **Eid N**, Davamani F. Human β-defensin-1 activates autophagy in human colon cancer cells *via* regulation of long non-coding RNA TCONS_00014506. *World J Gastrointest Oncol* 2024; **16**: 2894-2901 [PMID: 39072156 DOI: 10.4251/wjgo.v16.i7.2894]
12 **Kato S**, Fushimi K, Yabuki Y, Maru Y, Hasegawa S, Matsuura T, Kurotaki D, Suzuki A, Kobayashi N, Yoneda M, Higurashi T, Enaka M, Tamura T, Hippo Y, Nakajima A. Precision modeling of gall bladder cancer patients in mice based on orthotopic implantation of organoid-derived tumor buds. *Oncogenesis* 2021; **10**: 33 [PMID: 33866327 DOI: 10.1038/s41389-021-00322-1]
13 **Lundgren L**, Henriksson M, Andersson B, Sandström P. Cost-effectiveness of gallbladder histopathology after cholecystectomy for benign disease. *BJS Open* 2020; **4**: 1125-1136 [PMID: 33136336 DOI: 10.1002/bjs5.50325]
14 **Salazar M**, Ituarte C, Abriata MG, Santoro F, Arroyo G. Gallbladder cancer in South America: epidemiology and prevention. *Chin Clin Oncol*

2019; **8**: 32 [PMID: 31431040 DOI: 10.21037/cco.2019.07.12]

15 **Patel K**, Dajani K, Vickramarajah S, Huguet E. Five year experience of gallbladder polyp surveillance and cost effective analysis against new European consensus guidelines. *HPB (Oxford)* 2019; **21**: 636-642 [PMID: 30416065 DOI: 10.1016/j.hpb.2018.10.008]

World Journal of Gastrointestinal Oncology

Submit a Manuscript: https://www.f6publishing.com

World J Gastrointest Oncol 2025 January 15; 17(1): 100199

DOI: 10.4251/wjgo.v17.i1.100199

ISSN 1948-5204 (online)

LETTER TO THE EDITOR

Controversies around the treatment of peritoneal metastases of colorectal cancer

Francisco J Morera-Ocon, Clara Navarro-Campoy, Ticiano Guastella, Francisco Landete-Molina

Specialty type: Oncology

Provenance and peer review: Invited article; Externally peer reviewed.

Peer-review model: Single blind

Peer-review report's classification

Scientific Quality: Grade A
Novelty: Grade A
Creativity or Innovation: Grade A
Scientific Significance: Grade A

P-Reviewer: Li S

Received: August 9, 2024
Revised: October 24, 2024
Accepted: November 7, 2024
Published online: January 15, 2025
Processing time: 124 Days and 22.7 Hours

Francisco J Morera-Ocon, Francisco Landete-Molina, Department of General Surgery, Hospital General de Requena, Requena 46340, Spain

Clara Navarro-Campoy, Department of Gynecology and Obstetrics, Hospital 9 Octubre, Valencia 46015, Spain

Ticiano Guastella, Department of Pathology, Hospital General de Requena, Requena 46340, Spain

Corresponding author: Francisco J Morera-Ocon, PhD, Surgeon, Surgical Oncologist, Department of General Surgery, Hospital General de Requena, Paraje Casablanca s/n, Requena 46340, Spain. fmoreraocon@gmail.com

Abstract

In this editorial we examine the article by Wu *et al* published in the *World Journal of Gastrointestinal Oncology*. Surgical resection for peritoneal metastases from colorectal cancer (CRC) has been gradually accepted in the medical oncology community. A randomized trial (PRODIGE 7) on cytoreductive surgery (CRS) with hyperthermic intraperitoneal chemotherapy (HIPEC) failed to prove any benefit of oxaliplatin in the overall survival of patients with peritoneal metastases from colorectal origin. Nevertheless, isolated systemic chemotherapy for CRC stage IV has demonstrated a reduced response in peritoneal metastases than that obtained in other metastatic sites such as the liver. Another tool is required in those patients to achieve more local control of the disease. Surgical groups in peritoneal surgery continue to use HIPEC in their procedures, using other agents than oxaliplatin for peritoneal cavity infusion, such as mitomycin C. These patients present with complex surgical issues to manage, and consequently a large burden of complications has to be anticipated. Therefore, identifying patients who will benefit from CRS with or without HIPEC would be of great interest.

Key Words: Colorectal cancer; Peritoneal metastasis; Hyperthermic intraoperative chemotherapy; Treatment strategies; Peritoneal Surface Oncology GroupInternational

Core Tip: Local control of peritoneal metastasis in colorectal cancer requires surgical resection to assist the outcome of systemic chemotherapy and target therapy. Despite the negative results of a randomized phase III trial studying the effect of oxaliplatin as a hyperthermic intraperitoneal chemotherapy (HIPEC) agent, HIPEC therapy may work in synergy with complete surgical resection to achieve locoregional control of the disease. Studies focusing on diagnostic tools to achieve better selection of patients who will benefit from comprehensive treatment (surgery, HIPEC, and systemic chemotherapy) are welcome.

Citation: Morera-Ocon FJ, Navarro-Campoy C, Guastella T, Landete-Molina F. Controversies around the treatment of peritoneal metastases of colorectal cancer. *World J Gastrointest Oncol* 2025; 17(1): 100199
URL: https://www.wjgnet.com/1948-5204/full/v17/i1/100199.htm
DOI: https://dx.doi.org/10.4251/wjgo.v17.i1.100199

TO THE EDITOR

The term "peritoneal carcinomatosis" has contributed to maintaining the nihilistic approach of the medical oncology community and general surgeons toward surgical resection as part in the treatment of colorectal cancer (CRC) peritoneal metastases. Until recently, surgery for these patients has only been considered as palliative treatment[1]. Nevertheless, the medical oncology community has always considered surgery as the standard treatment approach for patients with resectable oligometastatic disease of CRC origin, "even in the absence of randomized trials comparing surgical with non-surgical disease management", as written by the authors of ESMO consensus guidelines for the management of patients with metastatic CRC in 2016[2]. Consequently, when surgical treatment of liver metastases from CRC began, the strategy was easily embraced by the oncologic community, even before any dedicated randomized trial was complete. Peritoneal surgery, unlike liver surgery, has never received the same recognition.

The conventional therapy for patients with CRC peritoneal metastases is based on systemic chemotherapy that aims to obtain prolongation of survival and symptomatic relief. Keeping in mind that isolated modern chemotherapy regimens have poorer efficacy in patients with CRC peritoneal metastases than in patients with other metastatic sites[3,4], it would be desirable to make available a more aggressive locoregional therapy to address the peritoneal involvement.

DEVELOPMENT OF PERITONEAL SURGERY

In the 1980s and 1990s, surgical pioneers in peritoneal surface malignancies: Paul Sugarbaker[5], François Gilly[6], Dominique Elias[7], and Franz Zoetmulder[8], developed surgical techniques to address malignant involvement of the peritoneal cavity, naming those procedures cytoreductive surgery (CRS). Surgeons worldwide trained in this surgical expertise, and an international group (Peritoneal Surface Oncology Group International (PSOGI), 1998) and other national groups (for example the Grupo Español de Cirugía Oncológica Peritoneal (GECOP) 2007, in Spain) were founded. Within these surgical groups, the combination of hyperthermic intraperitoneal chemotherapy (HIPEC) with CRS has always been considered.

The rational for the association of CRS and HIPEC is to achieve a complete surgical resection of all macroscopic disease within the peritoneal cavity, and to treat the residual microscopic disease (or residual nodules less than 2.5 mm in diameter) with intraperitoneal chemotherapy[9].

Other surgical groups also perform peritoneal metastatic resection without the use of HIPEC[10-12]. The reason for not using HIPEC is mostly due to its presumed high morbidity. In 2016, Baratti *et al*[13] conducted a systematic review on CRC peritoneal metastases treatment, based on retrospectives studies, and showed the benefits of comprehensive treatment with CRS and HIPEC. For comparison purposes, only retrospective studies have ever been required for the acceptance of surgical treatment of CRC liver metastases. For CRS/HIPEC, there is a greater demand required to prove its benefits, and the lack of randomized trials has been underscored.

CONTROVERSIAL STUDIES ON CYTOREDUCTIVE SURGERY AND HIPEC

A phase III randomized trial was conducted by Verwaal *et al*[14] comparing CRS/HIPEC to the standard treatment at the time, *i.e.* systemic chemotherapy with 5-fluorouracil (5-FU) and leucovorin. The results revealed a median survival of 12.6 months in the standard therapy arm, and 22.3 months in the HIPEC group ($P = 0.032$), but the median follow-up was only 21.6 months. This study generated a great deal of criticism. It was mainly criticized as cases of peritoneal disease from mucinous appendicular neoplasia were present within the included patients in the HIPEC group, and the study was performed in the era of 5-FU. Subsequently, chemotherapy and target therapy for CRC have evolved since then with increased overall survival (OS).

The results of PRODIGE 7, a multicenter French randomized phase III trial comparing CRS/HIPEC with CRS alone for CRC peritoneal metastases, were presented at the ASCO meeting and published as an abstract in 2018[15]. Curiously, the

manuscript was not published until 2021[16].

The study included 133 patients in the CRS/HIPEC arm, and 132 patients in the CRS alone group. After a median follow-up of 63.8 months, the median OS was 41.7 months in the CRS/HIPEC group and 41.2 months in the CRS alone group (P = 0.99). The negative result for HIPEC in this study made us recall Thomas Henry Huxley at The Address at the Meeting of the British Association at Liverpool (1870), when he said: "But the great tragedy of Science-the slaying of a beautiful hypothesis by an ugly fact … was played, almost immediately, for the benefit of Buffon and Needham"[17]. In this case, the results of PRODIGE 7 were promptly "played for the benefit of" the anti-HIPEC adversaries[18].

In the PRODIGE 7 study, systemic 5-FU and folinic acid were delivered intravenously 20 minutes before intraperitoneal infusion of oxaliplatin at 43 ºC over 30 minutes[16]. From their results it appears that "the beautiful hypothesis" of the benefit of oxaliplatin as locoregional treatment for microscopic disease for 30 minutes was rejected because this HIPEC did not prolong survival (which became "the ugly fact"). Nevertheless, the hypothesis of HIPEC as adjuvant locoregional treatment in CRC with peritoneal involvement was not falsified by this trial. What the trial leads us to conclude is that HIPEC with oxaliplatin at that specific dose and perfusion time did not influence OS. Furthermore, the trial results show that a potential benefit of the regimen cannot be excluded. There was a trend towards better locoregional control of the disease in the first 18 months after surgery, as shown by the Kaplan Meier curves, corresponding to a decrease in peritoneal recurrence observed in the CRS/HIPEC group compared with CRS alone[19]. Additionally, the authors found in a post-hoc subgroup analysis that median overall and relapse-free survival were longer in patients with a peritoneal cancer index (PCI) of 11-15 in the CRS plus HIPEC group than in those in the CRS group. This result may encourage future research into the role of HIPEC in patients with a PCI of 11-15 and in whom complete or near-complete surgical resection is achieved.

Apart from OS results, the issue of morbidity and mortality is of importance when discussing the role of HIPEC. The morbidity at 30 days reported by the PRODIGE 7 study was not different between the groups, with 42% in the CRS/HIPEC group *vs* 32% in the CRS alone group (P = 0.083). The intra-abdominal complications were not different at 30 days (27% *vs* 18%, P = 0.084) and 60 days (6% *vs* 3%, P = 0.38) between the CRS/HIPEC and CRS alone groups, respectively. Four patients died within 30 days of CRS with or without HIPEC, two (2%) due to cardiac failure and massive pneumonia in the CR/HIPEC group, and 2 (2%) due to intraperitoneal hemorrhage and septic shock in the CRS alone group. The difference in morbidity was statistically significant for: neutropenia (17% *vs* 8%, P = 0.025), thrombocytopenia (9% *vs* 2%, P = 0.011), and late severe complications (day 31-60) (26% *vs* 15%, P = 0.035) in the CRS/HIPEC group and CRS alone group, respectively. It is striking that the higher complication rate in the HIPEC/CRS group was rapidly associated with the oxaliplatin intraperitoneal infusion, and was not considered to be related to 5-FU intravenous bolus administered to the anesthetized patient, as this was performed following the bidirectional chemotherapy protocol[20] used in the trial. It is well known that bolus administration of 5-FU is associated with hematological toxicities (anemia, neutropenia, and thrombocytopenia)[21-23]. Therefore, the effect of endovenous administration of 5-FU on postoperative complications should be studied before ascribing the higher morbidity shown in the CRS/HIPEC group to the sole administration of intraperitoneal chemotherapy agent.

The Group of Professor Bruno Camps from Valencia, Spain, one of the pioneers of CRS/HIPEC in this country, used mitomycin C for 60 minutes at 40 ºC, without the administration of systemic chemotherapy. No treatment-associated myelosuppression was observed in our patients.

Despite the negative results for HIPEC in the PRODIGE 7 trial, worldwide CRS/HIPEC surgical groups have not been discouraged and persevere using several HIPEC protocols in patients with CRC peritoneal metastases. These patients, mainly if metastases are metachronous, may require very complex surgical management, due to the disease itself and to previous surgical adhesions. Therefore, identifying patients who will benefit from CRS with or without HIPEC would be of great interest.

PROGNOSTIC MARKERS AND SURGICAL INDICATIONS FOR CRS/HIPEC

In the recent issue of *World Journal of Gastrointestinal Oncology*, Wu *et al*[24] published their work on markers related to the prognosis of patients with peritoneal metastasis of CRC. The authors performed a study aiming to investigate the association of preoperative inflammatory neutrophil-to-lymphocyte ratio (NLR) and nutritional markers (hemoglobin) with prognosis in patients with CRC peritoneal metastases. They undertook a retrospective study including a series of 133 patients with peritoneal metastases from CRC who underwent CRS and HIPEC. The protocol used in their institution was a mixture of 5-FU, oxaliplatin, and platinum, at 42ºC, for 60 minutes for patients with a completeness of cytoreduction (CC) score of CC 0 or CC 1 (non-macroscopic disease after resection, or residual tumor nodules of less 2.5 mm as the maximum diameter, respectively). They determined an optimal NLR cutoff value of 3.1 for predicting OS (high NLR group: NLR ≥ 3.1; low NLR group: NLR < 3.1). The authors observed a median OS for patients with high NLR of 7.9 months compared with 25.4 months for those with low NLR (P = 0.002). As revealed by the authors, there are currently no standardized NLR values for all patient cohorts and this could limit the conclusion of the study concerning the influence of NLR on OS.

Another finding in the study was that albumin level, unlike hemoglobin (Hb) level, was not an independent prognostic factor in their multivariate analysis, and therefore they proposed that Hb was a better indicator of nutritional status and prognosis than albumin. In their series, patients with normal Hb had a significantly longer median OS (18.5 months) than those with low Hb (6.3 months; P < 0.001)[24].

The study also provided a nomogram, which included the factors Hb, age, NLR, serum cancer antigen 19.9, and PCI [24], that translated the importance of these factors for assessment of surgical risk, as well as prognostic factors. The

consideration of these factors, mainly the PCI, will be necessary when the decision to proceed with CRS with or without HIPEC is taken.

CONCLUSION

In conclusion, CRS must be included in the treatment of selected patients with stage IV CRC with peritoneal metastases, in association with systemic chemotherapy. Thus, surgery should not be viewed only as palliative treatment, and therapeutic resection surgery must always be considered. The administration of HIPEC should be left to the discretion of the surgical group. Provided that there are no postoperative complications directly related to HIPEC, the administration of HIPEC should be encouraged mainly when CC 0 and CC 1 resections are obtained, and preferably in clinical trials.

FOOTNOTES

Author contributions: Morera-Ocon FJ drafted the manuscript; Morera-Ocon FJ and Navarro-Campoy C translated and completed the manuscript; Guastella T and Landete-Molina F reviewed the manuscript. All authors contributed to the manuscript revision and approved the submitted version.

Conflict-of-interest statement: The authors have nothing to disclose.

Country of origin: Spain

ORCID number: Francisco J Morera-Ocon 0000-0002-7378-5086; Clara Navarro-Campoy 0000-0003-3727-3312.

S-Editor: Qu XL
L-Editor: Webster JR
P-Editor: Zhao S

REFERENCES

1 **Cervantes A**, Adam R, Roselló S, Arnold D, Normanno N, Taïeb J, Seligmann J, De Baere T, Osterlund P, Yoshino T, Martinelli E; ESMO Guidelines Committee. Metastatic colorectal cancer: ESMO Clinical Practice Guideline for diagnosis, treatment and follow-up. *Ann Oncol* 2023; **34**: 10-32 [PMID: 36307056 DOI: 10.1016/j.annonc.2022.10.003]

2 **Van Cutsem E**, Cervantes A, Adam R, Sobrero A, Van Krieken JH, Aderka D, Aranda Aguilar E, Bardelli A, Benson A, Bodoky G, Ciardiello F, D'Hoore A, Diaz-Rubio E, Douillard JY, Ducreux M, Falcone A, Grothey A, Gruenberger T, Haustermans K, Heinemann V, Hoff P, Köhne CH, Labianca R, Laurent-Puig P, Ma B, Maughan T, Muro K, Normanno N, Österlund P, Oyen WJ, Papamichael D, Pentheroudakis G, Pfeiffer P, Price TJ, Punt C, Ricke J, Roth A, Salazar R, Scheithauer W, Schmoll HJ, Tabernero J, Taïeb J, Tejpar S, Wasan H, Yoshino T, Zaanan A, Arnold D. ESMO consensus guidelines for the management of patients with metastatic colorectal cancer. *Ann Oncol* 2016; **27**: 1386-1422 [PMID: 27380959 DOI: 10.1093/annonc/mdw235]

3 **Koopman M**, Antonini NF, Douma J, Wals J, Honkoop AH, Erdkamp FL, de Jong RS, Rodenburg CJ, Vreugdenhil G, Loosveld OJ, van Bochove A, Sinnige HA, Creemers GM, Tesselaar ME, Slee PHTJ, Werter MJ, Mol L, Dalesio O, Punt CJ. Sequential versus combination chemotherapy with capecitabine, irinotecan, and oxaliplatin in advanced colorectal cancer (CAIRO): a phase III randomised controlled trial. *Lancet* 2007; **370**: 135-142 [PMID: 17630036 DOI: 10.1016/S0140-6736(07)61086-1]

4 **Tol J**, Koopman M, Rodenburg CJ, Cats A, Creemers GJ, Schrama JG, Erdkamp FL, Vos AH, Mol L, Antonini NF, Punt CJ. A randomised phase III study on capecitabine, oxaliplatin and bevacizumab with or without cetuximab in first-line advanced colorectal cancer, the CAIRO2 study of the Dutch Colorectal Cancer Group (DCCG). An interim analysis of toxicity. *Ann Oncol* 2008; **19**: 734-738 [PMID: 18272912 DOI: 10.1093/annonc/mdm607]

5 **Sugarbaker PH**. Peritonectomy procedures. *Ann Surg* 1995; **221**: 29-42 [PMID: 7826158 DOI: 10.1097/00000658-199501000-00004]

6 **Gilly FN**, Beaujard A, Glehen O, Grandclement E, Caillot JL, Francois Y, Sadeghi-Looyeh B, Gueugniaud PY, Garbit F, Benoit M, Bienvenu J, Vignal J. Peritonectomy combined with intraperitoneal chemohyperthermia in abdominal cancer with peritoneal carcinomatosis: phase I-II study. *Anticancer Res* 1999; **19**: 2317-2321 [PMID: 10472351]

7 **Detroz B**, Elias D, Damia E, Debaene B, Rougier P, Lasser P. [Intraperitoneal hyperthermic chemotherapy (IPHC), a promising treatment of peritoneal carcinomatosis]. *Bull Cancer* 1994; **81**: 182-193 [PMID: 7894126]

8 **Zoetmulder FA**, Sugarbaker PH. Patterns of failure following treatment of pseudomyxoma peritonei of appendiceal origin. *Eur J Cancer* 1996; **32A**: 1727-1733 [PMID: 8983281 DOI: 10.1016/0959-8049(96)00178-5]

9 **Zoetmulder FA**. Cancer cell seeding during abdominal surgery: experimental studies. *Cancer Treat Res* 1996; **82**: 155-161 [PMID: 8849949 DOI: 10.1007/978-1-4613-1247-5_10]

10 **Evrard S**, Desolneux G, Bellera C, Esnaud T, Bécouarn Y, Collet D, Chafai N, Marchal F, Cany L, Lermite E, Rivoire M, Mathoulin-Pélissier S. Systemic chemotherapy plus cetuximab after complete surgery in the treatment of isolated colorectal peritoneal carcinoma: COCHISE phase

II clinical trial. *BMC Res Notes* 2019; **12**: 450 [PMID: 31331370 DOI: 10.1186/s13104-019-4476-9]

11 **Désolneux G**, Mazière C, Vara J, Brouste V, Fonck M, Béchade D, Bécouarn Y, Evrard S. Cytoreductive surgery of colorectal peritoneal metastases: outcomes after complete cytoreductive surgery and systemic chemotherapy only. *PLoS One* 2015; **10**: e0122816 [PMID: 25825874 DOI: 10.1371/journal.pone.0122816]

12 **Matsuda K**, Hotta T, Takifuji K, Yamamoto M, Nasu T, Togo N, Oka M, Tabuse K, Yamaue H. Clinical impact of a macroscopically complete resection of colorectal cancer with peritoneal carcinomatosis. *Surgery* 2012; **151**: 238-244 [PMID: 21176934 DOI: 10.1016/j.surg.2010.10.018]

13 **Baratti D**, Kusamura S, Pietrantonio F, Guaglio M, Niger M, Deraco M. Progress in treatments for colorectal cancer peritoneal metastases during the years 2010-2015. A systematic review. *Crit Rev Oncol Hematol* 2016; **100**: 209-222 [PMID: 26867984 DOI: 10.1016/j.critrevonc.2016.01.017]

14 **Verwaal VJ**, van Ruth S, de Bree E, van Sloothen GW, van Tinteren H, Boot H, Zoetmulder FA. Randomized trial of cytoreduction and hyperthermic intraperitoneal chemotherapy versus systemic chemotherapy and palliative surgery in patients with peritoneal carcinomatosis of colorectal cancer. *J Clin Oncol* 2003; **21**: 3737-3743 [PMID: 14551293 DOI: 10.1200/JCO.2003.04.187]

15 **Quenet F**, Elias D, Roca L, Goere D, Ghouti L, Pocard M, Facy O, Arvieux C, Lorimier G, Pezet D, Marchal F, Loi V, Meeus P, De Forges H, Stanbury T, Paineau J, Glehen O; UNICANCER-GI Group and the French BIG-Renape Group. A UNICANCER phase III trial of hyperthermic intra-peritoneal chemotherapy (HIPEC) for colorectal peritoneal carcinomatosis (PC): PRODIGE 7. *J Clin Oncol* 2018; **36**: LBA3503-LBA3503 [DOI: 10.1200/jco.2018.36.18_suppl.lba3503]

16 **Quénet F**, Elias D, Roca L, Goéré D, Ghouti L, Pocard M, Facy O, Arvieux C, Lorimier G, Pezet D, Marchal F, Loi V, Meeus P, Juzyna B, de Forges H, Paineau J, Glehen O; UNICANCER-GI Group and BIG Renape Group. Cytoreductive surgery plus hyperthermic intraperitoneal chemotherapy versus cytoreductive surgery alone for colorectal peritoneal metastases (PRODIGE 7): a multicentre, randomised, open-label, phase 3 trial. *Lancet Oncol* 2021; **22**: 256-266 [PMID: 33476595 DOI: 10.1016/S1470-2045(20)30599-4]

17 **Anonymous**. Address of Thomas Henry Huxley, at the meeting of the British Association at Liverpool, on the 14th of Sept., 1870. *Am J Sci* 1870; **s2-50**: 383-402 [DOI: 10.2475/ajs.s2-50.150.383]

18 **Evrard S**. Autopsy of an expert consensus: End of hyperthermic intraperitoneal chemotherapy in colorectal carcinomatosis. *Eur J Surg Oncol* 2018; **44**: 1845-1846 [PMID: 30172424 DOI: 10.1016/j.ejso.2018.07.061]

19 **Ceelen W**. HIPEC with oxaliplatin for colorectal peritoneal metastasis: The end of the road? *Eur J Surg Oncol* 2019; **45**: 400-402 [PMID: 30392745 DOI: 10.1016/j.ejso.2018.10.542]

20 **Elias D**, Bonnay M, Puizillou JM, Antoun S, Demirdjian S, El OA, Pignon JP, Drouard-Troalen L, Ouellet JF, Ducreux M. Heated intra-operative intraperitoneal oxaliplatin after complete resection of peritoneal carcinomatosis: pharmacokinetics and tissue distribution. *Ann Oncol* 2002; **13**: 267-272 [PMID: 11886004 DOI: 10.1093/annonc/mdf019]

21 **Khan M**, Alharbi S, Aljuhani S, Tunkar M, Morya A, Alnatsheh A, Alshamrani M, Felemban R. The Incidence of Hematological Toxicities in Colorectal Cancer Patients Treated With Fluoropyrimidine-Based Regimens at Princess Noorah Oncology Center. *Cureus* 2023; **15**: e44267 [PMID: 37772227 DOI: 10.7759/cureus.44267]

22 **Garg MB**, Lincz LF, Adler K, Scorgie FE, Ackland SP, Sakoff JA. Predicting 5-fluorouracil toxicity in colorectal cancer patients from peripheral blood cell telomere length: a multivariate analysis. *Br J Cancer* 2012; **107**: 1525-1533 [PMID: 22990653 DOI: 10.1038/bjc.2012.421]

23 **Gradishar WJ**, Vokes EE. 5-Fluorouracil cardiotoxicity: a critical review. *Ann Oncol* 1990; **1**: 409-414 [PMID: 2083185 DOI: 10.1093/oxfordjournals.annonc.a057793]

24 **Wu ZJ**, Lan B, Luo J, Ameti A, Wang H, Hu QY. Impact of preoperative inflammatory and nutritional markers on the prognosis of patients with peritoneal metastasis of colorectal cancer. *World J Gastrointest Oncol* 2024; **16**: 3865-3874 [PMID: 39350999 DOI: 10.4251/wjgo.v16.i9.3865]

World Journal of Gastrointestinal Oncology

Submit a Manuscript: https://www.f6publishing.com

World J Gastrointest Oncol 2025 January 15; 17(1): 100369

DOI: 10.4251/wjgo.v17.i1.100369

ISSN 1948-5204 (online)

LETTER TO THE EDITOR

Curcumin in gastric cancer treatment: A commentary on mechanistic insights and future directions

Xin-Yue Wei, Wen-Bo Cao, Sai-Jun Mo, Zhi-Yan Sun

Specialty type: Oncology

Provenance and peer review: Invited article; Externally peer reviewed.

Peer-review model: Single blind

Peer-review report's classification

Scientific Quality: Grade B
Novelty: Grade B
Creativity or Innovation: Grade B
Scientific Significance: Grade B

P-Reviewer: Tang X

Received: August 14, 2024
Revised: September 23, 2024
Accepted: October 21, 2024
Published online: January 15, 2025
Processing time: 119 Days and 20.3 Hours

Xin-Yue Wei, Department of Pathophysiology, School of Basic Medical Sciences, Zhengzhou University, Zhengzhou 450001, Henan Province, China

Wen-Bo Cao, School of Basic Medical Science, Zhengzhou University, Zhengzhou 450001, Henan Province, China

Sai-Jun Mo, Department of Basic Science of Oncology, School of Basic Medical Sciences, Zhengzhou University, Zhengzhou 450001, Henan Province, China

Zhi-Yan Sun, Department of Special Service, No. 988 Hospital of the Joint Service Support Force of PLA, Zhengzhou 450042, Henan Province, China

Co-first authors: Xin-Yue Wei and Wen-Bo Cao.

Co-corresponding authors: Sai-Jun Mo and Zhi-Yan Sun.

Corresponding author: Sai-Jun Mo, PhD, Associate Professor, Department of Basic Science of Oncology, School of Basic Medical Sciences, Zhengzhou University, No. 100 Science Avenue, Zhongyuan District, Zhengzhou 450001, Henan Province, China. sjmo@zzu.edu.cn

Abstract

The study by Yang *et al* presents a comprehensive investigation into the therapeutic potential of curcumin for gastric cancer (GC). Using network pharmacology, the researchers identified 48 curcumin-related genes, 31 of which overlap with GC targets. Key genes, including *ESR1*, *EGFR*, *CYP3A4*, *MAPK14*, *CYP1A2*, and *CYP2B6*, are linked to poor survival in GC patients. Molecular docking confirmed strong binding affinity of curcumin to these genes. *In vitro* experiments demonstrated that curcumin effectively inhibits the growth and proliferation of *BGC-823*, suggesting its therapeutic potential in GC through multiple targets and pathways.

Key Words: Curcumin; Gastric cancer; Network pharmacology; Mechanism of action; *In vitro* experiments

Core Tip: The study by Yang *et al* elucidates the therapeutic mechanisms of curcumin in gastric cancer treatment, identifying key targets and confirming their interactions with curcumin through molecular docking. This study provides a solid foundation for further exploration of curcumin's role in gastric cancer therapy.

Citation: Wei XY, Cao WB, Mo SJ, Sun ZY. Curcumin in gastric cancer treatment: A commentary on mechanistic insights and future directions. *World J Gastrointest Oncol* 2025; 17(1): 100369
URL: https://www.wjgnet.com/1948-5204/full/v17/i1/100369.htm
DOI: https://dx.doi.org/10.4251/wjgo.v17.i1.100369

TO THE EDITOR

We had the privilege of reading the article "Curcumin for gastric cancer: Mechanism prediction *via* network pharmacology, docking, and *in vitro* experiments[1]," authored by Yang *et al*[1], published in the *World Journal of Gastrointestinal Oncology*. This study explores the potential therapeutic mechanisms of curcumin for gastric cancer (GC) through network pharmacology, molecular docking, and *in vitro* experiments, offering new perspectives and approaches for GC treatment.

We would like to commend the authors for their work on elucidating the pharmacological mechanisms of curcumin. The article initially assesses the pharmacokinetic properties of curcumin using network pharmacology methods and predicts its potential targets through various databases. The cross-analysis with GC disease targets successfully identified multiple key genes associated with curcumin, laying the foundation for subsequent experimental validation, and providing a powerful tool for the modernization of research into natural medicinal materials. The identification of key genes such as ESR1 and EGFR, along with the validation of curcumin's binding affinity through molecular docking, presents a significant advancement in the field[2,3].

It is particularly noteworthy that this study goes beyond theoretical exploration and further verifies the interaction between curcumin and core targets through molecular docking and *in vitro* experiments. The inhibitory effects of curcumin on BGC-823 cells contribute to further evidence for the use of curcumin in cancer therapy[4]. The highlight of this study lies in its integration of multidisciplinary methods. By employing advanced network pharmacology, combined with molecular docking techniques and *in vitro* experimental validation, this interdisciplinary research approach provides a new strategy to explore the pharmacological effects of natural medicinal materials. Gene ontology enrichment analysis and Kyoto Encyclopedia of Genes and Genomes pathway analysis reveal that curcumin may act through multiple biological processes and signaling pathways. Furthermore, the analysis of patient survival data using Kaplan–Meier plots shows that high expression of certain core targets is correlated with poor prognosis in GC patients, providing clinical relevance for curcumin as a potential therapeutic agent.

However, we also have some exploratory opinions on certain aspects of the study. Firstly, regarding the pharmacokinetic properties of curcumin, although the article mentions the assessment results of Lipinski's Rule of Five, the discussion on the bioavailability and pharmacokinetic characteristics of curcumin in the body appears insufficient. Given that the bioavailability of curcumin has always been one of the challenges in its clinical application[5], future research that further explores its pharmacokinetic behavior in the body will be significant in promoting its clinical use.

Secondly, while the study's network pharmacology predicted multiple targets and validated them through molecular docking experiments, an in-depth discussion on the specific mechanisms by which these targets affect the occurrence and development of GC and how they synergistically influence the biological behavior of GC cells seems lacking. Future research that delves into the molecular mechanisms of action of these core targets will help to better understand the anti-cancer effects of curcumin.

In future experiments, the range of curcumin concentrations used in the article may need further optimization in animal models to simulate real clinical use and consider drug interactions and side effects. The study should also consider the potential genetic and epigenetic differences between patients, which may affect the efficacy and tolerance of curcumin. Lastly, although the *in vitro* experimental results are encouraging, the anti-cancer effects and mechanisms of curcumin in the body still need to be verified by more *in vivo* experiments. It is suggested that the authors consider conducting relevant animal model studies to further explore the *in vivo* anti-tumor effects of curcumin.

In summary, the research by Yang *et al*[1] provides valuable insights and directions for the application of curcumin in GC treatment. We commend this work and look forward to the authors conducting more in-depth investigations on the issues in their future studies.

ACKNOWLEDGEMENTS

We express our gratitude to the reviewers for their constructive feedback, which has significantly enhanced the quality of this manuscript.

FOOTNOTES

Author contributions: This study was conceptualized and the draft was written by Wei XY; Cao WB, Mo SJ, and Sun ZY participated in revising the manuscript; All authors have read and approved the final version of the manuscript. Wei XY proposed the study, designed and performed the analysis, and wrote the initial draft. Cao WB was responsible for proofreading and editing. Both authors made key and indispensable contributions to the completion of this project and are, therefore, eligible to be co-first authors thereof. Mo SJ and Sun ZY served as co-corresponding authors and played an important and indispensable role in various aspects, including writing the paper. Mo SJ applied for and obtained funding for this research project; she supervised the entire process of the project, searched for relevant materials, and revised and submitted the early versions of the manuscript. The collaboration between Mo SJ and Sun ZY was crucial for the publication of this manuscript and other manuscripts currently in preparation.

Supported by The College Students' Innovation and Entrepreneurship Competition, No. 2024cxcy504 and No. 202410459164.

Conflict-of-interest statement: All the authors report no relevant conflicts of interest for this article.

Country of origin: China

ORCID number: Sai-Jun Mo 0000-0001-7375-3562.

S-Editor: Li L
L-Editor: Filipodia
P-Editor: Zhao YQ

REFERENCES

1 **Yang PH**, Wei YN, Xiao BJ, Li SY, Li XL, Yang LJ, Pan HF, Chen GX. Curcumin for gastric cancer: Mechanism prediction *via* network pharmacology, docking, and in vitro experiments. *World J Gastrointest Oncol* 2024; **16**: 3635-3650 [PMID: 39171177 DOI: 10.4251/wjgo.v16.i8.3635]
2 **Li J**, Wang X, Xue L, He Q. Exploring the therapeutic mechanism of curcumin in prostate cancer using network pharmacology and molecular docking. *Heliyon* 2024; **10**: e33103 [PMID: 39022084 DOI: 10.1016/j.heliyon.2024.e33103]
3 **Liang Y**, Zhao J, Zou H, Zhang J, Zhang T. In vitro and in silico evaluation of EGFR targeting activities of curcumin and its derivatives. *Food Funct* 2021; **12**: 10667-10675 [PMID: 34604873 DOI: 10.1039/d1fo02002a]
4 **Liang T**, Zhang X, Xue W, Zhao S, Zhang X, Pei J. Curcumin induced human gastric cancer BGC-823 cells apoptosis by ROS-mediated ASK1-MKK4-JNK stress signaling pathway. *Int J Mol Sci* 2014; **15**: 15754-15765 [PMID: 25198898 DOI: 10.3390/ijms150915754]
5 **Lopresti AL**. The Problem of Curcumin and Its Bioavailability: Could Its Gastrointestinal Influence Contribute to Its Overall Health-Enhancing Effects? *Adv Nutr* 2018; **9**: 41-50 [PMID: 29438458 DOI: 10.1093/advances/nmx011]

World Journal of Gastrointestinal Oncology

Submit a Manuscript: https://www.f6publishing.com

World J Gastrointest Oncol 2025 January 15; 17(1): 101581

DOI: 10.4251/wjgo.v17.i1.101581

ISSN 1948-5204 (online)

LETTER TO THE EDITOR

Network pharmacology: Changes the treatment mode of "one disease-one target" in cancer treatment

Shuai Liu, Yong-Wei Yu

Specialty type: Oncology

Provenance and peer review: Unsolicited article; Externally peer reviewed.

Peer-review model: Single blind

Peer-review report's classification

Scientific Quality: Grade B
Novelty: Grade C
Creativity or Innovation: Grade C
Scientific Significance: Grade B

P-Reviewer: Pan D

Received: September 19, 2024
Revised: October 7, 2024
Accepted: October 31, 2024
Published online: January 15, 2025
Processing time: 83 Days and 18.7 Hours

Shuai Liu, Department of Cardiology, The First People's Hospital of Jiashan, Jiaxing 314100, Zhejiang Province, China

Yong-Wei Yu, Department of Critical Care Medicine, The First Affiliated Hospital of Zhejiang University School of Medicine, Hangzhou 310000, Zhejiang Province, China

Corresponding author: Yong-Wei Yu, PhD, Doctor, Department of Critical Care Medicine, The First Affiliated Hospital of Zhejiang University School of Medicine, No. 79 Qingchun Road, Hangzhou 310000, Zhejiang Province, China. yuyongwei@zju.edu.cn

Abstract

The article concluded that network pharmacology provides new ideas and insights into the molecular mechanism of traditional Chinese medicine (TCM) treatment of cancer. TCM is a new choice and hot spot in the field of cancer treatment. We have also previously published studies on TCM and network pharmacology. In this letter, we summarize the new paradigm of network pharmacology in cancer treatment mechanisms.

Key Words: Network pharmacology; Cancer; Multicomponent; Multitarget; Therapy

Core Tip: Cancer cannot be effectively treated against a single gene target because it involves the synergy of different gene groups. Network pharmacology provides strong evidence of "multicomponent-multitarget" synergistic effects for the treatment of cancer with Chinese medicine.

Citation: Liu S, Yu YW. Network pharmacology: Changes the treatment mode of "one disease-one target" in cancer treatment. *World J Gastrointest Oncol* 2025; 17(1): 101581
URL: https://www.wjgnet.com/1948-5204/full/v17/i1/101581.htm
DOI: https://dx.doi.org/10.4251/wjgo.v17.i1.101581

TO THE EDITOR

We read with great interest the article recently published on the *World Journal of Gastrointestinal Oncology*[1]. The authors suggest that gastric cancer (GC) is the third most common malignancy in terms of both morbidity and mortality. At the same time, due to the difficulty in early diagnosis of GC, the current therapeutic methods are limited[2]. Although some molecular targeted drugs can be used for certain patients with overexpression or activation of certain targets, the scope of application is still very limited. Traditional Chinese medicine (TCM) is designed on the basis of the integrity of the human body and has the characteristics of multicomponent, multitarget and multilevel action[3], which can improve the clinical symptoms and quality of life in GC patients, prolong the survival time of patients, and reduce the toxic side effects caused by radiotherapy and chemotherapy. The authors revealed the possible mechanism by which the TCM Xiaoji-anzhong decoction improves GC by the synergistic effect of multiple targets through network pharmacology.

In recent years, the incidence and mortality of cancer have been rising, and traditional treatments, including chemotherapy, radiotherapy and surgery, are often unable to effectively control the progression of cancer. In the past few decades, the development of cancer treatment has focused on the development of drugs for a single target, that is, the "one disease-one target" model[4]. However, this strategy has been limited in addressing the complex pathological mechanisms of cancer. Cancer is a multifactorial, multistep, and multigene mutation-driven disease that involves abnormal activation or inhibition of multiple biological pathways[5]. Single-target drugs often cannot effectively address the diversity and complexity of cancer.

LIMITATIONS OF THE TRADITIONAL “ONE DISEASE-ONE TARGET” MODEL

The traditional drug development model is usually based on a single relationship between drug targets and diseases, which means that each disease is directly related to one or a few targets and that drugs regulate the progression of the disease by acting on these targets. However, the pathogenesis of cancer involves multiple signalling pathways and complex gene-environment interactions. Therefore, single-target drugs often fail to achieve the expected results in clinical applications, especially in the face of cancer heterogeneity and drug resistance[6]. First, the heterogeneity of cancer means that even for the same type of cancer, there are significant differences in gene expression profiles and pathological characteristics between patients. This heterogeneity means that a certain targeted drug is effective for some patients but may be ineffective or even harmful to others. Second, tumor cells are highly adaptable, and long-term use of a single targeted drug often leads to drug resistance, which gradually weakens or even makes the treatment ineffective. In addition, cancer involves abnormalities in multiple biological processes, such as proliferation, apoptosis, metabolism, and immune escape, and these processes cannot be fully inhibited by regulating a single target.

THE RISE OF NETWORK PHARMACOLOGY

In response to these challenges in cancer treatment, network pharmacology has been developed. Network pharmacology is a research method based on systems biology and network science that aims to understand the impact of drugs on the entire biological system by analyzing the complex interactions between drugs, genes, targets and diseases. Unlike the traditional "one disease-one target" model, network pharmacology focuses on the overall regulation of multiple targets and biological pathways and uses multi omics data and computational models to identify potential multitarget drugs or drug combinations, thereby formulating more precise and comprehensive treatment strategies[7,8]. Network pharmacology reveals complex disease mechanisms, especially multiple pathway regulatory mechanisms in cancer, by constructing a "disease-gene-target-drug" network. It uses computational models and big data analysis to connect targets, pathways, drugs, and diseases to form a multidimensional interactive pharmacological network. On the basis of this model, researchers can screen for potential multitarget drugs and even design treatments that can regulate multiple pathways simultaneously, thereby improving the accuracy and efficacy of cancer treatment.

APPLICATION OF NETWORK PHARMACOLOGY IN CANCER THERAPY

In cancer treatment, network pharmacology can provide new ideas and tools for the development of personalized treatment plans. Through network analysis, researchers can identify key regulatory nodes and core pathways in cancer, thereby developing multifunctional drugs that act on multiple targets. These drugs can not only regulate the multiple pathway mechanisms of cancer but also reduce the drug resistance caused by the failure or mutation of a single target[9-11]: (1) Development of multitarget drugs: Unlike single-target drugs, multitarget drugs can act on multiple interrelated targets or signalling pathways at the same time. Through network pharmacology, researchers can discover key target combinations that are closely related to cancer pathological mechanisms, facilitating the design of more effective drugs. For example, some natural products or compound drugs may regulate multiple signalling pathways at the same time, and the screening and development of these compounds can be achieved through network pharmacology; (2) Optimization of drug combinations: In addition to developing new multitarget drugs, network pharmacology can also be used to optimize existing drug combinations. By analyzing the interactions between different drugs and their impact on cancer pathology networks, we can identify drug combinations with synergistic effects, thereby improving efficacy and

reducing side effects; and (3) Precision medicine and personalized treatment: Network pharmacology can provide personalized treatment options for cancer patients. By analyzing multi omics data such as patient genomes, transcriptomes, and proteomes, researchers can construct personalized disease networks and identify patient-specific pathological pathways and key targets. This personalized network analysis lays the foundation for precision medicine, allowing each patient to receive a tailored treatment plan to maximize the treatment effect.

SHORTCOMINGS AND FUTURE OF NETWORK PHARMACOLOGY

Although network pharmacology has shown great potential in cancer treatment, it still faces some challenges. First, network pharmacology requires a large amount of multi omics data support, and the integration of different types of omics data is still difficult. Second, the construction and analysis of complex network models require advanced computational tools and algorithms, which places high demands on the technical level of researchers. In addition, although multitarget drugs and combination therapies are expected to improve therapeutic effects, how to reduce their potential side effects and toxicity still needs further study. In the future, with the advancement of omics technology and the accumulation of data, network pharmacology is expected to play a more important role in cancer treatment. In particular, with the introduction of artificial intelligence and big data analysis technology, network pharmacology will be able to predict the mechanism of action and clinical effects of drugs more accurately, thereby leading to more breakthroughs in cancer treatment.

CONCLUSION

As an emerging research paradigm, network pharmacology has changed the traditional "one disease-one target" treatment model and provided a new perspective for the multitarget and multi pathway treatment of cancer. By integrating multiomics data and systems biology methods, network pharmacology can not only improve the efficiency of drug development but also promote the development of personalized medicine, thereby providing cancer patients with more accurate and effective treatment options. In the future, with the further development of technology, network pharmacology will play an increasingly important role in cancer treatment.

FOOTNOTES

Author contributions: Liu S wrote the manuscript; Yu YW designed the study and revised the manuscript; All listed authors consent to the submission.

Conflict-of-interest statement: All the authors report no relevant conflicts of interest for this article.

Country of origin: China

ORCID number: Shuai Liu 0009-0009-6551-0224; Yong-Wei Yu 0000-0001-8319-7707.

S-Editor: Li L
L-Editor: A
P-Editor: Zhao S

REFERENCES

1 **Chen GQ**, Nan Y, Ning N, Huang SC, Bai YT, Zhou ZY, Qian G, Li WQ, Yuan L. Network pharmacology study and in vitro experimental validation of Xiaojianzhong decoction against gastric cancer. *World J Gastrointest Oncol* 2024; **16**: 3932-3954 [PMID: 39350988 DOI: 10.4251/wjgo.v16.i9.3932]

2 **Zeng H**, Chen W, Zheng R, Zhang S, Ji JS, Zou X, Xia C, Sun K, Yang Z, Li H, Wang N, Han R, Liu S, Li H, Mu H, He Y, Xu Y, Fu Z, Zhou Y, Jiang J, Yang Y, Chen J, Wei K, Fan D, Wang J, Fu F, Zhao D, Song G, Chen J, Jiang C, Zhou X, Gu X, Jin F, Li Q, Li Y, Wu T, Yan C, Dong J, Hua Z, Baade P, Bray F, Jemal A, Yu XQ, He J. Changing cancer survival in China during 2003-15: a pooled analysis of 17 population-based cancer registries. *Lancet Glob Health* 2018; **6**: e555-e567 [PMID: 29653628 DOI: 10.1016/S2214-109X(18)30127-X]

3 **Ren X**, Yan CX, Zhai RX, Xu K, Li H, Fu XJ. Comprehensive survey of target prediction web servers for Traditional Chinese Medicine. *Heliyon* 2023; **9**: e19151 [PMID: 37664753 DOI: 10.1016/j.heliyon.2023.e19151]

4 **Setijono SR**, Kwon HY, Song SJ. MicroRNA, an Antisense RNA, in Sensing Myeloid Malignancies. *Front Oncol* 2017; **7**: 331 [PMID:

29441324 DOI: 10.3389/fonc.2017.00331]

5 **Breitkreutz D**, Hlatky L, Rietman E, Tuszynski JA. Molecular signaling network complexity is correlated with cancer patient survivability. *Proc Natl Acad Sci U S A* 2012; **109**: 9209-9212 [PMID: 22615392 DOI: 10.1073/pnas.1201416109]

6 **Pan R**, Tang X, Wang H, Huang Y, Huang K, Ling S, Zhou M, Cai J, Chen H, Huang Y. The Combination of Astragalus membranaceus and Ligustrazine Protects Against Thrombolysis-Induced Hemorrhagic Transformation Through PKCδ/Marcks Pathway in Cerebral Ischemia Rats. *Cell Transplant* 2020; **29**: 963689720946020 [PMID: 32749163 DOI: 10.1177/0963689720946020]

7 **Omolo CA**, Soni N, Fasiku VO, Mackraj I, Govender T. Update on therapeutic approaches and emerging therapies for SARS-CoV-2 virus. *Eur J Pharmacol* 2020; **883**: 173348 [PMID: 32634438 DOI: 10.1016/j.ejphar.2020.173348]

8 **Azmi AS**. Adopting network pharmacology for cancer drug discovery. *Curr Drug Discov Technol* 2013; **10**: 95-105 [PMID: 23237672 DOI: 10.2174/1570163811310020002]

9 **Wang Y**, Zhao T, Huang C, Liu F, Zhang Y, Kong D, Fan Z. Effect and mechanism of Banxia Xiexin decoction in colorectal cancer: A network pharmacology approach. *Phytomedicine* 2024; **123**: 155174 [PMID: 38039904 DOI: 10.1016/j.phymed.2023.155174]

10 **Saravanan KS**, Satish KS, Saraswathy GR, Kuri U, Vastrad SJ, Giri R, Dsouza PL, Kumar AP, Nair G. Innovative target mining stratagems to navigate drug repurposing endeavours. *Prog Mol Biol Transl Sci* 2024; **205**: 303-355 [PMID: 38789185 DOI: 10.1016/bs.pmbts.2024.03.025]

11 **Liu T**, Wang J, Tong Y, Wu L, Xie Y, He P, Lin S, Hu X. Integrating network pharmacology and animal experimental validation to investigate the action mechanism of oleanolic acid in obesity. *J Transl Med* 2024; **22**: 86 [PMID: 38246999 DOI: 10.1186/s12967-023-04840-x]

Published by **Baishideng Publishing Group Inc**
7041 Koll Center Parkway, Suite 160, Pleasanton, CA 94566, USA
Telephone: +1-925-3991568
E-mail: office@baishideng.com
Help Desk: https://www.f6publishing.com/helpdesk
https://www.wjgnet.com